ZooKeys 1182: 1–9 (2023)
DOI: 10.3897/zookeys.1182.109532

Research Article

First record of the genus *Passiena* (Araneae, Lycosidae) from China, with the first description of the male of *P. spinicrus* Thorell, 1890 from Malaysia

Bing Tan[1], Muhammad Irfan[1], Zhi-Sheng Zhang[1], Lu-Yu Wang[1]

1 *Key Laboratory of Eco-environments in Three Gorges Reservoir Region (Ministry of Education), School of Life Science, Southwest University, Chongqing 400715, China*
Corresponding authors: Zhi-Sheng Zhang (zhangzs327@qq.com); Lu-Yu Wang (wangluyu1989@163.com)

Abstract

The genus *Passiena* is recorded for the first time from China with *Passiena duani* **sp. nov.** (♂♀) from Guangxi described here. In addition, the male of *P. spinicrus* Thorell, 1890 is described for the first time based on a specimen from Malaysia and colour photographs of freshly collected material are also presented. Detailed morphological descriptions, photographs, genital illustrations, and a distribution map for the two species are provided.

Key words: New record, new species, morphology, taxonomy, wolf spider

Academic editor: Sarah Crews
Received: 14 July 2023
Accepted: 23 September 2023
Published: 11 October 2023

ZooBank: https://zoobank.org/0D3B2D4D-D1C4-488C-9814-2B05C263D105

Citation: Tan B, Irfan M, Zhang Z-S, Wang L-Y (2023) First record of the genus *Passiena* (Araneae, Lycosidae) from China, with the first description of the male of *P. spinicrus* Thorell, 1890 from Malaysia. ZooKeys 1182: 1–9. https://doi.org/10.3897/zookeys.1182.109532

Introduction

Lycosidae is the sixth largest spider family with 2462 species in 132 genera distributed worldwide, including 310 species in 26 genera reported from China (World Spider Catalog 2023). In recent years, we have described several new genera of wolf spider from China, such as *Serratacosa* Wang, Peng & Zhang, 2021, *Sinacosa* Wang, Lu & Zhang, 2023 and *Sinartoria* Wang, Framenau & Zhang, 2021. Still, most of the lycosid diversity in China has not been fully documented.

The genus *Passiena* Thorell, 1890 contains five species from Cameroon, Indonesia, Laos, Malaysia, South Africa and Thailand (World Spider Catalog 2023). It is diagnosed by the male pedipalp with a unique group of soft spicules on the distal part of the palea (Lehtinen 2005). In this paper, *Passiena* is recorded for the first time in China, and the male of *P. spinicrus* Thorell, 1890, newly found in Malaysia, is described here. *Passiena duani* sp. nov. is predominantly found in the terrestrial habitat beneath forest canopies in Guangxi Province.

Materials and methods

All specimens were preserved in 75% ethanol and examined, illustrated, photographed and measured using a Leica M205A stereomicroscope equipped with a drawing tube, a Leica DFC450 camera, and Leica Application Suite software (Ver. 4.6). Male pedipalps and epigynes were examined and illustrated after dissection. Epigynes were cleared in pancreatin (Álvarez-Padilla and Hormiga 2007). Leg measurements are shown as: total length (femur, patella+tibia, metatarsus, tarsus). All measurements are in millimetres. Map was created using the online mapping software SimpleMappr (Shorthouse 2010) (Fig. 5). Specimens examined here are deposited in the spider collection at the School of Life Sciences, Southwest University, Chongqing, China (**SWUC**).

Abbreviations used in the text and figures: **ALE–**anterior lateral eye; **AME–**anterior median eye; **PLE–**posterior lateral eye; **PME–**posterior median eye; **A–**atrium; **Ap–**anterior apophysis of palea; **CO–**copulatory opening; **C–**conductor; **E–**embolus; **FD–**fertilization duct; **HS–**head of spermatheca; **H–**hood; **MA–**median apophysis; **Pt–**tip of posterior apophysis; **St–**subtegulum; **TA–**terminal apophysis; **T–**tegulum; **Se–**septum; **SS–**stalk of spermatheca.

Taxonomy

Family Lycosidae Sundevall, 1833
Genus *Passiena* Thorell, 1890 (帕狼蛛属)

Passiena duani sp. nov. (段氏帕狼蛛)

https://zoobank.org/6CE69B00-418B-4697-B35E-C2347209460E
Figs 1A, B, 2A–D, 3A–I, 5

Type material. ***Holotype*** (male): China, Guangxi Zhuang Autonomous Region, Chongzuo City, Ningming County, Chengzhong Town, Panlong, 22.2347°N, 107.0538°E, elev. 138 m, 25 April 2023, L.Y. Wang and Q.L. Lu leg. (SWUC-T-LY-13-01); ***Paratypes*** (3 males and 4 females): 2 males and 3 females, same data as holotype; 1 male and 1 female (SWUC-T-LY-13-07~08), Ningming County, Tuolong Township, Nongna Village, 22.2325°N, 107.0558°E, elev. 152 m, 19 June 2017, L.Y. Wang and R.B. Wu leg. (SWUC-T-LY-13-02~06).

Etymology. The specific name comes from the family name of Dr Meichun Duan, who gave much support to our research on spiders; noun in apposition.

Diagnosis. The new species resembles *P. bayi* Omelko & Marusik, 2020, *P. torbjoerni* Lehtinen, 2005 (Figs 2A–D, 3C–I; Omelko and Marusik 2020, figs 19–29) and *P. spinicrus* Thorell, 1890 (4C–I) in having similar median apophysis and terminal apophysis of the male pedipalp and variable sclerotization of the lateral plates at the base of the epigyne (Figs 2A–D, 3C–I, 4C–I; Omelko and Marusik 2020, figs 30–35). However, it can be distinguished by the combination of the following characters: 1) apical edge of anterior apophysis of palea as long as the stalk of posterior apophysis of palea (Fig. 3G) vs. about half the length of the stalk of posterior apophysis of palea in *P. bayi*, *P. torbjoerni* and *P. spinicrus* (Omelko and Marusik 2020, figs 25, 26; Fig. 4G); 2) cymbium apex with two claws (Fig. 3G) vs. with one claw in *P. bayi*, *P. torbjoerni* and *P. spinicrus* (Omelko and Marusik 2020, figs 27, 28; Fig. 4G); and 3) epigynal septum stem length/septum base width ratio 1.2 in *P. duani* sp. nov. and *P. torbjoerni* (Figs 2C, D, 3H, I; Omelko and Marusik 2020, figs 33, 34) vs. septum stem length/septum base width ratio 1.5 in *P. bayi* (Omelko and Marusik 2020, figs 30, 31) and *P. spinicrus* (Fig. 4H, I).

Figure 1. Live photo of *Passiena duani* sp. nov. (**A, B**) and *P. spinicrus* Thorell, 1890 (**C, D**) **A, C** male **B, D** female. Live photos taken by Qian-Le Lu (**A, B**) and Lu-Yu Wang (**C, D**).

Description. Male (holotype, Fig. 1A, 3A). Total length 4.08. Prosoma 2.05 long, 1.59 wide; opisthosoma 1.98 long, 1.30 wide. Carapace greyish brown. Eye sizes and interdistances: AME 0.09, ALE 0.07, PME 0.30, PLE 0.25; AME–AME 0.09, AME–ALE 0.04, PME–PME 0.33, PME–PLE 0.32. Clypeus height 0.18. Chelicerae dark brown, with three promarginal and three retromarginal teeth. Endites and labium dark brown, longer than wide. Sternum yellow brown, with sparse brown setae. Legs yellow brown. Tibia I with six pairs of ventral spines and metatarsus I with four pairs of ventral spines; tibia II with five pairs of ventral spines, metatarsus II with three pairs of ventral spines. Leg measurements: I 6.14 (1.63, 2.21, 1.48, 0.82); II 5.47 (1.54, 1.79, 1.36, 0.78); III 5.23 (1.46, 1.57, 1.43, 0.77); IV 8.02 (2.07, 2.38, 2.49, 1.08). Leg formula: 4123. Opisthosoma oval. Dorsum greyish brown, with black markings. Venter yellow brown.

Pedipalp (Figs 2A, B, 3C–G): Cymbium proximal part brown, distal part yellowish with two large claws on the tip. Subtegulum distinct in ventral view, located baso-prolaterally. Conductor somewhat membranous, somewhat tongue-shaped in ventral view and triangular in retrolateral view. Terminal apophysis terminates at approx. 1 o'clock position in ventral view. Embolus originating on the dorsal side of the bulb, long, prolaterally accompanied with

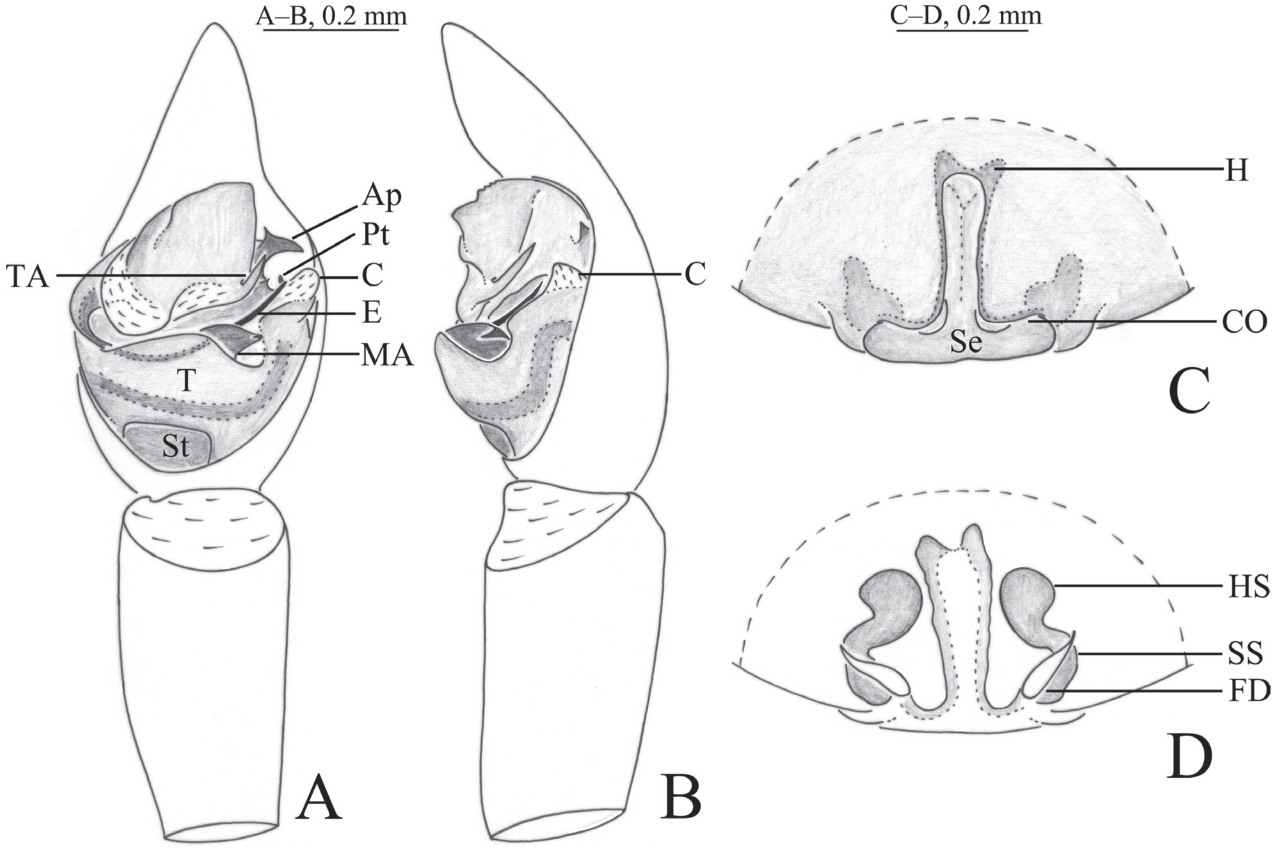

Figure 2. *Passiena duani* sp. nov., male holotype (**A, B**) and female paratype (**C, D**) **A** pedipalp, ventral view **B** same, retrolateral view **C** epigyne, ventral view **D** same, dorsal view.

a membrane, terminating at approx. 2 o'clock position; palea with two apophyses, anterior apophysis with smooth apical edge sharply pointed, and posterior one claw-like.

Female (one paratype, SWUC-T-LY-13-02, Fig. 1B, 3B). Total length 4.57. Prosoma 2.36 long, 1.83 wide; opisthosoma 2.28 long, 1.65 wide. Eye sizes and interdistances: AME 0.12, ALE 0.09, PME 0.35, PLE 0.27; AME–AME 0.10, AME–ALE 0.07, PME–PME 0.33, PME–PLE 0.38. Clypeus height 0.23. Leg measurements: **I** 6.87 (1.92, 2.43, 1.65, 0.87); **II** 6.12 (1.58, 2.18, 1.53, 0.83); **III** 5.96 (1.68, 1.77, 1.70, 0.81); **IV** 9.28 (2.28, 2.75, 2.98, 1.27). Leg formula: 4123. Tibia **I** with six pairs of ventral spines and metatarsus **I** with four pairs of ventral spines; tibia **II** with six pairs of ventral spines, metatarsus **II** with four pairs of ventral spines. Except genitalia, all other morphological characteristics same as in male.

Epigyne (Figs 2C–D, 3H–**I**). Anterior pocket with 2 hoods, septum reversed T-shaped with distinct stem becoming very thick in its anterior part and narrow posteriorly; stem 1.2 times longer than base width. Copulatory openings located posteriorly at the base of atrium transverse edges. Spermathecal heads sub-oval with the antero-lateral part angled, heads 2 times longer than septum base. Spermathecal stalks thick, short, slightly curved. Fertilization ducts teardrop-shaped.

Distribution. Currently known only from the type locality, Ningming County, Guangxi, China (Fig. 5).

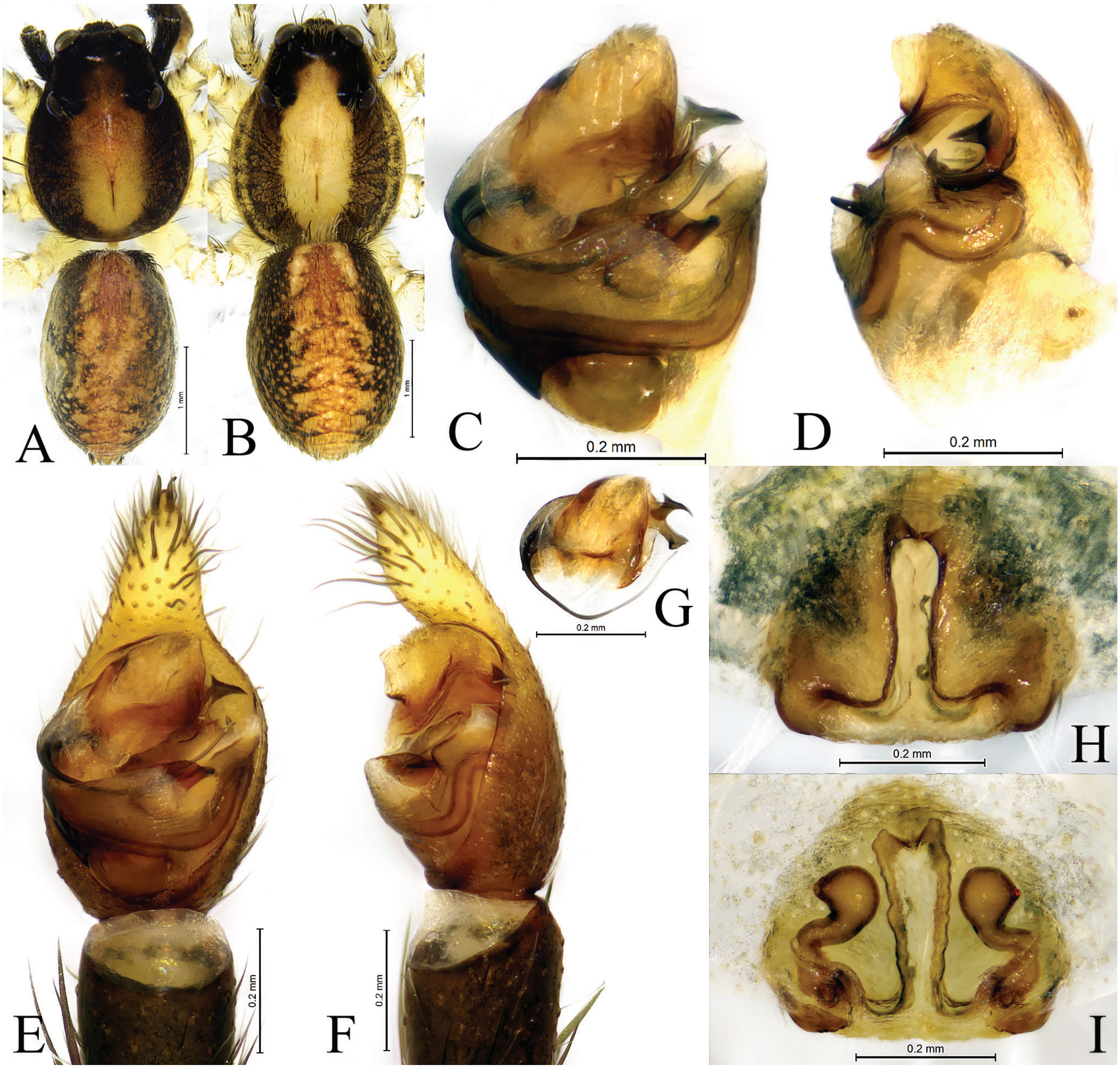

Figure 3. *Passiena duani* sp. nov., male holotype (**A, C–G**) and female paratype (**B, H, I**) **A** male habitus, dorsal view **B** female habitus, dorsal view **C, E** pedipalp, ventral view **D, F** same, retrolateral view **G** embolus and terminal apophysis, ventral view **H** epigyne, ventral view **I** same, dorsal view.

Passiena spinicrus **Thorell, 1890**
Figs 1C, D, 4, 5

Passiena spinicrus Thorell, 1890: 140 (♀); Lehtinen 2005: 402, figs 5–10 (♀); Omelko and Marusik 2020: 480, figs 6, 15, 18, 35 (♀).

Material examined. Malaysia: 6 males and 4 females, Borneo, Sabah, Trus Madi Mountain, 5.4669°N, 116.4488°E, elev. 760 m, 12 October 2015, G.Q. Huang and L.Y. Wang leg. (MLXY-15-15); 2 males and 1 female, Borneo, Sabah, Keningau, apin-apin, 5.4669°N, 116.2752°E, elev. 346 m, 17 October 2015, G.Q. Huang and L.Y. Wang leg. (MLXY-15-25); 4 males and 5 females, Borneo, Kalabakan, Maliau Basin, 4.54°N, 117.0272°E, elev. 321 m, 18 October 2015, G.Q.

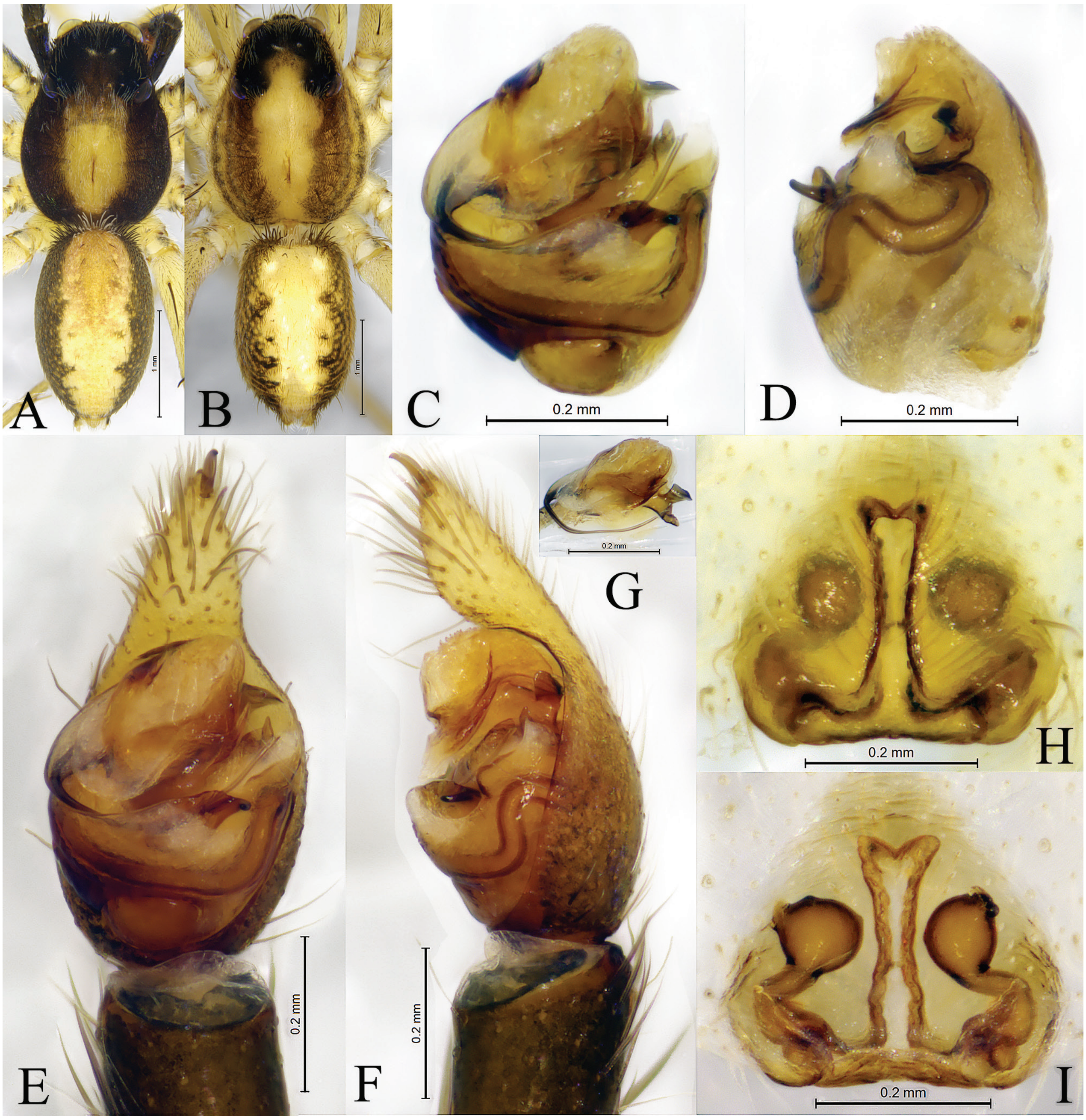

Figure 4. *Passiena spinicrus* Thorell, 1890, male (**A, C–G**) and female (**B, H, I**). **A** male habitus, dorsal view **B** female habitus, dorsal view **C** bulb, ventral view **D** same, retrolateral view **E** pedipalp, ventral view **F** same, retrolateral view **G** embolic division, ventral view **H** epigyne, ventral view **I** same, dorsal view.

Huang and L.Y. Wang leg. (MLXY-15-29); 1 male and 1 female, Borneo, Sabah, Sandakan, 5.8788°N, 118.0536°E, elev. 41 m, 19 October 2015, G.Q. Huang and L.Y. Wang leg. (MLXY-15-35).

Description. Male (Figs 1C, 4A) total length 3.91. Prosoma 2.16 long, 1.61 wide; opisthosoma 1.74 long, 1.02 wide. Carapace gray brown. Eye sizes and interdistances: AME 0.12, ALE 0.08, PME 0.34, PLE 0.28; AME–AME 0.10, AME–ALE 0.06, PME–PME 0.34, PME–PLE 0.37. Clypeus height 0.24. Chelicerae black brown, with three promarginal and three retromarginal teeth. Endites and labium black brown, longer than wide. Sternum yellow brown, with sparse brown hairs. Legs yellow brown. Tibia I with six pairs of ventral spines

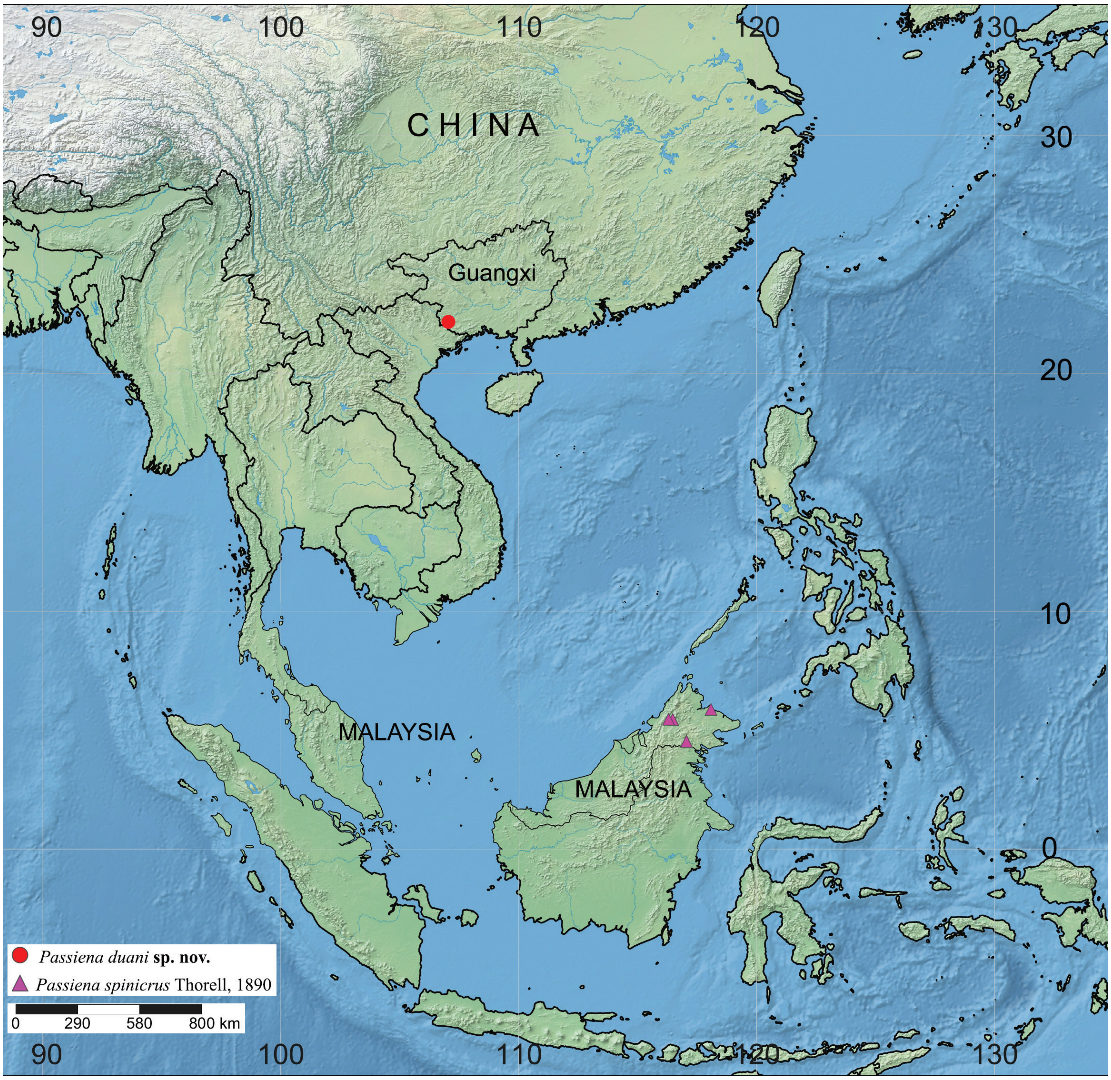

Figure 5. Map showing distribution records of *Passiena duani* sp. nov. and *P. spinicrus* Thorell, 1890.

and metatarsus I with four pairs of ventral spines; tibia II with six pairs of ventral spines, metatarsus II with four pairs of ventral spines. Leg measurements: I 6.63 (1.65, 2.39, 1.69, 0.90); II 5.98 (1.66, 1.99, 1.54, 0.79); III 5.75 (1.55, 1.82, 1.60, 0.78); IV 8.87 (2.22, 2.59, 2.87, 1.19). Leg formula: 4123. Opisthosoma oval. Dorsum greyish brown, with black markings. Venter yellow brown.

Pedipalp (Fig. 4C–G): Cymbium proximal part brown, distal part yellowish with two large claws on the tip. Subtegulum distinct in ventral view, located baso-prolaterally. Conductor somewhat membranous and tongue-shaped in ventral view and triangular in retrolateral view. Terminal apophysis terminates at approx. 1 o'clock position in ventral view. Embolus originating on the dorsal side of the bulb, long, prolaterally accompanied with a membrane, terminating at approx. 2 o'clock position; palea with two apophyses, anterior apophysis ax-shaped, and the posterior apex strongly curved.

Female (Figs 1D, 4B) total length 4.21. Prosoma 2.20 long, 1.77 wide; opisthosoma 1.89 long, 1.23 wide. Eye sizes and interdistances: AME 0.12, ALE 0.09, PME 0.33, PLE 0.29; AME–AME 0.08, AME–ALE 0.05, PME–PME 0.32, PME–PLE 0.37. Clypeus height 0.21. Legs yellow brown. Tibia I with six pairs of ventral spines and metatarsus I with four pairs of ventral spines; tibia II with six pairs of ventral spines, metatarsus II with three pairs of ventral spines. Leg measurements: I 6.96 (1.92, 2.56, 1.66, 0.82); II 6.36 (1.77, 2.19, 1.57, 0.83); III 6.02 (1.64, 1.89, 1.68, 0.81); IV 9.04 (2.38, 2.56, 2.87, 1.23). Leg formula: 4123.

Epigyne (Fig. 4H, I). Anterior pocket with 2 hoods, septum reversed T-shaped with distinct stem becoming very thick in its anterior part and narrow at the center. Copulatory openings located posteriorly at the base of atrium transverse edges. Spermathecal heads globular with the antero-lateral part angled, heads 2 times longer than septum base. Spermathecal stalks thick, short, slightly curved. Fertilization ducts extending postero-laterally.

Distribution. Malaysia, Indonesia (Borneo) (Fig. 5).

Discussion

In all known species of the genus *Passiena*, it is observed that the reproductive organs of both male and female individuals exhibit a remarkable resemblance, hence posing a considerable challenge in terms of distinguishing between congeners. The majority of species can be distinguished solely based on the morphology of the palea apophyses in the male pedipalps and the spermathecae shape in epigynes as can be seen in the study carried out by Omelko and Marusik (2020). Logunov and Ponomarev (2020) and Lehtinen (2005) used morphological traits to place this genus into the subfamily Lycosinae. However, no molecular analysis of *Passiena* was included in the largest phylogenetic analysis of Lycosidae by Piacentini and Ramírez (2019). It is highly recommended that future studies undertake a revision of *Passiena*, taking into consideration both molecular and morphological data.

Acknowledgements

Many thanks are given to Mr Sheng Du (Xinjiang), Run-Biao Wu (SWUC formerly) for their assistance during the field work and collection.

Additional information

Conflict of interest

The authors have declared that no competing interests exist.

Ethical statement

No ethical statement was reported.

Funding

This research was supported by the Science & Technology Fundamental Resources Investigation Program (Grant No. 2022FY202100), the Fundamental Research Funds for the Central Universities (SWU120051), the Key Natural Science Foundation of Chongqing (cstc2019jcyj-zdxmX0006), the Investigation Project of Basic Science and Technology (2018FY100305), Chongqing Provincial Funding for Postdoc (cstc2021jcyj-bsh0196) and Foreign Youth Talent Program Funding (QN2022168002L).

Author contributions

All authors have contributed equally.

Author ORCIDs

Bing Tan https://orcid.org/0009-0003-0517-1116
Muhammad Irfan https://orcid.org/0000-0003-0445-9612
Zhi-Sheng Zhang https://orcid.org/0000-0002-9304-1789
Lu-Yu Wang https://orcid.org/0000-0002-5250-3473

Data availability

All of the data that support the findings of this study are available in the main text.

References

Álvarez-Padilla F, Hormiga G (2007) A protocol for digesting internal soft tissues and mounting spiders for scanning electron microscopy. The Journal of Arachnology 35(3): 538–542. https://doi.org/10.1636/Sh06-55.1

Lehtinen PT (2005) Review of the Oriental wolf spider genus *Passiena* (Lycosidae, Pardosinae). The Journal of Arachnology 33(2): 398–407. https://doi.org/10.1636/05-11.1

Logunov DV, Ponomarev AV (2020) *Karakumosa* gen. nov., a new Central Asian genus of fossorial wolf spiders (Araneae: Lycosidae: Lycosinae). Revue Suisse de Zoologie 127(2): 275–313. https://doi.org/10.35929/RSZ.0021

Omelko MM, Marusik YM (2020) A new species and new records of wolf spiders (Araneae: Lycosidae) from Laos. The Raffles Bulletin of Zoology 68: 479–487. https://doi.org/10.26107/RBZ-2020-0066

Piacentini LN, Ramírez MJ (2019) Hunting the wolf: A molecular phylogeny of the wolf spiders (Araneae, Lycosidae). Molecular Phylogenetics and Evolution 136: 227–240. https://doi.org/10.1016/j.ympev.2019.04.004

Shorthouse DP (2010) SimpleMappr, an online tool to produce publication-quality point maps. https://www.simplemappr.net [Accessed on 23 Sep. 2023]

Sundevall CJ (1833) Conspectus *Arachnidum*. C. F. Berling, Londini Gothorum [= Lund], 1–39.

Thorell T (1890) Diagnoses aranearum aliquot novarum in Indo *Malesia inventarum*. Annali del Museo Civico di Storia Naturale di Genova 30: 132–172.

Wang LY, Framenau VW, Zhang ZS (2021a) A further study on the wolf spider subfamily Artoriinae from China (Araneae: Lycosidae). Zootaxa 4964(3): 571–584. https://doi.org/10.11646/zootaxa.4964.3.8

Wang LY, Peng XJ, Zhang ZS (2021b) *Serratacosa*, a new genus of Lycosidae (Araneae) from the southern slopes of the Eastern Himalayas. European Journal of Taxonomy 762: 96–107. https://doi.org/10.5852/ejt.2021.762.1455

Wang LY, Lu QL, Zhang ZS (2023) *Sinacosa*, a new trapdoor-building genus of Lycosidae (Araneae) from China. Acta Arachnologica Sinica 32(1): 1–7. https://doi.org/10.3969/j.issn.1005-9628.2023.01.001

World Spider Catalog (2023) World Spider Catalog. Natural History Museum Bern. http://wsc.nmbe.ch [version 24] [Accessed on September 02, 2023]

ZooKeys 1182: 11–18 (2023)
DOI: 10.3897/zookeys.1182.108243

Research Article

Cryptotermes pugnus (Blattodea, Isoptera, Kalotermitidae), a new drywood termite species from the Brazilian Caatinga dry forest and key to South American *Cryptotermes* Banks, 1909

Rudolf H. Scheffrahn[1], Alexandre Vasconcellos[2]

1 *Fort Lauderdale Research and Education Center, University of Florida, 3205 College Avenue Davie, Florida 33314, USA*
2 *Laboratório de Termitologia, Departamento de Sistemática e Ecologia, Centro de Ciências Exatas e da Natureza, Universidade Federal da Paraíba, Paraíba, Brazil*
Corresponding author: Rudolf H. Scheffrahn (rhsc@ufl.edu)

Abstract

A new termite species, *Cryptotermes pugnus* **sp. nov.**, is described from northeastern Brazil. The winged imago of *C. pugnus* is distinguished from most congeners by the lack of arolia and the multiple branches connecting the median vein to the radial sector. The soldier is unique among South American *Cryptotermes* by its cuboidal head capsule and very rugose postclypeus. The new species constitutes the fourteenth *Cryptotermes* species on the continent for which we provide a key to soldiers.

Key words: Arolium, Bahia, imago, Paraíba, soldier, South America, venation

Academic editor: Fred Legendre
Received: 19 June 2023
Accepted: 25 September 2023
Published: 11 October 2023

ZooBank: https://zoobank.org/B49C6966-A3DE-415E-9D6A-B9EACEECBA99

Citation: Scheffrahn RH, Vasconcellos A (2023) *Cryptotermes pugnus* (Blattodea, Isoptera, Kalotermitidae), a new drywood termite species from the Brazilian Caatinga dry forest and key to South American *Cryptotermes* Banks, 1909. ZooKeys 1182: 11–18. https://doi.org/10.3897/zookeys.1182.108243

Introduction

The cosmopolitan termite genus *Cryptotermes* Banks, 1906 is most diverse in the Neotropics with 32 of the 72 species described worldwide (Constantino 2020). Three of the Neotropical species are exotic pests, including *C. brevis* (Walker, 1853) (only the populations outside its endemic region of coastal Chile and Peru), *C. dudleyi* Banks, 1918, and *C. havilandi* (Sjostedt, 1900) with a previous fourth, *C. domesticus* Haviland, 1898, now deemed absent from the New World (Scheffrahn et al. 2009; Scheffrahn 2021). Until now, mainland South America (and Trinidad and Tobago) was habitat to 11 endemic *Cryptotermes* species: *C. aequacornis* Scheffrahn & Křeček, 1999; *C. brevis*; *C. camelus* Scheffrahn, 2021; *C. chacoensis* Roisin, 2003; *C. colombianus* Casalla et al., 2016; *C. contognathus* Constantino, 2000; *C. cubicoceps* (Emerson, 1925); *C. cylindroceps* Scheffrahn & Křeček, 1999; *C. mangoldi* Scheffrahn & Křeček, 1999; *C. rhicnocephalus* Bacchus, 1987; and *C. verruculosus* (Emerson, 1925). *Cryptotermes mangoldi* and *C. cylindroceps* were originally described from the West Indies until Casalla et al. (2016) reported their mainland distribution. Here, we describe a new endemic mainland species, *C. pugnus* sp. nov., from northeastern Brazil and provide a key to the described *Cryptotermes* from South America.

Material and methods

Photomicrographs were taken as multilayer montages using a Leica M205C stereomicroscope controlled by Leica Application Suite v. 3 software. Preserved specimens were taken from 85% ethanol and suspended in a pool of Purell Hand Sanitizer to position the specimens on a transparent Petri dish background. Comparisons with other South American *Cryptotermes* species were made from specimens in the University of Florida Termite Collection (Scheffrahn 2019).

Taxonomy

Cryptotermes pugnus **Scheffrahn & Vasconcellos, sp. nov.**
https://zoobank.org/B7EB068D-34FD-4B36-A5B9-C37A230F05FD

Comparison. The imago of *C. pugnus* groups with *C. brevis*, *C. chacoensis* Roisin, 2003, *C. kirbyi* Moszkowski, 1955, and *C. darwini* (Light, 1935) in having the arolium absent between the tarsal claws (Fig. 1C). The forewing venation of the *C. pugnus* imago is atypical for most of the genus in having several branches splitting from the media and intersecting the radial sector (Fig. 1D). This character is only known from *C. brevis*, *C. darwini* (see Light 1935), and *C. kirbyi* (see Bacchus 1987). The latter two species may be found in future studies to by synonyms of *C. brevis*. Roisin (2003) did not describe the venation of *C. chacoensis*.

Among mainland South American *Cryptotermes* soldiers, *C. pugnus* is unique in having, in dorsal view, a cuboidal head capsule and a very rugose, rounded and projecting postclypeus (Fig. 2). The postclypeus of *C. brevis* and *C. chacoensis* soldiers are closest to *C. pugnus*, but the head capsules of the former two are constricted (Fig. 3). Along with *C. pugnus*, only *C. aequacornis*, *C. cylindroceps*, and *C. rhicnocephalus* have both frontal and genal horns projecting the same length anteriorly (Fig. 3H, L, M).

Description. ***Imago*** (Fig. 1A–D). Head capsule and pronotum pale yellow brown. Compound eye obtusely triangular; ocellus light yellow, about half diameter of eye, roundly ellipsoid, and touching eye margin. Vertex with a few short setae. Pronotum wider than head capsule; anterior margin shallowly concave. Pronotum lateral margins with about one dozen setae each. Antennae with 15 articles, basal article relative lengths 2 = 3 > 4 = 5. Forewing with subcosta joining costal margin at about 1/8 of wing length from suture. Wing membrane pale; veins a shade darker. Costa, subcostal, radius, and radial sector sclerotized; unsclerotized media with several branches intersecting radial sector; media terminating at radial sector about 3/4 wing length, then appearing as a separate branch near tip of wing. Arolium absent. Measurements (mm, mean, n = 3). Head maximum width with eyes 0.96; head maximum width without eyes 0.88; pronotum maximum width 0.94; eye maximum diameter 0.23; ocellus maximum diameter 0.12; total body length 5.3; right forewing length from scale 6.90; body length with wings 8.74.

Soldier (Fig. 2A–E). Head capsule, in dorsal view, strongly rugose; dark castaneous brown from postclypeus grading to orange-brown at occiput. Head capsule widest at posterior third, narrowest at frontal flange. Frontal flange (ridge)

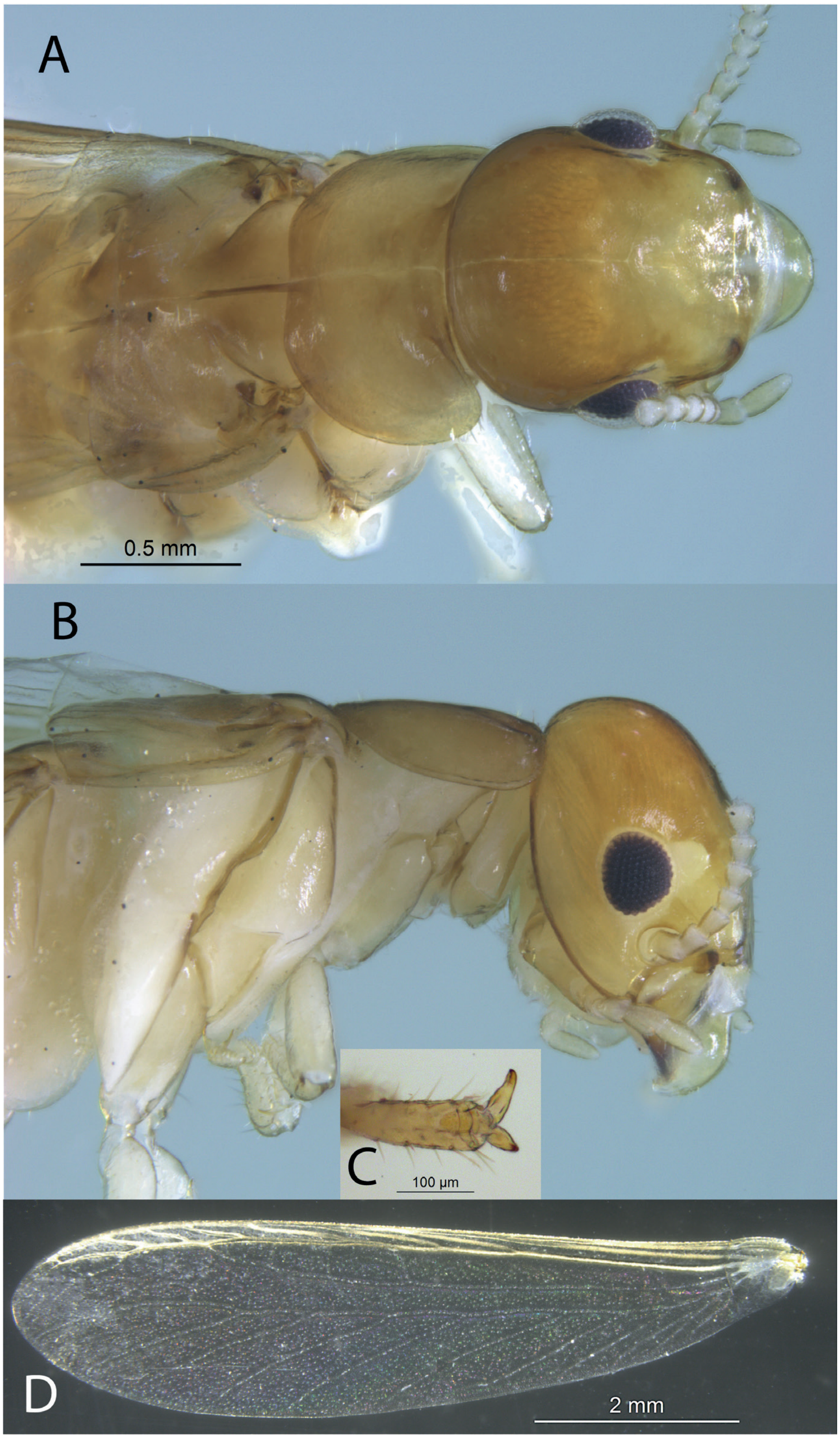

Figure 1. Imago of *Cryptotermes pugnus* sp. nov. (SA470) **A** dorsal view of head and pronotum **B** lateral view of head and pronotum **C** distal tarsomere of foreleg **D** left forewing.

V-shaped with deep median cleft. Posterior margin of head capsule truncate, posterolateral corners forming right angles, lateral margins nearly parallel combining to form cuboidal appearance. In lateral view, frontal flange elevated, vertex unevenly concave; frontal horns visible as blunt knobs. Genal horns evenly rounded, slightly posterior to frontal horns (Fig. 2E). Pronotum angled sharply

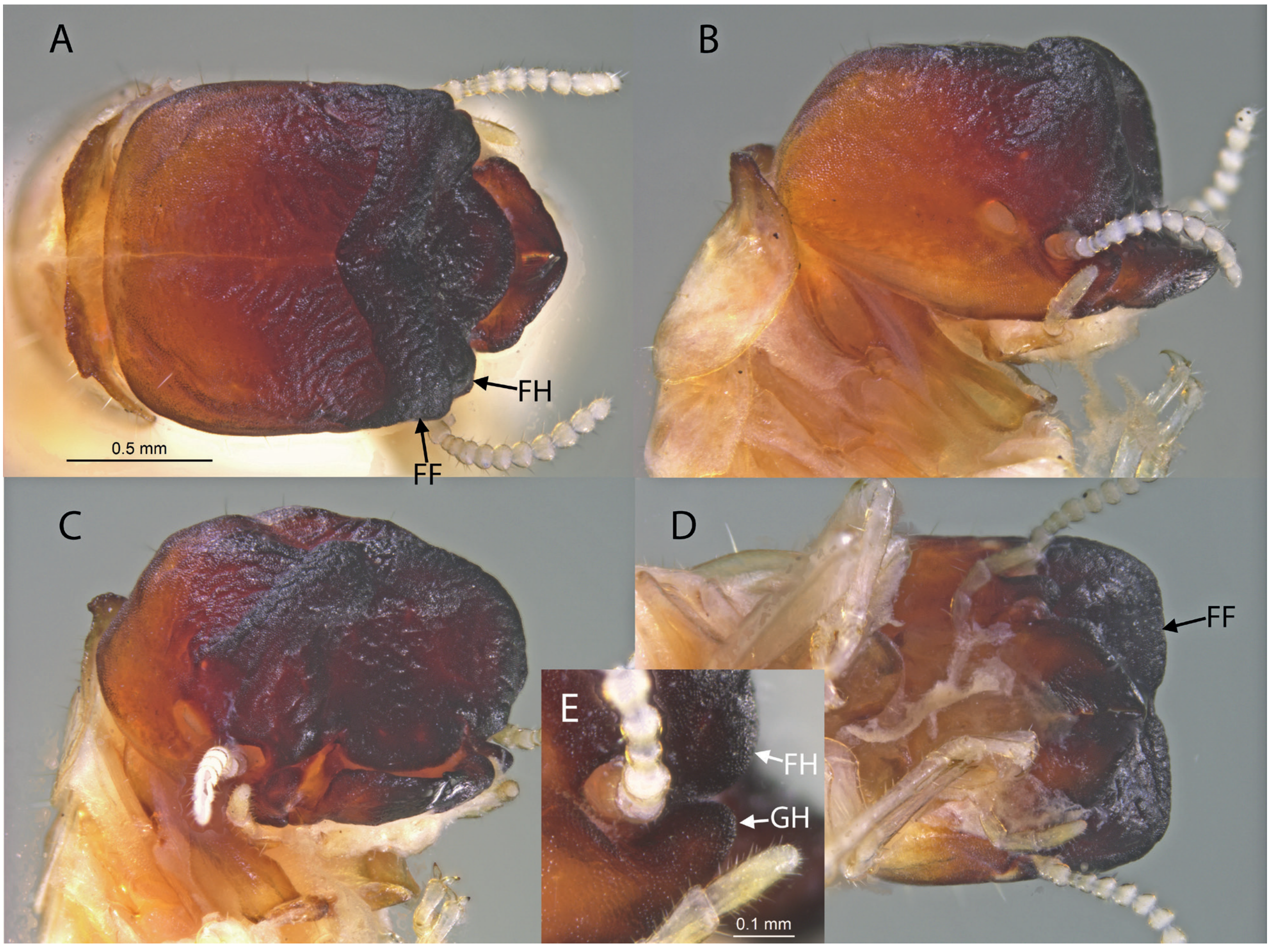

Figure 2. Soldier of *Cryptotermes pugnus* sp. nov. (SA470) **A** dorsal view of head and pronotum **B** lateral view of head and pronotum **C** oblique view of head and pronotum **D** ventral view of head and pronotum **E** lateral view of cephalic horns. FF = frontal flange, FH = frontal horn, and GH = genal horn.

from vertex, narrower than head; anterior margin dark and ruffle; incised in middle with rounded anterior lobes. Eye spots large, narrowly elliptical. In oblique view (Fig. 2C) frons concave. Postclypeus evenly convex, strongly rugose, projecting well beyond frontal flange (Fig. 2A). Antennae with 8 or 9 articles, third fused or divided; or with 10 or 11 articles, third fused or divided. Mandibles wide and short for the genus; rugose, rounded basal hump at half-length when seen from below, outer margin of blade angles about 50°. Measurements (mm, mean, n = 2). Head length to tip of mandibles 1.57; head length to tip genal horns 1.20, frontal flange width 1.11; frontal horns, outside span 0.90; genal horns, outer span 0.95; head width, maximum 1.20; head width, minimum (behind frontal flange) 1.10; head height, excluding postmentum 0.88; pronotum, maximum length 0.95; pronotum, maximum width 1.12; left mandible length, tip to ventral condyle 0.53.

Type materials. ***Holotype*:** Brazil • Soldier; Paraíba, São José dos Cordeiros; -7.39056, -36.80833; 526 m a.s.l.; 17 Aug. 2000; A. Vasconcellos leg.; two soldiers (one labelled holotype, Fig. 2), three imagos, and three pseudergates; University of Florida Termite Collection (UFTC) no. SA470, subsample from Federal University of Paraíba Termite Collection (FUPTC) no. 2052. ***Paratypes*:** Brazil

• Bahia, Curaçá; −9.123, −39.691; 366 m a.s.l.; 4 May 2011; A. Vasconcellos leg.; one soldier and pseudergates; FUPTC no. 4345.

Etymology. Named after the pug dog. The oblique view of the soldier (Fig. 2C) resembles this short-nosed breed.

Key to South American *Cryptotermes* soldiers

1 In dorsal (or ventral) view, genal horns form anterolateral knobs of head capsule; vertex smooth (introduced species) (Fig. 3A, B) **2**

— In dorsal view, genal horns eclipsed by frontal horn or frontal flange (e.g. Fig. 3H) **3**

2 Mandibles project more than one third length of head capsule (Fig. 3A) .... ***C. dudleyi***

— Mandibles project about one fourth length of head capsule (Fig. 3B) .... ***C. havilandi***

3 Mandibles barely project beyond frons or frontal horns (Fig. 3C, D) **4**

— Mandibles clearly project beyond frons or frontal horns (e.g. Fig. 3H) **5**

4 Frontal horns not visible (Fig. 3C) .... ***C. colombianus***

— Frontal horns visible (Fig. 3D) .... ***C. contognathus***

5 Vertex excavated; with deeply folding rugosity (e.g. Fig. 3H) **6**

— Vertex not excavated; rugosity more shallow (e.g. Fig. 3M) **10**

6 Head constricted behind frontal flange (Fig. 3E, F) **7**

— Head not constricted behind frontal flange (Fig. 3G–I) **8**

7 Genal horns visible from above, mandibles with lateral humps; Gran Chaco region (Fig. 3E) .... ***C. chacoensis***[*]

— Genal horns not visible from above, mandibles without lateral humps; widespread (Fig. 3F) .... ***C. brevis***[*]

8 Frontal horns barely extend beyond anterolateral margin of frontal flange (Fig. 3G) .... ***C. cubicoceps***

— Frontal horns extend well beyond anterolateral margin of frontal flange (Fig. 3H, I) **9**

9 Anterior margin of postclypeus linear; outer span of mandibles <1/2 width of head (Fig. 3H) .... ***C. aequacornis***

— Anterior margin of postclypeus rounded; outer span of mandibles >1/2 width of head (Fig. 3I) .... ***C. pugnus* sp. nov.**[*]

10 In lateral view, frontal flange emerges above vertex as a rounded mound (Fig. 3J, K) **11**

— In lateral view, frontal flange forms angular intersection with vertex (Fig. 3L–N) **12**

11 Frontal flange semicircular; humid Chaco (Fig. 3J) .... ***C. camelus***

— Frontal flag quadrant (Fig. 3K) .... ***C. verruculosus***

12 Lateral margin of vertex linear in lateral view (Fig. 3L) .... ***C. cylindroceps***

— Lateral margin of vertex concave (Fig. 3M–O) **13**

13 Flange without elevated rim (Fig. 3M) .... ***C. rhicnocephalus***

— Flange with elevated rim (Fig. 3N, O) **14**

14 Frontal horn not projecting beyond frontal flange (Fig. 3N) .... ***C. fatulus***

– Frontal horn projects beyond frontal flange (Fig. 3O) .... ***C. mangoldi***

---

[*] Imago without arolia (*C. camelus* imago unknown).

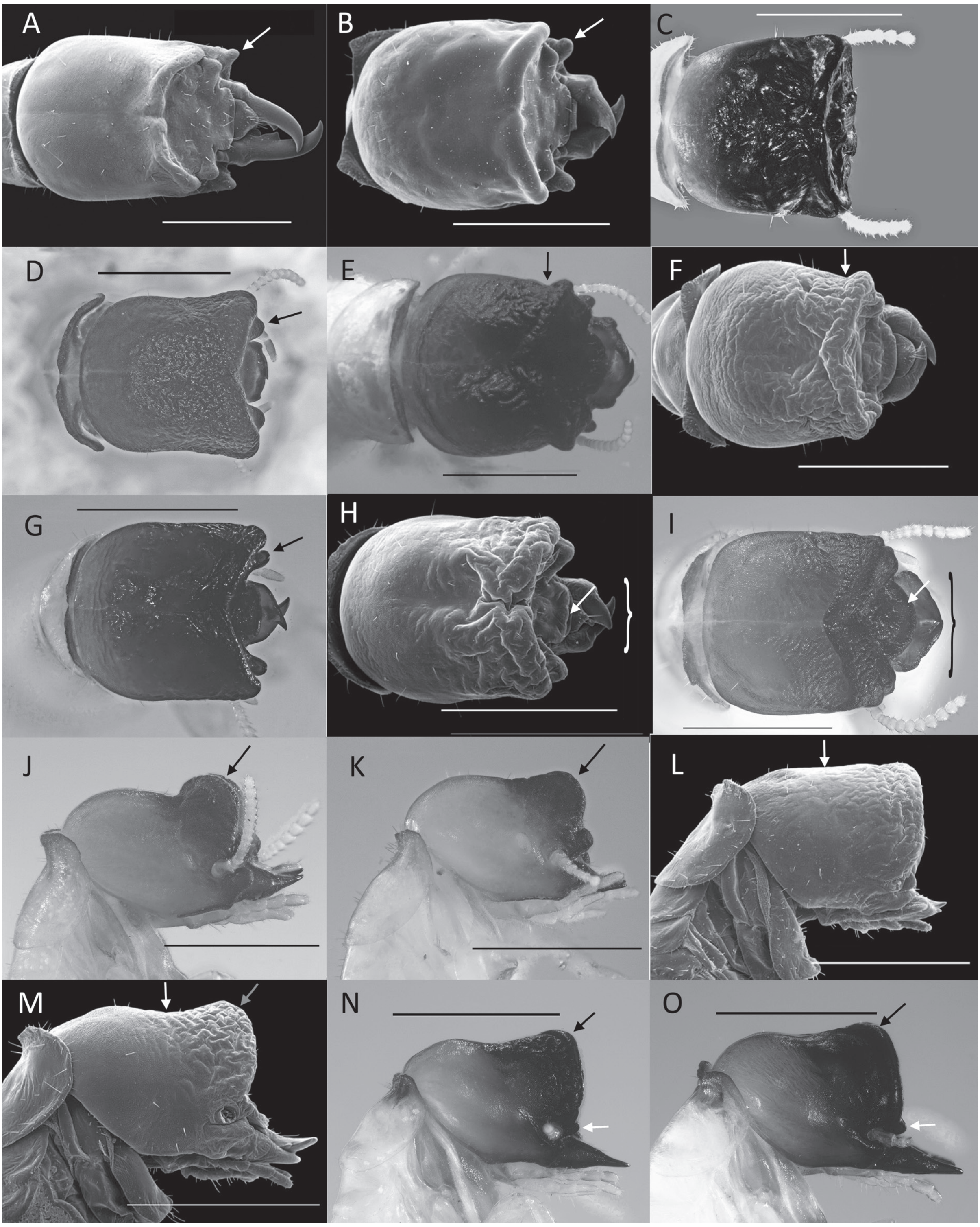

Figure 3. South American *Cryptotermes* soldier head capsules **A** *C. dudleyi* (arrow: genal horn) **B** *C. havilandi* (arrow: genal horn) **C** *C. colombianus* **D** *C. contognathus* (arrow: frontal horn) **E** *C. chacoensis* (arrow: constriction) **F** *C. brevis* (arrow: constriction) **G** *C. cubicoceps* (arrow: frontal horn) **H** *C. aequacornis* (arrow: postclypeus; bracket: outer span of mandibles) **I** *C. pugnus* sp. nov. (arrow: postclypeus; bracket: outer span of mandibles) **J** *C. camelus* (arrow: frontal flange) **K** *C. verruculosus* (arrow: frontal flange) **L** *C. cylindroceps* (arrow: lateral margin of vertex) **M** *C. rhicnocephalus* (white arrow: vertex concave, grey arrow: frontal flange without elevated rim) **N** *C. fatulus* (black arrow: frontal flange with elevated rim; white arrow: frontal horn) **O** *C. mangoldi* (black arrow: frontal flange with elevated rim; white arrow: frontal horn with elevated rim). **A, B, F, H, L, M** modified from Scheffrahn and Křeček (1999); C modified from Casalla et al. (2016). Scale bars: 1 mm.

Discussion

Cryptotermes pugnus is the second species of the genus described from Brazil and the first from the Caatinga dry forest, with records for two ecoregions, which have different geomorphological history and climatic parameters, "Planalto da Borborema" (São José dos Cordeiros, Paraíba State) and "Depressão Sertaneja Meridional" (Curaçá, Bahia State) (Silva et al. 2018). There is also a record of *C. havilandi* from the Caatinga dry forest (Vasconcellos unpublished data), an exotic species which probably originated in tropical West Africa (Scheffrahn et al. 2003). There are no records of *C. pugnus* infestations in buildings, either in urban or agricultural environments. Other kalotermitids reported from the Caatinga include two undescribed species of *Glyptotermes* Froggatt, 1897, *Rugitermes* cf. *niger* Oliveira, 1979, an undescribed species of *Rugitermes* Holmgren, 1911 (Bandeira et al. 2003), and *Tauritermes bandeirai* Scheffrahn & Vasconcellos, 2022 (Scheffrahn and Vasconcellos 2020).

Small colonies of *C. pugnus* were found on adult individuals of *Cenostigma nordestinum* E. Gagnon & G.P. Lewis, an endemic tree of the Caatinga dry forest, which presents hard, highly dense (>0.84 g/cm^3) wood and individuals that can exceed 10 m in height (Silva et al. 2009). Due to the hardness of the wood, access to *C. pugnus* colonies is difficult, requiring the use of an ax and/or chainsaw. Possibly because of this, its colonies are rarely found. At the type locality, there are records of *C. pugnus* alate flights from late December to early February (Lucena et al. 2022).

Acknowledgements

We thank Reginaldo Constantino for image of *C. contognathus* (Fig. 3D).

Additional information

Conflict of interest

The authors have declared that no competing interests exist.

Ethical statement

No ethical statement was reported.

Funding

This study was supported by the University of Florida. The second coauthor thanks CNPq for the research grant (proc.309820/2020-0).

Author contributions

Scheffrahn wrote first draft. Vasconcellos did field work and inproved first draft.

Author ORCIDs

Alexandre Vasconcellos https://orcid.org/0000-0001-7211-7097

Data availability

All of the data that support the findings of this study are available in the main text.

References

Bacchus S (1987) TDRI Tropical Pest Bulletin 7: a Taxonomic and Biometric Study of the Genus *Cryptotermes* (Isoptera: Kalotermitidae). Tropical Development and Research Institute, London, 91 pp.

Bandeira AG, Vasconcellos A, Silva MP, Constantino R (2003) Effects of habitat disturbance on the termite fauna in a highland humid forest in the Caatinga domain, Brazil. Sociobiology 42: 117–128.

Casalla R, Scheffrahn R, Korb J (2016) *Cryptotermes colombianus* a new drywood termite and distribution record of *Cryptotermes* in Colombia. ZooKeys 596: 39–52. https://doi.org/10.3897/zookeys.596.9080

Constantino R (2020) Termite Database. Brasília, University of Brasília. [Updated Dec. 2020; cited 22 May 2023] http://termitologia.net

Light SF (1935) The Templeton Crocker Expedition of the California Academy of Sciences, 1932. No. 20. The termites. Proceedings of the California Academy of Sciences (Fourth Series) 21: 233–256. [+ 1 pl.]

Lucena EF, Silva IS, Monteiro SR, Moura FM, Vasconcellos A (2022) Accumulated precipitation and air density are linked to termite (Blattodea) flight synchronism in a Seasonally Dry Tropical Forest in north-eastern Brazil. Austral Entomology 61(1): 78–85. https://doi.org/10.1111/aen.12577

Roisin Y (2003) *Cryptotermes chacoensis*, a new species from native South American inland habitats (Isoptera: Kalotermitidae). Sociobiology 42: 319–327.

Scheffrahn RH (2019) UF termite database. University of Florida termite collection. https://www.termitediversity.org/ [Accessed 22 September 2023]

Scheffrahn RH (2021) *Cryptotermes camelus* (Isoptera: Kalotermitidae), a new drywood termite species from the Bolivian Chaco. Zootaxa 4938(1): 145–147. https://doi.org/10.11646/zootaxa.4938.1.9

Scheffrahn RH, Křeček J (1999) Termites of the genus *Cryptotermes* Banks (Isoptera: Kalotermitidae) from the West Indies. Insecta Mundi 13: 111–171.

Scheffrahn RH, Vasconcellos A (2020) *Tauritermes bandeirai*: A new drywood termite (Isoptera, Kalotermitidae) from the Caatinga and Atlantic Forest of Brazil. ZooKeys 954: 75–83. https://doi.org/10.3897/zookeys.954.52335

Scheffrahn RH, Jones SC, Křeček J, Chase JA, Mangold JR, Su NY (2003) Taxonomy, distribution, and notes on the termites (Isoptera: Kalotermitidae, Rhinotermitidae, Termitidae) of Puerto Rico and the U.S. Virgin Islands. Annals of the Entomological Society of America 96(3): 181–201. https://doi.org/10.1603/0013-8746(2003)096[0181:TDANOT]2.0.CO;2

Scheffrahn RH, Křeček J, Ripa R, Luppichini P (2009) Endemic origin and vast anthropogenic dispersal of the West Indian drywood termite. Biological Invasions 11(4): 787–799. https://doi.org/10.1007/s10530-008-9293-3

Silva LBD, Santos FDARD, Gasson P, Cutler D (2009) Anatomia e densidade básica da madeira de *Caesalpinia pyramidalis* Tul. (Fabaceae), espécie endêmica da caatinga do Nordeste do Brasil. Acta Botanica Brasílica 23(2): 436–445. https://doi.org/10.1590/S0102-33062009000200015

Silva JMC, Leal IR, Tabarelli M (2018) Caatinga: the Largest Tropical Dry Forest Region in South America. Springer, Cham, 482 pp. https://doi.org/10.1007/978-3-319-68339-3

ZooKeys 1182: 19–34 (2023)
DOI: 10.3897/zookeys.1182.111296

Research Article

Redescription of the hispidoberycid, *Hispidoberyx ambagiosus* Kotlyar, 1981 from Taiwan, with comments on its morphology (Beryciformes, Stephanoberycoidei, Hispidoberycidae)

Yo Su[1], Chien-Hsiang Lin[2], Hsuan-Ching Ho[3,4,5]

1 *Department of Marine Biotechnology and Resources, National Sun Yat-sen University, Kaohsiung, Taiwan*
2 *Biodiversity Research Center, Academia Sinica, Taipei, Taiwan*
3 *Department and Graduate Institute of Aquaculture, National Kaohsiung University of Science Technology, Kaohsiung, Taiwan*
4 *Institute of Marine Biology, National Donghwa University, Pingtung, Taiwan*
5 *Research Associate, Australian Museum, Sydney, Australia*
Corresponding author: Hsuan-Ching Ho (ogcoho@gmail.com)

Abstract

A rare spiny-scale pricklefish, *Hispidoberyx ambagiosus* Kotlyar, 1981, is redescribed based on four specimens collected from Taiwan. Their sampling locality represents the northernmost record of the family, which extends the family's distribution from the eastern Indian Ocean and the South China Sea to northeastern Taiwan in the northwestern Pacific Ocean. A detailed description of these specimens and the first description of its sagittal otoliths are provided. In addition, the specimens are compared with other known specimens. Intraspecific variation of some morphological characters are discussed.

Key words: biodiversity, biogeography, ichthyology, otolith, taxonomy

Academic editor: Nina Bogutskaya
Received: 17 August 2023
Accepted: 24 September 2023
Published: 11 October 2023

ZooBank: https://zoobank.org/070C7452-A3AC-4BC2-84F3-CE119FC3279D

Citation: Su Y, Lin C-H, Ho H-C (2023) Redescription of the hispidoberycid, *Hispidoberyx ambagiosus* Kotlyar, 1981 from Taiwan, with comments on its morphology (Beryciformes, Stephanoberycoidei, Hispidoberycidae). ZooKeys 1182: 19–34. https://doi.org/10.3897/zookeys.1182.111296

Introduction

The fish order Beryciformes (Nelson et al. 2016) currently comprises eight families and about 123 valid species distributed worldwide (Fricke et al. 2023). Most members are deep-sea fishes, some of which live at depths to 5308 m (Kotlyar 1996). The monotypic family Hispidoberycidae was established by Kotlyar (1981) to accommodate the new genus and new species *Hispidoberyx ambagiosus* Kotlyar, 1981. The species was described based on the holotype and a non-type specimen collected from off the northwestern tip of Sumatra and the south coast of Java in the eastern Indian Ocean.

Specimens of *H. ambagiosus* appear to be extremely rare in collections worldwide, with only five specimens known from the South China Sea and East Indian Ocean (Yang et al. 1988; Kotlyar 1991, 1996, 2004). Known specimens were collected from depths of 560–1019 m, and ecology and biology of the species are still poorly known. Kotlyar (1991, 1996) described some osteological features and reviewed all available information on the family and its presumed relationships.

Recently, four specimens initially identified as *Barbourisia rufa* Parr, 1945 were found in the Pisces collection of the Biodiversity Research Center, Academia

Sinica, Taipei, Taiwan (ASIZP). After a detailed examination, these specimens are re-identified as *H. ambagiosus* based on their unique characteristics. These specimens represent the first record of the species, genus, and family from Taiwan, as well as the third formal record in history. A detailed description of these specimens and the first description of its sagittal otoliths are provided; these specimens are also compared to the data of other known specimens.

Materials and methods

Classification of taxonomic rank follow Nelson et al. (2016). Terminology and methodology follow Kotlyar (1996) and Su et al. (2023), with body depths measured at greatest depth and both dorsal- and anal-fin origins and body width additionally measured at lateral-line origin. Measurements of forehead length follow Su et al. (2022) and are abbreviated as HF1 and HF2. Counts of paired-fin characters and lateral-line scales were presented as left/right whenever available. Vertebral counts follow Kotlyar (1991), with the second ural centrum counted as the last vertebra. Only vertebrae with ribs are included in the counts of precaudal vertebrae. The counts of vertebrae were determined by x-radiograph. Terminology of lateral-line canals follow Jakubowski (1974) and Kotlyar (1991). In addition, terminology and description of otoliths follow Lin and Chang (2012) and Nolf (2013). The distribution map was generated from Ocean Data View (Schlitzer 2023).

Measurements were taken using 150 mm digital calipers or 300 mm calipers and rounded to the nearest 0.1 mm. Morphometric data were presented as a percentage of standard length (SL) and/or as a percentage of head length (HL), except where otherwise indicated. Specimens are deposited at Academia Sinica, Biodiversity Research Center, Taipei, Taiwan (**ASIZP**), and the Pisces Collection, National Museum of Marine Biology and Aquarium, Pingtung, Taiwan (**NMMB-P**). The sagittal otoliths of ASIZP 81665 were taken and deposited at the marine paleontology lab, Biodiversity Research Center with catalog number CHLOL 969.

Results

Family Hispidoberycidae Kotlyar, 1981
Chinese name: 刺金眼鯛科

***Hispidoberyx ambagiosus* Kotlyar, 1981**
Figs 1–8, Tables 1, 2
English name: Spiny-scale pricklefish
New Chinese name: 神秘刺金眼鯛

Literature records. *Hispidoberyx ambagiosus* Kotlyar, 1981: 413 (type locality: off northwestern tip of Sumatra, eastern Indian Ocean, 3°46'00"N, 95°00'00"E, depth 800–875 m. Holotype: ZMMU-P 15416): Yang et al. 1988: 3 (new record from the South China Sea). Kotlyar 1991: 100 (osteology). Kotlyar 1996: 252 (in part). Paxton in Randall and Lim 2000: 600 (listed). Kotlyar 2004: 1 (description). Kimura 2020 (phylogeny).

Specimens examined. ASIZP 63512, 134.8 mm SL, bottom trawl, depth 650–800 m, 10 Jun. 1999, coll. D.-M. Chen. ASIZP 64539, 154.7 mm SL, bottom

Figure 1. Fresh specimens of *Hispidoberyx ambagiosus* Kotlyar, 1981 **A** ASIZP 64539, 154.7 mm SL (after a few months of refrigeration) **B** ASIZP 81665, 162.0 mm SL. Photographed by J.-F. Huang. Not to scale.

trawl, 28 Aug. 2002, coll. H.-C. Ho. ASIZP 76178, 153.5 mm SL, bottom trawl, 24 Apr. 2015, coll. M.-Y. Lee. ASIZP 81665, 162.0 mm SL, bottom trawl, 25 July 2020, coll. C.-H. Lin et al. All collected from Daxi fishing port (ca 24°53'37"N, 121°55'26"E), Yilan, northeastern Taiwan.

Otolith (a pair of sagittae): CHLOL 969, otolith length 2.2 (left) and 2.3 (right) mm, taken from ASIZP 81665.

Description of Taiwanese specimens. Meristic and morphometric data are provided in Tables 1 and 2.

Dorsal-fin elements V, 10–11, first 2 spines fused in 2 specimens (Fig. 3A). Pectoral-fin elements 12/12–13, uppermost 2 and lowermost 1 or 2 rays unbranched. Pelvic-fin elements I, 7/I, 7. Anal fin-elements II–III, 10, first 2 spines fused in all specimens (Fig. 4B; 1 specimen unavailable). Principal caudal-fin rays 10 + 9, uppermost and lowermost rays unbranched; procurrent caudal-fin rays 9–10 on both upper and lower lobes. Gill rakers on outer face of first arch 4–5 + 1 + 10–13 = 15–19 (total). Pseudobranchial filaments 10–11. Lateral-line scales 33–36/33–36; scale rows above lateral line 15–18; scale rows below lateral line 27–31. Vertebrae 13 + 23 = 36; branchiostegal rays 8.

Body slender for stephanoberycoid, greatest depth 3.4–3.9 in SL, depth at dorsal- and anal-fin origins 3.6–4.5 and 4.5–5.5 in SL, respectively; body laterally compressed and oval in trunk section, its width 4.4–4.7 in SL. Head somewhat oval, length 3.2–3.3 in SL; its height 1.4–1.5 in HL; upper profile of head nearly straight, gently curved to dorsal-fin origin; forehead flat, HF1 14.3–20.3 and HF2 5.3–5.9 in HL; eye diameter 4.8–5.8 in HL; tip of snout slightly rounded, not extending before premaxilla, its length 3.3–3.5 in HL; interorbital width 2.8–2.9 in HL.

Mouth oblique, upper-jaw length 1.5 in HL; posterior end of maxilla rounded, reaching vertical through posterior margin of eye; lower jaw slightly larger than upper jaw and protruding before upper jaw, length 1.3–1.5 in HL. Two nostrils at same horizontal through center of eye; both nostrils rounded, slightly oval,

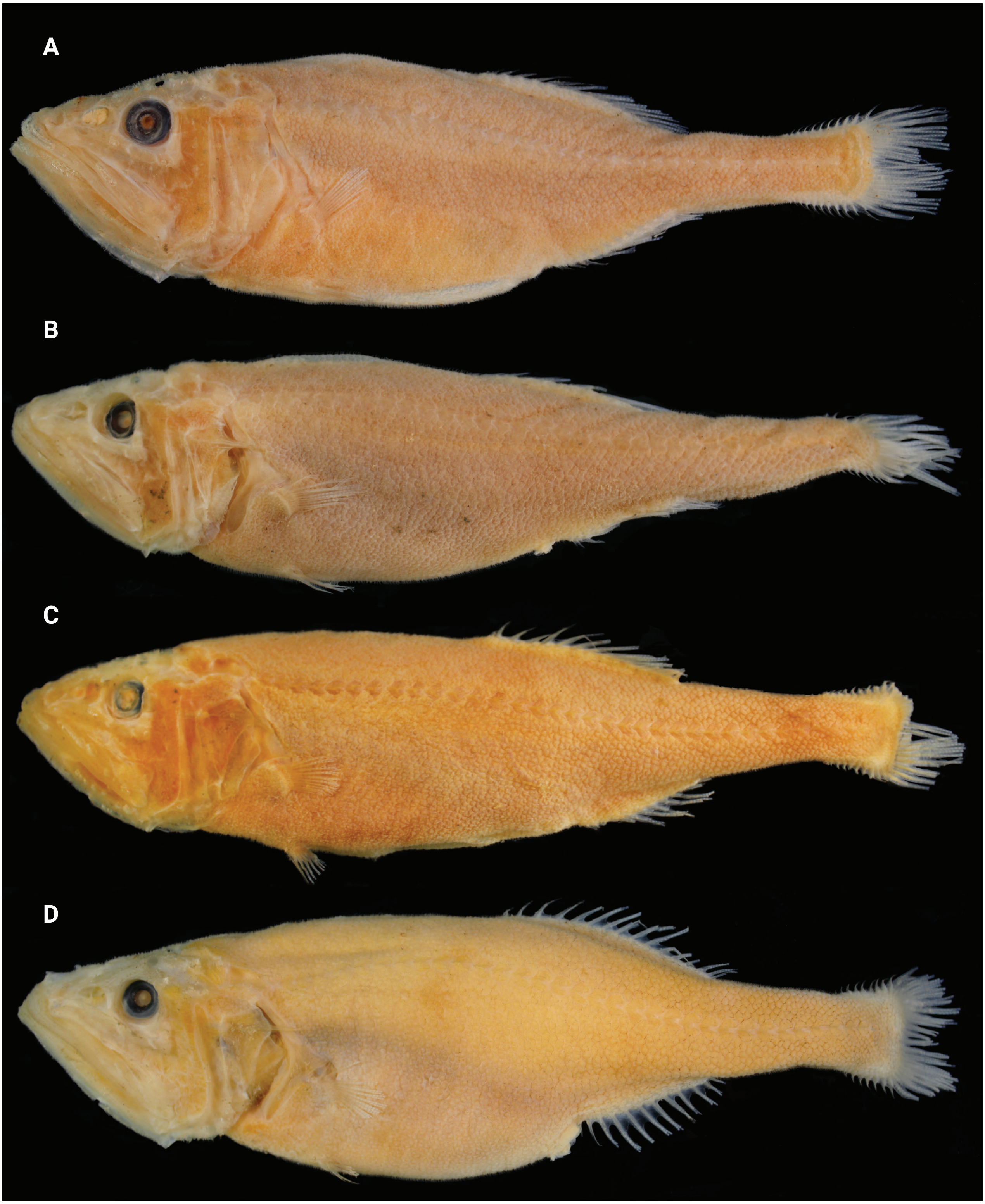

Figure 2. Preserved specimens of *Hispidoberyx ambagiosus* Kotlyar, 1981. **A** ASIZP 63512, 134.8 mm SL **B** ASIZP 64539, 154.7 mm SL **C** ASIZP 76178, 153.5 mm SL **D** ASIZP 81665, 162.0 mm SL. Not to scale.

with posterior nostril much larger than anterior one; both nostrils immediately in front of eye. Tominaga's organ (Fig. 4; *sensu* Paxton et al. 2001) present in olfactory chamber, mostly embedded behind nasal organ (Fig. 4). Nasal organ large and oval, bearing leaf-like appendages.

Table 1. Meristic characters of *Hispidoberyx ambagiosus* Kotlyar, 1981. Data of other specimens were retrieved from Kotlyar (1981, 1996) and Yang et al. (1988). Paired characters are presented as left/right whenever available.

	This study				**Kotlyar (1981)**	**Yang et al. (1988)**	**Kotlyar (1996)**
	ASIZP 63512	**ASIZP 64539**	**ASIZP 76178**	**ASIZP 81665**	**Holotype; non-type (*n* = 2)**	**(*n* = 2)**	**Holotype; non-types (*n* = 3)**
Dorsal-fin elements	V, 11	V, 11	V, 11	V, 10	IV–V, 10	V, 10	IV–V, 10
Pectoral-fin elements	12/12	12/13	12/12	12/12	12	11–12	12–13
Anal-fin elements	III, 10	II, 10	III, 10	II, 10	III, 9	III, 9	II–III, 9
Pelvic-fin elements	I, 7/ I, 7	I, 7/ I, 7	I, 7/ I, 7	I, 7/ I, 7	I, 6	I, 7	I, 7
Caudal-fin elements	10+10+9+10	9+10+9+9	9+10+9+10	9+10+9+9	9+10+9+9	–	–
Gill rakers	5+1+11=17	5+1+11=17	5+1+13=19	4+1+10=15	5–6+1+12=18–19	6+1+9–11=16–18	5–6+1+9–12=15–19
Pseudobranchial filaments	11	11	10	10	–	–	–
Lateral-line scale	34/34	33/34	36/36	34/33	32	33–34	32–34
Scale rows above lateral line	16	15	15	18	–	–	–
Scale rows below lateral line	30	27	31	28	–	–	–
Vertebrae	13+23=36	13+23=36	13+23=36	13+23=36	12+22=34	–	12–13+22=34–35

Symphysis of premaxillae notched and edentate. Symphysis of dentaries slightly notched and edentate. Supramaxilla single, with long needle-like process extending anteriorly and rectangular process posteriorly; covering about half of posterior portion of maxilla.

Bony ridges associated with skeletons of head, jaws, snout, and operculum covered with small spinules. Bony ridges on head forming sensory canals (Fig. 5); supraorbital canal running from nasal, frontal, connected to coronal commissure at parietal bones, and divided into temporal and supratemporal canal on posttemporal bone, and joined together, connected to lateral line. Fenestration present on frontal bone connecting coronal commissure and temporal canal (Fig. 5; red arrow). Opercle with 1 strong central spine. Posttemporal bone without spine. Pectoral girdle smooth, without any spines. Premaxilla with villiform teeth, its outer surface completely exposed and bearing 2 or 3 ridges anteriorly on its ascending process; its end extending to posterior end of maxilla. Dentary with villiform teeth on its medial face. Palatine and vomer with villiform teeth.

Gill rakers rod-shaped, laterally compressed, their inner surfaces covered with small teeth; rakers on outer row of first arch longer than remainder, longest gill raker shorter than eye diameter; small bump-like rakers on inner surfaces of outer 3 arches; outer-row rakers gradually shorter from first to fourth arch, with very short rakers on outer row of fourth arch; no tooth patches present between rakers on all 4 arches. Narrow, villiform tooth patch present on fifth ceratobranchial. Long, oval tooth patch on third epibranchial arch. Large, teardrop-like villiform tooth patch on third pharyngobranchial. Small, rounded villiform tooth

Table 2. Morphometric characters of *Hispidoberyx ambagiosus* Kotlyar, 1981. Data of other specimens were retrieved from Kotlyar (1981, 1996) and Yang et al. (1988). Abbreviations: A, Anal-fin; C, Caudal-fin; D, Dorsal-fin; H, head length; HF, forehead height; P, Pectoral-fin; SL, standard length; V, Pelvic-fin.

	This study				**Kotlyar (1981)**	**Yang et al. (1988)**	**Kotlyar (1996)**
	ASIZP 63512	**ASIZP 64539**	**ASIZP 76178**	**ASIZP 81665**	**Holotype; Non-type (*n* = 2)**	***n* = 2**	**Holotype; Non-types (*n* = 3)**
SL (mm)	134.8	154.7	153.5	162.0	162–181	173–175	156–181
%SL							
HL	31.3	30.6	31.3	31.3	29.6–33.1	31.4–31.7	27.6–33.1
Head depth	22.8	21.9	21.3	21.6	–	–	21.0–22.1
Body width	9.1	11.0	10.2	11.1	–	–	–
Predorsal length	53.5	51.0	52.9	53.4	53.8–55.1	52.0–56.0	51.8–55.8
Prepectoral length	33.9	33.7	31.9	35.1	32.7–36.5	–	32.7–36.5
Prepelvic length	36.0	37.2	35.6	37.4	34.1–38.6	36.0–36.9	34.6–39.1
Preanal length	64.4	65.2	65.3	63.7	61.0–66.3	62.4–63.4	61.0–66.3
Snout length	9.6	9.4	8.9	9.6	12.2–12.3	12.1–12.7	11.2–12.3
Eye diameter	6.5	5.9	5.4	5.7	4.3–4.4	4.5–4.6	4.3–4.8
Interorbital width	11.4	10.5	11.0	10.9	–	9.8–19.0	9.0–11.0
Upper-jaw length	21.4	20.8	20.2	21.1	20.3–22.1	19.0–20.0	19.9–22.1
Lower-jaw length	23.2	22.8	21.5	23.1	22.2–24.9	–	21.5–24.9
HF1	2.0	2.1	1.9	1.5	–	–	1.6–4.3
HF2	5.9	5.2	5.6	5.4	–	–	–
Postorbital length	14.7	14.0	14.5	14.3	12.3–13.3	–	12.1–13.3
D–P length	27.9	23.3	25.9	26.6	–	–	–
D–V length	32.2	29.3	32.4	34.5	–	–	–
Body depth at D origin	27.7	22.1	23.4	28.1	–	–	–
Body depth at A origin	21.0	18.1	20.4	22.4	–	–	–
Greatest body depth	29.7	25.7	25.4	29.2	24.1–29.3	–	24.1–29.3
V spine	6.7	5.8	broken	6.2	–	–	–
P–V length	5.4	6.8	6.2	7.4	4.9–6.1	–	4.9–6.7
D–A length	23.1	22.0	23.8	24.2	–	–	–
V–A length	29.6	31.3	32.1	29.3	22.8–27.2	–	27.2–29.8
D length	22.1	22.6	22.3	24.0	21.6–22.1	–	21.6–22.1
First D spine	3.4	2.5	broken	2.4	–	–	–
Second D spine	4.6	4.4	3.3	3.1	–	–	–
Last D spine	7.6	6.1	5.2	broken	–	–	–
A length	15.4	13.8	14.3	15.4	12.3–13.8	–	12.3–13.8
Last A spine	broken	broken	broken	4.4	–	–	–
Postanal length	23.8	23.2	23.6	23.2	23.2–24.7	–	–
Postdorsal length	25.1	25.8	24.3	23.4	26.0–27.8	–	–
Caudal-peduncle height	8.2	8.3	7.7	8.1	8.0–8.3	8.5–8.6	8.0–8.3
longest gill raker	4.7	4.1	4.6	5.0	4.0–4.4	–	4.0–4.4
gill filaments at angle	2.0	2.0	2.1	1.5	–	–	–

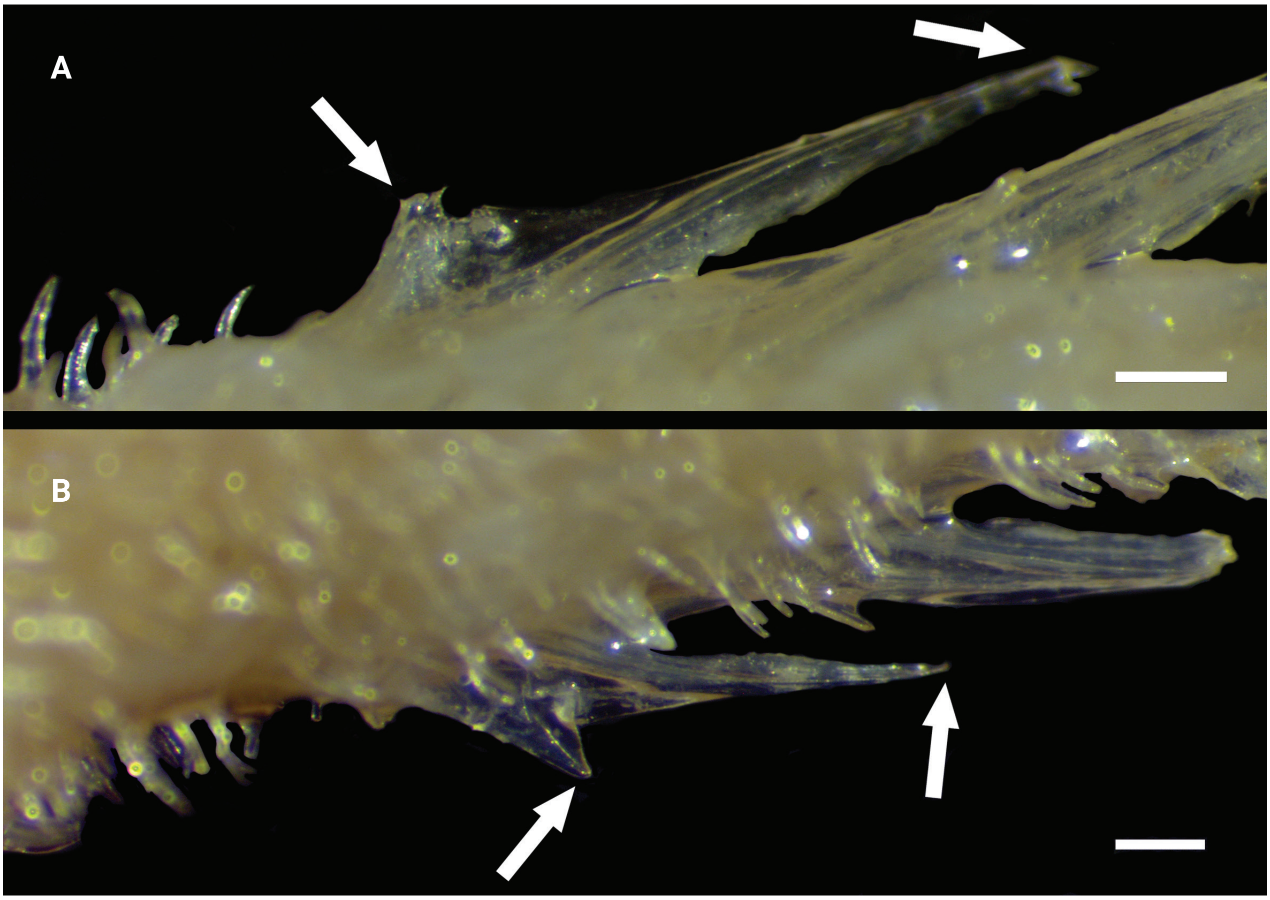

Figure 3. Close-up images of *Hispidoberyx ambagiosus* Kotlyar, 1981, ASIZP 63512, 134.8 mm SL, featuring the fusion of the first two spines on (**A**) dorsal and (**B**) and anal fins (tips indicated by arrows). Scale bar: 500 µm.

patch on fourth pharyngobranchial. Gill filaments on first arch short, about 1/3–1/2 length of longest opposite rakers. Pseudobranch present and short.

Prickle-like body scales adherent (Fig. 6A), covering entire body, operculum, and cheeks; spinules on body scales needle-like and curved backwards, their numbers variable: scales on nape with ca 2–7 spinules; scales on abdominal region with 2–7 spinules; scales on dorsum with 2–14 spinules; scales above anal-fin base with 4–11 spinules; scales on caudal peduncle with 3–16 spinules. Lateral-line scales shield shaped (Fig. 6B, C) with 2 posterior branches, each bearing 1–3 (modally 2) spines curving backwards; center of each scale with 2 or 3 (rarely 1) central spines curving and pointing backwards; all lateral-line scales distinctly larger than body scales; lateral-line canals opened at both anterior and posterior ends of scales. No scutes on abdominal region. No scales on gular region and isthmus. Predorsal scales not enlarged and not aligned in straight line.

Dorsal fin low, situated posteriorly, slightly anterior to anal-fin origin. Origin of pectoral fin situated lower than horizontal through ventral margin of eye. Origin of pelvic fin below and slightly behind pectoral-fin base. Both pectoral and pelvic fins short, their tips clearly anterior to vertical through anal-fin origin. Anal-fin base rather short, its end at same vertical through end of dorsal-fin base. Caudal fin moderately small, slightly forked. All fin rays fragile and possess spinules on lateral surfaces, except for procurrent caudal-fin rays (sometimes also absent on anterior most dorsal- and anal-fin spines).

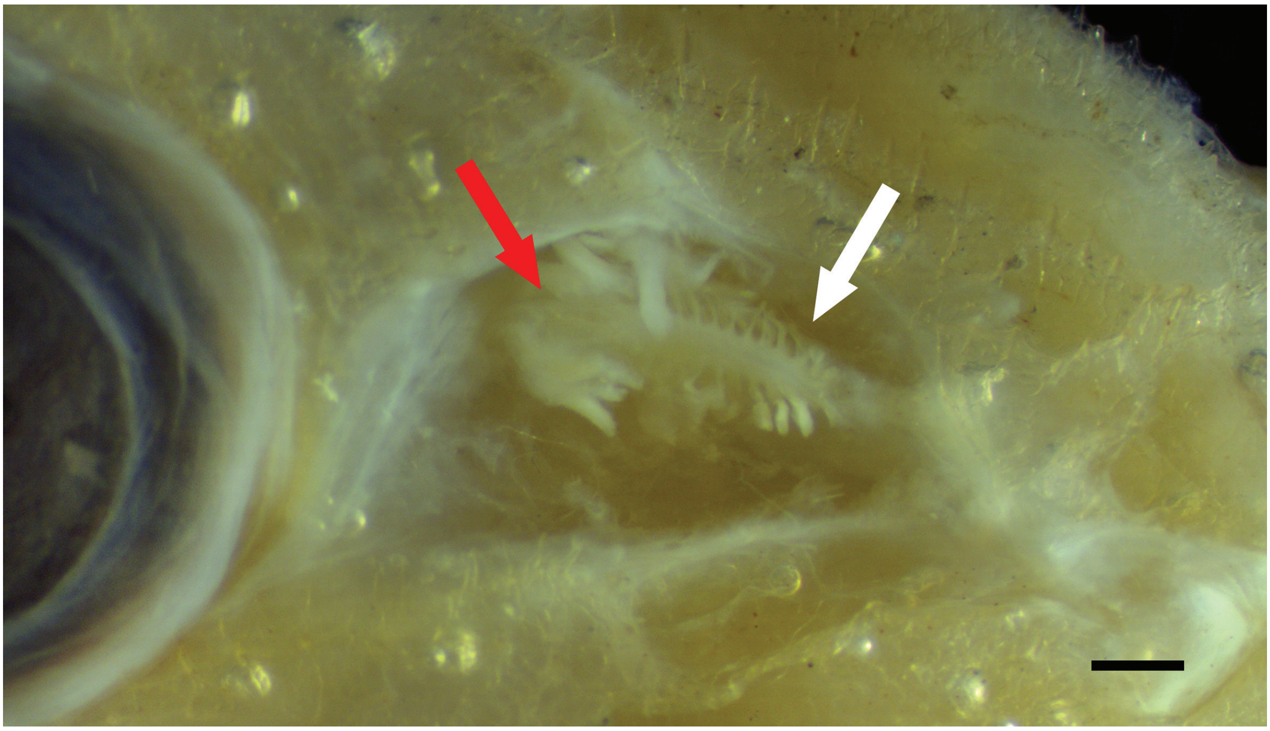

Figure 4. Close-up image of *Hispidoberyx ambagiosus* Kotlyar, 1981, ASIZP 63512, 134.8 mm SL, featuring the nasal organ (white arrow) in the right olfactory chamber. Red arrow indicates the position of Tominaga's organ (beneath and behind nasal organ). Anterior to right. Scale bar: 1 mm.

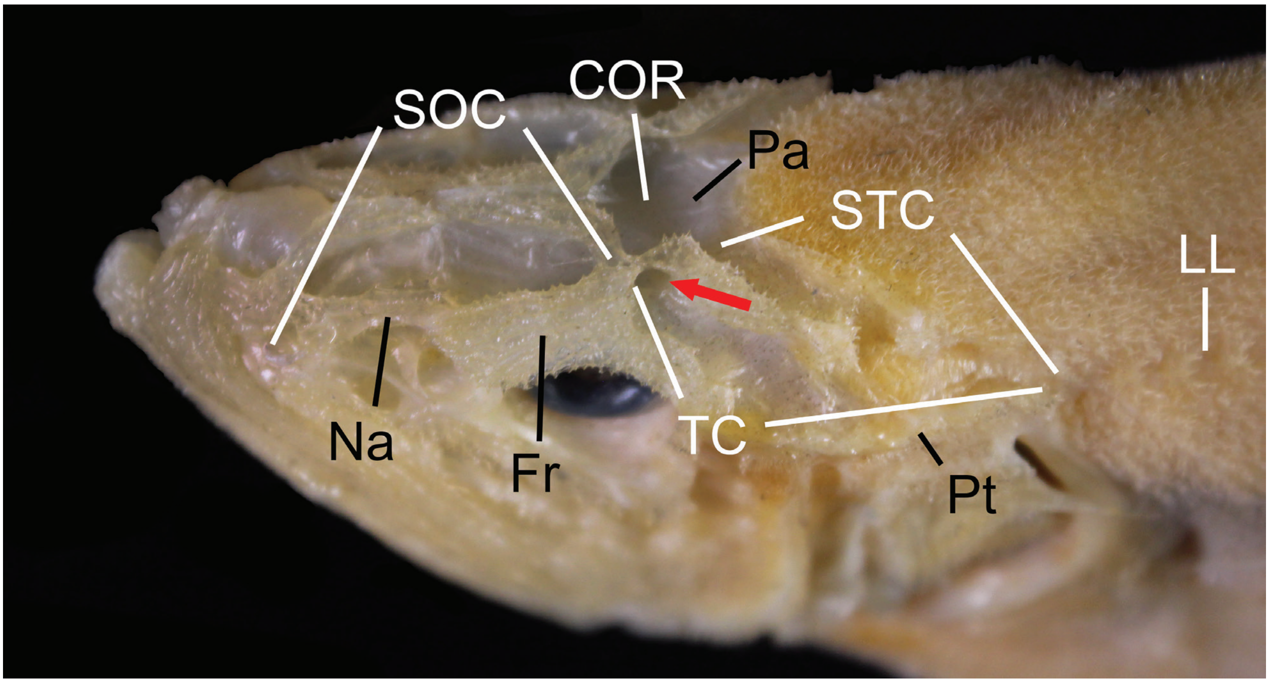

Figure 5. Dorsal-lateral view of *Hispidoberyx ambagiosus* Kotlyar, 1981, ASIZP 81665, 162.0 mm SL, showing sensory canals (white) on head and nearby bones (black). Red arrow indicates the fenestration connecting COR and TC. Abbreviations: COR, coronal commissure; Fr, frontal; LL, lateral line; Na, nasal; Pa, parietal; Pt, posttemporal; SOC, supraorbital canal; STC, supratemporal canal; TC, temporal canal. Anterior to left. Not to scale.

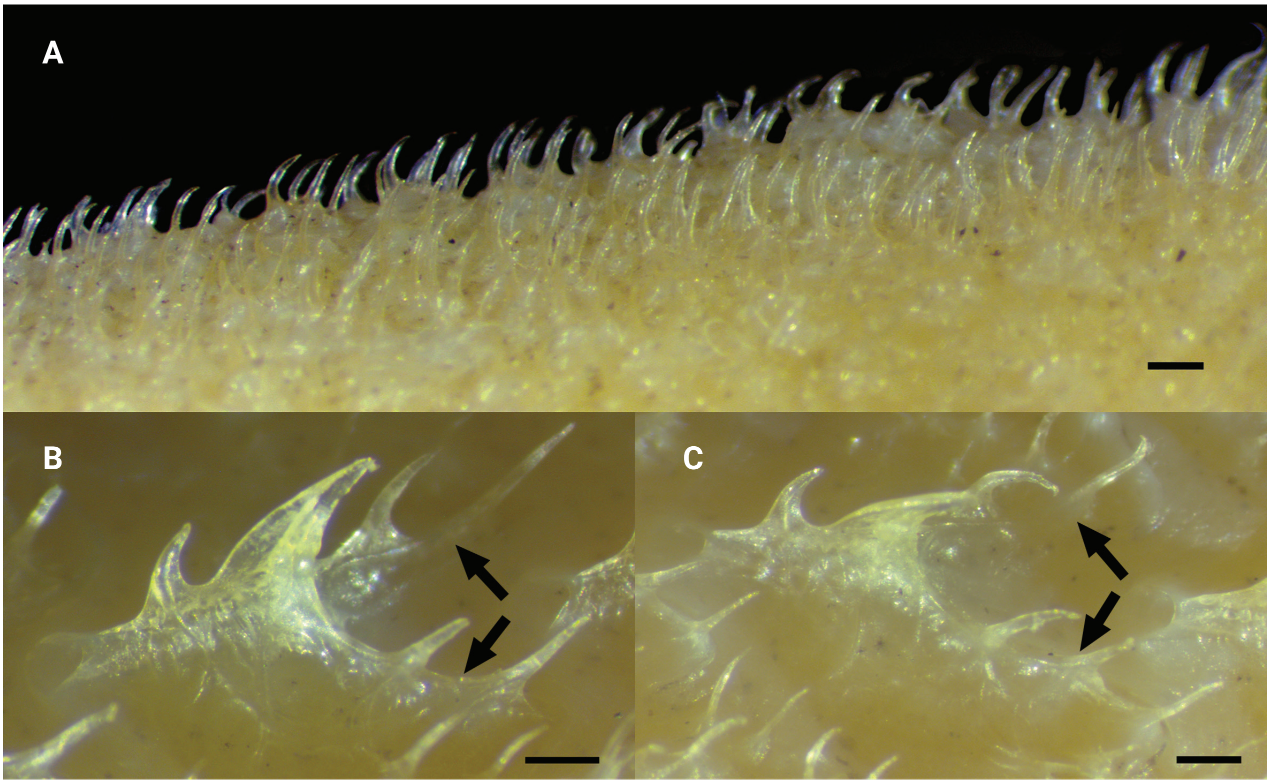

Figure 6. Body and lateral-line scales of *Hispidoberyx ambagiosus* Kotlyar, 1981, ASIZP 81665, 162.0 mm SL. **A** body scales on nape **B** lateral-line scales on anterior portion **C** lateral-line scales on posterior portion. Anterior to left. Scale bars: 500 µm.

Lateral line single, originating behind and slightly lower than posterior tip of posttemporal bone; its anterior portion slightly curved and raised, with downturn below dorsal-fin base, and nearly straight posterior portion; its end anterior to caudal-fin base. Anus situated immediately anterior to anal-fin origin. Caudal peduncle stout, length 1.3 in HL, height 3.7–4.1 in HL. Light organs absent. No trace of swim bladder.

Otoliths. (Fig. 7). Otoltihs triangular, with horizontal, long ventral rim, oblique posterior and anterior rims, and short but rounded dorsal rim. Slightly notched in anterior rim, forming brief but obtuse rostrum and antirostrum. All margins smooth. Otoliths notably thickened, with inner and outer faces nearly flat. Sulcus centrally positioned, not divided into ostium and cauda, open anteriorly, slightly bent upward posteriorly but not reaching posterior rim. Cristae not well delineated. Single, large colliculum centrally located, but shape of its posterior margin varies greatly; largely extended posteriorly in right otolith, but deeply indented in left one.

Coloration. When fresh (Fig. 1), entire body, including head, fin rays, and fin membranes uniformly pinkish to reddish. When preserved (Fig. 2), body uniformly pale, including entire oral cavity, gill rakers, inner face of operculum, stomach, and intestine. Membrane of kidney and ventral side of peritoneum scattered with pepper-like black pigments. Pelvic fin slightly dusky, while other fins pale.

Size. This is a moderately small species of stephanoberycoid, attaining at least 181 mm SL (holotype; Kotlyar 1981). Our largest specimen (ASIZP 81665; 162.0 mm SL) is a mature female with developing eggs, suggesting that it may mature at this size.

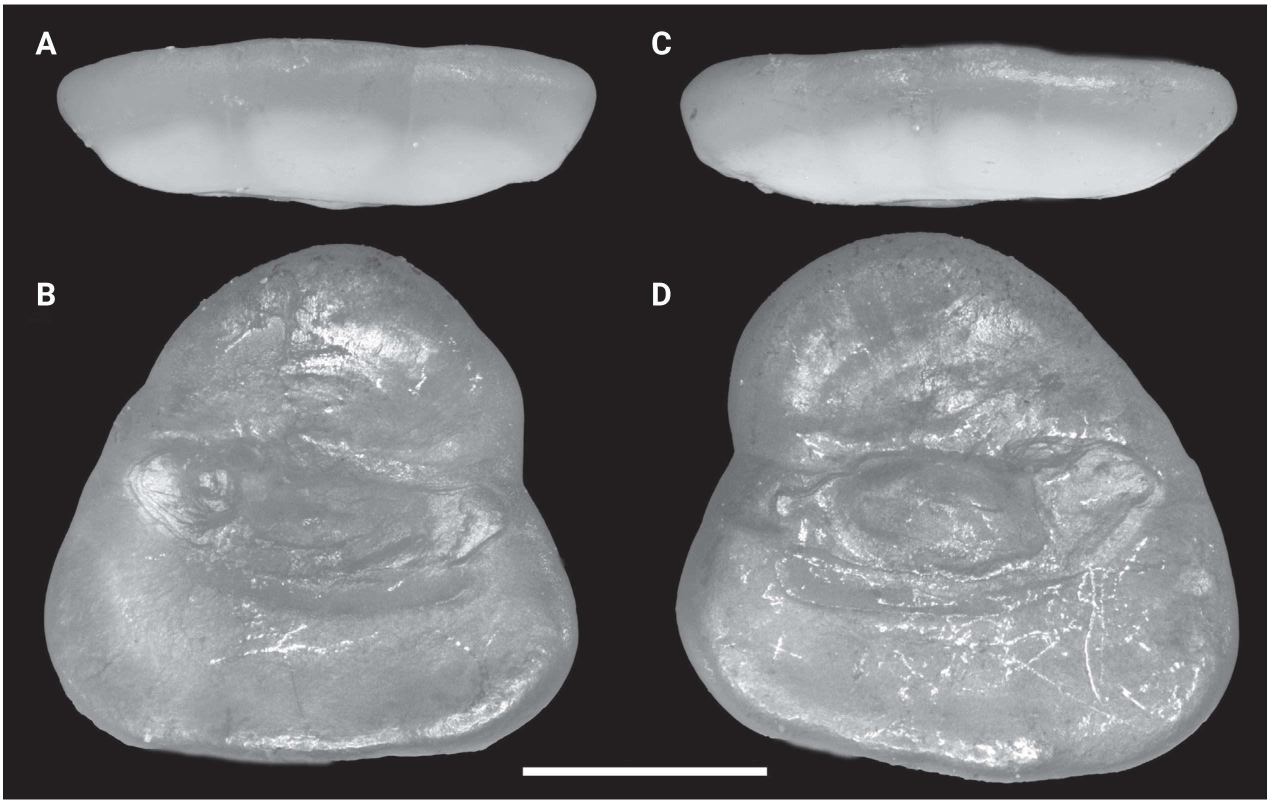

Figure 7. Otoliths (a pair of sagittae) of *Hispidoberyx ambagiosus* Kotlyar, 1981. Specimens (CHLOL 969) were taken from ASIZP 81665 **A, B** left otolith, 2.2 mm otolith length **C, D** right otolith, 2.3 mm otolith length **A, C** ventral views **B, D** inner (mesial) views. Scale bar: 1 mm.

Discussion

Distribution

Hispidoberyx ambagiosus was originally described from the eastern Indian Ocean (Kotlyar 1981) and subsequently recorded from the South China Sea (Yang et al. 1988; Kotlyar 1991). Our specimens represent the northernmost record of this species, suggesting a wide, but more or less restricted distribution in the western Pacific and eastern Indian Ocean; the known bathymetric range is 560–1019 m (Yang et al. 1988; Kotlyar 1991). With the new information presented here, the geographic range this species is now known to extend from the South China Sea to northeastern Taiwan, northwestern Pacific Ocean (Fig. 8).

Fin elements

The counts of fin rays of our specimens generally agree with those of Kotlyar (1996), with the exception that some of our specimens have one more dorsal-fin soft ray (10–11 vs 10 in Yang et al. 1988; Kotlyar 1996; Table 1) and consistently more anal-fin soft rays (10 vs 9). Notably, two of our specimens have their first two dorsal-fin spines and three specimens have their first two anal-fin spines fused as a single, double-tipped spine: we counted them as a single spine. Although Kotlyar (1981, 1991) did not mention such conditions, our specimens have the same number of fin spines (IV–V and II–III in dorsal and anal fins, respectively; Kotlyar 1981,

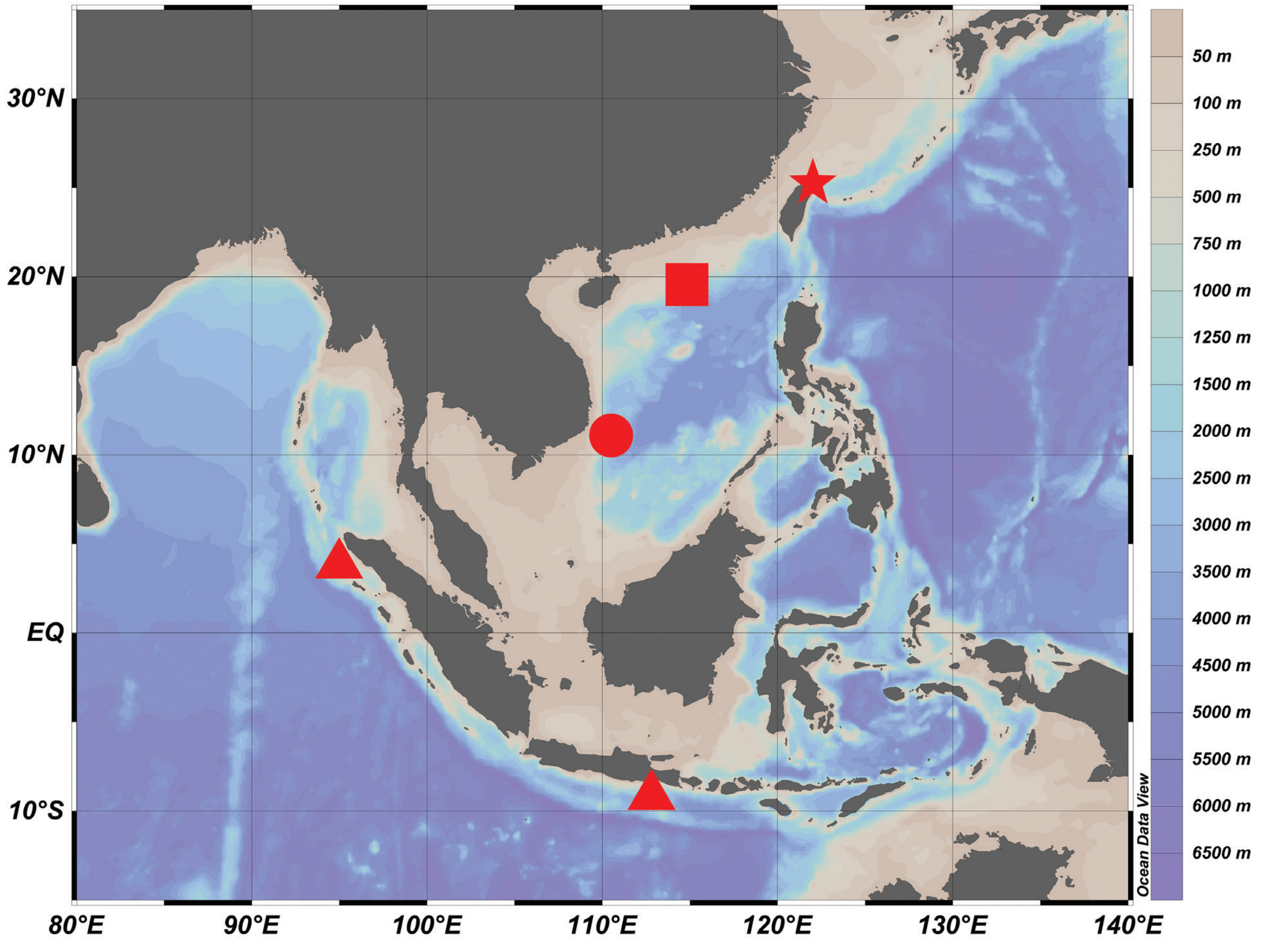

Figure 8. Distribution map of *Hispidoberyx ambagiosus* Kotlyar, 1981. Data source: star = this study; triangle = Kotlyar (1981); square = Yang et al. (1988); circle = Kotlyar (1991).

1996). Moreover, we found that all fin soft rays of our specimens are rather delicate, hindering precise measurements of them. These unique observations were not documented in previous works (Kotlyar 1981, 1991, 1996; Yang et al. 1988).

Lateral-line scales

The number of lateral-line scales generally agrees with the data provided by Kotlyar (1996), with the exception that one of our specimens has 36 lateral-line scales (vs 32–34 in Kotlyar 1996; Table 1). On the other hand, the overall shape of the lateral-line scales generally agrees with Kotlyar (1981: fig. 3). However, our specimens have longer posterior branches (Fig. 6B, C) and usually bear two spines (vs only 1 spine in all 3 scales, as illustrated by Kotlyar 1981: fig. 3). Additionally, we found all of the lateral-line scales opened at both anterior and posterior ends.

Body scales

All body scales of *H. ambagiosus* possess long, needle-like, recurved spinules on their surfaces. The numbers of those spinules are variable, however those on the anterior and ventral sides of the body tend to have fewer spinules. Moreover, we counted 3–8, 5–8, 4–10, and 7–16 spinules on caudal-peduncle scales in the 134.8, 153.5, 154.7, and 162.0 mm SL specimens, respectively, and similar phenomena were observed in scales above the anal-fin base, on the nape, and on scales of the dorsum. Therefore, we suggest that the number of spinules on these body scales slightly increases with body size.

Vertebrae

Because of the thickened body scales, it is difficult to determine the position of the first haemal spine. Therefore, we followed Kotlyar (1991) to include the vertebrae with pleural ribs as precaudal vertebrae and the remaining as caudal vertebrae. However, our specimens possess one additional caudal vertebra compared to previous works (23 vs 22 in Kotlyar 1981, 1991, 1996; Table 1). Although Kotlyar reported 22 caudal vertebrae in his original description, he subsequently (Kotlyar 1991) stated that the second ural centrum was not included in the original description. Nonetheless, Kotlyar (1991, 1996) provided the same number of caudal vertebrae (22) as in the original description, which may indicate that the number was not revised and caused this discrepancy in counting vertebrae numbers.

Tominaga's organ

The Tominaga's organ was first described as a structure with unknown function situated between the nasal rosette and the eye in *Rondeletia loricata* Goode & Bean, 1895 by Tominaga (1970) (Paxton et al. 2001). Later, Paxton et al. (2001) found this organ only exists in three species of Stephanoberycoidei, namely *Rondeletia bicolor* Abe & Hotta, 1963, *R. loricata*, and *Gibberichthys pumilus* Parr, 1933, and these authors proposed that Rondeletiidae and Gibberichthyidae are closely related. They also provided detailed descriptions and comparisons of this organ in the three species. Moreover, they suggested that the function of Tominaga's organ may be secretory (Paxton et al. 2001).

In this study, we confirm that Tominaga's organ is present in *H. ambagiosus* (Fig. 4). The nasal organ is visible when the nasal membrane is removed, and the overall shape is similar to those in Rondeletiidae and Gibberichthyidae (Paxton et al. 2001); as the Tominaga's organ lies beneath the skin behind the nasal organ, dissection is needed. Additionally, although not mentioned in the previous work (Ho et al. 2023), Tominaga's organ is also confirmed in *Gibberichthys latifrons* (Thorp, 1969).

Otoliths

In this study, the sagittal otoliths of *H. ambagiosus* have been both described and depicted for the first time (Fig. 7). Notably, their peculiar shape and highly specific sulcus configuration, characterized by a singular substantial colliculum, exhibit resemblances to features observed in otoliths of Rondeletiidae and Barbourisiidae (Rivaton and Bourret 1999; Nolf 2013). A particularly striking similarity is found with the otoliths of Cetomimidae (Fitch 1979). Noteworthy parallels can be drawn between the otoliths of *H. ambagiosus* and those of *Cetomimus*, *Ditropichthys*, and *Gyrinomimus* as illustrated by Fitch (1979). These include a triangular outline with an angled dorsal rim and an elongated ventral rim, the presence of a single substantial colliculum, and less prominently developed cristae. These shared features suggest a close relationship among Stephanoberycoidei.

Morphological variations

Variations in morphometric data of our specimens compared with those recorded by Kotlyar (1981, 1996) and Yang et al (1988) were observed. Compared with Kotlyar (1981 and 1996), our specimens have a longer eye diameter (5.4–6.5% SL vs 4.3–4.8% SL in Kotlyar 1996; Table 2); longer postorbital length (14.0–14.7% SL vs 12.1–13.3% SL); slightly longer pelvic-fin–anal-fin length (29.6–32.1% SL vs 27.2–29.8% SL); slightly longer dorsal-fin length (22.1–24.0% SL vs 21.6–22.1% SL); slightly longer anal-fin length (13.8–15.4% SL vs 12.3–13.8% SL); slightly longer longest gill-raker length (4.1–5.0% SL vs 4.0–4.4% SL); and a shorter postdorsal length (23.4–25.1% SL vs 26.0–27.8% SL in Kotlyar 1981). Since most of our specimens are smaller than specimens previously recorded (134.8–162.0 mm vs 156–181 mm in Yang et al. 1988; Kotlyar 1996), all morphometric differences we found are considered intraspecific variations.

Additionally, we suggest that the difference in snout length (8.9–9.6% SL vs 11.2–12.3 in Kotlyar 1996; Table 2) may be attributed to the difference in measuring landmarks. The anterior portion of the premaxilla protrudes before the snout, and thus we measured the snout length from the anterior tip of the lachrymal to the anterior margin of the eye only. It is very likely that both Kotlyar (1981, 1996) and Yang et al. (1988) included the premaxilla in their measurements of snout length, which, therefore, caused this discrepancy.

Record of *Barbourisia rufa* from Taiwan

The studied specimens were initially identified as *Barbourisia rufa*, with this species and *H. ambagiosus* both sharing a bright-red body coloration when fresh, and a rather big mouth with the posterior end of the maxilla exceeding a vertical through the posterior margin of the eye. However, *H. ambagiosus* is readily distinguished from *B. rufa* in having the pelvic fins anteriorly situated (vs posteriorly situated at the middle of trunk in *B. rufa*; Parr 1945), presence of dorsal- and anal-fin spines (vs fin spines absent on both fins), gill chamber and peritoneum pale (vs black), and opercle with single, strong central spine (vs opercle without spines).

Although the specimens reported here as *H. ambagiosus* were the basis for the inclusion of *B. rufa* in the Taiwanese fauna (Shao 2023), another *B. rufa* specimen (ASIZP 57678), previously considered lost (S.-P. Huang pers. comm.), was relocated in the National Museum of Marine Science and Technology, Keelung Taiwan (NMMST) for exhibition (J.-F. Huang pers. comm.), and we identify that specimen here as *B. rufa*. Therefore, *B. rufa* is retained in the ichthyofauna of Taiwan.

Comparative materials

Barbourisia rufa: ASIZP 57678, 312 mm SL, Bashi Channel, 21°30'00"N, 120°47'59.99"E, depth 300–400 m, 20 Jan. 1991, bottom trawl, coll. J.-W. Chen. *Gibberichthys latifrons*: NMMB-P37435, 100.7 mm SL, off Dong-gang fishing port (ca 22°22'22"N, 120°27'34"E), Pingtung, southwestern Taiwan, 26 Dec. 2022, bottom trawl, coll. K.-H. Wu.

Acknowledgements

We thank S.-P. Huang (ASIZP) for loans of specimens under his care, for searching for specimens, and for permission to dissect specimens; H.-W. Liu (ASIZ; BRCAS) for registering the specimen and providing various assistance; B.C. Mundy (NOAA) and M. Nakae (NSMT) for providing literature; H.-C. Lin (NSYSU) for providing resource materials and access to facilities; J.-F. Huang (NTOU) for providing fresh photos and information of the *B. rufa* specimen in NMMST, and taking x-radiographs.

Additional information

Conflict of interest

The authors have declared that no competing interests exist.

Ethical statement

No ethical statement was reported.

Funding

This study was supported by the National Science and Technology Council, Taiwan.

Author contributions

Y. S. and C.-H. Lin composed the manuscript; H.-C. Ho revised the manuscript, gave critical comments to the manuscript, and provided funding. All authors approved the manuscript.

Author ORCIDs

Yo Su https://orcid.org/0000-0002-3576-9229
Chien-Hsiang Lin https://orcid.org/0000-0002-9843-9729
Hsuan-Ching Ho https://orcid.org/0000-0003-1154-601X

Data availability

All of the data that support the findings of this study are available in the main text.

References

Abe T, Hotta H (1963) Description of a new deep-sea fish of the genus *Rondeletia* from Japan. Japanese Journal of Ichthyology 10(2–6): 43–48. [pls 6, 7]

Fitch JE (1979) The velvet whalefish, *Barbourisia rufa*, added to California's marine fauna, with notes on otoliths of whalefishes and possible related genera. Bulletin of the Southern California Academy of Sciences 78(1): 61–67.

Fricke R, Eschmeyer W, van der Laan R (2023) Catalog of fishes: genera, species, references. California Academy of Sciences, San Francisco, USA. http://researcharchive.calacademy.org/research/ichthyology/catalog/fishcatmain.asp

Goode GB, Bean TH (1895) On Cetomimidae and Rondeletiidae, two new families of bathybial fishes from the northwestern Atlantic. Scientific results of explorations by the U.S. Fish Commission steamer Albatross. Proceedings of the United States National Museum 17(1012): 451–454. [pl. 17] https://doi.org/10.5479/si.00963801.17-1012.451

Ho H-C, Su Y, Leung N-S, Lin T-Y (2023) New records of a rare gibberfish, *Gibberichthys latifrons* (Stephanoberyciformes, Gibberichthyidae), from the South China Sea, with comments on morphological characters. ZooKeys 1172: 47–59. https://doi.org/10.3897/zookeys.1172.102433

Jakubowski M (1974) Structure of the lateral-line canal system and related bones in the berycoid fish *Hoplostethus mediterraneus* Cuv. et Val. (Trachichthyidae, Pisces). Acta Anatomica 87(2): 261–274. https://doi.org/10.1159/000144173

Kimura K (2020) Reassessment of the phylogenetic position of the spiny-scale pricklefish *Hispidoberyx ambagiosus* (Beryciformes: Hispidoberycidae) [an abstract of dissertation and a summary of dissertation review] (Doctoral dissertation, Hokkaido University).

Kotlyar AN (1981) A new family, genus and species of Beryciformes, Hispidoberycidae fam. n. *Hispidoberyx ambagiosus* gen. et sp. n. (Beryciformes). Journal of Ichthyology 21(3): 9–13.

Kotlyar AN (1991) Osteology of *Hispidoberyx ambagiosus* (Hispidoberycidae) and its position within the Beryciformes. Journal of Ichthyology 31(5): 99–108.

Kotlyar AN (1996) Beryciform Fishes of the World Ocean. VNIRO Publishing, Moscow, 368 pp. [In Russian]

Kotlyar AN (2004) Family Hispidoberycidae Kotlyar, 1981 – Hispidoberycids. California Academy of Sciences Annotated Checklists of Fishes 26: 1–2.

Lin C-H, Chang C-W (2012) Otolith Atlas of Taiwan Fishes. National Museum of Marine Biology and Aquarium, Pingtung, 416 pp.

Nelson JS, Grande TC, Wilson MVH (2016) Fishes of the World. 5th edn., John Wiley and Sons, Hoboken, 707 pp. https://doi.org/10.1002/9781119174844

Nolf D (2013) The Diversity of Fish Otoliths, Past and Present. Royal Belgian Institute of Natural Sciences, Brussels, 222 pp.

Parr AE (1933) Deepsea Berycomorphi and Percomorphi from the waters around the Bahama and Bermuda islands. (Scientific results of the third oceanographic expedition of the “Pawnee” 1927.). Bulletin of the Bingham Oceanographic Collection Yale University 3: 1–51.

Parr AE (1945) Barbourisidae, a new family of deep sea fishes. Copeia 1945(3): 127–129. [pl. 1] https://doi.org/10.2307/1438273

Paxton JR, Johnson GD, Trnski T (2001) Larvae and juveniles of the deepsea “whalefishes” *Barbourisia* and *Rondeletia* (Stephanoberyciformes: Barbourisiidae, Rondeletiidae), with comments on family relationships. Records of the Australian Museum 53(3): 407–426. https://doi.org/10.3853/j.0067-1975.53.2001.1352

Randall JE, Lim KKP (2000) A checklist of the fishes of the South China Sea. Raffles Bulletin of Zoology Supplementary 8: 569–667.

Rivaton J, Bourret P (1999) Les otolithes des poissons de l’Indo-Pacifique. Institut de recherche pour le développement, Nouvelle-Calédonie, 378 pp.

Schlitzer R (2023) Ocean data view.

Shao K-T (2023) Taiwan Fish Database. WWW Web electronic publication. http://fishdb.sinica.edu.tw

Su Y, Lin H-C, Ho H-C (2022) *Hoplostethus roseus*, a new roughy fish from the western Pacific based on morphology and DNA barcoding (family Trachichthyidae). Journal of Fish Biology 101(3): 441–452. https://doi.org/10.1111/jfb.15086

Su Y, Lin H-C, Ho H-C (2023) New records of two roughy fish species of *Hoplostethus* and a confirmed record of *H. crassispinus* Kotlyar, 1980 (Trachichthyiformes, Trachichthyidae) from Taiwan. ZooKeys 1149: 85–101. https://doi.org/10.3897/zookeys.1149.96233

Thorp CH (1969) A new species of mirapinnaform fish (family Kasidoroidae) from the western Indian Ocean. Journal of Natural History 3(1): 61–70. https://doi.org/10.1080/00222936900770071

Tominaga Y (1970) On the glandular organs before the eyes of the red-coated whalefish, *Rondeletia loricata*. Zoological Magazine (Tokyo) 79(11–12): 368. [In Japanese]

Yang Y-R, Zeng B-G, Paxton JR (1988) Additional specimens of the deepsea fish *Hispidoberyx ambagiousus* [sic] (Hispidoberycidae, Berciformes [sic]) from the South China Sea, with comments on the family relationships. Uo (Japanese Society of Ichthyologists) 38: 3–8.

ZooKeys 1182: 35–134 (2023)
DOI: 10.3897/zookeys.1182.104258

Review Article

The Nereididae (Annelida) – diagnoses, descriptions, and a key to the genera

Robin S. Wilson[1,2], Christopher J. Glasby[3,4], Torkild Bakken[5]

1 Sciences Department, Museums Victoria Research Institute, Museums Victoria, GPO Box 666 Melbourne, Victoria 3001, Australia
2 The University of Melbourne, Melbourne, Victoria 3010, Australia
3 Museum and Art Gallery Northern Territory, PO Box 4646, Darwin NT 0801, Australia
4 Australian Museum Research Institute, Australian Museum, 1 William Street, Sydney, NSW 2010, Australia
5 Norwegian University of Science and Technology, NTNU University Museum, NO-7491 Trondheim, Norway
Corresponding author: Robin S. Wilson (rwilson@museum.vic.gov.au)

Abstract

Nereididae is among the most familiar of marine annelid families, common and well-studied in most marine environments but paradoxically no recent key or identification guide exists to the world's genera. Here updated generic descriptions, a list of characters, a linear key to genera, and minimal diagnoses that distinguish each genus from all others in the family are provided. This information is generated from a Delta database of 186 morphological characters and a link is provided to downloadable software allowing the same data to be interrogated using the open-source Delta program Intkey – a nonlinear multiple entry point computerised interactive key. For each genus the recent literature is also summarised, comments on taxonomic status provided, and published keys to species cited. Nexus format matrices are provided for all 45 genera and 158 Nereididae species, representing all genera, scored for 146 multistate characters from the same character list to facilitate future phylogenetic studies.

Key words: Computer taxonomy, diagnosis, identification tools, natural language descriptions, polychaete, taxonomic verification, Taxonomic Information System

This article is part of:
Guides to Australian Annelida

Academic editor: Greg Rouse
Received: 29 March 2023
Accepted: 31 July 2023
Published: 11 October 2023

ZooBank: https://zoobank.org/76D0717B-0197-4A85-A30F-A58338D1ED7B

Citation: Wilson RS, Glasby CJ, Bakken T (2023) The Nereididae (Annelida) – diagnoses, descriptions, and a key to the genera. ZooKeys 1182: 35–134. https://doi.org/10.3897/zookeys.1182.104258

Table of contents

Introduction

The Nereididae is probably the best-known of all the families of marine annelids ("polychaetes") – the family includes many species that are commonly encountered world-wide, intertidally, and also in diverse habitats from ephemeral freshwaters to abyssal depths (Bakken et al. 2022; Rouse et al. 2022). Nereididae are also frequent study subjects in teaching laboratories, and some species are commonly studied as laboratory animals (Fischer et al. 2010) (although now known to comprise complexes of multiple species; see Systematic account of Nereididae genera). Nereididae are almost invariably used as exemplars of marine Annelida in invertebrate zoology textbooks (Marshall and Williams 1972; Ruppert et al. 1994; Rouse and Giribet 2016). Nereididae are significant ecologically especially in intertidal flats (Compton et al. 2013; Choi et al. 2014) where they form significant components to the diet of fish and shorebirds (Iwamatsu et al. 2007; Alves et al. 2013; Duijns et al. 2013) and are aquaculture species of importance for fish bait and for aquaculture species for human consumption (Yoshida 1984; Olive 1994; Lim et al. 2021). A number of nereidid species are accidental introductions, or their introduced status is cryptic (Einfeldt et al. 2014; Villalobos-Guerrero and Carrera-Parra 2015; Tosuji et al. 2019; Kurt et al. 2021).

Taxonomic research on Nereididae is active, with nearly 100 papers published in the past decade, and the family currently comprises 45 genera and 719 species (Read and Fauchald 2023). Prominent among recent studies are investigations using molecular evidence leading to discovery of cryptic species (Glasby et al. 2013; Villalobos-Guerrero and Bakken 2018; Tosuji et al. 2019; Teixeira et al. 2022a, 2022b) and new phylogenetic hypotheses (Tosuji et al. 2018; Alves et al. 2020, 2023; Villalobos-Guerrero et al. 2022b). The past decade has also seen description of 40 new species, revision of eight genera and a review of the diversity, biology, anatomy, and ecology of the family Bakken et al. (2022).

Despite this recent taxonomic progress, identification of nereidid specimens remains a challenge, especially to non-specialists. Genus-level identification is difficult because no key to genera has been published since Fauchald (1977) and our own interactive key, now 20 years out of date (Wilson et al. 2003). Identification difficulties are compounded by the wide recognition that several of the most species-rich genera are assemblages of unrelated species (Bakken and Wilson 2005; Bakken et al. 2022; Rouse et al. 2022). It is clear that a number of genera will be revised when further molecular systematic studies are completed. But it is also clear that achieving sufficient taxon sampling in those molecular studies is a significant challenge and that the composition of many genera and identity of many species is likely to remain doubtful for a significant number of years. Yet the need for identification tools is widespread, not least by those conducting new molecular systematics studies to resolve problematic taxa. For these reasons we provide this review with the following aims:

- to provide updated descriptions of all genera; these correct one error in Bakken et al. (2022) and also include additional characters (see Systematic account of genera);
- to provide a dichotomous key to genera (see Key to genera of Nereididae) and a downloadable interactive identification tool (= Taxonomic Information System) using the Delta Intkey software (Wilson et al. 2023);
- to discriminate all genera based on minimal diagnoses (see Systematic account of genera);
- to provide a character list (see Nereididae characters) and Nexus format data matrices (Wilson et al. 2023) for inclusion in future phylogenetic studies requiring morphological evidence.

Methods

We used the Delta (Descriptive Language for Taxonomy) suite of programs to create and manage taxonomic data to support objective and quantitative description and discrimination of Nereididae taxa (Dallwitz 1974, 1980; Dallwitz et al. 1993; Dallwitz and Paine 2015). The original implementation of the Delta software by Australia's Commonwealth Scientific and Industrial Research Organisation (CSIRO) is still available as Windows only software via Dallwitz (2020). The Delta software was ported to Java by the Atlas of Living Australia as Open-Delta (Atlas of Living Australia 2014) as Windows/Mac OS/Linux software and this is the version we use. A third implementation of Delta, although lacking interactive identification software, is Cavalcanti (2022). The implementation of Delta is approximately identical in Dallwitz (2020) and Atlas of Living Australia (2014) so the guide of Coleman et al. (2010), although based on Windows software, is a very useful introduction for any Delta installation.

Delta comprises several separate applications: the Delta Editor manages taxon by character data and generates outputs via scripts (called Action Sets). For the purposes of this paper, principal outputs are natural language descriptions and diagnoses of taxa (see below and Systematic account of Nereididae genera), linear keys (see below and Key to genera of Nereididae), interactive keys and Nexus files (Wilson et al. 2023) and annotated character lists (see Nereididae characters, below).

For each genus we include two Delta outputs: a description and a diagnosis – terms that have been used loosely in much of the taxonomic literature, where typically "diagnoses" are merely descriptions. Our descriptions are Delta-generated natural language outputs, use all character states known for a genus based on the sources we list as interpreted against our character list. These are concatenations of character states recorded for each taxon.

We concur with Borkent (2021) that diagnoses should be minimal statements that precisely distinguish taxa – typically from other taxa of the same rank – and ours do so. Borkent (2021) did not identify tools for the non-trivial task of generating such diagnoses but the Delta system has that capability: the DiagLevel setting specifies the minimum number of characters for which the diagnostic description should differ from all the other taxa (Dallwitz 1989). The diagnoses provided below include, for all genera, 'minimal diagnoses' which as the name implies, are a list of those characters which alone are sufficient to distinguish the given genus from all others. These minimal diagnoses were generated using the Intkey setting DiagLevel=1. For many genera, the setting could be increased to DiagLevel=2, thus generating additional characters which, for those genera, can be used to verify a 'minimal diagnosis' that may have been tentatively achieved by the user (perhaps when viewing damaged specimens, or when interpreting some characters was uncertain). These additional diagnostic characters providing an additional secondary level of verification are termed 'secondary diagnosis' in the generic accounts below. Our intended use of the diagnosis is to verify identifications by detecting errors that may have been made while using a key (Borkent 2021; also see comment below at the beginning of Key to genera of Nereididae).

The key was generated by the Delta Confor program with the following settings: RBASE = 2.00 ABASE = 1.00 REUSE = 1.01 VARYWT = 0.80; Number of confirmatory characters = 2. Following the recommendation of Dallwitz and Paine (2015) these settings were arrived at by iterative modification: balancing length of key (RBASE), evenness of subdivisions based on abundance indices, (ABASE, not used here), minimising re-use of characters (REUSE) and treatment of variable characters (VARYWT); Dallwitz (1974) provides further details.

Characters and character states are described and illustrated in the following section. The downloadable Intkey interactive key associated with this paper includes a more comprehensive set of character state illustrations. Two Nexus files are provided as Suppl. materials 1, 2 and as part of Wilson et al. (2023). One Nexus file contains all 45 genera, the second contains 158 species representing all nereidid genera (these are the 158 species for which we have the most complete data). Delta truncates character and character state labels in Nexus outputs to 30 characters; these truncated labels were replaced with full names from original Delta text files using shell scripts provided by Buz Wilson (pers. comm. 2 September 2023) and subsequent manual editing. Both Nexus files use the same 146 unordered multistate characters; both exclude meristic characters since their coding for phylogenetic analyses requires additional data and assumptions (e.g., Lawing et al. 2008) and was beyond the scope of this project. All these information sources are generated from the same Delta database that was used for the diagnoses and descriptions.

Interactive keys are implemented in the Delta suite by the Intkey application (Dallwitz et al. 1995; Coleman et al. 2010) which requires binary files generated from the Delta Editor (Penev et al. 2009). Our Intkey files for Nereididae are available as a separate download (Wilson et al. 2023) and require prior installation of the (recommended) Open-Delta software (Atlas of Living Australia 2014) or the original Delta programs (Dallwitz 2020). This paper serves as an alternative for those unable to install the Delta software.

Results and discussion

Annotated characters of Nereididae

We identified 186 morphological characters to characterise nereidid taxa. Characters are given as they are described in the Delta Editor with annotations and illustrations as required, elaborating features in more detail. We have illustrated characters that we consider the most useful for identification using specimens lodged with the Museum & Art Gallery of the Northern Territory (NTM) and Museum Victoria (NMV), or derived from the literature as credited in the figure captions. Some characters are included even though their potential to inform higher level relationships are not yet tested, for example: palpophore surface (character 4), and prostomium longitudinal groove (character 9). We have also included some characters useful for distinguishing species (principally counts of papillae and paragnaths on the eversible pharynx). Meristic characters, in particular paragnath counts, are thus far rarely used to characterise nereidid genera – typically such characters require data from large numbers of specimens if they are to be the basis of robust taxonomic conclusions (Wilson 1993; Wilson and Glasby 1993).

This character list is also the basis of the Nexus format files provided by Wilson et al. (2023). That Nexus file excludes meristic characters for the reasons set out above, thus the 186 characters listed below are reduced to 146 multistate characters in Nexus outputs. Nexus file labels of character descriptions in some are abbreviated for convenience in phylogenetic software; all Nexus character labels are provided below in square brackets.

Prostomium, pharynx, and ventrum – characters 1–20 (Fig. 1A–P)

1. Antennae [NEXUS: antennae]

   1. present.
   2. absent.

All Nereididae have a pair of antennae excepting *Unanereis* Day, 1962 in which a single antenna is present as illustrated in Day (1962: fig. 3a) (*Unanereis macgregori*) and Ben Amor (1980: fig. A) (*Unanereis zghali*). Bakken et al. (2022) discussed the possibility that presence of a single antenna is a developmental anomaly seen occasionally in Nereididae specimens, in which case both species of *Unanereis* may be referable to *Ceratonereis* or *Solomononereis*.

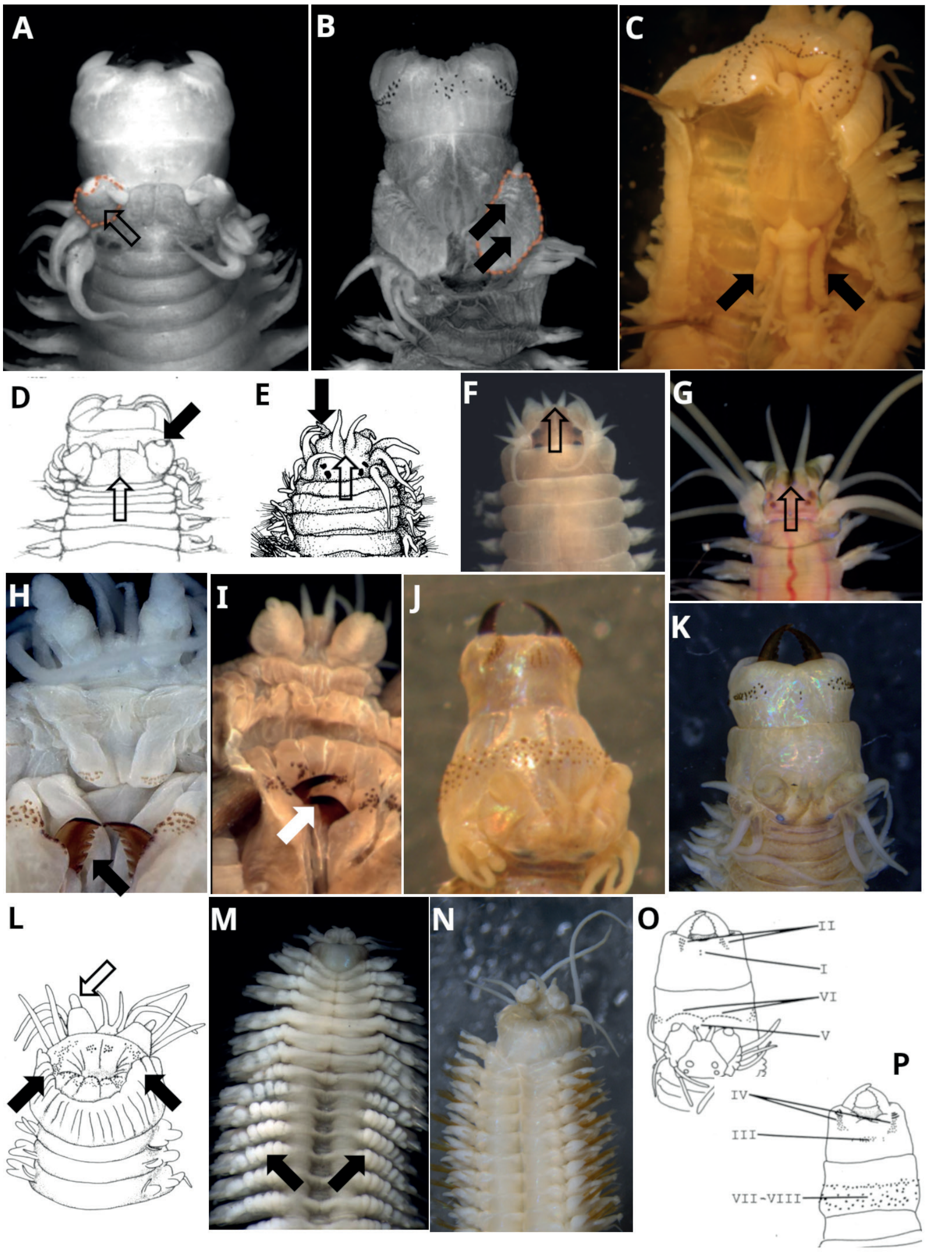

Figure 1. Prostomium, pharynx **A** barrel-shaped palps (orange dashed outline) and palpophore surface with a single transverse groove (open arrow) *Namalycastis abiuma* LNG M16Q3 **B** subconical palps (orange dashed outline) and palpophore surface with several oblique grooves (filled arrows) *Neanthes glandicincta* MD165 anterior **C** caecal glands (filled arrows) in ventral dissection of *Perinereis vallata* NMV F108784 **D** spherical palpostyles (filled arrow) and prostomium with longitudinal groove (open arrow) *Namalycastis abiuma* **E** acutely conical palpostyles (filled arrow) and indented prostomium (open arrow) *Gymnonereis minyami* **F** prostomium anterior margin entire *Nereis* sp. **G** prostomium anterior margin indented (open arrow) *Ceratonereis* sp. **H** dentate jaws (filled arrow) *Platynereis bicanaliculata* NTM W17252 **I** smooth/crenulate jaws (white arrow) *Leonnates crinitus* NTM W3330 **J** everted pharynx a truncate cone with greatest width at margin of tentacular belt (= "frustrum-shaped") *Alitta* sp. NMV F94547 **K** everted pharynx cylindrical *Simplisetia aequisetis* NMV F94248 **L** ventral peristomial flap (filled arrows) and palpostyles subconical to oval-shaped (open arrow) *Cheilonereis peristomialis* **M** ventrum of anterior chaetigers with rows of tubercles extending to the base of each neuropodium (filled arrows) *Australonereis ehlersi* **N** ventrum of anterior chaetigers smooth *Neanthes* sp. NMV F182608 **O** dorsal view pharynx with numbering following Kinberg *Perinereis vallata* **P** ventral view pharynx with numbering following Kinberg *Perinereis vallata*. Sources: **A, B, F, H, I, M** C. Glasby photographs **C, J, K, N** R. Wilson photographs **D** modified after C. Glasby (1999) **E** modified after Hutchings and Reid (1990) **G** Leon Altoff photograph **L, O, P** R. Wilson drawings. Not to scale; body widths of these example specimens are in the range 2–5 mm wide excluding parapodia.

2. Palps [NEXUS: palp orientation]

1. anteriorly directed.
2. ventrally directed.

In most nereidids the palps are anteriorly directed and both palpophore and palpostyles are typically easily seen in dorsal view e.g., Villalobos-Guerrero et al. (2022b: fig. 5b, c) for *Nereis agulhana*. However, in some taxa, e.g., *Micronereis* and some *Kainonereis* and *Platynereis* species, the palps are distinctly ventrally directed and not fully visible in dorsal view. Examples of ventrally directed palps are Paxton (1983: fig. 15) for *Micronereis bansei*, Conde-Vela et al. (2018: fig. 3b, c) for *Kainonereis alata* and Read (2007: fig. 6a, b) for *Platynereis australis*. Caution is required utilising this character alone for identification since, at least in *Kainonereis* and *Platynereis*, this condition seems to be expressed in epitokes and not always confirmed for atokes. Furthermore, it is plausible that palps which may have been ventrally directed in live epitokes may be distorted into an anteriorly directed palps orientation as an artefact caused by preservation with pharynx extended (Read 2007: figs 2a, 3a); Read (2007) did not make use of this character to separate New Zealand species of *Platynereis*.

3. Palpophore [NEXUS: palpophore form]

1. barrel-shaped, approximately equal width from base to palpostyle (not overly large compared with palpostyle; Fig. 1A).
2. massive subconical, flattened palpostyle (minute by comparison; Fig. 1B).

Although palpophore shape has been considered in recent revisionary works at the generic and species group levels, there has been no convincing arguments identifying particular shapes. At least four characteristic shapes have been documented: oval (*Perinereis* species complex) sub-ovoid (*Composetia*, *Leonnates*), obtusely conical (*Leonnates*, *Parasetia*, *Potamonereis*), and subconical (*Parasetia*, *Neanthes*) (Villalobos-Guerrero 2019; Villalobos-Guerrero et al. 2021, 2022a, b). However, some genera were found to be polymorphic for the states recognised and the states themselves can be difficult to distinguish, especially if specimens are preserved in a distorted condition. Other authors have distinguished palpophores on the basis of size: e.g., the palpophores of *Potamonereis* have been referred to as massive (as in *Potamonereis kumensenis* (Sato, 2020)). The present 2-state system is an attempt to describe more effectively the variation in the family. Thus, barrel-shaped palpophores (most genera) have an approximately equal width from base to palpostyle. They are not overly large compared to the size of the palpostyle, and in some cases may be of similar length and usually they have a transverse groove (Fig. 1A). Variability in length of barrel-shaped palpophores may be an indication that this character needs to be further divided into additional states. Subconical, dorso-ventrally flattened palpophores (*Alitta*, *Hediste*, *Leonnates*, *Neanthes micromma*, *Neanthes glandicincta*; Fig. 1B) tend to be massive compared to the size of the palpostyle, have a maximum width at mid to mid-end of palp, and usually have longitudinal striae. *Neanthes* is polymorphic for this character and *Dendronereis* is uncertain.

4. Palpophore surface [NEXUS: palpophore surface]

1. without grooves or striae (palps short, compact; Fig. 1D).
2. with a single transverse groove (palpophores well developed (Fig. 1A).
3. with several oblique grooves or striae (palpophores well developed; Fig. 1B).

The presence of a transverse groove (Fig. 1A, open arrow) or multiple striae (Fig. 1B, filled arrows) on the palpophore, as noted by Villalobos-Guerrero and Idris (2021) is present in many nereid genera with biarticulated palps. The depth of the groove is variable depending on how extended the palps were on fixation. Sometimes many finer transverse grooves (striae) are visible although they may be faint if the palps are extended. In general, we observed that barrel-shaped forms have a single transverse groove which is perpendicular to the long axis of the palpophore, and that subconical, flattened forms possess multiple striae which are at an oblique angle.

5. Palpostyles [NEXUS: palpostyles]

1. present.
2. absent (palps undivided, minute).

A biarticulate palp with a distinct distal palpostyle is present in all Nereididae except members of the genus *Micronereis* which have an undivided roughly spherical palp that is also ventrally located on the anterior prostomium; see Paxton (1983: fig. 15; *Micronereis bansei*).

6. Palpostyles for m [NEXUS: palpostyles form]

1. spherical.
2. subconical.
3. acutely conical.

Palpostyles (present in all genera except *Micronereis*) are recognised as having three shapes: spherical, subconical (in most nereidids; could also be referred to as oval-shaped), and acutely conical. The palpostyles are spherical in members of the Namanereidinae, as illustrated by Glasby (1999: fig. 10a; *Namalycastis abiuma*). Some members of the genera *Ceratocephale* and *Gymnonereis* have palpostyles that are acutely conical e.g., Hutchings and Reid (1990: fig. 6a; *Ceratocephale aureola*), Hutchings and Reid (1990: fig. 9a; *Gymnonereis minyami*), Wilson and Glasby (1993: fig. 8a; *Perinereis caeruleis*). This character is also useful for species separation across several unrelated genera of Nereididae.

7. Eyes [NEXUS: eyes]

1. present (Fig. 1E).
2. absent (Fig. 1D).

Two pairs of eyes are present in most Nereididae but they are absent in a number of species found at bathyal and abyssal depths and subterranean and cave-dwelling Namanereidinae. Examples of the former are illustrated by Hartman and Fauchald (1971: pl. 4 fig. a; *Ceratocephale abyssorum*, as *Pisionura abyssorum*) and Hartmann-Schröder (1975: fig. 22; *Neanthes bioculata*).

8. Prostomium anterior margin [NEXUS: prostomium anterior margin]

   1. entire (Fig. 1F).
   2. indented (Fig. 1E, G, open arrows).

The prostomium in Nereididae is usually entire on the anterior margin e.g., in *Composetia marmorata* (Glasby 2015: fig. 1G, H) but in 13 genera there is a conspicuous indentation between the antennae, as illustrated by Hutchings and Reid (1990: fig. 10a; *Gymnonereis yurieli*), Glasby (1999: fig. 12a; *Namalycastis borealis*) and Glasby (2015: fig. 1A–E; *Ceratonereis* spp.).

9. Prostomium longitudinal groove [NEXUS: prostomium longitudinal groove]

   1. present (Fig. 1D open arrow).
   2. absent (Fig. 1E, F).

10. Tentacular belt length [NEXUS: tentacular belt length]

   1. equal to or less than length of chaetiger 1.
   2. greater than length of chaetiger 1.

Terminology for characters 10 and 11 follows Villalobos-Guerrero et al. (2022a) who as part of a revision of *Composetia* showed that the body part referred to widely in the literature as “tentacular segment”, “achaetigerous segment” and “apodous segment” comprises two segments plus the peristomium. While some genera are polymorphic for this character, others consistently have one or the other state. A short tentacular belt (state 1) distinguishes *Namalycastis* and *Namanereis* from most other nereidids.

11. Tentacular belt [NEXUS: tentacular belt divided]

   1. fused, separate segments not recognisable.
   2. represented by two distinct segments each carrying a pair of tentacular cirri.

12. Tentacular cirri comprising [NEXUS: tentacular cirri number]

   1. four pairs.
   2. three pairs.

13. Tentacular cirrophores [NEXUS: tentacular cirrophores]

   1. present.
   2. absent (cirri undivided).

14. Tentacular cirri extending to chaetiger (number)

Small variations in the length of these cirri on the tentacular belt is often not a useful statistic, but may assist in recognising taxa which have very long tentacular cirri (e.g., *Ceratonereis* spp. and *Platynereis* spp.). Generally the posterodorsal pair is the longest.

15. Ventral peristomial flap [NEXUS: ventral peristomial flap]

1. present (Fig. 1L, filled arrows).
2. absent.

16. Ventrum of anterior chaetigers [NEXUS: ventrum anterior chaetigers]

1. smooth (Fig. 1N).
2. with rows of tubercles extending to the base of each neuropodium (Fig. 1M).

17. Oesophageal caeca [NEXUS: oesophageal caeca]

1. present (Fig. 1C).
2. absent.

Oesophageal caeca (equivalent terms are caecal glands, oesophageal pouches) are a pair of organs that are prominent and easily visible if present, but only by dissection. The oesophageal caeca are located immediately posterior to the muscular pharynx. at the start of the oesophagus. Their utility in taxonomy was first suggested by Savigny (1822) but Khlebovich (2001) was the first to use these structures in the taxonomy of Nereididae.

18. Jaws [NEXUS: jaw dentition]

1. with smooth or slightly crenulate cutting edge (Fig. 1I).
2. with dentate cutting edge (Fig. 1H).

Variation in jaw morphology is as yet not well understood. Some taxa have jaws with smooth or faintly crenulate cutting edge, while others have distinctly or indistinctly toothed jaws. In some taxa the jaws are robust and dark (e.g., *Neanthes* spp., *Perinereis* spp.), while others have finer, translucent jaws (e.g., *Ceratocephale* spp., some *Simplisetia* spp.). However, many taxa are intermediate between these conditions, and abrasion may falsely result in the appearance of “smooth” jaws. Differences in the chemical composition of nereidid jaws may offer the best opportunity to distinguish taxa, but these studies have yet to be undertaken systematically.

19. Everted pharynx shape [NEXUS: everted pharynx form]

1. cylindrical (Fig. 1K).
2. a truncate cone, tapering, greatest width at margin of tentacular segment (Fig. 1J).

This character was introduced by Villalobos-Guerrero et al. (2021) using the term “frustrum-shaped” however we prefer simpler language (and frustrum can also refer to a truncate pyramid).

20. Maxillary ring of pharynx [NEXUS: maxillary ring of pharynx]

1. divided into discrete Areas (Fig. 1O, P).
2. undivided.

Pharyngeal papillae and paragnaths – characters 21–82 (Fig. 2A–G)

21. Maxillary ring of pharynx with papillae [NEXUS: maxillary ring papillae]

1. present.
2. absent.

22. Maxillary ring of pharynx with papillae [NEXUS: maxillary papillae arrangement]

1. solitary.
2. in tufts.

23. Maxillary ring of pharynx with papillae number

A count of the total number of papillae on the maxillary ring helps to discriminate taxa and is practical even when the arrangement in discrete Areas is unclear, as is often the case in Gymnonereidinae.

24. Undivided maxillary ring – total number of paragnaths present

Micronereis is the only nereidid genus with paragnaths present on an undivided maxillary ring. In this genus the pharynx is not fully eversible and specimens are small – the number of paragnaths present can only be recorded as a single number, if it can be determined at all.

25. Maxillary ring paragnaths [NEXUS: maxillary ring paragnaths]

1. present.
2. absent.

26. Maxillary ring of pharynx with P-bar paragnaths (Fig. 2A) [NEXUS: maxillary ring Pbars]

1. present, usually in regular comb-like rows.
2. absent.

27. Area I conical paragnaths (Fig. 2B) [NEXUS: Area I conical paragnaths]

1. present.
2. absent.

28. Area I conical paragnaths: number
29. Area II conical paragnaths [NEXUS: Area II conical paragnaths]

   1. present.
   2. absent.

30. Area II conical paragnaths: number
31. Area II rod-like paragnaths (Fig. 2C) [NEXUS: Area II rodlike paragnaths]

   1. present.
   2. absent.

32. Area II rod-like paragnaths: number
33. Area III conical paragnaths [NEXUS: Area III conical paragnaths]

   1. present.
   2. absent.

34. Area III conical paragnaths: number
35. Area III conical paragnaths: isolated lateral groups [NEXUS: Area III lateral groups]

   1. present.
   2. absent.

In many taxa Area III paragnaths include a few paragnaths positioned as distinct groups on each side of the main group.

36. Area III rod-like paragnaths [NEXUS: Area III rodlike paragnaths]

   1. present.
   2. absent.

37. Area III rod-like paragnaths: number
38. Area IV paragnaths [NEXUS: Area IV paragnaths]

   1. present.
   2. absent.

39. Area IV conical paragnaths [NEXUS: Area IV conical paragnaths]

   1. present.
   2. absent.

40. Area IV conical paragnaths: number
41. Area IV smooth bar-like paragnaths (Fig. 2D) [NEXUS: Area IV smooth bars]

   1. present.
   2. absent.

These are the smooth bar paragnaths of Bakken et al. (2009) and are not formed by fusion of separate conical paragnaths but are apparently present throughout development in the form of smooth bars in all those taxa in which they occur. When they occur on Area IV, cones are also usually present (sometimes lacking, see Tosuji et al. 2019), as illustrated in Hutchings et al. (1991: fig. 3B; *Perinereis amblyodonta*) and Villalobos-Guerrero et al. (2022b: fig. 4B; *Neanthes capensis*).

Thus, bar-like paragnaths are distinct from "melted paragnaths" described and illustrated by Bakken et al. (2009: fig. 2c) which are formed by partial fusion of distinct paragnaths and occur most often in epitokes and are not considered to have taxonomic value. Glasby et al. (2011) clarified that the term "melted" should apply only to conical paragnaths mounted on a plate-like basement while Conde-Vela and Salazar-Vallejo (2015) introduced the term "merged paragnaths" for forms where a basement is not present. We have not used merged or melted paragnaths here since their intra-specific variability is incompletely understood.

42. Area IV smooth bar-like paragnaths: number

Paragnaths on Area IV are typically roughly conical in shape, though variations range from flattened domes of irregular shape to tooth-like paragnaths. In some taxa, particularly species of *Neanthes* and *Perinereis*, in addition to cones a separate patch of bar-shaped paragnaths occurs at the maxillary end of Area IV; these bars are counted separately.

43. Area IV rod-like paragnaths [NEXUS: Area IV rodlike paragnaths]

1. present.
2. absent.

44. Area IV rod-like paragnaths: number
45. Oral ring papillae [NEXUS: oral ring papillae]

1. present.
2. absent.

46. Oral ring papillae: number
47. Oral ring papillae arrangement [NEXUS: oral ring papillae arrangement]

1. solitary.
2. arranged in tufts.

48. Area V papillae [NEXUS: Area V papillae]

1. present.
2. absent.

49. Area V papillae: number

In *Ceratocephale* spp., Area V and VI contain up to three papillae in total; these are here interpreted as all occurring in Area V, with VI = 0,0.

50. Area VI papillae [NEXUS: Area VI papillae]

1. present.
2. absent.

51. Area VI papillae: number
52. Areas VII-VIII papillae [NEXUS: Areas VIIVIII papillae]

1. present.
2. absent.

53. Areas VII-VIII papillae: number
54. Areas VII-VIII papillae arranged [NEXUS: Areas VIIVIII papillae rows]

1. in a single row.
2. in a double row.

Where a double row of papillae is present, the 2nd (posterior) row may be hard to see unless the pharynx is completely everted.

55. Oral ring paragnaths [NEXUS: oral ring paragnaths]

1. present.
2. absent.

56. Oral ring paragnaths (discrete or continuous) [NEXUS: oral ring paragnaths arranged]

1. with Areas V, VI and VII-VIII discrete.
2. comprising a continuous ring dorsally and ventrally, discrete groups not recognisable.

57. Oral ring paragnaths on Areas V and VI (discrete or continuous) [NEXUS: Areas VVI paragnaths]

1. form discrete groups.
2. continuous, not recognisably distinct.

58. Oral ring pyramidal paragnaths (Fig. 2E) [NEXUS: oral ring pyramidal paragnaths]

1. present.
2. absent.

Pyramidal paragnaths have a quadrangular base and taper to a pointed apex (Bakken et al. 2009: 309).

59. Crown-shaped oral ring paragnaths (Fig. 2F) [NEXUS: oral ring crown paragnaths]

1. present.
2. absent.

60. Crown-shaped oral ring paragnaths: number
61. Area V conical paragnaths [NEXUS: Area V conical paragnaths]

1. present.
2. absent.

62. Area V conical paragnaths: number
63. Area V conical paragnaths arranged [NEXUS: Area V cones arranged]

1. in a triangle.
2. in a longitudinal line.
3. irregularly.

64. Area VI paragnaths [NEXUS: Area VI paragnaths]

1. present.
2. absent.

65. Area VI paragnaths arranged [NEXUS: Area VI paragnaths arranged]

1. in a roughly circular group.
2. in lines or arcs.

Area VI paragnaths are usually arranged in a circular or irregular compact group (sometimes of only one or two paragnaths). In some species of *Neanthes*, an alternative arrangement of cones occurs: a distinct line or arc.

66. Area VI conical paragnaths [NEXUS: Area VI conical paragnaths]

1. present.
2. absent.

67. Area VI conical paragnaths: number
68. Area VI smooth bars (Fig. 2D) [NEXUS: Area VI smooth bars]

1. present.
2. absent.

Tosuji et al. (2019) demonstrated that in some species of *Perinereis*, long smooth bars in Area VI may shorten in length with growth of the worm to the extent that Area VI paragnaths in mature forms show a mixture of short bars and cones, so care must be exercised in using this character.

69. Area VI smooth bars: number

70. Area VI shield-shaped bars (Fig. 2G) [NEXUS: Area VI shield-shaped bars]

1. present.
2. absent.

Shield-shaped bars are laterally compressed and have a pointed or rounded apex (Bakken et al. 2009: 311).

71. Area VI shield-shaped bars: number
72. Area VI rod-shaped paragnaths [NEXUS: Area VI rod paragnaths]

1. present.
2. absent.

73. Area VI rod-shaped paragnaths: number of rows
74. Areas VII-VIII paragnaths [NEXUS: Areas VIIVIII paragnaths]

1. present.
2. absent.

75. Areas VII-VIII conical paragnaths [NEXUS: Areas VIIVIII cone paragnaths]

1. present.
2. absent.

76. Areas VII-VIII conical paragnaths: number

Areas VII-VIII typically forms a continuous ventro-lateral band of paragnaths and is recorded as such. In a few taxa the Areas VII-VIII band of paragnaths is extended through the dorsal region and encircles the oral ring of the pharynx; in this case even though the band nominally extends through the dorsal Areas V and VI, they are indistinguishable and the count is recorded for Areas VII-VIII.

77. Areas VII-VIII conical paragnaths arranged [NEXUS: Areas VIIVIII cones arranged]

1. in isolated patches.
2. in one or more irregular lines forming a continuous band.

In a few nereidid species, e.g., *Cheilonereis peristomialis* Benham, 1916, the paragnaths on Areas VII-VIII are arranged in distinct isolated patches. In other nereidids the arrangement is an irregular but continuous band made up one or more rows deep.

78. Areas VII-VIII conical paragnaths (size distribution) [NEXUS: Areas VIIVIII cones sizes]

1. similar in size, or irregular mix of large and small paragnaths in a single band.
2. differentiated, with a separate band of minute paragnaths also present.

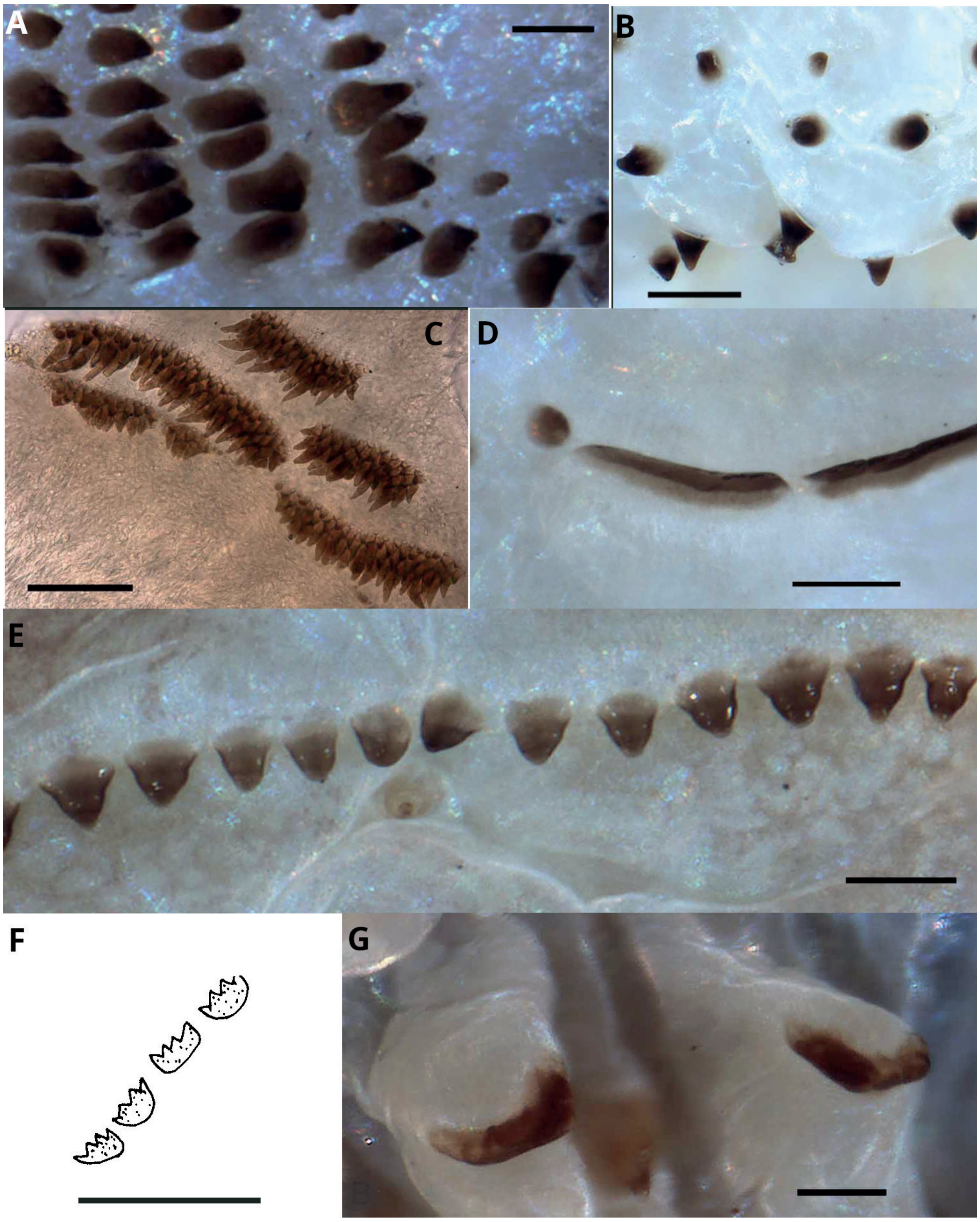

Figure 2. Paragnaths **A** P-bar paragnaths *Pseudonereis anomala* **B** conical paragnaths *Pseudonereis trimaculata* **C** rod-like paragnaths *Platynereis polyscalma* **D** smooth bar paragnaths *Perinereis vancaurica* **E** pyramidal paragnaths *Perinereis akuna* **F** crown paragnaths *Micronereis piccola* **G** shield-shaped paragnaths *Pseudonereis trimaculata*. Sources: **A–E, G** emended from Bakken et al. (2009: figs 2–5) **F** emended from Paxton (1983: fig. 4). Scale bars: 0.1 mm (**A–E, G**); 200 µm (**F**).

Typically the paragnaths on Areas VII-VIII comprise a variety of sizes irregularly arranged. However, in some taxa there is differentiation into an anterior band of paragnaths similar in size to elsewhere on the proboscis, and a separate band of minute paragnaths.

79. Areas VII-VIII P-bar paragnaths (Fig. 2A) [NEXUS: Areas VIIVIII Pbars]

1. present.
2. absent.

80. Areas VII-VIII P-bar paragnaths (interspersed/discrete) [NEXUS: Areas VIIVIII Pbar arrangement]

1. interspersed with conical paragnaths.
2. forming a separate band.

81. Areas VII-VIII rod-shaped paragnaths (Fig. 2C) [NEXUS: Areas VIIVIII rod paragnaths]

1. present.
2. absent.

82. Areas VII-VIII rod-shaped paragnaths: number of rows

Dorsal lamellae and parapodia – characters 83–128 (Fig. 3A–G)

83. Transverse dorsal lamellae (Fig. 3A) [NEXUS: transverse dorsal lamellae]

1. present.
2. absent.

84. Transverse dorsal lamellae, commencing chaetiger
85. Transverse dorsal lamellae, last present chaetiger
86. Transverse dorsal lamellae, mid-dorsal papilla [NEXUS: middorsal papilla]

1. present.
2. absent.

It has been shown by Blake (1985) and Hilbig (1997) (for *Ceratocephale loveni*) and by Hylleberg and Nateewathana (1988) (for *Ceratocephale andaman*) that presence/absence of mid-dorsal papilla is variable and likely to be related to size or sexual maturity. However, the description of *Ceratocephale papillata* de León-González & Góngora-Garza, 1992 is based on 155 specimens, all of which have mid-dorsal papilla. In other species of *Ceratocephale*, observations on mid-dorsal papillae should be interpreted with caution.

87. Transverse dorsal lamellae mid-dorsal papilla commencing chaetiger
88. Notopodium [NEXUS: notopodium development]

1. with at least one distinct ligule or lobe.
2. strongly reduced, without distinct lobes or ligules.

According to nautical wisdom, boats are defined as vessels able to be carried on ships. Parapodial lobes and ligules are distinguished according to a similar logic: lobes can be carried on ligules, but not vice versa. In general, ligules are larger and flatter than the smaller, conical lobes.

89. Dorsal notopodial ligule (Fig. 3E) [NEXUS: dorsal notopodial ligule]

1. present.
2. absent.

90. Dorsal notopodial ligule, first present [NEXUS: dorsal notopodial ligule first]

1. chaetiger 1.
2. chaetiger 3.
3. chaetiger 4.
4. chaetiger 5.

91. Dorsal notopodial ligule, length on anterior chaetigers [NEXUS: dorsal notopodial ligule anterior]

1. markedly elongate.
2. not markedly elongate.
3. markedly reduced.

92. Dorsal notopodial ligule, length on posterior chaetigers [NEXUS: dorsal notopodial ligule posterior]

1. markedly elongate (Fig. 3D).
2. not markedly elongate.

93. Dorsal notopodial ligule, breadth on posterior chaetigers [NEXUS: dorsal notopodial ligule posterior width]

1. markedly broader (Fig. 3G).
2. not markedly broader.

94. Dorsal notopodial ligule, reduction on posterior chaetigers [NEXUS: dorsal notopodial ligule posterior size]

1. absent (Fig. 3B).
2. markedly reduced.
3. not markedly reduced (Fig. 3F).

95. Dorsal notopodial ligule (divided into branchiae or not) [NEXUS: dorsal notopodial branchiae]

1. divided into numerous branchial filaments (Fig. 3H).
2. not divided into numerous branchial filaments.

Only in *Dendronereides* is the dorsal notopodial ligule divided into numerous branchial filaments. The branchial structures of *Dendronereides* and *Dendronereis* are therefore not homologous.

96. Prechaetal notopodial lobe (Fig. 3B, F) [NEXUS: prechaetal notopodial lobe]

1. present.
2. absent.

The prechaetal notopodial lobe is here defined as a digitiform process that is anterior to the acicular notopodial lobe and is not supported by the notopodial acicula (see character 100 Notopodial acicular process).

97. Prechaetal notopodial lobe, development [NEXUS: prechaetal notopodial lobe size]

1. smaller than dorsal notopodial ligule on anterior chaetigers, usually reduced or absent posteriorly.
2. approximately equal to length of dorsal notopodial ligule at least on anterior chaetigers (thus notopodium of three similar sized ligules/lobes).

98. Prechaetal notopodial lobe distribution [NEXUS: prechaetal noto lobe location]

1. present on all chaetigers (may be reduced in size on posterior chaetigers).
2. restricted to a limited number of anterior chaetigers.

99. Prechaetal notopodial lobe, reducing in size posteriorly, last present at approx. chaetiger
100. Notopodial acicular process (Fig. 3E open arrow) [NEXUS: notopodial acicular process]

1. present.
2. absent.

The notopodial acicular process, if present, is a small digitiform process formed around the tip of the acicula and is located between the acicular and ventral notopodial ligules (see character 97 Prechaetal notopodial lobe development).

101. Notopodial acicular process reducing in size posteriorly, last present on chaetiger
102. Notopodial acicular ligule (Fig. 3E–G) [NEXUS: acicular notopodial ligule]

1. present.
2. absent.

The acicular notopodial ligule is here considered to be that fleshy ligule ventral to the acicula in the notopodium. It is present in Nereidinae, but absent in *Ceratocephale*, *Gymnonereis*, *Micronereis* and *Stenoninereis*. Males of some species of *Micronereis* have a process on the ventral side of the notopodial acicular lobe; this dimorphic character is here considered not homologous with the ventral notopodial ligule of most nereidids.

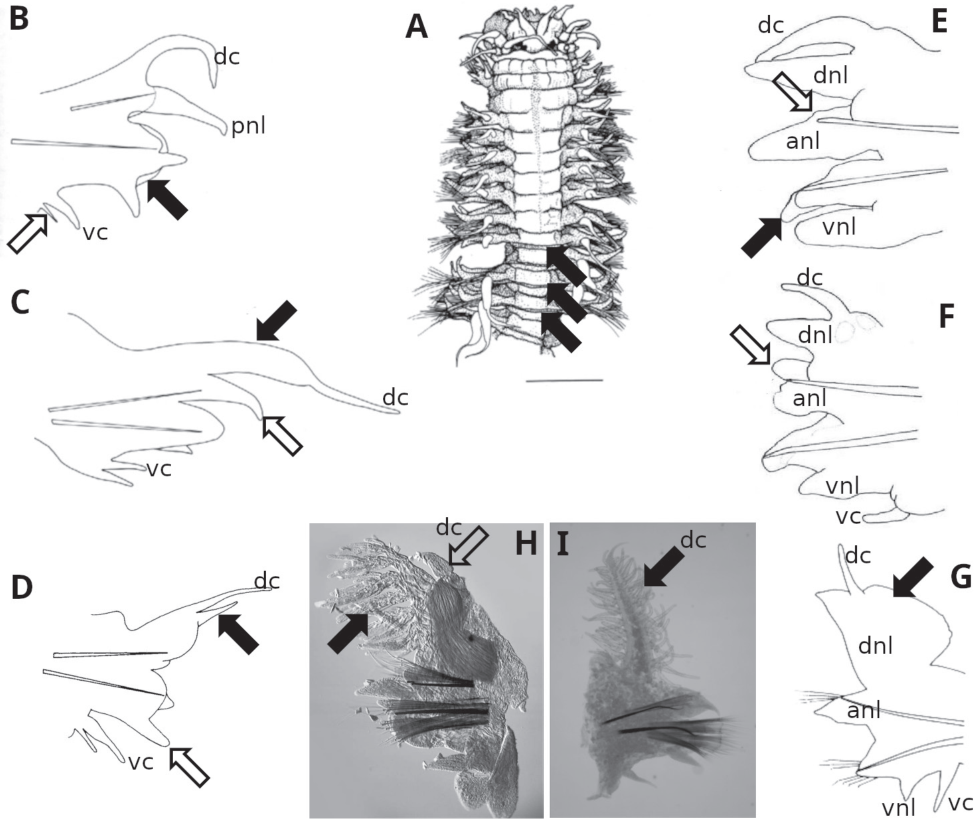

Figure 3. Parapodia **A** transverse dorsal lamellae (filled arrows) *Ceratocephale setosa* **B** flattened post-chaetal neuropodial lobe (filled arrow), accessory ventral cirrus (open arrow) anterior parapodium anterior view *Ceratocephale setosa* **C** cirrophore of dorsal cirrus enlarged and vascularised (filled arrow), acicular notopodial ligule present (open arrow) posterior parapodium anterior view *Ceratocephale setosa* **D** dorsal notopodial ligule (= accessory dorsal cirrus of some authors) (filled arrow) ventral neuropodial ligule (open arrow) *Gymnonereis minyami* chaetiger 34 anterior view **E** notopodial acicular process (open arrow) digitiform neuropodial postchaetal lobe (filled arrow) *Neanthes tasmani* chaetiger 30 anterior view (ventral cirrus missing) **F** notopodial prechaetal lobe (open arrow) digitiform neuropodial postchaetal lobe (filled arrow) *Neanthes tasmani* chaetiger 30 anterior view **G** dorsal notopodial ligule markedly broader on posterior chaetigers (filled arrow) chaetiger 78 *Alitta succinea* USNM 27799 **H** dorsal notopodial ligule divided into branchiae (filled arrow) dorsal cirrus (open arrow) *Dendronereides heteropoda* chaetiger 19 anterior view **I** dorsal cirrus divided into branchial filaments (filled arrow) *Dendronereis* sp chaetiger 14 anterior view. Sources: **A–D** Hutchings and Reid (1990) **E, F** modified after Bakken (2002) **G** R. Wilson drawing **H, I** C. Glasby photographs. Abbreviations: anl, acicular notopodial ligule; dc, dorsal cirrus; dnl, dorsal notopodial ligule; pnl, prechaetal notopodial ligule; vnl, ventral neuropodial ligule; vc, ventral cirrus. Not to scale; maximum body width excluding parapodia of 3A specimen ~ 1.2 mm; for remaining figures acicula lengths in the range 0.1–0.4 mm.

103. Acicular notopodial ligule development [NEXUS: acicular notopodial ligule form]

1. similar to or shorter than neuropodial acicular ligule.
2. prolonged, distinctly longer than neuropodial acicular ligule.
3. reduced, much shorter than neuropodial acicular ligule.

104. Dorsal cirrus (divided into branchiae or not) [NEXUS: dorsal cirrus branchiae]

1. divided into numerous branchial filaments (Fig. 3I).
2. not divided into numerous branchial filaments.

Only in *Dendronereis* does the dorsal cirrus form numerous branchial filaments. The branchial structures of *Dendronereides* and *Dendronereis* are therefore not homologous.

105. Dorsal cirrus (Fig. 3B, F) length on chaetiger 10–20 relative to length of acicular notopodial ligule
106. Dorsal cirrus: sub-terminally attached to dorsal notopodial ligule on posterior chaetigers, or not [NEXUS: dorsal cirrus subterminal]

1. sub-terminally attached to dorsal margin of dorsal notopodial ligule on posterior chaetigers (Fig. 3G).
2. not sub-terminally attached to dorsal notopodial ligule on posterior chaetigers.

107. Dorsal cirrus terminally attached to dorsal notopodial ligule on posterior chaetigers, or not [NEXUS: dorsal cirrus terminal]

1. terminally attached to dorsal notopodial ligule on posterior chaetigers.
2. not terminally attached to dorsal notopodial ligule on posterior chaetigers.

108. Dorsal cirrus terminally attached, or not [NEXUS: dorsal cirrus terminal all]

1. terminally attached throughout, so that dorsal notopodial ligule has appearance of a cirrophore for the dorsal cirrus.
2. not terminally attached throughout all chaetigers.

109. Dorsal cirrus (with/without cirrophore) [NEXUS: dorsal cirrophore]

1. simple, lacking basal cirrophore (Fig. 3C, filled arrow).
2. arising from basal cirrophore.

110. Cirrophore of dorsal cirrus length [NEXUS: dorsal cirrophore development]

1. short, at most as long as ventral notopodial ligule.
2. much longer than ventral notopodial ligule (Fig. 3D).

111. Cirrophore of dorsal cirrus enlargement [NEXUS: dorsal cirrophore vascular]

1. enlarged and vascularised (Fig. 3C, filled arrow).
2. not enlarged and vascularised.

112. Cirrophore of dorsal cirrus (expanded and leaflike, or cylindrical) [NEXUS: dorsal cirrophore expanded]

1. expanded and leaflike (Fig. 3C, filled arrow).
2. cylindrical throughout.

113. Cirrophore of dorsal cirrus expanded commencing approx. chaetiger

114. Neuropodial prechaetal lobe [NEXUS: neuropodial prechaetal lobe]

1. present.
2. absent.

Terminology after Hylleberg and Nateewathana (1988); characteristically present in the gymnonereids *Ceratocephale* and *Gymnonereis*. A structure of the same name is described as being present in descriptions (mostly prior to 1988), for example in some species of *Ceratonereis* but we contend that these are misinterpretations.

115. Neuropodial prechaetal lobe present on chaetigers
116. Neuropodial prechaetal lobe development [NEXUS: neuropodial prechaetal lobe form]

1. projecting beyond postchaetal lobe (at least in anterior chaetigers).
2. not projecting beyond the postchaetal lobe.

117. Neuropodial postchaetal lobe (Fig. 3E, filled arrow) [NEXUS: neuropodial postchaetal lobe]

1. present.
2. absent.

118. Neuropodial postchaetal lobe [NEXUS: neuropodial postchaetal lobe length]

1. projecting beyond end of the acicular ligule (Fig. 3E, filled arrow).
2. not projecting beyond end of the acicular ligule.

119. Neuropodial postchaetal lobe distribution [NEXUS: neuropodial postchaetal lobe distribution]

1. present throughout all chaetigers.
2. restricted to anterior chaetigers.

120. Neuropodial postchaetal lobe form [NEXUS: neuropodial postchaetal lobe form]

1. digitiform (Fig. 3E filled arrow).
2. flattened.

121. Neuropodial postchaetal lobe reducing posteriorly, last present on chaetigers
122. Ventral neuropodial ligule of anterior chaetigers [NEXUS: ventral neuropodial ligule anterior]

1. present (Fig. 3E).
2. absent.

123. Ventral neuropodial ligule of anterior chaetigers development [NEXUS: ventral neuropodial ligule anterior length]

1. approx. as long as acicular neuropodial ligule (Fig. 3E).
2. short, up to half length of acicular neuropodial ligule.

124. Ventral neuropodial ligule on posterior chaetigers [NEXUS: ventral neuropodial ligule posterior]

1. present.
2. absent.

125. Ventral neuropodial ligule on posterior chaetigers development [NEXUS: ventral neuropodial ligule posterior length]

1. similar to length of acicular neuropodial ligule.
2. longer than acicular neuropodial ligule.
3. short, up to half length of acicular neuropodial ligule (Fig. 3G).

126. Accessory ventral cirrus (Fig. 3B, open arrow) [NEXUS: accessory ventral cirrus]

1. present (i.e., double ventral cirri).
2. absent.

127. Accessory ventral cirrus commencing chaetiger
128. Relative length of paired ventral cirri [NEXUS: accessory ventral cirri length]

1. superior ventral cirrus of chaetigers 10–20 longer than inferior cirrus (Fig. 3B, D).
2. superior ventral cirrus of chaetigers 10–20 and inferior cirrus similar in length (Fig. 3C).
3. superior ventral cirrus of chaetigers 10–20 shorter than inferior cirrus.

In most *Ceratocephale* the superior cirrus is always the longer of the pair, especially on the first few chaetigers. However, in at least one species, *Ceratocephale papillata*, the superior cirrus is shorter than the inferior cirrus on anterior-most 10–20 chaetigers.

Aciculae and chaetae – characters 129–178 (Fig. 4A–Q)

129. Notoaciculae on chaetigers 1 and 2 [NEXUS: notoaciculae chaetigers 1 2]

1. present.
2. absent.

Presence of notoaciculae in chaetigers 1 and 2 is difficult to observe and failure to mention this character in published descriptions cannot be taken as evidence of absence. It is necessary to manipulate the parapodia with transmitted light, or, preferably in small specimens, to remove and mount parapodia on slides. In *Ceratonereis mirabilis* and related species, notoaciculae of chaetigers 1 and 2 are present, but are short and translucent even though those of subsequent chaetigers are dark and extend to the tip of the acicular ligule. *Namalycastis* and *Namanereis* have notoacicula in chaetigers 1 and 2, although like notoaciculae in remaining chaetigers, they sit just above the neuroaciculae in the upper part of the neuropodium.

130. Notochaetae of chaetigers 3 and 4 [NEXUS: notochaetae chaetigers 3 4]

1. present.
2. absent.

131. Notochaetae: heterogomph spinigers [NEXUS: notochaetae heterogomph spinigers]

1. present.
2. absent.

Chaetal shaft with heterogomph articulation is illustrated in Fig. 4B. Equivalent to long-bossed heterogomph sensu Conde-Vela (2021); see character 133 Notochaetae: sesquigomph spinigers. The chaetal shaft boss is the structure indicated with a filled arrow on Fig. 4B, C, L.

132. Notochaetae: homogomph spinigers [NEXUS: notochaetae homogomph spinigers]

1. present.
2. absent.

Chaetal shaft with homogomph articulation is illustrated in Fig. 4A. Equivalent to short-bossed heterogomph sensu Conde-Vela (2021).

133. Notochaetae: sesquigomph spinigers [NEXUS: notochaetae sesquigomph spinigers]

1. present.
2. absent.

Chaetal shaft with sesquigomph articulation is illustrated in Fig. 4C. Despite the advance in quantifying chaetal articulation by Conde-Vela (2021) we retain the terms homogomph/ heterogomph/ sesquigomph due to their near-universal usage in the literature over the near-equivalents proposed by Conde-Vela (2021). It would also be desirable to compare inter- and intra-specific variation between verified Nereididae species before adopting new terms and a revised assessment of their taxonomic significance.

134. Notochaetae: homogomph falcigers (Fig. 4K–Q) [NEXUS: notochaetae homogomph falcigers]

1. present.
2. absent.

135. Notochaetae: homogomph falcigers with terminal tendon (Fig. 4K, filled arrow) [NEXUS: notochaetae homogomph falcigers tendon]

1. present.
2. absent.

136. Notochaetae: homogomph falcigers first present at chaetiger
137. Notochaetae: homogomph falcigers articulation [NEXUS: notochaetae homogomph falcigers articulation]

1. fused on some chaetigers (present as a simple chaeta).
2. with blade free throughout.

138. Notochaetae: homogomph falcigers with smooth blade (Fig. 4M) [NEXUS: notochaetae homogomph falcigers blade smooth]

1. present.
2. absent.

139. Notochaetae: homogomph falcigers with bidentate blade and large adjacent terminal and subterminal teeth (Fig. 4N) [NEXUS: notochaetae homogomph falcigers bidentate]

1. present.
2. absent.

140. Notochaetae: homogomph falcigers with bidentate blade and large widely-separated terminal and subterminal teeth (Fig. 4O) [NEXUS: notochaetae homogomph falcigers bidentate gap]

1. present.
2. absent.

141. Notochaetae: homogomph falcigers with multidentate blade with ≥ 2 large lateral teeth, first lateral tooth subequal to terminal tooth, subsequent teeth usually decreasing in size (Fig. 4P) [NEXUS: notochaetae homogomph falcigers multidentate large]

1. present.
2. absent.

142. Notochaetae: homogomph falcigers with multidentate blade with ≥ 2 small lateral teeth, first and subsequent lateral teeth much smaller than terminal tooth (Fig. 4Q) [NEXUS: notochaetae homogomph falcigers multidentate small]

1. present.
2. absent.

143. Notochaetae: sesquigomph falcigers (Fig. 4L) [NEXUS: notochaetae sesquigomph falcigers]

1. present.
2. absent.

144. Notochaetae: sesquigomph falcigers from chaetiger
145. Notochaetae: sesquigomph falcigers blade form [NEXUS: notochaetae sesquigomph falcigers bifid]

1. distally bifid (Fig. 4K, L open arrows).
2. with a single distal tooth/.

146. Neurochaetae dorsal fascicle: heterogomph spinigers [NEXUS: neurochaetae dorsal fascicle heterogomph spinigers]

1. present.
2. absent.

147. Neurochaetae dorsal fascicle: homogomph spinigers [NEXUS: neurochaetae dorsal fascicle homogomph spinigers]

1. present.
2. absent.

148. Neurochaetae dorsal fascicle: sesquigomph spinigers [NEXUS: neurochaetae dorsal fascicle sesquigomph spinigers]

1. present.
2. absent.

149. Neurochaetae dorsal fascicle: sesquigomph falcigers [NEXUS: neurochaetae dorsal fascicle sesquigomph falcigers]

1. present.
2. absent.

150. Neurochaetae dorsal fascicle: sesquigomph falcigers blades [NEXUS: neurochaetae dorsal fascicle sesquigomph falcigers smooth]

1. serrated.
2. smooth.

151. Neurochaetae dorsal fascicle: heterogomph falcigers in anterior chaetigers [NEXUS: neurochaetae dorsal fascicle heterogomph falcigers anterior]

1. present.
2. absent.

152. Neurochaetae dorsal fascicle: heterogomph falcigers on posterior chaetigers [NEXUS: neurochaetae dorsal fascicle heterogomph falcigers posterior]

1. present.
2. absent.

153. Neurochaetae dorsal fascicle: heterogomph falcigers blades [NEXUS: neurochaetae dorsal fascicle heterogomph falcigers smooth]

1. smooth/
2. serrated/

154. Neurochaetae dorsal fascicle: heterogomph falcigers blades with teeth [NEXUS: neurochaetae dorsal fascicle heterogomph falcigers teeth]

1. only slightly longer proximally than distally.
2. much longer proximally than distally.

155. Neurochaetae dorsal fascicle: heterogomph falcigers blades with number of teeth
156. Neurochaetae dorsal fascicle: simple chaetae (fused falcigers) (Fig. 4I, J) [NEXUS: neurochaetae dorsal fascicle falcigers fused]

1. present.
2. absent.

157. Neurochaetae dorsal fascicle: simple chaetae (fused falcigers) present from chaetiger
158. Neurochaetae dorsal fascicle: homogomph falcigers in anterior chaetigers [NEXUS: neurochaetae dorsal fascicle homogomph falcigers anterior]

1. present.
2. absent.

159. Neurochaetae dorsal fascicle: homogomph falcigers on posterior chaetigers [NEXUS: neurochaetae dorsal fascicle homogomph falcigers posterior]

1. present.
2. absent.

160. Neurochaetae ventral fascicle: sesquigomph falcigers [NEXUS: neurochaetae ventral fascicle sesquigomph falcigers]

1. present.
2. absent.

161. Neurochaetae ventral fascicle: sesquigomph falcigers blade [NEXUS: neurochaetae ventral fascicle sesquigomph falcigers bifid]

1. distally bifid.
2. with a single distal tooth.

162. Neurochaetae ventral fascicle: heterogomph spinigers [NEXUS: neurochaetae ventral fascicle heterogomph spinigers]

1. present.
2. absent.

163. Neurochaetae ventral fascicle: heterogomph spinigers in anterior chaetigers with blades [NEXUS: neurochaetae ventral fascicle heterogomph spinigers anterior serrated]

1. evenly serrated throughout.
2. coarsely serrated proximally.

164. Neurochaetae ventral fascicle: heterogomph spinigers on posterior chaetigers with blades [NEXUS: neurochaetae ventral fascicle heterogomph spinigers posterior serrated] /

1. finely serrated proximally.
2. coarsely serrated proximally.

165. Neurochaetae ventral fascicle: homogomph spinigers [NEXUS: neurochaetae ventral fascicle homogomph spinigers]

1. present.
2. absent.

166. Neurochaetae ventral fascicle: sesquigomph spinigers [NEXUS: neurochaetae ventral fascicle sesquigomph spinigers]

1. present.
2. absent.

167. Neurochaetae ventral fascicle: heterogomph falcigers [NEXUS: neurochaetae ventral fascicle heterogomph falcigers]

1. present.
2. absent.

168. Neurochaetae ventral fascicle: heterogomph falcigers blade [NEXUS: neurochaetae ventral fascicle heterogomph falcigers bowed]

1. tapering, with straight margin (Fig. 4G).
2. bowed, with convex margin (Fig. 4H).

This character was introduced by Villalobos-Guerrero et al. (2022a: fig. 1e, f) and is valuable for distinguishing *Composetia* and similar taxa. Other Nereididae, for example many species illustrated in Pettibone (1971) appear intermediate between bowed and straight-bladed forms or appear to be variable depending on which chaetiger is examined and are difficult to score.

169. Neurochaetae ventral fascicle: anterior chaetigers heterogomph falcigers with long blades (Fig. 4D) [NEXUS: neurochaetae ventral fascicle heterogomph falcigers anterior long]

1. present.
2. absent.

Definitions of blade length of falcigers were introduced by Bakken and Wilson (2005) depending on length of the free margin of the blade relative to the part within the articulation (Fig. 4D–F) but has not been widely adopted. Here we use simpler terms; "long blades" is equivalent to "Type 0" of Bakken and Wilson (2005).

170. Neurochaetae ventral fascicle: anterior chaetigers heterogomph falcigers with extra-long blades (Fig. 4E) [NEXUS: neurochaetae ventral fascicle heterogomph falcigers anterior xlong]

1. present.
2. absent.

The term "extra-long blades" is equivalent to "Type 1" of Bakken and Wilson (2005).

171. Neurochaetae ventral fascicle: anterior chaetigers heterogomph falcigers with short blades (Fig. 4F) [NEXUS: neurochaetae ventral fascicle heterogomph falcigers anterior short]

1. present.
2. absent.

The term "short blades" is equivalent to "Type 2" of Bakken and Wilson (2005).

172. Neurochaetae ventral fascicle: posterior chaetigers heterogomph falcigers with long blades [NEXUS: neurochaetae ventral fascicle heterogomph falcigers posterior long]

1. present.
2. absent.

173. Neurochaetae ventral fascicle: posterior chaetigers heterogomph falcigers with extra-long blades [NEXUS: neurochaetae ventral fascicle heterogomph falcigers posterior xlong]

1. present.
2. absent.

174. Neurochaetae ventral fascicle: posterior chaetigers heterogomph falcigers with short blades [NEXUS: neurochaetae ventral fascicle heterogomph falcigers posterior short]

1. present.
2. absent.

175. Neurochaetae ventral fascicle: heterogomph falcigers blade [NEXUS: neurochaetae ventral fascicle heterogomph falcigers tendon]

1. with recurved terminal tooth and distinct tendon.
2. lacking distinct tendon on terminal tooth.

176. Neurochaetae ventral fascicle: heterogomph falcigers blade [NEXUS: neurochaetae ventral fascicle heterogomph falcigers bifid]

1. terminally bifid.
2. with a single terminal tooth.

177. Neurochaetae ventral fascicle: homogomph falcigers in anterior chaetigers [NEXUS: neurochaetae ventral fascicle homogomph falcigers anterior]

1. present.
2. absent.

178. Neurochaetae ventral fascicle: homogomph falcigers on posterior chaetigers [NEXUS: neurochaetae ventral fascicle homogomph falcigers posterior]

1. present.
2. absent.

Pygidium and appendages – character 179

A trilobate pygidium is present in *Namanereis* while other Namanereidinae, and some *Nicon* species, have a bilobate pygidium. Other nereidids are commonly described as having a funnel-shaped pygidium, which may be crenulated or multi-incised (perhaps indicating specimens approaching epitoky). For the majority of Nereididae the form of the pygidium is unknown, often because specimens were incomplete posteriorly. Thus, we have not included a character describing the form of the pygidium.

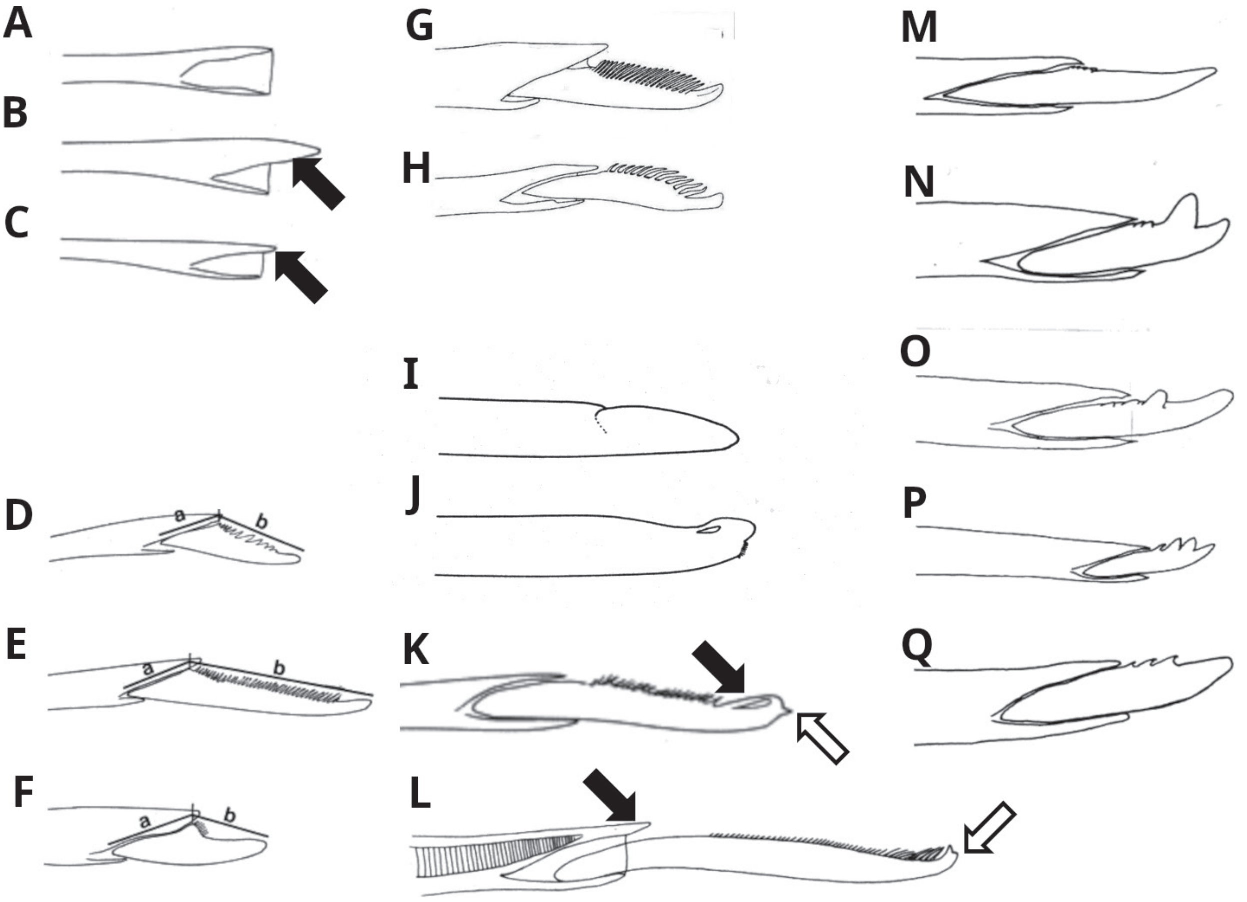

Figure 4. Chaetae **A** chaetal shaft homogomph articulation *Perinereis vallata* spiniger NMV F53971 **B** chaetal shaft heterogomph articulation *Perinereis vallata* falciger NMV F53971 (= long-bossed heterogomph sensu Conde-Vela (2021) filled arrow points to boss **C** chaetal shaft sesquigomph articulation *Ceratonereis mirabilis* (= short-bossed heterogomph sensu Conde-Vela (2021) filled arrow points to boss **D** heterogomph falcigers with long blades (a < b; = Type 0 of Bakken and Wilson (2005)) **E** heterogomph falcigers with extra-long blades (2× a < b; = Type 1 of Bakken and Wilson (2005)) **F** heterogomph falcigers with short blades (a ≥ b; = Type 2 of Bakken and Wilson (2005)) **G** heterogomph falciger blade with straight margin **H** heterogomph falciger blade with bowed margin **I** fused heterogomph falciger chaetiger 70 *Hediste diversicolor* complex AHF, Gilleleje, Denmark **J** fused falciger chaetiger 40 *Simplisetia aequisetis* NMV F53970 **K** homogomph falciger with terminal tendon (filled arrow) and with terminal secondary tooth (open arrow; = bifid) *Platynereis antipoda* notopodial falciger chaetiger 66 NMV F50116 **L** sesquigomph falciger with terminal tendon absent but bifid with secondary terminal tooth (open arrow) and boss (filled arrow) *Ceratonereis mirabilis* median chaetiger **M** homogomph falciger with smooth blade *Nereis cirriseta* chaetiger 74 **N** homogomph falcigers with bidentate blade and large adjacent terminal and subterminal teeth *Nereis bifida* chaetiger 71 **O** homogomph falciger with bidentate blade and large widely-separated terminal and subterminal teeth *Nereis triangularis* chaetiger 24 **P** homogomph falciger with multidentate blade with ≥ 2 large lateral teeth, first lateral tooth subequal to terminal tooth, subsequent teeth decreasing in size *Nereis denhamensis* anterior chaetiger **Q** homogomph falciger with multidentate blade with ≥ 2 small lateral teeth, first and subsequent lateral teeth much smaller than terminal tooth *Nereis apalie* chaetiger 74. Sources: **A–F, I–K, M–J** R. Wilson drawings **G, H** edited after Villalobos-Guerrero et al. (2021: fig. 1e, f) **L** after Perkins (1980: fig. 1d) **M–P** redrawn after Hutchings and Turvey (1982) **Q** after Wilson (1985: fig. 1E). Not to scale; maximum widths of chaetal shafts (at articulation) are in the range 0.01–0.03 mm.

179. Anal cirri form [NEXUS: anal cirri form]

1. cirriform or conical.
2. short, stout and appearing as an extension of the pygidium.
3. flattened, resembling posterior dorsal cirri.

Epitokal modifications and reproduction – characters 180–186

Although some epitokal features may be diagnostic at the genus level (Pamungkas and Glasby 2015), they are too poorly known across the family to be used in the present keys. Read (2007), Pamungkas and Glasby (2015) and Conde-Vela et al. (2018) demonstrated their utility in discriminating species across several genera. The seven characters presented below represent the basic characters for documenting epitokal reproductive forms.

180. Dorsal cirrophores of chaetigers 5–7 of epitokes [NEXUS: dorsal cirrophores chaetigers 5 7]

   1. unmodified.
   2. modified into flattened elytriform discs.
   3. modified into spherical globular structures.

181. Natatory region in males commences chaetiger
182. Natatory region in males comprises number of chaetigers
183. Natatory region in females commences chaetiger
184. Natatory region in females comprises number of chaetigers
185. Pygidium of male epitokes [NEXUS: pygidium of male epitokes]

   1. unmetamorphosed.
   2. with pygidial rosette.

Male epitokes may have the pygidium modified to form a pygidial rosette with multiple rows of short papillae. The unmodified form is illustrated by Villalobos-Guerrero and Bakken (2018: figs 6E, 17L) and the pygidial rosette is illustrated in Villalobos-Guerrero and Bakken (2018: fig. 14C, D).

186. Oocyte shape [NEXUS: oocyte form]

   1. spherical.
   2. ovoid.

Oocytes are typically spherical in Nereididae but in many *Namanereis* species they are ovoid.

Key to genera of Nereididae

It is easy to reach an incorrect identification using a linear (usually dichotomous) key – one always reaches a name, irrespective of errors that may have been made. Thus, it is wise to doubt, and some form of verification is highly desirable. Our recommendation is that after reaching a genus determination using the key below, the next step should be to compare the specimen at hand with the diagnosis of the genus that has been tentatively identified; if specimen and diagnosis match, the user can have increased confidence in the identification. See Methods above for further discussion. As discussed in the Introduction, several Nereididae genera are widely recognised as likely para- or polyphyletic groups. They are polymorphic for characters which distinguish other nereidid genera and therefore key out in more than one couplet.

1(0) Maxillary ring paragnaths present (Fig. 1B) **2**
– Maxillary ring paragnaths absent (Fig. 1A) **24**
2(1) Oral ring paragnaths present (Fig. 1J) **3**
– Oral ring paragnaths absent (Fig. 1A) **13**
3(2) Dorsal notopodial ligule markedly broader on posterior chaetigers (Fig. 3G) **4**
– Dorsal notopodial ligule not markedly broader on posterior chaetigers **7**
4(3) Palpophore barrel-shaped, approximately equal width from base to palpostyle (not overly large compared with palpostyle) (Fig. 1A); maxillary ring of pharynx with P-bar paragnaths present, usually in regular comb-like rows (Fig. 2A); Areas VI shield-shaped bars present (Fig. 2G) .... ***Pseudonereis* Kinberg, 1865**
– Palpophore massive subconical, flattened (palpostyle is minute by comparison) (Fig. 1B); maxillary ring of pharynx with P-bar paragnaths absent; Area VI shield-shaped bars absent **5**
5(4) Ventral peristomial flap present (Fig. 1L); Areas VII-VIII conical paragnaths differentiated, with a separate band of minute paragnaths also present; prechaetal notopodial lobe (Fig. 3B) restricted to a limited number of anterior chaetigers .... ***Cheilonereis* Benham, 1916**
– Ventral peristomial flap absent; Areas VII-VIII conical paragnaths similar in size, or irregular mix of large and small paragnaths in a single band; prechaetal notopodial lobe (Fig. 3B) present on all chaetigers **6**
6(5) Notochaetae sesquigomph (Fig. 4C) spinigers present; neurochaetae dorsal fascicle heterogomph (Fig. 4B) spinigers present; neurochaetae dorsal fascicle sesquigomph (Fig. 4C) spinigers present .... ***Nectoneanthes* Imajima, 1972**
– Notochaetae sesquigomph (Fig. 4C) spinigers absent; neurochaetae dorsal fascicle heterogomph (Fig. 4B) spinigers absent; neurochaetae dorsal fascicle sesquigomph (Fig. 4C) spinigers absent .... ***Alitta* Kinberg, 1865**
7(3) Antennae present; palpostyles present; maxillary ring of pharynx divided into discrete Areas (Fig. 1O, P) **8**
– Antennae absent palpostyles absent (palps undivided, minute) maxillary ring of pharynx undivided .... ***Micronereis* Claparède, 1863**
8(7) Notochaetae homogomph falcigers (fig. 4M–Q) present **9**
– Notochaetae homogomph falcigers absent **10**
9(8) Area II rod-like paragnaths present (Fig. 2C); Area III rod-like paragnaths present (Fig. 2C); Area IV conical paragnaths absent .... ***Platynereis* Kinberg, 1865**
– Area II rod-like paragnaths absent; Area III rod-like paragnaths absent; Area IV conical paragnaths present (Fig. 2B) .... ***Nereis* Linnaeus, 1758**
10(8) Oral ring papillae present; neurochaetae dorsal fascicle heterogomph falcigers in anterior chaetigers absent .... ***Imajimainereis* de León-González & Solis-Weiss, 2000**
– Oral ring papillae absent; neurochaetae dorsal fascicle heterogomph falcigers (Fig. 4D–F) in anterior chaetigers present **11**

11(10) Area VI smooth bars present .... ***Perinereis* Kinberg, 1865**

– Area VI smooth bars absent **12**

12(11) Neurochaetae dorsal fascicle simple chaetae (fused falcigers) (Fig. 4I) present .... ***Hediste* Malmgren, 1867**

– Neurochaetae dorsal fascicle simple chaetae (fused falcigers) absent .... ***Neanthes* Kinberg, 1865**

13(2) Oral ring papillae present **14**

– Oral ring papillae absent **16**

14(13) Ventral neuropodial ligule on posterior chaetigers similar to length of acicular neuropodial ligule (Fig. 3E) **15**

– Ventral neuropodial ligule on posterior chaetigers short, up to half length of acicular neuropodial ligule (Fig. 3F, G) .... ***Wuinereis* Khlebovich, 1996**

15(14) Neurochaetae dorsal fascicle homogomph (Fig. 4A) spinigers present .... ***Leonnates* Kinberg, 1865**

– Neurochaetae dorsal fascicle homogomph spinigers absent .... ***Paraleonnates* Khlebovich & Wu, 1962**

16(13) Notochaetae sesquigomph (Fig. 4C) spinigers present; neurochaetae dorsal fascicle homogomph (Fig. 4A) spinigers absent; prostomium anterior margin indented (Fig. 1G) **17**

– Notochaetae sesquigomph spinigers absent; neurochaetae dorsal fascicle homogomph (Fig. 4A) spinigers present; prostomium anterior margin entire (Fig. 1G) **18**

17(16) Area II rod-like paragnaths (Fig. 4C) present; notochaetae homogomph (Fig. 4A) falcigers present; Area I conical paragnaths present (Fig. 2B) .... ***Solomononereis* Gibbs, 1971**

– Area II rod-like paragnaths absent; notochaetae homogomph falcigers absent; Area I conical paragnaths absent .... ***Ceratonereis* Kinberg, 1865**

18(16) Notochaetae homogomph falcigers present .... ***Nereis* Linnaeus, 1758**

– Notochaetae homogomph falcigers absent **9**

19(18) Neurochaetae dorsal fascicle heterogomph falcigers in anterior chaetigers present (Fig. 4M–Q) **20**

– Neurochaetae dorsal fascicle heterogomph falcigers in anterior chaetigers absent **23**

20(19) Neurochaetae dorsal fascicle simple chaetae (fused falcigers) (Fig. 4J) present .... ***Simplisetia* Hartmann-Schröder, 1985**

– Neurochaetae dorsal fascicle simple chaetae (fused falcigers) absent **21**

21(20) Dorsal cirrus terminally attached to dorsal notopodial ligule (Fig. 3C) on posterior chaetigers; neuropodial prechaetal lobe (Fig. 3B) present; neuropodial postchaetal lobe flattened (Fig. 3B) .... ***Unanereis* Day, 1962**

– Dorsal cirrus not terminally attached to dorsal notopodial ligule on posterior chaetigers; neuropodial prechaetal lobe absent; neuropodial postchaetal lobe digitiform (Fig. 3F) **22**

22(21) Notoaciculae on chaetigers 1 and 2 present .... ***Potamonereis* Villalobos-Guerrero, Conde-Vela & Sato, 2022**

– Notoaciculae on chaetigers 1 and 2 absent .... ***Neanthes* Kinberg, 1865**

23(19) Palpophore barrel-shaped, approximately equal width from base to palpostyle (not overly large compared with palpostyle) (Fig. 1A); oesophageal caeca present (Fig. 1C); jaws with dentate cutting edge (Fig. 1H)............ ***Composetia* Hartmann-Schröder, 1985**
– Palpophore massive subconical, flattened (palpostyle is minute by comparison) (Fig. 1B); oesophageal caeca absent; jaws with smooth or slightly crenulate cutting edge (Fig. 1I)............ ***Parasetia* Villalobos-Guerrero, Conde-Vela & Sato, 2022**
24(1) Prostomium anterior margin entire (Fig. 1F)............**25**
– Prostomium anterior margin indented (Fig. 1G)............**41**
25(24) Maxillary ring of pharynx with papillae present............**26**
– Maxillary ring of pharynx with papillae absent............**29**
26(25) Neurochaetae ventral fascicle sesquigomph (Fig. 4C) spinigers present............**27**
– Neurochaetae ventral fascicle sesquigomph spinigers absent............**28**
27(26) Oral ring papillae present; tentacular cirri 3 pairs ventrum of anterior chaetigers smooth (Fig. 1N)............***Lycastonereis* Rao, 1981**
– Oral ring papillae absent; tentacular cirri 4 pairs; ventrum of anterior chaetigers with rows of tubercles extending to the base of each neuropodium (Fig. 1M)............***Australonereis* Hartman, 1954**
28(26) Area V papillae present; dorsal notopodial ligule divided into numerous branchial filaments (Fig. 3H); ventral neuropodial ligule of anterior chaetigers absent............***Dendronereides* Southern, 1921**
– Area V papillae absent dorsal notopodial ligule not divided into numerous branchial filaments; ventral neuropodial ligule (Fig. 3E–G) of anterior chaetigers present............***Olganereis* Hartmann-Schröder, 1977**
29(25) Dorsal notopodial ligule (Fig. 3E–G) commences chaetiger 1............***Leptonereis* Kinberg, 1865**
– Dorsal notopodial ligule (Fig. 3E–G) commences chaetiger 3............**30**
– Dorsal notopodial ligule (Fig. 3E–G) commences chaetiger 4............**38**
– Dorsal notopodial ligule (Fig. 3E–G) commences chaetiger 5............**40**
30(29) Notochaetae homogomph falcigers (Fig. 4M–Q) present............**31**
– Notochaetae homogomph falcigers absent............**33**
31(30) Oral ring paragnaths (Fig. 1O, P) present............***Eunereis* Malmgren, 1865**
– Oral ring paragnaths absent............**32**
32(31) Dorsal notopodial ligule (Fig. 3E) markedly reduced on posterior chaetigers; neurochaetae ventral fascicle heterogomph (Fig. 4B) spinigers absent............***Rullierinereis* Pettibone, 1971**
– Dorsal notopodial ligule (Fig. 3E) not markedly reduced on posterior chaetigers neurochaetae ventral fascicle heterogomph (Fig. 4B) spinigers present............***Kainonereis* Chamberlin, 1919**
33(30) Oral ring paragnaths (Fig. 1O, P) present............***Eunereis* Malmgren, 1865**
– Oral ring paragnaths (Fig. 1O, P) absent............**34**
34(33) Neuropodial postchaetal lobe (Fig. 3B, E) present............**35**
– Neuropodial postchaetal lobe absent............**36**
35(34) Oral ring papillae present............***Websterinereis* Pettibone, 1971**
– Oral ring papillae absent............***Nicon* Kinberg, 1865**

36(34) Dorsal notopodial ligule markedly broader on posterior chaetigers (Fig. 3G); dorsal cirrus terminally attached to dorsal notopodial ligule on posterior chaetigers (Fig. 3C); dorsal notopodial ligule markedly elongate on posterior chaetigers (Fig. 3C) .... ***Leptonereis* Kinberg, 1865**

– Dorsal notopodial ligule not markedly broader on posterior chaetigers dorsal cirrus not terminally attached to dorsal notopodial ligule on posterior chaetigers dorsal notopodial ligule not markedly elongate on posterior chaetigers **37**

37(36) Neurochaetae dorsal fascicle homogomph spinigers (Fig. 4A) present; neurochaetae ventral fascicle sesquigomph (Fig. 4C) spinigers present; palpophore surface with a single transverse groove (palpophores well developed) (Fig. 1A)... ***Micronereides* Day, 1963**

– Neurochaetae dorsal fascicle homogomph (Fig. 4A) spinigers absent; neurochaetae ventral fascicle sesquigomph spinigers (Fig. 4C) absent; palpophore surface without grooves or striae (palps short, compact) (Fig. 4D) ....***Namanereis* Chamberlin, 1919**

38(29) Dorsal notopodial ligule markedly broader on posterior chaetigers (Fig. 3G); dorsal cirrus terminally attached (Fig. 3G) to dorsal notopodial ligule on posterior chaetigers; neuropodial postchaetal lobe absent.. .... ***Leptonereis* Kinberg, 1865**

– Dorsal notopodial ligule not markedly broader on posterior chaetigers (Fig. 3E); dorsal cirrus not terminally attached to dorsal notopodial ligule on posterior chaetigers; neuropodial postchaetal lobe present **39**

39(38) Notochaetae homogomph falcigers (Fig. 4A) present; neurochaetae ventral fascicle falcigers blade bowed, with convex margin (Fig. 4H)...... .... ***Kainonereis* Chamberlin, 1919**

– Notochaetae homogomph falcigers absent; neurochaetae ventral fascicle falcigers blade tapering, with straight margin (Fig. 4G) .... ***Sinonereis* Wu & Sun, 1979**

40(29) Dorsal notopodial ligule markedly broader on posterior chaetigers (Fig. 3E); dorsal notopodial ligule not markedly reduced on posterior chaetigers; dorsal cirrus terminally attached to dorsal notopodial ligule on posterior chaetigers (Fig. 3C) .... ***Leptonereis* Kinberg, 1865**

– Dorsal notopodial ligule not markedly broader on posterior chaetigers; dorsal notopodial ligule markedly reduced on posterior chaetigers; dorsal cirrus not terminally attached to dorsal notopodial ligule on posterior chaetigers..***Typhlonereis* Hansen, 1879**

41(24) Dorsal cirrus simple, lacking basal cirrophore **42**

– Dorsal cirrus arising from basal cirrophore..**46**

42(41) Ventral neuropodial ligule on posterior chaetigers present (Fig. 3E–G) ...**43**

– Ventral neuropodial ligule on posterior chaetigers absent **45**

43(42) Maxillary ring of pharynx with papillae present; dorsal notopodial ligule not markedly reduced on posterior chaetigers (Fig. 3E, F); notoaciculae on chaetigers 1 and 2 absent..**44**

– Maxillary ring of pharynx with papillae absent; dorsal notopodial ligule markedly reduced on posterior chaetigers notoaciculae on chaetigers 1 and 2 present..***Kinberginereis* Pettibone, 1971**

44(43) Dorsal notopodial ligule commences chaetiger 1; dorsal notopodial ligule not markedly broader on posterior chaetigers (Fig. 3E, F); maxillary ring of pharynx with papillae in tufts ....***Laeonereis*** **Hartman, 1945**

– Dorsal notopodial ligule commences chaetiger 3; dorsal notopodial ligule markedly broader on posterior chaetigers (Fig. 3G); maxillary ring of pharynx with papillae solitary ....***Tylonereis*** **Fauvel, 1911**

45(42) Palpophore barrel-shaped, approximately equal width from base to palpostyle (not overly large compared with palpostyle) (Fig. 1A); notochaetae sesquigomph (Fig. 4C) spinigers present; neurochaetae dorsal fascicle homogomph spinigers absent .... ***Tylorrhynchus*** **Grube, 1866**

– Palpophore massive subconical, flattened (palpostyle is minute by comparison) (Fig. 1B); notochaetae sesquigomph spinigers absent; neurochaetae dorsal fascicle homogomph (Fig. 4A) spinigers present............... ....***Dendronereis*** **Peters, 1854**

46(41) Oral ring papillae present notoaciculae on chaetigers 1 and 2 absent; ventral neuropodial ligule of anterior chaetigers present (Fig. 3E–G)...........**47**

– Oral ring papillae absent notoaciculae on chaetigers 1 and 2 present; ventral neuropodial ligule of anterior chaetigers absent......................**49**

47(46) Dorsal notopodial ligule (Fig. 3E) present, commences chaetiger 1 .....**48**

– dorsal notopodial ligule absent.............***Ceratocephale*** **Malmgren, 1867**

48(47) Notochaetae sesquigomph (Fig. 4C) spinigers present; neurochaetae ventral fascicle sesquigomph (Fig. 4C) spinigers present; neurochaetae dorsal fascicle sesquigomph (Fig. 4C) spinigers present........................ ....***Gymnonereis*** **Horst, 1919**

– Notochaetae sesquigomph spinigers absent; neurochaetae ventral fascicle sesquigomph spinigers absent; neurochaetae dorsal fascicle sesquigomph spinigers absent........................... ***Tambalagamia*** **Pillai, 1961**

49(46) Neuropodial postchaetal lobe (Fig. 3B, F) present; antennae form cirriform (usually extending to or past palpophore) (Fig. 1G); palpophore surface with a single transverse groove (palpophores well developed) (Fig. 1A) .... ***Stenoninereis*** **Wesenberg-Lund, 1958**

– Neuropodial postchaetal lobe absent antennae form subconical (usually shorter than palpophore) (Fig. 1F); palpophore surface without grooves or striae (palps short, compact) (Fig. 1D).................................. ....***Namalycastis*** **Hartman, 1959**

Systematic account of Nereididae genera

Alitta Kinberg, 1865

Nereis (*Alitta*) auctt.

Type species. *Nereis virens* Sars, 1835.

WoRMS URL. https://www.marinespecies.org/polychaeta/aphia.php?p=taxdetails&id=234848.

Sources. Villalobos-Guerrero and Carrera-Parra (2015); Villalobos-Guerrero and Bakken (2018).

Diagnosis. Dorsal notopodial ligule markedly broader on posterior chaetigers; palpophore massive subconical, flattened (palpostyle is minute by comparison); ventral peristomial flap absent; notochaetae sesquigomph spinigers absent (minimal diagnosis; secondary diagnosis not attained).

Description. Palpophore massive subconical, flattened (palpostyle is minute by comparison). Palpophore surface with a single transverse groove (palpophores well developed) or with several oblique grooves or striae (palpophores well developed); palpostyles subconical. Prostomium anterior margin entire. Tentacular belt greater than length of chaetiger 1. Tentacular cirri cirrophores present.

Jaws with dentate cutting edge.

Maxillary ring of pharynx with papillae absent. Maxillary ring paragnaths present. Area I conical paragnaths present (absent occasionally in some specimens of *A. virens* species complex); II conical paragnaths present; III conical paragnaths present; III rod-like paragnaths absent; IV paragnaths present; IV conical paragnaths present; IV smooth bar-like paragnaths absent. Oral ring papillae absent. Oral ring paragnaths present; with Areas V, VI, and VII-VIII discrete. Oral ring pyramidal paragnaths absent, or present. Area V conical paragnaths present, or absent; arranged in a longitudinal line, or irregularly. Area VI paragnaths present; paragnaths arranged in a roughly circular group, or in lines or arcs; conical paragnaths present. Areas VII-VIII paragnaths present; conical paragnaths present; P-bar paragnaths absent, or present.

Dorsal notopodial ligule markedly elongate on posterior chaetigers, or not markedly elongate on posterior chaetigers; markedly broader on posterior chaetigers; not markedly reduced on posterior chaetigers. Prechaetal notopodial lobe present; smaller than dorsal notopodial ligule on anterior chaetigers, usually reduced or absent posteriorly, or approximately equal to length of dorsal notopodial ligule at least on anterior chaetigers (thus notopodium of three similar sized ligules/lobes); present on all chaetigers. Notopodial acicular process absent. Dorsal cirrus sub-terminally attached to dorsal margin of dorsal notopodial ligule on posterior chaetigers; not terminally attached to dorsal notopodial ligule on posterior chaetigers.

Neuropodial prechaetal lobe absent. Neuropodial postchaetal lobe present; projecting beyond end of the acicular ligule; present throughout all chaetigers; digitiform. Ventral neuropodial ligule of anterior chaetigers present. Ventral neuropodial ligule of anterior chaetigers approx. as long as acicular neuropodial ligule. Ventral neuropodial ligule on posterior chaetigers present. Ventral neuropodial ligule on posterior chaetigers similar to length of acicular neuropodial ligule, or short, up to half length of acicular neuropodial ligule.

Notoaciculae on chaetigers 1 and 2 present, or absent. Notochaetae of chaetigers 3 and 4 present. Notochaetae: homogomph spinigers present. Neurochaetae dorsal fascicle: heterogomph spinigers absent; homogomph spinigers present; dorsal fascicle heterogomph falcigers in anterior chaetigers present; on posterior chaetigers present, or absent. Neurochaetae ventral fascicle: heterogomph spinigers present; spinigers in anterior chaetigers with blades evenly serrated throughout; on posterior chaetigers with blades finely serrated proximally; heterogomph falcigers present; anterior chaetigers heterogomph falcigers with long blades absent; anterior chaetigers heterogomph falcigers with extra-long blades present; anterior chaetigers heterogomph falcigers with short blades absent; posterior chaetigers heterogomph falcigers with long blades absent; posterior chaetigers heterogomph falcigers with extra-long blades present; posterior chaetigers heterogomph falcigers with short blades absent; ventral fascicle heterogomph falcigers blade with recurved terminal tooth and distinct tendon, or lacking distinct tendon on terminal tooth; ventral fascicle heterogomph falcigers blade with a single terminal tooth.

Anal cirri form cirriform or conical.

Remarks. The modern concept of *Alitta* is due to Khlebovich (1996) but the generic description and the species included have been emended by Villalobos-Guerrero and Carrera-Parra (2015) and Villalobos-Guerrero and Bakken (2018); the description here is based on that of the latter two studies. *Alitta* now contains eight species all occurring in either the North Pacific or North Atlantic Oceans. *Alitta succinea* (Leuckart, 1847) has been reported as a supposed introduced species from numerous cosmopolitan localities but as summarised by Villalobos-Guerrero and Carrera-Parra (2015: 165–166) many of these represent misidentifications of related species.

There is no identification guide for all species of *Alitta* but the four species in the *A. virens* species complex can be identified using the keys to atokes and to epitokes in Villalobos-Guerrero and Bakken (2018).

***Australonereis* Hartman, 1954**

Type species. *Nereis* (*Leonnates*) *ehlersi* Augener, 1913.

WoRMS URL. https://www.marinespecies.org/polychaeta/aphia.php?p=taxdetails&id=324844.

Sources. Hutchings and Reid (1990).

Diagnosis. Ventrum of anterior chaetigers with rows of tubercles extending to the base of each neuropodium (minimal diagnosis). Dorsal notopodial ligule commences chaetiger 1; prostomium anterior margin entire; maxillary ring of pharynx with papillae present (secondary diagnosis).

Description. Palpophore barrel-shaped, approximately equal width from base to palpostyle (not overly large compared with palpostyle). Ventrum of anterior chaetigers with rows of tubercles extending to the base of each neuropodium.

Maxillary ring of pharynx with papillae present (sometimes with horny tips); solitary; 50–110 papillae in total. Maxillary ring paragnaths absent. Oral ring papillae absent. Oral ring paragnaths absent.

Dorsal notopodial ligule present; commences chaetiger 1; not markedly elongate on posterior chaetigers; not markedly broader on posterior chaetigers; not markedly reduced on posterior chaetigers. Prechaetal notopodial lobe present; smaller than dorsal notopodial ligule on anterior chaetigers, usually reduced or absent posteriorly; restricted to a limited number of anterior chaetigers. Notopodial acicular process absent. Dorsal cirrus not sub-terminally attached to dorsal notopodial ligule on posterior chaetigers; not terminally attached to dorsal notopodial ligule on posterior chaetigers; not terminally attached throughout all chaetigers.

Neuropodial prechaetal lobe absent. Neuropodial postchaetal lobe present; projecting beyond end of the acicular ligule; digitiform. Ventral neuropodial ligule of anterior chaetigers present.

Notoaciculae on chaetigers 1 and 2 absent. Notochaetae: homogomph spinigers present. Neurochaetae dorsal fascicle: heterogomph spinigers absent; homogomph spinigers present; sesquigomph spinigers present. Neurochaetae dorsal fascicle: sesquigomph falcigers present; blades serrated; heterogomph falcigers in anterior chaetigers absent; on posterior chaetigers absent. Neurochaetae ventral fascicle: sesquigomph falcigers present; heterogomph spinigers absent; homogomph spinigers absent; sesquigomph spinigers present; heterogomph falcigers absent.

Anal cirri form cirriform or conical.

Remarks. *Australonereis* is a monotypic genus. The single species *A. ehlersi* (Augener, 1913) occurs only in southern Australian estuaries where these large and often locally abundant worms are instantly recognisable by the conspicuous rows of tuberculae on the ventral surface; living specimens are also much more fragile than those belonging to other genera of Nereididae and readily fragment in the field.

***Ceratocephale* Malmgren, 1867**

Chaunorhychus Chamberlin, 1919.
Pisionura Hartman & Fauchald, 1971.

Type species. *Ceratocephale loveni* Malmgren, 1867.

WoRMS URL. https://www.marinespecies.org/polychaeta/aphia.php?p=taxdetails&id=129371.

Sources. Hylleberg and Nateewathana (1988); Hutchings and Reid (1990: table 9); Santos (2007).

Diagnosis. Transverse dorsal lamellae present; dorsal notopodial ligule absent (minimal diagnosis). Dorsal cirrus arising from basal cirrophore; dorsal notopodial ligule commences chaetiger 3 (secondary diagnosis).

Description. Palpophore barrel-shaped, approximately equal width from base to palpostyle (not overly large compared with palpostyle). Palpostyles subconical, or acutely conical. Eyes present, or absent. Prostomium anterior margin indented. Tentacular belt equal to or less than length of chaetiger 1.

Jaws with dentate cutting edge.

Maxillary ring of pharynx with papillae absent. Maxillary ring paragnaths absent. Oral ring papillae present. Oral ring papillae arrangement solitary. Area V three papillae present (close together); VI papillae present, or absent; VII-VIII seven papillae present, arranged in a single row. Oral ring paragnaths absent. In *Ceratocephale* spp., Areas V and VI contain up to three papillae in total; these are here interpreted as all occurring in Area V, with VI = 0,0.

Transverse dorsal lamellae present (in all species except *C. abyssorum*); commencing chaetiger 4–10.

Dorsal notopodial ligule absent. Prechaetal notopodial lobe present; present on all chaetigers. Notopodial acicular process absent. Dorsal cirrus arising from basal cirrophore; cirrophore of dorsal cirrus enlarged and vascularised; cirrophore of dorsal cirrus expanded and leaflike.

Neuropodial postchaetal lobe present; projecting beyond end of the acicular ligule; present throughout all chaetigers; digitiform. Ventral neuropodial ligule of anterior chaetigers present. Ventral neuropodial ligule of anterior chaetigers approx. as long as acicular neuropodial ligule, or short, up to half length of acicular neuropodial ligule. Ventral neuropodial ligule on posterior chaetigers present. Ventral neuropodial ligule on posterior chaetigers short, up to half length of acicular neuropodial ligule. Accessory ventral cirrus present; commencing chaetiger 1–3. Conspicuous neuropodial prechaetal ligule present.

Notoaciculae on chaetigers 1 and 2 absent. Notochaetae: homogomph spinigers present; sesquigomph spinigers present, or absent. Neurochaetae dorsal fascicle: heterogomph spinigers absent; homogomph spinigers present; sesquigomph spinigers present; heterogomph falcigers in anterior chaetigers absent; on posterior chaetigers absent. Neurochaetae ventral fascicle: heterogomph spinigers absent; homogomph spinigers present, or absent; heterogomph falcigers absent.

Anal cirri form cirriform or conical.

Remarks. The definition of *Ceratocephale* used here follows Santos (2007). Bakken et al. (2022) noted the possible synonymy of *Tambalagamia* Pillai, 1961 and suggested that a revision was required. Further evidence of morphological diversity of key characters also suggests that *Ceratocephale* as presently constituted may not be a natural group: according to Santos et al. (2005), in *Ceratocephale* the tentacular belt is shorter than the subsequent chaetigers however this is not so for all species: e.g. *Ceratocephale papillata* de León-González & Góngora-Garza, 1992, nor in *C. loveni* Malmgren, 1867 or *C. pacifica* (Hartman, 1960) based on Hilbig (1997); and *C. bansei* Khlebovich, 1966 may be the only species of *Ceratocephale* with papillae on Area VI of the pharynx.

Ceratocephale currently includes 12 accepted species recorded from all oceans except the Arctic Ocean and from intertidal to abyssal depths (Read and Fauchald 2023). There is no identification guide to all species although Hylleberg and Nateewathana (1988) have a key to the six species then known. Hutchings and Reid (1990) allow identification of the three Australian species currently described although we know of two additional undescribed Australian *Ceratocephale* species.

Ceratonereis Kinberg, 1865

Ceratonereis (*Ceratonereis*) auctt.

Type species. *Ceratonereis mirabilis* Kinberg, 1865.

WoRMS URL. https://www.marinespecies.org/polychaeta/aphia.php?p=taxdetails&id=129372.

Sources. Hartmann-Schröder (1985).

Diagnosis. Notochaetae: sesquigomph falcigers present; dorsal cirrus sub-terminally attached to dorsal margin of dorsal notopodial ligule on posterior chaetigers (minimal diagnosis). Neurochaetae dorsal fascicle: sesquigomph falcigers present; palpophore barrel-shaped, approximately equal width from base to palpostyle (not overly large compared with palpostyle) (secondary diagnosis).

Description. Palpophore barrel-shaped, approximately equal width from base to palpostyle (not overly large compared with palpostyle) (elongate). Palpophore surface with a single transverse groove (palpophores well developed). Prostomium anterior margin indented.

Oesophageal caeca absent.

Jaws with dentate cutting edge.

Maxillary ring of pharynx with papillae absent. Area I conical paragnaths absent; II conical paragnaths present; III conical paragnaths present; IV paragnaths present; IV conical paragnaths present. Oral ring papillae absent. Oral ring paragnaths absent.

Dorsal notopodial ligule not markedly elongate on posterior chaetigers; not markedly broader on posterior chaetigers; markedly reduced on posterior chaetigers, or not markedly reduced on posterior chaetigers. Prechaetal notopodial lobe absent. Notopodial acicular process absent. Dorsal cirrus sub-terminally attached to dorsal margin of dorsal notopodial ligule on posterior chaetigers; arising from basal cirrophore; cirrophore of dorsal cirrus short, at most as long as ventral notopodial ligule, or much longer than ventral notopodial ligule; cirrophore of dorsal cirrus not enlarged and vascularised; cirrophore of dorsal cirrus cylindrical throughout.

Neuropodial postchaetal lobe present; projecting beyond end of the acicular ligule; restricted to anterior chaetigers; digitiform or flattened. Ventral neuropodial ligule of anterior chaetigers present. Ventral neuropodial ligule of anterior chaetigers approx. as long as acicular neuropodial ligule, or short, up to half length of acicular neuropodial ligule. Ventral neuropodial ligule on posterior chaetigers present. Ventral neuropodial ligule on posterior chaetigers similar to length of acicular neuropodial ligule, or short, up to half length of acicular neuropodial ligule.

Notoaciculae on chaetigers 1 and 2 present. Notochaetae: homogomph spinigers absent; sesquigomph spinigers present; sesquigomph falcigers present; blade distally bifid, or with a single distal tooth. Neurochaetae dorsal fascicle: heterogomph spinigers absent; homogomph spinigers absent; sesquigomph spinigers present; sesquigomph falcigers present; heterogomph falcigers in anterior chaetigers present. Neurochaetae ventral fascicle: heterogomph spinigers present; homogomph spinigers absent; heterogomph falcigers present; anterior chaetigers heterogomph falcigers with short blades absent; heterogomph falcigers blade lacking distinct tendon on terminal tooth; heterogomph falcigers blade terminally bifid, or with a single terminal tooth.

Anal cirri form cirriform or conical.

Remarks. *Ceratonereis* as currently defined follows the concept of Perkins (1980) and Hartmann-Schröder (1985). Previously the genus ("*Ceratonereis* sensu lato") had included unrelated nereidid species with superficially similar paragnath configuration. Those disparate species (none of which have the indented prostomium characteristic of *Ceratonereis* sensu stricto) are now moved to genera *Composetia* Hartmann-Schröder (1985) and *Simplisetia* Hartmann-Schröder (1985). This restricted definition of *Ceratonereis* is probably monophyletic (Bakken and Wilson 2005) and comprises 43 species which are known from all oceans (Read and Fauchald 2023).

There is no identification guide to the species of *Ceratonereis* and many nominal species are poorly known and some still may belong to other genera. Distinguishing species relies heavily on differences in chaetae and in parapodial structures; pigmentation pattern in living specimens is often distinctive and would probably be most helpful.

Conde-Vela (2021) includes a key to American species of *Ceratonereis*. Glasby (2015) provides a key that includes four species of *Ceratonereis* known from tropical Australia.

Cheilonereis Benham, 1916

Type species. *Nereis cyclurus* Harrington, 1897.

WoRMS URL. https://www.marinespecies.org/polychaeta/aphia.php?p=taxdetails&id=156851.

Sources. Bakken et al. (2022).

Diagnosis. Ventral peristomial flap present (minimal diagnosis). Areas VII-VIII conical paragnaths differentiated, with a separate band of minute paragnaths also present; dorsal notopodial ligule markedly broader on posterior chaetigers (secondary diagnosis).

Description. Palpophore massive subconical, flattened (palpostyle is minute by comparison). Tentacular belt greater than length of chaetiger 1. Ventral peristomial flap present.

Oesophageal caeca present.

Jaws with dentate cutting edge.

Maxillary ring of pharynx with papillae absent. Maxillary ring paragnaths present. Area I conical paragnaths present; II conical paragnaths present; IV paragnaths present; IV conical paragnaths present. Oral ring papillae absent. Oral ring paragnaths present; with Areas V, VI and VII-VIII discrete; on Area V and VI form distinct groups. Area V conical paragnaths absent. Area VI paragnaths present; paragnaths arranged in a roughly circular group; conical paragnaths present; smooth bars absent. Areas VII-VIII paragnaths present; conical; arranged in isolated patches, or in one or more irregular lines forming a continuous band; conical paragnaths differentiated, with a separate band of minute paragnaths also present (present as patches in *C. peristomialis*).

Dorsal notopodial ligule markedly elongate on posterior chaetigers; markedly broader on posterior chaetigers; not markedly reduced on posterior chaetigers. Prechaetal notopodial lobe present; smaller than dorsal notopodial ligule on anterior chaetigers, usually reduced or absent posteriorly; restricted to a limited number of anterior chaetigers. Dorsal cirrus sub-terminally attached to dorsal margin of dorsal notopodial ligule on posterior chaetigers.

Neuropodial postchaetal lobe absent, or present; projecting beyond end of the acicular ligule; present throughout all chaetigers; flattened. Ventral neuropodial ligule of anterior chaetigers present. Ventral neuropodial ligule of anterior chaetigers approx. as long as acicular neuropodial ligule. Ventral neuropodial ligule on posterior chaetigers present. Ventral neuropodial ligule on posterior chaetigers similar to length of acicular neuropodial ligule.

Notoaciculae on chaetigers 1 and 2 absent. Notochaetae: homogomph spinigers present; homogomph falcigers present; homogomph falcigers with multidentate blade with two or more small lateral teeth, first and subsequent lateral teeth much smaller than terminal tooth present. Neurochaetae dorsal fascicle: heterogomph spinigers absent; homogomph spinigers present; heterogomph falcigers in anterior chaetigers present; on posterior chaetigers present; blades serrated. Neurochaetae ventral fascicle: heterogomph spinigers present; homogomph spinigers absent; heterogomph falcigers present; anterior chaetigers heterogomph falcigers with long blades absent; anterior chaetigers heterogomph falcigers with extra-long blades present; anterior chaetigers heterogomph falcigers with short blades absent; posterior chaetigers heterogomph falcigers with long blades present; posterior chaetigers heterogomph falcigers with extra-long blades absent; posterior chaetigers heterogomph falcigers with short blades absent; heterogomph falcigers blade lacking distinct tendon on terminal tooth.

Anal cirri form cirriform or conical.

Remarks. The genus *Cheilonereis* has two species, *C. cyclurus* (Harrington, 1897) from the NW Pacific and *C. peristomialis* Benham, 1916 from the SE Pacific; both species are commensals of hermit crabs. *Cheilonereis* species are characterised by the presence of a ventral collar or flap that partly covers the ventral paragnaths of the oral ring when the pharynx is extended (see photo by Dave Cowles, Walla Walla University: https://inverts.wallawalla.edu/Annelida/Nereidae/Cheilonereis_cyclurus_DLC2018-13.jpg also included as part of Wilson et al. (2023)); this structure is unknown in other Nereididae and it is plausible that the ventral flap is adaptive in some way for their commensal life style.

Composetia Hartmann-Schröder, 1985

Ceratonereis (*Composetia*) Hartmann-Schröder, 1985.

Type species. *Nereis costae* Grube, 1840.

WoRMS URL. https://www.marinespecies.org/polychaeta/aphia.php?p=taxdetails&id=324848.

Sources. Villalobos-Guerrero et al. (2022a).

Diagnosis. Neurochaetae ventral fascicle homogomph spinigers present; maxillary ring paragnaths present; oral ring paragnaths absent; Neurochaetae dorsal fascicle: heterogomph falcigers in anterior chaetigers absent; oesophageal caeca present (minimal diagnosis; secondary diagnosis not attained).

Description. Palpophore barrel-shaped, approximately equal width from base to palpostyle (not overly large compared with palpostyle). Palpophore surface with a single transverse groove (palpophores well developed). Prostomium longitudinal groove present; anterior region entire, sub-quadrangular, longitudinal groove present; prostomial posterior region subequal to or longer than anterior region. Tentacular belt greater than length of chaetiger 1.

Oesophageal caeca present.

Jaws with dentate cutting edge.

Maxillary ring of pharynx with papillae absent. Maxillary ring paragnaths present. Area I conical paragnaths present; II conical paragnaths present; III conical paragnaths present; IV paragnaths present; IV conical paragnaths present. Oral ring papillae absent. Oral ring paragnaths absent.

Dorsal notopodial ligule not markedly broader on posterior chaetigers; not markedly reduced on posterior chaetigers. Prechaetal notopodial lobe present; smaller than dorsal notopodial ligule on anterior chaetigers, usually reduced or absent posteriorly; present on all chaetigers, or restricted to a limited number of anterior chaetigers. Notopodial acicular process absent. Dorsal cirrus not sub-terminally attached to dorsal notopodial ligule on posterior chaetigers.

Neuropodial postchaetal lobe present; projecting beyond end of the acicular ligule; restricted to anterior chaetigers. Ventral neuropodial ligule of anterior chaetigers present. Ventral neuropodial ligule of anterior chaetigers approx. as long as acicular neuropodial ligule. Ventral neuropodial ligule on posterior chaetigers present. Ventral neuropodial ligule on posterior chaetigers similar to length of acicular neuropodial ligule.

Notoaciculae on chaetigers 1 and 2 absent. Notochaetae: homogomph spinigers present. Neurochaetae dorsal fascicle: heterogomph spinigers absent; homogomph spinigers present; heterogomph falcigers in anterior chaetigers absent; on posterior chaetigers absent. Neurochaetae ventral fascicle: heterogomph spinigers absent; homogomph spinigers present; heterogomph falcigers present; falcigers blade tapering, with straight margin; anterior chaetigers heterogomph falcigers with long blades absent; anterior chaetigers heterogomph falcigers with extra-long blades present; anterior chaetigers heterogomph falcigers with short blades absent; posterior chaetigers heterogomph falcigers with long blades absent; posterior chaetigers heterogomph falcigers with extra-long blades present; posterior chaetigers heterogomph falcigers with short blades absent; heterogomph falcigers blade lacking distinct tendon on terminal tooth; homogomph falcigers on posterior chaetigers present, or absent.

Anal cirri form cirriform or conical.

Remarks. The description here follows the revised concept of *Composetia* of Villalobos-Guerrero et al. (2022a) who removed several former species of *Composetia* sensu Hartmann-Schröder, 1985 to two new genera: *Parasetia* and *Potamonereis*. *Composetia* currently includes 11 species which collectively are widely distributed around the globe; however, many species have not yet been re-evaluated against the revised concept of Villalobos-Guerrero et al. (2022a) the genus remains as an assemblage of dissimilar species Villalobos-Guerrero et al. (2022a).

The only identification guide is the tabular comparisons of Villalobos-Guerrero et al. (2022a).

Dendronereides **Southern, 1921**

Type species. *Dendronereides heteropoda* Southern, 1921.

WoRMS URL. https://www.marinespecies.org/polychaeta/aphia.php?p=taxdetails&id=206894.

Sources. Southern (1921); Hutchings and Reid (1990).

Diagnosis. Dorsal notopodial ligule divided into numerous branchial filaments (minimal diagnosis).

Ventral neuropodial ligule of anterior chaetigers absent; maxillary ring of pharynx with papillae present; prostomium anterior margin entire (secondary diagnosis).

Description. Palpophore barrel-shaped, approximately equal width from base to palpostyle (not overly large compared with palpostyle). Palpophore surface with a single transverse groove (palpophores well developed).

Jaws with dentate cutting edge.

Maxillary ring of pharynx with papillae present; solitary. Maxillary ring paragnaths absent. Oral ring papillae present. Oral ring papillae arrangement solitary. Area V papillae present; VI papillae present; VII-VIII papillae present. Oral ring paragnaths absent.

Dorsal notopodial ligule present. Dorsal notopodial ligule divided into numerous branchial filaments. Dorsal cirrus not sub-terminally attached to dorsal notopodial ligule on posterior chaetigers; not terminally attached throughout all chaetigers.

Ventral neuropodial ligule of anterior chaetigers absent. Ventral neuropodial ligule on posterior chaetigers absent.

Notochaetae: homogomph spinigers present; sesquigomph spinigers present, or absent. Neurochaetae dorsal fascicle: heterogomph spinigers present, or absent; homogomph spinigers present; sesquigomph spinigers present, or absent; heterogomph falcigers in anterior chaetigers present, or absent; homogomph falcigers in anterior chaetigers present, or absent. Neurochaetae ventral fascicle: heterogomph spinigers present, or absent; homogomph spinigers present, or absent; heterogomph falcigers present, or absent; heterogomph falcigers blade lacking distinct tendon on terminal tooth; homogomph falcigers on posterior chaetigers present, or absent.

Remarks. *Dendronereides* is the only nereidid genus in which the dorsal notopodial ligule is transformed into "branchial" filaments; the genus contains three species which occur in tropical estuaries of the Indo-Pacific. There is no taxonomic review or identification guide for the species of *Dendronereides*.

Dendronereis Peters, 1854

Type species. *Dendronereis arborifera* Peters, 1854.

WoRMS URL. https://www.marinespecies.org/polychaeta/aphia.php?p=taxdetails&id=206700.

Sources. Hsueh (2019b).

Diagnosis. Dorsal cirrus divided into numerous branchial filaments (minimal diagnosis). Ventral neuropodial ligule on posterior chaetigers absent; palpophore massive subconical, flattened (palpostyle is minute by comparison); prostomium anterior margin indented (secondary diagnosis).

Description. Palpophore massive subconical, flattened (palpostyle is minute by comparison). Prostomium anterior margin indented.

Maxillary ring of pharynx with papillae present, or absent. Maxillary ring paragnaths absent. Oral ring papillae present. Oral ring paragnaths absent.

Dorsal notopodial ligule not markedly elongate on posterior chaetigers; not markedly broader on posterior chaetigers; not markedly reduced on posterior chaetigers. Prechaetal notopodial lobe present; smaller than dorsal notopodial ligule on anterior chaetigers, usually reduced or absent posteriorly. Dorsal cirrus divided into numerous branchial filaments. Dorsal cirrus not sub-terminally attached to dorsal notopodial ligule on posterior chaetigers; not terminally attached to dorsal notopodial ligule on posterior chaetigers; not terminally attached throughout all chaetigers.

Ventral neuropodial ligule of anterior chaetigers present. Ventral neuropodial ligule of anterior chaetigers approx. as long as acicular neuropodial ligule. Ventral neuropodial ligule on posterior chaetigers absent. Neuropodia of branchial chaetigers divided into five lobes, plus ventral cirrus, plus two smaller cirri on ventral neuropodial lobe (not arising from same location as ventral cirri). Posteriorly becoming simpler, eventually with a single neuropodial lobe and ventral cirrus.

Notochaetae: homogomph spinigers present. Neurochaetae dorsal fascicle: heterogomph spinigers absent; homogomph spinigers present; heterogomph falcigers in anterior chaetigers absent; on posterior chaetigers absent. Neurochaetae ventral fascicle: heterogomph spinigers absent; homogomph spinigers present; heterogomph falcigers absent.

Remarks. Species belonging to *Dendronereis* are easily recognised as this is the only genus of Nereididae in which the dorsal cirrus is transformed into branchial filaments. Bakken et al. (2022) incorrectly stated that maxillary ring paragnaths may be present or absent; they are always absent as per the corrected description and diagnosis above.

Five species of *Dendronereis* are known, all occurring in shallow waters of the Indo-Pacific. Hsueh (2019b) provides a key to all known species.

Eunereis Malmgren, 1865

Nereis (*Eunereis*) Malmgren, 1865.

Type species. *Nereis longissima* Johnston, 1840.

WoRMS URL. https://www.marinespecies.org/polychaeta/aphia.php?p=taxdetails&id=129373.

Sources. Hsueh (2018); Bakken et al. (2022).

Diagnosis. Oral ring paragnaths present; maxillary ring paragnaths absent (minimal diagnosis; secondary diagnosis not attained).

Description. Palpophore barrel-shaped, approximately equal width from base to palpostyle (not overly large compared with palpostyle). Palpophore surface with a single transverse groove (palpophores well developed). Tentacular belt greater than length of chaetiger 1.

Jaws with dentate cutting edge.

Maxillary ring of pharynx with papillae absent. Maxillary ring paragnaths absent. Oral ring papillae present, or absent. Oral ring paragnaths present; with Areas V, VI, and VII-VIII discrete, or comprising a continuous ring dorsally and ventrally, discrete groups not recognisable; on Areas V and VI form distinct groups. Area V conical paragnaths present, or absent. Area VI paragnaths present; arranged in a roughly circular group; conical paragnaths present, or absent; smooth bars present, or absent. Areas VII-VIII paragnaths present, or absent; conical paragnaths present; conical paragnaths arranged in isolated patches, or in one or more irregular lines forming a continuous band; conical paragnaths similar in size, or irregular mix of large and small paragnaths in a single band; rod-shaped paragnaths absent.

Dorsal notopodial ligule not markedly elongate on posterior chaetigers; not markedly broader on posterior chaetigers; markedly reduced on posterior chaetigers, or not markedly reduced on posterior chaetigers. Prechaetal notopodial lobe present, or absent; smaller than dorsal notopodial ligule on anterior chaetigers, usually reduced or absent posteriorly; restricted to a limited number of anterior chaetigers. Notopodial acicular process present, or absent. Dorsal cirrus not sub-terminally attached to dorsal notopodial ligule on posterior chaetigers; not terminally attached to dorsal notopodial ligule on posterior chaetigers; not terminally attached throughout all chaetigers; simple, lacking basal cirrophore.

Neuropodial prechaetal lobe absent. Neuropodial postchaetal lobe absent, or present; projecting beyond end of the acicular ligule; restricted to anterior chaetigers; digitiform. Ventral neuropodial ligule of anterior chaetigers present.

Ventral neuropodial ligule of anterior chaetigers approx. as long as acicular neuropodial ligule. Ventral neuropodial ligule on posterior chaetigers present. Ventral neuropodial ligule on posterior chaetigers similar to length of acicular neuropodial ligule.

Notoaciculae on chaetigers 1 and 2 absent. Notochaetae: homogomph spinigers present; homogomph falcigers present, or absent. Neurochaetae dorsal fascicle: heterogomph spinigers absent; homogomph spinigers present; heterogomph falcigers in anterior chaetigers present; on posterior chaetigers present; blades serrated. Neurochaetae ventral fascicle: heterogomph spinigers present; homogomph spinigers absent; heterogomph falcigers present; falcigers blade tapering, with straight margin; anterior chaetigers heterogomph falcigers with long blades absent; anterior chaetigers heterogomph falcigers with extra-long blades present; anterior chaetigers heterogomph falcigers with short blades absent; posterior chaetigers heterogomph falcigers with long blades present, or absent; posterior chaetigers heterogomph falcigers with extra-long blades present, or absent; posterior chaetigers heterogomph falcigers with short blades absent; heterogomph falcigers blade lacking distinct tendon on terminal tooth.

Anal cirri form cirriform or conical.

Remarks. The description here follows Hsueh (2018) with additional information on the straight/bowed blade falcigers character introduced (for *Composetia*) by Villalobos-Guerrero et al. (2022a).

Eunereis is the only Nereididae genus with paragnaths present only on the oral ring. *Eunereis* includes species which in other respects, especially chaetal characters, are similar to either of the genera *Neanthes* or *Nereis* suggesting a review is necessary.

Eunereis includes ten accepted species which encompass wide geographic and bathymetric distributions. There is no published identification guide to all species.

Gymnonereis Horst, 1919

Gymnorhynchus Horst, 1919 (replaced homonym).

Type species. *Gymnorhynchus sibogae* Horst, 1918.

WoRMS URL. https://www.marinespecies.org/polychaeta/aphia.php?p=taxdetails&id=324851.

Sources. Pettibone (1970); Hutchings and Reid (1990).

Diagnosis. Accessory ventral cirrus present; neurochaetae ventral fascicle sesquigomph spinigers present (minimal diagnosis). Notochaetae sesquigomph spinigers present; dorsal notopodial ligule present (secondary diagnosis).

Description. Palpophore barrel-shaped, approximately equal width from base to palpostyle (not overly large compared with palpostyle). Palpophore surface with a single transverse groove (palpophores well developed); palpostyles subconical, or acutely conical. Prostomium anterior margin indented.

Jaws with smooth or slightly crenulate cutting edge or with dentate cutting edge.

Maxillary ring of pharynx with papillae absent. Maxillary ring paragnaths absent. Oral ring papillae present. Oral ring papillae arrangement solitary. Area V papillae present; VI papillae present; VII-VIII papillae present. Oral ring paragnaths absent.

Transverse dorsal lamellae absent, or present.

Dorsal notopodial ligule present; commences chaetiger 1; not markedly elongate on posterior chaetigers; not markedly broader on posterior chaetigers; markedly reduced on posterior chaetigers (but cirrophore of dorsal cirrus is expanded and looks like an expanded notopodial lobe unless progressive change is noted over many chaetigers). Prechaetal notopodial lobe present; smaller than dorsal notopodial ligule on anterior chaetigers, usually reduced or absent posteriorly; present on all chaetigers. Notopodial acicular process present. Dorsal cirrus not sub-terminally attached to dorsal notopodial ligule on posterior chaetigers; not terminally attached to dorsal notopodial ligule on posterior chaetigers; not terminally attached throughout all chaetigers; arising from basal cirrophore.

Neuropodial prechaetal lobe present; extending beyond postchaetal lobe (at least in anterior chaetigers). Neuropodial postchaetal lobe present; not projecting beyond end of the acicular ligule; present throughout all chaetigers; flattened. Ventral neuropodial ligule of anterior chaetigers present. Ventral neuropodial ligule of anterior chaetigers approx. as long as acicular neuropodial ligule. Ventral neuropodial ligule on posterior chaetigers present. Ventral neuropodial ligule on posterior chaetigers similar to length of acicular neuropodial ligule, or short, up to half length of acicular neuropodial ligule. Accessory ventral cirrus present.

Notoaciculae on chaetigers 1 and 2 absent. Notochaetae: homogomph spinigers present, or absent; sesquigomph spinigers present. Neurochaetae dorsal fascicle: heterogomph spinigers absent; homogomph spinigers present, or absent; sesquigomph spinigers present. Neurochaetae dorsal fascicle: sesquigomph falcigers present, or absent; blades serrated; heterogomph falcigers in anterior chaetigers absent; on posterior chaetigers absent. Neurochaetae ventral fascicle: sesquigomph falcigers present, or absent; heterogomph spinigers absent; homogomph spinigers present, or absent; sesquigomph spinigers present; heterogomph falcigers absent.

Anal cirri form cirriform or conical.

Remarks. The genus *Gymnonereis* is diagnosed by the presence of accessory dorsal and ventral cirri and notochaetae comprising sesquigomph spinigers (although as discussed by Darbyshire 2014 it is not clear that these chaetae are alike in all species). *Gymnonereis* is most similar to *Tambalagamia* and the two have been combined by some authors, *Gymnonereis* being the senior synonym (Pettibone 1970; Hylleberg and Nateewathana 1988).

Gymnonereis is a genus of seven species, predominantly occurring in the southern hemisphere and the tropical Indo-Pacific and from shallow water (~ 60 m or less). There is no published key to all species although several regional keys exist (Hylleberg and Nateewathana 1988; Hutchings and Reid 1990).

Hediste Malmgren, 1867

Nereis (*Hediste*) Malmgren, 1867.

Type species. *Nereis diversicolor* Müller, 1776.

WoRMS URL. https://www.marinespecies.org/polychaeta/aphia.php?p=taxdetails&id=146968.

Sources. Sato and Nakashima (2003).

Diagnosis. Neurochaetae dorsal fascicle simple chaetae (fused falcigers) present; palpophore massive subconical, flattened (palpostyle is minute by comparison) (minimal diagnosis; secondary diagnosis not attained).

Description. Palpophore massive subconical, flattened (palpostyle is minute by comparison). Palpophore surface with a single transverse groove (palpophores well developed). Tentacular belt greater than length of chaetiger 1.

Jaws with dentate cutting edge.

Maxillary ring of pharynx with papillae absent. Area I conical paragnaths present; II conical paragnaths present; III conical paragnaths present; III rod-like paragnaths absent; IV paragnaths present; IV conical paragnaths present; IV rod-like paragnaths absent. Oral ring papillae absent. Oral ring paragnaths present; with Areas V, VI, and VII-VIII discrete; on Areas V and VI form distinct groups. Area V conical paragnaths absent. Area VI paragnaths present; paragnaths arranged in a roughly circular group, or in lines or arcs; conical paragnaths present; smooth bars absent. Area VII-VIII paragnaths present; conical paragnaths present; conical paragnaths arranged in one or more irregular lines forming a continuous band; conical paragnaths similar in size, or irregular mix of large and small paragnaths in a single band; rod-shaped paragnaths absent.

Dorsal notopodial ligule not markedly elongate on posterior chaetigers; not markedly broader on posterior chaetigers; not markedly reduced on posterior chaetigers. Prechaetal notopodial lobe present; smaller than dorsal notopodial ligule on anterior chaetigers, usually reduced or absent posteriorly; restricted to a limited number of anterior chaetigers. Notopodial acicular process absent. Dorsal cirrus not sub-terminally attached to dorsal notopodial ligule on posterior chaetigers; not terminally attached to dorsal notopodial ligule on posterior chaetigers; not terminally attached throughout all chaetigers.

Neuropodial postchaetal lobe absent, or present; projecting beyond end of the acicular ligule; restricted to anterior chaetigers; digitiform. Ventral neuropodial ligule of anterior chaetigers present. Ventral neuropodial ligule of anterior chaetigers approx. as long as acicular neuropodial ligule. Ventral neuropodial ligule on posterior chaetigers present. Ventral neuropodial ligule on posterior chaetigers similar to length of acicular neuropodial ligule.

Notoaciculae on chaetigers 1 and 2 absent. Notochaetae: homogomph spinigers present. Neurochaetae dorsal fascicle: heterogomph spinigers absent; homogomph spinigers present; heterogomph falcigers in anterior chaetigers present; on posterior chaetigers present; blades serrated; simple chaetae (fused falcigers) present. Neurochaetae ventral fascicle: heterogomph spinigers present or absent; homogomph spinigers absent; homogomph falcigers present or absent; heterogomph falcigers present; anterior chaetigers heterogomph falcigers with long blades absent; anterior chaetigers heterogomph falcigers with extra-long blades present; anterior chaetigers heterogomph falcigers with short blades absent; posterior chaetigers heterogomph falcigers with long blades absent; posterior chaetigers heterogomph falcigers with extra-long blades present; posterior chaetigers heterogomph falcigers with short blades absent; heterogomph falcigers blade lacking distinct tendon on terminal tooth.

Anal cirri form cirriform or conical.

Remarks. *Hediste* species are characterised by the “simple” neuropodial falcigers (with fused articulation) which are present in posterior chaetigers and by having paragnaths on both rings of the pharynx. The most recent taxonomic treatments are Sato and Nakashima (2003) and Teixeira et al. (2022a) who described a total of four new species, broadened the generic diagnosis, and demonstrated the power of morphometric methods to discriminate cryptic species.

Hediste is a genus of estuarine nereidids which occur in the northern hemisphere. Seven species of *Hediste* are currently described but despite recent publications, the most widespread species, *H. diversicolor* (O.F. Müller, 1776) still contains cryptic species not yet described (Tosuji et al. 2018; Teixeira et al. 2022a). A key to Asian species of *Hediste* is provided by Sato and Nakashima (2003) and Teixeira et al. (2022a) provide a key to European species.

Imajimainereis de León-González & Solis-Weiss, 2000

Type species. *Imajimainereis pacifica* de León-González & Solís-Weiss, 2000.

WoRMS URL. https://www.marinespecies.org/polychaeta/aphia.php?p=taxdetails&id=325837.

Sources. de León-González and Solís-Weiss (2000).

Diagnosis. Oral ring paragnaths present; oral ring papillae present; neurochaetae dorsal fascicle heterogomph spinigers present (minimal diagnosis). Neurochaetae dorsal fascicle heterogomph falcigers in anterior chaetigers absent; Area VI papillae absent; palpophore barrel-shaped, approximately equal width from base to palpostyle (not overly large compared with palpostyle) (secondary diagnosis).

Description. Palpophore barrel-shaped, approximately equal width from base to palpostyle (not overly large compared with palpostyle). Tentacular belt greater than length of chaetiger 1.

Jaws with dentate cutting edge.

Maxillary ring of pharynx with papillae absent. Area I conical paragnaths present; II conical paragnaths present; III conical paragnaths present; III rod-like paragnaths absent; IV paragnaths present; IV conical paragnaths present; IV rod-like paragnaths absent. Oral ring papillae present. Oral ring papillae arrangement solitary. Area V papillae absent; VI papillae absent; VII-VIII papillae present. Oral ring paragnaths present; with Areas V, VI, and VII-VIII discrete; on Areas V and VI form distinct groups. Area V conical paragnaths absent. Area VI paragnaths present; paragnaths arranged in a roughly circular group; conical paragnaths present; smooth bars absent. Areas VII-VIII paragnaths present; conical paragnaths present; conical paragnaths arranged in one or more irregular lines forming a continuous band; conical paragnaths similar in size, or irregular mix of large and small paragnaths in a single band; rod-shaped paragnaths absent.

Dorsal notopodial ligule not markedly elongate on posterior chaetigers; not markedly broader on posterior chaetigers; not markedly reduced on posterior chaetigers. Prechaetal notopodial lobe present; smaller than dorsal notopodial ligule on anterior chaetigers, usually reduced or absent posteriorly. Dorsal cirrus not sub-terminally attached to dorsal notopodial ligule on posterior chaetigers; not terminally attached to dorsal notopodial ligule on posterior chaetigers; not terminally attached throughout all chaetigers.

Neuropodial postchaetal lobe present. Ventral neuropodial ligule of anterior chaetigers present. Ventral neuropodial ligule of anterior chaetigers approx.

as long as acicular neuropodial ligule. Ventral neuropodial ligule on posterior chaetigers present. Ventral neuropodial ligule on posterior chaetigers similar to length of acicular neuropodial ligule.

Notoaciculae on chaetigers 1 and 2 absent. Notochaetae: homogomph spinigers present. Neurochaetae dorsal fascicle: heterogomph spinigers present; homogomph spinigers present; heterogomph falcigers in anterior chaetigers absent; on posterior chaetigers present; blades serrated; blades with teeth only slightly longer proximally than distally. Neurochaetae ventral fascicle: heterogomph spinigers present; homogomph spinigers present; heterogomph falcigers present; anterior chaetigers heterogomph falcigers with long blades absent; anterior chaetigers heterogomph falcigers with extra-long blades absent; anterior chaetigers heterogomph falcigers with short blades absent; posterior chaetigers heterogomph falcigers with long blades absent; posterior chaetigers heterogomph falcigers with extra-long blades present; posterior chaetigers heterogomph falcigers with short blades absent.

Remarks. *Imajimainereis* contains a single species, *I. pacifica* de León-González & Solís-Weiss, 2000, which differs from all other Nereididae by having both papillae and paragnaths on the oral ring and neurochaetae including heterogomph spinigers.

Imajimainereis is recorded from the Gulf of California, eastern Pacific Ocean (de León-González and Solís-Weiss 2000).

Kainonereis Chamberlin, 1919

Type species. *Kainonereis alata* Chamberlin, 1919.

WoRMS URL. https://www.marinespecies.org/polychaeta/aphia.php?p=taxdetails&id=324852.

Sources. Conde-Vela et al. (2018); Chamberlin (1919).

Diagnosis. Dorsal cirrophores of chaetigers 5–7 of epitokes modified into flattened elytriform discs (minimal diagnosis). Notochaetae homogomph falcigers present; maxillary ring paragnaths absent; oral ring paragnaths absent; dorsal notopodial ligule not markedly reduced on posterior chaetigers (secondary diagnosis).

Description. Palps anteriorly directed, or ventrally directed. Palpophore barrel-shaped, approximately equal width from base to palpostyle (not overly large compared with palpostyle). Prostomium the antennae are separate but sometimes basally fused in male epitokes. Tentacular cirri articulated.

Jaws with dentate cutting edge.

Maxillary ring of pharynx with papillae absent. Maxillary ring paragnaths absent. Oral ring paragnaths absent.

Dorsal notopodial ligule commences chaetiger 3, or chaetiger 4 (from chaetiger 4 in males, 3 in females); not markedly elongate on posterior chaetigers; not markedly reduced on posterior chaetigers. Prechaetal notopodial lobe present (subconical to digitate in atokes, rounded in epitokes). Dorsal cirrus not sub-terminally attached to dorsal notopodial ligule on posterior chaetigers.

Neuropodial prechaetal lobe absent. Neuropodial postchaetal lobe present; present throughout all chaetigers. Ventral neuropodial ligule of anterior chaetigers present. Ventral neuropodial ligule of anterior chaetigers approx.

as long as acicular neuropodial ligule. Ventral neuropodial ligule on posterior chaetigers present.

Notoaciculae on chaetigers 1 and 2 absent. Notochaetae: homogomph spinigers present; homogomph falcigers present (in males, on anterior chaetigers); homogomph falcigers with multidentate blade with two or more small lateral teeth, first and subsequent lateral teeth much smaller than terminal tooth present. Neurochaetae dorsal fascicle: heterogomph spinigers absent; homogomph spinigers present; heterogomph falcigers in anterior chaetigers present. Neurochaetae ventral fascicle: heterogomph spinigers present; homogomph spinigers absent; heterogomph falcigers present; falcigers blade bowed, with convex margin.

Pygidium bilobate. Anal cirri form cirriform or conical.

Epitokes. Dorsal cirrophores of chaetigers 5–7 of epitokes modified into flattened elytriform discs. Natatory epitokal modifications in males commence chaetiger 15. Natatory epitokal modifications in females commence chaetiger 15.

Remarks. *Kainonereis* was originally described for an epitokous specimen in which dorsal cirri of chaetigers 5–7 were expanded into elytra-like structures. Unless epitokes are available *Kainonereis* is not separable from *Nicon* and *Websterinereis* (this does not imply that *Kainonereis* is invalid). A revision by Conde-Vela et al. (2018) redefined the genus and included atokous characters; five species are now recognised and epitokes can be identified using the key of Conde-Vela et al. (2018).

***Kinberginereis* Pettibone, 1971**

Type species. *Nereis* (*Leptonereis*) *inermis* Hoagland, 1920.

WoRMS URL. https://www.marinespecies.org/polychaeta/aphia.php?p=taxdetails&id=843657.

Sources. Pettibone (1971); Bakken et al. (2022).

Diagnosis. Neurochaetae ventral fascicle heterogomph spinigers in anterior chaetigers with blades coarsely serrated proximally; oral ring papillae present; maxillary ring of pharynx with papillae absent (minimal diagnosis). Prostomium anterior margin indented; prechaetal notopodial lobe approximately equal to length of dorsal notopodial ligule at least on anterior chaetigers (thus notopodium of three similar sized ligules/lobes); antennae form cirriform (usually extending to or past palpophore); maxillary ring paragnaths absent (secondary diagnosis).

Description. Palpophore barrel-shaped, approximately equal width from base to palpostyle (not overly large compared with palpostyle) (elongate). Prostomium anterior margin indented.

Jaws with dentate cutting edge, 20 teeth.

Maxillary ring of pharynx with papillae absent. Maxillary ring paragnaths absent. Oral ring papillae present. Oral ring papillae number two in total; arrangement solitary. Area V papillae absent; VI papillae present, one papilla (a single fleshy nob on each side); VII-VIII papillae absent. Oral ring paragnaths absent.

Dorsal notopodial ligule present; markedly reduced on posterior chaetigers. Prechaetal notopodial lobe present; approximately equal to length of dorsal notopodial ligule at least on anterior chaetigers (thus notopodium of three similar sized ligules/lobes); present on all chaetigers. Dorsal cirrus not sub-terminally attached to dorsal notopodial ligule on posterior chaetigers.

Neuropodial prechaetal lobe present. Neuropodial postchaetal lobe present; projecting beyond end of the acicular ligule; flattened. Ventral neuropodial ligule of anterior chaetigers present. Ventral neuropodial ligule of anterior chaetigers approx. as long as acicular neuropodial ligule. Ventral neuropodial ligule on posterior chaetigers present. Ventral neuropodial ligule on posterior chaetigers similar to length of acicular neuropodial ligule.

Notoaciculae on chaetigers 1 and 2 present. Notochaetae: homogomph spinigers present. Neurochaetae dorsal fascicle: heterogomph spinigers absent; homogomph spinigers present; heterogomph falcigers in anterior chaetigers absent; on posterior chaetigers absent. Neurochaetae ventral fascicle: heterogomph spinigers present; spinigers in anterior chaetigers with blades coarsely serrated proximally; homogomph spinigers absent; heterogomph falcigers absent.

Remarks. The most recent taxonomic treatment of *Kinberginereis* is the original description of Pettibone (1971). *Kinberginereis* is most similar to *Kainonereis*, atokes differing only in that *Kinberginereis* has an indented prostomium but the prostomium of *Kainonereis* is entire. Epitokes of *Kainonereis* are distinctive in having elytriform expansion of dorsal cirrophores of chaetigers 5–7 but epitokes of *Kinberginereis* are unknown.

Kinberginereis includes a single species, *K. inermis* (Hoagland, 1920) described from a single specimen from shallow water in the Philippines; the only subsequent reports are unverified occurrence records now in the Smithsonian National Museum of Natural History from the Gulf of Mexico.

Laeonereis **Hartman, 1945**

Type species. *Nereis culveri* Webster, 1879.

WoRMS URL. https://www.marinespecies.org/polychaeta/aphia.php?p=taxdetails&id=181592.

Sources. Pettibone (1971); Conde-Vela (2021).

Diagnosis. Maxillary ring of pharynx with papillae in tufts (minimal diagnosis). Dorsal notopodial ligule commences chaetiger 1; neurochaetae ventral fascicle homogomph falcigers on posterior chaetigers present (secondary diagnosis).

Description. Palpophore barrel-shaped, approximately equal width from base to palpostyle (not overly large compared with palpostyle). Prostomium anterior margin indented; longitudinal groove present.

Jaws with dentate cutting edge.

Maxillary ring of pharynx with papillae present; in tufts. Maxillary ring paragnaths absent. Oral ring papillae present. Oral ring papillae arrangement solitary. Area V papillae absent; VI papillae present; VII-VIII papillae present or absent (may be absent in juveniles). Oral ring paragnaths absent. Papillae triangular or conical on Area VI, rounded on Areas VII-VIII.

Dorsal notopodial ligule present; commences chaetiger 1; not markedly elongate on posterior chaetigers; not markedly broader on posterior chaetigers; not markedly reduced on posterior chaetigers. Prechaetal notopodial lobe present; smaller than dorsal notopodial ligule on anterior chaetigers, usually reduced or absent posteriorly; restricted to a limited number of anterior chaetigers. Notopodial acicular process absent. Dorsal cirrus not sub-terminally attached to dorsal notopodial ligule on posterior chaetigers; not terminally attached to dorsal notopodial ligule on posterior chaetigers; not terminally attached throughout all chaetigers.

Neuropodial prechaetal lobe absent. Neuropodial postchaetal lobe present; projecting beyond end of the acicular ligule; restricted to anterior chaetigers. Ventral neuropodial ligule of anterior chaetigers present. Ventral neuropodial ligule of anterior chaetigers approx. as long as acicular neuropodial ligule. Ventral neuropodial ligule on posterior chaetigers present. Ventral neuropodial ligule on posterior chaetigers similar to length of acicular neuropodial ligule.

Notoaciculae on chaetigers 1 and 2 absent. Notochaetae: homogomph spinigers present. Neurochaetae dorsal fascicle: heterogomph spinigers absent; homogomph spinigers present; heterogomph falcigers in anterior chaetigers absent; on posterior chaetigers absent; homogomph falcigers in anterior chaetigers present, or absent; on posterior chaetigers present, or absent. Neurochaetae ventral fascicle: heterogomph spinigers absent; homogomph spinigers present; heterogomph falcigers absent; homogomph falcigers on posterior chaetigers present (with long blades).

Pygidium funnel-shaped, crenulated, or multi-incised, with ventral incision. Anal cirri cirriform or conical.

Remarks. The description and diagnosis of *Laeonereis* here is derived from the revision of Conde-Vela (2021) which is only slightly modified from that of Pettibone (1971) who recognised a single species of *Laeonereis*. Simultaneously with the publication of the morphological revision of *Laeonereis* by Conde-Vela (2021), Sampieri et al. (2021) published a molecular study of *Laeonereis* (but with no morphological component) and revealed seven or nine molecular OTUs. It is tantalising that Sampieri et al. (2021) and Conde-Vela (2021) discovered very similar species-level diversity from within the same geographic range but frustrating that neither apparently was aware of the others' research.

Currently eight species of *Laeonereis* are recognised, largely confined to the Atlantic coasts of North and South America; they can be identified using the key of Conde-Vela (2021).

Leonnates Kinberg, 1865

Nereis (*Leonnates*) auctt.
Laevispinereis He & Wu, 1989.

Type species. *Leonnates indicus* Kinberg, 1865.

WoRMS URL. https://www.marinespecies.org/polychaeta/aphia.php?p=taxdetails&id=129374.

Sources. Qiu and Qian (2000); Villalobos-Guerrero et al. (2022a).

Diagnosis. Oral ring papillae present; maxillary ring paragnaths present; oral ring paragnaths absent; ventral neuropodial ligule on posterior chaetigers similar to length of acicular neuropodial ligule; neurochaetae dorsal fascicle homogomph spinigers present (minimal diagnosis; secondary diagnosis not attained).

Description. Palpophore barrel-shaped, approximately equal width from base to palpostyle (not overly large compared with palpostyle), or massive subconical, flattened (palpostyle is minute by comparison). Palpophore surface with a single transverse groove (palpophores well developed). Prostomium anterior margin entire or indented (indented only in *L. persicus* and *L. stephensoni*); longitudinal groove present; anterior region sub-quadrangular or sub-rectangular. Tentacular belt greater than length of chaetiger 1.

Oesophageal caeca absent.

Jaws with smooth or slightly crenulate cutting edge or with dentate cutting edge.

Maxillary ring of pharynx with papillae present, or absent; solitary. Maxillary ring paragnaths present. Area I conical paragnaths present, or absent; II conical paragnaths present; III conical paragnaths present, or absent; III rod-like paragnaths absent; IV paragnaths present; IV conical paragnaths present; IV smooth bar-like paragnaths present, or absent; IV rod-like paragnaths absent. Oral ring papillae present. Oral ring papillae arrangement solitary. Area V papillae present, or absent; VI papillae present; VII-VIII papillae present. Oral ring paragnaths absent.

Dorsal notopodial ligule not markedly elongate on posterior chaetigers; not markedly broader on posterior chaetigers; not markedly reduced on posterior chaetigers. Prechaetal notopodial lobe present; smaller than dorsal notopodial ligule on anterior chaetigers, usually reduced or absent posteriorly, or approximately equal to length of dorsal notopodial ligule at least on anterior chaetigers (thus notopodium of three similarly sized ligules/lobes); present on all chaetigers, or restricted to a limited number of anterior chaetigers. Notopodial acicular process absent. Dorsal cirrus not sub-terminally attached to dorsal notopodial ligule on posterior chaetigers; not terminally attached to dorsal notopodial ligule on posterior chaetigers; not terminally attached throughout all chaetigers.

Neuropodial prechaetal lobe absent. Neuropodial postchaetal lobe present; projecting beyond end of the acicular ligule; present throughout all chaetigers or restricted to anterior chaetigers; digitiform. Ventral neuropodial ligule of anterior chaetigers present. Ventral neuropodial ligule of anterior chaetigers approx. as long as acicular neuropodial ligule. Ventral neuropodial ligule on posterior chaetigers present. Ventral neuropodial ligule on posterior chaetigers similar to length of acicular neuropodial ligule.

Notoaciculae on chaetigers 1 and 2 absent. Notochaetae: homogomph spinigers present; homogomph falcigers present, or absent. Neurochaetae dorsal fascicle: heterogomph spinigers present, or absent (present in *L. fujianensis*); homogomph spinigers present; sesquigomph spinigers present, or absent (present in *L. fujianensis*); sesquigomph falcigers present, or absent; heterogomph falcigers in anterior chaetigers present, or absent; on posterior chaetigers present, or absent; homogomph falcigers in anterior chaetigers present, or absent; on posterior chaetigers present, or absent. Neurochaetae ventral fascicle: sesquigomph falcigers present, or absent; blade with a single distal tooth; heterogomph spinigers present, or absent; homogomph spinigers present, or absent; sesquigomph spinigers present, or absent; heterogomph falcigers present, or absent; falcigers blade bowed, with convex margin; heterogomph falcigers blade lacking distinct tendon on terminal tooth; homogomph falcigers in anterior chaetigers present, or absent; on posterior chaetigers present, or absent. Ventral fascicle neuropodial falcigers apparently vary considerably between species.

Anal cirri form cirriform or conical.

Remarks. The current description and diagnosis follow Qiu and Qian (2000) and emendments by Villalobos-Guerrero et al. (2022a). Original descriptions sometimes report the presence of sesquigomph falcigers and spinigers but as noted by Qiu and Qian (2000) some of these interpretations are inconsistent, with the same chaetal forms being given different names by some authors. However Qiu and Qian (2000) also do not interpret these terms consistently: they do not use the term sesquigomph yet their figures 3B and 3E (*Leonnates indicus* Kinberg, 1865), 5E (*L. nierstraszi* Horst, 1924), 7B (*L. decipiens* Fauvel, 1929), 9D (*L. persicus* Wesenberg-Lund, 1949, and 14D (*L. crinitus* Hutchings & Reid, 1991, albeit damaged) all show sesquigomph articulation as accepted by other authors, e.g. Villalobos-Guerrero et al. (2022a: fig. 12i, j; *Parasetia irritabilis* (Webster, 1879)), Bakken et al. (2022: figs 7.13.3.3.3: C, 7.13.3.3.4: C), de León-González and Salazar-Vallejo (2003: fig. 1E, F) (*Leonnates crosnieri* de León-González & Salazar-Vallejo, 2003).

Leonnates includes 13 species with the greatest diversity in the tropical Indo-Pacific. Qiu and Qian (2000) provide a key to the seven species known at that time.

***Leptonereis* Kinberg, 1865**

Nereis (*Leptonereis*) auctt.

Type species. *Leptonereis laevis* Kinberg, 1865.

WoRMS URL. https://www.marinespecies.org/polychaeta/aphia.php?p=taxdetails&id=152401.

Sources. Hartman 1945; Pettibone 1971.

Diagnosis. Dorsal cirrus terminally attached to dorsal notopodial ligule on posterior chaetigers; maxillary ring paragnaths absent (minimal diagnosis). Dorsal notopodial ligule markedly broader on posterior chaetigers; prostomium anterior margin entire; maxillary ring of pharynx with P-bar paragnaths absent (secondary diagnosis).

Description. Palpophore barrel-shaped, approximately equal width from base to palpostyle (not overly large compared with palpostyle).

Maxillary ring of pharynx with papillae absent. Maxillary ring paragnaths absent. Oral ring papillae absent. Oral ring paragnaths absent.

Dorsal notopodial ligule present; markedly elongate on posterior chaetigers; markedly broader on posterior chaetigers; not markedly reduced on posterior chaetigers. Dorsal cirrus not sub-terminally attached to dorsal notopodial ligule on posterior chaetigers; terminally attached to dorsal notopodial ligule on posterior chaetigers; not terminally attached throughout all chaetigers.

Neuropodial postchaetal lobe absent. Ventral neuropodial ligule of anterior chaetigers present. Ventral neuropodial ligule of anterior chaetigers approx. as long as acicular neuropodial ligule. Ventral neuropodial ligule on posterior chaetigers present. Ventral neuropodial ligule on posterior chaetigers similar to length of acicular neuropodial ligule.

Notochaetae: homogomph spinigers present. Neurochaetae homogomph and heterogomph spinigers and heterogomph falcigers, but their distribution in dorsal and ventral fascicles is unknown.

Remarks. The description of *Leptonereis* given here follows the most recent treatment (Pettibone 1971) which in turn was based on new descriptions and figures of the type by Kinberg (1910) and Hartman (1945). However, many characters including articulation of the chaetae remain unverified.

Leptonereis includes a single species, *L. laevis* Kinberg, 1865, based on a single specimen from Guayaquil, Ecuador and now recorded from tropical east Pacific coasts of North and South America.

Lycastonereis Rao, 1981

Type species. *Lycastonereis indica* Rao, 1981.

WoRMS URL. https://www.marinespecies.org/polychaeta/aphia.php?p=taxdetails&id=324857.

Sources. Rao (1981); Conde-Vela (2019a).

Diagnosis. Tentacular cirri three pairs; palpophore surface with a single transverse groove (palpophores well developed) (minimal diagnosis). Neurochaetae dorsal fascicle homogomph falcigers on posterior chaetigers present; maxillary ring paragnaths absent; prostomium anterior margin entire (secondary diagnosis).

Description. Palpophore barrel-shaped, approximately equal width from base to palpostyle (not overly large compared with palpostyle). Palpophore surface with a single transverse groove (palpophores well developed). Prostomium anterior margin entire. Tentacular belt greater than length of chaetiger 1. Tentacular cirri three pairs.

Jaws with dentate cutting edge.

Maxillary ring of pharynx with papillae present. Maxillary ring paragnaths absent. Oral ring papillae present. Oral ring papillae arrangement solitary. Area V papillae absent; VI papillae present; VII-VIII papillae present, arranged in a single row. Oral ring paragnaths absent.

Dorsal notopodial ligule markedly reduced or absent on posterior chaetigers. Prechaetal notopodial lobe present; restricted to a limited number of anterior chaetigers.

Neuropodial prechaetal lobe absent. Neuropodial postchaetal lobe present; not projecting beyond end of the acicular ligule; digitiform. Ventral neuropodial ligule of anterior chaetigers present. Ventral neuropodial ligule of anterior chaetigers approx. as long as acicular neuropodial ligule. Ventral neuropodial ligule on posterior chaetigers present. Ventral neuropodial ligule on posterior chaetigers short, up to half length of acicular neuropodial ligule.

Notoaciculae on chaetigers 1 and 2 absent. Notochaetae: homogomph spinigers present. Neurochaetae dorsal fascicle: heterogomph spinigers absent; homogomph spinigers present; dorsal fascicle heterogomph falcigers in anterior chaetigers absent; on posterior chaetigers absent; dorsal fascicle homogomph falcigers in anterior chaetigers present; on posterior chaetigers present; ventral fascicle heterogomph spinigers absent; homogomph spinigers present; sesquigomph spinigers present. Neurochaetae ventral fascicle: heterogomph falcigers absent; homogomph falcigers in anterior chaetigers present; on posterior chaetigers present.

Remarks. This easily diagnosed genus from estuaries in India includes a single species. Conde-Vela (2019a) provides a redescription based on non-type material which is topotypic and shares the unusual morphological characters of the original description including the presence of only three pairs of tentacular cirri. Conde-Vela (2019a) also clarified the surname of the author, which is Rao, not ‘Nageswara-Rao’ or ‘Nageswara Rao’ as stated in much of the literature. Although the double surname is a more precise authority name, we follow Conde-Vela (2019a) because Rao appears to be an uncommon name among polychaete taxon authors and thus not easily confused.

Micronereides Day, 1963

Type species. *Micronereides capensis* Day, 1963.

WoRMS URL. https://www.marinespecies.org/polychaeta/aphia.php?p=taxdetails&id=324861.

Sources. Day (1963).

Diagnosis. Tentacular belt represented by two distinct segments each carrying a pair of tentacular cirri (minimal diagnosis). Dorsal notopodial ligule absent; neurochaetae ventral fascicle sesquigomph spinigers present (secondary diagnosis).

Description. Palpophore barrel-shaped, approximately equal width from base to palpostyle (not overly large compared with palpostyle). Eyes absent. Prostomium with eyes, if not absent, indistinct and likely to be missed. Tentacular belt equal to or less than length of chaetiger 1; represented by two distinct segments each carrying a pair of tentacular cirri.

Jaws with dentate cutting edge, seven teeth.

Maxillary ring of pharynx with papillae absent. Maxillary ring paragnaths absent. Oral ring papillae absent. Oral ring paragnaths absent.

Dorsal notopodial ligule absent. Prechaetal notopodial lobe absent. Notopodial acicular process absent.

Neuropodial prechaetal lobe absent. Neuropodial postchaetal lobe absent. Ventral neuropodial ligule of anterior chaetigers present. Ventral neuropodial ligule of anterior chaetigers short, up to half length of acicular neuropodial ligule. Ventral neuropodial ligule on posterior chaetigers present. Ventral neuropodial ligule on posterior chaetigers similar to length of acicular neuropodial ligule. Dorsal notopodial ligule elongate, exceeding length of dorsal cirrus.

Notochaetae: homogomph spinigers present. Neurochaetae dorsal fascicle: heterogomph spinigers absent; homogomph spinigers present; heterogomph falcigers in anterior chaetigers absent; on posterior chaetigers absent; ventral fascicle heterogomph spinigers absent; homogomph spinigers present; sesquigomph spinigers present (possibly, chaetae need re-examination).

Remarks. *Micronereides* was erected to contain *M. capensis* Day, 1963 a small nereidid lacking pharyngeal papillae or paragnaths and in which tentacular cirri arise from two distinct anterior segments (unique among Nereididae). A revised diagnosis was provided by Banse (1977) including the observation that accessory ventral cirri are present on anterior segments thus placing the genus in Gymnonereidinae.

The genus is still only known from a single species, *M. capensis*, recorded from shelf depths in the South Atlantic Ocean.

Micronereis Claparède, 1863

Notophycus Knox & Cameron, 1970.
Phyllodocella Fauchald & Belman, 1972.
Quadricirra Banse, 1977.

Type species. *Micronereis variegata* Claparède, 1863.

WoRMS URL. https://www.marinespecies.org/polychaeta/aphia.php?p=taxdetails&id=129375.

Sources. Paxton (1983).

Diagnosis. Palpostyles absent (palps undivided, minute) (minimal diagnosis). Maxillary ring of pharynx undivided (secondary diagnosis).

Description. Antennae absent. Palps ventrally directed. Palpophore surface with a single transverse groove (palpophores well developed); palpostyles absent (palps undivided, minute).

Jaws with dentate cutting edge.

Maxillary ring of pharynx undivided.

Maxillary ring of pharynx with papillae absent; undivided maxillary ring with two paragnaths in total. Oral ring papillae absent. Oral ring paragnaths present; on Areas V and VI not recognisably distinct. Crown-shaped oral ring paragnaths present. Area V conical paragnaths absent.

Dorsal notopodial ligule absent. Prechaetal notopodial lobe absent. Notopodial acicular process absent. Acicular notopodial ligule absent.

Neuropodial postchaetal lobe absent. Ventral neuropodial ligule of anterior chaetigers absent. Ventral neuropodial ligule on posterior chaetigers absent.

Notoaciculae on chaetigers 1 and 2 absent (only confirmed as yet for *M. bansei*). Notochaetae: homogomph spinigers present; homogomph falcigers present or absent; homogomph falcigers with multidentate blade with two or more small lateral teeth, first and subsequent lateral teeth much smaller than terminal tooth present. Neurochaetae dorsal fascicle: heterogomph spinigers absent; homogomph spinigers present; heterogomph falcigers in anterior chaetigers absent; homogomph falcigers in anterior chaetigers present; on posterior chaetigers present. Neurochaetae ventral fascicle: heterogomph spinigers absent; homogomph spinigers present; heterogomph falcigers absent.

Anal cirri form cirriform or conical.

Remarks. *Micronereis* is a genus of small nereidids generally associated with algal turfs in intertidal and shallow (to ~ 30 m) marine waters. *Micronereis* species differ from other Nereididae in lacking antennae and having a pharynx that is not fully eversible. They are sexually dimorphic and males have distinctive neurochaetae that function as copulatory hooks not found in other Nereididae.

Micronereis currently includes ten accepted species which collectively have a wide global distribution. Paxton (1983) revised the genus and included a key to males but three more species have since been recognised.

Namalycastis Hartman, 1959

Type species. *Lycastis abiuma* Grube, 1872.

WoRMS URL. https://www.marinespecies.org/polychaeta/aphia.php?p=taxdetails&id=129376.

Sources. Glasby (1999).

Diagnosis. Palpophore surface without grooves or striae (palps short, compact); antennae form subconical (shorter than palpophore) (minimal diagnosis). Prostomium anterior margin indented (secondary diagnosis).

Description. Palpophore barrel-shaped, approximately equal width from base to palpostyle (not overly large compared with palpostyle). Palpophore surface without grooves or striae (palps short, compact) or with a single transverse groove (palpophores well developed); palpostyles spherical. Prostomium anterior margin indented; longitudinal groove present. Tentacular belt equal to or less than length of chaetiger 1.

Jaws with dentate cutting edge.

Maxillary ring of pharynx with papillae absent. Maxillary ring paragnaths absent. Oral ring papillae absent. Oral ring paragnaths absent.

Notopodium strongly reduced, without distinct lobes or ligules. Dorsal cirrus arising from basal cirrophore (weakly developed; only on anterior chaetigers).

Neuropodial postchaetal lobe absent. Ventral neuropodial ligule of anterior chaetigers absent. Ventral neuropodial ligule on posterior chaetigers absent.

Notoaciculae on chaetigers 1 and 2 present. Notochaetae: homogomph spinigers absent; sesquigomph spinigers present, or absent. Neurochaetae dorsal fascicle: heterogomph spinigers present (rarely), or absent; homogomph spinigers absent; sesquigomph spinigers present; heterogomph falcigers in anterior chaetigers present, or absent (rarely); on posterior chaetigers present, or absent; blades smooth, or serrated; blades with teeth only slightly longer proximally than distally. Neurochaetae ventral fascicle: heterogomph spinigers present; spinigers in anterior chaetigers with blades evenly serrated throughout, or coarsely serrated proximally (rarely); on posterior chaetigers with blades finely serrated proximally, or coarsely serrated proximally; homogomph spinigers absent; heterogomph falcigers present, or absent (rarely); anterior chaetigers heterogomph falcigers with long blades absent; anterior chaetigers heterogomph falcigers with extra-long blades present; anterior chaetigers heterogomph falcigers with short blades absent; posterior chaetigers heterogomph falcigers with long blades absent; posterior chaetigers heterogomph falcigers with extra-long blades present; posterior chaetigers heterogomph falcigers with short blades absent.

Pygidium with three incisions marking lateral and dorsal lobes. Anal cirri form cirriform or conical, or flattened, resembling posterior dorsal cirri.

Reproductive characters. Oocyte spherical.

Remarks. *Namalycastis* currently includes 33 accepted species recorded mainly from intertidal and supralittoral areas, including freshwater, of the tropics and subtropics. Together with sister-group *Namanereis*, they are one of only a few polychaetes to be found in association with riparian vegetation. Because they have an unadorned pharynx and a simplified parapodia, distinguishing species relies heavily on differences in chaetae, form of sensory organs of the head, and pigmentation patterns in living specimens. The modern concept of the subfamily and genus was introduced by Hartman (1959) and later reviewed by Glasby (1999), who included a key to all known species at the time. Since Glasby (1999) there have been five species described: *Namalycastis caetensis* Alves & Santos, 2016, *Namalycastis glasbyi* Fernando &

Rajasekaran, 2007, *Namalycastis jaya* Magesh, Kvist & Glasby, 2012, *Namalycastis occulta* Conde-Vela, 2013 and *Namalycastis rhodochorde* Glasby, Miura, Nishi & Junardi, 2007; however, *Namalycastis occulta* Conde-Vela, 2013 is now accepted as *Namanereis occulta* (Conde-Vela, 2013). Magesh et al. (2013) provided a key to Indian species and Conde-Vela (2013) provided a key to Caribbean species.

***Namanereis* Chamberlin, 1919**

Cryptonereis Gibbs, 1971.
Lycastella Feuerborn, 1932.
Lycastilla Solís-Weiss & Espinasa, 1991.
Lycastoides Jakubova, 1930.
Lycastopsis Augener, 1922.

Type species. *Lycastis quadraticeps* Blanchard in Gay, 1849.

WoRMS URL. https://www.marinespecies.org/polychaeta/aphia.php?p=taxdetails&id=129377.

Sources. Glasby (1999).

Diagnosis. Palpophore surface without grooves or striae (palps short, compact); prostomium anterior margin entire (minimal diagnosis). Palpostyles spherical; dorsal cirrus simple, lacking basal cirrophore (secondary diagnosis).

Description. Antennae present, or absent (rarely). Palpophore barrel-shaped, approximately equal width from base to palpostyle (not overly large compared with palpostyle). Palpophore surface without grooves or striae (most species; palps short, compact) or with a single transverse groove (palpophores well developed); palpostyles spherical. Eyes present, or absent. Tentacular belt equal to or less than length of chaetiger 1. Tentacular cirri four pairs, or three pairs.

Jaws forms with a crenulate cutting edge have 2 teeth proximally, with smooth or slightly crenulate cutting edge or with dentate cutting edge.

Maxillary ring of pharynx with papillae absent. Maxillary ring paragnaths absent. Oral ring papillae absent. Oral ring paragnaths absent.

Notopodium strongly reduced, without distinct lobes or ligules.

Neuropodial postchaetal lobe absent. Ventral neuropodial ligule of anterior chaetigers absent. Ventral neuropodial ligule on posterior chaetigers absent.

Notoaciculae on chaetigers 1 and 2 present. Notochaetae: homogomph spinigers absent; sesquigomph spinigers present (rarely), or absent. Neurochaetae dorsal fascicle: heterogomph spinigers present (rarely), or absent; homogomph spinigers absent; sesquigomph spinigers present, or absent; heterogomph falcigers in anterior chaetigers present; on posterior chaetigers present; blades serrated; blades with teeth only slightly longer proximally than distally, or much longer proximally than distally. Neurochaetae ventral fascicle: heterogomph spinigers present (rarely), or absent; spinigers in anterior chaetigers with blades evenly serrated throughout; on posterior chaetigers with blades finely serrated proximally; homogomph spinigers absent; heterogomph falcigers present (some forms with very long blades = pseudospinigers); anterior chaetigers heterogomph falcigers with long blades present; anterior chaetigers heterogomph falcigers with extra-long blades present; anterior chaetigers heterogomph falcigers with short blades absent; posterior chaetigers heterogomph falcigers with long blades present, or absent; posterior chaetigers heterogomph falcigers with extra-long blades present, or absent; posterior chaetigers heterogomph falcigers with short blades absent.

Pygidium with three incisions marking lateral and dorsal lobes. Anal cirri form cirriform or conical, or short, stout and appearing as an extension of the pygidium.

Reproductive characters. Oocyte spherical (rarely), or ovoid.

Remarks. *Namanereis* currently includes 27 accepted species recorded mainly from intertidal, supralittoral and terrestrial areas, including the freshwaters of streams, caves, and underground aquifers. Although mainly found in the tropics and subtropics one species, *Namanereis quadraticeps* (Blanchard in Gay 1849), has a circum-subantarctic/temperate distribution. Together with sister-group *Namalycastis*, they are one of only a few polychaetes to be found in association with riparian vegetation. Because they have an unadorned pharynx and a simplified parapodia, distinguishing species relies heavily on differences in chaetae and form of sensory organs of the head. The modern concept of the subfamily and genus was introduced by Hartman (1959) and reviewed by Glasby (1999), the latter who included a key to all known species at the time. Since Glasby (1999) there have been seven species described: *Namanereis canariarum* Núñez, Glasby & Naranjo, 2020, *Namanereis christopheri* Conde-Vela, 2017, *Namanereis gesae* Fiege & Van Damme, 2002, *Namanereis llanetensis* Núñez, Glasby & Naranjo, 2020, *Namanereis occulta* (Conde-Vela, 2013), *Namanereis pilbarensis* Glasby, Fiege & Van Damme, 2014, and *Namanereis socotrensis* Glasby, Fiege & Van Damme, 2014, making this genus one of the most studied in the last 20 or so years. As noted by Alves et al. (2018) in a morphological phylogenetic study of the subfamily, *Lycastoides alticola* Johnson, 1903 is also part of the *Namanereis* clade, but the species cannot take the name *Namanereis*, as *Lycastoides* is the senior genus (Read and Fauchald 2023). Conde-Vela (2017) provides an updated key to *Namanereis* species of the World.

Neanthes Kinberg, 1865

Nereis (*Neanthes*) auctt.
Nereis (*Neanthioides*) Rioja, 1918.
Praxithea Malmgren, 1867.

Type species. *Neanthes vaalii* Kinberg, 1865.

WoRMS URL. https://www.marinespecies.org/polychaeta/aphia.php?p=taxdetails&id=129378.

Sources. Bakken et al. (2022).

Diagnosis. Maxillary ring paragnaths present; neurochaetae dorsal fascicle heterogomph falcigers in anterior chaetigers present; dorsal notopodial ligule not markedly broader on posterior chaetigers; oral ring papillae absent; notochaetae homogomph falcigers absent; notochaetae sesquigomph falcigers absent; neurochaetae dorsal fascicle simple chaetae (fused falcigers) absent; Area VI smooth bars absent; notoaciculae on chaetigers 1 and 2 absent (minimal diagnosis; secondary diagnosis not attained).

Description. Palpophore barrel-shaped, approximately equal width from base to palpostyle (not overly large compared with palpostyle), or massive subconical, flattened (palpostyle is minute by comparison) (rarely). Palpophore surface without grooves or striae or with a single transverse groove (palpophores well developed) or with several oblique grooves or striae (palpophores well developed). Eyes present, or absent. Tentacular belt greater than length of chaetiger 1.

Oesophageal caeca present, or absent.

Jaws with dentate cutting edge.

Maxillary ring of pharynx with papillae absent. Maxillary ring paragnaths present. Area I conical paragnaths present; II conical paragnaths present, or absent; III conical paragnaths present, or absent; III rod-like paragnaths absent; IV paragnaths present, or absent; IV conical paragnaths present, or absent; IV smooth bar-like paragnaths present, or absent; IV rod-like paragnaths absent. Oral ring papillae absent. Oral ring paragnaths present, or absent; with Areas V, VI, and VII-VIII discrete, or comprising a continuous ring dorsally and ventrally, discrete groups not recognisable; on Areas V and VI form distinct groups, or not recognisably distinct. Area V conical paragnaths present, or absent. Area VI paragnaths present, or absent; paragnaths arranged in a roughly circular group, or in lines or arcs; conical paragnaths present; smooth bars absent. Areas VII-VIII paragnaths present, or absent; conical paragnaths present; conical paragnaths arranged in one or more irregular lines forming a continuous band; conical paragnaths similar in size, or irregular mix of large and small paragnaths in a single band, or differentiated, with a separate band of minute paragnaths also present; rod-shaped paragnaths absent.

Dorsal notopodial ligule markedly elongate on anterior chaetigers, or not markedly elongate on anterior chaetigers; markedly elongate on posterior chaetigers, or not markedly elongate on posterior chaetigers; not markedly broader on posterior chaetigers; markedly reduced on posterior chaetigers, or not markedly reduced on posterior chaetigers. Prechaetal notopodial lobe present, or absent; smaller than dorsal notopodial ligule on anterior chaetigers, usually reduced or absent posteriorly, or approximately equal to length of dorsal notopodial ligule at least on anterior chaetigers (thus notopodium of three similar sized ligules/lobes); present on all chaetigers, or restricted to a limited number of anterior chaetigers. Notopodial acicular process present, or absent; reducing in size posteriorly, last present on chaetiger 5–25. Dorsal cirrus sub-terminally attached to dorsal margin of dorsal notopodial ligule on posterior chaetigers, or not sub-terminally attached to dorsal notopodial ligule on posterior chaetigers; not terminally attached to dorsal notopodial ligule on posterior chaetigers; not terminally attached throughout all chaetigers.

Neuropodial prechaetal lobe absent. Neuropodial postchaetal lobe absent, or present; projecting beyond end of the acicular ligule, or not projecting beyond end of the acicular ligule; present throughout all chaetigers, or restricted to anterior chaetigers; digitiform. Ventral neuropodial ligule of anterior chaetigers present. Ventral neuropodial ligule of anterior chaetigers approx. as long as acicular neuropodial ligule, or short, up to half length of acicular neuropodial ligule. Ventral neuropodial ligule on posterior chaetigers present, or absent. Ventral neuropodial ligule on posterior chaetigers similar to length of acicular neuropodial ligule, or short, up to half length of acicular neuropodial ligule.

Notoaciculae on chaetigers 1 and 2 absent. Notochaetae: homogomph spinigers present. Neurochaetae dorsal fascicle: heterogomph spinigers present, or absent; homogomph spinigers present; heterogomph falcigers in anterior chaetigers present; on posterior chaetigers present, or absent; blades serrated. Neurochaetae ventral fascicle: heterogomph spinigers present, or absent; homogomph spinigers present, or absent; heterogomph falcigers present; anterior chaetigers heterogomph falcigers with long blades present, or absent; anterior chaetigers heterogomph falcigers with extra-long blades present, or absent; anterior chaetigers heterogomph falcigers with short blades present, or absent; posterior chaetigers heterogomph falcigers with long blades present, or absent; posterior chaetigers heterogomph falcigers with extra-long blades present, or absent; posterior chaetigers heterogomph falcigers with short blades present, or absent; heterogomph falcigers blade lacking distinct tendon on terminal tooth.

Anal cirri form cirriform or conical.

Remarks. *Neanthes*, even after removing some species to *Alitta* and *Pseudonereis*, was found by Bakken and Wilson (2005) to contain morphologically dissimilar species. Our diagnosis here compounds the problem since the description is expanded to include species with variable palpophore morphology (*N. gisserana* (Horst, 1924) and *N. glandicincta* (Southern, 1921)) and with elongate dorsal notopodial lobe on all chaetigers (*N. articulata* Knox, 1960, *N. crucifera* (Grube, 1878), and *N. mossambica* Day, 1957) or only on posterior chaetigers (*N. mancorae* Berkeley & Berkeley, 1961 and *N. noodti* Hartmann-Schröder, 1962). Furthermore, *Neanthes* includes a subset of species having well-developed prechaetal notopodial lobes, giving the notopodia a tri-lobed appearance, which differs from the majority of bilobed species (Bakken 2006). However, the genus must still comprise several unrelated groups. *Neanthes* currently includes 88 species. There are no comprehensive keys or identification guides but there are several tabular comparisons of subsets of species, for example Asian species (Hsueh 2019a; Villalobos-Guerrero and Idris 2021) and deep-sea species (Shimabukuro et al. 2017).

Nectoneanthes Imajima, 1972

Type species. *Nereis* (*Alitta*) *oxypoda* Marenzeller, 1879.

WoRMS URL. https://www.marinespecies.org/polychaeta/aphia.php?p=taxdetails&id=324862.

Sources. Sato (2013).

Diagnosis. Dorsal notopodial ligule markedly broader on posterior chaetigers; notochaetae sesquigomph spinigers present (minimal diagnosis). Palpophore massive subconical, flattened (palpostyle is minute by comparison); neurochaetae dorsal fascicle heterogomph spinigers present (secondary diagnosis).

Description. Palpophore massive subconical, flattened (palpostyle is minute by comparison).

Jaws with dentate cutting edge.

Maxillary ring of pharynx with papillae absent. Area I conical paragnaths present; II conical paragnaths present; III conical paragnaths present; III rod-like paragnaths absent; IV paragnaths present; IV conical paragnaths present; IV rod-like paragnaths absent. Oral ring paragnaths present; with Areas V, VI and

VII-VIII discrete; on Areas V and VI form distinct groups. Area V conical paragnaths present. Area VI paragnaths present; paragnaths arranged in a roughly circular group; conical paragnaths present; smooth bars absent. Areas VII-VIII paragnaths present; conical paragnaths present; conical paragnaths arranged in one or more irregular lines forming a continuous band; conical paragnaths similar in size, or irregular mix of large and small paragnaths in a single band; rod-shaped paragnaths absent.

Dorsal notopodial ligule markedly elongate on posterior chaetigers; markedly broader on posterior chaetigers. Prechaetal notopodial lobe present; approximately equal to length of dorsal notopodial ligule at least on anterior chaetigers (thus notopodium of three similar sized ligules/lobes); present on all chaetigers. Dorsal cirrus sub-terminally attached to dorsal margin of dorsal notopodial ligule on posterior chaetigers; not terminally attached to dorsal notopodial ligule on anterior or posterior chaetigers.

Neuropodial prechaetal lobe absent. Neuropodial postchaetal lobe present; projecting beyond end of the acicular ligule; present throughout all chaetigers; digitiform. Ventral neuropodial ligule of anterior chaetigers present. Ventral neuropodial ligule of anterior chaetigers approx. as long as acicular neuropodial ligule. Ventral neuropodial ligule on posterior chaetigers present. Ventral neuropodial ligule on posterior chaetigers similar to length of acicular neuropodial ligule. Notopodial dorsal ligule with prominent ovoid lobe medial to the dorsal cirrus in middle and posterior parapodia.

Notoaciculae on chaetigers 1 and 2 present. Notochaetae: homogomph spinigers present; sesquigomph spinigers present. Neurochaetae dorsal fascicle: heterogomph spinigers present; homogomph spinigers present; sesquigomph spinigers present. Neurochaetae ventral fascicle: heterogomph spinigers present; homogomph spinigers present; heterogomph falcigers present (in small specimens); falcigers blade tapering, with straight margin; anterior chaetigers heterogomph falcigers with long blades absent; anterior chaetigers heterogomph falcigers with extra-long blades present; anterior chaetigers heterogomph falcigers with short blades absent; posterior chaetigers heterogomph falcigers with long blades absent; posterior chaetigers heterogomph falcigers with extra-long blades present; posterior chaetigers heterogomph falcigers with short blades absent.

Anal cirri form cirriform or conical.

Remarks. *Nectoneanthes* was treated as a synonym of *Neanthes* by Wilson (1988) and Bakken and Wilson (2005). Sato (2013) showed Wilson (1988) to be incorrect in treating *Nectoneanthes oxypoda* (Marenzeller, 1879) as an epitokal form and resurrected *Nectoneanthes* and described a second species for the genus. The description by Sato (2013) is followed here.

Sato (2013) provided a key to the two species of *Nectoneanthes*; both species occur on the north-west Pacific coast, with *N. oxypoda* also recorded by Sato (2013) from southern Australia and the Persian Gulf.

Nereis **Linnaeus, 1758**

Heteronereis Örsted, 1843.
Johnstonia Quatrefages, 1850.

Lycoris Lamarck, 1818.
Naumachius Kinberg, 1865.
Nereis (*Nereis*) auctt.
Thoosa Kinberg, 1865.

Type species. *Nereis pelagica* Linnaeus, 1758.

WoRMS URL. https://www.marinespecies.org/polychaeta/aphia.php?p=taxdetails&id=129379.

Sources. Bakken et al. (2022).

Diagnosis. Notochaetae homogomph falcigers present; maxillary ring paragnaths present; Area II rod-like paragnaths absent; dorsal notopodial ligule not markedly elongate on posterior chaetigers; antennae present; oral ring papillae absent (minimal diagnosis; secondary diagnosis not attained).

Description. Palpophore barrel-shaped, approximately equal width from base to palpostyle (not overly large compared with palpostyle). Palpophore surface with a single transverse groove (palpophores well developed). Eyes present, or absent. Tentacular belt greater than length of chaetiger 1.

Oesophageal caeca present, or absent.

Jaws with smooth or slightly crenulate cutting edge or with dentate cutting edge.

Maxillary ring of pharynx with papillae absent. Maxillary ring paragnaths present. Area I conical paragnaths present, or absent; II conical paragnaths present, or absent; III conical paragnaths present, or absent; III rod-like paragnaths absent; IV paragnaths present; IV conical paragnaths present; IV smooth bar-like paragnaths present, or absent; IV rod-like paragnaths absent. Oral ring papillae absent. Oral ring paragnaths present, or absent; Areas V, VI, and VII-VIII discrete, forming distinct groups. Area V conical paragnaths present, or absent; arranged in a triangle, or in a longitudinal line. Area VI paragnaths present, or absent; paragnaths arranged in a roughly circular group; conical paragnaths present; smooth bars absent. Areas VII-VIII paragnaths present, or absent; conical paragnaths present; conical paragnaths arranged in one or more irregular lines forming a continuous band; conical paragnaths similar in size, or irregular mix of large and small paragnaths in a single band; rod-shaped paragnaths absent.

Dorsal notopodial ligule not markedly elongate on posterior chaetigers; not markedly broader on posterior chaetigers; markedly reduced on posterior chaetigers, or not markedly reduced on posterior chaetigers. Prechaetal notopodial lobe present, or absent; smaller than dorsal notopodial ligule on anterior chaetigers, usually reduced or absent posteriorly; restricted to a limited number of anterior chaetigers. Notopodial acicular process absent. Dorsal cirrus not sub-terminally attached to dorsal notopodial ligule on posterior chaetigers; not terminally attached to dorsal notopodial ligule on posterior chaetigers; not terminally attached throughout all chaetigers.

Neuropodial prechaetal lobe absent. Neuropodial postchaetal lobe absent. Ventral neuropodial ligule of anterior chaetigers present. Ventral neuropodial ligule of anterior chaetigers approx. as long as acicular neuropodial ligule. Ventral neuropodial ligule on posterior chaetigers present. Ventral neuropodial ligule on posterior chaetigers similar to length of acicular neuropodial ligule, or short, up to half length of acicular neuropodial ligule.

Notoaciculae on chaetigers 1 and 2 absent. Notochaetae: homogomph spinigers present; homogomph falcigers present. Neurochaetae dorsal fascicle: heterogomph spinigers absent; homogomph spinigers present; heterogomph falcigers in anterior chaetigers present, or absent; on posterior chaetigers present; blades serrated; blades with teeth only slightly longer proximally than distally. Neurochaetae ventral fascicle: heterogomph spinigers present, or absent; spinigers in anterior chaetigers with blades evenly serrated throughout; on posterior chaetigers with blades finely serrated proximally; homogomph spinigers absent; heterogomph falcigers present, or absent; anterior chaetigers heterogomph falcigers with long blades present, or absent; anterior chaetigers heterogomph falcigers with extra-long blades present, or absent; anterior chaetigers heterogomph falcigers with short blades absent; posterior chaetigers heterogomph falcigers with long blades present, or absent; posterior chaetigers heterogomph falcigers with extra-long blades present, or absent; posterior chaetigers heterogomph falcigers with short blades present, or absent; heterogomph falcigers blade lacking distinct tendon on terminal tooth.

Anal cirri form cirriform or conical.

Remarks. *Nereis* is the type taxon of the family Nereididae. It is a large assemblage of species, currently with 226 species attributed to the genus, many that probably belong in other genera. There are no revisions of the genus, or parts of it, or any that delineate species into informal subgroups. The description here follows Bakken et al. (2022). Some species are treated as part of revisions of single species or of several similar species (e.g., Salazar-Vallejo et al. 2021), or in treatments of species belonging to the genus in a regional perspective (e.g., Hsueh 2020).

Species of *Nereis* have been found from the littoral zone to abyssal areas, and from a wide range of habitats.

No complete identification guide to species is available but several useful keys of restricted scope have been published: Ramírez-Hernández et al. (2015) has a key to 22 species occurring in the Grand Caribbean, Hsueh (2020) includes a key to 32 species reported from East Asia, and Salazar-Vallejo et al. (2021) has a key to the 11 species previously confused with *N. falsa* de Quatrefages, 1866.

Nicon Kinberg, 1865

Type species. *Nicon pictus* Kinberg, 1865.

WoRMS URL. https://www.marinespecies.org/polychaeta/aphia.php?p=taxdetails&id=173735.

Sources. Pettibone (1971).

Diagnosis. Maxillary ring paragnaths and papillae absent; neuropodial postchaetal lobe present; dorsal notopodial ligule commences chaetiger 3; dorsal notopodial ligule not markedly reduced on posterior chaetigers; oral ring paragnaths absent; notochaetae homogomph falcigers absent (minimal diagnosis; secondary diagnosis not attained).

Description. Palpophore barrel-shaped, approximately equal width from base to palpostyle (not overly large compared with palpostyle). Palpophore surface with a single transverse groove (palpophores well developed). Eyes present, or absent. Tentacular belt greater than length of chaetiger 1.

Jaws with dentate cutting edge.

Maxillary ring of pharynx with papillae and paragnaths absent. Oral ring papillae and paragnaths absent.

Dorsal notopodial ligule present, or absent; not markedly elongate on posterior chaetigers; not markedly broader on posterior chaetigers; not markedly reduced on posterior chaetigers. Prechaetal notopodial lobe present, or absent; smaller than dorsal notopodial ligule on anterior chaetigers, usually reduced or absent posteriorly; restricted to a limited number of anterior chaetigers. Notopodial acicular process absent. Dorsal cirrus not sub-terminally attached to dorsal notopodial ligule on posterior chaetigers; not terminally attached to dorsal notopodial ligule on posterior chaetigers; not terminally attached throughout all chaetigers.

Neuropodial prechaetal lobe absent. Neuropodial postchaetal lobe present; projecting beyond end of the acicular ligule; present throughout all chaetigers, or restricted to anterior chaetigers; digitiform. Ventral neuropodial ligule of anterior chaetigers present. Ventral neuropodial ligule of anterior chaetigers approx. as long as acicular neuropodial ligule. Ventral neuropodial ligule on posterior chaetigers present. Ventral neuropodial ligule on posterior chaetigers similar to length of acicular neuropodial ligule.

Notoaciculae on chaetigers 1 and 2 absent. Notochaetae: homogomph spinigers present. Neurochaetae dorsal fascicle: heterogomph spinigers present, or absent; homogomph spinigers present; heterogomph falcigers in anterior chaetigers present, or absent; on posterior chaetigers present, or absent; blades serrated; simple chaetae (fused falcigers) present, or absent; homogomph falcigers in anterior chaetigers present, or absent. Neurochaetae ventral fascicle: sesquigomph falcigers present, or absent; heterogomph spinigers present, or absent; homogomph spinigers present, or absent; heterogomph falcigers present; anterior chaetigers heterogomph falcigers with long blades absent; anterior chaetigers heterogomph falcigers with extra-long blades present; anterior chaetigers heterogomph falcigers with short blades absent; posterior chaetigers heterogomph falcigers with long blades present, or absent; posterior chaetigers heterogomph falcigers with extra-long blades present, or absent; posterior chaetigers heterogomph falcigers with short blades absent; heterogomph falcigers blade with recurved terminal tooth and distinct tendon, or lacking distinct tendon on terminal tooth; homogomph falcigers in anterior chaetigers present, or absent.

Pygidium bilobate. Anal cirri form cirriform or conical.

Remarks. *Nicon* is not a species-rich genus: of the 700+ species of Nereididae, only ten belong to the genus *Nicon* and those ten species are from diverse habitats and widespread regions (Read and Fauchald 2023). *Nicon* species exhibit more morphologically diversity than seen in many genera of Nereididae and with only a single species included in the most recent study (Wang et al. 2021), both their phylogenetic placement within Nereididae and their monophyly are doubtful.

The two most recent studies describing new *Nicon* species, de León-González and Trovant (2013) and Wang et al. (2021), both also provided keys to the then-known species.

Olganereis Hartmann-Schröder, 1977

Type species. *Ceratocephala edmondsi* Hartman, 1954.

WoRMS URL. https://www.marinespecies.org/polychaeta/aphia.php?p=taxdetails&id=324865.

Sources. Hartmann-Schröder (1977).

Diagnosis. Maxillary ring of pharynx with papillae present; dorsal notopodial ligule markedly reduced on posterior chaetigers; ventral neuropodial ligule of anterior chaetigers present (minimal diagnosis). Ventral neuropodial ligule of anterior chaetigers short, up to half length of acicular neuropodial ligule; oral ring papillae present; prostomium anterior margin entire; Area V papillae absent (secondary diagnosis).

Description. Palpophore barrel-shaped, approximately equal width from base to palpostyle (not overly large compared with palpostyle). Tentacular belt greater than length of chaetiger 1.

Jaws with dentate cutting edge.

Maxillary ring of pharynx with papillae present; solitary. Maxillary ring paragnaths absent. Oral ring papillae present. Oral ring papillae arrangement solitary. Area V papillae absent; VI papillae present; VII-VIII papillae present. Oral ring paragnaths absent.

Dorsal notopodial ligule present; commences chaetiger 3; not markedly elongate on posterior chaetigers; not markedly broader on posterior chaetigers; markedly reduced on posterior chaetigers.

Neuropodial prechaetal lobe present. Ventral neuropodial ligule of anterior chaetigers present. Ventral neuropodial ligule of anterior chaetigers short, up to half length of acicular neuropodial ligule. Ventral neuropodial ligule on posterior chaetigers present. Ventral neuropodial ligule on posterior chaetigers similar to length of acicular neuropodial ligule.

Notochaetae: homogomph spinigers present. Neurochaetae dorsal fascicle: heterogomph spinigers absent; homogomph spinigers present; heterogomph falcigers in anterior chaetigers present; on posterior chaetigers present; blades serrated; blades with teeth only slightly longer proximally than distally. Neurochaetae ventral fascicle: heterogomph spinigers present; spinigers in anterior chaetigers with blades evenly serrated throughout; on posterior chaetigers with blades finely serrated proximally; homogomph spinigers absent; heterogomph falcigers present; falcigers blade bowed, with convex margin; heterogomph falcigers blade with recurved terminal tooth and distinct tendon.

Anal cirri form cirriform or conical.

Remarks. *Ceratocephala edmondsi* Hartman, 1954 (misspelling for *Ceratocephale*) was separated into the new genus *Olganereis* by Hartmann-Schröder (1977) because of the lack of accessory ventral cirri and presence of papillae on both oral and maxillary rings of the pharynx (characters present in *Ceratocephale* species).

Olganereis is monotypic and the sole species *O. edmondsi* (Hartman, 1954) occurs in estuaries in southern Australia. The only other Australian nereidid with papillae on both rings of the pharynx is *Dendronereides heteropoda* Southern, 1921 from tropical estuaries and in which the dorsal notopodial ligule is divided into 'branchial' filaments.

Paraleonnates Khlebovich & Wu, 1962

Ganganereis Misra, 1999.
Periserrula Paik, 1977.

Type species. *Paraleonnates uschakovi* Chlebovitsch & Wu, 1962.

WoRMS URL. https://www.marinespecies.org/polychaeta/aphia.php?p=taxdetails&id=324866.

Sources. Hong et al. (2012).

Diagnosis. Neurochaetae dorsal fascicle homogomph spinigers absent; oral ring papillae present; prostomium anterior margin entire (minimal diagnosis; secondary diagnosis not attained).

Description. Palpophore barrel-shaped, approximately equal width from base to palpostyle (not overly large compared with palpostyle). Palpophore surface with a single transverse groove (palpophores well developed).

Jaws with dentate cutting edge.

Maxillary ring of pharynx with papillae absent. Maxillary ring paragnaths present. Area I conical paragnaths present, or absent; II conical paragnaths present; III conical paragnaths present; III rod-like paragnaths absent; IV paragnaths present; IV conical paragnaths present; IV rod-like paragnaths absent. Oral ring papillae present. Oral ring papillae arrangement solitary. Area V papillae present, or absent; VI papillae present; VII-VIII papillae present. Oral ring paragnaths absent.

Dorsal notopodial ligule not markedly elongate on posterior chaetigers; not markedly broader on posterior chaetigers; not markedly reduced on posterior chaetigers. Prechaetal notopodial lobe present; approximately equal to length of dorsal notopodial ligule at least on anterior chaetigers (thus notopodium of three similar sized ligules/lobes). Dorsal cirrus not sub-terminally attached to dorsal notopodial ligule on posterior chaetigers; not terminally attached to dorsal notopodial ligule on posterior chaetigers; not terminally attached throughout all chaetigers.

Neuropodial postchaetal lobe present; projecting beyond end of the acicular ligule. Ventral neuropodial ligule of anterior chaetigers present. Ventral neuropodial ligule of anterior chaetigers approx. as long as acicular neuropodial ligule. Ventral neuropodial ligule on posterior chaetigers present. Ventral neuropodial ligule on posterior chaetigers similar to length of acicular neuropodial ligule.

Notochaetae: homogomph spinigers present. Neurochaetae dorsal fascicle: heterogomph spinigers present; homogomph spinigers absent. Neurochaetae ventral fascicle: heterogomph spinigers present; homogomph spinigers absent; heterogomph falcigers present, or absent; heterogomph falcigers blade lacking distinct tendon on terminal tooth; homogomph falcigers in anterior chaetigers present, or absent; on posterior chaetigers present, or absent.

Anal cirri form cirriform or conical.

Remarks. The most recent taxonomic treatments of *Paraleonnates* are those of Hong et al. (2012) and Conde-Vela (2019a) which form the basis of the description and diagnosis provided here. *Paraleonnates* is a genus of four species which occur in shallow muddy habitats, typically estuaries and mangroves, in the Indo-Pacific.

Conde-Vela (2019a) provides a key to three species of *Paraleonnates* but omits *Paraleonnates tenuipalpa* (Pflugfelder, 1933) which had been moved to *Paraleonnates* by Glasby et al. (2009); however, Glasby et al. (2009: 15) also note that *P. tenuipalpa* may be a senior synonym of *Paraleonnates bolus* (Hutchings & Reid, 1991).

Parasetia **Villalobos-Guerrero, Conde-Vela & Sato, 2022**

Type species. *Nereis irritabilis* Webster, 1879.

WoRMS URL. https://www.marinespecies.org/polychaeta/aphia.php?p=taxdetails&id=1600661.

Sources. Villalobos-Guerrero et al. (2022a).

Diagnosis. Neurochaetae dorsal fascicle sesquigomph falcigers present; palpophore massive subconical, flattened (palpostyle is minute by comparison); oral ring papillae absent (minimal diagnosis). Neurochaetae ventral fascicle sesquigomph falcigers present; neuropodial postchaetal lobe not projecting beyond end of the acicular ligule (secondary diagnosis).

Description. Palpophore massive subconical, flattened (palpostyle is minute by comparison). Prostomium longitudinal groove present; anterior region entire, hemispherical, longitudinal groove present; prostomial posterior region as long as anterior region. Tentacular belt greater than length of chaetiger 1.

Oesophageal caeca absent.

Jaws with smooth or slightly crenulate cutting edge.

Everted pharynx a truncate cone, tapering, greatest width at margin of tentacular belt.

Maxillary ring paragnaths present. Area I conical paragnaths absent; II conical paragnaths present; III conical paragnaths present; IV paragnaths present; IV conical paragnaths present. Oral ring paragnaths absent.

Dorsal notopodial ligule not markedly reduced on posterior chaetigers. Prechaetal notopodial lobe present; restricted to a limited number of anterior chaetigers. Notopodial acicular process present, or absent.

Neuropodial prechaetal lobe absent. Neuropodial postchaetal lobe present; not projecting beyond end of the acicular ligule; restricted to anterior chaetigers; digitiform. Ventral neuropodial ligule of anterior chaetigers present. Ventral neuropodial ligule of anterior chaetigers approx. as long as acicular neuropodial ligule. Ventral neuropodial ligule on posterior chaetigers present. Ventral neuropodial ligule on posterior chaetigers similar to length of acicular neuropodial ligule.

Notoaciculae on chaetigers 1 and 2 absent. Notochaetae: homogomph spinigers present. Neurochaetae dorsal fascicle: heterogomph spinigers absent; homogomph spinigers present; sesquigomph falcigers present; heterogomph falcigers in anterior chaetigers absent; on posterior chaetigers absent. Neurochaetae ventral fascicle: sesquigomph falcigers present; heterogomph spinigers present; homogomph spinigers absent; heterogomph falcigers absent; falcigers blade bowed, with convex margin.

Anal cirri form cirriform or conical.

Remarks. *Parasetia* was established by Villalobos-Guerrero et al. (2022a) for *Nereis irritabilis* Webster, 1878, removed from *Composetia* due to absence of oesophageal caeca and other morphological differences from a redefined *Composetia*. *Parasetia irritabilis* (Webster, 1878) occurs on the Atlantic coast of North America down to a depth of ~ 50 m.

***Perinereis* Kinberg, 1865**

Arete Kinberg, 1865.
Gnatholycastis Ehlers, 1920.
Lipephile Malmgren, 1867.
Nereis (*Lipephile*) Malmgren, 1867.
Nereis (*Perinereis*) auctt.

Type species. *Perinereis novaehollandiae* Kinberg, 1865.

WoRMS URL. https://www.marinespecies.org/polychaeta/aphia.php?p=taxdetails&id=129380.

Sources. Bakken et al. (2022); de León-González and Goethel (2013).

Diagnosis. Palpophore massive subconical, flattened (palpostyle is minute by comparison); oral ring paragnaths present; Area VI smooth bars present; antennae present (minimal diagnosis; secondary diagnosis not attained).

Description. Palpophore massive subconical, flattened (palpostyle is minute by comparison). Palpophore surface with a single transverse groove (palpophores well developed). Tentacular belt greater than length of chaetiger 1.

Jaws with smooth or slightly crenulate cutting edge or with dentate cutting edge.

Maxillary ring of pharynx with papillae absent. Maxillary ring paragnaths present. Area I conical paragnaths present or absent; II conical paragnaths present or absent; III conical paragnaths present; III rod-like paragnaths absent; IV paragnaths present; IV conical paragnaths present or absent; IV smooth bar-like paragnaths present, or absent; IV rod-like paragnaths absent. Oral ring papillae absent. Oral ring paragnaths present; with Areas V, VI, and VII-VIII discrete; on Areas V and VI form distinct groups. Area V conical paragnaths present, or absent; arranged in a triangle, or in a longitudinal line. Area VI paragnaths present, arranged in lines or arcs; conical paragnaths present, or absent; smooth bars present. Areas VII-VIII paragnaths present, or absent; conical paragnaths present; conical paragnaths arranged in one or more irregular lines forming a continuous band; conical paragnaths similar in size, or irregular mix of large and small paragnaths in a single band; rod-shaped paragnaths absent.

Dorsal notopodial ligule markedly elongate on posterior chaetigers, or not markedly elongate on posterior chaetigers; not markedly broader on posterior chaetigers; not markedly reduced on posterior chaetigers. Prechaetal notopodial lobe present, or absent; smaller than dorsal notopodial ligule on anterior chaetigers, usually reduced or absent posteriorly; restricted to a limited number of anterior chaetigers. Dorsal cirrus sub-terminally attached to dorsal margin of dorsal notopodial ligule on posterior chaetigers, or not sub-terminally attached to dorsal notopodial ligule on posterior chaetigers; not terminally attached to dorsal notopodial ligule on posterior chaetigers; not terminally attached throughout all chaetigers.

Neuropodial prechaetal lobe absent. Neuropodial postchaetal lobe absent, or present; projecting beyond end of the acicular ligule; present throughout all chaetigers, or restricted to anterior chaetigers. Ventral neuropodial ligule of anterior chaetigers present. Ventral neuropodial ligule of anterior chaetigers approx. as long as acicular neuropodial ligule. Ventral neuropodial ligule on posterior chaetigers present. Ventral neuropodial ligule on posterior chaetigers similar to length of acicular neuropodial ligule, or short, up to half length of acicular neuropodial ligule.

Notoaciculae on chaetigers 1 and 2 absent. Notochaetae: homogomph spinigers present. Neurochaetae dorsal fascicle: heterogomph spinigers absent; homogomph spinigers present; heterogomph falcigers in anterior chaetigers present; on posterior chaetigers present; blades serrated; blades with teeth only slightly longer proximally than distally, or much longer proximally than distally. Neurochaetae ventral fascicle: heterogomph spinigers present, or absent; spinigers in anterior chaetigers with blades evenly serrated throughout, or coarsely serrated proximally; on posterior chaetigers with blades finely serrated proximally; homogomph spinigers absent; heterogomph falcigers present; anterior chaetigers heterogomph falcigers with long blades present, or absent; anterior chaetigers heterogomph falcigers with extra-long blades present, or absent; anterior chaetigers heterogomph falcigers with short blades present, or absent; posterior chaetigers heterogomph falcigers with long blades present, or absent; posterior chaetigers heterogomph falcigers with extra-long blades present, or absent; posterior chaetigers heterogomph falcigers with short blades present, or absent; heterogomph falcigers blade lacking distinct tendon on terminal tooth.

Anal cirri form cirriform or conical.

Remarks. The genus *Perinereis* contains 97 species and is thus one of the most species-rich in the family (Elgetany et al. 2022). Species of *Perinereis* are recorded from global locations but are most common in shallow water, particularly where algae occur. There is much morphological diversity within the genus, notably in respect of the form of Area VI paragnaths and of notopodial lobes, so for practical identification purposes informal groupings of species have been proposed (Hutchings et al. 1991). One such grouping, the *Perinereis nuntia* species complex, has been the subject of several recent studies combing morphological and molecular evidence and is probably not monophyletic (Tosuji et al. 2019; Villalobos-Guerrero 2019; Elgetany et al. 2022). The monophyly of the other informal groupings remains untested. Glasby (2015) provides a key to Nereididae from tropical eastern Australia and Villalobos-Guerrero (2019) presents a key to 20 species then known in the *Perinereis nuntia* species complex. Most other keys to species of *Perinereis* are now of limited use since they predate the most recent 20 or so papers which add significantly to knowledge of diversity within the genus.

Platynereis **Kinberg, 1865**

Iphinereis Malmgren, 1865.
Pisenoe Kinberg, 1866.
Leontis Malmgren, 1867.
Nectonereis Verrill, 1873.
Uncinereis Chamberlin, 1919.
Nereis (*Platynereis*) auctt.

Type species. *Platynereis magalhaensis* Kinberg, 1865.

WoRMS URL. https://www.marinespecies.org/polychaeta/aphia.php?p=taxdetails&id=129381.

Sources. Bakken et al. (2022); Read (2007).

Diagnosis. Areas VII-VIII rod-shaped paragnaths present (minimal diagnosis). Notochaetae homogomph falcigers with terminal tendon present (secondary diagnosis).

Description. Palps anteriorly directed, or ventrally directed. Palpophore barrel-shaped, approximately equal width from base to palpostyle (not overly large compared with palpostyle). Palpophore surface with a single transverse groove (palpophores well developed). Tentacular belt greater than length of chaetiger 1.

Jaws with dentate cutting edge.

Maxillary ring of pharynx with papillae absent. Maxillary ring paragnaths present. Area II rod-like paragnaths present; III conical paragnaths absent; III rod-like paragnaths present; IV paragnaths present; IV conical paragnaths absent; IV rod-like paragnaths present. Oral ring papillae present, or absent. Oral ring paragnaths present; on Area V and VI form distinct groups. Area V conical paragnaths absent. Area VI paragnaths present; conical paragnaths absent; rod-shaped paragnaths present. Areas VII-VIII paragnaths present; conical paragnaths absent; conical paragnaths arranged in isolated patches, or in one or more irregular lines forming a continuous band; rod-shaped paragnaths present.

Dorsal notopodial ligule not markedly elongate on posterior chaetigers; not markedly broader on posterior chaetigers; not markedly reduced on posterior chaetigers. Dorsal cirrus sub-terminally attached to dorsal margin of dorsal notopodial ligule on posterior chaetigers; not terminally attached to dorsal notopodial ligule on posterior chaetigers; not terminally attached throughout all chaetigers.

Neuropodial postchaetal lobe absent. Ventral neuropodial ligule of anterior chaetigers present. Ventral neuropodial ligule of anterior chaetigers approx. as long as acicular neuropodial ligule. Ventral neuropodial ligule on posterior chaetigers present. Ventral neuropodial ligule on posterior chaetigers similar to length of acicular neuropodial ligule.

Notoaciculae on chaetigers 1 and 2 absent. Notochaetae: homogomph spinigers present; homogomph falcigers present; with terminal tendon present; articulation fused on some chaetigers (present as a simple chaeta), or with blade free throughout. Neurochaetae dorsal fascicle: heterogomph spinigers absent; homogomph spinigers present; heterogomph falcigers in anterior chaetigers present; on posterior chaetigers present; blades serrated; blades with teeth only slightly longer proximally than distally. Neurochaetae ventral fascicle: heterogomph spinigers present; spinigers in anterior chaetigers with blades evenly serrated throughout; on posterior chaetigers with blades finely serrated proximally; homogomph spinigers absent; heterogomph falcigers present; anterior chaetigers heterogomph falcigers with long blades absent; anterior chaetigers heterogomph falcigers with extra-long blades present; anterior chaetigers heterogomph falcigers with short blades absent; heterogomph falcigers blade lacking distinct tendon on terminal tooth.

Anal cirri form cirriform or conical.

Remarks. Species belonging to *Platynereis* are easily recognised by the small rod-like paragnaths in tight rows on the pharynx; 36 species are recognised. No revisions have been published, but regional studies using molecular data to revise species to resolve the complex taxonomy, and taxonomic history of this genus have been appearing (Wäge et al. 2017; Kara et al. 2020; Teixeira et al. 2022b). Morphological characters from reproductive specimens (epitokes) may be important to distinguish species (Read 2007). Species of *Platynereis* are found in tropical, temperate and sub-Arctic waters, primarily in shallow water among algae.

Potamonereis Villalobos-Guerrero, Conde-Vela & Sato, 2022

Type species. *Composetia kumensis* Sato, 2020.

WoRMS URL. https://www.marinespecies.org/polychaeta/aphia.php?p=taxdetails&id=1600677.

Sources. Villalobos-Guerrero et al. (2022a).

Diagnosis. Maxillary ring paragnaths present; neuropodial postchaetal lobe not projecting beyond end of the acicular ligule; notoaciculae on chaetigers 1 and 2 present; prostomium anterior margin entire (minimal diagnosis; secondary diagnosis not attained).

Description. Palpophore barrel-shaped, approximately equal width from base to palpostyle (not overly large compared with palpostyle). Prostomium longitudinal groove present; anterior region entire, hemispherical, longitudinal groove present; prostomial posterior region shorter than anterior region. Tentacular belt greater than length of chaetiger 1.

Oesophageal caeca absent.

Jaws with dentate cutting edge.

Everted pharynx a truncate cone, tapering, greatest width at margin of tentacular belt.

Maxillary ring paragnaths present. Area I conical paragnaths present, or absent; II conical paragnaths present; III conical paragnaths present; III conical paragnaths isolated lateral groups absent; IV paragnaths present; IV conical paragnaths present. Oral ring paragnaths absent.

Prechaetal notopodial lobe absent. Dorsal cirrus not sub-terminally attached to dorsal notopodial ligule on posterior chaetigers.

Neuropodial prechaetal lobe absent. Neuropodial postchaetal lobe present; not projecting beyond end of the acicular ligule; restricted to anterior chaetigers; digitiform. Ventral neuropodial ligule of anterior chaetigers present.

Notoaciculae on chaetigers 1 and 2 present. Notochaetae: homogomph spinigers present. Neurochaetae dorsal fascicle: heterogomph spinigers present, or absent; homogomph spinigers present; heterogomph falcigers in anterior chaetigers present; on posterior chaetigers present. Neurochaetae ventral fascicle: heterogomph spinigers present; homogomph spinigers absent; heterogomph falcigers present; falcigers blade tapering, with straight margin.

Anal cirri form cirriform or conical.

Remarks. *Potamonereis* was established by Villalobos-Guerrero et al. (2022a) for two former species of *Composetia* in which oesophageal caeca are absent and which have a truncate-conical pharynx, and other morphological differences (at the same time those authors redefined *Composetia*). Both species of *Potamonereis* occur in the North-west Pacific in Japanese estuaries.

***Pseudonereis* Kinberg, 1865**

Phyllonereis Hansen, 1882.

Type species. *Pseudonereis gallapagensis* Kinberg, 1865.

WoRMS URL. https://www.marinespecies.org/polychaeta/aphia.php?p=taxdetails&id=129382.

Sources. Conde-Vela (2018); Villalobos-Guerrero and Idris (2020).

Diagnosis. Maxillary ring of pharynx with P-bar paragnaths present, usually in regular comb-like rows (minimal diagnosis). Area VI shield-shaped bars present (secondary diagnosis).

Description. Palpophore barrel-shaped, approximately equal width from base to palpostyle (not overly large compared with palpostyle). Palpophore surface with a single transverse groove (palpophores well developed). Tentacular belt greater than length of chaetiger 1.

Jaws with dentate cutting edge.

Maxillary ring of pharynx with papillae absent. Maxillary ring paragnaths present; of pharynx with P-bar paragnaths present, usually in regular comb-like rows. Area I conical paragnaths present; II conical paragnaths present; III conical paragnaths present; III rod-like paragnaths absent; IV paragnaths present; IV conical paragnaths present; IV rod-like paragnaths absent. Oral ring papillae absent. Oral ring paragnaths present; with Areas V, VI and VII-VIII discrete; on Area V and VI form distinct groups. Area V conical paragnaths present, or absent. Area VI paragnaths present; paragnaths arranged in lines or arcs; conical paragnaths present, or absent; smooth bars present, or absent; shield-shaped bars present. Areas VII-VIII paragnaths present; conical paragnaths present; conical paragnaths arranged in one or more irregular lines forming a continuous band; conical paragnaths similar in size, or irregular mix of large and small paragnaths in a single band; P-bar paragnaths absent, or present.

Dorsal notopodial ligule markedly elongate on posterior chaetigers; markedly broader on posterior chaetigers; not markedly reduced on posterior chaetigers. Prechaetal notopodial lobe present, or absent. Notopodial acicular process absent. Dorsal cirrus not sub-terminally attached to dorsal notopodial ligule on posterior chaetigers; terminally attached to dorsal notopodial ligule on posterior chaetigers; not terminally attached throughout all chaetigers.

Neuropodial prechaetal lobe absent. Neuropodial postchaetal lobe absent, or present; projecting beyond end of the acicular ligule; restricted to anterior chaetigers; digitiform, or flattened. Ventral neuropodial ligule of anterior chaetigers present. Ventral neuropodial ligule on posterior chaetigers present. Ventral neuropodial ligule on posterior chaetigers similar to length of acicular neuropodial ligule, or short, up to half length of acicular neuropodial ligule.

Notoaciculae on chaetigers 1 and 2 absent. Notochaetae: homogomph spinigers present; homogomph falcigers present, or absent. Neurochaetae dorsal fascicle: heterogomph spinigers present, or absent; homogomph spinigers present, or absent; heterogomph falcigers in anterior chaetigers present; on posterior chaetigers present; blades serrated; blades with teeth only slightly longer proximally than distally. Neurochaetae ventral fascicle: homogomph spinigers absent; heterogomph falcigers present; heterogomph falcigers blade lacking distinct tendon on terminal tooth.

Anal cirri form cirriform or conical.

Remarks. *Pseudonereis* species are characterised by presence of both P-bars and comb-like rows of paragnaths in Areas II-IV (Villalobos-Guerrero and Idris 2020). The genus was found to be a monophyletic group and could be diagnosed from morphological characters (Bakken and Wilson 2005; Bakken 2007). More species have been described in recent years, and the genus description has been emended (Glasby 2015; Conde-Vela 2018; Villalobos-Guerrero and Idris 2020). The description used here follows Villalobos-Guerrero and Idris (2020). Kara et al. (2018) investigated relationships between several species using molecular data.

Species in this genus are primarily found in tropical and subtropical waters, in shallow depths. Following the last work including revised species, the genus includes 19 species (Villalobos-Guerrero and Idris 2020).

Rullierinereis Pettibone, 1971

Profundilycastis Hartmann-Schröder, 1977.

Type species. *Leptonereis zebra* Rullier, 1963.

WoRMS URL. https://www.marinespecies.org/polychaeta/aphia.php?p=taxdetails&id=129383.

Sources. Pettibone (1971); Tanaka and Sato (2017).

Diagnosis. Notochaetae homogomph falcigers present; maxillary ring paragnaths absent; neurochaetae ventral fascicle heterogomph spinigers absent (minimal diagnosis; secondary diagnosis not attained).

Description. Palpophore barrel-shaped, approximately equal width from base to palpostyle (not overly large compared with palpostyle). Tentacular belt greater than length of chaetiger 1.

Jaws with dentate cutting edge.

Maxillary ring of pharynx with papillae absent. Maxillary ring paragnaths absent. Oral ring papillae present, or absent. Oral ring paragnaths absent.

Dorsal notopodial ligule present; commences chaetiger 3; not markedly elongate on posterior chaetigers (and may be fused with dorsal cirri); not markedly broader on posterior chaetigers; markedly reduced on posterior chaetigers. Dorsal cirrus not sub-terminally attached to dorsal notopodial ligule on posterior chaetigers; not terminally attached to dorsal notopodial ligule on posterior chaetigers; not terminally attached throughout all chaetigers.

Ventral neuropodial ligule of anterior chaetigers present. Ventral neuropodial ligule of anterior chaetigers approx. as long as acicular neuropodial ligule. Ventral neuropodial ligule on posterior chaetigers present. Ventral neuropodial ligule on posterior chaetigers similar to length of acicular neuropodial ligule.

Notochaetae: homogomph spinigers present; homogomph falcigers present (on posterior chaetigers). Neurochaetae dorsal fascicle: heterogomph spinigers absent; homogomph spinigers present; heterogomph falcigers in anterior chaetigers present; on posterior chaetigers present; blades serrated; blades with teeth only slightly longer proximally than distally. Neurochaetae ventral fascicle: heterogomph spinigers absent; homogomph spinigers absent; heterogomph falcigers present; anterior chaetigers heterogomph falcigers with long blades absent; anterior chaetigers heterogomph falcigers with extra-long blades present; anterior chaetigers heterogomph falcigers with short blades absent; posterior chaetigers heterogomph falcigers with long blades present; posterior chaetigers heterogomph falcigers with short blades present.

Anal cirri form cirriform or conical.

Remarks. *Rullierinereis* is a genus with similarities to *Nicon* and *Typhlonereis* but differing in having notopodial homogomph falcigers (Tanaka and Sato 2017). Fifteen species of *Rullierinereis* are recognised and they occur widely around the world from shallow water to abyssal depths (4800 m). Tanaka and Sato (2017) revised the generic description. The only key to species is that of Pettibone (1971), but since that time nine additional species have been described.

Simplisetia **Hartmann-Schröder, 1985**

Ceratonereis (*Simplisetia*) Hartmann-Schröder, 1985.

Type species. *Nereis* (*Ceratonereis*) *aequisetis* Augener, 1913.

WoRMS URL. https://www.marinespecies.org/polychaeta/aphia.php?p=taxdetails&id=324869.

Sources. Hartmann-Schröder (1985); Bakken and Wilson (2005).

Diagnosis. Neurochaetae dorsal fascicle simple chaetae (fused falcigers) present; palpophore barrel-shaped, approximately equal width from base to palpostyle (not overly large compared with palpostyle); maxillary ring paragnaths present (minimal diagnosis; secondary diagnosis not attained).

Description. Palpophore barrel-shaped, approximately equal width from base to palpostyle (not overly large compared with palpostyle). Palpophore surface with a single transverse groove (palpophores well developed).

Jaws with dentate cutting edge.

Maxillary ring of pharynx with papillae absent. Maxillary ring paragnaths present. Area I conical paragnaths present, or absent; II conical paragnaths present; III conical paragnaths present; III rod-like paragnaths absent; IV paragnaths present; IV conical paragnaths present; IV rod-like paragnaths absent. Oral ring papillae absent. Oral ring paragnaths absent.

Dorsal notopodial ligule not markedly elongate on posterior chaetigers; not markedly broader on posterior chaetigers (rarely markedly reduced on posterior chaetigers). Prechaetal notopodial lobe present, or absent; smaller than dorsal notopodial ligule on anterior chaetigers, usually reduced or absent posteriorly; restricted to a limited number of anterior chaetigers. Notopodial acicular process present, or absent. Dorsal cirrus not sub-terminally attached to dorsal notopodial ligule on posterior chaetigers; not terminally attached to dorsal notopodial ligule on posterior chaetigers; not terminally attached throughout all chaetigers.

Neuropodial postchaetal lobe absent, or present; projecting beyond end of the acicular ligule; restricted to anterior chaetigers; digitiform. Ventral neuropodial ligule of anterior chaetigers present. Ventral neuropodial ligule of anterior chaetigers approx. as long as acicular neuropodial ligule. Ventral neuropodial ligule on posterior chaetigers present. Ventral neuropodial ligule on posterior chaetigers similar to length of acicular neuropodial ligule, or short, up to half length of acicular neuropodial ligule.

Notoaciculae on chaetigers 1 and 2 absent. Notochaetae: homogomph spinigers present. Neurochaetae dorsal fascicle: heterogomph spinigers present, or absent (only in *S. lizardensis*); homogomph spinigers present; heterogomph falcigers in anterior chaetigers present; on posterior chaetigers present; simple chaetae (fused falcigers) present. Neurochaetae ventral fascicle: heterogomph spinigers present; homogomph spinigers present (only in *Simplisetia* sp. from Phuket), or absent; heterogomph falcigers present; anterior chaetigers heterogomph falcigers with long blades absent; anterior chaetigers heterogomph falcigers with extra-long blades present; anterior chaetigers heterogomph falcigers with short blades absent; posterior chaetigers heterogomph falcigers with long blades present, or absent; posterior chaetigers heterogomph falcigers with extra-long blades present, or absent; posterior chaetigers heterogomph falcigers with short blades present, or absent; heterogomph falcigers blade lacking distinct tendon on terminal tooth.

Anal cirri form cirriform or conical.

Remarks. *Simplisetia* is a genus of estuarine nereidids characterised by the presence of fused neuropodial falcigers in posterior chaetigers and absence of oral ring paragnaths. The fused falcigers are also present in another estuarine genus, *Hediste*, and the two genera may be related (Bakken and Wilson 2005) although they are easily separated by the presence of numerous oral ring paragnaths in *Hediste*.

Simplisetia currently includes ten species, seven of which occur in Australian estuaries. Significant differences occur among *Simplisetia* species in the form of the fused falcigers.

The interactive key of Wilson et al. (2003) allowed identification of the Australian species.

Sinonereis Wu & Sun, 1979

Type species. *Sinonereis heteropoda* Wu & Sun, 1979.

WoRMS URL. https://www.marinespecies.org/polychaeta/aphia.php?p=taxdetails&id=324879.

Sources. Conde-Vela and Wu (2019).

Diagnosis. Dorsal cirrophores of chaetigers 5–7 of epitokes modified into spherical globular structures (minimal diagnosis). Dorsal notopodial ligule commences chaetiger 4; dorsal notopodial ligule not markedly elongate on posterior chaetigers; notochaetae homogomph falcigers absent (secondary diagnosis).

Description. Palpophore barrel-shaped, approximately equal width from base to palpostyle (not overly large compared with palpostyle).

Jaws with dentate cutting edge.

Maxillary ring of pharynx with papillae absent. Maxillary ring paragnaths absent. Oral ring papillae absent. Oral ring paragnaths absent.

Dorsal notopodial ligule present; commences chaetiger 4; not markedly reduced on posterior chaetigers. Prechaetal notopodial lobe present; present on all chaetigers. Notopodial acicular process absent. Dorsal cirrus not sub-terminally attached to dorsal notopodial ligule on posterior chaetigers.

Neuropodial prechaetal lobe absent. Neuropodial postchaetal lobe present; not projecting beyond end of the acicular ligule; present throughout all chaetigers; digitiform. Ventral neuropodial ligule of anterior chaetigers present. Ventral neuropodial ligule of anterior chaetigers approx. as long as acicular neuropodial ligule. Ventral neuropodial ligule on posterior chaetigers present. Ventral neuropodial ligule on posterior chaetigers similar to length of acicular neuropodial ligule.

Notoaciculae on chaetigers 1 and 2 absent. Notochaetae: homogomph spinigers present. Neurochaetae dorsal fascicle: heterogomph spinigers absent; homogomph spinigers present; heterogomph falcigers in anterior chaetigers present; on posterior chaetigers present. Neurochaetae ventral fascicle: heterogomph spinigers present; homogomph spinigers absent; heterogomph falcigers present; falcigers blade tapering, with straight margin.

Anal cirri form cirriform or conical.

Epitokes. Dorsal cirrophores of chaetigers 5–7 of epitokes modified into spherical globular structures. Natatory epitokal modifications in males commence chaetiger 22. Females without natatory modifications.

Remarks. *Sinonereis* Wu & Sun, 1979 is a monotypic genus originally based on a single epitokous specimen. An emended description including atokous characters was provided by Conde-Vela and Wu (2019).

Solomononereis Gibbs, 1971

Type species. *Solomononereis marauensis* Gibbs, 1971.

WoRMS URL. https://www.marinespecies.org/polychaeta/aphia.php?p=taxdetails&id=324870.

Sources. Nateewathana (1992); Bakken and Wilson (2005).

Diagnosis. Area II rod-like paragnaths present; prostomium anterior margin indented (minimal diagnosis). Notochaetae homogomph falcigers present; dorsal notopodial ligule markedly reduced on posterior chaetigers (secondary diagnosis).

Description. Palpophore barrel-shaped, approximately equal width from base to palpostyle (not overly large compared with palpostyle). Prostomium anterior margin indented. Tentacular belt greater than length of chaetiger 1.

Jaws with dentate cutting edge.

Maxillary ring of pharynx with papillae absent. Maxillary ring paragnaths present. Area I conical paragnaths present; II conical paragnaths absent; II rod-like paragnaths present; III conical paragnaths absent; III rod-like paragnaths present; IV paragnaths present; IV conical paragnaths absent; IV rod-like paragnaths present. Oral ring papillae absent. Oral ring paragnaths absent.

Dorsal notopodial ligule not markedly elongate on posterior chaetigers; not markedly broader on posterior chaetigers; markedly reduced on posterior chaetigers. Prechaetal notopodial lobe absent. Notopodial acicular process absent. Dorsal cirrus not sub-terminally attached to dorsal notopodial ligule on posterior chaetigers; not terminally attached to dorsal notopodial ligule on posterior chaetigers; not terminally attached throughout all chaetigers.

Neuropodial postchaetal lobe absent. Ventral neuropodial ligule of anterior chaetigers present. Ventral neuropodial ligule of anterior chaetigers approx. as long as acicular neuropodial ligule. Ventral neuropodial ligule on posterior chaetigers present. Ventral neuropodial ligule on posterior chaetigers short, up to half length of acicular neuropodial ligule.

Notoaciculae on chaetigers 1 and 2 present. Notochaetae: homogomph spinigers absent; sesquigomph spinigers present; homogomph falcigers present; homogomph falcigers with multidentate blade with 2 or more small lateral teeth, first and subsequent lateral teeth much smaller than terminal tooth present; sesquigomph falcigers present, or absent. Neurochaetae dorsal fascicle: heterogomph spinigers absent; homogomph spinigers absent; sesquigomph spinigers present; heterogomph falcigers in anterior chaetigers absent; on posterior chaetigers present; blades serrated. Neurochaetae ventral fascicle: heterogomph spinigers present; homogomph spinigers absent; heterogomph falcigers absent.

Anal cirri form cirriform or conical.

Remarks. *Solomononereis* is a genus of Nereididae sharing some similarities to members of the larger genus *Ceratonereis*. *Solomononereis*, however, can be distinguished by the presence of rod-like paragnaths on the maxillary ring. *Solomononereis* contains two species, both occurring in the tropical Indo-Pacific to a depth of ~ 30 m. Nateewathana (1992) provides a tabular comparison enabling identification of the species.

Stenoninereis Wesenberg-Lund, 1958

Type species. *Stenoninereis martini* Wesenberg-Lund, 1958.

WoRMS URL. https://www.marinespecies.org/polychaeta/aphia.php?p=taxdetails&id=324872.

Sources. Pettibone (1971); Conde-Vela (2019b).

Diagnosis. Dorsal cirrus arising from basal cirrophore; ventral neuropodial ligule of anterior chaetigers absent; palpophore surface with a single transverse groove (palpophores well developed) (minimal diagnosis). Oral ring papillae absent; maxillary ring paragnaths absent; palpostyles subconical (secondary diagnosis).

Description. Palpophore barrel-shaped, approximately equal width from base to palpostyle (not overly large compared with palpostyle). Prostomium anterior margin indented; longitudinal groove absent. Tentacular belt equal to or less than length of chaetiger 1.

Jaws with dentate cutting edge.

Maxillary ring of pharynx with papillae absent. Maxillary ring paragnaths absent. Oral ring papillae absent. Oral ring paragnaths absent.

Dorsal notopodial ligule present; commences chaetiger 3; markedly reduced on posterior chaetigers. Prechaetal notopodial lobe absent. Notopodial acicular process absent. Dorsal cirrus not sub-terminally attached to dorsal notopodial ligule on posterior chaetigers; arising from basal cirrophore; cirrophore of dorsal cirrus much longer than ventral notopodial ligule (and ciliated); cirrophore of dorsal cirrus cylindrical throughout.

Neuropodial prechaetal lobe absent. Neuropodial postchaetal lobe present; not projecting beyond end of the acicular ligule; present throughout all chaetigers; flattened (rounded). Ventral neuropodial ligule of anterior chaetigers absent. Ventral neuropodial ligule on posterior chaetigers absent.

Notoaciculae on chaetigers 1 and 2 present. Notochaetae: homogomph spinigers absent; sesquigomph spinigers present. Neurochaetae dorsal fascicle: heterogomph spinigers absent; homogomph spinigers absent; sesquigomph spinigers present; heterogomph falcigers in anterior chaetigers absent; on posterior chaetigers absent. Neurochaetae ventral fascicle: heterogomph spinigers present; homogomph spinigers absent; heterogomph falcigers present; falcigers blade tapering, with straight margin; anterior chaetigers heterogomph falcigers with long blades absent; anterior chaetigers heterogomph falcigers with extra-long blades present; anterior chaetigers heterogomph falcigers with short blades absent; posterior chaetigers heterogomph falcigers with long blades absent; posterior chaetigers heterogomph falcigers with extra-long blades present; posterior chaetigers heterogomph falcigers with short blades absent. Neuropodial heterogomph spinigers with blades basally serrate, coarse teeth, larger teeth longer than blade width, 2/3 of the blade edentate and subulate. Neuropodial heterogomph falcigers with very long blades, increasing their length from upper to lower positions in the same fascicle; falcigers with blades smooth.

Anal cirri form cirriform or conical.

Remarks. *Stenoninereis* Wesenberg-Lund, 1958 was described for a single species, *S. martini* Wesenberg-Lund, 1958. The genus now includes four small species, all occurring in sinkholes in the Caribbean-Mexico-central America region. Species of *Stenoninereis* can be identified using the key of Conde-Vela (2019b).

***Tambalagamia* Pillai, 1961**

Type species. *Tambalagamia fauveli* Pillai, 1961.

WoRMS URL. https://www.marinespecies.org/polychaeta/aphia.php?p=taxdetails&id=324873.

Sources. Shen and Wu (1993).

Diagnosis. Transverse dorsal lamellae present; neurochaetae dorsal fascicle sesquigomph spinigers absent (minimal diagnosis). Dorsal cirrus arising from basal cirrophore; tentacular belt greater than length of chaetiger 1; notochaetae sesquigomph spinigers absent (secondary diagnosis).

Description. Palpophore barrel-shaped, approximately equal width from base to palpostyle (not overly large compared with palpostyle). Prostomium anterior margin indented. Tentacular belt greater than length of chaetiger 1.

Jaws with smooth or slightly crenulate cutting edge.

Maxillary ring of pharynx with papillae absent. Maxillary ring paragnaths absent. Oral ring papillae present. Oral ring papillae arrangement solitary. Area V papillae present; VII-VIII papillae present. Oral ring paragnaths absent.

Transverse dorsal lamellae present.

Dorsal notopodial ligule present; commences chaetiger 1. Prechaetal notopodial lobe present. Dorsal cirrus arising from basal cirrophore; cirrophore of dorsal cirrus enlarged and vascularised; cirrophore of dorsal cirrus cylindrical throughout.

Ventral neuropodial ligule of anterior chaetigers present. Accessory ventral cirrus present.

Notoaciculae on chaetigers 1 and 2 absent. Notochaetae: homogomph spinigers present. Neurochaetae dorsal fascicle: heterogomph spinigers absent; homogomph spinigers present; heterogomph falcigers in anterior chaetigers absent; on posterior chaetigers absent. Neurochaetae ventral fascicle: heterogomph spinigers absent; homogomph spinigers present; heterogomph falcigers absent.

Remarks. *Tambalagamia* Pillai, 1961 is similar to *Ceratocephale* and, especially to *Gymnonereis*, with double ventral cirri being shared characters. Pettibone (1970) and Hylleberg and Nateewathana (1988) considered *Tambalagamia* to be a junior synonym of *Gymnonereis*. We follow Bakken et al. (2022) and retain *Tambalagamia* as separate pending phylogenetic analysis with better taxon sampling of both genera. *Tambalagamia* currently includes three species which can be identified using the tabular comparison of Shen and Wu (1993).

Tylonereis **Fauvel, 1911**

Type species. *Tylonereis bogoyawlenskyi* Fauvel, 1911.

WoRMS URL. https://www.marinespecies.org/polychaeta/aphia.php?p=taxdetails&id=324874.

Sources. Fauvel (1911).

Diagnosis. Dorsal notopodial ligule markedly broader on posterior chaetigers; prostomium anterior margin indented (minimal diagnosis). Maxillary ring of pharynx with papillae present; dorsal notopodial ligule markedly elongate on posterior chaetigers (secondary diagnosis).

Description. Palpophore barrel-shaped, approximately equal width from base to palpostyle (not overly large compared with palpostyle). Prostomium anterior margin indented.

Jaws with smooth or slightly crenulate cutting edge.

Maxillary ring of pharynx with papillae present; in tufts. Maxillary ring paragnaths absent. Oral ring papillae present. Oral ring papillae arrangement solitary. Area V papillae absent; VI one papillae present; VII-VIII papillae present (in a single row). Oral ring paragnaths absent. Maxillary ring papillae absent on Areas I and II, with double rows on Areas III and IV.

Dorsal notopodial ligule present; commences chaetiger 3; markedly elongate on posterior chaetigers; markedly broader on posterior chaetigers; not markedly reduced on posterior chaetigers. Dorsal cirrus not sub-terminally attached to dorsal notopodial ligule on posterior chaetigers; not terminally attached to dorsal notopodial ligule on posterior chaetigers; not terminally attached throughout all chaetigers.

Ventral neuropodial ligule of anterior chaetigers present. Ventral neuropodial ligule of anterior chaetigers approx. as long as acicular neuropodial ligule. Ventral neuropodial ligule on posterior chaetigers present. Ventral neuropodial ligule on posterior chaetigers similar to length of acicular neuropodial ligule. The neuropodial acicular ligule has three or four distinct lobes; homology of these is unclear, therefore these structures are not scored in this description.

Notoaciculae on chaetigers 1 and 2 absent. Notochaetae: homogomph spinigers present. Neurochaetae dorsal fascicle: heterogomph spinigers absent; homogomph spinigers present; heterogomph falcigers in anterior chaetigers absent; on posterior chaetigers absent. Neurochaetae ventral fascicle: heterogomph spinigers absent; homogomph spinigers present; heterogomph falcigers absent.

Remarks. *Tylonereis* is one of several genera of Nereididae from tropical estuaries which have papillae on both maxillary and oral rings of the pharynx. The genus contains three species, all known from coastal lagoons and lakes of the tropical Indo-Pacific. Tan and Chou (1994) provide a key to species.

Tylorrhynchus Grube, 1866

Type species. *Nereis heterocheta* Quatrefages, 1866.

WoRMS URL. https://www.marinespecies.org/polychaeta/aphia.php?p=taxdetails&id=324876.

Sources. Pettibone (1971).

Diagnosis. Dorsal cirrus terminally attached throughout, so that dorsal notopodial ligule has appearance of a cirrophore for the dorsal cirrus (minimal diagnosis). Acicular notopodial ligule reduced, much shorter than neuropodial acicular ligule; maxillary ring of pharynx with papillae present (secondary diagnosis).

Description. Palpophore barrel-shaped, approximately equal width from base to palpostyle (not overly large compared with palpostyle). Prostomium anterior margin indented. Tentacular belt greater than length of chaetiger 1.

Jaws with dentate cutting edge.

Maxillary ring of pharynx with papillae present. Maxillary ring paragnaths absent. Oral ring papillae present. Oral ring paragnaths absent.

Dorsal notopodial ligule absent. Prechaetal notopodial lobe absent. Notopodial acicular process absent. Acicular notopodial ligule reduced, much shorter than neuropodial acicular ligule. Dorsal cirrus length ~ 5× acicular notopodial ligule at chaetigers 10–20; not sub-terminally attached to dorsal notopodial ligule on posterior chaetigers; terminally attached throughout, so that dorsal notopodial ligule has appearance of a cirrophore for the dorsal cirrus.

Ventral neuropodial ligule of anterior chaetigers absent. Ventral neuropodial ligule on posterior chaetigers absent. The single notopodial ligule (Pettibone 1971: fig. 25b, c, e) apparently has the notoacicula and therefore cannot be the dorsal notopodial ligule. The homology of the two acicular neuropodial lobes with those of other nereidids is unclear; therefore, these structures are not scored in this description.

Notochaetae: homogomph spinigers absent; sesquigomph spinigers present. Neurochaetae dorsal fascicle: heterogomph spinigers absent; homogomph spinigers absent; sesquigomph spinigers present; heterogomph falcigers in anterior chaetigers present; on posterior chaetigers present; blades serrated. Neurochaetae ventral fascicle: heterogomph spinigers present; spinigers in anterior chaetigers with blades coarsely serrated proximally; on posterior chaetigers with blades coarsely serrated proximally; homogomph spinigers absent; heterogomph falcigers present; anterior chaetigers heterogomph falcigers with long blades absent; anterior chaetigers heterogomph falcigers with extra-long blades present; anterior chaetigers heterogomph falcigers with short blades absent; posterior chaetigers heterogomph falcigers with long blades absent; posterior chaetigers heterogomph falcigers with extra-long blades present; posterior chaetigers heterogomph falcigers with short blades absent.

Epitokes. Epitokes formed by transformation of the anterior part of the body, with the posterior part cast off (Izuka 1903; Pettibone 1971).

Remarks. *Tylorrhynchus* is known from two species, both of which occur in estuarine and fresh waters of the western Pacific Ocean (Japan, China) and the nearby north-east Pacific Ocean (Khlebovich 1996). Additional information on the biology and timing of swarming is provided by Hanafiah et al. (2006). The best taxonomic resources are Izuka (1903) and Pettibone (1971), at which time a single species was recognised. *Tylorrhynchus* is unlike other Nereididae genera in several ways including the absence of a ventral neuropodial ligule.

Typhlonereis **Hansen, 1879**

Type species. *Typhlonereis gracilis* Hansen, 1879.

WoRMS URL. https://www.marinespecies.org/polychaeta/aphia.php?p=taxdetails&id=324877.

Sources. Bakken (2003).

Diagnosis. Notochaetae of chaetigers 3 and 4 absent (minimal diagnosis). Dorsal notopodial ligule commences chaetiger 5; dorsal notopodial ligule not markedly elongate on posterior chaetigers (secondary diagnosis).

Description. Tentacular belt greater than length of chaetiger 1. Tentacular cirri extend to chaetiger 2 (longest cirrus).

Jaws with dentate cutting edge.

Maxillary ring of pharynx with papillae absent. Maxillary ring paragnaths absent. Oral ring papillae absent. Oral ring paragnaths absent.

Dorsal notopodial ligule present; commences chaetiger 5; not markedly elongate on posterior chaetigers; not markedly broader on posterior chaetigers; markedly reduced on posterior chaetigers. Prechaetal notopodial lobe absent. Notopodial acicular process absent. Dorsal cirrus length ~ 1× acicular notopodial ligule at chaetigers 10–20; sub-terminally attached to dorsal margin of dorsal notopodial ligule on posterior chaetigers; not terminally attached to dorsal notopodial ligule on posterior chaetigers; not terminally attached throughout all chaetigers.

Neuropodial prechaetal lobe absent. Neuropodial postchaetal lobe absent. Ventral neuropodial ligule of anterior chaetigers present. Ventral neuropodial ligule of anterior chaetigers approx. as long as acicular neuropodial ligule. Ventral neuropodial ligule on posterior chaetigers present. Ventral neuropodial ligule on posterior chaetigers similar to length of acicular neuropodial ligule.

Notoaciculae on chaetigers 1 and 2 absent. Notochaetae of chaetigers 3 and 4 absent. Notochaetae: homogomph spinigers present. Neurochaetae dorsal fascicle: heterogomph spinigers absent; homogomph spinigers present; heterogomph falcigers in anterior chaetigers absent; on posterior chaetigers absent. Neurochaetae ventral fascicle: heterogomph spinigers present; homogomph spinigers absent; heterogomph falcigers present; anterior chaetigers heterogomph falcigers with long blades absent; anterior chaetigers heterogomph falcigers with extra-long blades present; anterior chaetigers heterogomph falcigers with short blades absent; posterior chaetigers heterogomph falcigers with long blades absent; posterior chaetigers heterogomph falcigers with extra-long blades present; posterior chaetigers heterogomph falcigers with short blades absent.

Remarks. *Typhlonereis* is known from a single species represented by six specimens from 2222 m in the far North-east Atlantic Ocean (Bakken 2003).

The sole species, *Typhlonereis gracilis*, redescribed by Bakken (2003), is similar to *Nicon* and *Rullierinereis* and perhaps will be shown to belong instead in one of those genera.

Unanereis Day, 1962

Type species. *Unanereis macgregori* Day, 1962.

WoRMS URL. https://www.marinespecies.org/polychaeta/aphia.php?p=taxdetails&id=129384.

Sources. Day (1962).

Diagnosis. Dorsal cirrus terminally attached to dorsal notopodial ligule on posterior chaetigers; dorsal notopodial ligule not markedly broader on posterior chaetigers (minimal diagnosis). Notochaetae sesquigomph falcigers present; prostomium anterior margin entire (secondary diagnosis).

Description. Antennae present (described as having a single antenna but this is here assumed to be a mistake; likely a developmental anomaly or simply missing). Tentacular belt greater than length of chaetiger 1.

Jaws with dentate cutting edge.

Maxillary ring of pharynx with papillae absent. Maxillary ring paragnaths present. Area II conical paragnaths present; III conical paragnaths present; III rod-like paragnaths absent; IV paragnaths present; IV conical paragnaths present; IV rod-like paragnaths absent. Oral ring papillae absent. Oral ring paragnaths absent.

Dorsal notopodial ligule markedly elongate on posterior chaetigers; not markedly broader on posterior chaetigers; not markedly reduced on posterior chaetigers. Dorsal cirrus not sub-terminally attached to dorsal notopodial ligule on posterior chaetigers; terminally attached to dorsal notopodial ligule on posterior chaetigers; not terminally attached throughout all chaetigers.

Neuropodial prechaetal lobe present; extending beyond postchaetal lobe (at least in anterior chaetigers). Neuropodial postchaetal lobe present; projecting beyond end of the acicular ligule; flattened. Ventral neuropodial ligule of anterior chaetigers present. Ventral neuropodial ligule of anterior chaetigers approx. as long as acicular neuropodial ligule. Ventral neuropodial ligule on posterior chaetigers present. Ventral neuropodial ligule on posterior chaetigers short, up to half length of acicular neuropodial ligule.

Notochaetae: homogomph spinigers present; sesquigomph falcigers present; blade distally bifid. Neurochaetae dorsal fascicle: heterogomph spinigers absent; homogomph spinigers present; heterogomph falcigers in anterior chaetigers present; on posterior chaetigers present. Neurochaetae ventral fascicle: heterogomph spinigers present; homogomph spinigers absent; heterogomph falcigers present; heterogomph falcigers blade terminally bifid.

Remarks. *Unanereis* Day, 1962 was described from a single specimen found in the tube of a species of Terebellidae. A second species, *U. zghali* Ben Amor, 1980, from a vertical rocky substrate including dendrophyllid coral *Astroides calycularis* and algae *Corallina mediterranea* but without an obvious host, has been described from the Mediterranean (Ben Amor 1980). As noted by several studies, the validity of *Unanereis* is doubtful and the genus may represent developmental anomalies in specimens belonging to *Ceratonereis* or *Solomononereis* (Bakken and Wilson 2005; Santos et al. 2005; Bakken et al. 2022).

Websterinereis Pettibone, 1971

Type species. *Nereis tridentata* Webster, 1879.

WoRMS URL. https://www.marinespecies.org/polychaeta/aphia.php?p=taxdetails&id=129385.

Sources. Pettibone (1971); de León-González and Balart (2016).

Diagnosis. Oral ring papillae present; neurochaetae dorsal fascicle heterogomph falcigers in anterior chaetigers present; maxillary ring paragnaths absent; maxillary ring of pharynx with papillae absent; notochaetae homogomph falcigers absent; oral ring paragnaths absent (minimal diagnosis; secondary diagnosis not attained).

Description. Palpophore barrel-shaped, approximately equal width from base to palpostyle (not overly large compared with palpostyle). Palpophore surface with a single transverse groove (palpophores well developed). Tentacular belt equal to or less than length of chaetiger 1, or greater than length of chaetiger 1.

Jaws with dentate cutting edge.

Maxillary ring of pharynx with papillae absent. Maxillary ring paragnaths absent. Oral ring papillae present. Oral ring papillae arrangement solitary. Area V papillae absent; VI papillae present; VII-VIII papillae present. Oral ring paragnaths absent.

Dorsal notopodial ligule present; commences chaetiger 3; not markedly elongate on posterior chaetigers; not markedly broader on posterior chaetigers; not markedly reduced on posterior chaetigers. Prechaetal notopodial lobe present; smaller than dorsal notopodial ligule on anterior chaetigers, usually reduced or absent posteriorly; restricted to a limited number of anterior chaetigers. Notopodial acicular process absent. Dorsal cirrus not sub-terminally attached to dorsal notopodial ligule on posterior chaetigers; not terminally attached to dorsal notopodial ligule on posterior chaetigers; not terminally attached throughout all chaetigers.

Neuropodial postchaetal lobe present; projecting beyond end of the acicular ligule; present throughout all chaetigers; digitiform. Ventral neuropodial ligule of anterior chaetigers present. Ventral neuropodial ligule of anterior chaetigers approx. as long as acicular neuropodial ligule. Ventral neuropodial ligule on posterior chaetigers present. Ventral neuropodial ligule on posterior chaetigers similar to length of acicular neuropodial ligule.

Notoaciculae on chaetigers 1 and 2 absent. Notochaetae: homogomph spinigers present. Neurochaetae dorsal fascicle: heterogomph spinigers absent; homogomph spinigers present; heterogomph falcigers in anterior chaetigers present; on posterior chaetigers present; blades serrated; blades with teeth only slightly longer proximally than distally. Neurochaetae ventral fascicle: heterogomph spinigers present; homogomph spinigers absent; heterogomph falcigers present; anterior chaetigers heterogomph falcigers with long blades absent; anterior chaetigers heterogomph falcigers with extra-long blades present; anterior chaetigers heterogomph falcigers with short blades absent; posterior chaetigers heterogomph falcigers with long blades present, or absent; posterior chaetigers heterogomph falcigers with extra-long blades absent; posterior chaetigers heterogomph falcigers with short blades present, or absent; heterogomph falcigers blade lacking distinct tendon on terminal tooth.

Anal cirri form cirriform or conical.

Remarks. *Websterinereis* is similar to *Rullierinereis* in having the anterior margin of prostomium entire, the maxillary ring bare and papillae on the oral ring; *Websterinereis* differs from *Rullierinereis* in lacking notopodial homogomph falcigers. There are five species of *Websterinereis* which are known from the Atlantic, Indian, and Pacific Oceans, mostly from shallow water (less than ~ 130 m) except for *W. glauca*, which is recorded to a maximum depth of 3310 m. The genus was revised by de León-González and Balart (2016) who provide a key to species.

Wuinereis Khlebovich, 1996

Type species. *Leonnates simplex* Monro, 1939.

WoRMS URL. https://www.marinespecies.org/polychaeta/aphia.php?p=taxdetails&id=1039985.

Sources. Bakken et al. (2022).

Diagnosis. Oral ring papillae present; maxillary ring paragnaths present; ventral neuropodial ligule on posterior chaetigers short, up to half length of acicular neuropodial ligule (minimal diagnosis; secondary diagnosis not attained).

Description. Palpophore barrel-shaped, approximately equal width from base to palpostyle (not overly large compared with palpostyle). Tentacular belt greater than length of chaetiger 1.

Jaws with dentate cutting edge.

Maxillary ring of pharynx with papillae absent. Maxillary ring paragnaths present. Area I conical paragnaths present; II conical paragnaths present; III conical paragnaths present; III conical paragnaths isolated lateral groups absent; IV paragnaths present; IV conical paragnaths present. Oral ring papillae present. Oral ring papillae arrangement solitary. Area V papillae present; VI papillae present; VII-VIII papillae present; VII-VIII papillae arranged in a double row. Oral ring paragnaths absent.

Dorsal notopodial ligule not markedly reduced on posterior chaetigers.

Ventral neuropodial ligule of anterior chaetigers present. Ventral neuropodial ligule of anterior chaetigers approx. as long as acicular neuropodial ligule. Ventral neuropodial ligule on posterior chaetigers present. Ventral neuropodial ligule on posterior chaetigers short, up to half length of acicular neuropodial ligule.

Notoaciculae on chaetigers 1 and 2 absent. Notochaetae: homogomph spinigers present. Neurochaetae dorsal fascicle heterogomph spinigers absent; homogomph spinigers present; heterogomph falcigers in anterior chaetigers present; on posterior chaetigers present. Neurochaetae ventral fascicle: heterogomph spinigers present; homogomph spinigers absent; heterogomph falcigers present; falcigers blade tapering, with straight margin.

Remarks. *Wuinereis* was established by Khlebovich (1996) for a single species formerly placed in *Leonnates*. The two genera (and also *Paraleonnates*) are similar in having only paragnaths on the maxillary ring and only papillae on the oral ring. *Wuinereis* can be separated by chaetal and parapodial characters as per the diagnosis given here. The sole species, *W. simplex* (Monro, 1939) is known only from Aldabra Atoll in the Indian Ocean.

Acknowledgements

We are very grateful to collection managers Melanie Mackenzie and Chris Rowley (Museums Victoria Research Institute) and Gavin Dally (formerly, The Museum and Art Gallery of the Northern Territory) for their ever-willing support, to Olga Biriukova (The Museum and Art Gallery of the Northern Territory) for her assistance with image editing, and to Leon Altoff (Field Naturalists Club of Victoria) and Dr Dave Cowles (Walla Walla University) for access to photographs of polychaetes and permission to use them. Dr G.D.F. (Buz) Wilson kindly shared shell scripts for manipulating Delta output. We are grateful to Dr Masanori Sato, Dr Greg Rouse, and Dr Nathalie Yonow for comments that helped to improve the manuscript.

Additional information

Conflict of interest

The authors have declared that no competing interests exist.

Ethical statement

No ethical statement was reported.

Funding

This study was supported in part by Australian Biological Resources Study Research Grant RG18-21 to Drs Chris Glasby and Robin Wilson.

Author contributions

Conceptualization: TB, CJG, RSW. Formal analysis: RSW, CJG. Funding acquisition: CJG, RSW. Methodology: TB, RSW. Writing – original draft: RSW. Writing – review and editing: TB, CJG, RSW.

Author ORCIDs

Robin S. Wilson https://orcid.org/0000-0002-9441-2131
Christopher J. Glasby https://orcid.org/0000-0002-9464-1938
Torkild Bakken https://orcid.org/0000-0002-5188-7305

Data availability

All of the data that support the findings of this study are available in the main text or Supplementary Information.

References

Alves JA, Gunnarsson TG, Potts PM, Sutherland WJ, Gill JA (2013) Sex-biases in distribution and resource use at different spatial scales in a migratory shorebird. Ecology and Evolution 3(4): 1079–1090. https://doi.org/10.1002/ece3.503

Alves PR, Glasby CJ, Santos CSG (2018) On the use of troglomorphic characters in Namanereidinae (Annelida; Nereididae) systematics. Zootaxa 4531(2): 195–210. https://doi.org/10.11646/zootaxa.4531.2.2

Alves PR, Halanych KM, Santos CSG (2020) The phylogeny of Nereididae (Annelida) based on mitochondrial genomes. Zoologica Scripta 49(3): 366–378. https://doi.org/10.1111/zsc.12413

Alves PR, Halanych KM, Silva EP, Santos CSG (2023) Nereididae (Annelida) phylogeny based on molecular data. Organisms, Diversity & Evolution 23(3): 529–541. https://doi.org/10.1007/s13127-023-00608-9

Atlas of Living Australia (2014) Open-delta. A Java port of the Delta – Description Language for Taxonomy suite of applications into Java. Canberra, Australia. https://github.com/AtlasOfLivingAustralia/open-delta [Accessed 29 April 2014]

Bakken T (2002) A new species of *Neanthes* (Polychaeta: Nereididae) from southern Australia. Memoirs of the Museum of Victoria 59(2): 327–331. https://doi.org/10.24199/j.mmv.2002.59.4

Bakken T (2003) Redescription and resurrection of *Typhlonereis gracilis* Hansen, 1879 (Polychaeta, Nereididae). Sarsia 88(5): 346–352. https://doi.org/10.1080/00364820310002894

Bakken T (2006) Redescription of two species of *Neanthes* (Polychaeta: Nereididae) possessing a large notopodial prechaetal lobe. Scientia Marina 70S3: 27–33. https://doi.org/10.3989/scimar.2006.70s327

Bakken T (2007) Revision of *Pseudonereis* (Polychaeta, Nereididae). Zoological Journal of the Linnean Society 150(1): 145–176. https://doi.org/10.1111/j.1096-3642.2007.00289.x

Bakken T, Wilson RS (2005) Phylogeny of nereidids (Polychaeta, Nereididae) with paragnaths. Zoologica Scripta 34(5): 507–547. https://doi.org/10.1111/j.1463-6409.2005.00200.x

Bakken T, Glasby CJ, Wilson RS (2009) A review of paragnath morphology in Nereididae (Polychaeta). Zoosymposia 2(1): 305–316. https://doi.org/10.11646/zoosymposia.2.1.21

Bakken T, Glasby CJ, Santos CSG, Wilson RS (2022) 7.13.3.3 Nereididae Blainville, 1818. In: Purschke G, Böggemann M, Westheide W (Eds) Handbook of Zoology (Vol. 4) Pleistoannelida, Errantia II. De Gruyter, Osnabrück, 259–307. https://doi.org/10.1515/9783110647167-010

Banse K (1977) Gymnonereidinae new subfamily: The Nereididae (Polychaeta) with bifid parapodial neurocirri. Journal of Natural History 11(6): 609–628. https://doi.org/10.1080/00222937700770541

Ben Amor Z (1980) Presence en Mediterranee du genre *Unanereis* Day, 1962 (Polychaeta, Nereidae) et description de *U. zghali* n. sp. Bulletin De L'Office National Des Peches Republique Tunisienne 4: 13–15.

Blake JA (1985) Polychaeta from the vicinity of deep-sea geothermal vents in the eastern Pacific. I. Euphrosinidae, Phyllodocidae, Hesionidae, Nereididae, Glyceridae, Dorvilleidae, Orbiniidae and Maldanidae. Bulletin of the Biological Society of Washington 6: 67–101.

Borkent A (2021) Diagnosing diagnoses – can we improve our taxonomy? ZooKeys 1071: 43–48. https://doi.org/10.3897/zookeys.1071.72904

Cavalcanti MJ (2022) Free DELTA. An Open Source System for Processing Taxonomic Descriptions. https://freedelta.sourceforge.net/ [Accessed 31 January 2023]

Chamberlin RV (1919) The Annelida Polychaeta. Memoirs of the Museum of Comparative Zoology, Harvard 48: 1–514. https://www.biodiversitylibrary.org/ia/memoirsofmuseumo4801harv

Choi C-Y, Battley Phil F, Potter Murray A, Ma Z, Liu W (2014) Factors Affecting the Distribution Patterns of Benthic Invertebrates at a Major Shorebird Staging Site in the Yellow Sea, China. Wetlands 34(6): 1085–1096. https://doi.org/10.1007/s13157-014-0568-4

Coleman CO, Lowry JK, Macfarlane T (2010) DELTA for Beginners: An introduction into the taxonomy software package DELTA. ZooKeys 45: 1–75. https://doi.org/10.3897/zookeys.45.263

Compton TJ, Holthuijsen S, Koolhaas A, Dekinga A, ten Horn J, Smith J, Galama Y, Brugge M, van der Wal D, van der Meer J, van der Veer HW, Piersma T (2013) Distinctly variable mudscapes: Distribution gradients of intertidal macrofauna across the Dutch Wadden Sea. Journal of Sea Research 82: 103–116. https://doi.org/10.1016/j.seares.2013.02.002

Conde-Vela VM (2013) *Namalycastis occulta* n. sp. and a new record of *N. borealis* (Polychaeta: Nereididae: Namanereidinae) from the Northwestern Caribbean Sea. Zootaxa 3721(5): 475–487. https://doi.org/10.11646/zootaxa.3721.5.3

Conde-Vela VM (2017) The troglomorphic adaptations of Namanereidinae (Annelida, Nereididae) revisited, including a redescription of *Namanereis cavernicola* (Solís-Weiss & Espinasa, 1991), and a new Caribbean species of *Namanereis* Chamberlin, 1919. Subterranean Biology 23: 19–28. https://doi.org/10.3897/subtbiol.23.13701

Conde-Vela VM (2018) New species of *Pseudonereis* Kinberg, 1865 (Polychaeta: Nereididae) from the Atlantic Ocean, and a review of paragnath morphology and methodology. Zootaxa 4471(2): 245–278. https://doi.org/10.11646/zootaxa.4471.2.2

Conde-Vela VM (2019a) Re-evaluation of the morphology of the monotypic genera *Lycastonereis* Rao, 1981 and *Ganganereis* Misra, 1999 (Annelida, Phyllodocida, Nereididae). Zootaxa 4567(3): 450–460. https://doi.org/10.11646/zootaxa.4567.3.2

Conde-Vela VM (2019b) Sinkhole and brackish water nereidid polychaetes: Revision of *Stenoninereis* Wesenberg-Lund, 1958 (Annelida). Subterranean Biology 30: 95–115. https://doi.org/10.3897/subtbiol.30.36273

Conde-Vela VM (2021) Revision of *Laeonereis* Hartman, 1945 (Annelida: Phyllodocida: Gymnonereidinae), with a review of shaft morphology in nereidids. Journal of Natural History 55(7–8): 381–455. https://doi.org/10.1080/00222933.2021.1903601

Conde-Vela V, Salazar-Vallejo S (2015) Redescriptions of *Nereis oligohalina* (Rioja, 1946) and *N. garwoodi* González-Escalante & Salazar-Vallejo, 2003 and description of *N. confusa* sp. n. (Annelida, Nereididae). ZooKeys 518: 15–49. https://doi.org/10.3897/zookeys.518.9564

Conde-Vela VM, Wu X (2019) Revision of *Sinonereis* Wu & Sun, 1979 (Annelida: Nereididae). Zoosystema 41(1): e153. https://doi.org/10.5252/zoosystema2019v4a9

Conde-Vela VM, Wu X, Salazar-Vallejo SI (2018) Reevaluation and New Species of *Kainonereis* Chamberlin, 1919 (Annelida: Polychaeta: Nereididae). Zoological Studies 57: 1–24. https://doi.org/10.6620/zs.2018.57-06

Dallwitz MJ (1974) A flexible computer program for generating identification keys. Systematic Zoology 23(1): 1–50. https://doi.org/10.2307/2412239

Dallwitz MJ (1980) A general system for coding taxonomic descriptions. Taxon 29(1): 41–46. https://doi.org/10.2307/1219595

Dallwitz MJ (1989) A flexible computer program for generating identification keys. DELTA Newsletter 3: 8–13. https://www.delta-intkey.com/www/dn03-facsimile.pdf [Accessed 30 January 2023]

Dallwitz MJ (2020) Installing and running the programs of the DELTA System. Reports, Division of Entomology CSIRO Australia. https://www.delta-intkey.com/www/programs.htm [Accessed 31 January 2023]

Dallwitz MJ, Paine TA (2015) Definition of the DELTA format. Reports, Division of Entomology CSIRO Australia. https://www.delta-intkey.com/www/standard.pdf [Accessed 31 January 2023]

Dallwitz MJ, Paine TA, Zurcher EJ (1993) User's guide to the DELTA System: a general system for processing taxonomic descriptions. Reports, Division of Entomology CSIRO Australia. https://www.delta-intkey.com/www/uguide.htm [Accessed 1 October 2023]

Dallwitz MJ, Paine TA, Zurcher EJ (1995) User's guide to Intkey: a program for interactive identification and information retrieval. Reports, Division of Entomology CSIRO Australia. https://www.delta-intkey.com/www/intkey-ug.htm [Accessed 1 October 2023]

Darbyshire T (2014) Intertidal and nearshore Nereididae (Annelida) of the Falkland Islands, southwestern Atlantic, including a new species of *Gymnonereis*. ZooKeys 427: 75–108. https://doi.org/10.3897/zookeys.427.7296

Day JH (1962) Polychaeta from several localities in the western Indian Ocean. Proceedings of the Zoological Society of London 139(4): 627–656. https://doi.org/10.1111/j.1469-7998.1962.tb01597.x

Day JH (1963) The polychaete fauna of South Africa Part 8. New species and records from grab samples and dredgings. Bulletin of the British Museum, Natural History. Zoology 10: 383–445. https://doi.org/10.5962/bhl.part.20530

de León-González JA, Balart EF (2016) A new species of *Websterinereis* from the Gulf of California and redescription of *Websterinereis foli* (Fauvel, 1930) (Annelida, Nereididae). ZooKeys 614: 15–26. https://doi.org/10.3897/zookeys.614.8843

de León-González J, Goethel C (2013) A new species of *Perinereis* (Polychaeta, Nereididae) from Florida, USA, with a key to all *Perinereis* from the American continent. ZooKeys 312: 1–11. https://doi.org/10.3897/zookeys.312.4535

de León-González JA, Salazar-Vallejo SI (2003) Four new nereidid species (Annelida, Polychaeta) collected during the MUSORSTOM cruises in the Indo-Pacific Ocean. Zoosystema 25: 365–375.

de León-González JA, Solís-Weiss V (2000) A review of the polychaete family Nereididae from western Mexico. Bulletin of Marine Science 67: 549–570.

de León-González JA, Trovant B (2013) A new species of *Nicon* Kinberg, 1866 (Polychaeta, Nereididae) from Ecuador, Eastern Pacific, with a key to all known species of the genus. ZooKeys 269: 67–76. https://doi.org/10.3897/zookeys.269.4003

Duijns S, Hidayati NA, Piersma T (2013) Bar-tailed Godwits *Limosa l. lapponica* eat polychaete worms wherever they winter in Europe. Bird Study 60(4): 509–517. https://doi.org/10.1080/00063657.2013.836153

Einfeldt AL, Doucet JR, Addison JA (2014) Phylogeography and cryptic introduction of the ragworm *Hediste diversicolor* (Annelida, Nereididae) in the Northwest Atlantic. Invertebrate Biology 133(3): 232–241. https://doi.org/10.1111/ivb.12060

Elgetany AH, Struck TH, Glasby CJ (2022) Three new species of the genus *Perinereis* (Annelida, Nereididae) from Egyptian coasts. ZooKeys 1132: 163–188. https://doi.org/10.3897/zookeys.1132.87629

Fauchald K (1977) The polychaete worms. Definitions and keys to the orders, families and genera. Natural History Museum of Los Angeles County, Science Series 28: 1–188. https://repository.si.edu/handle/10088/3435

Fauvel P (1911) Annèlides polychètes du golfe Persique recueillies par M.N. Bogoyawlensky. Archives de zoologie experimentale et generale sèrie 5, 6: 353–439. [pls19–21.]

Fischer AH, Henrich T, Arendt D (2010) The normal development of *Platynereis dumerilii* (Nereididae, Annelida). Frontiers in Zoology 7(1): 1–31. https://doi.org/10.1186/1742-9994-7-31

Glasby CJ (1999) The Namanereidinae (Polychaeta: Nereididae). Part 1, Taxonomy and Phylogeny. Records of the Australian Museum 25(Supplement 25): 1–129. https://doi.org/10.3853/j.0812-7387.25.1999.1354

Glasby CJ (2015) Nereididae (Annelida: Phyllodocida) of Lizard Island, Great Barrier Reef, Australia. Zootaxa 4019(1): 207–239. https://doi.org/10.11646/zootaxa.4019.1.11

Glasby CJ, Timm T, Muir AI, Gil J (2009) Catalogue of non-marine Polychaeta (Annelida) of the World. Zootaxa 2070(1): 1–52. https://doi.org/10.11646/zootaxa.2070.1.1

Glasby CJ, Wilson RS, Bakken T (2011) Redescription of the Indo-Pacific polychaete *Neanthes pachychaeta* (Fauvel, 1918) n. comb. (Annelida, Phyllodocida, Nereididae) and its synonyms. Zoosystema 33(3): 361–376. https://doi.org/10.5252/z2011n3a5

Glasby CJ, Wei N-WV, Gibb KS (2013) Cryptic species of Nereididae (Annelida: Polychaeta) on Australian coral reefs. Invertebrate Systematics 27(3): 245–264. https://doi.org/10.1071/IS12031

Hanafiah Z, Sato M, Nakashima H, Tosuji H (2006) Reproductive Swarming of Sympatric Nereidid Polychaetes in an Estuary of the Omuta-gawa River in Kyushu, Japan, with Special Reference to Simultaneous Swarming of Two Hediste Species. Zoological Science 23(2): 205–217. https://doi.org/10.2108/zsj.23.205

Hartman O (1945) The marine annelids of North Carolina. Duke University Marine Station Bulletin no. 2: 1–54.

Hartman O (1959) Catalogue of the Polychaetous Annelids of the World. Parts 1, 2. Occasional Papers of the Allan Hancock Foundation 23: 1–628.

Hartman O, Fauchald K (1971) Deep-water benthic polychaetous annelids off New England to Bermuda and other North Atlantic Areas. Part II. Allan Hancock Monographs in Marine Biology 6: 1–327. [pls1–34.]

Hartmann-Schröder G (1975) Polychaeten der Iberischen tiefsee, gesammelt auf der 3. Reise der Meteor im Jahre 1966. Mitteilungen aus dem Zoologischen Institut und Zoologische Museum der Universität Hamburg 72: 47–73.

Hartmann-Schröder G (1977) The genera *Ceratocephale* Malmgren, *Olganereis* n. gen., and *Profundilycastis* n. gen. (Nereidae, Polychaeta) with a key to the nereid genera without chitinous paragnaths. In: Reish DJ, Fauchald K (Eds) Essays on Polychaetous Annelids in Memory of Dr. Olga Hartman. Allan Hancock Press, Los Angeles, 141–155.

Hartmann-Schröder G (1985) Revision der gattung *Ceratonereis* Kinberg (Nereididae, Polychaeta) (mit besonderer beruksichtigung der arten mit eingeschnittenem prostomium). Mitteilungen aus dem Zoologischen Institut und Zoologische Museum der Universität Hamburg 82: 37–59.

Hilbig B (1997) Family Nereididae Johnston, 1845. In: Blake JA, Hilbig B, Scott PH (Eds) The Annelida Part 2 Oligochaeta and Polychaeta: Phyllodocida (Phyllodocidae to Paralacydoniidae). Taxonomic Atlas of the Benthic Fauna of the Santa Maria Basin and the Western Santa Barbara Channel. Santa Barbara Museum of Natural History, Santa Barbara, California, 291–316.

Hong J-S, Choi B-M, Kubo A, Sato M (2012) Redescription of the giant mud worm *Paraleonnates uschakovi* Khlebovich and Wu, 1962 (Polychaeta: Nereididae) with special reference to the synonymy of *Periserrula leucophryna* Paik, 1977 and the difference from *Paraleonnates bolus* (Hutchings and Reid, 1991). Zootaxa 3490(1): 49–62. https://doi.org/10.11646/zootaxa.3490.1.4

Hsueh P-W (2018) First records of *Composetia*, *Eunereis* and *Nectoneanthes* (Annelida: Nereididae) from Taiwan, with descriptions of two new species. Zootaxa 4531(2): 211–224. https://doi.org/10.11646/zootaxa.4531.2.3

Hsueh P-W (2019a) *Neanthes* (Annelida: Nereididae) from Taiwanese waters, with description of seven new species and one new species record. Zootaxa 4554(1): 173–198. https://doi.org/10.11646/zootaxa.4554.1.5

Hsueh P-W (2019b) Two new species of nereidids (Annelida, Polychaeta) from Taiwan. Zootaxa 4652(3): 544–556. https://doi.org/10.11646/zootaxa.4652.3.10

Hsueh P-W (2020) New species of *Nereis* (Annelida, Polychaeta, Nereididae) from Taiwanese waters. Zootaxa 4802(1): 1–31. https://doi.org/10.11646/zootaxa.4802.1.1

Hutchings PA, Reid A (1990) The Nereididae (Polychaeta) from Australia – Gymnonereinae *sensu* Fitzhugh, 1987: *Australonereis*, *Ceratocephale*, *Dendronereides*, *Gymnonereis*, *Nicon*, *Olganereis* and *Websterinereis*. Records of the Australian Museum 42(1): 69–100. https://doi.org/10.3853/j.0067-1975.42.1990.107

Hutchings PA, Turvey SP (1982) The Nereididae of South Australia. Transactions of the Royal Society of South Australia 106: 93–144.

Hutchings PA, Reid A, Wilson RS (1991) *Perinereis* from Australia (Polychaeta, Nereididae) from Australia, with redescriptions of six additional species. Records of the Australian Museum 43(3): 241–274. https://doi.org/10.3853/j.0067-1975.43.1991.47

Hylleberg J, Nateewathana A (1988) Polychaetes of Thailand. Nereididae (Part 2): *Ceratocephale* and *Gymnonereis*, with description of two new species and notes on the subfamily Gymnonereidinae. Research Bulletin – Phuket Marine Biological Center 49: 1–20.

Iwamatsu S, Suzuki A, Sato M (2007) Nereidid Polychaetes as the Major Diet of Migratory Shorebirds on the Estuarine Tidal Flats at Fujimae-Higata in Japan. Zoological Science 24(7): 676–685. https://doi.org/10.2108/zsj.24.676

Izuka A (1903) Observations on the Japanese Palolo, *Ceratocephale osawai*, n.sp. Journal of the College of Science of the Imperial University, Tokyo 17: 1–37. [2 plates.]

Kara J, Macdonald AHH, Simon CA (2018) Integrative taxonomic methods reveal an incorrect synonymisation of the South African *Pseudonereis podocirra* (Schmarda) as the widespread *Pseudonereis variegata* (Grube) from Chile. Invertebrate Systematics 32(6): 1282–1297. https://doi.org/10.1071/IS18016

Kara J, Santos CSG, Macdonald AHH, Simon CA (2020) Resolving the taxonomic identities and genetic structure of two cryptic *Platynereis* Kinberg species from South Africa. Invertebrate Systematics. https://doi.org/10.1071/IS19072

Khlebovich VV (1996) Fauna of Russia and Neighbouring Countries. Polychaetous Annelids (Vol. III). Polychaetes of the family Nereididae of the Russian Seas and the adjacent waters. NAUKA publishing house, St Petersburg, 225 pp.

Khlebovich VV (2001) Caecal glands in Nereididae and a new tribe of the subfamily Nereidinae (Polychaeta, Phyllodocida). Zoosystematica Rossica 10: 33–35.

Kinberg JGH (1910) Kongliga svenska fregatten Eugenies resa omkring jorden under befäl af C. A. Virgin åren 1851–1853. Vetenskapliga iakttagelser. II, Zoologi. 3 Annulater. Kungliga Svenska Vetenskapsakademien.

Kurt G, Rezzag-Mahcene H, Kus S, Daas T, Villalobos-Guerrero TF (2021) First record of the Lessepsian nereidid *Pseudonereis anomala* Gravier, 1899 (Annelida: Nereididae) in the western Mediterranean Sea. Cahiers de Biologie Marine 62: 17–26. https://doi.org/10.21411/CBM.A.4D8612

Lawing AM, Meik JM, Schargel WE (2008) Coding Meristic Characters for Phylogenetic Analysis: A Comparison of Step-Matrix Gap-Weighting and Generalized Frequency Coding. Systematic Biology 57(1): 167–173. https://doi.org/10.1080/10635150801898938

Lim JA, Loo PL, Tan KS, Ng NK (2021) Fish culture waste improves growth and fatty acid composition of the polychaete *Namalycastis* sp. (Nereididae) and its potential use as feed for mud crabs. Aquaculture Research 52(6): 2622–2639. https://doi.org/10.1111/are.15109

Magesh M, Kvist S, Glasby C (2013) Description and phylogeny of *Namalycastis jaya* sp. n. (Polychaeta, Nereididae, Namanereidinae) from the southwest coast of India. ZooKeys 238: 31–43. https://doi.org/10.3897/zookeys.238.4014

Marshall AJ, Williams WD [Eds] (1972) Textbook of Zoology Invertebrates (7th Edn.). The Macmillan Press, London, 874 pp. https://doi.org/10.1007/978-1-349-02495-7

Nateewathana A (1992) Polychaetes of Thailand. Nereididae (Part 3): *Solomononereis phuketensis* n. sp. From euhaline environments in the andaman sea. Research Bulletin – Phuket Marine Biological Center 57: 89–96.

Olive PJW (1994) Polychaeta as a world resource: A review of patterns of exploitation as sea angling baits, and the potential for aquaculture based production. Mèmoires du Musèum National d'Histoire Naturelle 162: 603–610.

Pamungkas J, Glasby CJ (2015) Taxonomy of reproductive Nereididae (Annelida) in multispecies swarms at Ambon Island, Indonesia. ZooKeys 520: 1–25. https://doi.org/10.3897/zookeys.520.9581

Paxton H (1983) Revision of the genus *Micronereis* Polychaeta Nereididae Notophycinae. Records of the Australian Museum 35(1): 1–18. https://doi.org/10.3853/j.0067-1975.35.1983.299

Penev L, Sharkey M, Erwin T, van Noort S, Buffington M, Seltmann K, Johnson N, Taylor M, Thompson F, Dallwitz M (2009) Data publication and dissemination of interactive keys under the open access model. ZooKeys 21: 1–17. https://doi.org/10.3897/zookeys.21.274

Perkins TH (1980) Review of species previously referred to *Ceratonereis mirabilis*, and descriptions of new species of *Ceratonereis*, *Nephtys* and *Goniada* (Polychaeta). Proceedings of the Biological Society of Washington 93: 1–49.

Pettibone MH (1970) Polychaeta Errantia of the Siboga Expedition. Part IV. Some additional polychaetes of the Polynoidae, Hesionidae, Nereidae, Goniadidae, Eunicidae, and Onuphidae, selected as new species by the late Dr. Hermann Augener with remarks on other related species. Siboga-Expeditie Monographie 24: 199–270.

Pettibone MH (1971) Revision of some species referred to *Leptonereis*, *Nicon*, and *Laeonereis* (Polychaeta: Nereididae). Smithsonian Contributions to Zoology 104(104): 1–53. https://doi.org/10.5479/si.00810282.104

Qiu J-W, Qian P-Y (2000) Revision of the genus *Leonnates* Kinberg, 1866 (Polychaeta: Nereididae), with descriptions and comments on other species described in *Leonnates*. Proceedings of the Biological Society of Washington 113: 1111–1146.

Ramírez-Hernández A, Hernandes-Alcantara P, Solis-Weiss V (2015) *Nereis alacranensis*, a new species of polychaete (Annelida, Nereididae) from Alacranes Reef, southern Gulf of Mexico, with a key to *Nereis* from the Grand Caribbean. Zootaxa 4012: 156–166. https://doi.org/10.11646/zootaxa.4012.1.8

Rao CAN (1981) On two new polychaetes (Nereidae: Annelida) from estuarine waters of India. Bulletin of the Zoological Survey of India 3: 213–217.

Read GB (2007) Taxonomy of sympatric New Zealand species of *Platynereis*, with description of three new species additional to *P. australis* (Schmarda) (Annelida: Polychaeta: Nereididae). Zootaxa 1558(1): 1–28. https://doi.org/10.11646/zootaxa.1558.1.1

Read GB, Fauchald K (2023) The World Polychaeta Database. https://www.marinespecies.org/polychaeta/ [Accessed 19 March, 2023]

Rouse GW, Giribet G (2016) Phylum Annelida: The Segmented (and Some Unsegmented) Worms. In: Brusca RC, Moore W, Schuster SM (Eds) Invertebrates. Sinauer Associates, Sunderland, Massachusett.

Rouse GW, Pleijel F, Tilic E (2022) Annelida. Oxford University Press, New York. https://doi.org/10.1093/oso/9780199692309.001.0001

Ruppert EE, Barnes RD, Barnes RD (1994) Invertebrate zoology (6th ed.). Saunders College Pub, Fort Worth, 1056 pp.

Salazar-Vallejo SI, De León-González JA, Conde-Vela VM (2021) Revision of the species confused with “*Nereis falsa*” de Quatrefages, 1866 (Annelida, Nereididae). European Journal of Taxonomy 779: 1–70. https://doi.org/10.5852/ejt.2021.779.1579

Sampieri BR, Vieira PE, Teixeira MAL, Seixas VC, Pagliosa PR, Amaral ACZ, Costa FO (2021) Molecular diversity within the genus *Laeonereis* (Annelida, Nereididae) along the west Atlantic coast: Paving the way for integrative taxonomy. PeerJ 9: e11364. https://doi.org/10.7717/peerj.11364

Santos CSG (2007) Nereididae from Rocas Atoll (North-east Brazil). Arquivos do Museu Nacional, Rio de Janeiro 65: 369–380.

Santos CSG, Pleijel F, Lana PC, Rouse GW (2005) Phylogenetic relationships within Nereididae (Annelida: Phyllodocida). Invertebrate Systematics 19(6): 557–576. https://doi.org/10.1071/IS05001

Sato M (2013) Resurrection of the genus *Nectoneanthes* Imajima, 1972 (Nereididae: Polychaeta), with redescription of *Nectoneanthes oxypoda* (Marenzeller, 1879) and description of a new species, comparing them to *Neanthes succinea* (Leuckart, 1847). Journal of Natural History 47(1–2): 1–50. https://doi.org/10.1080/00222933.2012.743609

Sato M, Nakashima A (2003) A review of Asian *Hediste* species complex (Nereididae, Polychaeta) with descriptions of two new species and a redescription of *Hediste japonica* (Izuka, 1908). Zoological Journal of the Linnean Society 137(3): 403–445. https://doi.org/10.1046/j.1096-3642.2003.00059.x

Savigny J-C (1822) Systeme des annélides, principalement de celles des cotes de l’Egypte et de la Syrie, offrant les caracteres tant distinctifs que naturels des Ordres, Familles et Genres, avec la Description des Especes. Description de l’Égypte ou Recueil des Observations et des Recherches qui ont été faites en Égypte pendant l’Expédition de l’Armée Française, publié par les Ordres de sa Majesté l’Empereur Napoléon le Grand, Histoire Naturelle, Paris 1(3): 1–128. https://biodiversitylibrary.org/page/41329897

Shen S, Wu B (1993) A new species of *Tambalagamia* (Polychaeta) from Nansha Islands in South China Sea. Oceanologia et Limnologia Sinica 24: 641–644.

Shimabukuro M, Santos CSG, Alfaro-Lucas JM, Fujiwara Y, Sumida PYG (2017) A new eyeless species of *Neanthes* (Annelida: Nereididae) associated with a whale-fall community from the deep Southwest Atlantic Ocean. Deep-sea Research. Part II, Topical Studies in Oceanography 146: 27–34. https://doi.org/10.1016/j.dsr2.2017.10.013

Southern R (1921) Polychaeta of the Chilka Lake and also of fresh and brackish waters in other parts of India. Memoirs of the Indian Museum Calcutta 5: 563–659. [pls 19–31.]

Tan LT, Chou LM (1994) A new species of polychaete worm, *Tylonereis heterochaeta* (Polychaeta, Nereididae) from Singapore. The Raffles Bulletin of Zoology 42: 663–668.

Tanaka M, Sato M (2017) *Rullierinereis imajimai* nom. nov., a replacement name for *R. profunda* Imajima, 2009, secondary homonym to *R. profunda* (Hartman, 1965), formerly *Namalycastis profundus*. Zootaxa 4341(3): e428. https://doi.org/10.11646/zootaxa.4341.3.9

Teixeira MAL, Bakken T, Vieira PE, Langeneck J, Sampieri BR, Kasapidis P, Ravara A, Nygren A, Costa FO (2022a) The curious and intricate case of the European *Hediste diversicolor* (Annelida, Nereididae) species complex, with description of two new species. Systematics and Biodiversity 20(1): e2116124. https://doi.org/10.1080/14772000.2022.2116124

Teixeira MAL, Langeneck J, Vieira PE, Hernández JC, Sampieri BR, Kasapidis P, Mucciolo S, Bakken T, Ravara A, Nygren A, Costa FO (2022b) Reappraisal of the hyperdiverse *Platynereis dumerilii* (Annelida: Nereididae) species complex in the Northern Atlantic, with the description of two new species. Invertebrate Systematics 36(11): 1017–1061. https://doi.org/10.1071/IS21084

Tosuji H, Bastrop R, Götting M, Park T, Hong J-S, Sato M (2018) Worldwide molecular phylogeny of common estuarine polychaetes of the genus *Hediste* (Annelida: Nereididae), with special reference to interspecific common haplotypes found in southern Japan. Marine Biodiversity. https://doi.org/10.1007/s12526-018-0917-2

Tosuji H, Nishinosono K, Hsieh H-L, Glasby CJ, Sakaguchi T, Sato M (2019) Molecular evidence of cryptic species diversity in the *Perinereis nuntia* species group (Annelida: Nereididae) with first records of *P. nuntia* and *P. shikueii* in southern Japan. Plankton & Benthos Research 14(4): 287–302. https://doi.org/10.3800/pbr.14.287

Villalobos-Guerrero TF (2019) Redescription of two overlooked species of the *Perinereis nuntia* complex and morphological delimitation of *P. nuntia* (Savigny in Lamarck, 1818) from the Red Sea (Annelida, Nereididae). Zoosystema 41(1): e465. https://doi.org/10.5252/zoosystema2019v41a24

Villalobos-Guerrero TF, Bakken T (2018) Revision of the *Alitta virens* species complex (Annelida: Nereididae) from the North Pacific Ocean. Zootaxa 4483(2): 201–257. https://doi.org/10.11646/zootaxa.4483.2.1

Villalobos-Guerrero T, Carrera-Parra LF (2015) Redescription of *Alitta succinea* (Leuckart, 1847) and reinstatement of *A. acutifolia* (Ehlers, 1901) n. comb. based upon morphological and molecular data (Polychaeta: Nereididae). Zootaxa 3919(1): 157–178. https://doi.org/10.11646/zootaxa.3919.1.7

Villalobos-Guerrero TF, Idris I (2020) Redescriptions of a neglected species of *Pseudonereis* Kinberg, 1865 (Annelida: Nereididae) and its similar congener from the Eastern Tropical Pacific. Journal of Natural History 54(23–24): 1559–1580. https://doi.org/10.1080/00222933.2020.1810800

Villalobos-Guerrero TF, Idris I (2021) Reproductive morphology and redescriptions of some *Neanthes* Kinberg, 1865 (Annelida: Nereididae) species from the southeastern Asian seas, with comparative synoptic tables of accepted species. The European Zoological Journal 88(1): 556–594. https://doi.org/10.1080/24750263.2021.1899318

Villalobos-Guerrero TF, Kara J, Idris I (2021) Redescriptions of *Neanthes* Kinberg, 1865 (Annelida: Errantia: Nereididae) species from worldwide regions. European Journal of Taxonomy 760 (1): 101–135. https://doi.org/10.5852/ejt.2021.760.1443

Villalobos-Guerrero TF, Conde-Vela VM, Sato M (2022a) Review of *Composetia* Hartmann-Schröder, 1985 (Annelida: Nereididae), with the establishment of two new similar genera. Journal of Natural History 55(37–38): 2313–2397. https://doi.org/10.1080/00222933.2021.1976295

Villalobos-Guerrero TF, Kara J, Simon C, Idris I (2022b) Systematic review of *Neanthes* Kinberg, 1865 (Annelida: Errantia: Nereididae) from southern Africa, including a preliminary molecular phylogeny of the genus. Marine Biodiversity 52(2): 1–21. https://doi.org/10.1007/s12526-021-01244-2

Wäge J, Valvassori G, Hardege JD, Schulze A, Gambi MC (2017) The sibling polychaetes *Platynereis dumerilii* and *Platynereis massiliensis* in the Mediterranean Sea: Are phylogeographic patterns related to exposure to ocean acidification? Marine Biology 164(10): e199. https://doi.org/10.1007/s00227-017-3222-x

Wang Y, Cheng H, Wang C (2021) A new eyeless species of *Nicon* (Annelida: Nereididae) from the deep Northwest Pacific Ocean. Acta Oceanologica Sinica 40(12): 20–26. https://doi.org/10.1007/s13131-021-1886-z

Wilson RS (1985) *Nereis* and *Platynereis* (Polychaeta: Nereididae) from Victoria with description of a new species of *Nereis*. Proceedings of the Royal Society of Victoria 97: 129–138.

Wilson RS (1988) Synonymy of the genus *Nectoneanthes* Imajima, 1972, with *Neanthes* Kinberg, 1866 (Polychaeta: Nereididae). Proceedings of the Biological Society of Washington 101: 4–10.

Wilson RS (1993) Systematics of the *Perinereis nuntia* complex (Polychaeta: Nereididae) in South-eastern Australia. Records of the Australian Museum 45(3): 241–252. https://doi.org/10.3853/j.0067-1975.45.1993.22

Wilson RS, Glasby CJ (1993) A revision of the *Perinereis nuntia* species group (Polychaeta: Nereididae). Records of the Australian Museum 45(3): 253–277. https://doi.org/10.3853/j.0067-1975.45.1993.23

Wilson RS, Bakken T, Glasby CJ (2003) Nereididae (Polychaeta)-A DELTA database of genera, and Australian species. In: Wilson RS, Hutchings PA, Glasby CJ (Eds) Polychaetes: An Interactive Identification Guide. CSIRO Publishing, Melbourne.

Wilson RS, Glasby CJ, Bakken T (2023) A Taxonomic Information System for Nereididae (Annelida): morphological datasets supporting description, interactive identification and phylogenetic analysis of the family. https://doi.org/10.5281/zenodo.7776745 [Accessed 12 September, 2023]

Yoshida S (1984) Studies on the biology and aquaculture of a common polychaete, *Perinereis nuntia* (Grube). Bull. Osaka Prefect. Fish. Exp. Stn. Osaka-Fu Suisan Shikenjo Kenkyu Hokoku 6: 1–64.

Supplementary material 1

Nereididae genera Nexus format

Authors: Robin S. Wilson, Christopher J. Glasby, Torkild Bakken

Data type: nex

Copyright notice: This dataset is made available under the Open Database License (http://opendatacommons.org/licenses/odbl/1.0/). The Open Database License (ODbL) is a license agreement intended to allow users to freely share, modify, and use this Dataset while maintaining this same freedom for others, provided that the original source and author(s) are credited.

Link: https://doi.org/10.3897/zookeys.1182.104258.suppl1

Supplementary material 2

Nereididae species Nexus format

Authors: Robin S. Wilson, Christopher J. Glasby, Torkild Bakken

Data type: nex

Copyright notice: This dataset is made available under the Open Database License (http://opendatacommons.org/licenses/odbl/1.0/). The Open Database License (ODbL) is a license agreement intended to allow users to freely share, modify, and use this Dataset while maintaining this same freedom for others, provided that the original source and author(s) are credited.

Link: https://doi.org/10.3897/zookeys.1182.104258.suppl2

ZooKeys 1182: 135–151 (2023)
DOI: 10.3897/zookeys.1182.110322

Research Article

Two new species of *Sinolachnus* Hille Ris Lambers (Hemiptera, Aphididae, Lachninae) from China

Zhao-Xu Li[1,2], Jing Chen[1], Li-Yun Jiang[1], Ge-Xia Qiao[1,2]

1 *Key Laboratory of Zoological Systematics and Evolution, Institute of Zoology, Chinese Academy of Sciences, No. 1-5 Beichen West Road, Chaoyang District, Beijing 100101, China*
2 *College of Life Science, University of Chinese Academy of Sciences, No. 19, Yuquan Road, Shijingshan District, Beijing 100049, China*
Corresponding authors: Ge-Xia Qiao (qiaogx@ioz.ac.cn); Li-Yun Jiang (jiangliyun@ioz.ac.cn)

Abstract

Two new *Sinolachnus* species from China, *Sinolachnus rubusis* Qiao & Li, **sp. nov.** feeding on *Rubus* sp. from Shaanxi and Sichuan Provinces, and *Sinolachnus yunnanensis* Qiao & Li, **sp. nov.** feeding on *Elaeagnus* sp. from Yunnan Province, are described and illustrated. Keys to *Sinolachnus* species distributed in China are presented. All examined specimens are deposited in the National Zoological Museum of China, Institute of Zoology, Chinese Academy of Sciences, Beijing, China.

Key words: Alate, aphid, apterous, key, morphology, taxonomy

Academic editor: Colin Favret
Received: 1 August 2023
Accepted: 21 September 2023
Published: 12 October 2023

ZooBank: https://zoobank.org/A6D2C0AF-86C0-41F8-926E-747239AF313A

Citation: Li Z-X, Chen J, Jiang L-Y, Qiao G-X (2023) Two new species of *Sinolachnus* Hille Ris Lambers (Hemiptera, Aphididae, Lachninae) from China. ZooKeys 1182: 135–151. https://doi.org/10.3897/zookeys.1182.110322

Introduction

The aphid genus *Sinolachnus* was established by Hille Ris Lambers (1956), with *Lachnus niitakayamensis* Takahashi as type species. Subsequently, Tao (1989) described a second species, *Sinolachnus taiwanus* Tao, only based on alatae collected by a malaise trap. Chakrabarti and Das (2015) reported a new species, *Sinolachnus elaeagnensis* Chakrabarti & Das from Bhutan, with descriptions of alate viviparous females and fourth instar nymphs. Kanturski et al. (2022 [2023]) revised the genus, proposed three new species, *Sinolachnus nipponicus* Kanturski, Yeh & Lee, *Sinolachnus takahashii* Kanturski, Yeh & Lee and *Sinolachnus yushanensis* Kanturski, Yeh & Lee, suggested two new combinations, *Sinolachnus plurisensoriatus* (Zhang) (from *Cinara* Curtis) and *Sinolachnus rubi* (Ghosh & Raychaudhuri) (from *Maculolachnus* Gaumont), and transferred the genus from Tuberolachnini Oestlund to Tramini Herrich-Schaeffer. So far, eight species are recorded in *Sinolachnus*, including five species distributed in China (Kanturski et al. 2022 [2023]).

Sinolachnus is distinguished within Lachninae by the presence of numerous protuberant secondary rhinaria on the antennae of alatae (Tao 1961; Ghosh 1982; Blackman and Eastop 1994), which was further demonstrated as a reliable characteristic of the genus (Kanturski et al. 2022 [2023]); other diagnostic generic characteristics were provided including the arrangement of accessory rhinaria on antennal segment VI and several "sense pegs" on the first tarsal segments.

Herein, two new species, *Sinolachnus rubusis* Qiao & Li, sp. nov. feeding on *Rubus* sp. (Rosaceae) from Shaanxi and Sichuan Provinces, and *Sinolachnus yunnanensis* Qiao & Li, sp. nov. feeding on *Elaeagnus* sp. (Elaeagnaceae) from Yunnan Province, China, are described and illustrated. Keys to apterae and alatae of *Sinolachnus* species distributed in China are provided.

Material and methods

Morphological description

Aphid terminology and the measurements in this paper generally follow Blackman and Eastop (1994) and Kanturski et al. (2022 [2023]). The unit of measurement is millimeter (mm). The following abbreviations are used:

Ant. I, II, III, IV, V, VIb	antennal segment I, II, III, IV, V and the base of segment VI, respectively;
PT	processus terminalis;
Ant. III BD	basal diameter of antennal segment III;
URS	ultimate rostral segment;
BW URS	basal width of ultimate rostral segment;
MW hind tibia	mid-width of hind tibia;
HT Ib	basal width of first hind tarsal segment;
HT Id	dorsal length of first hind tarsal segment;
HT Iv	ventral length of first hind tarsal segment;
HT II	second hind tarsal segment;
BW SIPH	basal width of siphunculus;
DW SIPH	distal width of siphunculus;
BW Cauda	basal width of cauda;
Frontal setae	the longest seta on vertex;
Setae on Ant. III	the longest seta on antennal segment III;
Setae on Hind tibia	the longest seta on hind tibia;
Setae on Tergite I	the longest marginal seta on abdominal tergite I;
Setae on Tergite VIII	the longest seta on abdominal tergite VIII.

Specimen depositories

The holotype and paratypes of the new species are deposited in the National Zoological Museum of China, Institute of Zoology, Chinese Academy of Sciences, Beijing, China.

Taxonomy

***Sinolachnus rubusis* Qiao & Li, sp. nov.**
https://zoobank.org/E2426EA3-0D93-4EA5-AFD9-9A5F9A1DD78F
Figs 1–35, Table 1

Type material. *Holotype*: apterous viviparous female, CHINA: Shaanxi Province (Baoji City, Tongtianhe National Forest Park, 34.2133°N, 106.5861°E, altitude 1650 m), 12 July 2016, No. 37534-1-1, on *Rubus* sp., coll. R. Chen and C.C. Du.

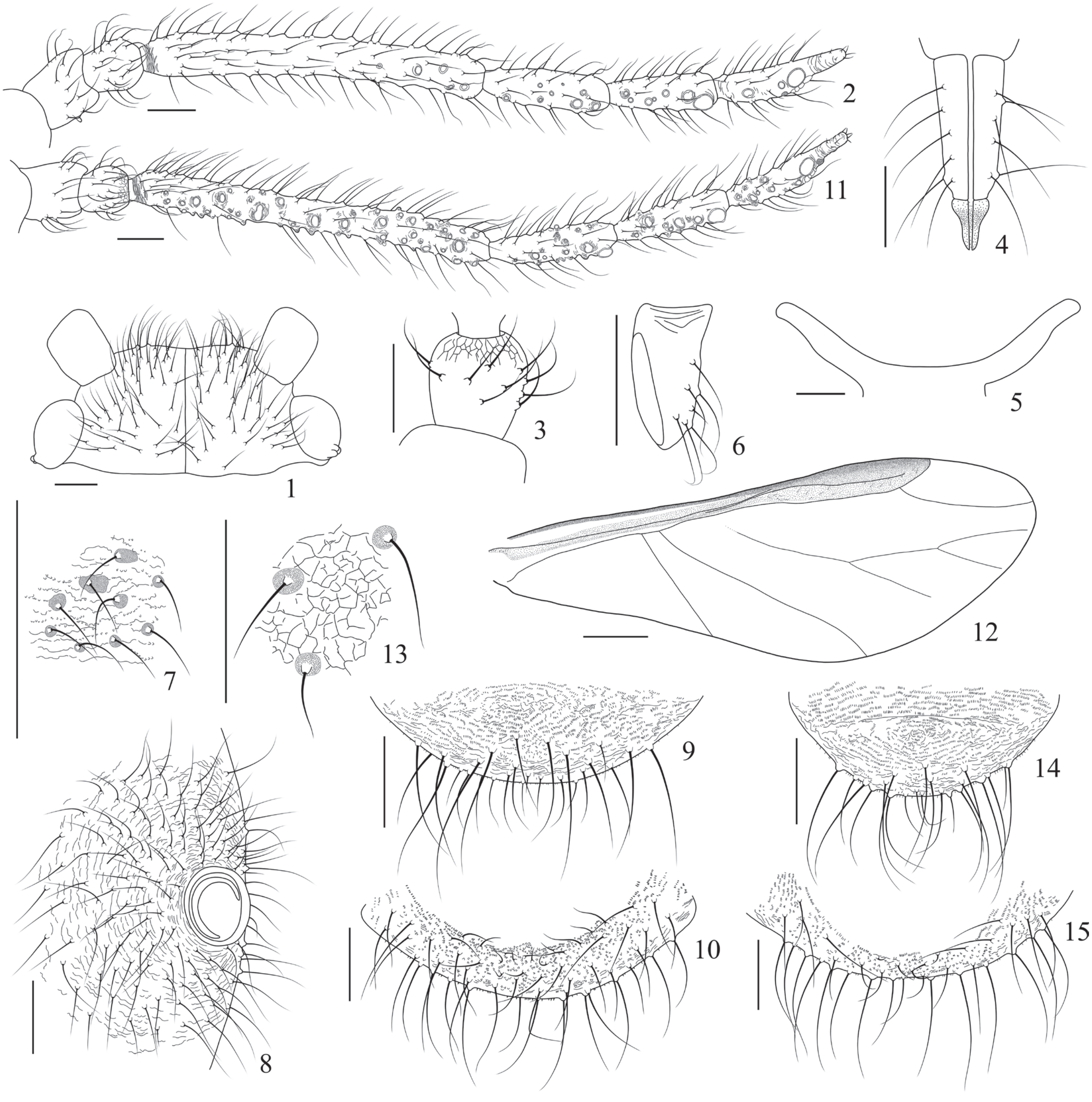

Figures 1–15. *Sinolachnus rubusis* Qiao & Li, sp. nov. Apterous viviparous female: **1** dorsal view of head **2** antenna **3** Ant. II, distal reticulations and setae shown **4** URS **5** mesosternal furca **6** hind first tarsal segment **7** spinulose imbrications and setae on abdominal tergites **8** siphunculus **9** cauda **10** anal plate. Alate viviparous female: **11** antenna **12** fore wing **13** reticulations and setae on abdominal tergites **14** cauda **15** anal plate. Scale bars: 0.10 mm (**1–11, 13–15**); 0.50 mm (**12**). (All figures were drawn according to type material No. 37534).

***Paratypes*:** seven apterous viviparous females and one alate viviparous female, with the same collection data as holotype; one apterous viviparous female and three alate viviparous females, CHINA: Sichuan Province (Ya'an City, Zhougong Mountain), 14 July 2018, No. 43462, on *Rubus* sp., coll. Yong Wang.

Etymology. The new species is named after the genus name of its host plant, *rubusis* being the masculine form.

Diagnosis. In apterae, abdominal tergites IV–VII with scattered sclerites, pleural and marginal sclerites often incompletely fused (Fig. 16). In alatae, antennae with fewer round and protuberant secondary rhinaria in various sizes, Ant. III–VI with 29–54, 5–18, 3–14, 4–8 secondary rhinaria, respectively; abdominal tergite VII without sclerites.

Description. Apterous viviparous female: Body oval, reddish-brown in life, dorsal patches and siphunculi dark brown (Fig. 34).

Mounted specimens. Head, antennal segments except basal half of Ant. III, rostral segments III–V, pronotum, mesonotum, distal half of tibiae, tarsi, siphunculi, cauda, anal plate and genital plate dark brown; other parts pale brown; coxae, trochanters, femora and basal half of tibiae pale yellowish-brown; setae on metanotum and abdominal tergites bearing dark base-sclerites. For morphometric data, see Table 1.

Head. Head dorsum smooth, with an obvious dark median suture. Head with 88–111 long and pointed dorsal setae. Frons round. Ocular tubercles well developed (Figs 1, 18). Antennae almost smooth (Figs 2, 19), distal part of Ant. II with polygonal reticulations on dorsal (Fig. 3), basal part of Ant. III and PT with transverse striae. Antennal setae fine, long and pointed, Ant. I–VI each with 20–28, 18–30, 94–139, 30–40, 34–40, 25–35+2–3 setae, respectively; apex of PT with 3–5 short blunt setae. Primary rhinaria elliptical, Ant. VI with 3–6 accessory rhinaria around primary rhinaria; secondary rhinaria almost round and protuberant in various sizes, basal diameter of secondary rhinaria about 0.006–0.038 mm, Ant. III–VI with 1–8, 2–11, 0–6 and 0–7 secondary rhinaria, respectively, along the distal part of Ant. III, the middle and distal part of Ant. IV, the entire length of Ant. V and Ant. VIb, respectively. Rostrum long, beyond hind coxae; URS wedge-shaped (Figs 4, 20), with 2–3 pairs of primary setae and 10–14 accessory setae.

Thorax. Pronotum and mesonotum with a few scattered spinules; metanotum with spinulose imbrications and small scattered sclerites, pleural and marginal sclerites sometimes fused. Dorsal setae numerous, fine and pointed. Mesosternal furca with a short stem (Figs 5, 21). Legs normal, with long and pointed setae. First tarsal chaetotaxy: 12–16, 9–14, 8–10; first fore tarsal segments with 6–9 peg-like setae and 5–8 long setae, first mid-tarsal segments with 3–6 peg-like setae and 5–9 long setae, first hind tarsal segments with 1–3 peg-like setae and 6–9 long setae.

Abdomen. Abdominal tergites I–VI with spinulose imbrications (Figs 7, 23), tergites VII, VIII and venter with spinulose stripes. Abdominal tergites I–III with a few small scattered sclerites, sclerites on tergite III more obvious than tergites I and II; tergites IV–VII with scattered sclerites, pleural and marginal sclerites often incompletely fused (Fig. 16), sometimes sclerites reduced (Fig. 17); tergite VIII with a transverse band; intersegmental muscle sclerites small and dark. Dorsal setae numerous, long and pointed. Abdominal tergite VIII with 31–54 setae. Spiracles round to oval, open or closed, on brown spiracular plates. Siphunculi truncate, on dark brown seta-bearing cones, with flange and transverse striae (Figs 8, 24), surrounding by 88–142 setae. Cauda round with spinulose stripes, with 28–36 long or short setae (Figs 9, 25). Anal plate broadly round with spinules, with 66–88 long or short setae (Figs 10, 26). Genital plate transverse elliptical with spinulose stripes, with 100–129 setae (Fig. 27). Genopophyses three, each with 10–14, 9–12, 8–13 setae, respectively.

Alate viviparous female: Body elongate-oval, brown in life, with dark brown siphunculi (Fig. 35).

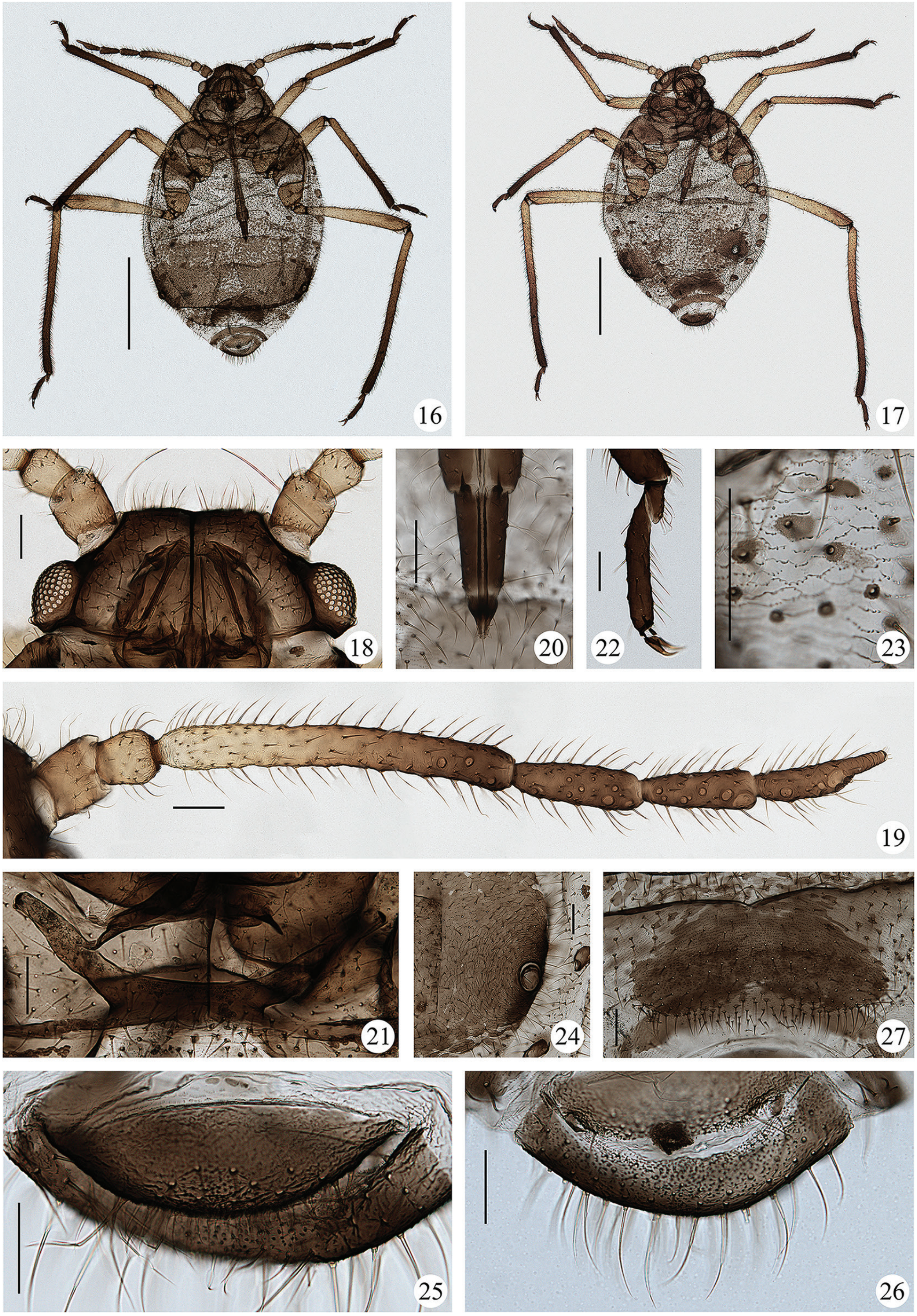

Figures 16–27. *Sinolachnus rubusis* Qiao & Li, sp. nov. Apterous viviparous female: **16** dorsal view of body with large fused sclerites **17** dorsal view of body with scattered sclerites **18** dorsal view of head **19** antenna **20** URS **21** mesosternal furca **22** hind tarsi and claws **23** spinulose imbrications on abdominal tergites **24** siphunculus **25** cauda **26** anal plate **27** genital plate. Scale bars: 1.00 mm (**16, 17**); 0.10 mm (**18–27**). (All figures were photographed according to type material No. 37534)

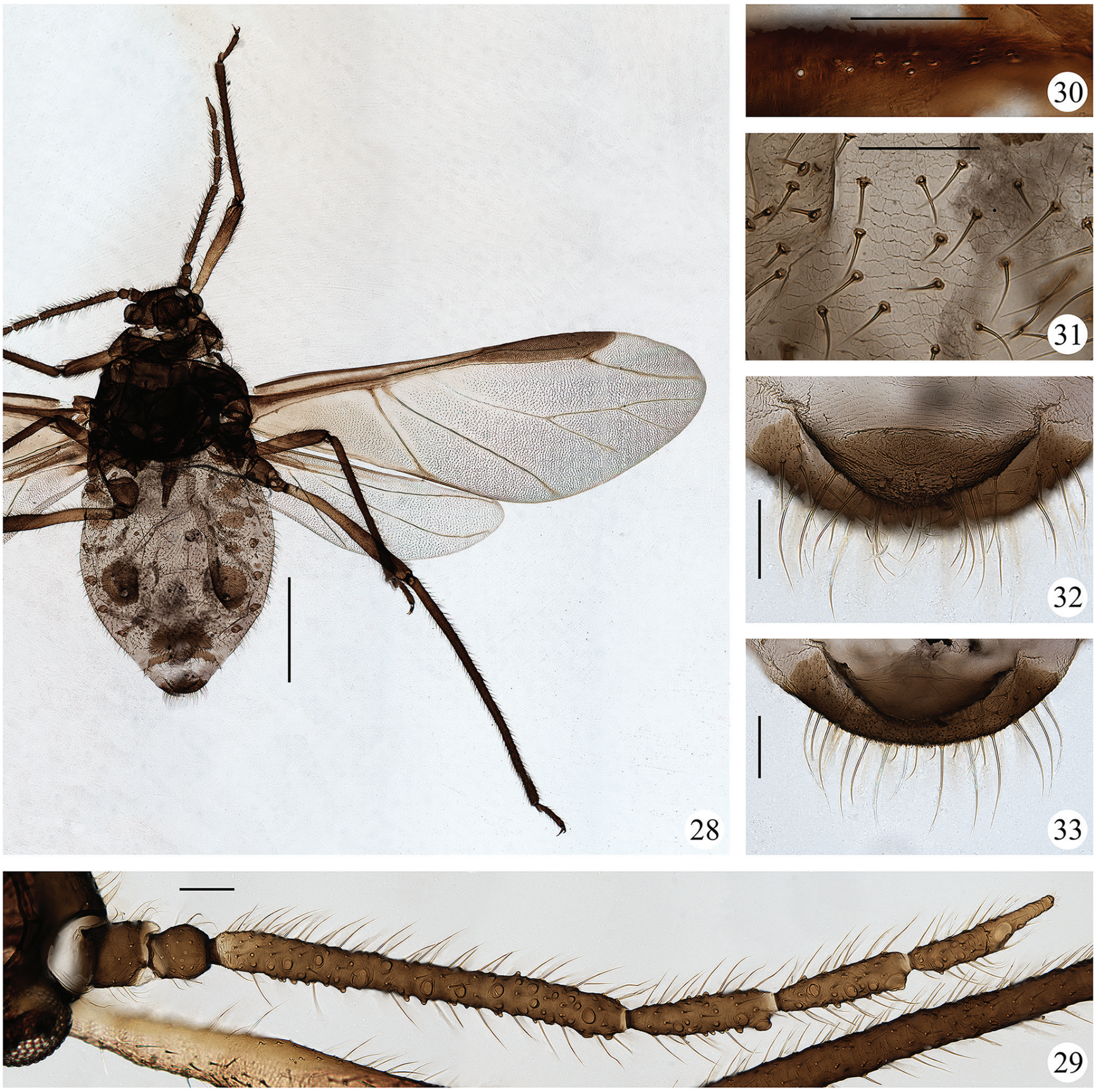

Figures 28–33. *Sinolachnus rubusis* Qiao & Li, sp. nov. Alate viviparous female: **28** dorsal view of body **29** antenna **30** sensilla on subcostal of fore wing **31** reticulations on abdominal tergites **32** cauda **33** anal plate. Scale bars: 1.00 mm (**28**); 0.10 mm (**29–33**). (All figures were photographed according to type material No. 37534)

Mounted specimens. Head, antennae, rostral segments III–V, thorax, legs except basal half of tibiae, siphunculi, cauda, anal plate and genital plate dark brown, other parts pale brown; dorsal setae on abdominal tergites bearing dark base-sclerites. For morphometric data, see Table 1.

Head. Head dorsum smooth with an obvious dark median suture. Head with 70–88 long and pointed dorsal setae. Frons flat. Ocular tubercles well developed. Antennae almost smooth (Figs 11, 29), distal part of Ant. II with polygonal reticulations and distinct on dorsal, obvious or weak on ventral; basal part of Ant. III and PT with transverse striae. Antennal setae long and pointed, Ant. I–VI each with 22–24, 18–29, 88–129, 21–38, 33–43, 24–32+2–3 setae, respectively; apex of PT with 4–6 short blunt setae. Primary rhinaria elliptical,

Figures 34–35. *Sinolachnus rubusis* Qiao & Li, sp. nov. **34** a colony on the root of the host, visited by ants **35** alate viviparous female.

Ant. VI with 5 accessory rhinaria around primary rhinaria; secondary rhinaria almost round and protuberant in various sizes, basal diameter of secondary rhinaria about 0.008–0.046 mm, Ant. III–VI with 29–54, 5–18, 3–14, 4–8 secondary rhinaria respectively along the entire length of Ant. III–V and base of Ant. VI. Rostrum long, reaching hind coxae; URS wedge-shaped, with 3 pairs of primary setae and 9–12 accessory setae.

Thorax. Legs normal, with long and pointed setae. First tarsal chaetotaxy: 10–15, 10, 6–9; first fore tarsal segments with 6–11 peg-like setae and 4 or 5 long setae, first mid-tarsal segments with 4 or 5 peg-like setae and 5 or 6 long setae, first hind tarsal segments with 2 peg-like setae and 4–7 long setae. Wings with scaly imbrications entirely (Fig. 28); campaniform sensilla near the base of subcosta slightly protuberant (Fig. 30), fore wings and hind wings with 10–13 and 11–20 campaniform sensilla on basal part, respectively; fore wings with pale media twice branched and faint on basal part (Fig. 12), pterostigma with 25–27 setae; hind wings with two oblique veins.

Abdomen. Abdominal tergites smooth, tergites I–VI with polygonal reticulations (Figs 13, 31), tergites VII, VIII and venter with spinulose stripes. Abdominal tergites II–IV each with 1 pair of marginal sclerites, sclerites on tergite IV relatively smaller, tergite VIII with a transverse band; intersegmental muscle sclerites small and dark. Dorsal setae on abdomen long and pointed, relatively sparse than on venter. Abdominal tergite VIII with 29–33 setae. Spiracles round and closed, on brown spiracular plates. Siphunculi truncate, on dark brown seta-bearing cones, with flange and transverse striae, surrounding by 123–156 setae. Cauda elliptical with spinulose stripes, with 26–30 long or short setae (Figs 14, 32). Anal plate broadly round with spinules, with 54–64 setae (Figs 15, 33). Genital plate transverse elliptical with spinulose stripes, with 87–105 setae. Genopophyses three, each with 12, 14, 12 setae.

Distribution. China (Shaanxi, Sichuan).

Host plant. *Rubus* sp. (Rosaceae).

Biology. The species feeds on roots of host plants and was visited by ants.

Comments. Apterae of the new species are related to *Sinolachnus rubi* in having abdominal tergites with scattered sclerites and sometimes fused. *Sinolachnus rubi* was originally regarded as a member of *Maculolachnus*, but transferred to *Sinolachnus* by Kanturski et al. (2022 [2023]). Based on the detailed

Table 1. Morphometric data of *Sinolachnus rubusis* Qiao & Li, sp. nov. (measurements in mm, with means in brackets).

	Characters	**Apterous viviparous females (*N* = 9)**	**Alate viviparous females (*N* = 4)**
Length (mm)	Body length	3.19–3.67 (3.42)	3.65–3.69 (3.67)
	Body width	1.97–2.47 (2.25)	1.73–1.85 (1.79)
	Antenna	1.56–1.84 (1.71)	1.66–1.88 (1.73)
	Ant. I	0.14–0.17 (0.15)	0.14–0.15 (0.14)
	Ant. II	0.11–0.13 (0.12)	0.10–0.11 (0.10)
	Ant. III	0.59–0.77 (0.69)	0.69–0.79 (0.72)
	Ant. IV	0.20–0.26 (0.23)	0.21–0.28 (0.24)
	Ant. V	0.21–0.26 (0.22)	0.23–0.26 (0.24)
	Ant. VIb	0.16–0.22 (0.19)	0.18–0.20 (0.19)
	PT	0.09–0.11 (0.10)	0.09–0.10 (0.09)
	URS	0.24–0.26 (0.25)	0.23–0.25 (0.24)
	Hind femur	1.15–1.34 (1.27)	1.35–1.44 (1.40)
	Hind tibia	1.90–2.28 (2.13)	2.28–2.51 (2.39)
	HT Ib	0.05–0.06 (0.05)	0.05
	HT Id	0.02	0.02
	HT Iv	0.10–0.12 (0.11)	0.10–0.11 (0.10)
	HT II	0.31–0.37 (0.33)	0.31–0.35 (0.33)
	BW SIPH	0.36–0.43 (0.40)	0.41–0.44 (0.42)
	DW SIPH	0.11–0.12 (0.11)	0.10
	Cauda	0.13–0.15 (0.14)	0.12–0.13 (0.12)
	BW Cauda	0.31–0.40 (0.36)	0.26–0.32 (0.28)
	Ant. III BD	0.04–0.05 (0.05)	0.04–0.05 (0.04)
	MW hind tibia	0.09–0.10 (0.09)	0.08–0.09 (0.08)
	Frontal setae	0.09–0.12 (0.10)	0.10–0.11 (0.11)
	Setae on Tergite I	0.09–0.11 (0.10)	0.10–0.13 (0.11)
	Setae on Tergite VIII	0.11–0.14 (0.13)	0.11–0.13 (0.12)
	Setae on Ant. III	0.08–0.10 (0.09)	0.10–0.11 (0.10)
	Setae on Hind tibia	0.09–0.10 (0.09)	0.11–0.12 (0.11)
Ratio (times)	Body length/Body width	1.40–1.62 (1.52)	1.99–2.11 (2.05)
	Whole antenna/Body	0.44–0.57 (0.50)	0.45–0.51 (0.48)
	Hind femur/Ant. III	1.74–1.93 (1.85)	1.82–1.94 (1.88)
	Hind tibia/Body	0.56–0.69 (0.62)	0.62–0.68 (0.65)
	PT/Ant. VIb	0.41–0.62 (0.51)	0.44–0.54 (0.49)
	URS/BW URS	2.63–3.37 (2.90)	2.93–3.21 (3.10)
	URS/HT II	0.65–0.81 (0.75)	0.71–0.77 (0.75)
	HT Ib/HT Id	2.26–3.47 (2.68)	2.25–2.71 (2.44)
	HT Ib/HT Iv	0.42–0.48 (0.46)	0.41–0.48 (0.44)
	Frontal setae/Ant. III BD	1.87–2.86 (2.18)	2.28–2.80 (2.56)
	Setae on Tergite I/Ant. III BD	1.89–2.43 (2.16)	2.32–3.18 (2.64)
	Setae on Tergite VIII/Ant. III BD	2.49–3.09 (2.78)	2.66–3.05 (2.88)
	Setae on Ant. III/Ant. III BD	1.74–2.38 (1.96)	2.21–2.65 (2.42)
	Setae on Hind tibia/MW hind tibia	0.95–1.09 (1.01)	1.30–1.57 (1.43)
	DW SIPH/BW SIPH	0.26–0.32 (0.29)	0.23–0.24 (0.23)
	Cauda/BW Cauda	0.38–0.43 (0.41)	0.40–0.50 (0.44)

description, the new species obviously differs from *S. rubi* as follows: femora and basal half of tibiae pale yellowish-brown, distal half of tibiae dark brown (the latter: basal half of femora slightly pale, distal half of femora and tibiae dark brown); HT Ib 2.26–3.47 times as long as HT Id (the latter: 1.80–2.00 times); HT II 0.31–0.37 mm in length, URS 0.65–0.81 times as long as HT II (the latter: HT II 0.23–0.28 mm in length, URS 0.83–0.96 times as long as HT II); abdominal tergites I–III with a few small scattered sclerites, tergites IV–VII with scattered sclerites, pleural and marginal sclerites often incompletely fused (the latter: abdominal tergites with many small scattered sclerites, often fused in spinal parts, form bands on tergites I and VII), tergite VIII with 31–54 setae (the latter: 18–20 setae). In addition, two mentioned species specially infest *Rubus* sp., the new species feeds on roots of host plants, while *S. rubi* was recorded from apical stems.

Sinolachnus yunnanensis **Qiao & Li, sp. nov.**

https://zoobank.org/2CA4D6AA-7B90-4CCF-9D72-0A608A74904D
Figs 36–64, Table 2

Type material. ***Holotype*:** apterous viviparous female, CHINA: Yunnan Province (Nujiang Lisu Autonomous Prefecture, 26.4401°N, 99.3911°E, alt. 2341 m), 28 July 2022, No. 54113-1-1, on *Elaeagnus* sp., coll. S. Xu and Ying Wang; ***Paratypes*:** one alate viviparous female, others same as holotype; two apterous viviparous females and one alate viviparous female, CHINA: Yunnan Province (Nujiang Lisu Autonomous Prefecture, 26.5618°N, 99.4392°E, alt. 2774 m), 1 August 2022, No. 54211, on *Elaeagnus* sp., coll. S. Xu and Ying Wang; two apterous viviparous females, CHINA: Yunnan Province (Diqing Tibetan Autonomous Prefecture, 27.3449°N, 99.2376°E, alt. 2529 m), 2 August 2022, No. 54223-1-1, on *Elaeagnus* sp., coll. S. Xu and Ying Wang; two apterous viviparous females, CHINA: Yunnan Province (Diqing Tibetan Autonomous Prefecture, 27.3407°N, 99.2448°E, alt. 2558 m), 2 August 2022, No. 54230-1-1, on *Elaeagnus* sp., coll. S. Xu and Ying Wang; two apterous viviparous females, CHINA: Yunnan Province (Diqing Tibetan Autonomous Prefecture, 27.2209°N, 99.2755°E, alt. 2152 m), 3 August 2022, No. 54252-1-1, on *Elaeagnus* sp., coll. S. Xu and Ying Wang; one apterous viviparous female and one apterous nymph, CHINA: Yunnan Province (Diqing Tibetan Autonomous Prefecture, 27.1958°N, 99.3338°E, alt. 2395 m), 4 August 2022, No. 54260-1-1, on *Elaeagnus* sp., coll. S. Xu and Ying Wang; two apterous viviparous females, CHINA: Yunnan Province (Diqing Tibetan Autonomous Prefecture, 27.1965°N, 99.3306°E, alt. 2347 m), 4 August 2022, No. 54271-1-1, on *Elaeagnus* sp., coll. S. Xu and Ying Wang; two apterous viviparous females, CHINA: Yunnan Province (Diqing Tibetan Autonomous Prefecture, 27.1976°N, 99.3210°E, alt. 2289 m), 4 August 2022, No. 54272-1-1, on *Elaeagnus* sp., coll. S. Xu and Ying Wang; two apterous viviparous females, CHINA: Yunnan Province (Diqing Tibetan Autonomous Prefecture, 27.2708°N, 99.2311°E, alt. 2215 m), 4 August 2022, No. 54279-1-1, on *Elaeagnus* sp., coll. S. Xu and Ying Wang; CHINA: Yunnan Province (Lijiang City, 26.7731°N, 100.0227°E, alt. 2880 m), 12 August 2022, No. 54424-1-1, on *Elaeagnus* sp., coll. S. Xu and Ying Wang.

Etymology. The new species is named after its distribution location, *yunnanensis* being the masculine form.

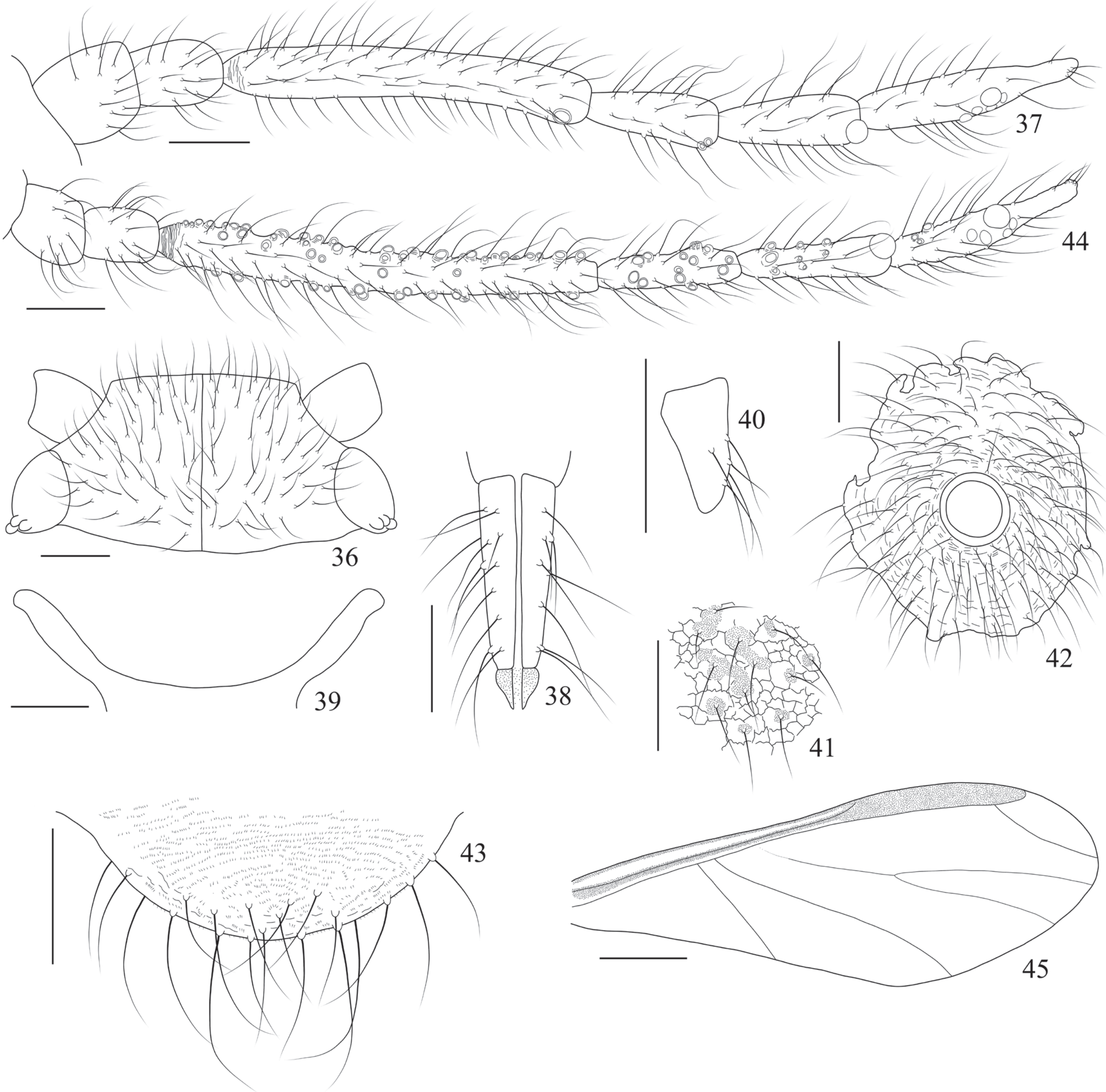

Figures 36–45. *Sinolachnus yunnanensis* Qiao & Li, sp. nov. Apterous viviparous female: **36** dorsal view of head **37** antenna **38** URS **39** mesosternal furca **40** hind first tarsal segment **41** reticulations and setae bearing dark base-sclerites on spinal part of abdominal tergites **42** siphunculus **43** cauda. Alate viviparous female: **44** antenna **45** fore wing. Scale bars: 0.10 mm (**36–44**); 0.50 mm (**45**). (Figs 36, 37 and 40 were drawn according to type material No. 54272, Figs 38 and 39 according to No. 54223, Fig. 41 according to No. 54224, Figs 42–44 according to No. 54211, Fig. 45 according to No. 54113)

Diagnosis. Body relatively small, less than 3 mm in length. PT with 2–6 long setae on basal part. Abdominal tergites of apterous viviparous females often with small scattered spinal sclerites and sometimes fused or unobvious. Alate viviparous females with fewer secondary rhinaria, Ant. III–VI with 70–80, 14, 8, 3 secondary rhinaria, respectively; fore wings with media once branched; abdominal tergite VII with a broad transverse patch with irregular margin.

Description. Apterous viviparous female: Body oval, with densely long setae, reddish-brown in life (Figs 61–63), apical or whole antennae and legs, siphunculi, and a transverse patch on abdominal tergite VII dark brown.

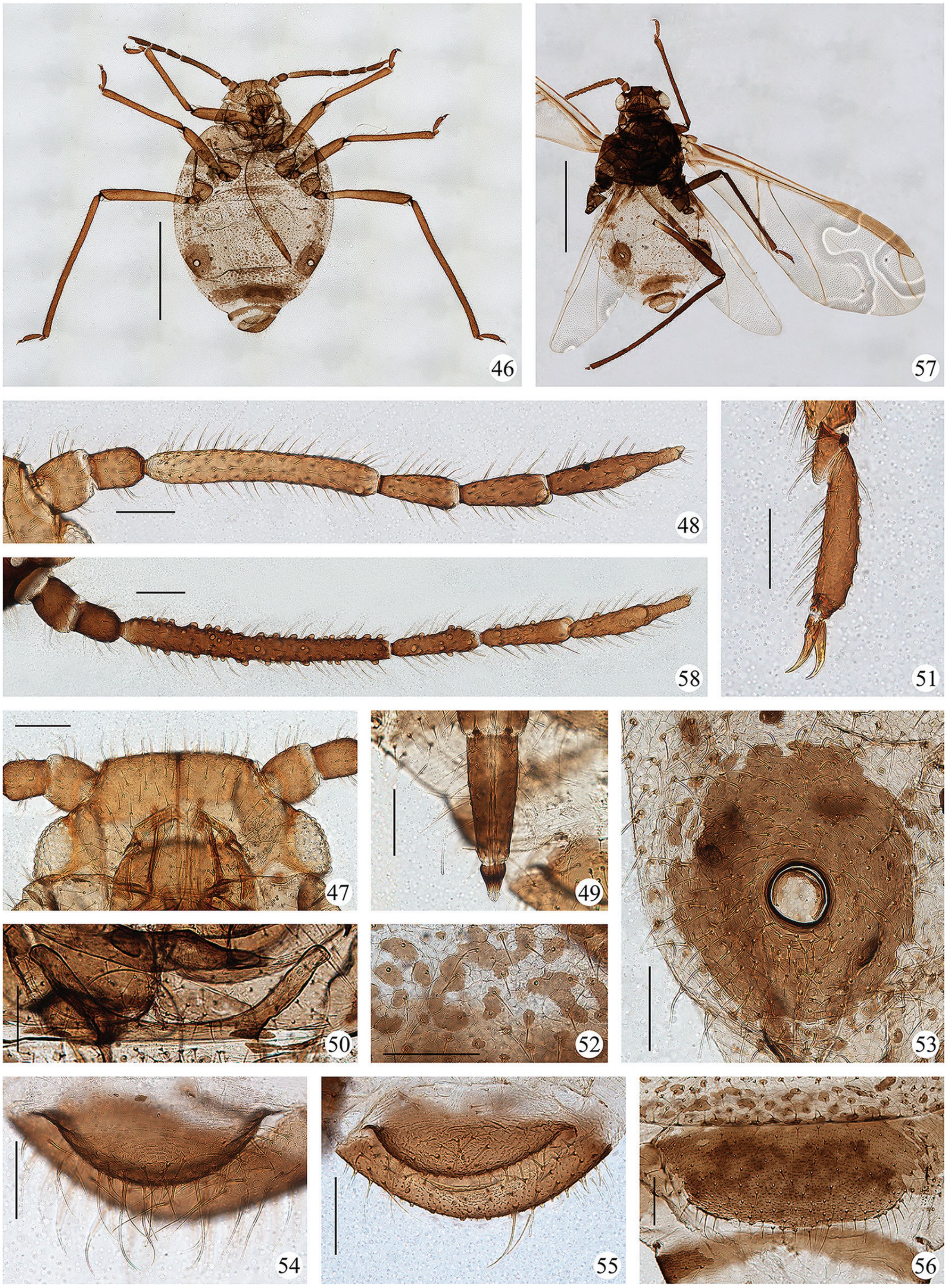

Figures 46–58. *Sinolachnus yunnanensis* Qiao & Li, sp. nov. Apterous viviparous female: **46** dorsal view of body with large sclerites **47** dorsal view of head **48** antenna **49** URS **50** mesosternal furca **51** hind tarsi and claws **52** reticulations and setae bearing dark base-sclerites on spinal part of abdominal tergites **53** siphunculus **54** cauda **55** anal plate **56** genital plate. Alate viviparous female: **57** dorsal view of body **58** antenna. Scale bars: 1.00 mm (**46, 57**); 0.10 mm (**47–56, 58**). (Fig. 46 was photographed according to type material No. 54424, Figs 47, 48, 51 and 52 according to No. 54272, Figs 49 and 50 according to No. 54223, Figs 53, 54, 56 and 58 according to No. 54211, Fig. 55 according to No. 54252, Fig. 57 according to No. 54113)

Mounted specimens. Head, antennae, rostral segments III–V, pronotum, mesonotum, legs, siphunculi, cauda, anal plate and genital plate dark brown; other parts pale brown; setae on metanotum and abdominal tergites, and some on venter of abdomen bearing dark base-sclerites. For morphometric data, see Table 2.

Head. Head dorsum smooth, with an obvious dark median suture. Head with 104–137 long and pointed dorsal setae. Frons round. Ocular tubercles well developed (Figs 36, 47). Antennae almost smooth (Figs 37, 48), basal part of Ant. III and PT with transverse striae. Antennal setae fine, long and pointed, Ant. I–VI each with 22–30, 28–35, 106–131, 27–38, 29–40, 28–36+3–8 setae, respectively; PT with 5 short blunt setae at apex. Primary rhinaria round, Ant. VI with 4 or 5 accessory rhinaria around primary rhinaria; secondary rhinaria often absent, Ant. III and IV with 1 or 2, Ant. VI with 1 round and protuberant secondary rhinarium occasionally. Rostrum long, reach abdominal segment V; URS elongate wedge-shaped (Figs 38, 49), with 3 pairs of primary setae and 18–26 accessory setae.

Thorax. Metanotum with small scattered sclerites on spino-pleural part, and 1 pair of marginal sclerites. Dorsal setae long and pointed. Mesosternal furca with a short stem (Figs 39, 50). Legs normal, with long and pointed setae. First tarsal chaetotaxy: 9–12, 8–10, 5–8; first fore tarsal segments with 3–7 peg-like setae and 3–7 long setae, first mid-tarsal segments with 2–4 peg-like setae and 5–8 long setae, first hind tarsal segments with 0–2 peg-like setae and 4–6 long setae.

Abdomen. Abdominal tergites I–VI with reticulations, tergites VII, VIII and venter with spinulose stripes. Abdominal tergite I and marginal part of tergite II with small scattered sclerites; tergites II–V with scattered spinal sclerites, sometimes fused (Figs 41, 52) or unobvious; tergite VI often with scattered spino-pleural sclerites, sometimes fused; tergite VII with a broad transverse patch with irregular margin; tergite VIII with a narrow band, sometimes separated in the middle; intersegmental muscle sclerites small and dark. Dorsal setae fine, long and pointed. Abdominal tergite VIII with 36–65 setae. Spiracles oval, closed, on brown spiracular plates. Siphunculi truncate, on dark brown seta-bearing cones, with flange and transverse striae (Figs 42, 53), surrounding by 135–195 setae. Cauda round with spinulose stripes, with 33–45 long or short setae (Figs 43, 54). Anal plate broadly round with spinules, with 77–95 long or short setae (Fig. 55). Genital plate transverse elliptical, anterior part slightly concaved, with spinulose stripes, with 120–148 setae (Fig. 56). Genopophyses three, each with 6–7, 6–10, 6–7 setae.

Alate viviparous female: Body elongate oval, head and thorax blackish brown, abdomen brown in life (Fig. 64); antennae, legs, siphunculi and patches on abdominal tergites VII and VIII blackish-brown.

Mounted specimens. Head, antennae, rostral segments III–V, thorax, legs except basal part of femora, siphunculi, cauda, anal plate and genital plate dark brown, other parts pale brown; dorsal and ventral setae on abdomen bearing dark base-sclerites. For morphometric data, see Table 2.

Head. Head dorsum smooth, with an obvious dark median suture. Head with 71–79 long and pointed dorsal setae. Frons flat. Ocular tubercles well developed. Antennae almost smooth (Figs 44, 58), basal part of Ant. III and PT with transverse striae. Antennal setae fine, most long and pointed, few short and blunt, Ant. I–VI each with 19–23, 30, 101, 33, 32, 32+7 setae, respectively; PT with 5 short blunt setae at apex. Primary rhinaria round, Ant. VI with 4 accessory rhinaria around primary rhinaria; secondary rhinaria round and protuberant, Ant. III–VI with 70–80, 14,

Figures 59–64. *Sinolachnus yunnanensis* Qiao & Li, sp. nov. **59, 60** host plant **61–63** apterous viviparous females and nymphs on stems of host plants near the ground **64** alate viviparous female.

8, 3 secondary rhinaria, respectively. Rostrum long, reach abdominal segment IV; URS elongate wedge-shaped, with 3 pairs of primary setae and 18 accessory setae.

Thorax. Legs normal, with long and pointed setae. First tarsal chaetotaxy: 7–10, 6–10, 4; first fore tarsal segments with 4 or 5 peg-like setae and 3–5 long setae, first mid-tarsal segments with 2–5 peg-like setae and 4 or 5 long setae, first hind tarsal segments with none or 1 peg-like setae and 3 or 4 long setae. Wings with scaly imbrications entirely (Fig. 57); campaniform sensilla near the base of subcosta slightly protuberant, fore wings and hind wings each with 10–14 and 7–9 campaniform sensilla on basal part, respectively; fore wings with pterostigma elongate, pale media once branched and faint on basal part (Fig. 45); hind wings with two oblique veins.

Table 2. Morphometric data of *Sinolachnus yunnanensis* Qiao & Li, sp. nov. (measurements in mm, with means in brackets).

	Characters	Apterous viviparous females (*N* = 10)	Alate viviparous females (*N* = 2)
Length (mm)	Body length	1.94–2.64 (2.34)	2.45–2.49 (2.47)
	Body width	1.15–1.68 (1.48)	0.99–1.27 (1.13)
	Antenna	0.93–1.39 (1.17)	1.38
	Ant. I	0.09–0.12 (0.11)	0.10–0.11 (0.10)
	Ant. II	0.08–0.11 (0.10)	0.10
	Ant. III	0.33–0.52 (0.41)	0.55–0.60 (0.58)
	Ant. IV	0.11–0.19 (0.15)	0.18
	Ant. V	0.12–0.20 (0.16)	0.19
	Ant. VIb	0.13–0.17 (0.15)	0.16
	PT	0.07–0.10 (0.09)	0.09
	URS	0.20–0.25 (0.23)	0.22–0.23 (0.22)
	Hind femur	0.58–0.96 (0.78)	0.98–0.99 (0.99)
	Hind tibia	1.00–1.73 (1.34)	1.76–1.78 (1.77)
	HT Ib	0.03–0.04 (0.04)	0.03
	HT Id	0.01–0.02 (0.01)	0.01–0.02 (0.01)
	HT Iv	0.06–0.09 (0.08)	0.06–0.07 (0.07)
	HT II	0.18–0.24 (0.21)	0.24
	BW SIPH	0.28–0.39 (0.35)	0.28–0.33 (0.30)
	DW SIPH	0.08–0.09 (0.08)	0.07
	Cauda	0.08–0.10 (0.09)	0.09–0.10 (0.09)
	BW Cauda	0.25–0.32 (0.29)	0.23–0.26 (0.24)
	Ant. III BD	0.02–0.03 (0.03)	0.03
	MW hind tibia	0.05–0.07 (0.06)	0.05
	Frontal setae	0.09–0.12 (0.10)	0.10–0.11 (0.10)
	Setae on Tergite I	0.09–0.11 (0.10)	/
	Setae on Tergite VIII	0.09–0.13 (0.11)	0.10–0.12 (0.11)
	Setae on Ant. III	0.10–0.12 (0.10)	0.10–0.11 (0.11)
	Setae on Hind tibia	0.09–0.13 (0.11)	0.10–0.12 (0.11)
Ratio (times)	Body length/Body width	1.47–1.69 (1.59)	1.96–2.47 (2.22)
	Whole antenna/Body	0.45–0.55 (0.50)	0.56
	Hind femur/Ant. III	1.68–2.01 (1.88)	1.66–1.78 (1.72)
	Hind tibia/Body	0.48–0.67 (0.57)	0.72
	PT/Ant. VIb	0.51–0.71 (0.59)	0.57
	URS/BW URS	3.00–3.72 (3.39)	2.93–3.55 (3.24)
	URS/HT II	1.03–1.15 (1.11)	0.92
	HT Ib/HT Id	2.40–3.60 (2.93)	2.07–2.82 (2.44)
	HT Ib/HT Iv	0.43–0.56 (0.49)	0.47–0.48 (0.48)
	Frontal setae/Ant. III BD	3.29–4.83 (3.98)	3.75
	Setae on Tergite I/Ant. III BD	3.07–4.58 (3.82)	/
	Setae on Tergite VIII/Ant. III BD	3.61–5.33 (4.24)	4.14
	Setae on Ant. III/Ant. III BD	3.19–4.86 (4.07)	3.93
	Setae on Hind tibia/MW hind tibia	1.48–2.14 (1.77)	1.91–2.30 (2.10)
	DW SIPH/BW SIPH	0.20–0.28 (0.23)	0.25
	Cauda/BW Cauda	0.28–0.32 (0.30)	0.37–0.40 (0.39)

Abdomen. Abdominal tergites smooth, reticulations obvious or not; tergites VII, VIII and venter with spinulose stripes. Abdominal tergites I–III each with 1 pair of marginal sclerites, tergites V and VI with a few scattered spinal sclerites, tergite VII with a broad transverse patch with irregular margin; tergite VIII with a narrow band; intersegmental muscle sclerites small and dark. Setae on abdominal tergites fine, most long and pointed, few short and blunt, dorsal setae sparser than on venter. Abdominal tergite VIII with 28 setae. Spiracles oval and closed, on brown spiracular plates. Siphunculi truncate, on dark brown seta-bearing cones, apical with few transverse striae and flange, surrounding by 140–156 setae. Cauda round with spinulose stripes, with 32–43 long or short setae. Anal plate broadly round with spinules, with 71–78 long or short setae. Genital plate transverse elliptical with spinulose stripes, with 110–124 setae. Genopophyses three, each with 7, 8, 7 setae.

Distribution. China (Yunnan).

Host plant. *Elaeagnus* sp. (Elaeagnaceae).

Biology. The species colonizes branches and stems of host plants near the ground under ant nests.

Comments. Apterae of the new species resemble *Sinolachnus rubi*, which is only known from apterous viviparous females, in having abdominal tergites with scattered spinal sclerites, sometimes fused, but differs from it as follows: body relatively small, 1.94–2.64 mm in length (the latter: 2.70–3.40 mm); Ant. VI 0.50–0.66 times as long as Ant. III (the latter: 0.40–0.42 times); secondary rhinaria often absent, Ant. III and IV with 1 or 2, Ant. VI with 1 occasionally (the latter: Ant. III–VI with 1–7, 1–6, 1–5, 1–3 secondary rhinaria, respectively); Setae on Ant. III 3.19–4.86 times as long as Ant. III BD (the latter: 2.12–2.75 times); URS with 18–26 secondary setae (the latter: URS with 11 or 12 secondary setae); Setae on Hind tibiae 1.48–2.14 times as long as MW hind tibia (the latter: 0.90–1.20 times); HT Ib 2.40–3.60 times as long as HT Id (the latter: 1.80–2.00 times); abdominal tergite VIII with 36–65 setae (the latter: 18–20 setae), Setae on Tergite VIII 3.61–5.33 times as long as Ant. III BD (the latter: 2.70–3.40 times).

Alatae of the new species resemble *S. nipponicus*, which is only known from alate viviparous females, in having the body relatively small (body length less than 3.00 mm), Ant. III with fewer secondary rhinaria (66–88 secondary rhinaria), PT with several long setae on basal part, media of fore wings once branched, but differs from it as follows: PT 0.57 times as long as Ant. VIb (the latter: 0.73–0.83 times); Ant. VIb with 32 setae (the latter: 21–23 setae); Setae on Hind tibiae 0.10–0.12 mm (the latter: 0.070–0.075 mm); abdominal tergites V and VI with few scattered spinal sclerites, tergite VII with a broad transverse patch with irregular margin (the latter: abdominal tergites I–VII without spinal and pleural patches); genital plate transverse elliptical (the latter: genital plate with irregular and divided proximal part).

Keys to the species of *Sinolachnus* in China

Apterous viviparous females

1 Body length 1.94–2.64 mm; antenna 0.93–1.39 mm in length; Ant. IV with 0–2 secondary rhinaria **2**

– Body length 2.77–3.67 mm; antenna 1.48–1.84 mm in length; Ant. IV with 2–11 secondary rhinaria **3**

2 Ant. IV slightly longer than Ant. V, Ant. VI 0.44 times as long as Ant. III, Ant. V with 1 secondary rhinarium .... ***S. niitakayamensis* (Takahashi)**

– Ant. IV slightly shorter than Ant. V, Ant. VI 0.50–0.66 times as long as Ant. III, Ant. V without secondary rhinaria .... ***S. yunnanensis* Qiao & Li, sp. nov.**

3 URS 0.65–0.81 times as long as HT II, with 10–14 accessory setae; first tarsal segments with 8–16 setae; abdominal tergites with sclerites .... ***S. rubusis* Qiao & Li, sp. nov.**

– URS 0.92–1.02 times as long as HT II, with 20–24 accessory setae; first tarsal segments with 1–8 setae; abdominal tergites without sclerites....... .... ***S. yushanensis* Kanturski, Yeh & Lee**

Alate viviparous females

1 Media of fore wings once branched.. **2**

– Media of fore wings twice branched... **5**

2 Ant. III–V with 70–80, 14, 8 secondary rhinaria, respectively; Setae on Ant. III 3.93 times as long as Ant. III BD, basal part of PT with 5 long setae .... ***S. yunnanensis* Qiao & Li, sp. nov.**

– Ant. III with more than 100, Ant. IV and V each with more than 20 secondary rhinaria; Setae on Ant. III 2.10–2.85 times as long as Ant. III BD, basal part of PT without long setae **3**

3 Ant. III with 220–255 and Ant. IV with 50–70 secondary rhinaria; fore wings with scaly imbrications mostly on distal part..................................... .... ***S. takahashii* Kanturski, Yeh & Lee**

– Secondary rhinaria on Ant. III more than 200, on Ant. IV less than 40; fore wings with scaly imbrications entirely **4**

4 PT 0.57–0.62 times as long as Ant. VIb, Ant. VI with 4–6 secondary rhinaria; URS 0.79–0.82 times as long as HT II; hind wings with 9–11 pseudo-sensoria on basal part .... ***S. niitakayamensis* (Takahashi)**

– PT 0.35–0.42 times as long as Ant. VIb, Ant. VI with 7–16 secondary rhinaria; URS 0.88–0.96 times as long as HT II; hind wings with 17–19 pseudo-sensoria on basal part ....***S. yushanensis* Kanturski, Yeh & Lee**

5 Body length about 2 mm; antenna about 0.68 times as long as body length; fore wings with scaly imbrications mostly on distal part ...***S. taiwanus* Tao**

– Body length more than 3 mm; antenna 0.45–0.58 times as long as body length; fore wings with scaly imbrications entirely **6**

6 Antenna 0.58 times as long as body length; Ant. III–VI with 280–285, 62–81, 64–89, 22–39 small secondary rhinaria, respectively; abdominal tergite VII with a sclerotic band........................ ***S. plurisensoriatus* (Zhang)**

– Antenna 0.45–0.51 times as long as body length; Ant. III–VI with 29–54, 5–18, 3–14, 4–8 secondary rhinaria, respectively, secondary rhinaria in various sizes; abdominal tergite VII without sclerites .... ***S. rubusis* Qiao & Li, sp. nov.**

Acknowledgements

Thanks are due to F.D. Yang for making slides and to all collectors, S. Xu, Ying Wang, Yong Wang, R. Chen and C.C. Du for their assistance in aphid specimen collection and taking pictures in the field.

Additional information

Conflict of interest

The authors have declared that no competing interests exist.

Ethical statement

No ethical statement was reported.

Funding

The work was supported by the National Natural Science Foundation of China (Grant Nos. 32030014, 31970451), Survey of Wildlife Resources in Key Areas of Tibet (ZL202203601), the Key Collaborative Research Program of the Alliance of International Science Organizations (Grant No. ANSO-CR-KP-2020-04) and the Second Tibetan Plateau Scientific Expedition and Research (STEP) program (Grant No. 2019QZKK0501) and the Youth Innovation Promotion Association of Chinese Academy of Sciences (Grant No. 2020087).

Author contributions

G.X.Q., Z.X.L., L.Y.J. and J.C. conceived the research. G.X.Q. and Z.X.L. checked the specimens. Z.X.L., L.Y.J. and J.C. did the morphological description and made the drawings of features, and took photographs. All authors discussed the results and provided edits and approval of the manuscript.

Author ORCIDs

Zhao-Xu Li https://orcid.org/0000-0002-9252-4877
Jing Chen https://orcid.org/0000-0002-7584-5249
Li-Yun Jiang https://orcid.org/0000-0002-2527-9613
Ge-Xia Qiao https://orcid.org/0000-0002-7300-6812

Data availability

All of the data that support the findings of this study are available in the main text.

References

Blackman RL, Eastop VF (1994) Aphids on the World's Trees: An Identification and Information Guide. CAB international, Wallingford, 987 pp. https://doi.org/10.1079/9780851988771.0000

Chakrabarti S, Das D (2015) A new species and new records of aphids (Hemiptera) from Bhutan. Oriental Insects 48(3–4): 327–336. https://doi.org/10.1080/00305316.2015.1013183

Ghosh AK (1982) Homoptera: Aphidoidea. Part 2. Subfamily Lachninae. The Fauna of India and the Adjacent Countries. Zoological Survey of India, Calcutta, 167 pp.

Hille Ris Lambers D (1956) Lachnids from Elaeagnaceae (Homoptera: Aphidoidea). Zeitschrift für Angewandte Entomologie 39(4): 467–473. https://doi.org/10.1111/j.1439-0418.1956.tb01264.x

Kanturski M, Yeh HT, Lee Y (2022) Morphology, taxonomy, and systematic position of the enigmatic aphid genus *Sinolachnus* (Hemiptera: Aphididae, Lachninae). The European Zoological Journal 90 [2023]: 10–59. https://doi.org/10.1080/24750263.2022.2157897

Tao CC (1961) Aphid fauna of China. Science Yearbook of the Taiwan Museum 4: 35–44.

Tao CC (1989) Aphids from Taiwan collected by Malaise trap (Homoptera: Aphidae). Journal of the National Taiwan Museum 42(2): 21–29.

ZooKeys 1182: 153–164 (2023)
DOI: 10.3897/zookeys.1182.105716

Research Article

New species of the genus *Trichosetodes* Ulmer, 1915 (Trichoptera, Leptoceridae) from Ratanakiri province, Cambodia, based on morphological and molecular data

Pongsak Laudee[1], Hans Malicky[2], Chamroeun Kong[3], Masaki Takenaka[4], Koji Tojo[4]

1 *Faculty of Innovative Agriculture and Fishery Establishment Project, Prince of Songkla University, Surat Thani Campus, Surat Thani, Muang District Province, 84100, Thailand*
2 *Sonnengasse 13, A-3293 Lunz am See, Austria*
3 *Kampong Speu Institute of Technology, Amleang, Kampong Speu Province, Cambodia*
4 *Department of Biology, Faculty of Science, Shinshu University, Asahi 3-1-1, Matsumoto, Nagano 390-8621, Japan*
Corresponding author: Pongsak Laudee (pongsak.l@psu.ac.th)

Abstract

Three new species of *Trichosetodes*, namely *T. carmelae* **sp. nov.**, *T. katiengensis* **sp. nov.** and *T. ratanakiriensis* **sp. nov.** are described and illustrated by male specimens. The male genitalia of *T. carmelae* **sp. nov.** can be distinguished from the other 16 species of the genus found in Southeast Asia by the shape of the phallicata. The phallicata of *T. carmelae* **sp. nov.** bears a tuft of long hairs in the middle of the dorsal edge. *Trichosetodes katiengensis* **sp. nov.** can be distinguished from the other species in Southeast Asia by the shape of the phallicata which is divided into dorsal and ventral branches in lateral view, and *T. ratanakiriensis* **sp. nov.** by the characters of the left inferior appendage and the shape of segment IX. The posterior end of the left inferior appendage of *T. ratanakiriensis* **sp. nov.** is not forked and the ventral and lateral views of the posteroventral lobes of segment IX are rounded. Illustrations of male genitalia of *Trichosetodes kampongspeuensis* Malicky & Kong, 2020 are provided for comparison. The molecular diversity of new *Trichosetodes* species was analyzed using the mitochondrial large subunit ribosomal rRNA gene region (16S rRNA). In terms of their genetic divergence, *T. ratanakiriensis* **sp. nov.** and *T. kampongspeuensis* exhibited remarkable proximity, with only a 1.4% distance. On the contrary, *T. carmelae* **sp. nov.** displayed genetic disparity exceeding 6.3% when compared to both *T. ratanakiriensis* **sp. nov.** and *T. kampongspeuensis*.

Key words: Aquatic insects, biodiversity, caddisfly, Mekong River basin, morphology, ribosomal mRNA, taxonomy

Academic editor: Ana Previšić
Received: 30 April 2023
Accepted: 21 September 2023
Published: 12 October 2023

ZooBank: https://zoobank.org/863375EB-2502-4A93-A561-7FDFA26FAD1D

Citation: Laudee P, Malicky H, Kong C, Takenaka M, Tojo K (2023) New species of the genus *Trichosetodes* Ulmer, 1915 (Trichoptera, Leptoceridae) from Ratanakiri province, Cambodia, based on morphological and molecular data. ZooKeys 1182: 153–164. https://doi.org/10.3897/zookeys.1182.105716

Introduction

Trichosetodes Ulmer is a genus of Trichoptera in the family Leptoceridae, which can be identified by the crescent shape of the abdominal segment IX from the lateral view, finger-like preanal appendages and a tuft of long hairs anterodorsally on abdominal segment IX (Schmid 1987; Gibon 1991; Malicky 2006a; Malicky and Graf 2020). Fifty-five species have been described worldwide. However, while *Trichosetodes* spp. has been mainly found from Oriental regions, three and thirteen species have been reported from the East Palearctic and Afrotropical regions, respectively (Malicky 2010; Mey and De Moor 2019; Kimura and Kuranishi 2020; Laudee et al. 2020; Malicky and Graf 2020; Morse 2023). In Asia, *T. atisudhara* Schmid, 1987, *T. compositus* Martynov, 1936, and *T. pandrosus* Malicky, 2006 were reported from Nepal (Malicky 2006b), and *T. japonicus* Tsuda, 1942 from Japan and the Korean Peninsula (Kimura and Kuranishi 2020; Park and Kong 2020). Yang et al. (2016) reported that seven species of *Trichosetodes*, namely *T. bicornis* Yang & Morse, 2000, *T. falcatus* Yang & Morse, 2000, *T. insularis* Schmid, 1987, *T. lasiophyllus* Yang & Morse, 1989, *T. phylloideus* Yang & Morse, 2000, *T. rhamphodes* Yang & Morse, 2000 and *T. serrayus* Yang & Morse, 2000 were found from several parts of China. In India, thirteen species of *Trichosetodes* have been recorded from several areas (Saini et al. 2001). In Southeast Asia, Malicky (2010) reported that 12 species of *Trichosetodes* were collected from Thailand, Laos, Peninsular Malaysia, Sumatra (Indonesia) and Java (Indonesia). Oláh (2013) described two new species of *Trichosetodes*, namely *T. harmas* Oláh, 2013 and *T. sotet* Oláh, 2013 from Vietnam. In Myanmar, Malicky and Laudee (2017) described a new species of *Trichosetodes*, *T. asphor* Malicky & Laudee, 2017, which was found from Taninthayi Division. Recently, *T. kampongspeuensis* Malicky & Kong, 2020 in Laudee et al. (2020) from Cambodia was described.

Presented herein is a report encompassing selected findings derived from an extensive investigation into the caddisfly biodiversity within the Mekong River and its network of tributaries. This study led to the collection and subsequent description of three distinct *Trichosetodes* species originating from the Katieng Waterfall, situated within the confines of Cambodia's Ratanakiri Province.

Material and methods

Male adult caddisfly specimens were collected overnight with a UV pan light trap (12V, 10W) near Katieng Waterfall and its stream, in Ratanakiri Province, Cambodia. The adult Trichoptera specimens were collected and preserved in 70% ethanol. Adult male genitalia of the new species were excised and macerated in 10% KOH at 60 °C for 30–60 min. The male genitalia of the new species were drawn with pencil while using a compound microscope with a drawing tube, and then final vector-graphic illustrations were prepared from the pencil templates with Adobe Illustrator 2023 software.

The holotypes and some paratypes of the new species were stored in 70% ethanol and were deposited at the Princess Maha Chakri Sirindhorn Natural History Museum, Prince of Songkla University, Hat Yai Campus, Hat Yai District, Songkhla Province, Thailand (**PSUNHM**). Some paratypes are deposited in the collection of Hans Malicky, Lunz am See, Austria (**CHM**), the National Museum, Prague, Czech Republic (**NMPC**) and the Clemson University Arthropod Collection, Clemson, South Carolina, USA (**CUAC**). Terminology of structure of genitalia follows Yang and Morse (2000).

The DNA was extracted from the ethanol-preserved tissue of the specimens, and purified using the DNeasy Blood & Tissue Kit (Qiagen, Hilden, Germany), according to the manufacturer's instructions. The region of mitochondrial DNA (mtDNA) coding 16S rRNA region was amplified by a polymerase chain reaction (PCR) using the primer set 16S rRNA: 5'- TRA CYG TRC AAA GGT AGC -3' and 5’- CCG GTY TRA ACT CAR ATC ATG T -3’ (Takenaka et al. 2023). Regarding each reaction, 1.0 μL of 10× Ex Taq buffer, 0.8 μL dNTP mixture (included 25 mM $MgCl_2$), 0.05 μL of 5 U/μL Ex Taq polymerase (TAKARA, Shiga), 0.25 μL of each primer and 2.0 μL of extracted DNA for in total 10 μL were applied. The PCR protocol was: 94 °C for 2 min; 35× (94 °C for 1 min, 50 °C for 1 min, 72 °C for 1 min); and 72 °C for 3 min. The PCR products were purified using ExoSAP-IT Express (Thermo Fisher Scientific K.K., Tokyo, Japan). Purified DNA fragments were sequenced directly by an automated method using a BigDye Terminator v.1.1 Cycle Sequencing Kit (Applied Biosystems, Foster City, CA, USA) on an automated DNA Sequencer (ABI 3130 or 3130xl DNA Analyzer; Perkin Elmer/Applied Biosystems).

All sequences obtained have been submitted to the DNA data bank of Japan (DDBJ database) (GenBank accession numbers: *Trichosetodes carmelae* sp. nov., C761851; *T. ratanakiriensis* sp. nov., LC761852; *T. kampongspeuensis*, LC761853). Regarding the outgroup, we included the DNA sequence data of *Setodes brevicaudatus* Yang & Morse, 1989 (GenBank accession numbers: OL678050 and NC069285). Sequence alignment and editing were performed using MEGA v.7.0.26 (Kumar et al. 2016) and CLC Workbench software (CLC bio, Aarhus, Denmark). All sequence data were aligned using MAFFT v.7.222 (Katoh and Standley 2013). Phylogenetic analyses based on the mtDNA 16S rRNA (434 bp) were performed by the Neighbor-Joining (NJ) method using MEGA v.7.0.26 (Kumar et al. 2016) with 1000 bootstrap cycles. Genetic distances (*p*-distance) between the species were calculated using MEGA v.7.0.26 (Kumar et al. 2016).

Systematics

***Trichosetodes carmelae* Laudee & Malicky, sp. nov.**
https://zoobank.org/78DA92FF-BAEB-4BD3-9097-AE4E453A4255
Fig. 1

Type material. *Holotype*. Male. Cambodia: Ratanakiri Province: Banlung, Katieng Waterfall, 13°40'38"N, 106°58'33"E, elev. 203 m, 13.v.2022, Pongsak Laudee. (PSUNHM). ***Paratypes*:** Same data as holotype, 6 males: 2 males (PSUNHM), 2 males (CHM), 2 males (CUAC).

Diagnosis. The male genitalia of the new species are moderately similar to those of *T. sotet* Oláh, 2013 described in Vietnam in the form of segment IX and inferior appendages, as well as of *T. insularis* Schmid, 1987 in the form of segment IX and segment X; but the phallicata or aedeagus is clearly different. The phallicata of *T. sotet* and *T. insularis* are divided into subbasodorsal branch and subbasoventral branch, whereas such features are missing in *T. carmelae*. The phallicata in *T. carmelae* bears tuft of long hairs in the middle of dorsal edge, which does not occur in *T. sotet*. The phallicata in *T. carmelae* is slightly bent upward subapically, while it is curved downward in *T. sotet*.

Description. Length of each male forewing 4.5 mm (*N* = 5); specimens in alcohol with head, thorax, abdomen, legs, forewings light brown.

Male genitalia (Fig. 1A–D). Segment IX right trapezoid, anterior margin convex dorsally and truncated ventrally, posterior margin truncated in lateral view (Fig. 1A); rectangular with pair of notches anteriorly in ventral view (Fig. 1C).

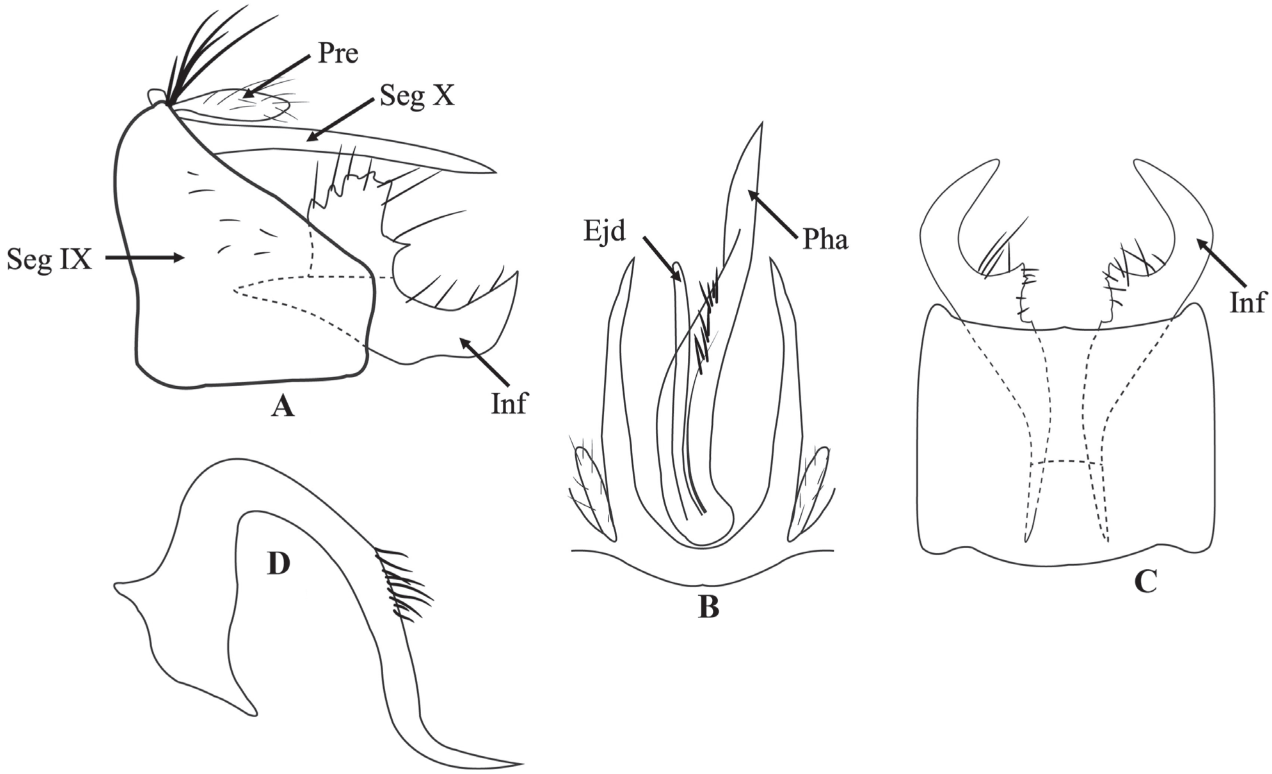

Figure 1. *Trichosetodes carmelae* sp. nov. male genitalia **A** segment IX and inferior appendages, left lateral **B** segment X and phallus, dorsal **C** segment IX and inferior appendages, ventral **D** phallus, left lateral. Abbreviations: Pre = preanal appendages (paired), Pha = phallicata, Seg IX = segment IX, Seg X = segment X, Inf = inferior appendage (paired), Ejd = ejaculatory duct.

Preanal appendages thumb-like covered with hairs (Fig. 1A, B). Segment X produced in pair of javelin-like processes each with acute apex (Fig. 1A, B). Inferior appendages each with dorsal and ventral lobes, dorsal lobe broad rectangular, serrated dorsally with small triangular process, ventral lobe slender with acute apex directed dorsad in lateral view (Fig. 1A); in ventral view, claw-like, bent inward, each with inner broad tooth sub-basally (Fig. 1C). phallicata in dorsal view, slender, lancet-like, acute apex, with isolated bunch of long hair in the middle; ejaculatory duct tube-like, about half as long as phallicata length (Fig. 1B); in lateral view, phallus typically large, axe-like, broad basally, strongly curved backward subbasally, with isolated bunch of long hairs dorsally, bent subapically, sharp apex (Fig. 1D).

Etymology. The species name is dedicated to Dr Carmela R. Centrino who works for United Nations Industrial Development, Vienna International Centre for Southeast Asian Countries.

Trichosetodes katiengensis Laudee & Malicky, sp. nov.

https://zoobank.org/A1F2CDD2-ABBA-4CDF-A5E9-87E5C3D3CDE3
Fig. 2

Type material. ***Holotype*. Male.** Cambodia: Ratanakiri Province: Banlung, Katieng Waterfall, 13°40'38"N, 106°58'33"E, elev. 203 m, 13.v.2022, Pongsak Laudee. (CHM). ***Paratypes*:** same data as holotype. 2 males: 1 male (PSUNHM), 1 male (CHM).

Diagnosis. The male genitalia of the new species are moderately similar to those of *Trichosetodes pales* Malicky & Chaibu, 2006 described in Thailand, in the form of segment IX and inferior appendages, however, the phallus is clearly different. The phallicata of *T. pales* is divided into a dorsal branch, median branch and ventral branch, however, these features are missing in *T. katiengensis*. In addition, ventral lobes of inferior appendages are truncated and pointed in *T. pales* in both ventral and lateral views.

Description. Length of each male forewing 3.5–4.0 mm (*N* = 3); specimens in alcohol with head, thorax, abdomen, legs, forewings dark brown.

Male genitalia (Fig. 2A–D). Segment IX with pair of thumb-like lobes posteriorly in dorsal view (Fig. 2B); right trapezoid, anterior margins convex with small lobe anterodorsally, posterior margin slightly truncated in lateral view (Fig. 2A); square with shallow notches anteriorly in ventral view (Fig. 2C). Preanal appendages thumb-like covered with hairs (Fig. 2A, B). Segment X not evident. Inferior appendages with dorsal and ventral lobes, dorsal lobe triangular in lateral view with sharp process basoposteriorly, ventral lobe tubular and truncated apically in lateral view (Fig. 2A); in ventral view, horn-like, bent inward, truncated apically (Fig. 2C). In dorsal view, phallus complex, phallicata divided into dorsal and ventral branches; dorsal branch with outer edge denticulated and ventral branch undulated with acute apex; ejaculatory duct short and thin (Fig. 2B). In lateral view, phallicata sickle-like with dorsal and ventral branches, dorsal branch of phallicata straight, covered with numerous short protrusions subapically, apex with small spines; ventral branch of phallicata claw-like, curved downward, acute apex; ejaculatory duct curved tube-like (Fig. 2D).

Etymology. The species is named for the type locality, Katieng Waterfall.

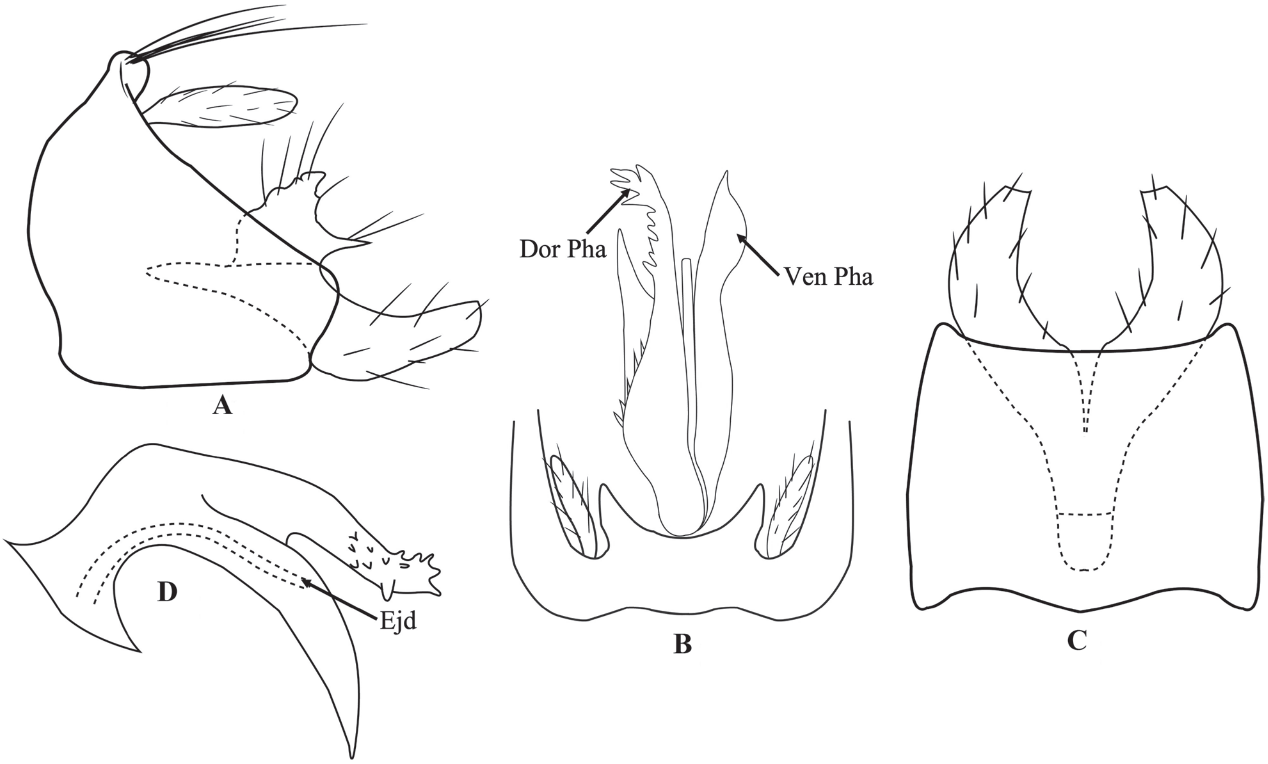

Figure 2. *Trichosetodes katiengensis* sp. nov. male genitalia **A** segment IX and inferior appendages, left lateral **B** segment IX and phallus, dorsal **C** segment IX and inferior appendages, ventral **D** phallus. Abbreviations: Dor Pha = dorsal branch of phallicata, Ven Pha = ventral branch of phallicata, Ejd = ejaculatory duct.

Trichosetodes ratanakiriensis **Laudee & Malicky, sp. nov.**

https://zoobank.org//873AF5A4-76F5-423D-8E48-4A45AD10BBB1
Fig. 3

Type material. *Holotype*. Male. Cambodia: Ratanakiri Province: Banlung, Katieng Waterfall, 13°40'38"N, 106°58'33"E, elev. 203 m, 13.v.2022, Pongsak Laudee. (CHM). ***Paratypes*:** same data as holotype. 33 males: 18 males (PSUNHM), 5 males (CHM), 5 males (CUAC), 5 males (NMPC).

Diagnosis. The male genitalia of *T. ratanakiriensis* are moderately similar to those of *T. pandareos* Malicky, 2006 described in Laos and *T. kampongspeuensis* Malicky & Kong, 2020 (Fig. 4), however it can be differentiated by the shape of left inferior appendage and the shape of segment IX. The left inferior appendage is forked in *T. pandareos* whereas this feature is missing in *T. ratanakiriensis*. In addition, the prolongations of the subapicoventral part of segment IX are symmetric in *T. pandareos* but asymmetric in *T. ratanakiriensis* in ventral view. Compared to *T. kampongspeuensis*, *T. ratanakiriensis* exhibits a longer, cylindrical right inferior appendage with a sharp apex in lateral view, whereas in *T. kampongspeuensis*, this appendage is oval and splits into two at the tip. The prolongations of subapical part of segment IX in ventral view are thin in *T. kampongspeuensis* but prominent in *T. ratanakiriensis*.

Description. Length of each male forewing 5 mm (N = 12); specimens in alcohol with head, thorax, abdomen, legs, forewings dark brown.

Male genitalia (Fig. 3A–D). Segment IX square with U-shaped incision anteriorly in dorsal view (Fig. 3C); in left lateral view, complicated shape, strong-

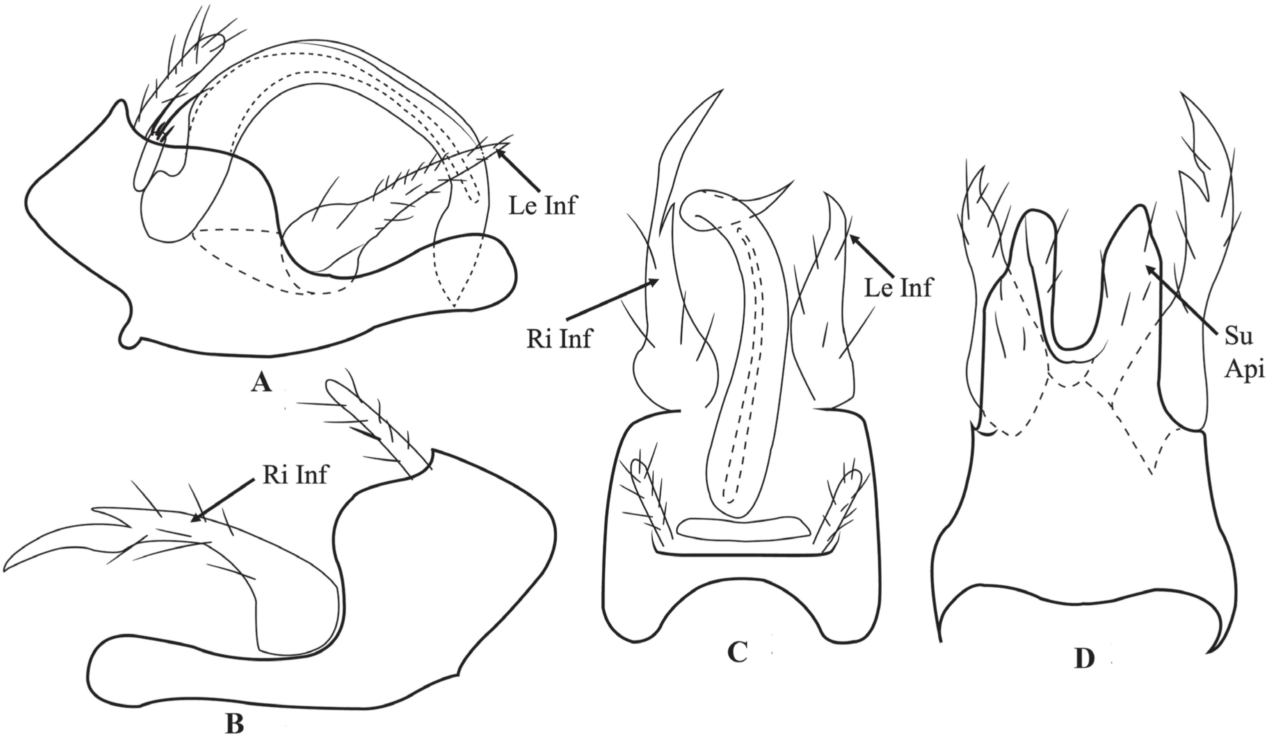

Figure 3. *Trichosetodes ratanakiriensis* sp. nov. male genitalia **A** segment IX and inferior appendages, left lateral **B** segment IX and inferior appendages, right lateral **C** segment IX and phallus, dorsal **D** segment IX, ventral. Abbreviations: Le Inf = left inferior appendages, Ri Inf = right inferior appendage, Su Api = subspicoventral part of segment IX.

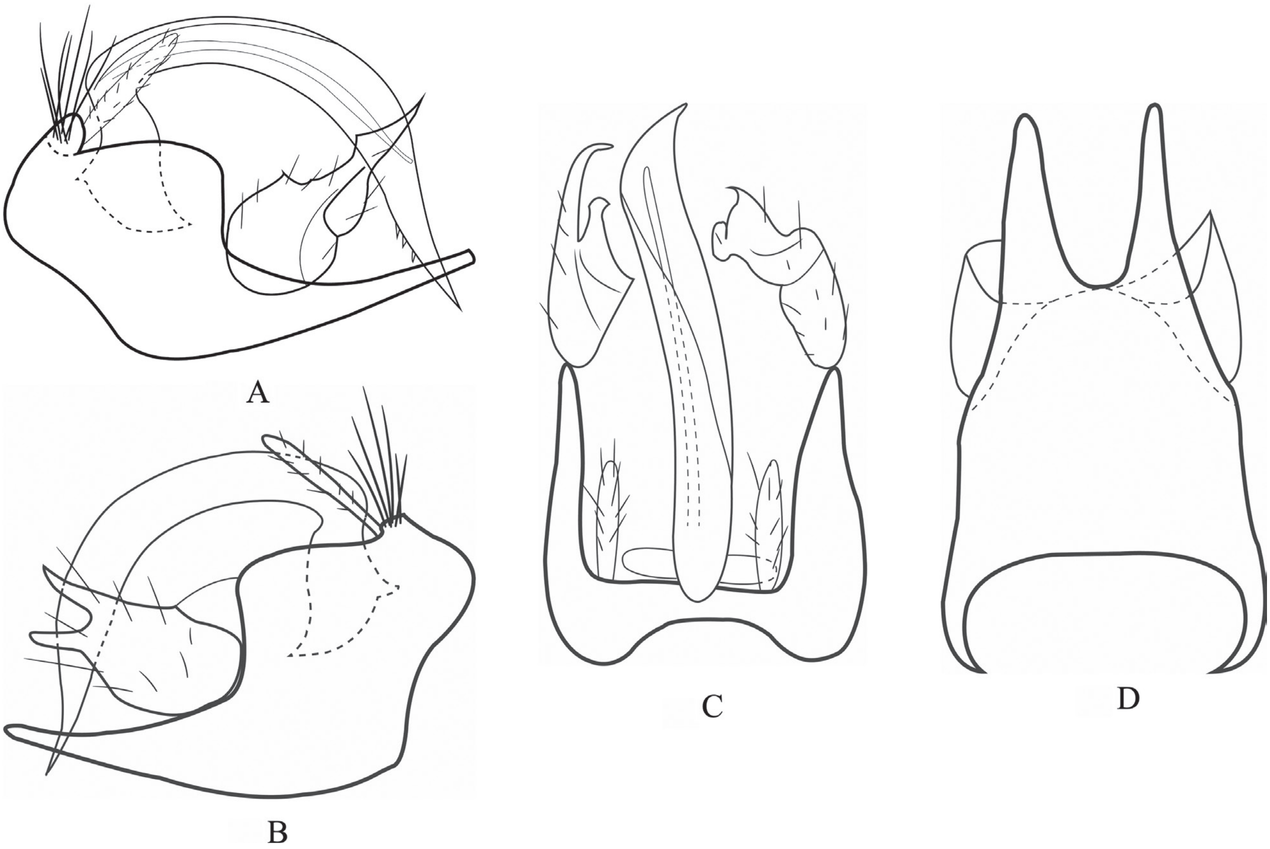

Figure 4. *Trichosetodes kampongspeuensis* male genitalia **A** segment IX and inferior appendages, left lateral **B** segment IX and inferior appendages, right lateral **C** segment IX and phallus, dorsal **D** segment IX, ventral.

ly convex anteriorly, undulated edge dorsally, curved downward ventrally with pimple sub-anteroventrally, long cylindrical subapicoventrally, rounded apically (Fig. 3A); in right lateral view the same as left lateral view but without pimple (Fig. 3B); in ventral view, vertical profile rectangular with 1/3 of height in U-shaped incision apically, rounded apex (Fig. 3D). Preanal appendages slender covered with hairs (Fig. 3A, B). Segment X not evident. Inferior appendages asymmetrical; circular basally, conical apically in left lateral view (Fig. 3A); in right lateral view, cylindrical with expanded basally, curved downward with tooth at dorsal edge subapically, pointed apically (Fig. 3B); in dorsal and ventral view, left inferior appendage claw-like, right inferior appendage long claw-like with an inner tooth. Phallicata large, tubular, curved and bent subapically, pointed apically in dorsal view; in lateral view, upside down U-shaped, pointed apically.

Etymology. The species is named for the type locality, Ratanakiri Province.

Molecular analysis

The molecular diversity of the new *Trichosetodes* species was analyzed using the mitochondrial large subunit ribosomal rRNA gene region (16S rRNA). Based on genetic distance (*p*-distance) of this gene fragment, *T. ratanakiriensis* sp. nov. and *T. kampongspeuensis* have a close genetic relationship, whereas *T. carmelae* sp. nov. showed greater genetic divergence from both *T. ratanakiriensis* sp. nov. and *T. kampongspeuensis* (Table 1). The estimated phylogenetic relationships based on the mtDNA 16S rRNA are shown in Fig. 5, where

Table 1. Genetic distances (*p*-distances) between *Trichosetodes* spp. from the Mekong River basin.

	T. kampongspeuensis	*T. ratanakiriensis*
T. ratanakiriensis	0.014	
T. carmelae	0.070	0.063

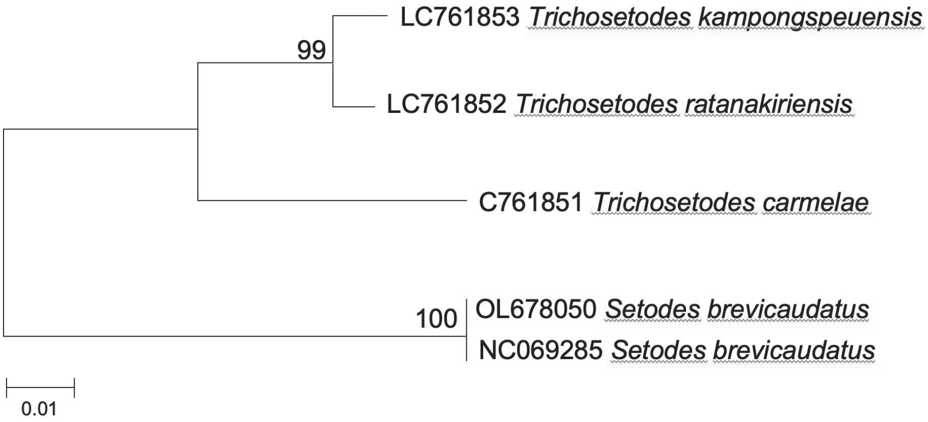

Figure 5. Estimated phylogenetic relationships using the Neighbor-Joining clustering method for *Trichosetodes* spp. based on the mtDNA 16S rRNA region. Sequences of *Setodes brevicaudatus* were included as outgroups. Each node's bootstrap value is shown (based on 1000 replicates). The scale bar indicates genetic distance (*p*-distance).

all three *Trichosetodes* sp. nov. were genetically differentiated. The monophyly of *T. ratanakiriensis* sp. nov. and *T. kampongspeuensis* was highly supported by the bootstrap value (NJ BP). In addition, *T. carmelae* sp. nov. was differentiated from the monophyletic clade of *T. ratanakiriensis* sp. nov. and *T. kampongspeuensis* (Fig. 5).

Discussion

Alongside the previously known *T. kampongspeuensis*, there are now a total of four species of *Trichosetodes* recorded in Cambodia. The three new species are known from a single locality, and such restricted distribution could be attributed to limited regional data availability, thus indicating the need for a comprehensive survey of aquatic invertebrate diversity in the Mekong River basin. Additionally, considering the known distribution of 19 *Trichosetodes* species in Southeast Asia (Fig. 7; Malicky 2010; Oláh 2013; Malicky and Laudee 2017; Morse 2023), such restricted distribution could also be attributed to potentially high endemism of this particular genus in the region (Laudee et al. 2022).

Trichosetodes carmelae sp. nov., *T. katiengensis* sp. nov. and *T. ratanakiriensis* sp. nov. were collected from a waterfall with cover by montane evergreen rainforest in eastern Cambodia. According to the habitat characteristics where they were collected, the three new species of *Trichosetodes* are potentially rhithral species that live in waterfalls and small streams where the substrate is dominated by bedrock, boulders and sand (Fig. 6). Moreover, all four species of *Trichosetodes* recorded from Cambodia were collected from waterfalls (Laudee et al. 2020). Furthermore, *T. asphor* was also collected from a fast-flowing stream (Malicky

Figure 6. Stream and waterfall at the collection site of *Trichosetodes* spp. in Ratanakiri Province, Cambodia, Mekong River basin.

and Laudee 2017). However, larvae of *T. japonicus* which is widely distributed in East Asia including Honshu and Fukuoka Prefectures (Japan), Korean Peninsula and Far East of Russia were mainly found from middle to lower sections of rivers with slow current (Kawai and Tanida 2018). The larvae and pupae of *T. imperfectus* Ulmer, 1951 from Sumatra, Indonesia were described by Ulmer (1955). Thus, as our collections are based on light trapping and larval stages are still unknown, we cannot exclude the possibility that *T. carmelae*, *T. katiengensis* and *T. ratanakiriensis* inhabit a wide range of habitats, such as larger river sections, lakes and reservoirs like some other Asian species (Kawai and Tanida 2018).

The molecular analysis, centered on the mtDNA 16S rRNA region, consistently mirrored the morphological distinctions observed among the newly identified species. While *T. ratanakiriensis* sp. nov. and *T. kampongspeuensis* share similarities in male genitalia characteristics, they exhibit distinct genital mor-

Figure 7. Distribution map of Trichosetodes spp. recorded from Southeast Asia. Abbreviations: **Asterix** = *T. anaksepuluh* Malicky & Chantaramongkol, 1995, **Plus** = *T. sisyphos* Malicky & Taeng-On, 2006, **White up-pointing triangle** = *T. pales* Malicky & Chaibu, 2006, **White circle** = *T. palinurus* Malicky & Chantaramongkol, 2006, **Black circle** = *T. hubertbruckneri* Malicky, 2006, **Black square** = *T. pallas* Malicky & Chantaramongkol, 2006, **White square** = *T. pan* Malicky, 2006, **Black up-pointing triangle** = *T. pandareos* Malicky 2006, **Black down-pointing triangle** = *T. pandion* Malicky & Chantaramongkol, 2006, **White down-pointing triangle** = *T. asphor* Malicky & Laudee, 2017, **Black star** = *T. harmas* Oláh, 2013, **White star** = *T. sotet* Oláh, 2013, **Black moon** = *T. kampongspeuensis* Malicky & Kong, 2020, **White moon** = *T. handschini* Ulmer, 1951, **Black right-pointing triangle** = *T. thienemanni* Ulmer, 1951, **White right-pointing triangle** = *T. anavadya* Schmid, 1987, **Black left-pointing triangle** = *T. carmelae* sp. nov., **White left-pointing triangle** = *T. katiengensis* sp. nov., **Multiplication X** = *T. ratanakiriensis* sp. nov.

phologies in contrast to *T. carmelae* sp. nov. Concerning the genetic distance calculated from the mtDNA 16S rRNA region, *T. ratanakiriensis* sp. nov. and *T. kampongspeuensis* demonstrated remarkable proximity, with a mere 1.4% divergence. On the contrary, the male genitalia traits of *T. carmelae* sp. nov. markedly differed from those of *T. ratanakiriensis* sp. nov. and *T. kampongspeuensis*, with molecular analysis indicating genetic distances exceeding 6.3%. Our results imply that the mtDNA16S rRNA gene fragment used to infer genetic divergence in Leptoceridae studied proved to be a good tool for supplementing taxonomy and diversity studies of Trichoptera (Takenaka et al. 2023).

Acknowledgments

We would like to thank Prof. Dr Vladimir Ivanov and an anonymous reviewer for providing very useful suggestions to improve the manuscript. We would like to thank Assoc. Prof. Dr Seppo Karrila for linguistic assistance.

Additional information

Conflict of interest

The authors have declared that no competing interests exist.

Ethical statement

No ethical statement was reported.

Funding

This research is supported by the Thailand Research Fund (TRF), project number DBG 6180021.

Author contributions

Conceptualization, Pongsak Laudee and Hans Malicky; Insect collection, Pongsak Laudee and Chamroeun Kong; Insect Identification, Pongsak Laudee and Hans Malicky; DNA analysis, Pongsak Laudee and Masaki Takenaka; Data Analysis and Manuscript Preparation, Pongsak Laudee, Hans Malicky, Koji Tojo and Masaki Takenaka

Author ORCIDs

Pongsak Laudee https://orcid.org/0000-0003-3819-7980
Chamroeun Kong https://orcid.org/0000-0002-4141-7270
Masaki Takenaka https://orcid.org/0000-0002-9565-524X
Koji Tojo https://orcid.org/0000-0002-9362-604X

Data availability

All of the data that support the findings of this study are available in the main text or Supplementary Information.

References

Gibon FM (1991) Trichoptères d'Afrique Occidentale et du Cameroun. Le genre *Trichosetodes* (Leptoceridae). Bulletin de la Société Entomologique de France 96(4): 347–353. https://doi.org/10.3406/bsef.1991.17740

Katoh K, Standley DM (2013) MAFFT Multiple sequence alignment Software Version 7: Improvements in performance and usability. Molecular Biology and Evolution 30(4): 772–780. https://doi.org/10.1093/molbev/mst010

Kawai T, Tanida K (2018) Aquatic Insects of Japan: Manual with Keys and Illustrations. Tokai University Press, Kanagawa, 1730 pp.

Kimura G, Kuranishi R (2020) Effect of visible light sticks for collecting of adult caddisflies (Trichoptera): A preliminary field study. Zoosymposia 18(1): 153–159. https://doi.org/10.11646/zoosymposia.18.1.19

Kumar S, Stecher G, Tamura K (2016) MEGA7: Molecular evolutionary genetics analysis version 7.0 for bigger datasets. Molecular Biology and Evolution 33(7): 1870–1874. https://doi.org/10.1093/molbev/msw054

Laudee P, Kong C, Malicky H (2020) New species of caddisflies (Trichoptera: Psychomyiidae, Hydropsychidae, Leptoceridae) from Mekong tributaries, Cambodia. Zootaxa 4853(1): 133–138. https://doi.org/10.11646/zootaxa.4853.1.9

Laudee P, Malicky H, Seetapan K, Thamsaenanupap P, Karnkasem S, Vongsombath C, Oo SSL, Kong C, Zalyan P, Morse JC (2022) Distribution of *Ecnomus* McLachlan, 1864 (Trichoptera, Ecnomidae) from the Lower Mekong River with a description of *Ecnomus stungtrengensis* new species. Biodiversity Data Journal 10: e94936. https://doi.org/10.3897/BDJ.10.e94936

Malicky H (2006a) Beiträge zur Kenntnis asiatischer Leptoceridae (Trichoptera: *Adicella*, *Athripsodes*, *Ceraclea*, *Leptocerus*, *Oecetis*, *Parasetodes*, *Tagalopsyche*, *Triaenodes*, *Trichosetodes*). Linzer Biologische Beitrage 38: 1507–1530.

Malicky H (2006b) Caddisflies from Bardia National Park, Nepal, with a preliminary survey of Nepalese species (Insecta, Trichoptera). Entomofauna 27(20): 241–264.

Malicky H (2010) Atlas of Southeast Asian Trichoptera. Biology Department, Faculty of Science, Chiang Mai University, Chiang Mai, 346 pp.

Malicky H, Graf W (2020) Drei neue Köcherfliegen-Arten der Gattung *Trichosetodes* (Trichoptera, Leptoceridae) aus Afrika. Acta ZooBot Austria 157: 257–260.

Malicky H, Laudee P (2017) Fünf neue Köcherfliegen (Trichoptera) aus Laos und Myanmar. Linzer Biologische Beitrage 49(2): 1447–1452.

Mey W, De Moor FC (2019) The Trichoptera (Insecta) of the lower Kunene River in Namibia and Angola. Zoosymposia 14(1): 134–150. https://doi.org/10.11646/zoosymposia.14.1.16

Morse JC (2023) Trichoptera World Checklist. https://trichopt.app.clemson.edu/welcome.php#ol [accessed 10 July 2023]

Oláh J (2013) On the Trichoptera of Vietnam, with description of 52 new species. Annales Historico-Naturales Musei Nationalis Hungarici 105: 55–134.

Park S, Kong S (2020) A checklist of Trichoptera (Insecta) of the Korean Peninsula. Journal of Species Research 9(3): 288–323.

Saini MS, Kaur M, Bajwa PK (2001) An updated check-list of the Indian Trichoptera along with an illustrated key to its families. Records of the Zoological Survey of India 99(1–4): 201–256. https://doi.org/10.26515/rzsi/v99/i1-4/2001/159643

Schmid F (1987) Considérations diverses sur quelques genres léptocerins (Trichoptera, Leptoceridae). Bulletin de l'Institut royal des sciences naturelles de Belgique. Entomologie and biologie 57(Supplement): 1–147.

Takenaka M, Yano K, Suzuki T, Tojo K (2023) Development of novel PCR primer sets for DNA barcoding of aquatic insects, and the discovery of some cryptic species. Limnology 24(2): 121–136. https://doi.org/10.1007/s10201-022-00710-5

Ulmer G (1955) KÖcherfliegen (Trichopteren) von den Sunda-Inseln (Teil II). Archiv fÜr Hydrobiologie supplement 21(3/4): 408–608.

Yang L, Morse JC (2000) Leptoceridae (Trichoptera) of the People's Republic of China. Memoirs of the American Entomological Institute, 309 pp.

Yang L, Sun C, Morse JC (2016) An amended checklist of the caddisflies of China (Insecta, Trichoptera). Zoosymposia 10(1): 451–479. https://doi.org/10.11646/zoosymposia.10.1.42

ZooKeys 1182: 165–181 (2023)
DOI: 10.3897/zookeys.1182.97346

Research Article

Five new species of *Bryaxis* Kugelann (Coleoptera, Staphylinidae, Pselaphinae) from Korea and a nomenclatural note on *Bryaxis mahunkai* Löbl

Yeon-Jae Choi[1], Sun-Jae Park[2], Seung-Gyu Lee[3], Jong-Seok Park[1]

1 *Department of Biological Sciences and Biotechnology, Chungbuk National University, Cheongju 28644, Republic of Korea*
2 *Climate Change and Environmental Biology Research Division, National Institute of Biological Resources, Incheon 22689, Republic of Korea*
3 *Biodiversity Education Division, National Institute of Biological Resources, Incheon 22689, Republic of Korea*
Corresponding author: Jong-Seok Park (jpark16@cbnu.ac.kr)

Abstract

The genus *Bryaxis* Kugelann (Goniaceritae: Bythinini) is the most species-rich genus of the subfamily Pselaphinae and is mainly distributed in the Palearctic region. Although previous studies have documented 14 species in the Korean Peninsula, the true diversity, ecology, and immature stages of the genus are still inadequately known. In this study, five new Korean species are described: *B. grandinodus* **sp. nov.**, *B. uljinensis* **sp. nov.**, *B. fabaiformis* **sp. nov.**, *B. girinensis* **sp. nov.**, and *B. nemorosus* **sp. nov.** Illustrations of the habitus and other morphological details, and a distribution map are provided. In addition, *Bryaxis leechanyoungi* Nomura & Lee, 1993 is proposed as a new synonym of *B. mahunkai* Löbl, 1975 based on the original description and illustrations of diagnostic characters.

Key words: *B. fabaiformis* sp. nov., *B. girinensis* sp. nov., *B. grandinodus* sp. nov., *B. nemorosus* sp. nov., *B. uljinensis* sp. nov., diversity, morphology, new synonym, Palearctic, taxonomy

Academic editor: Adam Brunke
Received: 9 November 2022
Accepted: 16 June 2023
Published: 13 October 2023

ZooBank: https://zoobank.org/86F5AC45-D35E-4DDF-AB04-2BCBDEEE8407

Citation: Choi Y-J, Park S-J, Lee S-G, Park J-S (2023) Five new species of *Bryaxis* Kugelann (Coleoptera, Staphylinidae, Pselaphinae) from Korea and a nomenclatural note on *Bryaxis mahunkai* Löbl. ZooKeys 1182: 165–181. https://doi.org/10.3897/zookeys.1182.97346

Introduction

The genus *Bryaxis* Kugelann, 1794 is the most species-rich pselaphine genus, containing 385 species and 40 subspecies. Except for one adventive species recorded from North America (Chandler 2022) most species of the genus are distributed in the Palearctic and Oriental regions (Newton 2022; Yin 2023). In Northeast Asia, 36, 10, 18, and 19 species are recorded in Japan, the Russian Far East, China, and Taiwan, respectively (Schülke and Smetana 2015; Taru and Nomura 2021; Yin 2023). In Korea, *Bryaxis* comprises 14 species, 11 of which are endemic (Schülke and Smetana 2015; Ahn et al. 2017). Löbl (1974) first recorded this genus in Korea by describing two species, *B. pawlowskii* Löbl and *B. validicornides* Löbl. Nomura and Lee (1992, 1993) revised the Korean *Bryaxis* and described eight species, one of which was later synonymized (*B. coreanus* Nomura & Lee, 1992 with *B. koltzei* (Reitter, 1887); Nomura 1995). Members of Korean *Bryaxis* can be identified by the swollen antennal scape or pedicel with glandular nodule in males (Nomura and Lee 1992). All type specimens were collected from forest leaf litter.

Herein we describe five new species by providing illustrations of the habitus and diagnostic characters of each species and a distribution map. Moreover, we found a taxonomic problem regarding *Bryaxis leechanyoungi* Nomura & Lee, 1993, which is synonymized with *B. mahunkai* Löbl, 1975 in the present study.

Material and method

Eighty-seven specimens from Chungbuk National University Insect Collection (**CBNUIC**, Cheongju, Republic of Korea) and one specimen from Chungnam National University Insect Collection (**CNUIC**, Daejeon, Republic of Korea) were examined. The holotypes of all species described herein are deposited in the National Institute of Biological Resources (**NIBR**, Incheon, Republic of Korea). Depositions of paratypes and vouchers are indicated parenthetically. At least one specimen of each species was dissected to study the male genitalia and details of other characters. Terminology and nomenclature used follow Chandler (2001) for external characters and Lawrence et al. (2011) for genital characters. Numbering of abdominal sclerites indicate morphological segments. Specimen label data for the holotypes are transcribed verbatim. Data for other specimens are standardized for consistency. Specimens were observed using a Leica M80 and DM1000 LED optical microscope. Images were generated using Sony ILCE-7RM3 mirrorless camera and stacked with Zerene Stacker v. 1.04. The map of Korea was created using the Natural Earth quick start for QGIS v. 3 and open source QGIS v. 3.30.2. For comparison, localities of three dominant species in Korea, *Bryaxis mahunkai* Löbl, *B. koltzei* (Reitter) and *B. kimjongkuki* Nomura & Lee, were also marked.

Results

Subfamily Pselaphinae Latreille, 1802
Supertribe Goniaceritae Reitter, 1882
Tribe Bythinini Raffray, 1890

Genus *Bryaxis* Kugelann, 1794

Type species. *Pselaphus bulbifer* Reichenbach, 1816.

Bryaxis grandinodus Choi, Park, Lee & Park, sp. nov.

https://zoobank.org/296C6B58-60CE-41D9-BD87-AAC45B5AC0C5
Figs 1, 2A, C

Type materials (*N* = 11, 6♂♂, 5♀♀). *Holotype male*. “Korea: Jeonnam Prov. Dangsan-ri, Gyegok-myeon, Haenam-gun, 18 May 2019, 34°40'53.0"N, 126°38'56.3"E, 211 m, sifting leaf litter & deadwood debris, J.-S. Park, M.-H. Song” (NIBR). ***Paratypes*.** 2♂♂, 2♀♀ (CBNUIC, 1♂, 1♀ slide mounted, 1♂, 1♀ dried). “Korea: Jeonbuk Prov. Sinsi island. Sinsido-gil, Okdo-myeon, Gunsan-si, 4 Jul 2022, 35°49'12.2"N, 126°27'35.1"E, 36 m, sifting leaf & soil litter, M.-H. Song, U.-J. Byeon, J.-W. Kang, T.-Y. Jang”. 2♂♂ (CBNUIC, dried) “Korea: Jeonbuk Prov. Seonyu island. Seonyubuk-gil, Okdo-myeon, Gunsan-si, 16 Jun 2021,

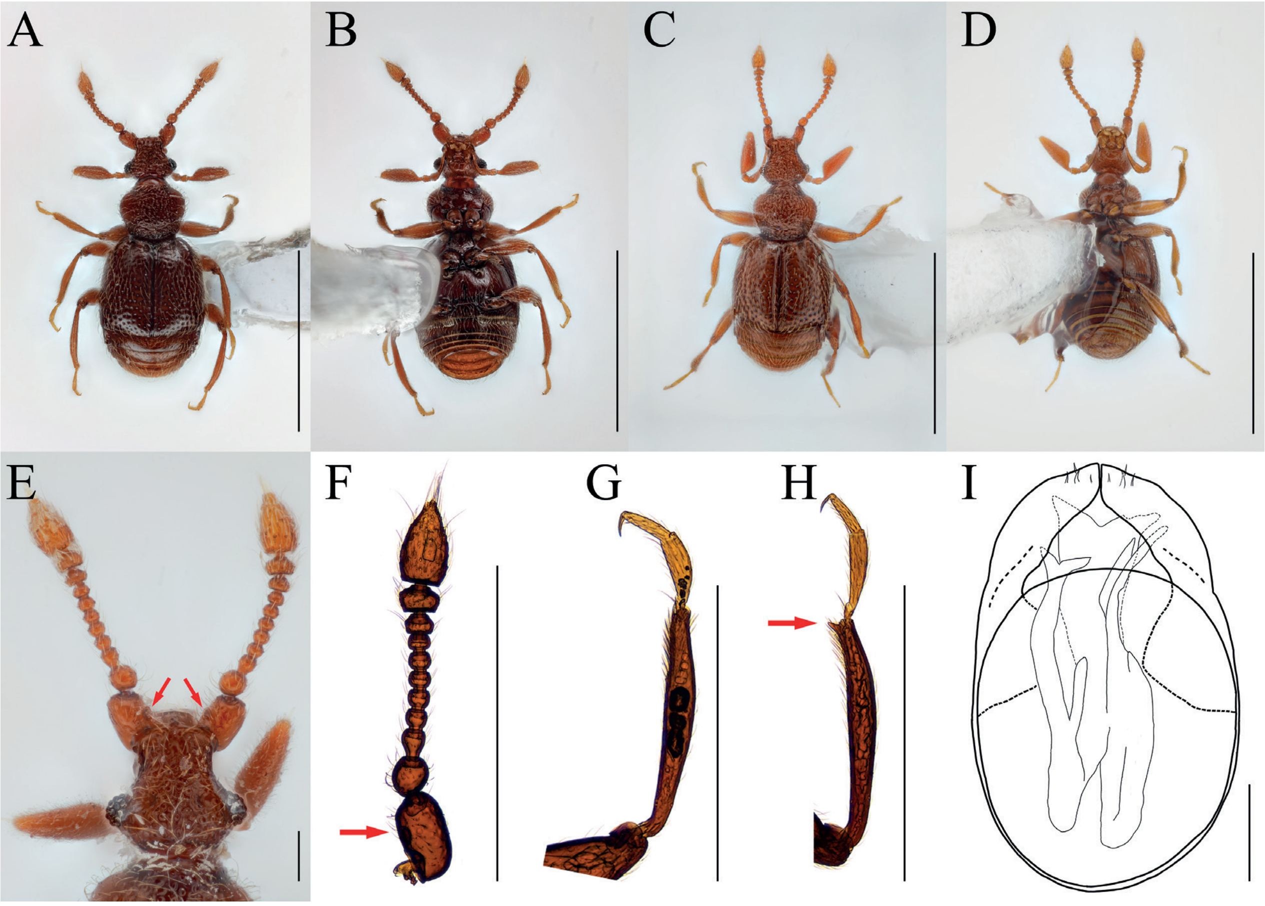

Figure 1. *Bryaxis grandinodus* Choi, Park, Lee & Park, sp. nov., male (**A, B, E–I**), female (**C, D**). **A, C** dorsal habitus **B, D** ventral habitus **E** head **F** antenna **G** fore leg **H** hind leg **I** aedeagus. Scale bars: 1 mm (**A–D**); 0.1 mm (**E, I**); 0.5 mm (**F–H**).

35°48'36.5"N, 126°24'57.4"E, 25 m, sifting leaf, soil litter & fungi, J.-W. Kang, J.-I. Shin". 1♂, 3♀♀ (CBNUIC, DNA grade). "Korea: Jeonbuk Prov. Seonyu island. 5-1, Seonyunam-gil, Okdo-myeon, Gunsan-si, 4 Jul 2022, 35°48'24.7"N, 126°24'40.3"E, 9 m, sifting leaf & soil litter, M.-H. Song, U.-J. Byeon, J.-W. Kang, T.-Y. Jang".

Diagnosis. Antennal scapes robust, with bowl-like glandular nodule on inner margin (Figs 1E, F, 2A, arrows), 2.45 times as long as pedicels; endophallus of male genitalia with three bifid struts, joined at base (Fig. 1I).

Description. Body reddish brown, antennae, maxillary palpi, and tarsi slightly lighter, length 1.2–1.32 mm, maximum width 0.51–0.58 mm (Fig. 1A–D). Setae on body yellowish, long. Head 0.92 times as long as wide (Fig. 1E). Frons with U-shaped impression between antennal tubercles; frontal foveae absent; frontal rostrum distinct anteriorly. Vertex slightly convex; longitudinal carina weak; vertexal foveae large. Eyes as long as tempora, with 23–26 facets. Maxillary palpi moderately developed; palpomeres II–III with tubercles; palpomere IV 0.23 mm long and about 3.15 times as long as wide, subcylindrical pseudosegment at apex. Antennae about 0.54 mm long; pedicels subglobose with long setae, 0.89 times as long as wide; antennomere III 1.12 times as long as wide; IV–VIII subequal in length; IX–X transverse, IX 0.64 times as long as wide and X 0.63 times as long as wide; XI largest, pointed at apex, 1.67 times as long as wide (Fig. 1F). Pronotum 0.84 times as long as wide and widest at basal 2/3, lateral antebasal

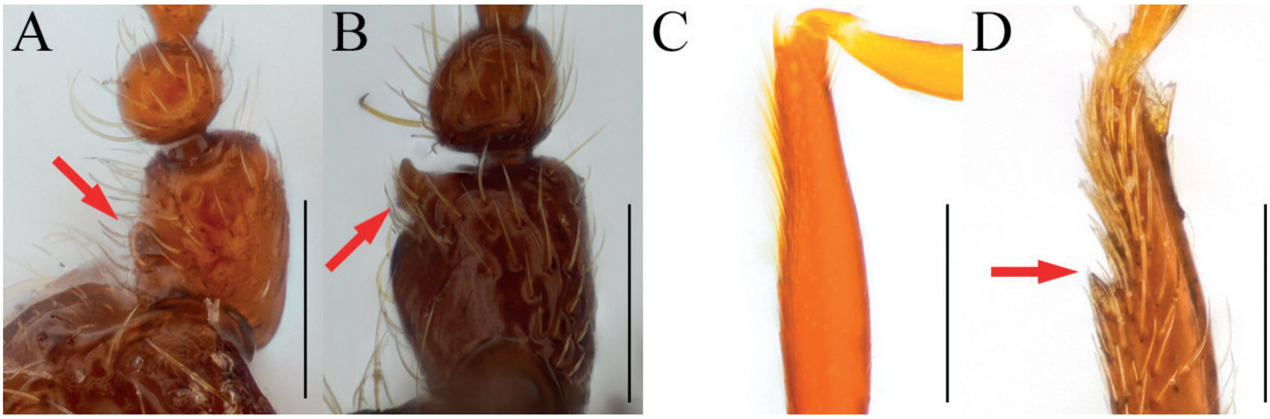

Figure 2. Diagnostic characters of *Bryaxis grandinodus* sp. nov. (**A, C**) and *B. koltzei* (Reitter) (**B, D**). **A, B** antennal scapes and pedicels **C, D** protibiae. Scale bars: 0.1 mm.

foveae connected by antebasal sulcus. Elytra slightly convex, 0.89 times as long as wide and widest at basal 1/4, each elytron with two basal foveae and subhumeral fovea. Legs slender; protibiae without spine (Figs 1G, 2C); metatibiae with spine at apex (Fig. 1H, arrow). Aedeagus large, 0.37 mm long and 1.69 times as long as wide; penis bulbous and dorsal diaphragm ovoid; parameres short and symmetrical, apices almost encountered, one robust seta and three fine setae on each apex; endophallus divided into three large struts, left dorsal strut branched at basal 1/3 and bifid at apex, right dorsal strut weakly branched basally and bifid dorso-ventrally at apex, ventral strut robust and bifid at apex (Fig. 1I).

***Sexual dimorphism*.** Female eyes shorter than tempora, composed of 11 facets; antennal scapes subcylindrical, without modification; metatibial spines absent.

Remarks. Adults of this species are very similar to *Bryaxis koltzei* (Reitter, 1887) in the general body characters, but can be distinguished by the shape of the antennal scapes and its glandular nodule (Fig. 2A, arrow) and the spineless protibiae in the male (Fig. 2C).

Comments. The localities of *B. grandinodus* sp. nov. probably overlap with those of *B. koltzei* (Reitter) given that the latter are distributed across the entire country (Fig. 11).

Etymology. The specific epithet is a combination of the Latin words *grandis* (“large”, masculine) and *nodus* (“knob”, masculine) and refers to the shape of the glandular nodules on the male antennal scapes.

Habitat. The holotype was collected by sifting leaf litter in mixed forest. Paratypes were collected by sifting leaf litter and soil.

Distribution. Korea (Haenam-gun, Jeollanam-do; Gunsan-si, Jeollabuk-do).

***Bryaxis uljinensis* Choi, Park, Lee & Park, sp. nov.**

https://zoobank.org/CF039CE1-2159-4BF5-8E6A-5B9508CBEAC5

Figs 3, 4A, C, E

Type materials (*N* = 7, 4♂♂, 3♀♀). *Holotype male*. “Korea: Gyeongbuk Prov. Onjeong-myeon, Uljin-gun, 8 Jun 2019, 36°43'23.0"N, 129°20'16.0"E, 180 m, sifting leaf litter near stream, J.-S. Park” (NIBR). ***Paratypes*.** 2♂♂ (CBNUIC, 1♂ slide mounted, 1♂ dried). “Korea: Gangwon Prov. Gujeol-ri, Yeoryang-myeon, Jeongseon-gun, 24 Apr 2020, 37°31'08.7"N, 128°46'42.8"E, 591 m, sifting leaf & soil litter, U.-J. Byeon, T.-Y. Jang". 1♂, 3♀♀ (CBNUIC, dried). "Korea: Gangwon Prov. Gujeol-ri, Yeoryang-myeon, Jeongseon-gun, 24 Apr 2020, 37°30'57.6"N, 128°45'18.8"E, 510 m, sifting ant colony, leaf & soil litter, Y.-J. Choi, U.-J. Byeon".

Diagnosis. Antennal pedicel strongly swollen, subglobose with subcylindrical glandular nodule on basal 1/3 of inner margin (Figs 3F, 4C, arrows); protibiae with spine on internal side of widest (Figs 3G, 4E, arrows); parameres of male genitalia robust and fan-shaped, bearing three setae on each (Fig. 3I).

Description. Body reddish brown, antennae, maxillary palpi, legs slightly lighter than body, length 1.25–1.31 mm, maximum width 0.53–0.60 mm (Fig. 3A–D). Setae on body yellowish, and short. Head 0.98 times as long as wide (Fig. 3E). Frons with small U-shaped impression between antennal tubercles; frontal foveae absent; frontal rostrum slightly distinct anteriorly. Vertex convex; longitudinal carina present; vertexal foveae small. Eyes large, longer than twice that of tempora, composed of 32–34 facets. Maxillary palpi moderately developed; palpomeres II–III smooth; palpomere IV 0.22 mm long and about 3.16 times as long as wide, subcylindrical pseudosegment at apex. Antennae about 0.53 mm long; scapes short without modification, 0.92 times as long as pedicels; pedicels long as wide; antennomere III–VIII subequal in length; IX 0.63 times as long as wide; X transverse, 0.61 times as long as wide; XI largest, pointed at apex, 1.61 times as long as wide (Fig. 3F). Pronotum 0.88 times as long as

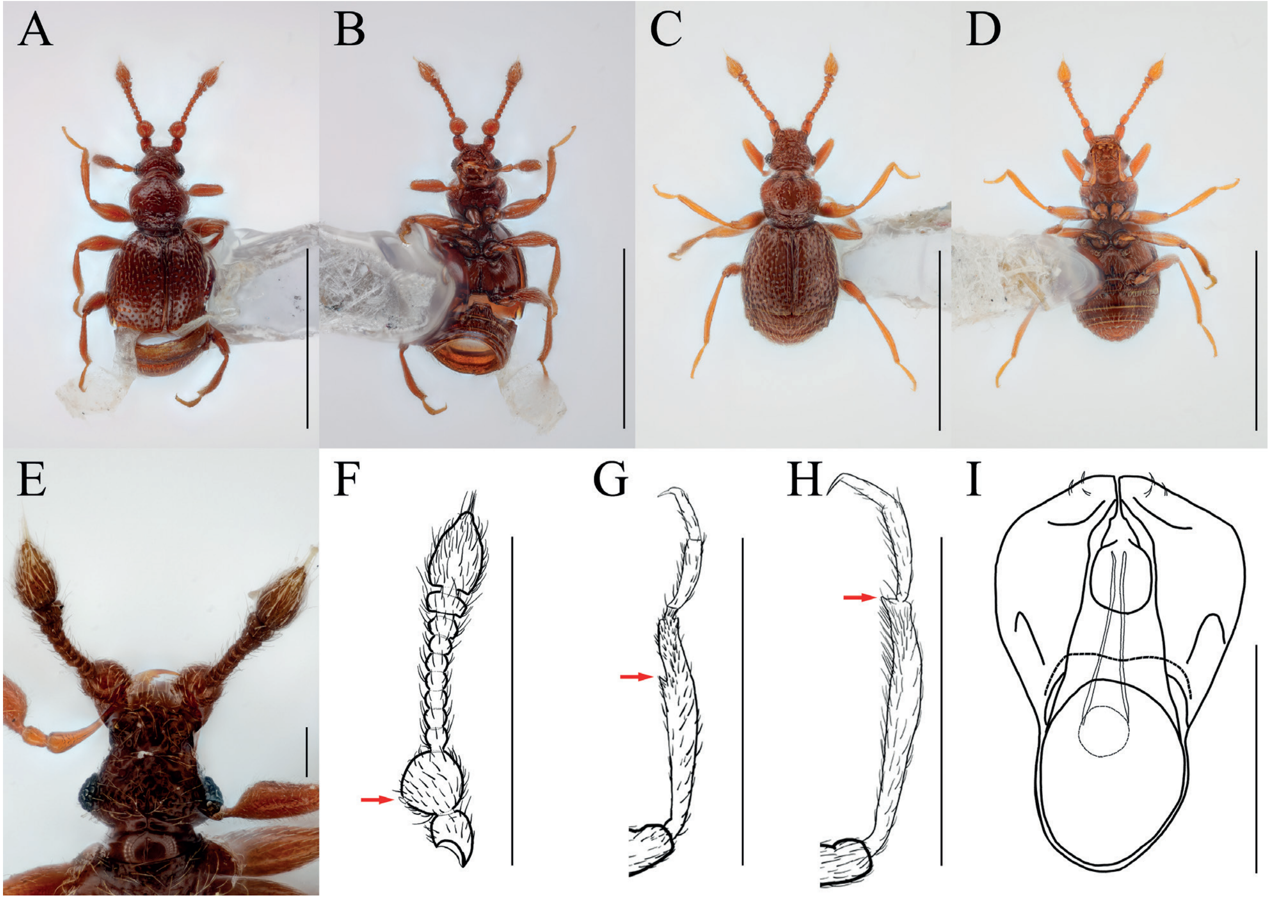

Figure 3. *Bryaxis uljinensis* Choi, Park, Lee & Park, sp. nov., male (**A, B, E–I**), female (**C, D**). **A, C** dorsal habitus **B, D** ventral habitus **E** head **F** antenna **G** fore leg **H** hind leg **I** aedeagus. Scale bars: 1 mm (**A–D**); 0.1 mm (**E, I**); 0.5 mm (**F–H**).

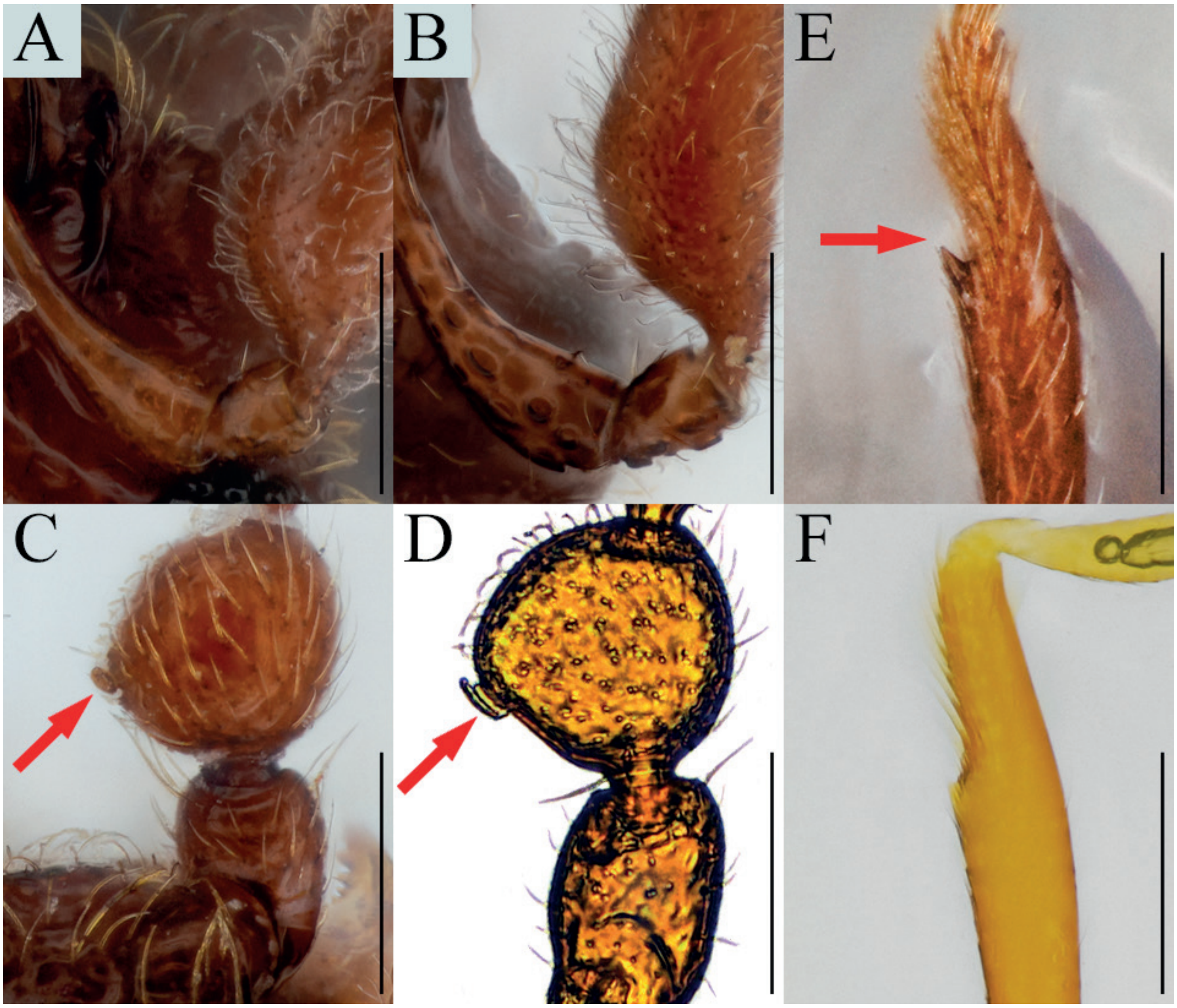

Figure 4. Diagnostic characters of *Bryaxis uljinensis* sp. nov. (**A, C, E**) and *B. mahunkai* Löbl (**B, D, F**). **A, B** maxillary palpi **C, D** antennal scapes and pedicels **E, F** protibiae. Scale bars: 0.1 mm.

wide and widest at basal 3/5, lateral antebasal foveae connected by antebasal sulcus. Elytra convex, 0.85 times as long as wide and widest at basal 1/3, each elytron with two basal foveae and subhumeral fovea. Legs robust; internal spine on widest of protibiae (Fig. 3G, arrow); metatibiae with spine on apical (Fig. 3H, arrow). Aedeagus small, 0.27 mm long and 1.61 times as long as wide; penis small fusiform and dorsal diaphragm bulbous; parameres symmetrical; endophallus composed with two convergent, slender struts (Fig. 3I).

***Sexual dimorphism*.** Female eyes slightly longer than tempora, composed of 15 facets; antennal pedicels simple; protibial spines and metatibial spines absent.

Remarks. Adults of this species are very similar to *Bryaxis mahunkai* Löbl, 1975 in having strongly swollen antennal pedicels (Fig. 4C, D). However, they can be distinguished by smooth maxillary palpomere II–III (Fig. 4A), apically symmetrical antennal scapes, pedicels less swollen apically and bearing smaller glandular nodules (Fig. 4C, arrow), fore legs with a tibial spine (Fig. 4E, arrow), and parameres wider than the penis (aedeagus in *B. mahunkai* as wide as penis; Fig. 10C, D).

Comments. The localities of *B. uljinensis* sp. nov. probably overlap with those of *B. mahunkai* Löbl given that the latter are nationally distributed (Fig. 11).

Etymology. This species is named after the type locality, Uljin-gun.

Habitat. The holotype was collected by sifting leaf litter in mixed forest. Paratypes were collected by sifting leaf litter, soil, and an ant colony.

Distribution. Korea (Uljin-gun, Gyeongsangbuk-do; Jeongseon-gun, Gangwon-do).

Bryaxis fabaiformis Choi, Park, Lee & Park, sp. nov.

https://zoobank.org/1110CCA6-D13F-45B9-A9EF-49B993E8DF44
Figs 5, 6A, C, E

Type materials (*N* = 4, 3♂♂, 1♀). *Holotype male*. "Korea: Gangwon Prov. Gujeol-ri, Yeoryang-myeon, Jeongseon-gun, 24 Apr 2020, 37°31'08.3"N, 128°46'43.0"E, 552 m, sifting soil & leaf litter, U.-J. Byeon, T.-Y. Jang" (NIBR). ***Paratypes*.** (CBNUIC, 1♂ slide mounted, 1♂, 1♀ dried). "Korea: Gangwon Prov. Gujeol-ri, Yeoryang-myeon, Jeongseon-gun, 24 Apr 2020, 37°31'08.3"N, 128°46'43.0"E, 552 m, sifting soil & leaf litter, U.-J. Byeon, T.-Y. Jang".

Diagnosis. Enlarged fabiform antennal pedicels with subcylindrical glandular nodule on inner margin in male (Figs 5E, F, 6A, arrows).

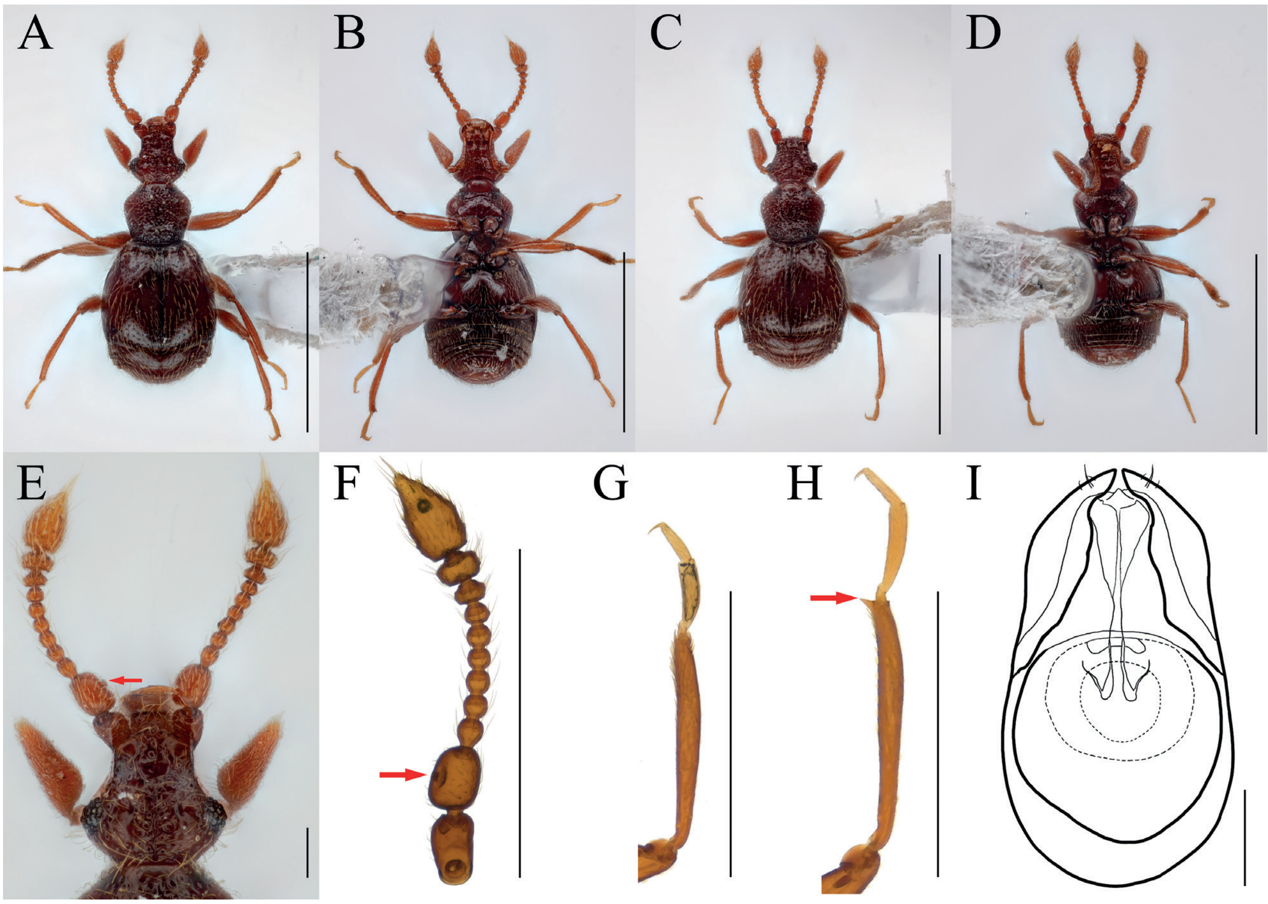

Figure 5. *Bryaxis fabaiformis* Choi, Park, Lee & Park, sp. nov. male (**A, B, E–I**), female (**C, D**). **A, C** dorsal habitus **B, D** ventral habitus **E** head **F** antenna **G** fore leg **H** hind leg **I** aedeagus. Scale bars: 1 mm (**A–D**); 0.1 mm (**E, I**); 0.5 mm (**F–H**).

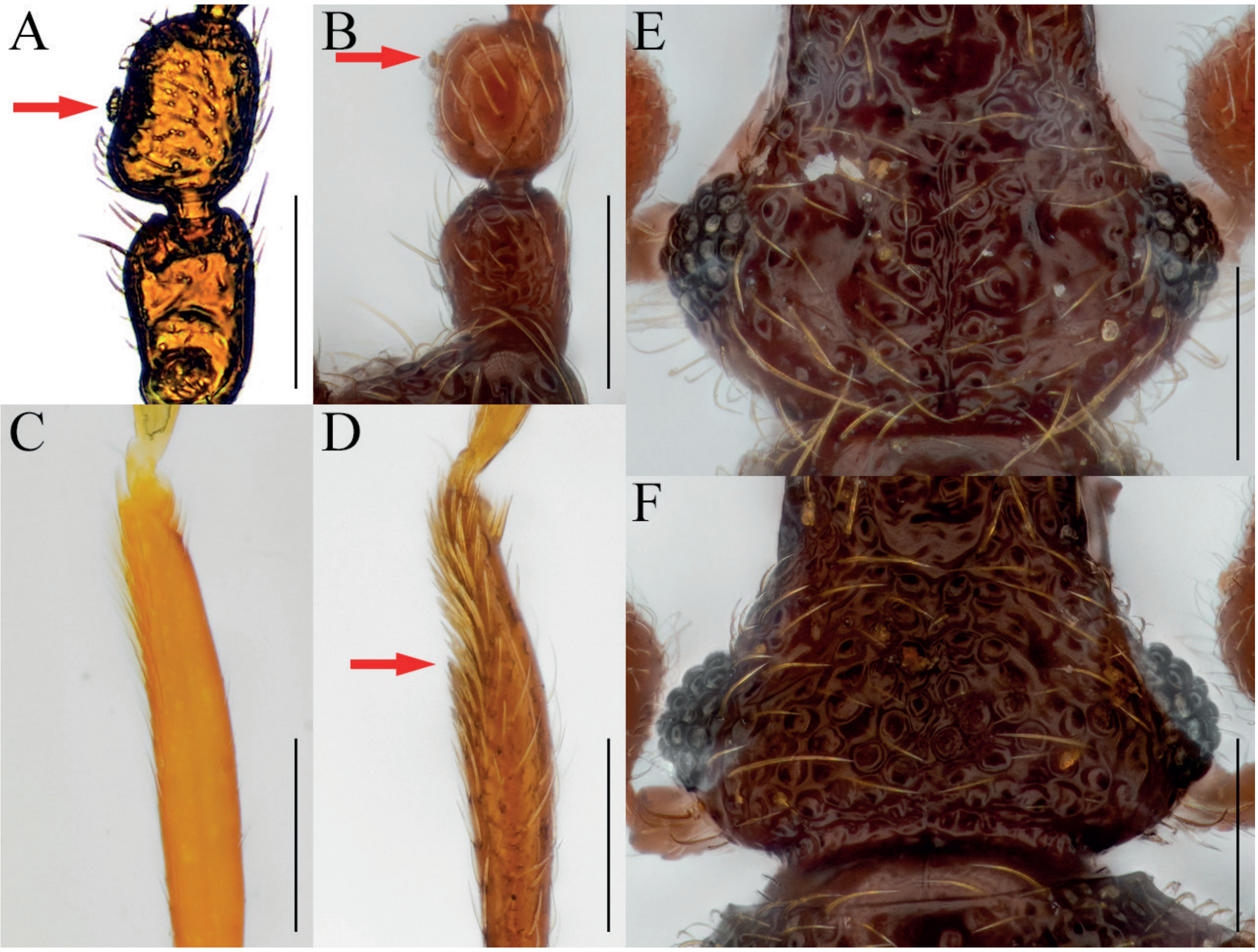

Figure 6. Diagnostic characters of *Bryaxis fabaiformis* sp. nov. (**A, C, E**) and *B. kimjongkuki* Nomura & Lee (**B, D, F**). **A, B** antennal scapes and pedicels **C, D** protibiae **E, F** heads. Scale bars: 0.1 mm.

Description. Body reddish brown, antennae, maxillary palpi, legs slightly lighter than body, length 1.29–1.41 mm, maximum width 0.60–0.64 mm (Fig. 5A–D). Setae on body golden and long. Head 0.84–1.00 times as long as wide (Fig. 5F). Frons with U-shaped impression between antennal tubercles; frontal foveae absent; frontal rostrum distinct anteriorly. Vertex weakly convex; longitudinal carina distinct; vertexal foveae enlarged. Eyes large with 31–32 facets. Maxillary palpi moderately developed; palpomeres II–III with sparse tubercles; palpomere IV 0.25–0.29 mm long and about 2.92–3.44 times as long as wide, subcylindrical pseudosegment at apex. Antennae about 0.58–0.61 mm long; scapes short, without modification, 0.73–1.11 times as long as pedicels; pedicels 1.02–1.19 times as long as wide; antennomere III 1.18–1.23 times as long as wide; IV–VIII subequal in length; IX–X transverse, IX 0.66–0.69 times as long as wide and X 0.62–0.63 times as long as wide; XI largest, pointed at apex, 1.65–1.75 times as long as wide (Fig. 5F). Pronotum 0.84–0.89 times as long as wide and widest at basal 3/5, lateral antebasal foveae connected by antebasal sulcus. Elytra convex, 0.85–0.94 times as long as wide and widest at basal 1/3, each elytron with two basal foveae and subhumeral fovea. Legs slender; protibiae without spine (Fig. 5G); metatibiae with spine at apex (Fig. 5H, arrow). Aedeagus robust, 0.43 mm long and 1.79 times as long as wide; penis bulbous and dorsal diaphragm circular; parameres small and symmetrical, each with three setae; endophallus comprising two symmetrical struts, each broadened basally and apically, and shortly branched basally (Fig. 5I).

***Sexual dimorphism*.** Female eyes slightly shorter than tempora, comprising 9 facets; antennal pedicels without modification; metatibial spines absent.

Remarks. Adults of this species are similar to those of *Bryaxis kimjongkuki* Nomura & Lee, 1993 in having the maxillary palpomere II–III with tubercles and asymmetrical antennal scapes. However, they can be recognized by having a rounded tempora as long as the eyes (Fig. 6E), a glandular nodule situated at the mid-level of the antennal pedicels (Fig. 6A, arrow), and protibiae without a spine (Fig. 6C).

Comments. The localities of *B. fabaiformis* sp. nov. probably overlap with those of *B. kimjongkuki* Nomura & Lee given that the latter species was abundantly collected near the type localities of the former (Fig. 11).

Etymology. The specific epithet is a combination of the Latin words *faba* ("bean", feminine) and *-formis* ("having the form of", masculine/feminine) and refers to the shape of antennal pedicels in the male.

Habitat. Specimens of this species were collected by sifting soil and leaf litter in mixed forest.

Distribution. Korea (Jeongseon-gun, Gangwon-do).

Bryaxis girinensis Choi, Park, Lee & Park, sp. nov.

https://zoobank.org/DB5551C4-3A0F-4F13-8D83-87BFBAA8741A
Figs 7, 9A, C, E

Type material (*N* = 1, 1♂). *Holotype male*. "Korea: Gangwon Prov. Bangdong-ri, Girin-myeon, Inje-gun, 23 Jun 2009, sifting flood debris, T.-K. Kim, CNUIC" (NIBR).

Diagnosis. Antennal pedicels less enlarged subglobose, with dorsolateral glandular nodule on subapical (Fig. 7C, D, arrows); protibiae with spine on internal side at widest point (Figs 7E, 9C, arrows); parameres of male genitalia with depression on lateral margin and three setae on apical (Fig. 7G).

Description. Body reddish brown, antennae, maxillary palpi, and tarsi slightly lighter, length 1.62 mm, maximum width 0.70 mm (Fig. 7A, B). Setae on body yellowish, long and dense. Head long as wide (Fig. 7C). Frons with U-shaped impression between antennal tubercles; frontal foveae absent; frontal rostrum distinct anteriorly. Vertex slightly convex; longitudinal carina present; vertexal foveae small. Eyes large with 34 facets. Maxillary palpi moderately developed; palpomeres II–III with dense tubercles; palpomere IV 0.25 mm long and about 3.30 times as long as wide, subcylindrical pseudosegment at apex. Antennae about 0.54 mm long; scapes subcylindrical, without modification, 1.83 times as long as pedicels; pedicels long as wide; antennomere III 1.70 times as long as wide; IV–VIII subequal in length; IX 0.89 times as long as wide; X 0.78 times as long as wide; XI largest, pointed at apex, 1.86 times as long as wide (Fig. 7D). Pronotum 0.79 times as long as wide and widest at basal 3/5, lateral antebasal foveae connected by antebasal sulcus. Elytra slightly convex, 0.98 times as long as wide and widest at basal 1/3, each elytron with two basal foveae and subhumeral fovea. Legs robust; metatibiae with spine at apex (Fig. 7E, arrow). Aedeagus large, 0.36 mm long and 2.05 times as long as wide; penis fusiform

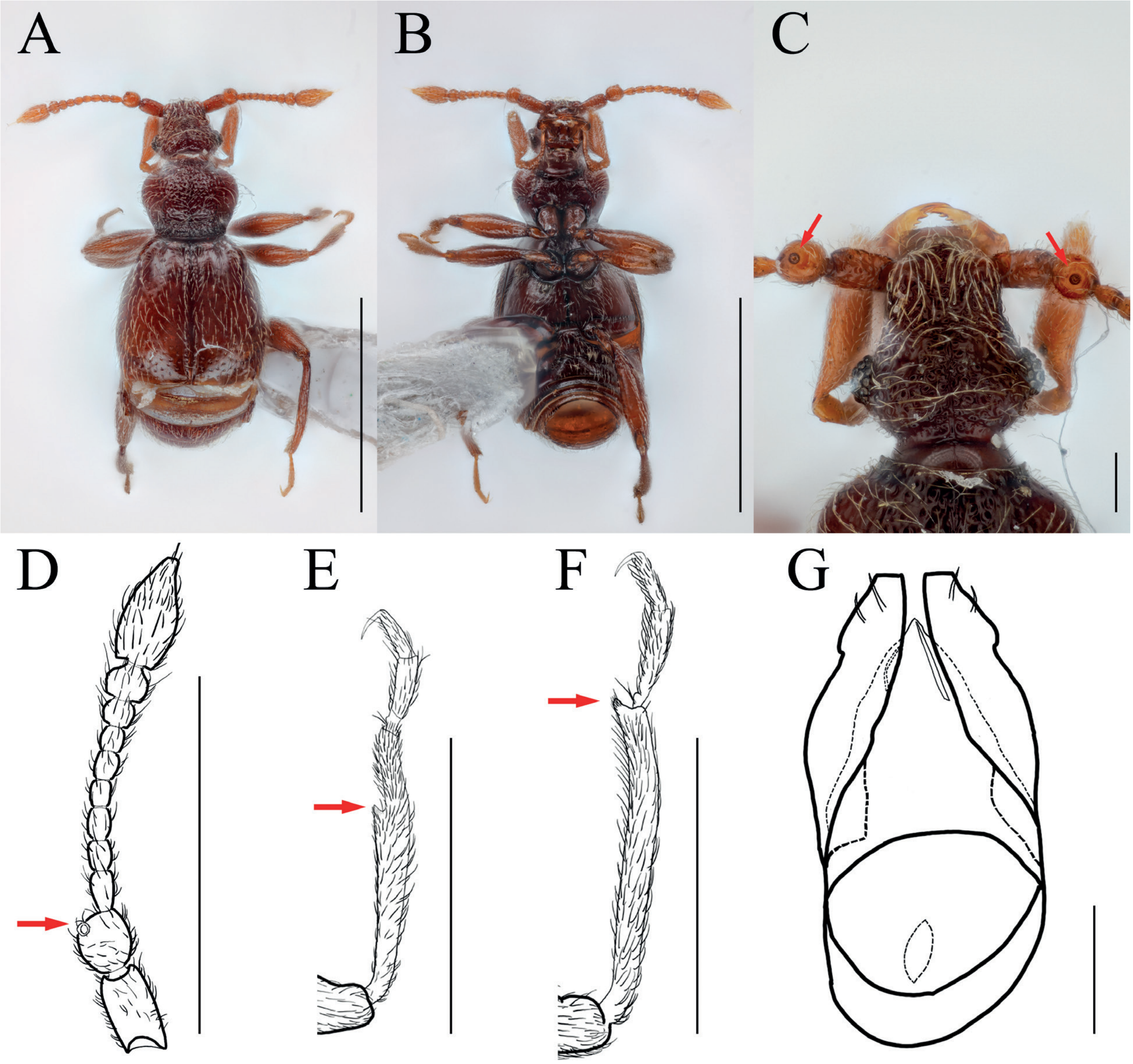

Figure 7. *Bryaxis girinensis* Choi, Park, Lee & Park, sp. nov. **A** dorsal habitus **B** ventral habitus **C** head **D** antenna **E** fore leg **F** hind leg **G** aedeagus. Scale bars: 1 mm (**A, B**); 0.1 mm (**C, G**); 0.5 mm (**D–F**).

and dorsal diaphragm transversely ovoid; parameres short and symmetrical, apices truncated; endophallus composed of two fine struts, asymmetrical (Fig. 7G).

***Sexual dimorphism*.** Unknown.

Remarks. The adult of this species is similar to *Bryaxis nemorosus* Choi, Park, Lee & Park sp. nov. in the shape of antennomeres IV–XI (Figs 7D, 8F). However, it can be distinguished by the robust setae on the body (Fig. 7A), large eyes as long as the tempora (Fig. 9E), a strongly tuberculate maxillary palpomere II (Fig. 9A), protibiae with a spine at the widest point (Fig. 9C, arrow), and a simple endophallus of the male genitalia (Fig. 7G).

Etymology. This species is named after the type locality, Girin-myeon, Inje-gun.

Habitat. The holotype was collected by sifting flood debris in mixed forest.

Distribution. Korea (Inje-gun, Gangwon-do).

Bryaxis nemorosus **Choi, Park, Lee & Park, sp. nov.**

https://zoobank.org/812B1845-BAEB-4E11-A8BD-7F51B922433F

Figs 8, 9B, D, F

Type materials (*N* = 5, 4♂♂, 1♀). ***Holotype male.*** "Korea: Jeonnam Prov. Mt. Doksil, Gageo island. Gageodo-gil, Heuksan-myeon, Sinan-gun, 13 Jul 2021, 34°05'06.1"N, 125°06'17.4"E, 468 m, sifting leaf & soil litter, J.-W. Seo" (NIBR). ***Paratype.*** 1♂ (CBNUIC, slide mounted). "Korea: Jeonnam Prov. Mt. Doksil, Gageo island. Gageodo-gil, Heuksan-myeon, Sinan-gun, 13 Jul 2021, 34°05'06.1"N, 125°06'17.4"E, 468 m, sifting leaf & soil litter, J.-W. Seo". 1♂ (CBNUIC, dried). "Korea: Jeonnam Prov. Mt. Doksil, Gageo island. Gageodo-gil, Heuksan-myeon, Sinan-gun, 8 Jul 2020, 34°05'35.0"N, 125°06'25.0"E, 590 m, sifting leaf & soil litter, T.-Y. Jang". 1♂ (CBNUIC, dried). "Korea: Jeonnam Prov. Mt. Doksil, Gageo island. Gageodo-gil, Heuksan-myeon, Sinan-gun, 8 Jul 2020, 34°04'40.0"N, 125°06'23.0"E, 540 m, sifting leaf & soil litter, U.-J. Byeon, T.-Y. Jang". 1♀ (CBNUIC, dried). "Korea: Jeonnam Prov. Mt. Doksil, Gageo island. Gageodo-gil, Heuksan-myeon, Sinan-gun, 7 Jul 2020, 34°04'34.7"N, 125°06'28.8"E, 534 m, sifting leaf & soil litter, T.-Y. Jang".

Diagnosis. Elongated head with small eyes situated on mid-length of head (Fig. 8E, arrow).

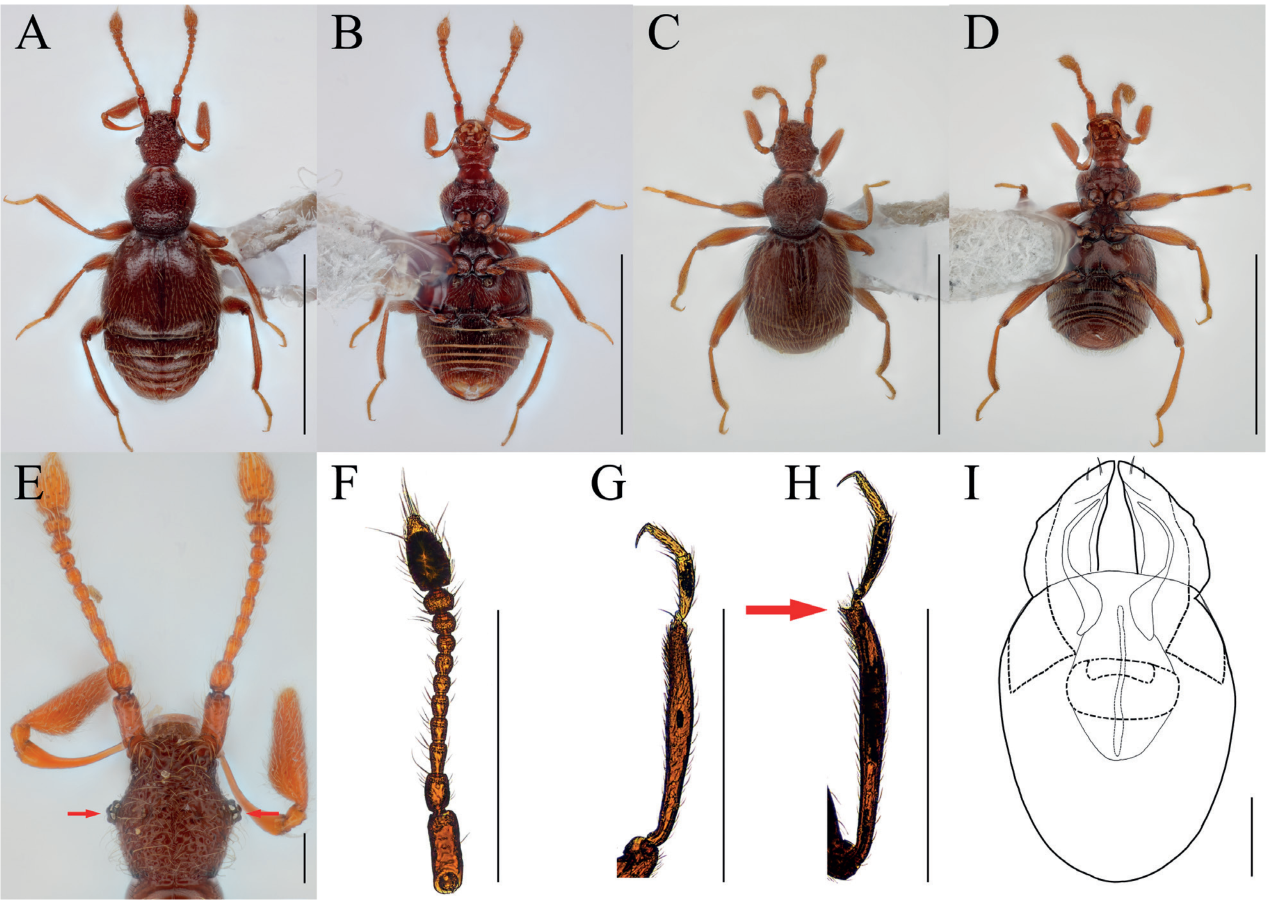

Figure 8. *Bryaxis nemorosus* Choi, Park, Lee & Park, sp. nov. male (**A, B, E–I**), female (**C, D**). **A, C** dorsal habitus **B, D** ventral habitus **E** head **F** antenna **G** fore leg **H** hind leg **I** aedeagus. Scale bars: 1 mm (**A–D**); 0.1 mm (**E, I**); 0.5 mm (**F–H**).

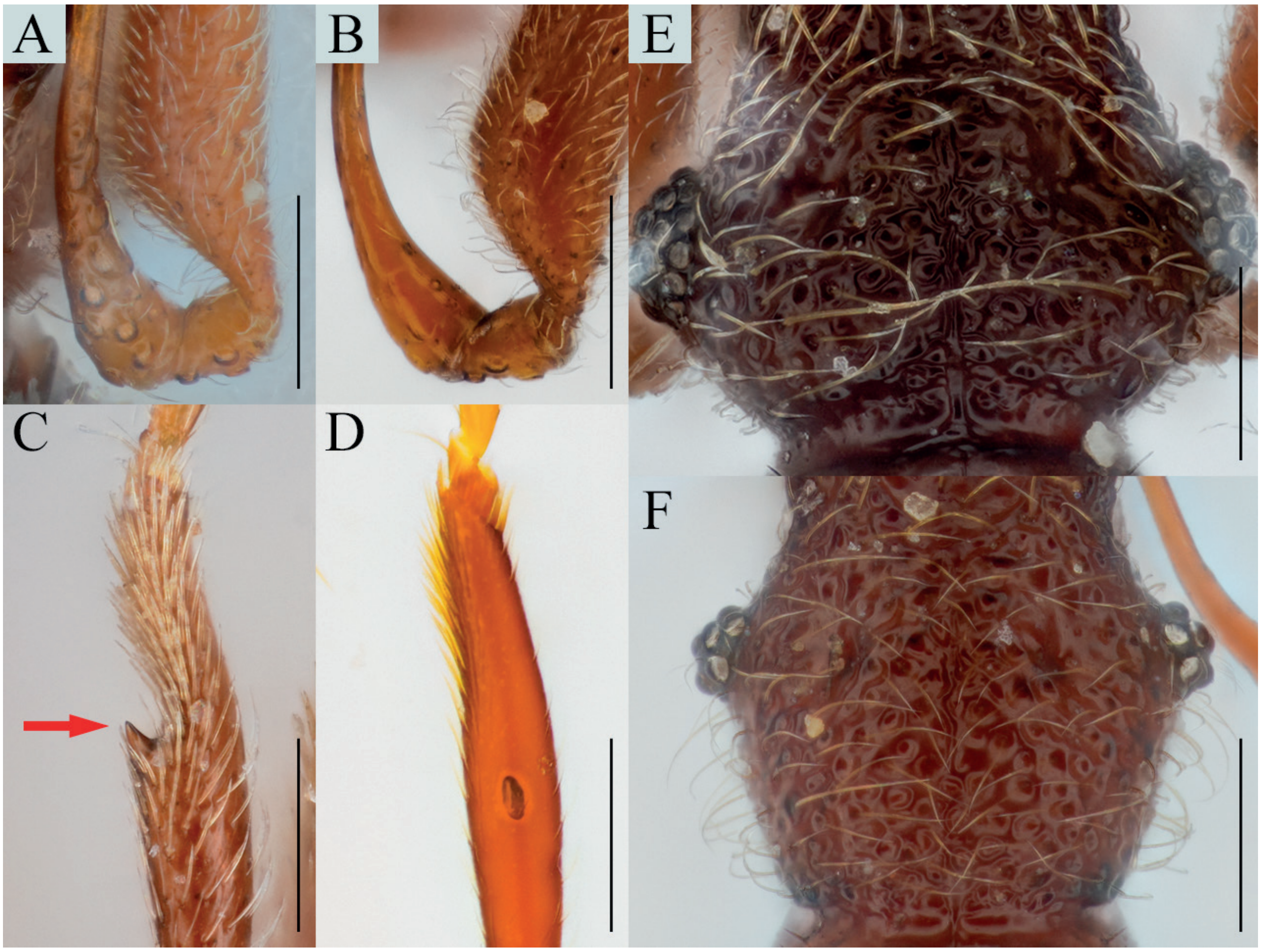

Figure 9. Diagnostic characters of *Bryaxis girinensis* sp. nov. (**A, C, E**) and *B. nemorosus* sp. nov. (**B, D, F**). **A, B** maxillary palpi **C, D** protibiae **E, F** heads. Scale bars: 0.1 mm.

Description. Body reddish brown, antennae, maxillary palpi, legs slightly lighter than body, length 1.57–1.58 mm, maximum width 0.61–0.67 mm (Fig. 8A–D). Setae on body yellowish. Head 1.15 times as long as wide (Fig. 8E). Frons with U-shaped impression between antennal tubercles; frontal foveae absent; frontal rostrum distinct anteriorly. Vertex weakly convex; longitudinal carina absent; vertexal foveae small. Eyes reduced with 9 facets. Maxillary palpi moderately developed; palpomeres II smooth; III with tubercles; palpomere IV 0.24–0.28 mm long and about 3.06–3.24 times as long as wide, subcylindrical pseudosegment at apex. Antennae about 0.61–0.68 mm long; scapes subcylindrical and elongated, 2–2.18 times as long as pedicels, without modification; pedicels subcylindrical, 1.38–1.40 times as long as wide; antennomere III 1.67–1.72 times as long as wide; IV–VII subequal in length; VIII subglobose as long as wide; IX 0.82–0.86 times as long as wide; X transverse, 0.64–0.65; XI largest, pointed at apex, 1.76–1.84 times as long as wide (Fig. 8F). Pronotum 0.85–0.89 times as long as wide and widest at basal 2/3, lateral antebasal foveae connected by antebasal sulcus. Elytra slightly convex, 0.87 times as long as wide and widest at basal 1/3, each elytron with two basal foveae and subhumeral fovea. Legs slender; protibiae without spine (Fig. 8G); metatibiae with spine on apical (Fig. 8H, arrow). Aedeagus robust, 0.53 mm long and 1.79 times as long as wide; penis bulbous and dorsal diaphragm small, transversely ovoid; parameres symmetrical, each bearing two setae; endophallus comprising simple strut basally and two symmetrical struts curved along with parameres, thickened basally (Fig. 8I).

***Sexual dimorphism*.** Female metatibial spines absent.

Remarks. Adults of this species are similar to that of *Bryaxis girinensis* Choi, Park, Lee & Park sp. nov. in the shape of antennomeres IV–XI (Figs 7D, 8F). However, they can be distinguished by having angular tempora much longer than the eyes (Fig. 9F), smooth maxillary palpomere II (Fig. 9B), unadorned antennal scapes and pedicels (Fig. 8F), slender protibiae without a spine (Fig. 9D), and an endophallus composed of three long struts (Fig. 8I).

Etymology. The specific epithet is the Latin word *nemorosus* ("wooded, shady", masculine) that refers to habitat where the types collected.

Habitat. Specimens of this species were collected by sifting leaf and soil litter in wet forest with dense canopy, which is located on an island.

Distribution. Korea (Gageo island, Sinan-gun, Jeollanam-do).

***Bryaxis mahunkai* Löbl, 1975**

Fig. 10

Bryaxis mahunkai Löbl, 1975: 117.
Bryaxis leechanyoungi Nomura & Lee, 1993: 27; syn. nov.

Material examined (*N* = 60, 34♂♂, 26♀♀). 1♂ (CBNUIC, dried). "Korea: Chungbuk Prov., Mt. Songnisan, Beopjusa-ro, Songnisan-myeon, Boeun-gun, 20 Sep 2019, 36°32'55.6"N, 127°51'19.8"E, 476 m, flood debris, Y.-J. Choi, J.-W. Kang". 2♂♂, 11♀♀ (CBNUIC, dried). "Korea: Gangwon Prov., Garakjae-ro, Hwachon-myeon, Hongcheon-gun, 5 May 2019, 37°46'26.0"N, 127°54'48.0"E, 240 m, sifting leaf litter near stream, J.-S. Park". 1♂ (CBNUIC, dried). "Korea: Gangwon Prov., Jangjeon-gil, Jinbu-myeon, Pyeongchang-gun, 11 Mar 2019, 37°27'58.0"N, 128°32'18.4"E, 901 m, sifting leaf litter & dead wood debris & moss, J.-W. Kang". 7♂♂, 7♀♀ (CBNUIC, dried). "Korea: Gyeongbuk Prov., Gowol-gil, Yeongyang-eup, Yeongyang-gun, 19 Mar 2019, 36°38'48.1"N, 129°09'18.7"E, 265 m, sifting leaf litter, Y.-J. Choi". 2♂♂ (CBNUIC, dried). "Korea: Gyeongbuk Prov., Yongmunsa-gil, Yongmun-myeon, Yecheon-gun, 1 Jun 2019, 36°43'45.0"N, 128°22'14.0"E, 358 m, sifting leaf litter & soil near stream, U.-J. Byeon". 7♂♂ (CBNUIC, dried). "Korea: Gyeonggi Prov., Mt. Bukhansan, Daeseomun-gil, Deogyang-gu, Goyang-si, 23 Aug 2019, 37°39'43.7"N, 126°59'11.2"E, 491 m, sifting leaf litter & soil & dead wood debris, Y.-J. Choi, T.-Y. Jang". 4♂♂ (CBNUIC, dried). "Korea: Gyeonggi Prov., Mt. Yeoninsan, Yongchu-ro, Gapyeong-eup, Gapyeong-gun, 15 Apr 2019, 37°51'29.5"N, 127°28'01.0"E, 193 m, sifting leaf litter & moss near stream, J.-Y. Kang, J.-W. Kang". 5♂♂, 3♀♀ (CBNUIC, dried). "Korea: Gangwon Prov., Hwanseon-ro, Singi-myeon, Samcheok-si, 23 Aug 2018, 37°20'22.6"N, 129°03'28.5"E, 172 m, sifting leaf litter near mountain stream, Y.-J. Choi". 5♂♂, 5♀♀ (CBNUIC, dried). "Korea: Jeonnam Prov., Mt. Heukseoksan, Biseuran-gil, Gyegok-myeon, Haenam-gun, 18 May 2019, 34°40'44.9"N, 126°37'10.9"E, 160 m, sifting mushroom & leaf litter & plant root under rock in bamboo forest, S.-H. Choi, U.-J. Byeon".

Remarks. Adult males of this species are characterized by the following combination of characters: maxillary palpomeres II–III tubercular ventrally; an-

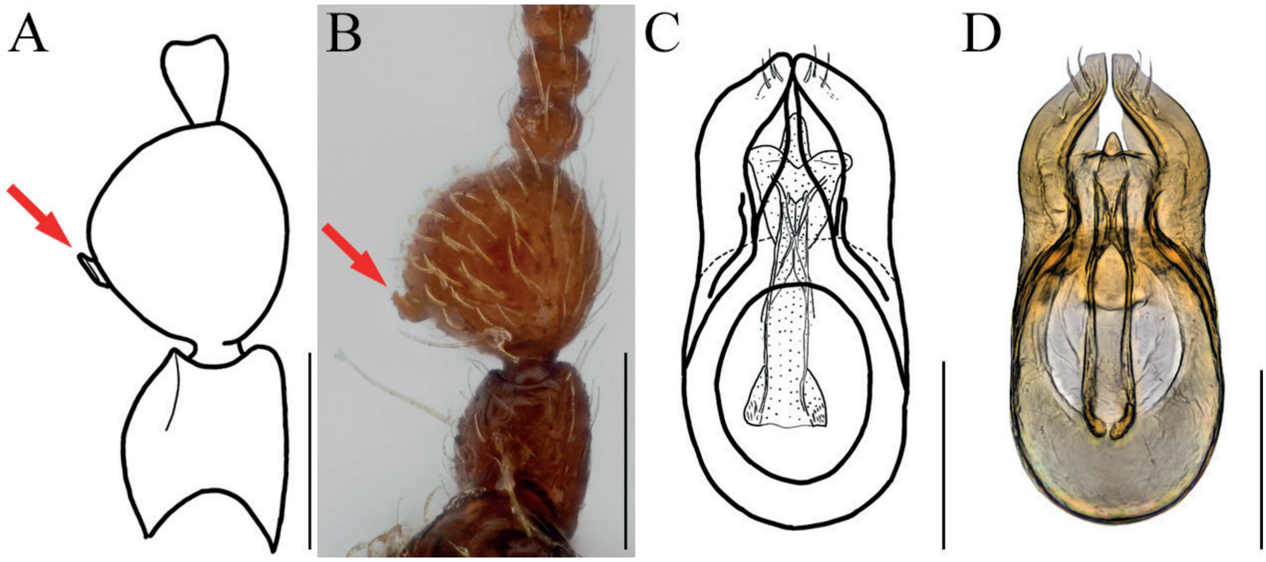

Figure 10. Diagnostic characters of *Bryaxis mahunkai* Löbl. **A, B** antennal scapes and pedicels **C, D** aedeagi. Scale bars: 0.1 mm.

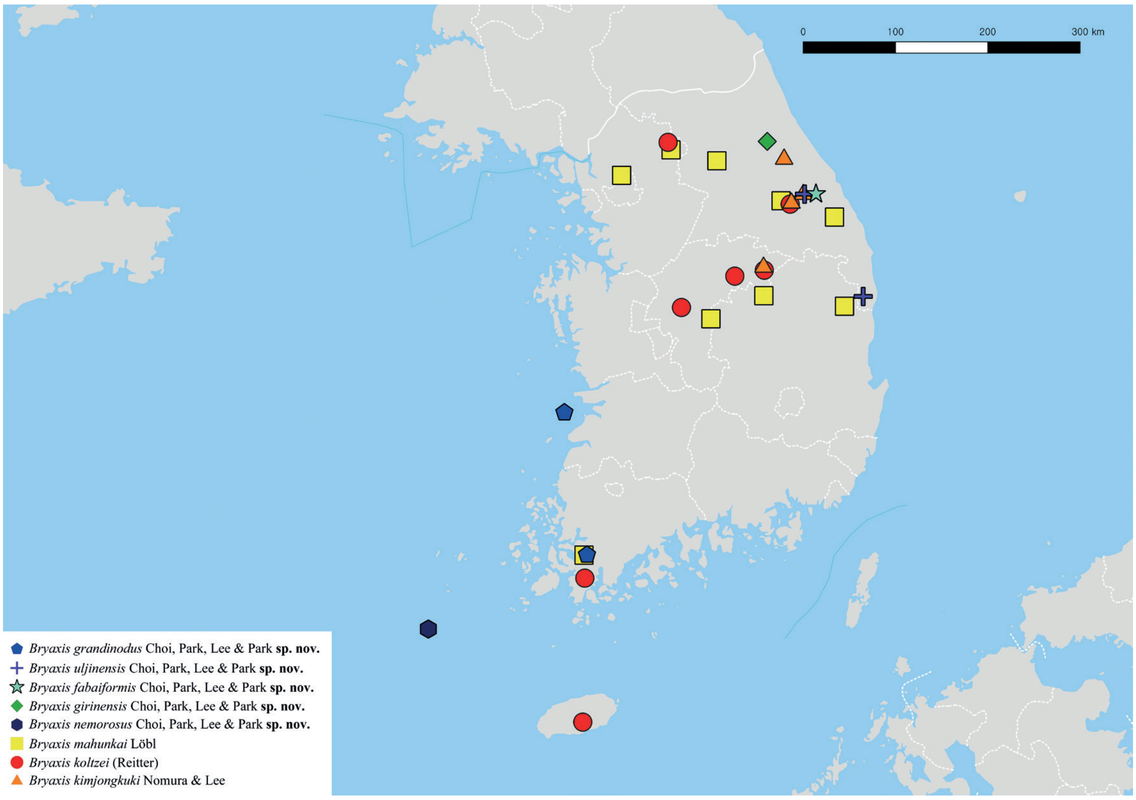

Figure 11. Collection localities. *Bryaxis grandinodus* sp. nov. (blue pentagon); *B. uljinensis* sp. nov. (purple cross); *B. fabaiformis* sp. nov. (sky-blue star); *B. girinensis* sp. nov. (green diamond); *B. nemorosus* sp. nov. (navy hexagon); *B. mahunkai* Löbl (yellow square); *B. koltzei* (Reitter) (red circle); *B. kimjongkuki* Nomura & Lee (orange triangle).

tennal scapes tubiform, more curved on the internal side; pedicels globularly enlarged and a glandular nodule situated at the basal 1/3 (Fig. 10A, B, arrows); parameres with four setae each; and an endophallus consisting of two slender struts, converging subapically (Fig. 10C, D).

Comments. Dorsal habitus of the holotype is available in Park and Jeon (2012; https://ecolibrary.me.go.kr/nibr/#/search/detail/5513253). Illustrations of antenna and aedeagus were obtained from Löbl (1975), and compared to those of specimens examined in this study. All specimens collected in Korea were recognized as *B. mahunkai* Löbl based on the antennal scapes (curved internally), pedicels (swollen and bearing upward glandular nodule), and the aedeagus (structure of endophallus).

Distribution. Korea (Kaesong-si, Gyeonggi-do; Gapyeong-gun, Gyeonggi-do; Goyang-si, Gyeonggi-do; Boeun-gun, Chungcheongbuk-do; Hongcheon-gun, Gangwon-do; Samcheok-si, Gangwon-do; Pyeongchang-gun, Gangwon-do; Yeongyang-gun, Gyeongsangbuk-do; Yecheon-gun, Gyeongsangbuk-do; Haenam-gun, Jeollanam-do).

Discussion

This study was the first revision of Korean *Bryaxis* since Nomura and Lee described eight new species in 1992–1993 [note that *Bryaxis coreanus* Nomura & Lee, 1992 was subsequently synonymized with *Bryaxis koltzei* (Reitter, 1887) (Nomura 1995)]. According to Kurbatov and Löbl (1995), subgenera *Arcobythus* Jeannel, 1958 and *Bythiniama* Jeannel, 1958 were synonymized with *Bryaxis* Kugelann due to the absence of informative characters to separate the genus into subgeneric groups. The adult males of *B. nemorosus* sp. nov. possess unadorned antennomeres and small eyes, which are thought to be linked to their shady habitat caused by the dense canopy. The features of this species are shown in cavernicolous species (e.g., elongated scapes and reduced eye sizes (Hlaváč 2006; Bekchiev and Hlaváč 2016). However, it is difficult to say whether it belongs to the same lineage as the other cavernicolous species, considering the isolated locality of *B. nemorosus* sp. nov.

This study added five new species based on 28 specimens. We were able to recollect only three of the species previously described. Of these, *B. koltzei* (Reitter) and *B. mahunkai* Löbl were very abundant over their ranges with hundreds of specimens collected. *Bryaxis koltzei* is a very widespread species present throughout much of eastern Asia, from Korea, north to Russian Far East, and Japan, while *B. mahunkai* is endemic to Korea. *Bryaxis kimjongkuki* Nomura & Lee, also endemic to Korea was less abundant than these two, with about 50 specimens collected throughout its range. Two species, *B. grandinodus* sp. nov. and *B. uljinensis* sp. nov., were distributed in two localities each (Fig. 11), suggesting the potential for a wide habitat range.

Acknowledgements

We appreciate Min-Sang Jang, Jun-Young Kang, Ji-Won Kang, Ui-Joung Byeon, Su-Ho Choi, Taeyoung Jang, Ji-Wook Kim, Min-Ho Song and Joong-In Shin for help to collect specimens examined in this study. R. Leschen provided feedback on a draft manuscript.

Additional information

Conflict of interest

The authors have declared that no competing interests exist.

Ethical statement

No ethical statement was reported.

Funding

This work was supported by a grant from the National Institute of Biological Resources (NIBR), funded by the Ministry of Environment (MOE) of the South Korea (NIBR202028201 and NIBR202002112).

Author contributions

Conceptualization, Y.-J. C. and J.-S. P.; Funding Acquisition, S.-J. P. and S.-G. L.; Investigation, Y.-J. C. and J.-S. P.; Resources, Y.-J. C. and J.-S. P.; Writing–Original Draft Preparation, Y.-J. C. and J.-S. P.; Writing–Review & Editing, Y.-J. C., S.-J. P., S.-G. L. and J.-S. P.; Visualization, Y.-J. C.; Project Administration, J.-S. P. and S.-J. P.

Author ORCIDs

Yeon-Jae Choi https://orcid.org/0000-0003-0172-1128
Sun-Jae Park https://orcid.org/0000-0003-3759-6517
Seung-Gyu Lee https://orcid.org/0000-0001-5576-2799
Jong-Seok Park https://orcid.org/0000-0003-2063-2534

Data availability

All of the data that support the findings of this study are available in the main text or Supplementary Information.

References

Ahn K-J, Cho Y-B, Kim Y-H, Yoo I-S, Newton AF (2017) Checklist of the Staphylinidae (Coleoptera) in Korea. Journal of Asia-Pacific Biodiversity 10(3): 279–336. https://doi.org/10.1016/j.japb.2017.06.006

Bekchiev R, Hlaváč P (2016) New and interesting species of the genus *Bryaxis* Kugelann, 1794 (Coleoptera, Staphylinidae, Pselaphinae) from Croatia. Zootaxa 4144(1): 109–116. https://doi.org/10.11646/zootaxa.4144.1.6

Chandler DS (2001) Biology, Morphology, and Systematics of the Ant-Like Litter Beetles of Australia (Coleoptera: Staphylinidae: Pselaphinae) (Vol. 15). Associated Publishers, Florida, 560 pp.

Chandler DS (2022) *Bryaxis pyrenaeus pyrenaeus* (Saulcy): European genus and species newly recorded for North America (Coleoptera: Staphylinidae: Pselaphinae). Coleopterists Bulletin 76(4): 510–512. https://doi.org/10.1649/001-065X-76.4.510

Hlaváč P (2006) A new cavernicolous species of the genus *Bryaxis* (Coleoptera: Staphylinidae: Pselaphinae) from the island of Mljet. Natura Croatica 17: 1–8.

Jeannel R (1958) Révision des Psélaphides du Japon. Mémoires du Muséum National d'Histoire Naturelle 18: 1–138.

Kugelann JG (1794) Verzeichniss der in einigen Gegeden Preussens bis jetzt entdeckten Käfer-Arten, nebst kurzen Nachrichten von denselben. Neustes Magazin für die Liebhaber der Entomologie, herausgegeben von D. H. Schneider 1: 513–582.

Kurbatov SA, Löbl I (1995) Contribution to the knowledge of the east Asian *Bryaxis* (Coleoptera, Staphylinidae, Pselaphinae). Archives de Science, Geneve 48: 161–172.

Latreille PA (1802) Histoire Naturelle, Génerale et Particulière, des Crustacés et des Insectes (Vol. 5). F. Dufart, Paris, 391 pp. https://doi.org/10.5962/bhl.title.15764

Lawrence JF, Ślipiński A, Seago AE, Thayer MK, Newton AF, Marvaldi AE (2011) Phylogeny of the Coleoptera based on morphological characters of adults and larvae. Annales Zoologici 61(1): 1–217. https://doi.org/10.3161/000345411X576725

Löbl I (1974) Beitrag zur Kenntnis der Pselaphidae (Coleoptera) der Koreanischen Volksdemokratischen Republik. Acta Zoologica Cracoviensia 19: 91–104.

Löbl I (1975) Beitrag zur Kenntnis der Pselaphiden von Korea (Coleoptera). Annales Historico-Naturales Musei Nationalis Hungarici 67: 113–118.

Newton AF (2022) StaphBase: Staphyliniformia world catalog database. In: Bánki O, Roskov Y, Döring M, Ower G, Vandepitte L, Hobern D, Remsen D, Schalk P, DeWalt RE, Keping M, Miller J, Orrell T, Aalbu R, Adlard R, Adriaenssens EM, Aedo C, Aescht E, Akkari N et al. (Eds) Catalogue of Life Checklist (Aug 2022). https://doi.org/10.48580/dfqt-3gk

Nomura S (1995) Taxonomic notes on *Bryaxis koltzei* (Reitter) and its allied new species from Japan (Coleoptera, Pselaphinae). Esakia 35: 129–134. https://doi.org/10.5109/2587

Nomura S, Lee C-E (1992) A revision of the family Pselaphidae (Coleoptera) from Cheju-do island, Korea. Esakia 32: 59–80. https://doi.org/10.5109/2557

Nomura S, Lee C-E (1993) A revision of the family Pselaphidae (Coleoptera) from South Korea. Esakia 33: 1–48. https://doi.org/10.5109/2561

Park S-J, Jeon M-J (2012) Coleoptera. In: Park S-J, Choi W-Y (Eds) Korean type specimens of insects deposited in Hungarian Natural History Museum. National Institute of Biological Resources, Incheon, 35–91.

Raffray A (1890) Étude sur les Psélaphides. In: Fauvel A (Ed.) Revue D’Entomologie. Henri Delesques, Caen, 81–172.

Reichenbach HGL (1816) Monographia Pselaphorum, Dissertatio Entomolgica. Impressit IB Hirschfeld, Lipsiae, 77 pp. https://doi.org/10.5962/bhl.title.50613

Reitter E (1882) Versuch einer systematischen Eintheilung der Clavigeriden und Pselaphiden. Verhandlungen des Naturforschenden Vereines in Brünn 20: 177–211. https://doi.org/10.1002/mmnd.48018820229

Reitter E (1887) Neue Coleopteran aus Europa, den angrenzenden Ländern und Sibirien, mit Bemerkungen der bekannte Arten. Deutsche Entomologische Zeitschrift 31(1): 241–288. https://doi.org/10.1002/mmnd.48018870141

Schülke M, Smetana A (2015) Staphylinidae Latreille. In: Löbl I, Löbl D (Eds) Catalogue of Palaearctic Coleoptera (Vol. 2/1–2) Revised and updated edition Hydrophiloidea–Staphylinoidea. Brill, Leiden, 304–1134.

Taru S, Nomura S (2021) A new species of the genus *Bryaxis* Kugelann, 1794 (Coleoptera, Staphylinidae, Pselaphinae) from Yakushima Island, Kagoshima Prefecture, off Kyushu, Southwestern Japan. Elytra. New Series 11: 39–46.

Yin Z-Y (2023) A new species of *Bryaxis* Kugelann from tropical China (Coleoptera: Staphylinidae: Pselaphinae). Zootaxa 5228(5): 595–598. https://doi.org/10.11646/zootaxa.5228.5.4

ZooKeys 1182: 183–205 (2023)
DOI: 10.3897/zookeys.1182.104943

Research Article

A taxonomic revision of the Old World genus *Dichoteleas* Kieffer (Hymenoptera, Scelionidae)

Johanna Schwartz[1], Simon Van Noort[2,3], Norman F. Johnson[1,4]

1 *Department of Entomology, The Ohio State University, Columbus, Ohio, USA*
2 *Research and Exhibitions Department, South African Museum, Iziko Museums of South Africa, Cape Town 8000, South Africa*
3 *Department of Biological Sciences, University of Cape Town, Private Bag, Rondebosch, 7701, South Africa*
4 *Department of Evolution, Ecology & Organismal Biology, The Ohio State University, 1315 Kinnear Road, Columbus, Ohio 43212, USA*
Corresponding author: Johanna Schwartz (schwartz.2085@osu.edu)

Abstract

The genus *Dichoteleas* Kieffer (Scelionidae: Scelioninae) is known only from the Old World: Kenya, Tanzania, Malawi, South Africa, Madagascar, southern India, the island of New Guinea, and eastern Australia. After revision, 10 species are recognized. Four species were previously recognized and are redescribed: *D. ambositrae* Risbec (Madagascar), *D. indicus* Saraswat (India: Kerala), *D. rugosus* Kieffer (Australia: Queensland), and *D. subcoeruleus* Dodd (Australia: Queensland). Six species are described as new: *D. fulgidus* **sp. nov.** (Indonesia: Papua Barat), *D. fuscus* **sp. nov.** (Papua New Guinea, Australia: Queensland), *D. hamatus* **sp. nov.** (Kenya, Tanzania, Malawi, South Africa)., *D. rubyae* **sp. nov.** (Madagascar), *D. striatus* **sp. nov.** (Madagascar), and *D. umbra* **sp. nov.** (Tanzania). *Dichoteleas pappi* Szabó is treated as a junior synonym of *D. rugosus.* An identification key to species of the genus is provided.

Key words: Egg-parasitoid, Platygastroidea, revision, Scelioninae, taxonomy, tropical

Academic editor: Zachary Lahey
Received: 13 April 2023
Accepted: 31 August 2023
Published: 13 October 2023

ZooBank: https://zoobank.org/5CE38750-EECC-4275-B53A-3ADB32DB908B

Citation: Schwartz J, Van Noort S, Johnson NF (2023) A taxonomic revision of the Old World genus *Dichoteleas* Kieffer (Hymenoptera, Scelionidae). ZooKeys 1182: 183–205. https://doi.org/10.3897/zookeys.1182.104943

Introduction

The genus *Dichoteleas* was first described by Jean-Jacques Kieffer in 1907 on the basis of a single male specimen collected in Mackay, North Queensland, Australia. It was distinguished from *Pentacantha* Ashmead (a genus of the subfamily Teleasinae) by the "Thorax mit drei spitzen Zähnen" (thorax with three pointed teeth) and the presence of the postmarginal vein on the forewing (Kieffer, 1907). Kieffer did not specify in his generic description on which parts of the mesosoma these teeth occur, but in his description of the sole species, *D. rugosus*, he indicated that the teeth are found on the sides of the mesoscutellum and medially on the metanotum. After collecting a female of the type species, Dodd (1926) added that the antennal club had 7 segments. Later, Masner (1976) proposed that *Dichoteleas* could be identified by its large hairless eyes, elongate maxillary palpi, and subtridentate mandibles.

In the years since its description, five species have been described in the genus. Three were described from Australia (*D. rugosus* Kieffer, *D. subcoeruleus* Dodd, and *D. pappi* Szabó), one from Madagascar (*D. ambositrae* Risbec), and one from India (*D. indicus* Saraswat). Only *D. subcoeruleus* was described based on more than a single sex, and none of these were based on more than five specimens. In their revision of Australian Scelioninae, Galloway and Austin (1984) noted that *D. pappi* may be a junior synonym of *D. rugosus*, since the species have similar ranges, and *Dichoteleas pappi* was described from one female specimen, while *D. rugosus* was described from a male.

Masner (1976) placed *Dichoteleas* in the tribe Calliscelionini of the subfamily Scelioninae, although he mentioned that the genus was “difficult to classify tribally.” He also cited a possible relationship with *Amblyscelio* Kieffer or *Neoscelio* Dodd. *Dichoteleas* was grouped with *Amblyscelio* and *Oxyteleia* Kieffer In the 4-gene analysis of Chen et al. (2021), but the bootstrap support for this was relatively weak. *Dichoteleas* is fairly unusual among platygastroids in that some of the species are distinctly metallic in color. To the best of our knowledge, all members of the subfamily Scelioninae are egg parasitoids of spiders or other insects, but there are currently no host records for *Dichoteleas* and little else is known of this group.

The goals of this paper are to incorporate information from newly collected specimens, revise the circumscription of described species on the basis of these new data, document and describe hypothesized new species within the genus, and to provide a comprehensive identification key for the species of *Dichoteleas*.

Methods

This work is based on specimens from the Australian National Insect Collection (**ANIC**; Canberra, Australia), Bernice P. Bishop Museum (**BPBM**; Honolulu, HI), California Academy of Sciences (**CAS**; San Francisco, CA), Canadian National Collection of Insects (**CNCI**; Ottawa, Canada), C.A. Triplehorn Insect Collection (**OSUC**; The Ohio State University, Columbus, OH), Hungarian Natural History Museum (**HNHM**; Budapest, Hungary), International Centre of Insect Physiology and Ecology (**ICIPE**, Nairobi, Kenya), Muséum National d’Histoire Naturelle (**MNHN**; Paris, France), South Australian Museum (**SAMA**; Adelaide, South Australia, Australia), South African Museum (**SAMC**; Iziko Museums of South Africa, Cape Town, South Africa), and Utah State University Insect Collection (**USU**; Logan, Utah).

Each specimen examined in this paper has a unique identifier consisting of a prefix (e.g., “OSUC”) and a number. The associated data for each specimen may be accessed at http://mbd-db.osu.edu using this unique identifier. Morphological terminology generally follows Mikó et al. (2007). The term claval formula (Bin 1981) refers to the apical antennomeres of the female that bear papillary sensilla on their ventral surface. The claval formula is the number of papillary sensilla on each antennomere separated by a dash, starting from the distal antennomere to the most proximal antennomere. The antennomere is also designated by number (from proximal to distal segment). A 5–segmented clava with 1 sensillum on the most distal antennomere and 2 sensilla on each of the remaining antennomeres would be represented with a claval formula of A12–A8: 1–2–2–2–2. Metasomal tergites are referred to by the letter T followed by a number, e.g., T1 is the first (i.e., basalmost) metasomal tergite.

The terminology for the surface sculpture follows (Harris, 1979). Species descriptions and a taxon by data matrix were generated using vSysLab (https://vsyslab.osu.edu). These descriptions were exported in the format of “Character: Character state(s).” The states of characters polymorphic for a species are separated by semicolons. Photographs of specimens were captured using a Leica Z16 APOA system and stacked with the Leica Application Suite software. Images of type specimens were provided by Elijah Talamas (Florida State Collection of Arthropods).

Our concept of species is based on the biological species concept as described by Mayr (1942). Species are populations whose individuals have the ability to interbreed in nature. Many morphological characters likely are the result of polygenic origin, and interbreeding populations exchange genes among themselves but not with other species. Thus, one would predict that separate species will eventually come to evolve differences in morphological character states, either randomly or through natural selection (Wild 2004). Other factors – including sexual dimorphism, under-sampling of intraspecific variability, genetically simple but discrete character states, and environmental influences – may suggest species differences. It is the task of the taxonomist in the early stages of the study of a group to tease apart such sources of variation, evaluate the evidence, and propose hypotheses of how many independent species exist and which characters can be used to distinguish them. Going forward, these hypotheses can be tested with new characters and new sources of characters.

Results

Key to species of *Dichoteleas*

1 Interantennal process produced anterodorsally, pinched laterally, surrounded by depression, central keel on frons present (Fig. 22); India .... ***Dichoteleas indicus***

– Interantennal process flattened against lower frons; central keel absent (Fig, 10) **2**

2 Median carina on T1–T4 present (Fig. 14), head metallic blue..................**3**

– Median carina on T1–T4 absent, head black (Fig. 21) **5**

3 Median mesoscutal line present (Fig. 37), axillular carinae xanthic; Australia (Queensland) ....***Dichoteleas subcoeruleus***

– Median mesoscutal line absent (Figs 11, 15), axillular carinae variable, concolorous with mesosoma or only slightly lighter **4**

4 Mesoscutum finely punctate (Fig. 15), pronotum metallic blue (Fig. 12), submedian carinae absent on frons (Fig. 13); Indonesia (West Papua) ....***Dichoteleas fulgidus* sp. nov.**

– Mesoscutum rugulose (Fig. 18), pronotum black to dark brown (Fig. 16); submedian carinae present on frons (Fig. 17); Papua New Guinea, Australia (Queensland) ....***Dichoteleas fuscus* sp. nov.**

5 Notaulus incomplete, pronotum xanthic (Fig. 11); Madagascar.................. .... ***Dichoteleas ambositrae***

– Notaulus complete, pronotum red, black, or brown (Fig. 28, 31, 34) **6**

6 Axillular carinae with a laterally compressed, posteroventral hooklike projection (Fig. 19); South Africa (Limpopo), Malawi, Kenya, Tanzania ....***Dichoteleas hamatus*** **sp. nov.**

– Axillular carinae triangular and pointed posteriorly or slightly curved inwardly (Fig. 28) **7**

7 Mesosoma red dorsally and darkened posteroventrally, areolate-rugose (Figs 26, 28); Madagascar ....***Dichoteleas rubyae*** **sp. nov.**

– Mesosoma dark brown to black, punctate or with longitudinal striations between notauli beginning posteriorly (Fig. 31, 40) **8**

8 Mesoscutum and scutellum smooth with sparse setation (Fig. 34); Madagascar .... ***Dichoteleas striatus*** **sp. nov.**

– Mesoscutum and scutellum setose and punctate (Fig. 31).......................**9**

9 Mandibles bidentate; mesoscutual humeral sulcus foveolate; mesoscutum with longitudinal striations between notauli beginning posteriorly (Figs 29, 30); Australia (Queensland)..........................***Dichoteleas rugosus***

– Mandibles tridentate; mesoscutual humeral sulcus present as an uninterrupted groove; mesoscutum punctate between notauli with xanthic posterolateral corners (Figs 39, 40); Tanzania ....***Dichoteleas umbra*** **sp. nov.**

Dichoteleas Kieffer

Dichoteleas Kieffer: 1907: 297: (original description. Type: *Dichoteleas rugosus* Kieffer, by monotypy); Brues: 1908: 28, 44: (diagnosis, list of species, keyed); Kieffer: 1908: 113: (keyed); Kieffer: 1910: 62: (keyed); Dodd: 1913: 131: (keyed); Kieffer: 1913: 23: (description); Dodd: 1926: 369: (description, key to species); Kieffer: 1926: 266, 351: (description, keyed); Muesebeck & Walkley: 1956: 346: (citation of type species); Masner: 1976: 30: (description); Mani & Sharma: 1982: 173: (description); Galloway & Austin: 1984: 7, 16: (diagnosis, list of species described from Australia, keyed); Johnson: 1992: 367: (cataloged, catalog of world species); Rajmohana: 2006: 116, 123: (description, keyed).

Description. ***Head*****.** Head shape in dorsal view: transverse. Vertex: smooth or rugose. Hyperoccipital carina: present or absent. Occipital carina: present, complete. OOL: lateral ocellus nearly contiguous with inner orbits, OOL < 0.5 OD. Upper frons: convex or with a slight concavity; smooth, striate, or areolate. Frontal depression: undifferentiated. Submedian carina: present or absent. Orbital carina: present. Inner orbits: diverging ventrally. IOS/EH: IOS less than EH. Interantennal process: short, often excavate medially. Central keel: present or absent. Antennal foramen: oriented laterally on interantennal process. Facial striae: present or absent. Malar sulcus: present. Malar striae: present or absent. Setation of compound eye: present or absent. Gena: narrows dorsally behind eye, convex. Clypeus shape: narrow, rectangular, lateral corners not produced. Anterior (or ventral) margin of clypeus: straight. Labrum: narrow, trapezoidal, ventral margin convex or straight. Number of mandibular teeth: 2 or 3. Arrangement of mandibular teeth: transverse. Number of maxillary palpomeres: 4. Shape of maxillary palpomeres: cylindrical. Number of labial palpomeres: 2.

Antenna**.** Number of antennomeres in female: 12. Number of antennomeres in male: 12. Insertion of radicle into A1: parallel to longitudinal axis of

A1. Shape of A1: cylindrical, not flattened. Length of A3 of female: distinctly longer than A2. Number of antennomeres with papillary sensilla in female: 7. Arrangement of sensilla on female clava: in longitudinal pairs. Claval formula: A12–A6:1–2–2–2–2–2–2. Shape of male flagellum: filiform. Sex segment of male antenna: A5.

***Mesosoma*.** Posterior apex of pronotum in dorsal view: bifid apically to articulate with tegula. Epomial carina: absent. Cervical pronotal area: oblique, visible dorsally, short. Lateral face of pronotum: weakly concave ventrally around the pronotal cervical sulcus. Netrion: present. Netrion shape: moderately wide, open ventrally. Anterior portion of mesoscutum: vertical, flexed ventrally to meet pronotum. Mesoscutum shape: pentagonal, excavate at base of wings. Skaphion: absent. Notauli: present, percurrent. Parapsidal lines: present. Antero-admedian lines: absent. Transscutal articulation: well-developed. Mesoscutal suprahumeral sulcus: present or absent. Mesoscutal humeral sulcus: present as an uninterrupted groove or foveolate. Shape of mesoscutellum: trapezoidal. Lateral mesoscutellar spines: present. Median mesoscutellar spine: absent. Axillular spines: present. Surface of mesoscutellum: convex throughout. Median longitudinal furrow on mesoscutellum: absent. Metascutellum: clearly differentiated. Shape of metascutellum: flattened laterally into a medially spine; flattened dorsoventrally into a triangular plate. Setation of metascutellum: absent. Metapostnotum: fused to propodeum. Lateral propodeal projection: absent. Medial propodeal projection: absent. Mesopleural carina: present. Mesal course of acetabular carina: not separating fore coxae. Mesopleural pit: present. Posterodorsal corner of mesopleuron: rounded.

***Legs*.** Number of mesotibial spurs: 1. Number of metatibial spurs: 1. Dorsal surface of metacoxa: smooth. Shape of metacoxa: cylindrical, ecarinate. Trochantellus: indicated by transverse sulcus on femur.

***Wings*.** Wing development of female: macropterous. Wing development of male: macropterous. Tubular veins in fore wing: present. Bulla of fore wing R: absent. Length of marginal vein of fore wing: punctiform, R terminating at costal margin. Origin of r-rs in fore wing: arises at the point where R meets costal margin. Development of R in hind wing: complete.

***Metasoma*.** Number of external metasomal tergites in female: 7. Number of external metasomal sternites in female: 7. Number of external metasomal tergites in male: 8. Number of external metasomal sternites in male: 7. Shape of metasoma: lanceolate. Laterotergites: present, narrow. Laterosternites: present. T1 of female: flat; produced anteriorly as a small hump. Relative size of metasomal segments: T2–T3 subequal in length, remaining terga shorter. Metasomal tergites with basal crenulae: T2. Sublateral carinae on tergites: present. Median longitudinal carina on metasomal terga: absent; present on T1–T4. Shape of female T6: slightly convex. Anterior margin of S1: not produced anteriorly, straight. Felt fields on S2: present; obscured by setation. Felt fields on S3: present; obscured by setation. Ovipositor: *Scelio*-type (Austin and Field 1997).

Generic diagnosis. *Dichoteleas* can be identified by its elongate maxillary palpi, lateral spines on the mesoscutellum, medial spine on the metascutellum, and well-developed postmarginal vein on the forewing. This taxon can be distinguished from *Neoscelio* by the short (or absent) setation on the eyes and the well-developed postmarginal vein. It may be distinguished from *Oxyteleia* and *Oreiscelio* since in *Dichoteleas* the metascutellum only has a single median spine. The New World genus *Pseudoheptascelio* may also be interpreted to have a bidentate mesoscutellum. In that group the stigmal vein (r-rs) arises from the submarginal vein before it reaches the costal margin of the fore wing. In *Dichoteleas*, the stigma vein arises from the costal margin.

Distribution. *Dichoteleas* species are known from Kenya, Tanzania, Malawi, northeastern South Africa, Madagascar, southern India, New Guinea and Far North Queensland in Australia (Figs 1–8). No specimens have yet been collected in other parts of sub-Saharan Africa, southeast Asia, or regions to the east of Papua New Guinea.

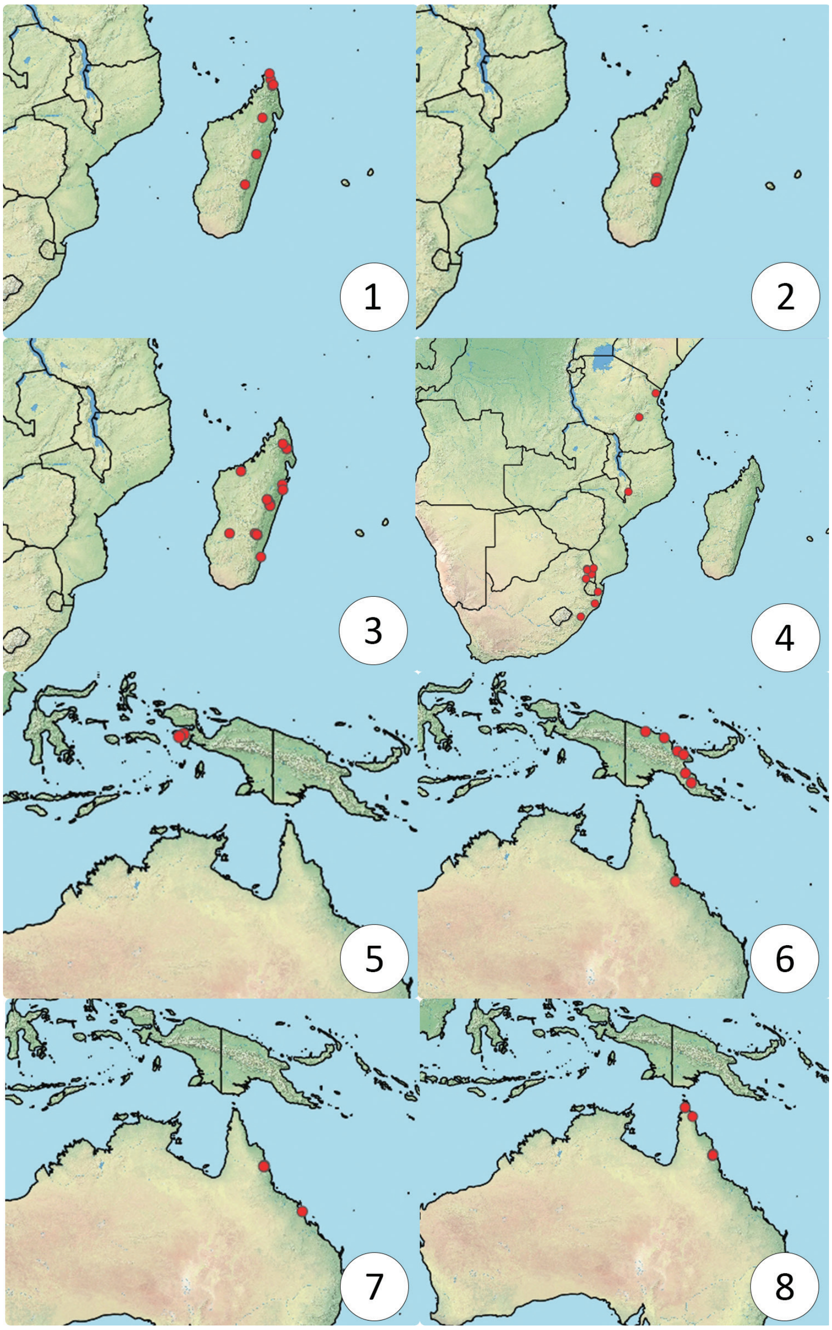

Figures 1–8. Distribution of *Dichoteleas* species **1** *D. rubyae* **2** *D. ambositrae* **3** *D. striatus* **4** *D. hamatus* **5** *D. fulgidus* **6** *D. fuscus* **7** *D. rugosus* **8** *D. subcoeruleus*.

Dichoteleas ambositrae **Risbec**

Figs 2, 9–11

Dichoteleia ambositrae Risbec, 1956: 261 (original description).
Dichoteleas ambositrae: Masner, 1976: 31 (type information); Johnson, 1992: 367 (catalogued, type information).

Description. Color of head: black. Hyperoccipital carina: present. Frontal depression: absent. Malar striae: absent. Facial striae: present. Setation of eyes: absent. Sculpture of frons: primarily smooth with weak transverse striations above the IAP. Setation of frons: mostly glabrous with sparse setation laterally. Submedian carina: absent. Interantennal process: undifferentiated. Central keel: absent. Transverse pronotal carina: absent. Color of pronotum: yellow. Pronotal cervical sulcus: present. Mesepimeral sulcus: present. Sulcus along mesopleural carina: foveolate. Mesoscutal suprahumeral sulcus: present. Mesoscutal humeral sulcus: present as an uninterrupted groove. Median mesoscutal line: absent. Color of mesoscutum: dark brown to black. Sculpture of mesoscutum: smooth without longitudinal striations. Notaulus: incomplete. Visibility of notaulus: unobscured. Parapsidal line: present. Sculpture of mesoscutellum: smooth. Shape of axillular carinae in lateral view: without a posteroventral hooklike projection. Color of axillular carina: yellow. Sculpture of T3–6: punctate. Median carina on T1–T4: absent.

Diagnosis. This species can be distinguished from *D. subcoeruleus*, *D. fulgidus*, *and D. fuscus* by the absence of the median carina on T1–T4. It can be distinguished from the other species by its xanthic pronotum and smooth mesoscutum.

Distribution. Madagascar (Ambositra, Fianarantsoa).

Material examined. ***Holotype***, female: **MADAGASCAR:** Ambositra, MNHN Paris EY32526; **MADAGASCAR**: 2 females, CASENT 2138155, 2138157 (CAS).

Dichoteleas fulgidus **sp. nov.**

https://zoobank.org/551D6CCD-7E66-496A-9B7C-53D007349DAC
Figs 5, 12–15

Description. Color of head: metallic blue. Hyperoccipital carina: present. Frontal depression: absent. Malar striae: absent. Facial striae: absent. Setation of eyes: absent. Sculpture of frons: smooth above interantennal prominence, areolate laterally. Setation of frons: sparsely setose throughout. Submedian carina: absent. Interantennal process: undifferentiated. Central keel: absent. Transverse pronotal carina: present. Color of pronotum: metallic blue. Pronotal cervical sulcus: absent. Mesepimeral sulcus: absent. Sulcus along mesopleural carina: absent. Mesoscutal suprahumeral sulcus: absent. Mesoscutal humeral sulcus: present as an uninterrupted groove. Median mesoscutal line: absent. Color of mesoscutum: metallic blue. Sculpture of mesoscutum: finely punctate without longitudinal striations. Notaulus: complete. Visibility of notaulus: unobscured. Parapsidal line: present. Sculpture of mesoscutellum: smooth. Shape of axillular carinae in lateral view: without a posteroventral hooklike projection. Color of axillular carina: metallic blue. Sculpture of T3–6: rugulose. Median carina on T1–T4: present.

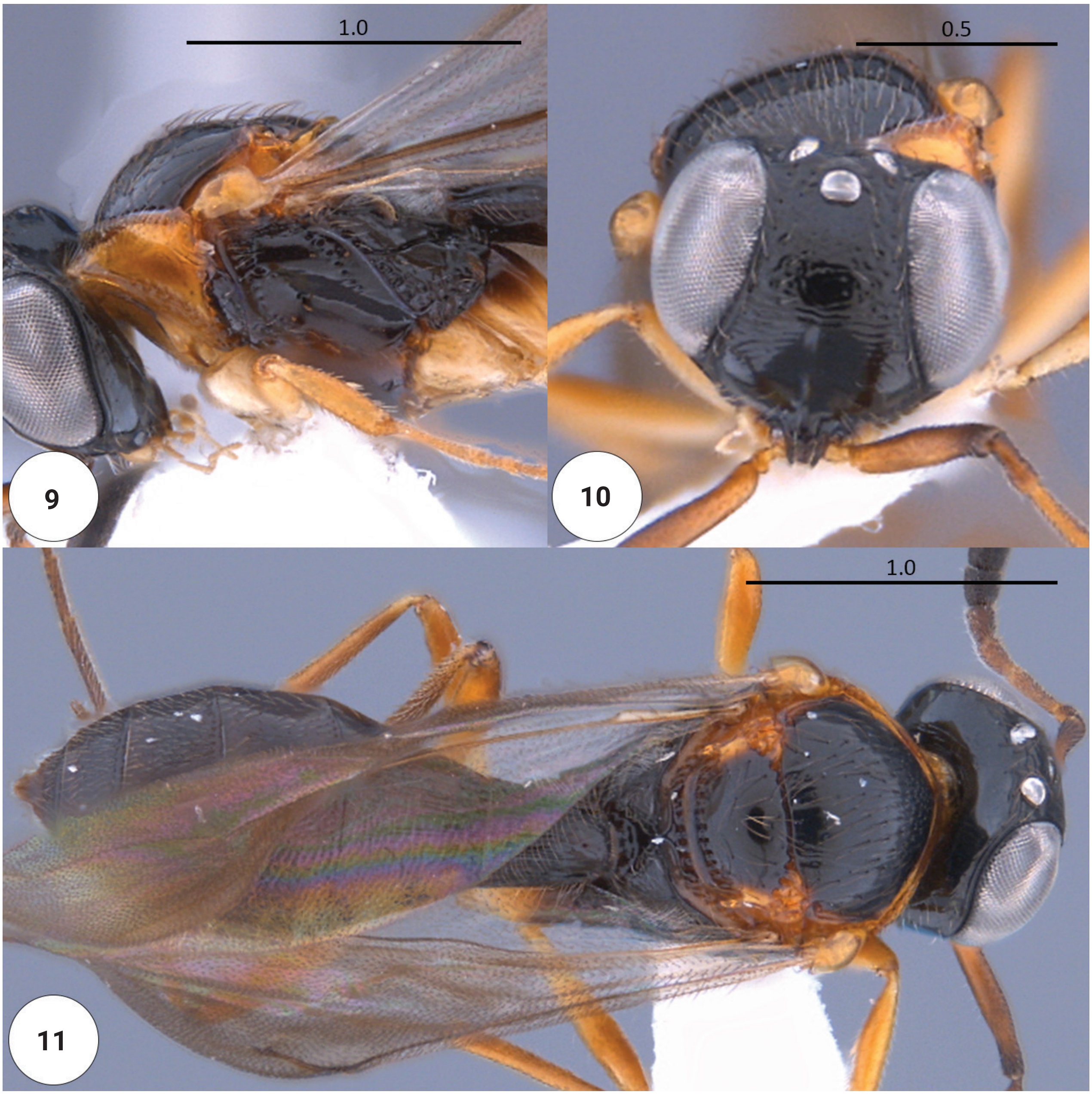

Figures 9–11. *Dichoteleas ambositrae* (F) (CASENT 2138155) **9** head, mesosoma, lateral view **10** head, anteroventral view **11** dorsal habitus.

Diagnosis. This species can be identified by the presence of a dorsal median carina on T1–T4 of the metasoma, and it may be distinguished from *D. subcoeruleus* and *D. fuscus* by the finely punctate sculpture of the mesoscutum.

Etymology. The epithet comes from the Latin word for "shiny," referring to the smooth, metallic luster of the mesosoma. This epithet is treated as an adjective.

Distribution. Indonesia (Papua Barat).

Material examined. ***Holotype***, female: **Indonesia:** FakFak S. coast of Bomberai, 100–700m; OSUC 234427 (BPBM). *Paratypes*. **Indonesia**: 3 males, OSUC 234420–234421, 234425 (BPBM).

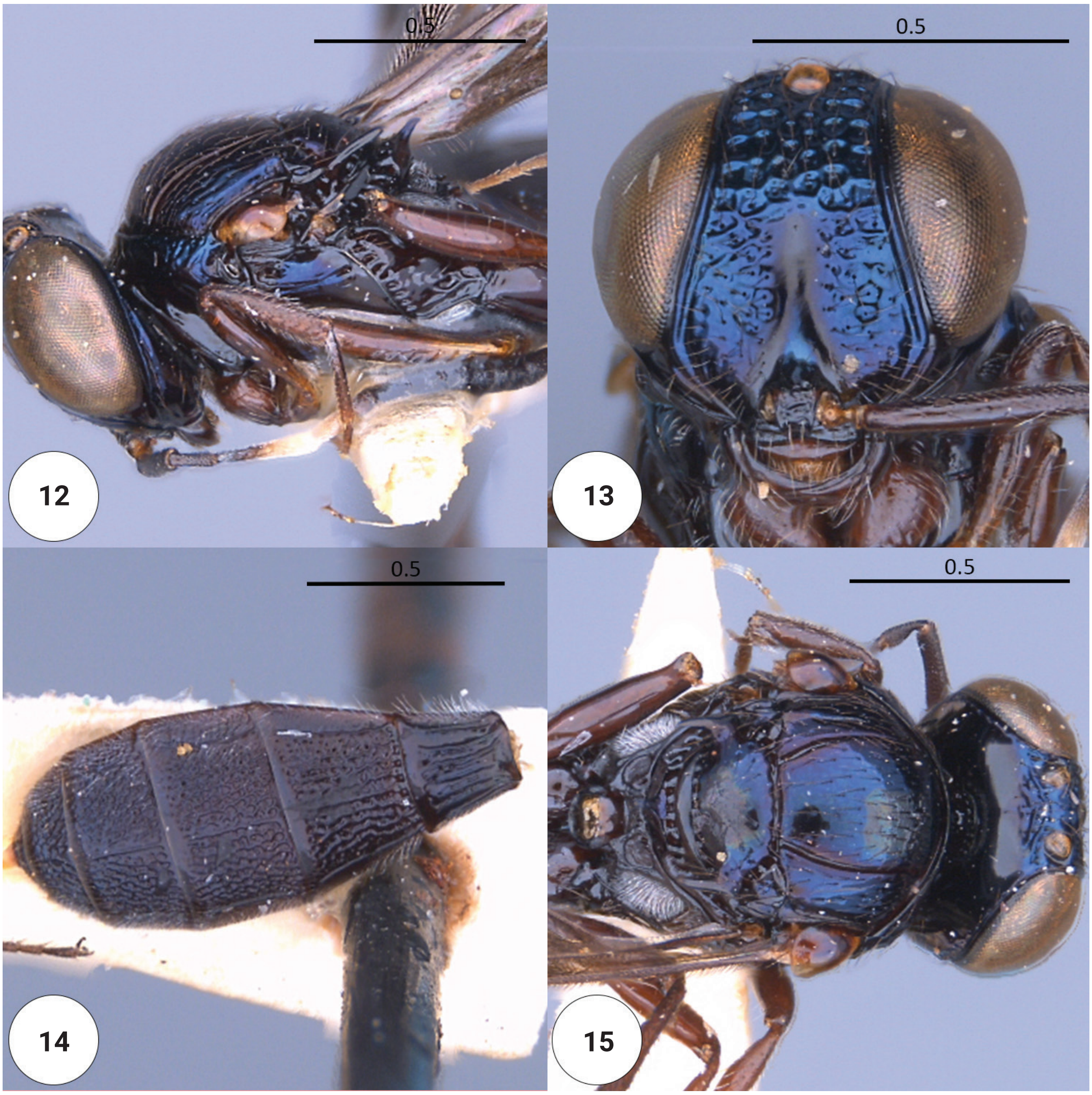

Figures 12–15. *Dichoteleas fulgidus* (F) (OSUC 0234427) **12** head, mesosoma, lateral view **13** head, anteroventral view **14** metasoma, dorsal view **15** head, mesosoma, dorsal view.

Dichoteleas fuscus **sp. nov.**
https://zoobank.org/8CA7BC20-6A81-4DBE-904A-2997CA6072F3
Figs 6, 16–18

Description. Color of head: metallic blue. Hyperoccipital carina: present. Frontal depression: absent. Malar striae: absent. Facial striae: absent. Setation of eyes: absent. Sculpture of frons: smooth above interantennal prominence, areolate laterally. Setation of frons: sparsely setose throughout. Submedian carina: present. Interantennal process: undifferentiated. Central keel: absent. Transverse pronotal carina: present. Color of pronotum: dark brown to black. Pronotal cervical sulcus: absent. Mesepimeral sulcus: absent. Sulcus

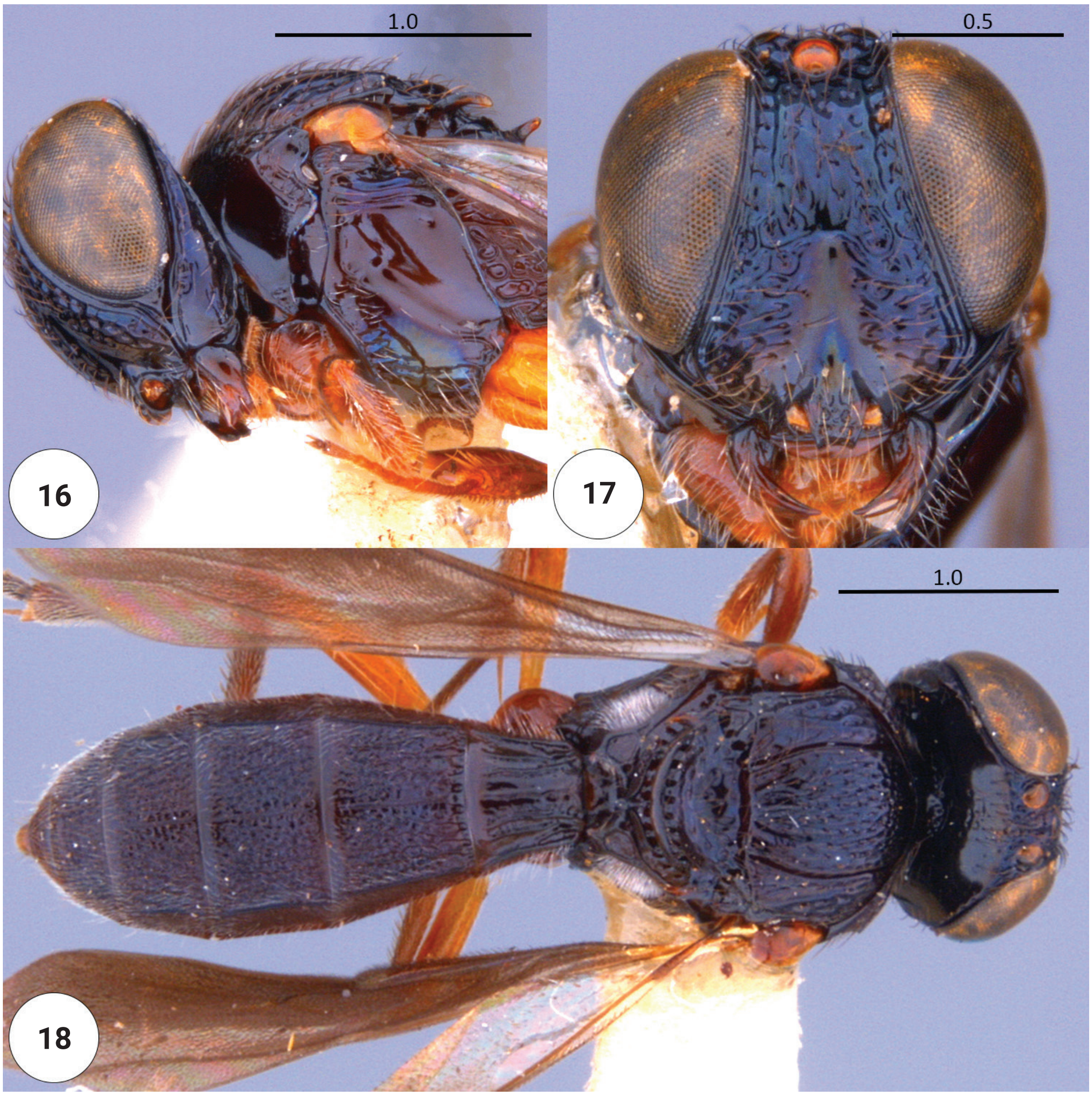

Figures 16–18. *Dichoteleas fuscus* (F) (OSUC 0234418) **16** head, mesosoma, lateral view **17** head, anteroventral view **18** dorsal habitus.

along mesopleural carina: absent. Mesoscutal suprahumeral sulcus: absent. Mesoscutal humeral sulcus: present as an uninterrupted groove. Median mesoscutal line: absent. Color of mesoscutum: dark brown to black. Sculpture of mesoscutum: rugulose. Notaulus: complete. Visibility of notaulus: unobscured. Parapsidal line: present. Sculpture of mesoscutellum: rugulose. Shape of axillular carinae: without a posteroventral hooklike projection. Color of axillular carina: brown. Sculpture of T3–6: rugulose. Median carina on T1–T4: present.

Diagnosis. This species can be identified by the dorsal median carina (T1–T4 of metasoma) and can be distinguished from *D. subcoeruleus* and *D. fulgidus* by the rugulose sculpture of the mesoscutum.

Etymology. The epithet comes from the Latin word for "dusky," referring to the darker, metallic color of the mesosoma (in comparison to *D. fulgidus*). This epithet is treated as an adjective.

Distribution. Papua New Guinea (Madang, Morobe, Northern, East Sepik), Australia (Queensland).

Material examined. ***Holotype***, female: **Papua New Guinea:** NE Finisterre Range, Saidor, Gabumi; OSUC 234417 (BPBM). ***Paratypes*.** **Australia:** 1 male, OSUC 875045 (CNCI). **Papua New Guinea:** 12 females, 4 males, OSUC 234413–234416, 234422–234424, 234426, 234428–234429 (BPBM), OSUC 875873–875876 (CNCI).

Dichoteleas hamatus **sp. nov.**

https://zoobank.org/09D49988-1679-4AC2-AC59-D5C47ED6E353
Figs 4, 19–21

Description. Color of head: black. Hyperoccipital carina: absent. Frontal depression: absent. Malar striae: present. Facial striae: present. Setation of eyes: sparse, with few scattered fine hairs. Sculpture of frons: smooth above interantennal prominence, areolate laterally. Setation of frons: sparsely setose throughout. Submedian carina: absent. Interantennal process: undifferentiated. Central keel: absent. Transverse pronotal carina: present. Color of pronotum: dark brown to black. Pronotal cervical sulcus: present. Mesepimeral sulcus: present. Sulcus along mesopleural carina: absent. Mesoscutal suprahumeral sulcus: absent. Mesoscutal humeral sulcus: present, foveolate. Median mesoscutal line: absent. Color of mesoscutum: dark brown to black. Sculpture of mesoscutum: areolate-rugose. Notaulus: complete. Visibility of notaulus: slightly obscured by mesoscutal sculpture. Parapsidal line: present. Sculpture of mesoscutellum: rugulose. Shape of axillular carinae in lateral view: with a sharp posteroventral hooklike projection. Color of axillular carina: brown. Sculpture of T3–6: rugulose and finely punctate. Median carina on T1–T4: absent.

Diagnosis. This species can be distinguished from *D. rugosus* by the distinct hooked projections on axillular carinae.

Etymology. The name *hamatus* is drawn from the Latin word for hooked, referring to the hooked projections on the axillular carinae. This epithet is treated as an adjective.

Distribution. Kenya (Coast), Malawi (Mulanje), South Africa (Limpopo), Tanzania (Uzungwa Mts., Tanga Amani Hills).

Material examined. ***Holotype***, female: **South Africa:** Guernsey Farm, Limpopo Prov.; OSUC 56306 (CNCI). *Paratypes*. **Kenya:** 1 female, ICIPE 32195 (ICIPE). **Malawi:** 1 female, OSUC 875032 (CNCI). **South Africa:** 20 females, 50 males, OSUC 874965–875031, 875037 (CNCI); SAM-HYM-P031302, SAM-HYM-P037851 (SAMC); USNMENT01197871 (USNM). **Tanzania:** 5 females, 1 male, OSUC 875033–875036, 875040-875041 (CNCI).

Dichoteleas indicus **Saraswat**

Figs 22–25

Dichoteleas indicus Saraswat, 1982: 350 (original description); Johnson, 1992: 367 (catalogued, type information).

Description. Color of head: black. Hyperoccipital carina: present. Frontal depression: absent. Malar striae: present. Facial striae: present. Setation

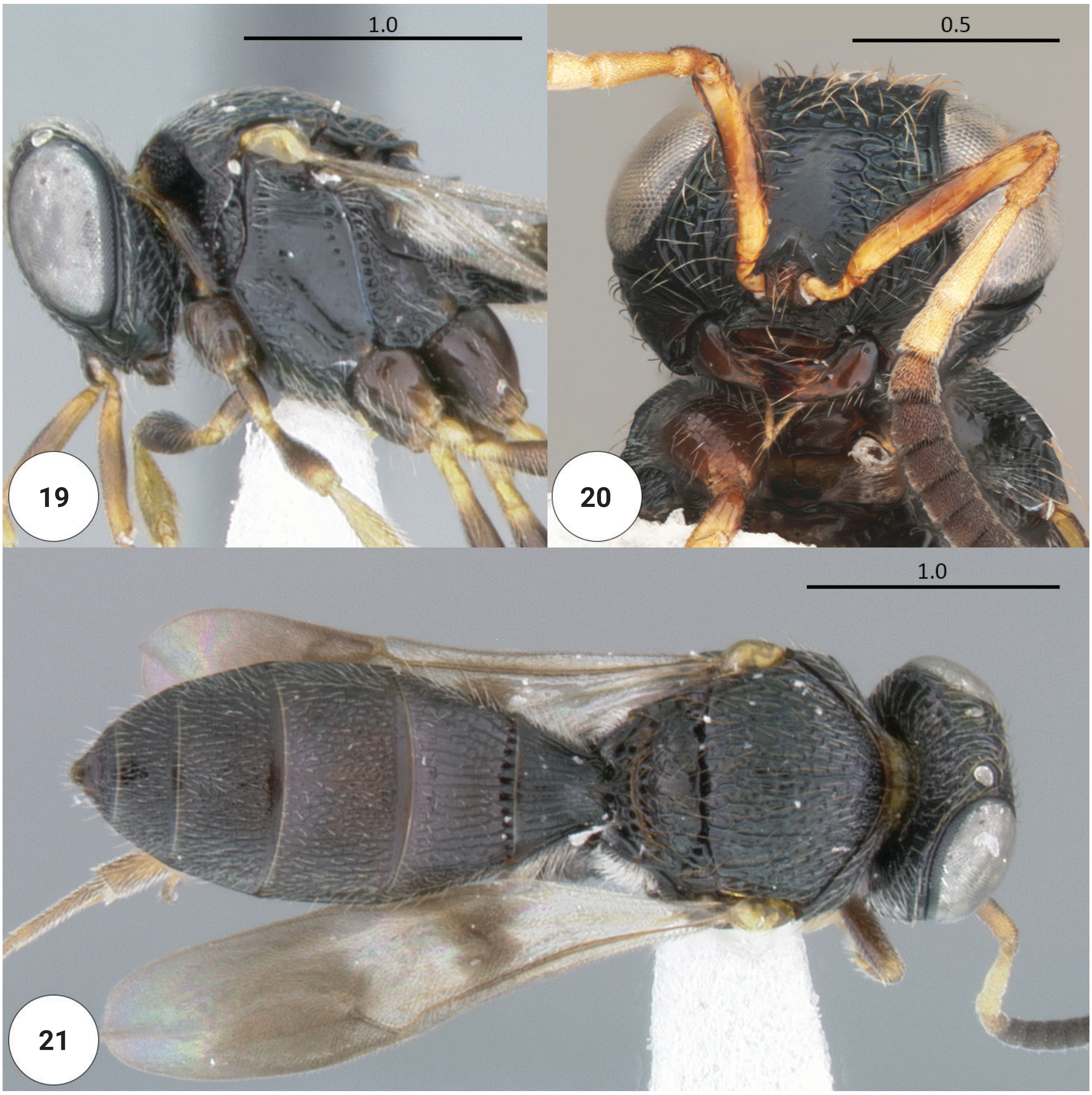

Figures 19–21. *Dichoteleas hamatus* (F) (OSUC 56306) **19** head, mesosoma, lateral view **20** head, anteroventral view **21** dorsal habitus.

of eyes: sparse, with few scattered fine hairs. Sculpture of frons: primarily rugulose. Setation of frons: sparsely setose throughout. Submedian carina: present. Interantennal process: produced anteriorly, margined by depression. Central keel: present. Transverse pronotal carina: present. Color of pronotum: dark brown to black. Pronotal cervical sulcus: present. Mesepimeral sulcus: absent. Sulcus along mesopleural carina: absent. Mesoscutal suprahumeral sulcus: absent. Mesoscutal humeral sulcus: present as an uninterrupted groove. Median mesoscutal line: present. Color of mesoscutum: dark brown to black. Sculpture of mesoscutum: rugulose. Notaulus: complete. Visibility of notaulus: slightly obscured by mesoscutal sculpture. Parapsidal line:

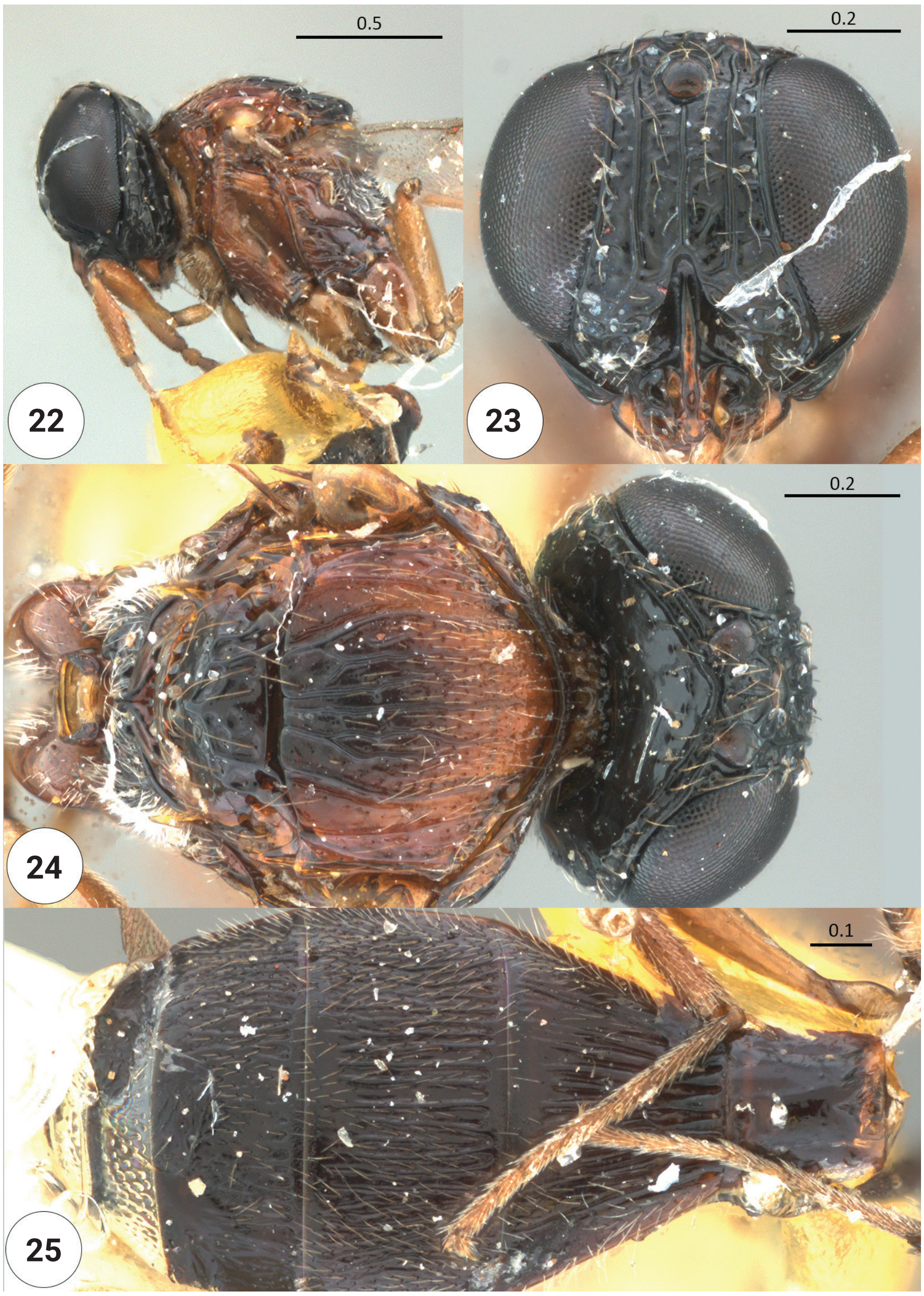

Figures 22–25. *Dichoteleas indicus* (M) (USNMENT 01109962) **22** mesosoma, lateral view **23** head, anteroventral view **24** head, mesosoma, dorsal view **25** metasoma, dorsal view.

present. Sculpture of mesoscutellum: rugulose. Shape of axillular carinae in lateral view: without a posteroventral hooklike projection. Color of axillular carina: yellow. Sculpture of T3–6: strigate and finely punctate. Median carina on T1–T4: absent.

Diagnosis. This species can be distinguished by the anteriorly produced interantennal process and the presence of the central keel.

Distribution. India (Kerala).

Material examined. Holotype, male: **India:** School of Entomology, St. John's College; USNMENT 01109962. **India:** 1 female, OSUC 875044 (CNCI).

Dichoteleas rubyae sp. nov.

https://zoobank.org/A33B1DD4-261B-4969-957E-26E7C3D654A1

Figs 1, 26–28

Description. Color of head: black. Hyperoccipital carina: absent. Frontal depression: present, shallow. Malar striae: present. Facial striae: present. Setation of eyes: absent. Sculpture of frons: smooth above interantennal prominence, areolate laterally. Setation of frons: sparsely setose throughout. Submedian carina: absent. Interantennal process: undifferentiated. Central keel: absent. Transverse pronotal carina: absent. Color of pronotum: red. Pronotal cervical sulcus: present. Mesepimeral sulcus: present. Sulcus along mesopleural carina: foveolate. Mesoscutal suprahumeral sulcus: present. Mesoscutal humeral sulcus: present, foveolate. Median mesoscutal line: absent. Color of mesoscutum: red. Sculpture of mesoscutum: areolate-rugose. Notaulus: complete. Visibility of notaulus: slightly obscured by mesoscutal sculpture. Parapsidal line: present. Sculpture of mesoscutellum: smooth. Shape of axillular carinae: without a posteroventral hooklike projection. Color of axillular carina: yellow. Sculpture of T3–6: rugulose and finely punctate. Median carina on T1– T4: absent.

Diagnosis. This species can be distinguished from *D. rugosus* by its reddish mesosoma and the smooth mesoscutellum.

Etymology. The epithet *rubyae* in honor of the first author's grandmother, Ruby Thomas. The name also refers to the red coloration of the mesosoma. This epithet is treated as a noun in the genitive case.

Distribution. Madagascar (Antsiranana, Ranomafana).

Material examined. ***Holotype***, female: **MADAGASCAR:** Prov. Antsiranana, Forêt de Binara, 375m; CASENT 2134207 (CAS). ***Paratypes*. MADAGASCAR:** 19 females, 7 males, CASENT 2043443–2043447, 2131300–2131302, 2134208–2134212, 2137245, 2137863 (CAS), OSUC 874887, 874942 (CNCI); CASENT 2042724–2042725, 2043436-2043442, 2134212, 2137245, 2137863 (OSUC).

Comments. There is some variation in the visibility of the notauli. In most specimens, the notauli were obscured by the mesoscutal sculpture, but one specimen (CASENT 2137863) had clearly defined notauli.

Dichoteleas rugosus Kieffer

Figs 7, 29–31

Dichoteleas rugosus Kieffer, 1907: 297 (original description); Kieffer, 1926: 351 (description, keyed); Dodd, 1926: 370 (description); Masner, 1965: 72 (type information); Galloway, 1976: 90 (type information); Johnson, 1992: 367 (catalogued, type information).

Dichoteleas pappi Szabó, 1971: 319 (original description); Galloway 1976: 90 (type information); Johnson, 1992: 367 (catalogued, type information), new synonymy.

Description. Color of head: black. Hyperoccipital carina: absent. Frontal depression: absent. Malar striae: present. Facial striae: present. Setation of eyes: absent. Sculpture of frons: smooth above interantennal prominence, areolate laterally. Setation of frons: sparsely setose throughout. Submedian

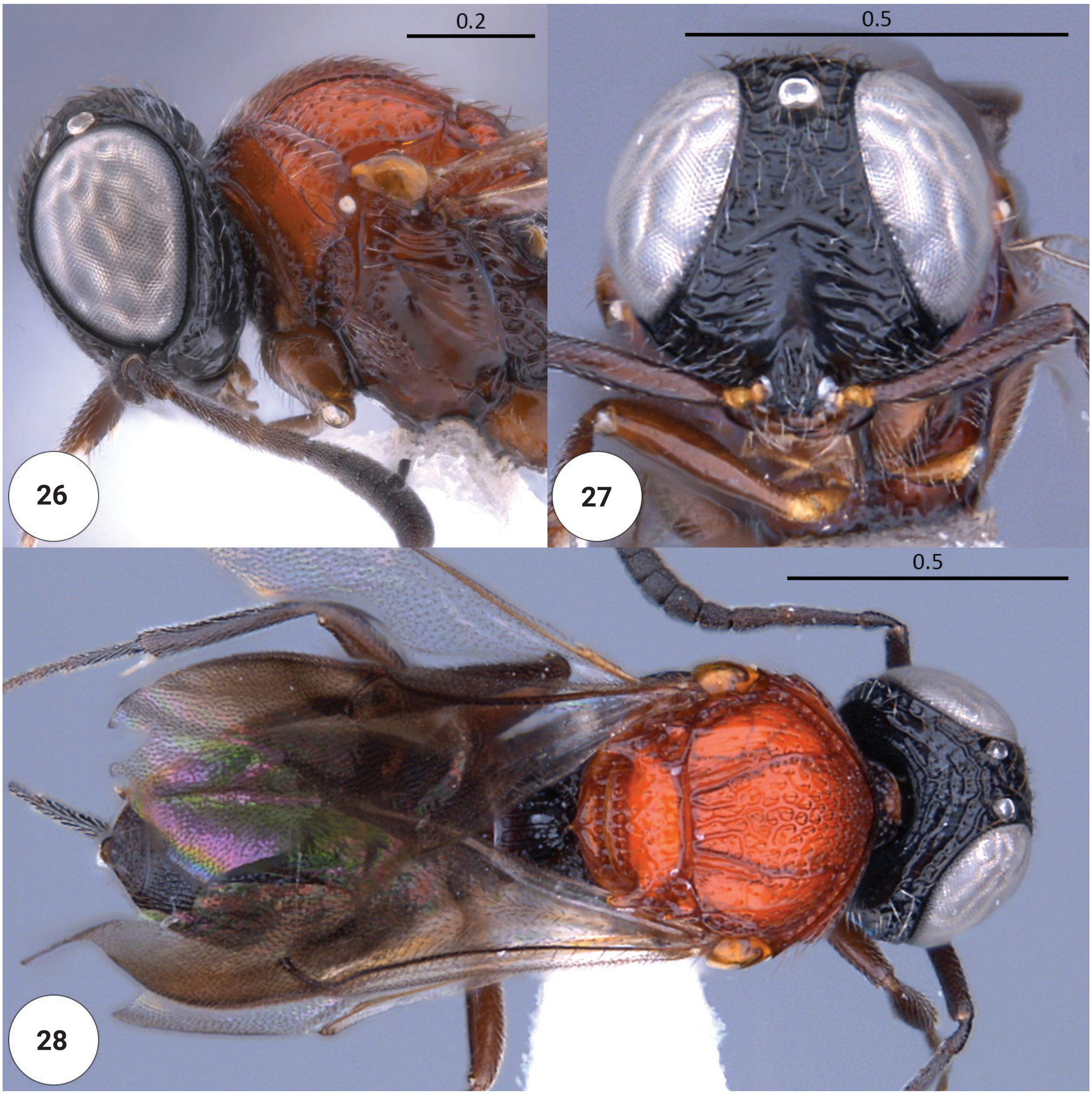

Figures 26–28. *Dichoteleas rubyae* (F) (CASENT 2137863) **26** head, mesosoma, lateral view **27** head, anteroventral view **28** dorsal habitus.

carina: absent. Interantennal process: undifferentiated. Central keel: absent. Transverse pronotal carina: present. Color of pronotum: dark brown to black. Pronotal cervical sulcus: present. Mesepimeral sulcus: present. Sulcus along mesopleural carina: foveolate. Mesoscutal suprahumeral sulcus: absent. Mesoscutal humeral sulcus: present, foveolate. Median mesoscutal line: absent. Color of mesoscutum: dark brown to black. Sculpture of mesoscutum: punctate with longitudinal striations between notauli. Notaulus: complete. Visibility of notaulus: unobscured. Parapsidal line: present. Sculpture of mesoscutellum: punctate. Shape of axillular carinae in lateral view: without a posteroventral hooklike projection. Color of axillular carina: brown. Sculpture of T3–6: rugulose and finely punctate. Median carina on T1–T4: absent.

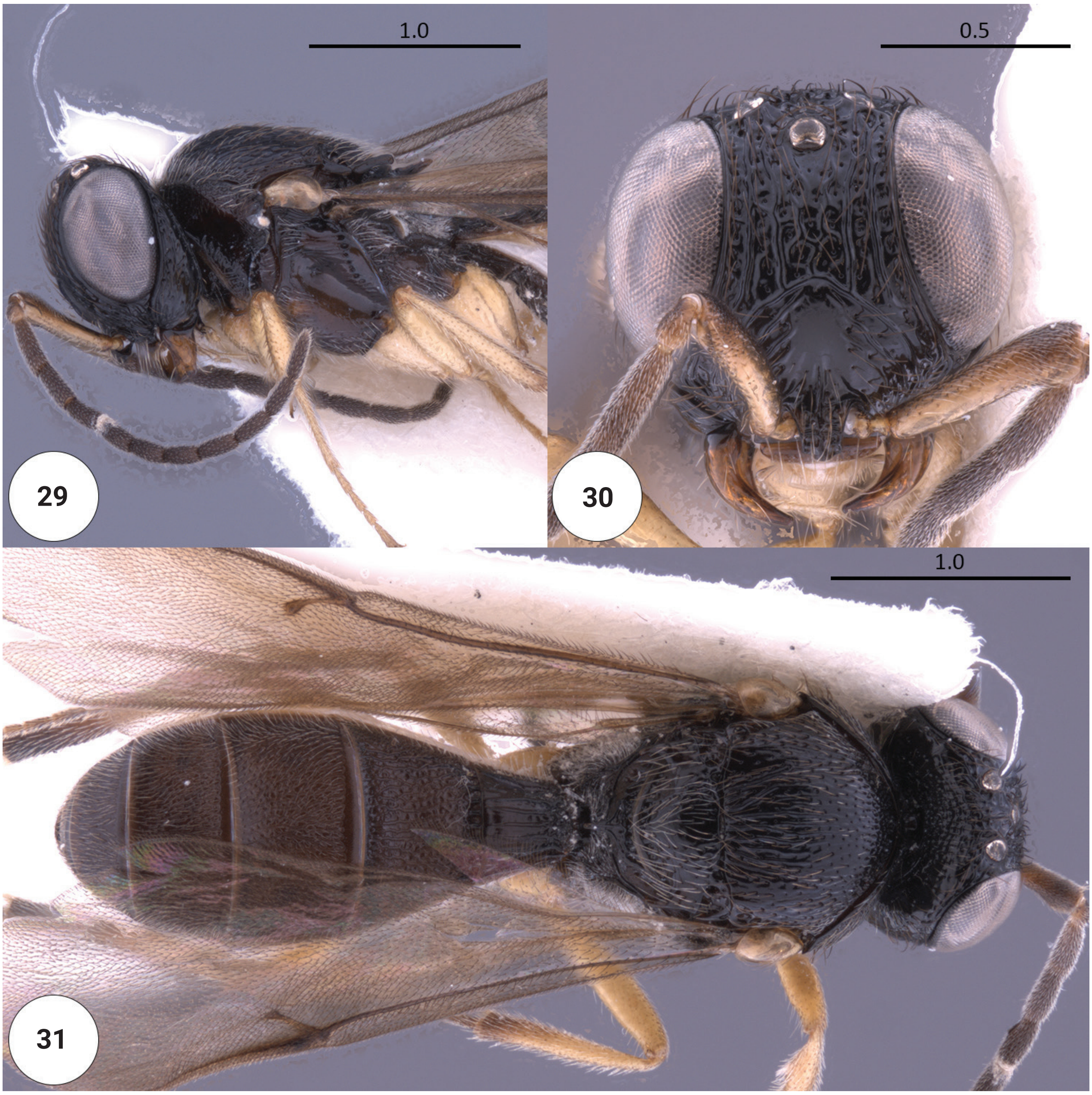

Figures 29–31. *Dichoteleas rugosus* (M) (OSUC 0367523) **29** head, mesosoma, lateral view **30** head, anteroventral view **31** dorsal habitus.

Diagnosis. *Dichoteleas rugosus* can be distinguished from *D. striatus* by its setose and punctate mesosoma and other *Dichoteleas* by its bidentate mandibles.

Distribution. Australia (Queensland).

Material examined. ***Holotype***, male, *D. rugosus*: **Australia:** QLD, Mackay; OCT-1897, B.M. TYPE HYM. 9.496.; **Australia:** 4 females, 2 males, OSUC 367523, 367536 (ANIC), OSUC 875046–875047, 875871–875872 (CNCI).

Comments. In the original description, Kieffer (1907) wrote that *D. rugosus* was missing parapsidal lines. They are present but obscured by the sculpture of the mesoscutum.

***Dichoteleas striatus* sp. nov.**

https://zoobank.org/985F5CD2-7A6E-4546-8CDA-FCFF2BBFE104
Figs 3, 32–34

Description. Color of head: black. Hyperoccipital carina: present. Frontal depression: absent. Malar striae: absent. Facial striae: present. Setation of eyes: absent. Sculpture of frons: primarily smooth with weak transverse striations above the IAP. Setation of frons: mostly glabrous with sparse setation laterally. Submedian carina: absent. Interantennal process: undifferentiated. Central keel: absent. Transverse pronotal carina: present. Color of pronotum: dark brown to black. Pronotal cervical sulcus: present. Mesepimeral sulcus: present. Sulcus along mesopleural carina: absent. Mesoscutal suprahumeral sulcus: present. Mesoscutal humeral sulcus: present as an uninterrupted groove. Median mesoscutal line: absent. Color of mesoscutum: dark brown; black. Sculpture of mesoscutum: primarily smooth with longitudinal striations between notauli. Notaulus: complete. Visibility of notaulus: slightly obscured by mesoscutal sculpture. Parapsidal line: present. Sculpture of mesoscutellum: smooth. Shape of axillular carinae in lateral view: without a posteroventral hooklike projection. Color of axillular carina: brown. Sculpture of T3–6: weakly strigate and finely punctate. Median carina on T1–T4: absent.

Diagnosis. This species can be distinguished from *D. ambositrae* by the longitudinal striations between the notauli and the black/brown pronotum and from *D. rugosus* by its glabrous mesosoma.

Etymology. The epithet refers to the longitudinal striations present on the mesoscutum. This epithet is treated as an adjective.

Distribution. Madagascar (Antananarivo, Antsiranana, Fianarantsoa, Mahajanga, Toamasina).

Material examined. ***Holotype***, female: **MADAGASCAR:** Prov. Fianarantsoa, 1130m, PN Ranomafana, radio tower; CASENT 2043988 (CAS). ***Paratypes***. **MADAGASCAR:** 93 females, 64 males, CASENT 2043198, 2043540, 2043564–2043565, 2043989, 2118400, 2118404, 2118444, 2131303–2131316, 2132729, 2132737, 2133921–2133922, 2134086, 2134150, 2134156, 2134161, 2134169, 2134198–2134200, 2134203– 2134204, 2134523, 2135869, 2135989, 2136263, 2136415, 2137236, 2137832, 2137876, 2137937, 2138216 (CAS); CASENT 2042824, 2042844–2042857, 2042967–2042976, OSUC 146657, 229802 (OSUC); OSUC 218026 (USU); OSUC 874879–874883, 874885–874886, 874888–874941, 874943–874964 (CNCI).

Comments. There was some variation in the length and the number of the longitudinal striations on the mesoscutum. In fewer than half of the specimens, the striations started anteriorly and terminated around the middle of the mesoscutum. In the majority of the specimens, the striations started anteriorly and terminated at the posterior margin of the mesoscutum.

***Dichoteleas subcoeruleus* Dodd**

Figs 8, 35–37

Dichoteleas subcoeruleus Dodd, 1926: 370, 371 (original description); Galloway 1976: 90 (type information); Johnson, 1992: 367 (catalogued, type information).

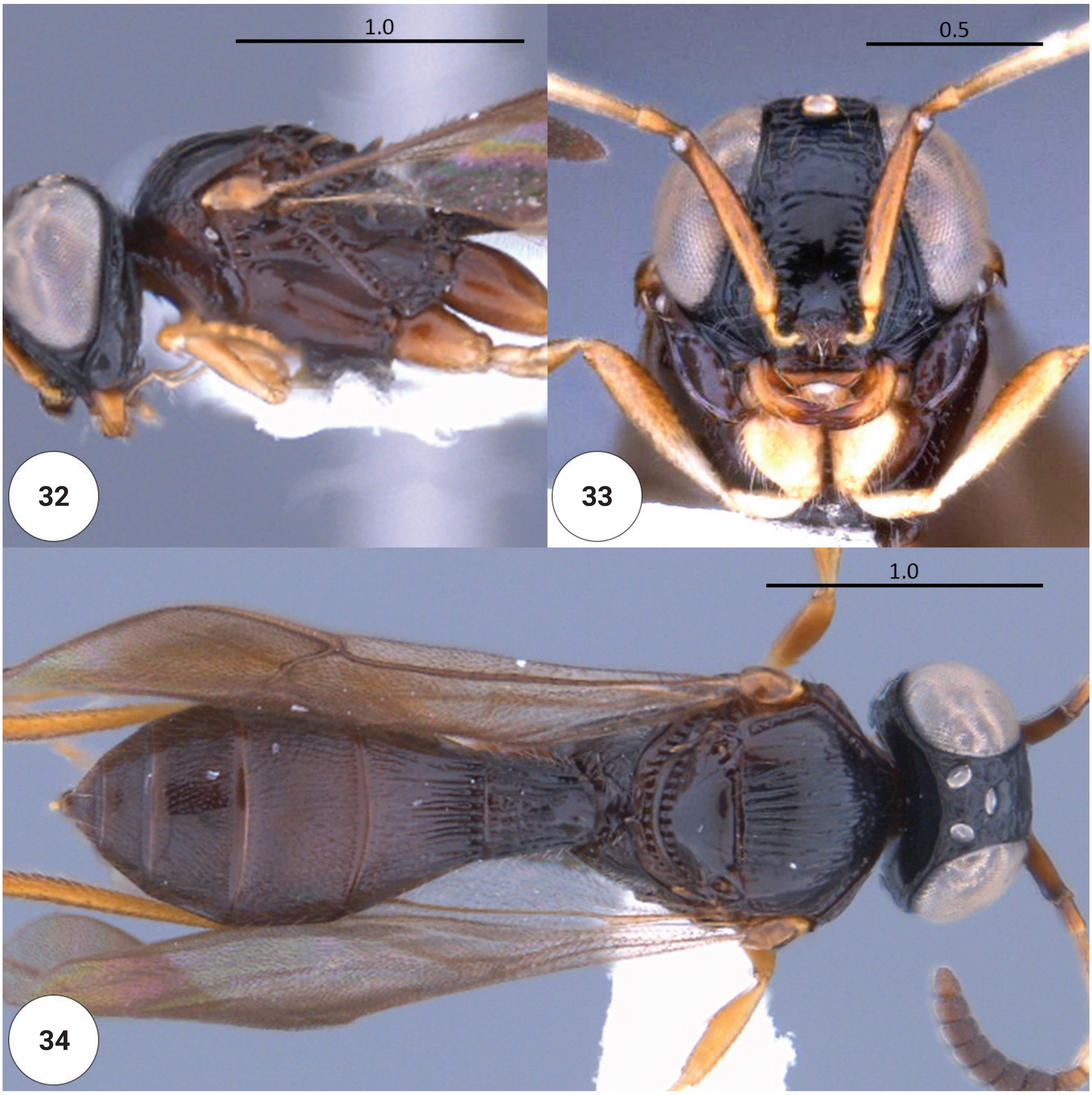

Figures 32–34. *Dichoteleas striatus* (F) (CASENT 2043988) **32** head, mesosoma, lateral view **33** head, anteroventral view **34** dorsal habitus.

Description. Color of head: metallic blue. Hyperoccipital carina: absent. Frontal depression: absent. Malar striae: absent. Facial striae: present. Setation of eyes: absent. Sculpture of frons: smooth above interantennal prominence, areolate laterally. Setation of frons: sparsely setose throughout. Submedian carina: present. Interantennal process: undifferentiated. Central keel: absent. Transverse pronotal carina: present. Color of pronotum: dark brown to black. Pronotal cervical sulcus: absent. Mesepimeral sulcus: present. Sulcus along mesopleural carina: foveolate. Mesoscutal suprahumeral sulcus: absent. Mesoscutal humeral sulcus: present as an uninterrupted groove. Median mesoscutal line: present. Color of mesoscutum: metallic blue. Sculpture of mesoscutum: rugulose. Notaulus: complete. Visibility of notaulus: unobscured.

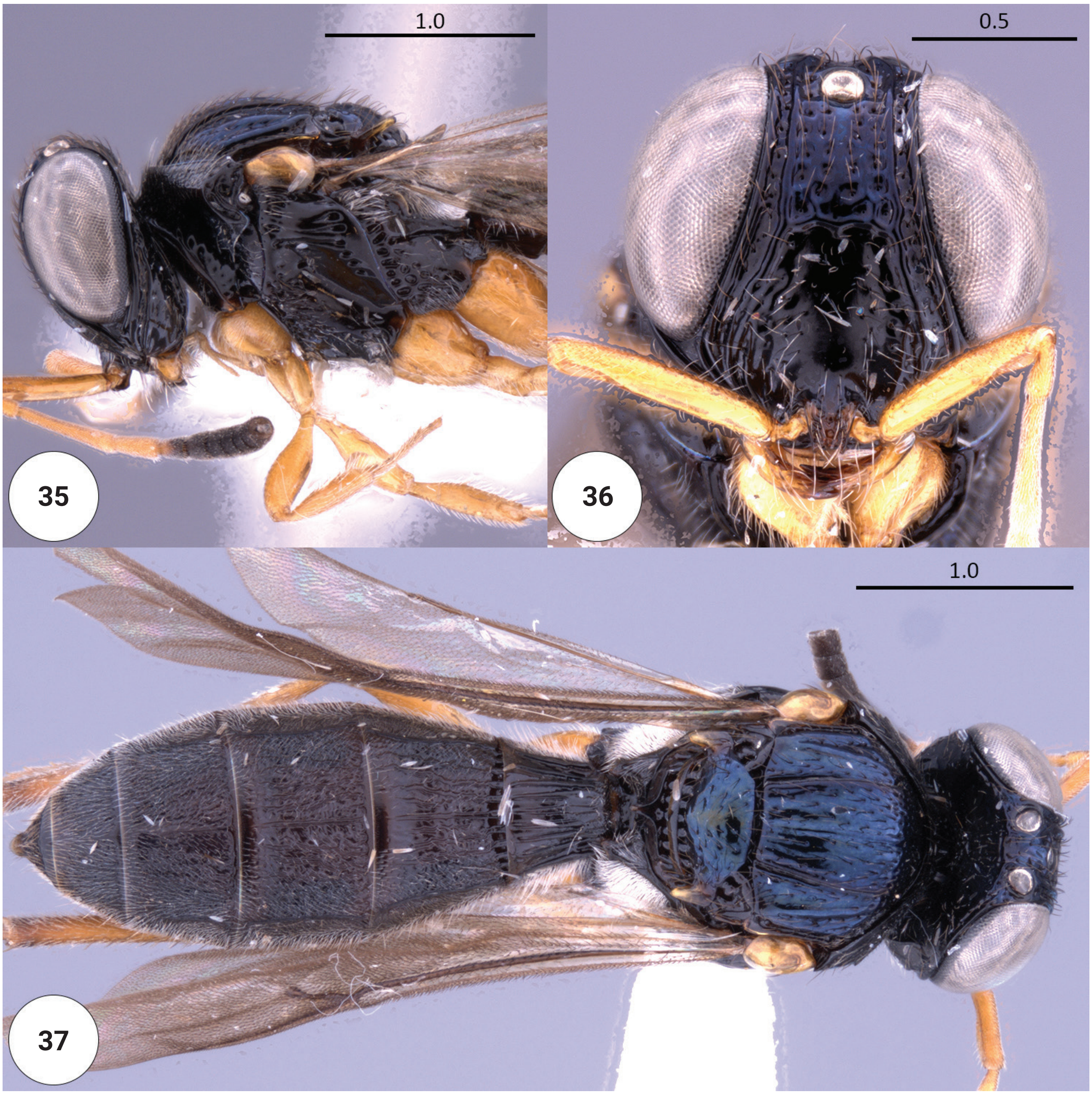

Figures 35–37. *Dichoteleas subcoeruleus* (F) (OSUC 0367538) **35** head, mesosoma, lateral view **36** head, anteroventral view **37** dorsal habitus.

Parapsidal line: present. Sculpture of mesoscutellum: smooth. Shape of axillular carinae in lateral view: without a posteroventral hooklike projection. Color of axillular carina: yellow. Sculpture of T3–4: rugulose and finely punctate. Median carina on T1–T4: present.

Diagnosis. This species can be distinguished by the presence of the median mesoscutal line and can be distinguished from *D. indicus* by the median carina on T1–T4.

Distribution. Australia (Queensland)

Material examined. ***Holotype***, female: **Australia:** Queensland, Mossman, SAMA 32-00145 (SAMA). **Australia:** 13 females, 4 males, OSUC 367522, 367527–367542 (ANIC).

Dichoteleas umbra **sp. nov.**

https://zoobank.org/C86B76DC-5B02-4FDF-842F-60F2E98B4B06
Figs 38–40

Description. Color of head: black. Hyperoccipital carina: present. Frontal depression: absent. Malar striae: present. Facial striae: present. Setation of eyes: absent. Sculpture of frons: smooth above interantennal prominence, areolate laterally. Setation of frons: sparsely setose throughout. Submedian carina: absent. Interantennal process: undifferentiated. Central keel: absent. Transverse pronotal carina: present. Color of pronotum: dark brown to black. Pronotal cervical sulcus: present. Mesepimeral sulcus: present. Sulcus along mesopleural carina: foveolate. Mesoscutal suprahumeral sulcus: absent. Mesoscutal humeral sulcus: present as an uninterrupted groove. Median mesoscutal line: absent. Color of mesoscutum: black with xanthic posterolateral corners. Sculpture of mesoscutum: punctate. Notaulus: complete. Visibility of notaulus: unobscured. Parapsidal line: present. Sculpture of mesoscutellum: smooth. Shape of axillular carinae in lateral view: without a posteroventral hooklike. Color of axillular carina: slighter lighter than mesoscutellum. Sculpture of T3–6: punctate. Median carina on T1–T4: absent.

Diagnosis. *D. umbra* can be distinguished from *D. rugosus* by the xanthic posterolateral corners of the mesoscutum. This species differs from *D. hamatus* and *D. striatus* by the punctate mesoscutum.

Etymology. The name *umbra* is from the Latin word for shadow or shade, referring to the dark color. This epithet is treated as a noun.

Distribution. Tanzania (Uluguru Mts.).

Material examined. ***Holotype***, female: **TANZANIA:** Uluguru Mts. Lupanga, East, 1300m; OSUC 875037 (CNCI). ***Paratypes***. **TANZANIA:** 1 female, 1 male, OSUC 875038-875039 (CNCI).

Comments on undescribed specimens:

There were a few specimens that did not fit into these species descriptions. We have chosen to not formally describe them because all were male and only 1–2 specimens were available.

Unknown 1

Material examined. MADAGASCAR: 1 male, CASENT2042862 (CAS).

Diagnosis. This specimen has an anteriorly produced IAP, similar to *D. indicus*, but it lacks a central keel and submedian carinae on the frons.

Unknown 2

Material examined. INDIA: 2 males, OSUC 875042, OSUC 875043 (CNCI).

Diagnosis. These specimens have a curved carina in the shape of an inverted “U” present on the frons. It appears to join the facial striae anteriorly. Submedian carinae are present, and there is a blunt medial projection on the mesoscutellum. The specimens were collected in southern India, Tamil Nadu state (Coimbatore and the Anaimlai Hills).

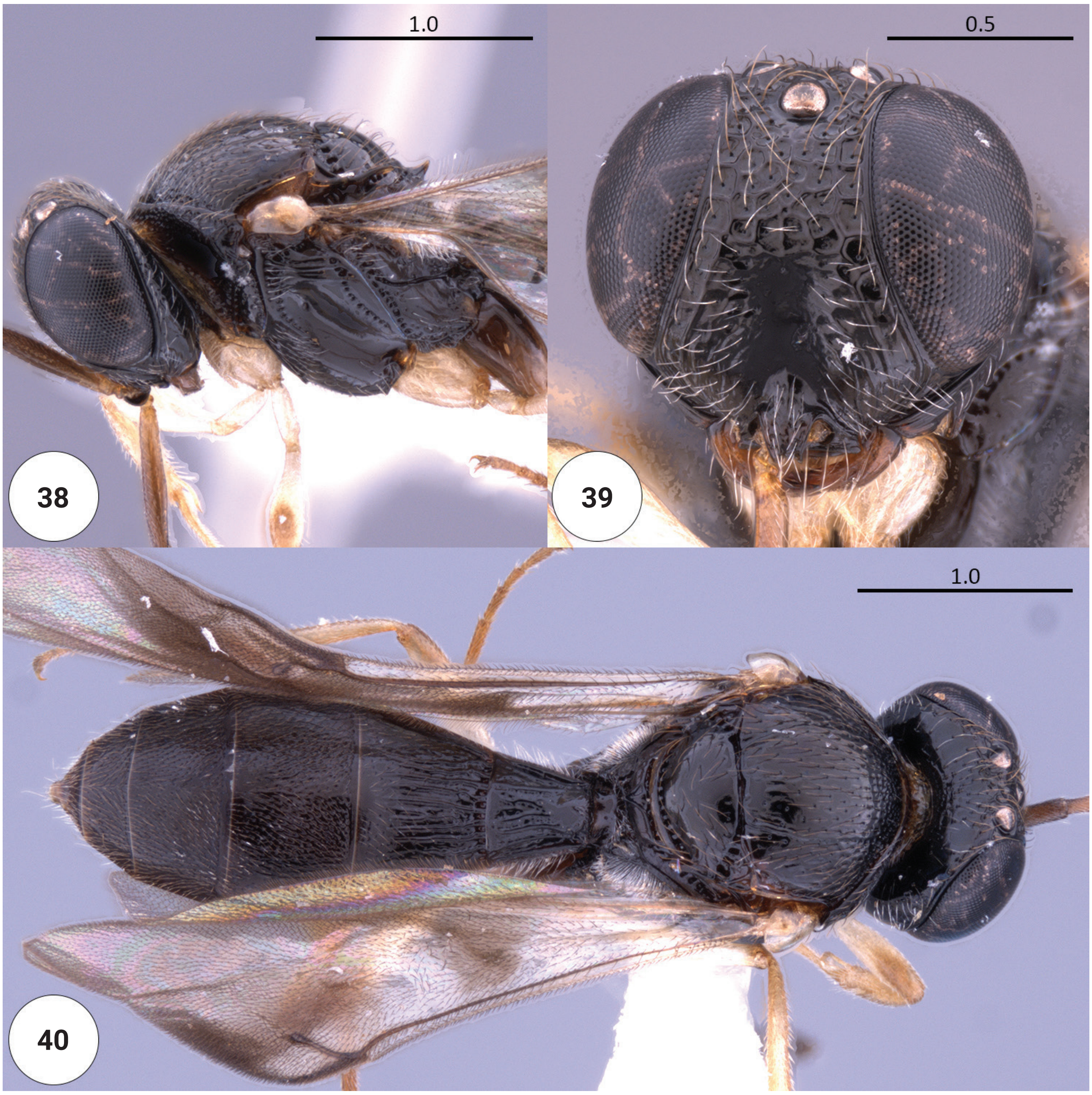

Figures 38–40. *Dichoteleas umbra* (F) (OSUC 875039) **38** head, mesosoma, lateral view **39** head, anteroventral view **40** dorsal habitus.

Acknowledgments

We thank the curators and collectors whose efforts were essential for this study. Special thanks to Luciana Musetti, Lubomír Masner, Kendall King, and Sara Hemly for critical support.

Additional information

Conflict of interest

The authors have declared that no competing interests exist.

Ethical statement

No ethical statement was reported.

Funding

No funding was reported.

Author contributions

J. Schwartz conducted the bulk of the taxonomic analysis and writing of the manuscript. S. van Noort provided supplementary information, images, and analysis of Afrotropical species. N. Johnson designed the project, guided the execution of the analysis, contributed to writing of the manuscript, and edited the final version.

Author ORCIDs

Simon Van Noort https://orcid.org/0000-0001-6930-9741
Norman F. Johnson https://orcid.org/0000-0003-1691-5187

Data availability

All of the data that support the findings of this study are available in the main text.

References

Austin AD, Field SA (1997) The ovipositor system of scelionid and platygastrid wasps (Hymenoptera: Platygastroidea): comparative morphology and phylogenetic implications. Invertebrate Systematics 11(1): 1–87. https://doi.org/10.1071/IT95048

Bin F (1981) Definition of female antennal clava based on its plate sensilla in Hymenoptera Scelionidae Telenominae. Redia (Firenze) 64: 245–261.

Brues CT (1908) Hymenoptera. Fam. Scelionidae. Genera Insectorum 80: 1–59. https://www.biodiversitylibrary.org/item/105248#page/202/mode/1up

Chen HY, Lahey Z, Talamas EJ, Valreio AA, Popovici OA, Musetti L, Klompen H, Polaszek A, Masner L, Austin AD, Johnson NF (2021) An integrated phylogenetic assessment of the parasitoid superfamily Platygastroidea (Hymenoptera: Proctotrupomorpha) results in a revised familial classification. Systematic Entomology 46(4): 1088–1113. https://doi.org/10.1111/syen.12511

Dodd AP (1913) Australian Hymenoptera Proctotrypoidea. No. 1. Transactions of the Royal Society of South Australia 37: 130–181.

Dodd AP (1926) New species of Australian Proctotrypoidea, with revisional notes. Proceedings of the Linnean Society of New South Wales 51: 369–381. https://doi.org/10.5281/zenodo.23802

Galloway ID (1976) the types of Australian species of the subfamily Scelioninae (Hymenoptera: Scelionidae). Queensland Journal of Agricultural and Animal Sciences 33(1): 83–114.

Galloway ID, Austin AD (1984) Revision of the Scelioninae (Hymenoptera: Scelionidae) in Australia. Australian Journal of Zoology Supplementary Series 99: 1–138. https://doi.org/10.1071/AJZS099

Harris RA (1979) A glossary of surface sculpturing. California Department of Food and Agriculture, Bureau of Entomology. Occasional Papers in Entomology 28: 1–31.

Johnson NF (1992) Catalog of world Proctotrupoidea excluding Platygastridae. Memoirs of the American Entomological Institute 51: 1–825.

Kieffer JJ (1907) Beschreibung neuer im British Museum zu London aufbewahrter Proctotrypiden. Berliner Entomologische Zeitschrift 51: 279–302. https://doi.org/10.1002/mmnd.47919060306

Kieffer JJ (1908) Révision des Scelionidae (Hyménoptères). Annales de la Société Scientifique de Bruxelles 32: 111–250. https://www.biodiversitylibrary.org/item/157108#page/457/mode/1up

Kieffer JJ (1910) Hymenoptera. Fam. Scelionidae. Addenda et corrigenda. Genera Insectorum 80: 61–112. https://biostor.org/reference/132766

Kieffer JJ (1913) Proctotrypidae (3e partie). Species des Hyménoptères d'Europe et d'Algérie 11: 161–304. https://doi.org/10.3406/lsoc.1980.1236

Kieffer JJ (1926) Scelionidae. Das Tierreich Vol. 48. Walter de Gruyter & Co., Berlin, 885 pp.

Mani MS, Sharma SK (1982) Proctotrupoidea (Hymenoptera) from India. A review. Oriental Insects 16(2): 135–258. https://doi.org/10.1080/00305316.1982.10434314

Masner L (1965) The types of Proctotrupoidea (Hymenoptera) in the British Museum (Natural History) and in the Hope Department of Entomology, Oxford. Bulletin of the British Museum (Natural History) Entomology Supplement 1: 1–154. https://doi.org/10.5962/p.97756

Masner L (1976) Revisionary notes and keys to world genera of Scelionidae (Hymenoptera: Proctotrupoidea). Memoirs of the Entomological Society of Canada 108(S97): 1–87. https://doi.org/10.4039/entm10897fv

Mayr E (1942) Systematics and the origin of species from the viewpoint of a zoologist. Columbia University Press, New York, USA.

Mikó I, Vilhelmsen L, Johnson NF, Masner L, Penzes Z (2007) Skeletomusculature of Scelionidae (Hymenoptera: Platygastroidea): head and mesosoma. Zootaxa 1571(1): 1–78. https://doi.org/10.11646/zootaxa.1571.1.1

Muesebeck CFW, Walkley LM (1956) Type species of the genera and subgenera of parasitic wasps comprising the superfamily Proctotrupoidea (order Hymenoptera). Proceedings of the United States National Museum 105(3359): 319–419. https://doi.org/10.5479/si.00963801.3359.319

Rajmohana K (2006) Studies on Proctotrupoidea and Platygastroidea (Hymenoptera: Insecta) of Kerala. Memoirs of the Zoological Survey of India 21(1): 1–153. https://doi.org/10.11609/JoTT.ZPJ.1570.2506-13

Risbec J (1956) Proctotrupides Scelionini de Madagascar. Revue Française d`Entomologie 23: 244–264. [Hyménoptères]

Saraswat GG (1982) Some Indian Proctotrupoidea (Hymenoptera: Scelionidae). Records of the Zoological Survey of India 79(3–4): 343–358. https://doi.org/10.26515/rzsi/v79/i3-4/1981/161731

Szabó JB (1971) Eine neue Art der australischen Scelioniden, *Dichoteleas pappi* sp. n. (Hym., Proctotrupoidea). Folia Entomologica Hungarica 24: 313–318.

Wild AL (2004) Taxonomy and distribution of the Argentine ant, *Linepithema humile* (Hymenoptera: Formicidae). Annals of the Entomological Society of America 97(6): 1204–1215. https://doi.org/10.1603/0013-8746(2004)097[1204:TADOTA]2.0.CO;2

ZooKeys 1182: 207–221 (2023)
DOI: 10.3897/zookeys.1182.104240

Research Article

Formosania immaculata, a new species of hillstream loach (Teleostei, Cypriniformes, Gastromyzontidae) from the Ou-Jiang River, Southeast China

Wei Sun[1*], Jia-Jun Zhou[2,3*], Jin-Quan Yang[1]

1 Shanghai Universities Key Laboratory of Marine Animal Taxonomy and Evolution, Shanghai Ocean University, Shanghai 201306, China
2 Zhejiang Forest Resource Monitoring Center, Hangzhou 310020, China
3 Zhejiang Forestry Survey Planning and Design Company Limited, Hangzhou 310020, China
Corresponding author: Jin-Quan Yang (jqyang@shou.edu.cn)

Abstract

Formosania immaculata, a new species, is described from the Ou-Jiang basin in Zhejiang Province, Southeast China. It is distinguished from other species of the genus by having a combination of the following characteristics: body without obvious mottling; snout length longer than postorbital length; abdominal scaleless area extending to middle of pectoral-fin base; shorter rostral barbels, the outermost pair length 112.9%–140.0% of eye diameter; and shorter lower lip papillae, length 19.9%–24.4% of eye diameter. Its validity is also affirmed by its distinct *Cytb* gene sequence divergence from all congeners and its monophyly recovered in a *Cytb* gene-based phylogenetic analysis.

Key words: cytochrome *b*, freshwater fish, key, molecular phylogeny, morphology, taxonomy

Academic editor: Yahui Zhao
Received: 29 March 2023
Accepted: 18 September 2023
Published: 16 October 2023

ZooBank: https://zoobank.org/39A9DC67-106B-42E1-B5BA-9F06DDA42CB3

Citation: Sun W, Zhou J-J, Yang J-Q (2023) *Formosania immaculata*, a new species of hillstream loach (Teleostei, Cypriniformes, Gastromyzontidae) from the Ou-Jiang River, Southeast China. ZooKeys 1182: 207–221. https://doi.org/10.3897/zookeys.1182.104240

Introduction

The genus *Formosania* (Cypriniformes: Gastromyzontidae) was formerly known as *Crossostoma* Sauvage, 1878. Because of the junior homonym of *Crossostoma* Morris & Lycett, 1851 (Gastropoda), Novak et al. (2006) suggested the replacement name *Formosania* Oshima, 1919 for the genus, and the type species is *Formosania davidi* (Sauvage, 1878). *Formosania* can be distinguished from other genera of the family Gastromyzontidae by having the following characters: snout with a fringe of 13 small barbels; one or two pairs of maxillary barbels; gill opening extending the ventral surface of the head; and dark lateral stripes or blotches on the body (Chen and Tang 2000).

This genus is a group of small loaches endemic to southern China that have adapted to fast-flowing mountain streams and has been considered to be restricted to Fujian and Guangdong Provinces and the west of Taiwan Island (Chen and Tang 2000). However, in the last ten years, two new species have been described from the Ou-Jiang River and the Feiyun-Jiang River in Zhejiang Province, north of Fujian Province (Wang et al. 2006; Zhang and Wang 2011). According to

---

[*] These authors contributed equally to this paper.

the Catalog of Fishes (https://researcharchive.calacademy.org/research/ichthyology/catalog/fishcatmain.asp), there are nine valid species in the genus, which are *Formosania davidi* (Sauvage, 1878), *F. lacustre* (Steindachner, 1908), *F. stigmata* (Nichols, 1926), *F. fascicauda* (Nichols, 1926), *F. tinkhami* (Herre, 1934), *F. paucisquama* (Zheng, 1981), *F. chenyiyui* (Zheng, 1991), *F. fasciolata* (Wang et al., 2006), and *F. galericula* (Zhang, 2011) (Nichols 1926; Chen 1980; Zheng 1981, 1991; Chen and Tang 2000; Wang et al. 2006; Zhang and Wang 2011).

While examining the fish collected from one stream flowing into the Ou-Jiang River in Wuyi County, Zhejiang Province, we found some specimens of *Formosania* that could not be assigned to any described species. Further morphological and molecular analyses of these specimens support them as belonging to a new species described herein.

Material and methods

Specimen sampling, preservation and morphological analysis

Specimens of the new species were captured in a fish survey conducted in June 2021. Among the 18 collected specimens, five were preserved in 95% ethyl alcohol for DNA extraction, and the remaining 13 specimens were fixed in 10% formalin for two days and then preserved in 70% ethyl alcohol for morphological examination. Two paratype specimens were deposited at the Zhejiang Museum of Natural History, Hangzhou City, Zhejiang Province, and the holotype and the remaining paratypes and alcohol-preserved specimens were deposited at Shanghai Ocean University, Shanghai City, China. Another eight congeneric species of mainland China, which were caught from other fish surveys, were also included for molecular analysis in this study. The three species (*Formosania davidi*, *F. galericula* and *F. fasciolata*) were used for morphological comparison with the new species because they are similar in morphology and geographically adjacent. The suffixes -Jiang and -Xi indicate rivers and streams, respectively, in Mandarin Chinese.

All measurements were taken point-to-point with a digital caliper and recorded to the nearest 0.1 mm, following Yi et al. (2014). Measurements and counts were made on the left side of the specimens whenever possible. Morphometric measurements were expressed as percentages of standard length (SL), head length (HL), or eye diameter. The numbers of fin rays and lateral-line scales were counted under a research microscope.

DNA extraction, PCR amplification and sequencing

Genomic DNA was extracted from the alcohol-preserved pectoral-fin tip, and the mitochondrial cytochrome *b* (*Cytb*) gene was selected for amplification and sequencing. The *Cytb* gene was amplified by polymerase chain reaction in 25 μL reactions containing 9.5 μL of H_2O, 1 μL of each primer, 1 μL of template DNA, and 12.5 μL of Taq Master Mix (Sangon Co.,Ltd., Shanghai, China). Polymerase chain reaction (PCR) was performed at 95 °C predenaturing (3 min), then at 94 °C denaturing (30 s), 54 °C annealing (45 s), 72 °C extension (1 min) for 35 cycles, and 72 °C final extension (5 min). The primer pairs used for amplification and sequencing were L14724 (GACTTGAAAAACCACCGTTG) and H15915 (CTCCGATCTCCGGATTACAAGAC) (Xiao et al. 2001). Amplified

Table 1. The samples used in this study with their localities, voucher information and GenBank numbers.

Species	River	Sampling localities	Voucher number	GenBank Accession No.	Source
Formosania chenyiyui	Han-jiang	Changting County, Fujian	SHOU20150001	OQ605797	This study
	Han-jiang	Fujian	–	MK135435	Wan et al. 2019
Formosania davidi	Min-jiang	Qingyuan County, Zhejiang	SHOU202106251	OQ605818	This study
	Min-jiang	Qingyuan County, Zhejiang	SHOU202106252	OQ605819	This study
	Min-jiang	Qingyuan County, Zhejiang	SHOU202106253	OQ605820	This study
	Min-jiang	Qingyuan County, Zhejiang	SHOU202106262	OQ605821	This study
	Min-jiang	Qingyuan County, Zhejiang	SHOU202106263	OQ605822	This study
Formosania fascicauda	Jiulong-jiang	Nanjing County, Fujian	SHOU202201065	OQ605796	This study
	–	–	–	AY392469	Wang 2004
	–	–	–	AY392470	Wang 2004
Formosania fasciolata	Feiyun-jiang	Taishun County, Zhejiang	SHOU202107001	OQ605808	This study
	Feiyun-jiang	Taishun County, Zhejiang	SHOU202107002	OQ605809	This study
	Feiyun-jiang	Taishun County, Zhejiang	SHOU202107003	OQ605810	This study
	Feiyun-jiang	Taishun County, Zhejiang	SHOU202107004	OQ605811	This study
	Feiyun-jiang	Taishun County, Zhejiang	SHOU202107005	OQ605812	This study
Formosania galericula	Ou-jiang	Qingyuan County, Zhejiang	SHOU202106273	OQ605803	This study
	Ou-jiang	Qingyuan County, Zhejiang	SHOU202106275	OQ605804	This study
	Ou-jiang	Qingyuan County, Zhejiang	SHOU202106276	OQ605805	This study
	Ou-jiang	Qingyuan County, Zhejiang	SHOU202106277	OQ605806	This study
	Ou-jiang	Qingyuan County, Zhejiang	SHOU202106293	OQ605807	This study
New species	Ou-jiang	Wuyi County, Zhejiang	SHOU202106312	OQ605813	This study
	Ou-jiang	Wuyi County, Zhejiang	SHOU202106313	OQ605814	This study
	Ou-jiang	Wuyi County, Zhejiang	SHOU202106314	OQ605815	This study
	Ou-jiang	Wuyi County, Zhejiang	SHOU202106315	OQ605816	This study
	Ou-jiang	Wuyi County, Zhejiang	SHOU202106316	OQ605817	This study
Formosania lacustre	–	Taiwan	–	AY392455	Wang 2004
	–	Taiwan	–	AY392456	Wang 2004
	–	Taiwan	–	AY392457	Wang 2004
	–	Taiwan	–	AY392458	Wang 2004
	–	Taiwan	–	AY392459	Wang 2004
Formosania paucisquama	Lian-jiang	Puning County, Guangdong	SHOU202110011	OQ605798	This study
	Rong-jiang	Jiexi County, Guangdong	SHOU202110028	OQ605799	This study
Formosania stigmata	Min-jiang	Yanping County, Fujian	SHOU202201013	OQ605800	This study
	Min-jiang	Yanping County, Fujian	SHOU202201019	OQ605801	This study
	Min-jiang	Yanping County, Fujian	SHOU202201027	OQ605802	This study
Formosania tinkhami	Zhu-jiang	Longmen County, Guangdong	SHOU202110086	OQ605795	This study
Vanmanenia stenosoma	–	–	–	KX056122	GenBank
Vanmanenia pingchowensis	–	Wuyuan, Jiangxi	IHCAS0000066	DQ105219	Tang et al. 2006

products were subsequently purified and utilized for sequencing by a commercial sequencing company. The obtained sequences were spliced using Seqman from DNASTAR's Lasergene (Burland 2000) and then checked by utilizing BLAST analysis in the GenBank database. After confirmation, the targeted sequences were submitted to the GenBank database (Table 1), and provided accession numbers.

Phylogenetic reconstruction

We sequenced 28 *Cytb* gene sequences of *Formosania* and retrieved 8 *Cytb* gene sequences of *Formosania* from GenBank. *Vanmanenia stenosoma* and *V. pingchowensis* were selected as outgroups for molecular phylogeny analysis (Table 1). A multiple sequence alignment was prepared for all sequences using MEGA v.11.0 (Tamura et al. 2021). The genetic distances (p-distance with 1000 bootstraps) of the sequences among taxa were also calculated by using MEGA v.11.0. The best substitution models (TIM2+R3) for maximum likelihood (ML) and the best substitution model (GTR+G+I) for Bayesian inference (BI) were selected in ModelFinder (Kalyaanamoorthy et al. 2017) by Akaike's information criterion (AIC). The phylogenetic trees were inferred using Bayesian inference (BI) and maximum likelihood (ML) approaches. Bayesian analyses were conducted using MrBayes (Ronquist et al. 2012). Four simultaneous Monte Carlo Markov chains were run for 2 million generations, with sampling one tree per 100 replicates for each run, and the first quarter of the trees were discarded as burn-in; the remaining trees from two independent runs were used to construct a consensus tree. The ML analyses were conducted using IQ-TREE (Nguyen et al. 2015) with a total of 20 000 bootstrap replications performed.

Results

Taxonomic account

Family Gastromyzontidae Hora,1950
Genus *Formosania* Oshima,1919

***Formosania immaculata* Sun, Zhou & Yang, sp. nov.**
https://zoobank.org/E62FDC2E-148C-45B3-8BC1-2AD18C2B486A
Figs 1, 2A, 5

Type material. *Holotype*. SHOU2021060325, 87.9 mm total length (TL), 77.4 mm standard length (SL), adult collected by Jia-Jun Zhou and Wei Sun on June 28, 2021, in Wuyi County, Jinhua City, Zhejiang Province, China (28.7179°N, 119.4939°E; c. 882 m a.s.l.).

***Paratypes*.** Twelve specimens from the same locality as the holotype, SHOU2021060326-060337, 43.2–68.7 mm SL, were collected by Wei Sun and Jia-Jun Zhou on June 28, 2021.

Description. Morphometric measurements for the specimens examined are given in Table 2. See Fig. 1A–C for lateral, dorsal, and ventral views of the body and Fig. 2A for its mouthpart structures.

Head depressed in lateral view; head width always greater than depth; head width 17.4–19.7% of SL. Snout obtuse in dorsal view and longer than postorbital length; snout length 114.5%–125.0% of postorbital length. Mouth inferior and arched. Lips fleshy, with upper lip wide, without obvious convex particles; lower lip with a pair of papillae and a pair of lobulated papillae (Fig. 2A). Upper lip connected to lower lip around the corners of mouth by a papillated flap and one pair of maxillary barbels at the corners of mouth. Upper jaw covered by upper lip. Rostral fold appeared at end of snout, with 13 well-developed rostral barbels

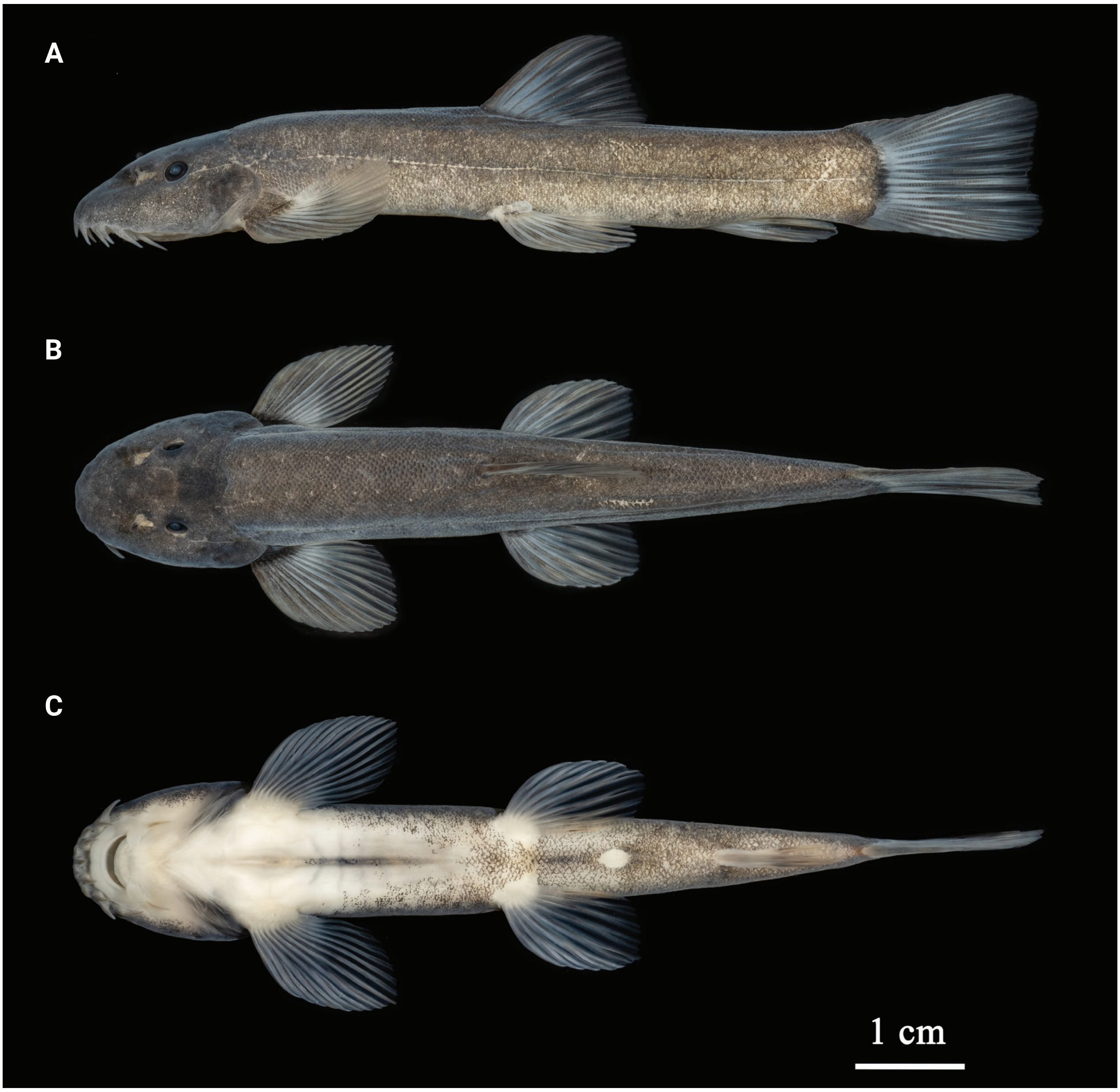

Figure 1. Lateral (**A**) dorsal (**B**) and ventral (**C**) views of *Formosania immaculata* sp. nov., holotype, adult, SHOU2021060325.

in an irregular row, covered with small spots. All rostral barbels connected with rostral fold. Outermost pair of rostral barbels longest and slightly longer than eye diameter, with a length of 112.9%–140.0% of eye diameter. Anterior and posterior nostrils adjacent with a well-developed flap on anterior ones. Eyes normal; diameter 13.7%–16.8% of HL. Gill openings reached ventral surface of head, with its upper extremity reaching the level of upper margin of orbit. Body elongated, the anterior part of body cylindrical and laterally compressed behind dorsal-fin base. The greatest depth of body at dorsal-fin origin and the least depth at caudal-fin base; body depth at dorsal-fin origin 16.1%–21.1% of SL. Body scaled but scales absent on head and before the middle of pectoral-fin base of abdomen. Scales minute, lateral line complete with 92–98 perforated scales. Caudal peduncle compressed laterally; length equal to peduncle depth.

Dorsal fin had three unbranched and eight branched rays; origin slightly in front of pelvic-fin insertion, situated slightly ahead to the midpoint between

Table 2. Morphometric measurements and meristic counts for *Formosania immaculata* sp. nov., *F. davidi*, *F. fasciolata* and *F. galericula*.

Characters	***F. immaculata* sp.nov. (*N*=13)**			***F. davidi* (*N*=15)**		***F. fasciolata* (*N*=8)**		***F. galericula* (*N*=11)**	
	Holotype	**Holotype+paratypes**							
		Range	**Mean+SD**	**Range**	**Mean+SD**	**Range**	**Mean+SD**	**Range**	**Mean+SD**
Standard length (mm)	77.4	43.2–77.4	61.7±7.80	58.5–75.4	67.8±6.08	50.4–73.4	58.9±7.85	50.5–67.3	59.0±4.63
% of standard length (SL)									
Body depth	17.9	16.1–21.1	17.6±1.29	17.3–19.2	18.4±0.59	16.2–17.4	16.8±0.41	13.5–18.4	15.5±1.37
Head length	22.9	22.5–25.9	23.6±1.05	21.1–24.5	23.1±0.99	22.7–27.0	24.2±1.48	22.7–26.3	24.5±1.00
Head depth	12.6	11.5–13.9	12.7±0.72	11.5–13.4	12.5±0.55	12.5–13.4	13.0±0.29	11.8–13.3	12.5±0.48
Head width	18.7	17.4–19.7	18.3±0.61	16.0–19.5	17.8±1.07	18.1–19.8	19.0±0.61	13.5–20.0	18.0±1.99
Length of caudal peduncle	12.2	12.2–14.3	13.2±0.65	10.5–13.9	11.8±1.01	10.2–12.8	11.1±0.82	10.4–13.0	11.8±0.83
Depth of caudal peduncle	12.4	12.4–14.3	12.9±0.59	11.3–13.2	12.2±0.58	12.2–13.8	13.1±0.56	10.2–12.7	11.3±0.65
Dorsal-fin length	20.7	19.6–22.4	20.9±0.90	20.2–23.1	21.4±0.96	20.2–23.2	21.8±1.03	19.6–22.4	21.2±0.84
Pectoral-fin length	23.5	22.0–25.0	23.7±0.92	22.3–24.2	23.3±0.53	22.8–27.4	24.5±1.47	22.4–26.7	25.0±1.31
Pelvic-fin length	20.3	19.0–21.2	19.9±0.65	19.2–21.6	20.2±0.80	19.8–22.2	21.0±0.90	19.1–21.8	20.8±0.87
Anal-fin length	19.1	16.8–19.1	18.1±0.74	17.7–20.5	19.3±1.04	18.1–22.1	19.6±1.18	17.1–19.8	18.4±0.99
Dorsal-fin base length	12.6	12.3–13.8	12.8±0.46	11.3–14.1	12.8±0.85	12.6–15.3	13.7±0.91	10.5–13.6	12.4±0.83
Pectoral-fin base length	7.5	6.6–8.4	7.3±0.58	6.2–8.0	6.8±0.57	6.3–8.1	7.4±0.61	6.4–8.5	7.3±0.58
Pelvic-fin base length	5.1	4.6–5.4	5.1±0.26	4.3–5.3	4.7±0.32	4.4–5.7	5.2±0.44	4.6–5.5	5.2±0.29
Anal-fin base length	7.4	6.4–8.1	7.1±0.51	6.3–8.0	7.3±0.59	5.9–8.6	7.2±1.03	6.0–7.7	6.9±0.49
Predorsal length	47.5	45.4–50.5	48.2±1.45	47.3–49.9	49.0±0.96	46.7–51.2	48.8±1.37	47.6–49.8	49.1±0.72
Prepectoral length	18.2	18.1–20.9	19.5±0.96	17.2–20.8	19.3±1.00	20.2–22.2	21.0±0.69	17.8–23.1	20.7±1.36
Prepelvic length	52.1	50.8–54.5	52.8±1.07	51.7–55.0	53.4±0.94	52.2–54.9	53.8±0.95	52.0–55.8	54.2±1.42
Preanal length	79.3	78.1–80.4	79.4±0.74	77.2–82.8	79.9±1.91	78.4–83.3	80.6±1.71	75.9–82.2	79.8±1.94
% of head length (HL)									
Snout length	47.8	44.6–48.2	46.0±0.93	40.7–44.8	43.2±1.35	42.2–43.8	43.2±0.49	39.9–45.9	43.1±1.96
Head depth	55.0	48.7–60.6	53.9±3.44	50.1–56.9	53.8±2.17	49.5–58.8	53.8±3.08	47.6–53.9	51.0±1.99
Eye diameter	13.9	13.7–16.8	15.1±1.07	13.1–15.8	14.3±0.90	14.8–17.7	16.3±0.92	15.1–17.3	15.9±0.81
Interorbital width	43.4	35.1–43.4	39.2±2.53	32.1–42.5	38.8±2.73	32.6–41.9	37.9±2.90	33.3–39.1	36.4±1.88
% of caudal peduncle length									
Depth of caudal peduncle	101.7	91.0–101.9	97.8±3.74	86.0–109.3	103.4±7.34	107.9–130.6	118.8±7.85	86.2–106.2	96.5±6.01
% of eye diameter									
the outermost pair of rostral barbels length	124.2	112.9–140.0	122.2±8.61	128.3–175.4	159.0±15.63	119.8–167.5	145.6±14.01	105.6–138.8	113.5±9.09
Maxillary barbels length	113.7	94.2–123.9	105.1±9.00	94.3–150.4	126.9±17.61	94.0–142.0	120.1±14.25	83.5–107.0	95.0±7.01
Lower lip papillae length	23.2	19.9–24.4	22.8±1.59	47.0–61.9	53.0±5.36	40.3–51.0	47.0±3.25	16.3–25.4	21.0±3.02
% of the postorbital length									
Snout length	124.3	114.5–125.0	119.6±3.62	97.7–102.7	100.6±1.46	99.6–103.5	101.6±1.43	96.4–102.4	99.3±1.78
Meristic counts									
Dorsal-fin rays	iii,8	iii,8		iii,8		iii,8		iii,8	
Pectoral-fin rays	i,14	i,13–14		i,14–15		i,14		i,13–14	
Pelvic-fin rays	i,8	i,8		i,8		i,8		i,8	
Anal-fin rays	ii,5	ii,5		ii,5		ii,5		ii,5	
Lateral-line scales	92	92–98		89–100		90–96		89–95	

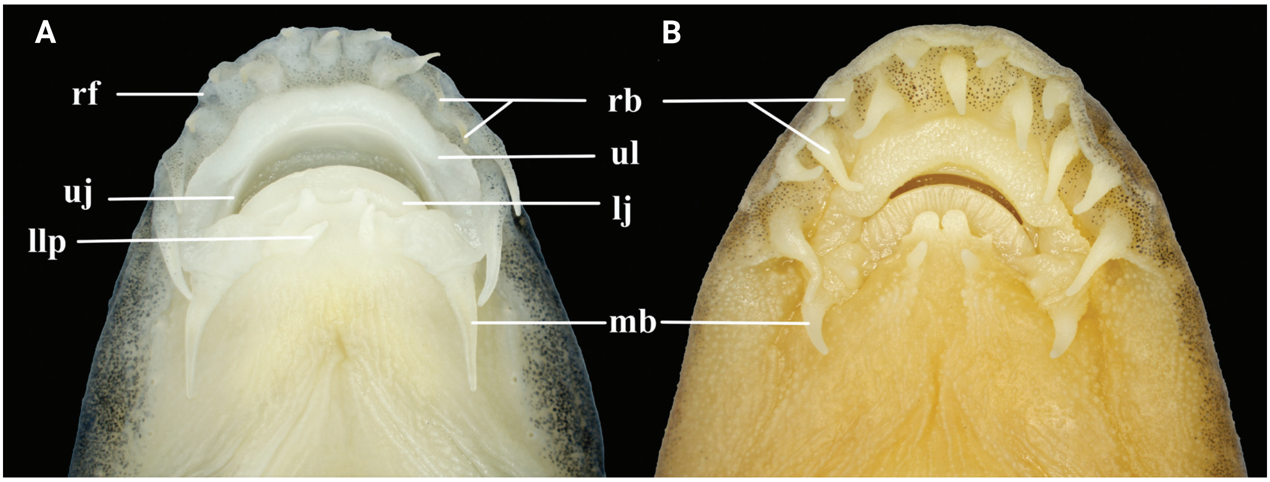

Figure 2. Ventral view of mouth of **A** *Formosania immaculata* sp. nov., SHOU2021060325, holotype **B** *Formosania stigmata*, SHOU2021060180. lj: lower jaw; llp: lower lip papilla; mb: maxillary barbel; rb: rostral barbel; rf: rostral fold; uj: upper jaw; ul: upper lip.

snout tip and caudal-fin base. Pectoral fin developed, with one unbranched and 13–14 branched rays. Pelvic fins long with one unbranched and eight branched rays, tips of depressed pelvic fins reaching anus when pelvic-fin rays extended backward. Anus in middle of pelvic-fin insertion and anal-fin insertion; anal fin with two unbranched and five branched rays, with the tip of anal fin closing or reaching to caudal-fin base. Caudal fin slightly forked; lower lobe slightly longer than upper lobe.

Coloration. In life, body slightly brown; fins and rostral barbels slightly red; with inconspicuous black blotches on back of head (Fig. 5). In 10% formalin-fixed specimens, dorsal and flank of head and body grayish-brown; ventral surface of head and abdomen white to yellowish with many black spots after pectoral fins; all fins hyaline and light gray, without obvious blotches (Fig. 1).

Diagnosis. *Formosania immaculata* sp. nov. resembles the *Formosania davidi* species group (*F. davidi*, *F. galericula* and *F. fasciolata*) in having 13 well-developed rostral barbels arranged in one irregular row (Fig. 2A), while other congeners arranged in 2 rows (Fig. 2B). It is distinguished from the three species in the *Formosania davidi* species group by having no obvious blotches or stripes (vs. having blotches or stripes) on the body and snout length longer than (vs. equal to) postorbital length (see Fig. 3 and Table 3). The new species differs from *F. davidi* in having shorter rostral barbels [outermost pair 112.9%–140.0% (average 122.2) vs. 128.3%–175.4% (average 159.0%) of eye diameter], shorter lower lip papillae [19.9%–24.4% (average 22.8) vs. 47.0%–61.9% (average 53.0%) of eye diameter] and narrower abdominal scaleless area (extending to middle of pectoral-fin base vs. extending slightly behind pectoral-fin axil) (see Table 3); from *F. fasciolata* in having shorter rostral barbels [outermost pair 112.9%–140.0% (average 122.2) vs. 119.8%–167.5% (average 145.6%)] of eye diameter, shorter lower lip papillae [19.9%–24.4% (average 22.8) vs. 40.3%–51.0% (average 47.0%) of eye diameter] and shorter depth of caudal peduncle [91.0%–101.9% (average 97.8%) vs. 107.9%–130.6% (average 118.8%) of caudal peduncle length]; and from *F. galericula* in having narrower abdominal scaleless area (extending to middle of pectoral-fin base vs. extending slightly behind pectoral-fin axil).

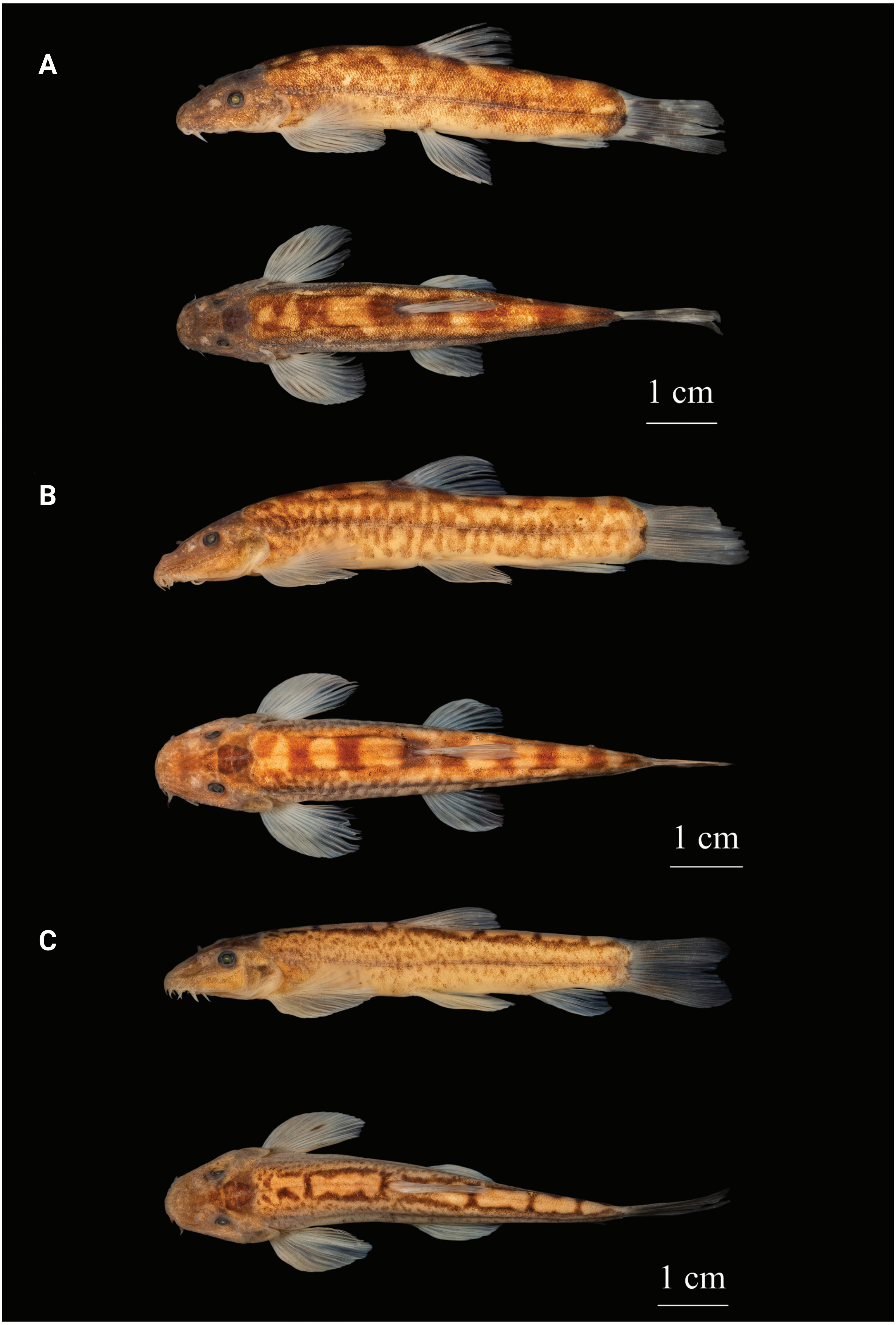

Figure 3. Lateral and dorsal views of **A** *Formosania davidi*, SHOU2021060176 **B** *Formosania fasciolata*, SHOU2021060200 **C** *Formosania galericula*, SHOU2021060169.

Table 3. Comparison of characters among *Formosania immaculata* sp. nov., *F. davidi*, *F. fasciolata* and *F. galericula*.

	***F. immaculata* sp. nov.**	***F. davidi***	***F. fasciolata***	***F. galericula***
Distribution	Ou-jiang	Min-jiang	Feiyun-jiang	Ou-jiang
Blotches on the back	Absent	7–9 black blotches	7–9 light-colored blotches	7–13 black blotches
Blotches on the flank	Absent	Irregular blotches	18–22 anomalistic stripes	Filled with irregular blotches
Pectoral-fin rays	i,13–14	i,14–15	i,14	i,13–14
Outermost pair of rostral barbels length (% of eye diameter)	112.9–140.0 (122.2±8.61)	128.3–175.4 (159.0±15.63)	119.8–167.5 (145.6±14.01)	105.6–138.8 (113.5±9.09)
Lower lip papillae length (% of eye diameter)	19.9–24.4 (22.8±1.59)	47.0–61.9 (53.0±5.36)	40.3–51.0 (47.0±3.25)	16.3–25.4 (21.0±3.02)
Depth of caudal peduncle (% of caudal peduncle length)	91.0–101.9 (97.8±3.74)	86.0–109.3 (103.4±7.34)	107.9–130.6 (118.8±7.85)	86.2–106.2 (96.5±6.01)
Abdominal scaleless area	Extending to the middle of the pectoral-fin base	Extending slightly behind the pectoral-fin axil	Extending to the middle of the pectoral-fin base	Extending slightly behind the pectoral-fin axil
Snout length (% of the postorbital length)	114.5–125.0 (119.6±3.62)	97.7–102.7 (100.6±1.46)	99.6–103.5 (101.6±1.43)	96.4–102.4 (99.3±1.78)

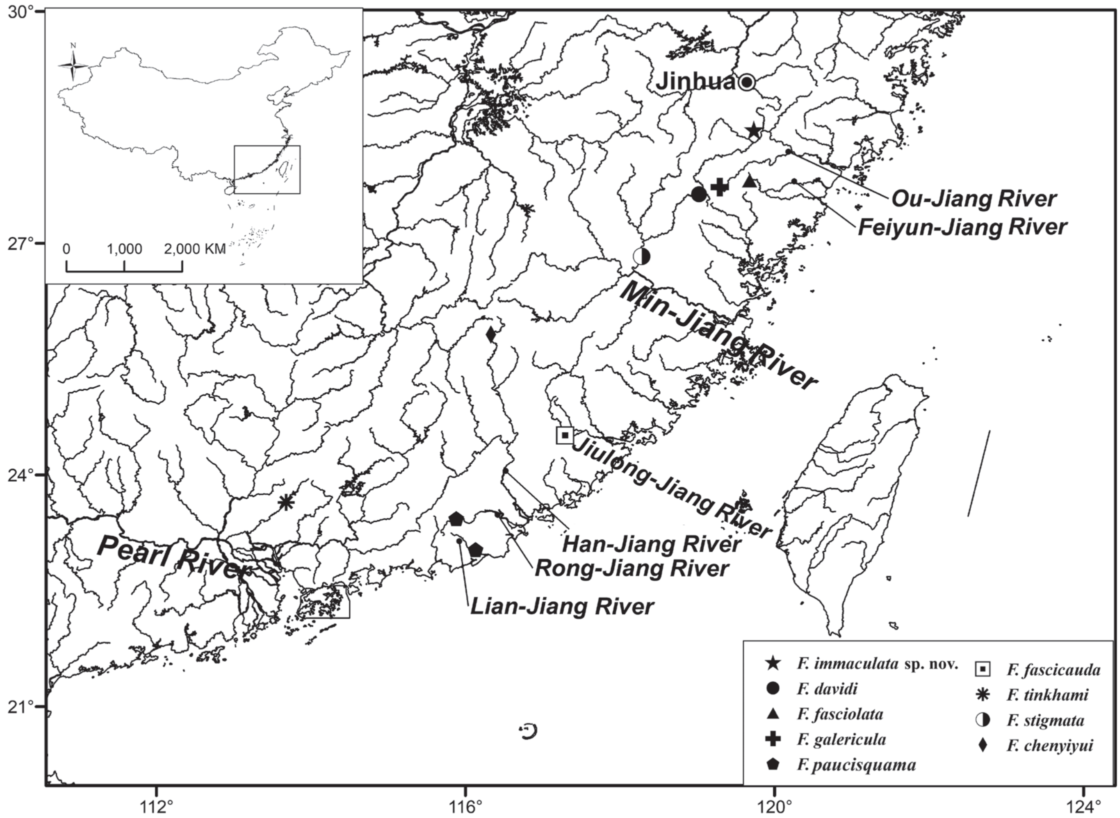

Figure 4. Map showing collection localities of nine species of *Formosania* involved in the present study. The names of rivers are italicized, and the city of Jinhua is highlighted.

Etymology. The specific epithet is the Latin form of the word *immaculate* here referring to the unique body of no blotches or stripes. We propose the Chinese common name Wú Bān Yīng Kǒu Qiū (无斑缨口鳅).

Distribution and habitat. The new species is known only from the upper reaches of the Xuanping-Xi, a stream tributary to the Ou-Jiang River, in Wuyi County, Zhejiang Province, China (Fig. 4). It inhabits fast-flowing streams with gravelly and pebbly substrates (Fig. 5).

Figure 5. Habitat and live specimen of *Formosania immaculata* sp. nov.

Molecular analysis

Thirty-six *Cytb* gene sequences of *Formosania* were used for phylogenetic analysis. After alignment and trimming, 1141 bp (base pairs) of the *Cytb* gene was obtained. There were 854 conserved sites, 287 variable sites, 15 singleton sites, and 272 parsimony-informative sites. The mean frequency of four nucleotides was A=25.8%, T=28.2%, C= 30.0%, and G=16.0%; the base composition was A-T rich (54.0%).

The two phylogenetic analysis methods (BI and ML) showed an identical topology (Fig. 6). The monophyly of the genus was well supported (94% bootstrap value and 100% posterior probability). Both phylogenetic trees revealed that *Formosania chenyiyui* is sister to the remaining species of *Formosania*. The remaining nine species formed a monophyletic clade with strong support and then separated into three groups. Samples of *F. immaculata* sp. nov. were monophyletic and belonged to a group of species with robust support (100% bootstrap value and 100% posterior probability). This group is defined here as the *F. davidi* species group, and our molecular data suggest that it includes *F. davidi*, *F. galericula* and *F. fasciolata*.

Formosania immaculata sp. nov. had minimal genetic distance with the three similar species, 4.5% with *F.* davidi, 4.5% with *F. galericula*, and 4.7% with *F. fasciolata*, which was greater than the genetic distance among the three similar species (2.5%–3.0%) (Table 4). The mean genetic distance of the new species from all sampled species was 8.6%, far greater than the minimum distance (2.3%), detected here between *F. stigmata* and *F. paucisquama*. *Formosania chenyiyui* has the greatest genetic divergence from all other species (16.2%–19.1%).

Discussion

Formosania species usually inhabit hill streams with relatively fast-flowing currents. Except for *F. fascicauda* and *F. stigmata* and even *F. lacustre*, the rest of the species are limited in distribution, only being found in a single river or a few adjacent rivers (Chen and Tang 2000; Tang and Chen 2000; Wang et al. 2006; Teng 2010; Zhang and Wang 2011). *Formosania immaculata* sp. nov. is known only from the upper reaches of the Xuanping-Xi, a northern stream tributary of the Ou-Jiang

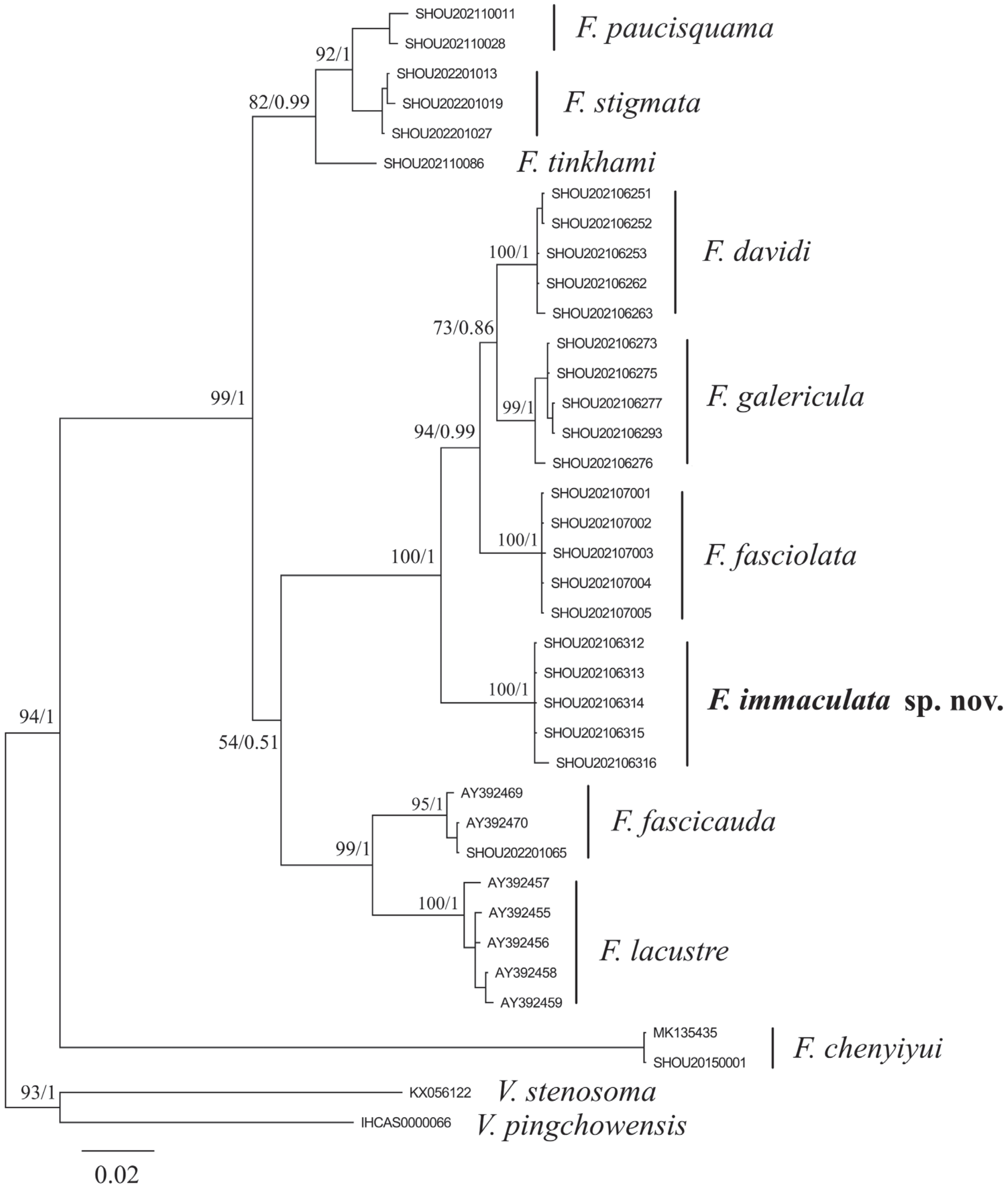

Figure 6. Bayesian inference tree based on mitochondrial *Cytb* gene sequences of 10 *Formosania* species. Maximum likelihood and Bayesian inference analyses resulted in congruent trees. Bootstrap and posterior probability values are shown beside nodes on the tree if 50% or higher.

River, in Wuyi County, Zhejiang Province, Southeast China, which is currently the northernmost species of *Formosania*. Another species, *F. galericula*, also occurs in the same river system, but it is only found in some southern tributaries of the Ou-Jiang River. *Formosania fasciolata* is known from the Feiyun-Jiang basin, adjacent to southern the Ou-Jiang River. The last similar species, *F. davidi*, is only distributed in the Min-Jiang River system, a close neighbor of the Feiyun-Jiang River. The new species can be assigned to the *F. davidi* group by sharing 13 rostral barbels in one irregular row, in addition to its distribution in the same or adjacent water systems.

Table 4. Genetic distances of *Cytb* computed by MEGA among 10 species of *Formosania*.

	1	2	3	4	5	6	7	8	9
F. immaculata sp. nov.									
F. davidi	0.045								
F. galericula	0.045	0.025							
F. fasciolata	0.047	0.030	0.029						
F. stigmata	0.091	0.089	0.090	0.091					
F. paucisquama	0.089	0.095	0.092	0.093	0.023				
F. fascicauda	0.093	0.091	0.091	0.094	0.070	0.071			
F. lacustre	0.094	0.092	0.090	0.095	0.074	0.077	0.045		
F. tinkhami	0.085	0.088	0.091	0.092	0.031	0.036	0.068	0.074	
F. chenyiyui	0.189	0.191	0.184	0.186	0.165	0.172	0.184	0.173	0.162

In addition, the new species can be easily distinguished from the *Formosania davidi* species group and the rest of the congeneric species by lacking blotches or stripes on the back or flank. In terms of morphometric characteristics, *F. galericula* is most similar to the new species. However, *F. immaculata* sp. nov. can be distinguished from *F. galericula* in possessing a longer snout (114.5–125.0 vs. 96.4%–102.4% of postorbital length) and narrower abdominal scaleless area (extending to middle of pectoral-fin base vs. extending slightly behind pectoral-fin axil) (Table 3).

The validity of *Formosania immaculata* sp. nov. is confirmed by its significant genetic divergence from congeners (Table 4). It has significant genetic distance from other congeners (4.5%–18.9%), far greater than the minimum calculated here between *F. stigmata* and *F. paucisquama* (2.3%), and greater than the genetic distance among the three species in the same group (2.5%–3.0%).

The validity of *Formosania immaculata* sp. nov. is also confirmed by its monophyly in the phylogenetic analysis based on the *Cytb* gene (Fig. 6). There are no reports on the complete phylogenetic and phylogeographic studies of this genus at present. Only Wang et al. (2007) and Teng (2010) have conducted a phylogeographic study on three or four species, which did not include any species in *F. davidi* group. Our results suggest that it should be reasonable for the new species to be designated to the *F. davidi* group for the aforementioned morphological and geographical reasons, which indicates that they originated from a recent common ancestor.

Diagnostic key to species of *Formosania*

1 Rostral barbels number unstable, ranging from 12 to 15, their length less than half of the eye diameter; two lengthwise-ribbon-like stripes on back, one in front of the dorsal-fin axil and one behind.. ....***F. chenyiyui* (Ting-Jiang River)**

– Rostral barbels number stable, always 13, their length great than half of the eye diameter; saddle-like or irregular stripes on back **2**

2 Rostral barbels arranged in two rows, the front row on top of the rostral fold, the back row in the center of the rostral groove; two pairs of maxillary barbels, the inside pair are papillae...**3**

– Rostral barbels arranged in an irregular row, the base of which connected with the rostral fold; one pair of maxillary barbels.....................................**7**

3 Cloud-like stripes on side.. **4**

– Wavy-longitudinal-like stripes or blotches on side....................................... **6**

4 Caudal peduncle stout, its depth greater than its length............................. ....***F. lacustre* (Mulan-Xi and Jin-Jiang Rivers, Taiwan Island)**

– Caudal peduncle slender, its depth less than or equal to its length........... **5**

5 86–105 perforated scales; narrower abdominal scaleless area extending slightly behind the pectoral-fin axil.. .... ***F. stigmata* (From Min-jiang to Han-jiang Rivers)**

– 76–83 perforated scales; narrower abdominal scaleless area extending to the middle of pectoral-fin base.. ....***F. paucisquama* (Lian-Jiang, Rong-Jiang and Han-Jiang Rivers)**

6 Several black-and-white and wavy-longitudinal-like stripes on side; 6–8 saddle-like stripes on back ....***F. fascicauda* (Jiulong-Jiang River)**

– Two or three rows of blotches on side; 5–7 irregular stripes on back ....***F. tinkhami* (Pearl River)**

7 No obvious blotches or stripes on body; snout length 1.2 times greater than the postorbital length............***F. immaculata* sp. nov. (Ou-Jiang River)**

– With obvious blotches or stripes on body; snout length equal to the postorbital length **8**

8 Caudal peduncle stout, its depth greater than its length; 18–22 anomalistic stripes on side; narrower abdominal scaleless area extending to the middle of pectoral-fin base .... ***F. fasciolata* (Feiyun-Jiang and Ou-Jiang Rivers)**

– Caudal peduncle slender, its depth less than or equal to its length; with irregular blotches on side; narrower abdominal scaleless area extending slightly behind the pectoral-fin axil... **9**

9 Length of longest rostral barbel about 1.5 times greater than the eye diameter; 7–9 saddle-like stripes on back ....***F. davidi* (Min-Jiang River)**

– Length of longest rostral barbel equal to the eye diameter; 7–13 irregular stripes on back ....***F. galericula* (Ou-Jiang River)**

Comparative materials

Formosania davidi: SHOU2021060096-106, SHOU2021060176-179, 15, 58.5–75.4 mm SL; Qingyuan County, Min-Jiang River System, Zhejiang Province, China.

Formosania fascicauda: SHOU202201083-091, 9, 53.4–69.1 mm SL; Nanjing County, Jiulong-Jiang River System, Fujian Province, China.

Formosania fasciolata: SHOU2021060193-200, 8, 50.8–73.4 mm SL; Liguang stream in Wuyanling National Nature Reserve (type locality), Taishun County, Feiyun-Jiang River System, Zhejiang Province, China.

Formosania galericula: SHOU2021060165-175, 11, 50.5–67.4 mm SL; unnamed stream in Hehu village (type locality), Qingyuan County, Ou-Jiang River System, Zhejiang Province, China.

Formosania paucisquama: SHOU202110011-013, 4, 50.3–64.4 mm SL; unnamed stream in Da'nan Mountain (type locality), Puning County, Lian-Jiang River System, Guangdong Province, China.

Formosania stigmata: SHOU2021060180-183, 4, 56.0–84.8 mm SL; Qingyuan County, Min-Jiang River System, Zhejiang Province, China.

Formosania tinkhami: SHOU202110086-090, 5, 44.6–58.1 mm SL; unnamed stream in Nankun Mountain (type locality), Longmen County, Pearl River System, Guangdong Province, China.

Acknowledgments

We thank Yi-Rong Zhu from Wuyi Niutoushan Herbarium of Zhejiang for help with specimen collection.

Additional information

Conflict of interest

The authors have declared that no competing interests exist.

Ethical statement

No ethical statement was reported.

Funding

This research was funded by a grant from the National Natural Science Foundation of China (No. 31872207).

Author contributions

Sun W contributed to the experimental work, data analysis and drafting of the manuscript. Zhou JJ performed specimen collection and photograph. Yang JQ was responsible for review and editing.

Author ORCIDs

Jia-Jun Zhou https://orcid.org/0000-0003-1038-1540
Jin-Quan Yang https://orcid.org/0000-0003-0387-1824

Data availability

All of the data that support the findings of this study are available in the main text.

References

Burland TG (2000) DNASTAR's Lasergene sequence analysis software. Methods in Molecular Biology (Clifton, N.J.) 132: 71–91. https://doi.org/10.1385/1-59259-192-2:71

Chen YY (1980) Systematic studies of the fishes of the family Homalopteridae of China II. Classification of the fishes of the subfamily Gastromyzononae. Acta Hydrobiologica Sinica 7(1): 95–120. [In Chinese]

Chen YY, Tang WQ (2000) Gastromyzonidae. In: Yue PQ (Ed.) Fauna Sinica (Osteichtyes: Cypriniformes III). Science Press, Beijing, 465–476.

Kalyaanamoorthy S, Minh BQ, Wong TK, Haeseler A, Jermiin LS (2017) ModelFinder: Fast model selection for accurate phylogenetic estimates. Nature Methods 14(6): 587–589. https://doi.org/10.1038/nmeth.4285

Nguyen L, Schmidt H, von Haeseler A, Minh B (2015) IQ-TREE: A fast and effective stochastic algorithm for estimating maximum-likelihood phylogenies. Molecular Biology and Evolution 32(1): 268–274. https://doi.org/10.1093/molbev/msu300

Nichols JT (1926) Some Chinese fresh-water fishes. XVIII. New species in recent and earlier Fukien collections. American Museum Novitates 224: 1–7.

Novak J, Hanel L, Rican O (2006) *Formosania*: A replacement name for *Crossostoma* sauvage, 1878 (Teleostei), a junior homonym of *Crossostoma* Morris & Lycett, 1851 (Gastropoda). Cybium 30(1): 92–92.

Ronquist F, Teslenko M, Van DMP, Ayres DL, Darling A, Höhna S, Larget B, Liu L, Suchard MA, Huelsenbeck JP (2012) MrBayes 3.2: efficient Bayesian phylogenetic inference and model choice across a large model space. Systematic Biology 61(3): 539–542. https://doi.org/10.1093/sysbio/sys029

Tamura K, Stecher G, Kumar S (2021) MEGA 11: Molecular Evolutionary Genetics Analysis Version 11. Molecular Biology and Evolution 38(7): 3022–3027. https://doi.org/10.1093/molbev/msab120

Tang WQ, Chen YY (2000) Study on taxonomy of Homalopteridae. Journal of Shanghai Fisheries University 9(1): 1–9. [In Chinese]

Tang QY, Liu HZ, Mayden R, Xiong BX (2006) Comparison of evolutionary rates in the mitochondrial DNA cytochrome *b* gene and control region and their implications for phylogeny of the Cobitoidea (Teleostei: Cypriniformes). Molecular Phylogenetics and Evolution 39(2): 347–357. https://doi.org/10.1016/j.ympev.2005.08.007

Teng HY (2010) Phylogeography study on the Genus *Formosania*. PhD Thesis, Department of Life Science, National Tsing Hua University, Hsinchu, Taiwan.

Wan H, Song XJ, Tang WQ (2019) Complete mitochondrial genome of *Formosania chenyiyui* (Osteichthyes: Gastromyzontidae). Mitochondrial DNA. Part B, Resources 4(1): 935–936. https://doi.org/10.1080/23802359.2019.1579059

Wang TY (2004) Taxonomy, evolution and phylogeography of Balitoridae in East Asia. PhD Thesis, Department of Life Science, National Tsing Hua University, Hsinchu, Taiwan.

Wang HG, Fan ZY, Chen Y (2006) A new species of the genus *Crossostoma* from Zhejiang, China (Cypriniformes, Homalopteridae, Gastromyzoninae). Acta Zootaxonomica Sinica 31(4): 902–905. [In Chinese]

Wang TY, Tzeng CS, Teng HY, Chang T (2007) Phylogeography and identification of a 187-bp-long duplication within the mitochondrial control region of *Formosania lacustre* (Teleostei: Balitoridae). Zoological Studies (Taipei, Taiwan) 46(5): 569–582. http://zoolstud.sinica.edu.tw/Journals/46.5/569.pdf

Xiao W, Zhang Y, Liu H (2001) Molecular systematics of Xenocyprinae (Teleostei: Cyprinidae): taxonomy, biogeography, and coevolution of a special group restricted in east Asia. Molecular Phylogenetics and Evolution 18(2): 163–173. https://doi.org/10.1006/mpev.2000.0879

Yi WJ, Zhang E, Shen JZ (2014) *Vanmanenia maculata*, a new species of hillstream loach from the Chang-Jiang Basin, South China (Teleostei: Gastromyzontidae). Zootaxa 3802(1): 85–97. https://doi.org/10.11646/zootaxa.3802.1.7

Zhang XF, Wang HG (2011) A new species of the genus *Crossostoma* from Zhejiang Province, China (Cypriniformes:Homalopteridae). Journal of Shanghai Ocean University 20(1): 85–88. [In Chinese]

Zheng CY (1981) The homalopterid fishes from Guangdong Province, China (continuation). Journal of Jinan University 3(1): 55–63. [In Chinese]

Zheng CY (1991) A taxonomic study on the genus *Crossostoma* (Pisces: Homalopteridae) with description of a new species. Journal of Jinan University 12(1): 77–82. [In Chinese]

ZooKeys 1182: 223–235 (2023)
DOI: 10.3897/zookeys.1182.109744

Research Article

Remarks on the genus *Phymatodiscus* Berlese, 1917, with the description of Phymatodiscidae fam. nov. and *Bardizon eotvosi* gen. nov., sp. nov. from Indonesia (Acari, Mesostigmata)

Jenő Kontschán[1,2], Sergey G. Ermilov[3]

1 HUN-REN Centre for Agricultural Researches, Plant Protection Institute, H-1025, Budapest, PO Box. 102, Hungary
2 Department of Plant Sciences, Albert Kázmér Faculty of Mosonmagyaróvár, Széchenyi István University, Vár square 2., H-9200 Mosonmagyaróvár, Hungary
3 Institute of Environmental and Agricultural Biology (X-BIO), Tyumen State University, Lenina str. 25, 625000 Tyumen, Russia
Corresponding author: Jenő Kontschán (kontschan.jeno@atk.hu)

Abstract

Phymatodiscidae **fam. nov.** is diagnosed, with *Phymatodiscus* as the type genus. A new genus, *Bardizon* **gen. nov.**, with *Bardizon eotvosi* **sp. nov.** (from Indonesia) as the type species, is erected to accommodate the *Phymatodiscus* species with an eye-like dorsal depression. Six *Phymatodiscus* species are reclassified as *Bardizon*: *B. aokii* (Hiramatsu, 1985), **comb. nov.**, *B. haradai* (Hiramatsu, 1985), **comb. nov.**, *B. oculatus* (Hirschmann, 1977), **comb. nov.**, *B. kuni* (Kontschán & Starý, 2011), **comb. nov.**, *B. insolitus* (Kontschán & Ripka, 2016), **comb. nov.**, and *B. malayicus* (Kontschán & Starý, 2012), **comb. nov.** The new species differs from the previously described congeners in the sculptural pattern, the shapes of the dorsal and ventral setae, and the sculptural pattern of the sternal shield of the male and the genital shield of the female. A list of all known phymatodiscid species is presented. *Phymatodiscus titanicus* (Berlese, 1905) is moved to the genus *Bostocktrachys*: *B. titanicus* (Berlese, 1905), **comb. nov.** (family Trachyuropodidae).

Key words: Soil mites, South-East Asia, taxonomy

Academic editor: Farid Faraji
Received: 19 July 2023
Accepted: 3 September 2023
Published: 17 October 2023

ZooBank: https://zoobank.org/03903FB4-E814-40C9-BE6E-47A34FFB0277

Citation: Kontschán J, Ermilov SG (2023) Remarks on the genus *Phymatodiscus* Berlese, 1917, with the description of Phymatodiscidae fam. nov. and *Bardizon eotvosi* gen. nov., sp. nov. from Indonesia (Acari, Mesostigmata). ZooKeys 1182: 223–235. https://doi.org/10.3897/zookeys.1182.109744

Introduction

The genus *Phymatodiscus* was erected by Berlese (1917) for *Discopoma miranda* Berlese, 1905. Decades later, Hirschmann (1977) revised this genus and transferred two previously described species, *Discopoma conifera* Canestrini, 1897 and *Trachyuropoda titanica* Berlese, 1905, to this taxon. In parallel to the new combinations, Hirschmann (1977) also described four new species from New Guinea. A couple of years later Hiramatsu (1979) described a new species from Japan and two new species from the island of Borneo, Indonesia (Hiramatsu 1985). After a long hiatus, Kontschán and Starý (2011, 2012) described a new species from Vietnam and another new species from Malaysia, and Kontschán and Ripka (2016) discovered and described a new species from Singapore.

In recent years numerous contributions have added more than 30 new species to the Uropodina mite fauna of Southeast Asia (e.g. Kontschán and Starý 2011, 2012; Kontschán and Kiss 2015; Kontschán and Ripka 2016; Kontschán 2018, 2021; Kontschán and Ermilov 2023a, 2023b, 2023c), but knowledge of this group is still far from complete. The present paper contributes towards our understanding of a poorly investigated group of Uropodina mites from Southeast Asia and is based on the collections of the Natural History Museum in Geneva, Switzerland.

Materials and methods

The specimens of the new species were cleared in lactic acid for a week and afterwards, investigated on half-covered deep slides with a Leica 1000 microscope. Drawings were made with the aid of a drawing tube on a Leica 1000 microscope. Photographs were taken with Keyence 5000 digital microscope. All specimens are stored in 75% ethanol and deposited in the Natural History Museum in Geneva. All measurements and the scale bars of the figures are given in micrometres (µm).

Abbreviations

Setae and pores: ***h*** = hypostomal setae, ***st*** = sternal setae, ***ad*** = adanal setae, ***ps*** = post-anal seta, ***p*** = pores, ***lf*** = lyriform fissures.

Systematics

Phymatodiscidae fam. nov.
https://zoobank.org/28862C32-19BC-4A8F-A157-10F1070E16AA

Phymatodiscidae Hirschmann, 1979: 69 (*nomen nudum*).
Phymatodiscidae—Halliday 2016: 355.

Type genus. *Phymatodiscus* Berlese, 1917.

Diagnosis. Idiosoma oval, dorsal shield fused with marginal shield in anterior area. Central area of dorsal shield elevated from neighbouring regions and subdivided with a transversal furrow in longer apical and shorter caudal parts. Transversal furrow forms a pair of eye-like depressions in some species. Genital shield of female scutiform; genital shield of male rounded and situated between coxae IV. Prestigmatid part of peritreme hooked. Corniculi horn-like; internal malae longer than corniculi and densely pilose. Gnathosomal setae in one longitudinal row; *h1* near anterior margin of gnathosoma; setae *h2*, *h3*, and *h4* far from setae *h1* and near each other. Setae *h1* smooth and needle-like; *h2* short and robust; *h3* long and smooth or serrate; *h4* divided into two or three short, serrate branches. Chelicerae with 1–3 teeth on both digits; internal sclerotized pore associated with levantor tendon present. Setae *v1* on palp trochanter long, pilose.

Distribution. All known phymatodiscid species occur in New Guinea, Indonesia, Malaysia, Vietnam, and Singapore.

Remarks. Hirschmann (1979) first introduced a family name, Phymatodiscidae, but it was simply listed and without formal description, diagnosis, or designation of a type genus. Following Halliday's (2016) suggestion about

Hirschmann's family name, a *nomen nudum*, we maintain the original name but formally establish it here as a new family. Phymatodiscidae currently includes two genera.

Genus Phymatodiscus Berlese, 1917

Discopoma (*Phymatodiscus*) Berlese, 1917: 12.

Type species. *Discopoma miranda* Berlese, 1905: 159, by original designation.

Diagnosis. Phymatodiscid species lacking a pair of eye-like dorsal depressions. Margins of idiosoma with or without many prolongations.

List of the known species

Remarks. One species, *Phymatodiscus titanicus* (Berlese, 1905), is transferred here from the family Phymatodiscidae to the family Trachyuropodidae Berlese, 1917. According to the dorsal characteristics (only these were illustrated by Berlese 1905: fig. 13), our opinion is that this species belongs to the genus *Bostocktrachys*, as *B. titanicus* (Berlese, 1905) comb. nov., given that Berlese's species has strongly sclerotized idiosoma and a deep transversal furrow on the dorsal shield (Kontschán and Ermilov 2023c).

Phymatodiscus coniferus (Canestrini, 1897)

Discopoma conifera Canestrini, 1897: 461, 470.
Phymatodiscus coniferus—Hirschmann 1977: 60–61.

Occurrence and biology. This species has been found in New Guinea, but its habitat is unknown (Canestrini 1897).

Phymatodiscus ignesemovens Hirschmann, 1977

Phymatodiscus ignesemovens Hirschmann, 1977: 64.

Occurrence and biology. This species has been found in New Guinea, but its habitat is unknown (Hirschmann 1977).

Phymatodiscus iriomotensis Hiramatsu, 1979

Phymatodiscus iriomotensis Hiramatsu, 1979: 108–109.

Occurrence and biology. This species was described from leaf litter in Japan (Hiramatsu 1985).

Phymatodiscus mirabilis Hirschmann, 1977

Phymatodiscus mirabilis Hirschmann, 1977: 64–65.

Occurrence and biology. This species has been found in New Guinea, but its habitat is unknown (Hirschmann 1977).

Phymatodiscus mirandus **(Berlese, 1905)**

Discopoma miranda Berlese, 1905: 159.
Discopoma (*Phymatodiscus*) *miranda*—Berlese 1917: 12.
Trachyuropoda miranda—Hirschmann and Zirngiebl-Nicol 1967: 21.
Phymatodiscus mirandus—Hirschmann 1977: 60–61.

Occurrence and biology. This species has been found in Java, Indonesia, but its habitat is unknown (Berlese 1905).

Phymatodiscus polyglottis **Hirschmann, 1977**

Phymatodiscus polyglottis Hirschmann, 1977: 63–64.

Occurrence and biology. This species has been found in New Guinea, but its habitat is unknown (Hirschmann 1977).

Bardizon **gen. nov.**

https://zoobank.org/D896ACBC-5F95-4111-8362-F9A395FEC90D

Diagnosis. Phymatodiscid species with one pair of eye-like dorsal depressions.

Type species. *Bardizon eotvosi* sp. nov.

Etymology. The name was suggested by the older son of the first author and derives from small chocolates, which are similar in shape to the idiosoma of these mites.

Gender. Male.

List of the known species

Bardizon aokii **(Hiramatsu, 1985) comb. nov.**

Phymatodiscus aokii Hiramatsu, 1985: 270–273.

Occurrence and biology. This species has been described from soil from Borneo (Indonesia) (Hiramatsu 1985).

Bardizon haradai **(Hiramatsu, 1985) comb. nov.**

Phymatodiscus haradai Hiramatsu, 1985: 273–275.

Occurrence and biology. This species has been described from soil from Borneo (Indonesia) (Hiramatsu 1985).

***Bardizon oculatus* (Hirschmann, 1977) comb. nov.**

Phymatodiscus oculatus Hirschmann, 1977: 62–63.

Occurrence and biology. This species has been found in New Guinea, where its habitat is unknown (Hirschmann 1977).

***Bardizon kuni* (Kontschán & Starý, 2011) comb. nov.**

Phymatodiscus kuni Kontschán & Starý, 2011: 15–16.

Occurrence and biology. This species was collected in Vietnam, in a tropical rain forest (Kontschán and Starý 2011).

***Bardizon insolitus* (Kontschán & Ripka, 2016) comb. nov.**

Phymatodiscus insolitus Kontschán & Ripka, 2016: 292–296.

Occurrence and biology. This species was found in Singapore, where it was collected from soil (Kontschán and Ripka 2016).

***Bardizon malayicus* (Kontschán & Starý, 2012) comb. nov.**

Phymatodiscus malayicus Kontschán & Starý, 2012: 184–188.

Occurrence and biology. This species was collected in Malaysia from leaf litter (Kontschán and Starý 2012).

***Bardizon eotvosi* sp. nov.**

https://zoobank.org/7146CC65-14C0-4BCC-91E0-3C6BDC5B3268
Figs 1–4

Materials examined. *Holotype*. Female. INDONESIA, East Kalimantan Prov., Berau Ditrict, 1 km off the Tanjungredeb–Tnajungselor road, ca 45 km N of Tanjungredebm 2°29.5'N, 117°28.766'E, 190 m elev., primary forest, 29 September 2008, P. Schwendinger leg. ***Paratypes*.** One female and eight males, with the same collection data as the holotype.

Diagnosis. Dorsal shield bearing smooth setae except two pairs of apically pilose setae near caudal margin. Surface of dorsal shield smooth, but web-like sculptural pattern situated anterior and posterior to eye-like dorsal depressions. Male sternal shield anterior to genital opening, and female genital shield covered by web-like sculptural pattern.

Description. Female (n = 2). Length of idiosoma 1570–1610, width at level of coxae IV 1130–1145, colour reddish-brown. Shape of idiosoma pentagonal, its caudal margin curved.

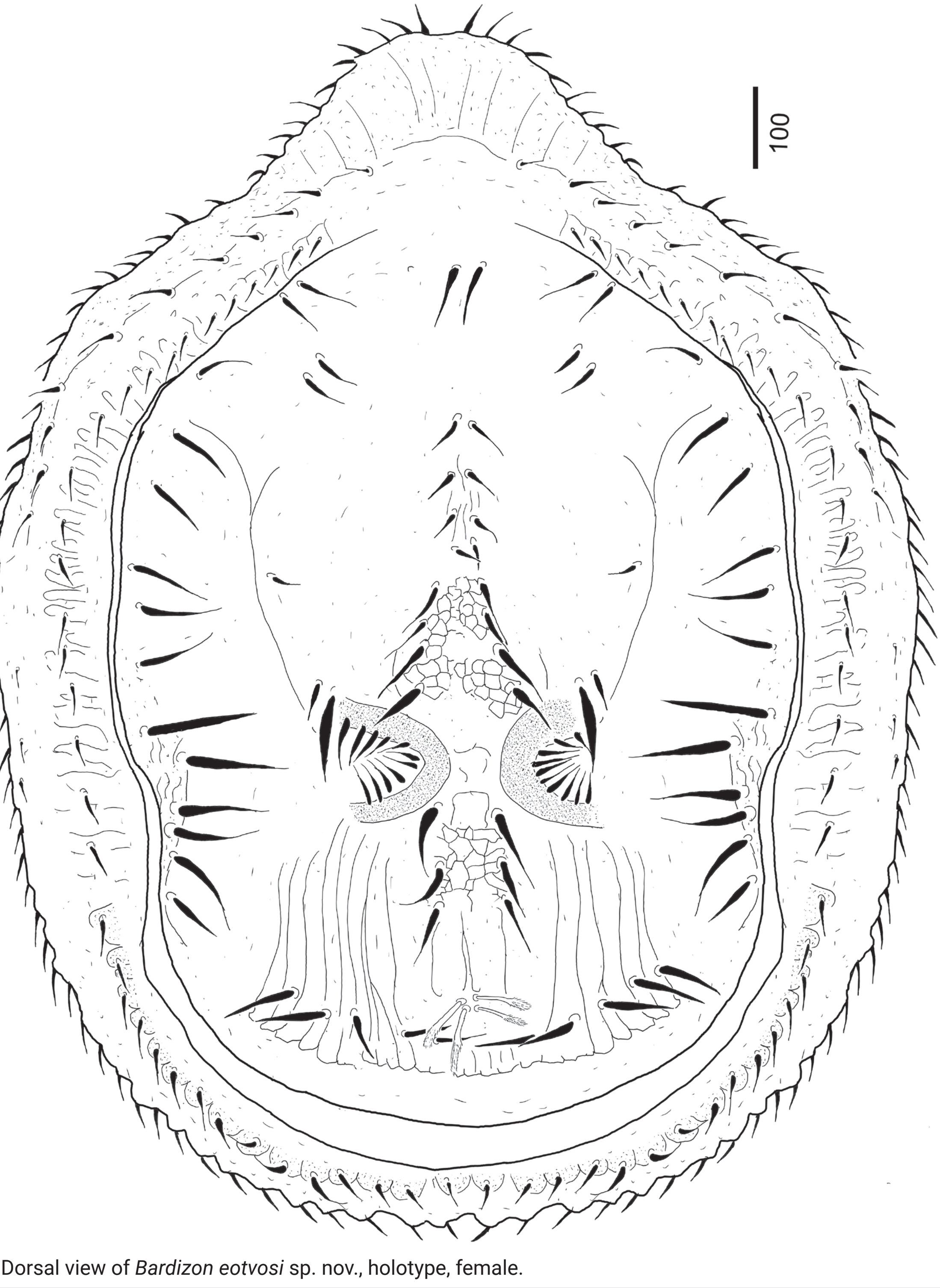

Figure 1. Dorsal view of *Bardizon eotvosi* sp. nov., holotype, female.

Dorsal idiosoma (Figs 1, 4A, B). Marginal and dorsal shields fused anteriorly. Central area elevated from neighbouring regions on dorsal shield (Fig. 4B). One pair of eye-like depressions on elevated central part; margins of depressions covered by smooth, short (ca 42–45), needle-like setae. Majority of dorsal shield with smooth surface; web-like sculptural pattern situated only anterior and posterior to eye-like dorsal depressions on central area and some longitudinal lines present posterior to eye-like depressions. Dorsal shield bearing 35–38 pairs of smooth (ca 70–124 long) and two pairs of apically pilose (ca 75–80 long)

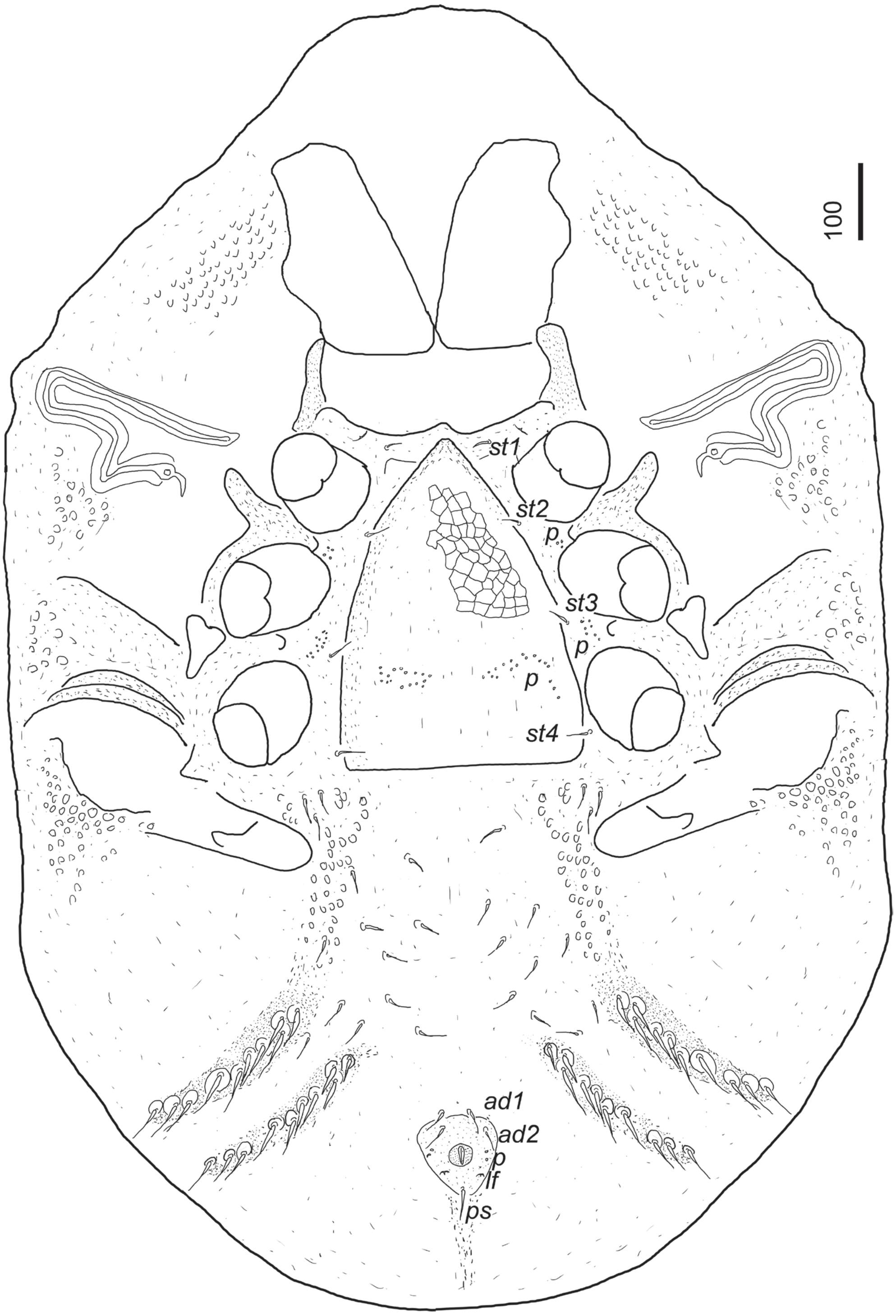

Figure 2. Ventral view of *Bardizon eotvosi* sp. nov., holotype, female.

setae. Longer (ca 110–125), smooth setae at level of oval depressions and near lateral margin of dorsal shield; apically pilose setae near posterior margin of dorsal shield. Marginal shield with some rounded platelets bearing short (ca 18–22), smooth setae on laterocaudal area and some reticulated sculptural pattern on marginal shield anterior to platelets. Other setae on marginal shield similar in shape and length to setae situated on platelets.

Ventral idiosoma (Figs 2, 4C, D). Four pairs of sternal setae present. All sternal setae smooth, needle-like, and ca 23–28 long. Setae *st1* inserted near anterior margin of sternal shield; *st2* at level of posterior margin of coxae II; *st3* at level of posterior margin of coxae III; *st4* at level of posterior margin of coxae IV. Sternal shield smooth, two pairs of field of poroid-like structures between coxae II and III and coxae III and IV. One pair of lyriform fissures visible near *st1*. About 13–16 pairs of ventral setae short (ca 25–34), smooth, and needle-like. About 10–14 pairs of smooth, ca 41–48 long and needle-like setae placed on small platelets.; these setae on two pairs of strongly sclerotized, slightly elevated ventral grooves posterior to pedofossae IV. Surface of ventral shield ornamented by oval pits posterior to coxae IV; other part of surface smooth. Anal opening oval (30–32 long and 28–30 wide); anal valves smooth, without euanal setae. Adanal (ca 27–29 long) and postanal (ca 38–41 long) setae smooth and needle-like. Two pairs of poroid-like structures and one pair of lyriform fissures situated lateral to anal opening. Anal area slightly elevated from neighbouring regions.

Genital shield scutiform, length 430–440, basal width 300–315, situated between coxae II and IV; surface of genital shield covered by web-like structures. Stigmata situated between coxae II and III. Presitgmatid part of peritremes with two bends; postsigmatid part very short. Pedofossae deep, their surface smooth, with separate furrow for tarsi IV. Some oval pits situated outside margin of pedofossae. Tritosternum with narrow base; its laciniae subdivided into two pilose lateral branch and one smooth central branch (Fig. 3A).

Gnathosoma (Fig. 3A, B). Corniculi smooth and horn-like; internal malae narrow and pilose, longer than corniculi. Hypostomal setae *h1* and *h3* smooth and needle-like (48–55 long); *h2* short (ca 16–18) and robust; and *h4* (36–39) antler-shaped. Deutosternal groove wide until *h3*, afterwards narrow; three rows of denticles posterior to setae *h3*. Chelicerae with internal sclerotized nodes. One central teeth situated on both cheliceral digit,, fixed digit as long as movable digit. Palp trochanter setae *v1* short and robust (ca 32–34); *v2* very long and pilose (ca 118–122). Other setae on palp segments smooth. Palp apothele with two branches (Fig. 3B). Epistome marginally pilose.

Legs (Fig. 3C–F). Length of legs (from base of coxae to apex of tarsi): I 665–680, II 525–540, III 485–500, IV 505–518. Leg I with ambulacral claws, but shorter than other legs. On all legs majority of setae needle-like, but some setae serrate and several setae pilose on other leg segments.

Male (n = 8). Body 1570–1610 long and 1090–1115 wide at level of coxae.

***Dorsal idiosoma*.** As for the female.

Ventral idiosoma (Figs 3G, 4E). Intercoxal area, with sternal setae and genital shield as in Fig. 3G. Sternal setae smooth and needle-like. Setae *st1* (ca 16–18) near anterior margin of sternal shield; *st2* (ca 25–26) at level of posterior margin of coxae II; *st3* (ca 26–28) at level of posterior margin of coxae III; *st4* (ca 30–84) at level of central area of coxae IV; *st5* (ca 25–27) near posterior margin of genital shield. Surface of sternal shield with web-like sculptural pattern anterior to genital opening and with oval pits posterior to genital opening. One pair of lyriform fissures and one pair of poroid-like structures near *st1*, two pairs of field of poroid-like structures between coxae II and III and coxae III and IV. Genital shield rounded (ca 70–73 × 67–69), its surface smooth, without eugenital setae, and situated between coxae IV.

Other characters as in female.

Developmental stages. Unknown.

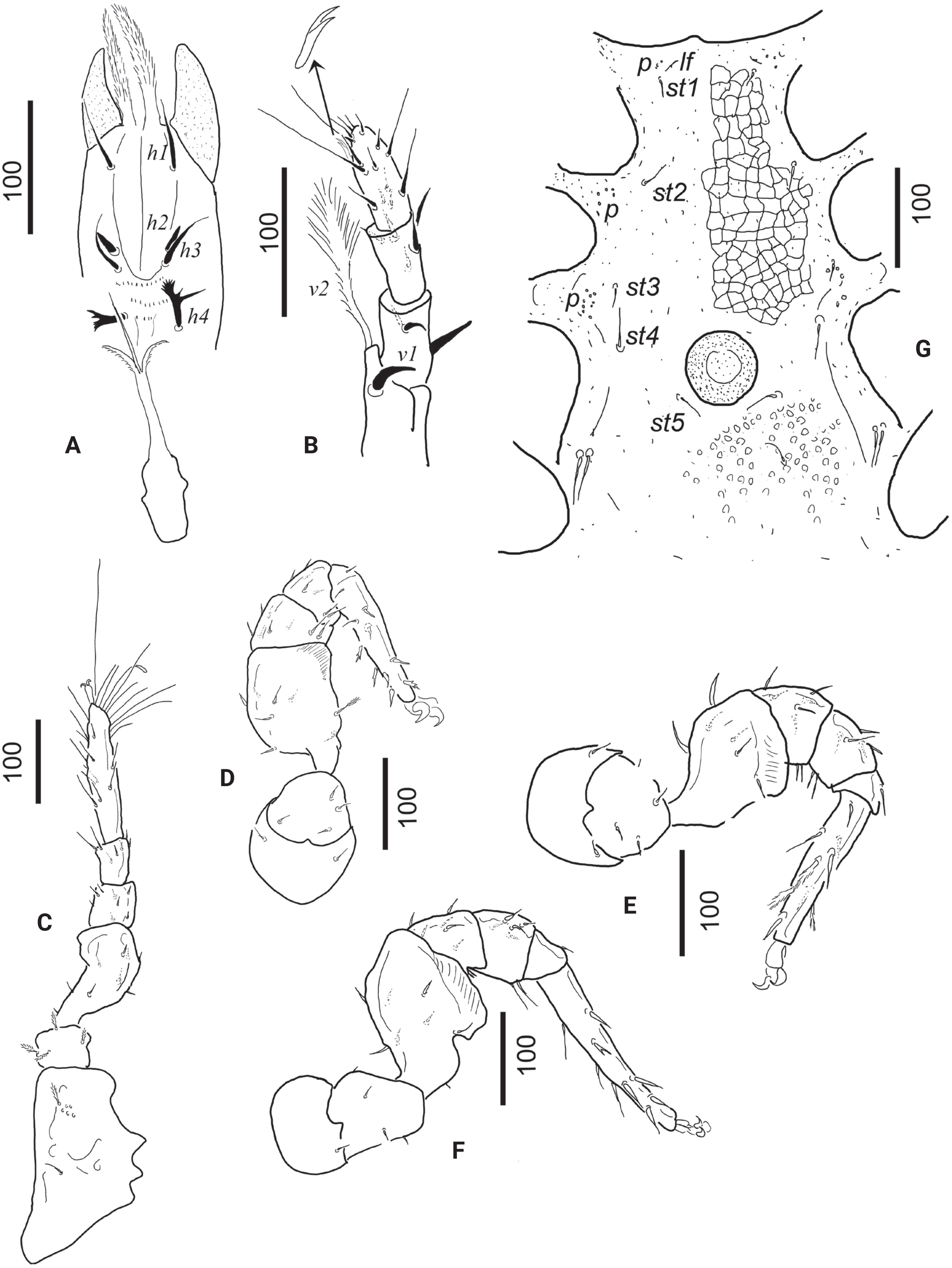

Figure 3. Dorsal view of *Bardizon eotvosi* sp. nov., holotype, female **A** ventral view of gnathosoma **B** ventral view of palp (arrow shows the palp apothele) **C** leg I in ventral view **D** leg II in ventrolateral view **E** leg III in ventrolateral view **F** leg IV in ventrolateral view **G** intercoxal area of male paratype.

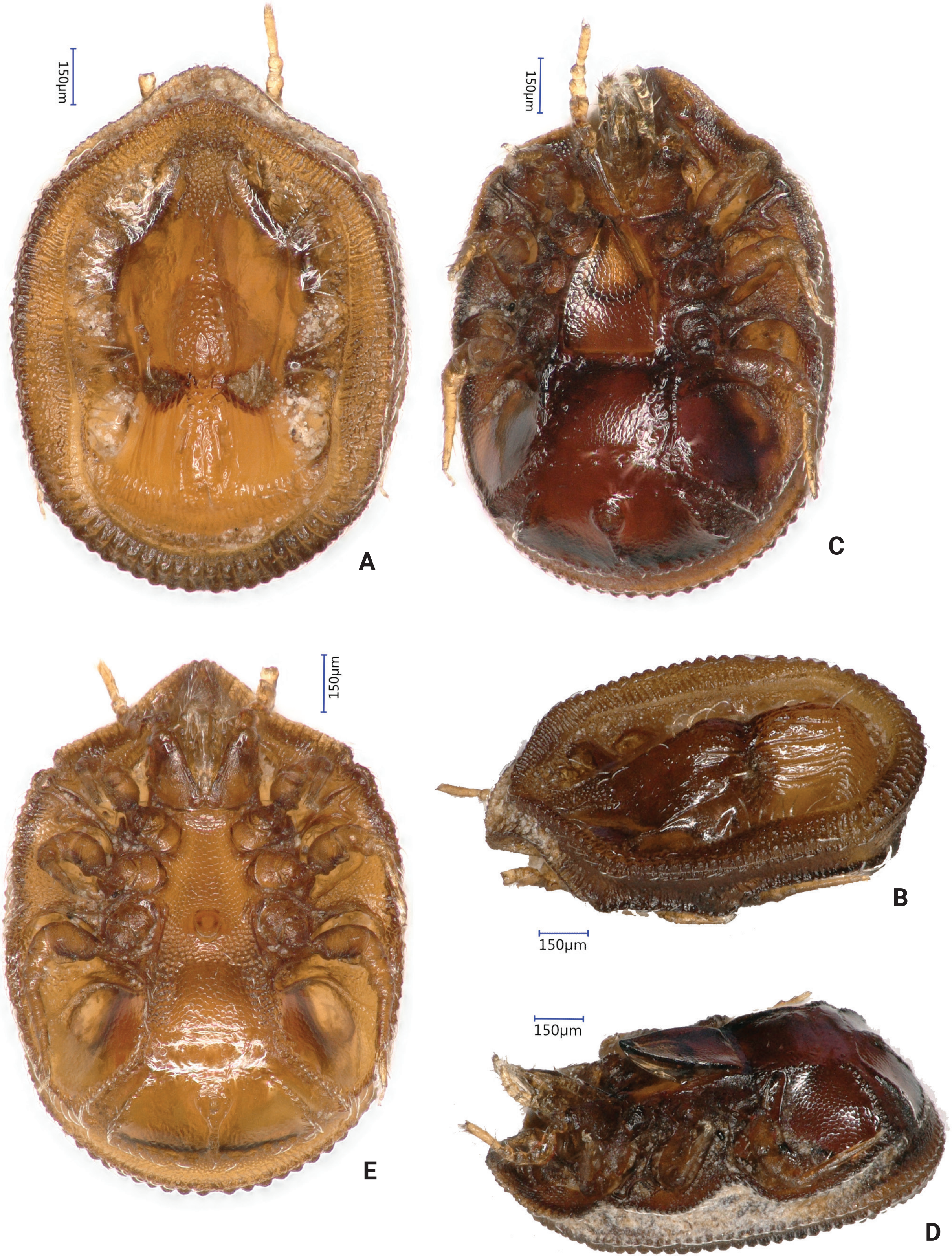

Figure 4. Photos about *Bardizon eotvosi* sp. nov., holotype, female **A** dorsal view of idiosoma **B** dorsolateral view of idiosoma **C** ventral view of idiosoma **D** lateroventral view of idiosoma **E** ventral view of idiosoma of male paratype.

Etymology. The new species is dedicated to Baron Loránd Eötvös (1848–1919), scientist, physicist, the president of the Hungarian Academy of Sciences (1889–1905) and Minister of the Culture (1894–1895) on the 125th anniversary of his birth.

Remarks. The new species is most similar to *B. akoii* (Hiramatsu, 1985), the most important differences being summarized in Table 1.

Table 1. Most important differences between the species *Bardizon aokii* and *B. eotvosi* sp. nov.

	B. aokii	***B. eotvosi***
Majority of dorsal setae	finely pilose	smooth
Surface of anterior area of dorsal shield	with oval pits	smooth
Surface dorsal shield anterior and posterior to the eye-like depressions	smooth	with web-like sculptural pattern
Oval pits posterior to coxae IV	absent	present
Surface of male sternal shield anterior to genital opening	smooth	with web-like sculptural pattern
Surface of male sternal shield posterior to genital opening	smooth	with oval pits
Apical bend of peritreme	wide and angular	hooked

Key to the known species of the family Phymatodiscidae

1 Dorsal idiosoma with one pair of eye-like depression (genus *Bardizon*) **2**
– Dorsal idiosoma without eye-like depressions (genus *Phymatodiscus*) **8**
2 Surface of female genital shield smooth, only bearing some pits **3**
– Surface of female genital shield ornamented with web-like sculptural pattern **7**
3 Eye-like transversal furrows large, visible, and bordered with long setae **4**
– Eye-like transversal furrows small, hidden, and not bordered with setae ..... ***B. insolitus***
4 Dorsal setae uniform in length **5**
– Dorsal setae not uniform in length **6**
5 Setae on marginal shield situated in multiple rows; two pairs of long and narrow setae on caudal area of dorsal shield ..... ***B. haradai***
– Setae on marginal shield situated in only one row; two pairs of robust setae on caudal area of dorsal shield ..... ***B. oculatus***
6 Setae *h1* marginally serrate; setae on margin of eye-like transversal furrows smooth ..... ***B. kuni***
– Setae *h1* smooth; setae on margin of eye-like transversal furrows marginally pilose ..... ***B. malayicus***
7 Surface of anterior area of dorsal shield without oval pits ..... ***B. eotvosi***
– Surface of anterior area of dorsal shield with oval pits ..... ***B. aokii***
8 Margin of idiosoma with several long prolongations **9**
– Margin of idiosoma without prolongation ..... ***P. polyglottis***
9 Marginal prolongations situated only on caudal margin ..... ***P. iriomotensis***
– Marginal prolongations situated on entire margin **10**
10 Prolongations cone-like **11**
– Prolongations not cone-like **12**
11 Margin with more than 14 prolongations ..... ***P. mirabilis***
– With fewer than 14 prolongations ..... ***P. coniferus***
12 Margin with more than 14 prolongations ..... ***P. mirandus***
– With fewer than 14 prolongations ..... ***P. ignesemovens***

Acknowledgements

We are very grateful to Dr Peter Schwendinger (MHNG) for his kind hospitality during JK's stay in Geneva. We would like to thank Dr Jason Dunlop for his linguistic correction of the manuscript.

Additional information

Conflict of interest

The authors have declared that no competing interests exist.

Ethical statement

No ethical statement was reported.

Funding

No funding was reported.

Author contributions

JK and SGE wrote the manuscript, JK did the illustration.

Author ORCIDs

Jenő Kontschán https://orcid.org/0000-0001-8274-4238
Sergey G. Ermilov https://orcid.org/0000-0002-0913-131X

Data availability

All of the data that support the findings of this study are available in the main text.

References

Berlese A (1905) Acari nuovi. Manipulus IV. (Acari di Giava). Redia (Firenze) 2: 154–176.

Berlese A (1917) Intorno agli Uropodidae Fasc. 1. Redia (Firenze) 113: 7–16.

Canestrini G (1897) Nuovi Acaroidei della N. Guinea. Természetrajzi Füzetek 20: 401–462.

Halliday RB (2016) Catalogue of families and their type genera in the mite suborder Uropodina (Acari: Mesostigmata). Zootaxa 4061(4): 347–366. https://doi.org/10.11646/zootaxa.4061.4.2

Hiramatsu N (1979) Gangsystematik der Parasitiformes. Teil 333. Stadien einer neuen *Phymatodiscus*-Art aus Japan (Dinychini, Uropodinae). Acarologie. Schriftenreihe für Vergleichende Milbenkunde 25: 108–109.

Hiramatsu N (1985) Zwei neue *Phymatodiscus*-Arten (Acari, Uropodidae) aus Borneo. Kontyu 53(2): 270–276.

Hirschmann W (1977) Gangsystematik der Parasitiformes. Teil 254. Die Gattung *Phymatodiscus* (Berlese, 1917), Teilgang and Stadien von 4 neuen *Phymatodiscus*-Arten aus Neuguinea (Dinychini, Uropodinae). Acarologie. Schriftenreihe für Vergleichende Milbenkunde 23: 60–65.

Hirschmann W (1979) Stadiensystematik der Parasitiformes. Teil 1. Stadienfamilien und Stadiengattungen der Atrichopygidiina, erstellt im Vergleich zum Gangsystem Hirschmann, 1979. Acarologie. Schriftenreihe für Vergleichende Milbenkunde 26: 57–70.

Kontschán J (2018) Two new species of *Angulobaloghia* Hirschmann, 1979 (Acari: Rotundabaloghiidae) from Brunei. Systematic and Applied Acarology 23(7): 1366–1374. https://doi.org/10.11158/saa.23.7.13

Kontschán J (2021) *Rotundabaloghia* (*Rotundabaloghia*) *dogani* sp. nov. from Hong Kong (Acari: Mesostigmata: Rotundabaloghiidae). Acarological Studies 3(1): 32–36. https://doi.org/10.47121/acarolstud.839531

Kontschán J, Ermilov SG (2023a) Resurrection of the genus *Micherdzinskiiobovella* Hirschmann, 1989, with the description of *M. petofii* sp. n. from Singapore (Acari: Mesostigmata: Urodinychidae). Acta Zoologica Academiae Scientiarum Hungaricae 69(2): 127–138. https://doi.org/10.17109/AZH.69.2.127.2023

Kontschán J, Ermilov SG (2023b) New *Angulobaloghia* species and records (Acari: Mesostigmata: Rotundabaloghiidae) from the Oriental region. Acarologia 63(1): 253–261. https://doi.org/10.24349/nwhs-7n23

Kontschán J, Ermilov SG (2023c) Catalogue of trachyuropodid mites (Acari: Mesostigmata: Uropodina: Trachyuropodidae) of the world, with the description of *Trachyibana kozari* n. sp. from Singapore. Acta Phytopathologica et Entomologica Hungarica 58(1): 18–50. https://doi.org/10.1556/038.2023.00183

Kontschán J, Kiss B (2015) Five new rotundabaloghiid mites (Acari: Uropodina) from South-East Asia. Zootaxa 4021(4): 515–528. https://doi.org/10.11646/zootaxa.4021.4.2

Kontschán J, Ripka G (2016) Three new Uropodina mites (Acari: Mesostigmata) from Singapore. Revue Suisse de Zoologie 123(2): 291–301. https://doi.org/10.5281/zenodo.155303

Kontschán J, Starý J (2011) Uropodina species from Vietnam (Acari: Mesostigmata). Zootaxa 2807(1): 1–28. https://doi.org/10.11646/zootaxa.2807.1.1

Kontschán J, Starý J (2012) New Uropodina species and records from Malaysia (Acari: Mesostigmata). Acta Zoologica Academiae Scientiarum Hungaricae 58(2): 177–192. https://doi.org/10.5281/zenodo.5735765

ZooKeys 1182: 237–258 (2023)
DOI: 10.3897/zookeys.1182.102866

Research Article

Water beetles (Coleoptera) associated with Afrotemperate Forest patches in the Garden Route National Park, South Africa

Matthew S. Bird[1], David T. Bilton[1,2], Musa C. Mlambo[3], Renzo Perissinotto[4]

1 Department of Zoology, University of Johannesburg, Auckland Park 2006, Johannesburg, South Africa
2 Marine Biology and Ecology Research Centre, School of Marine Science and Engineering, Plymouth University, Drake Circus, Plymouth PL4 8AA, UK
3 Department of Freshwater Invertebrates, Albany Museum, Department of Zoology and Entomology, Rhodes University, Makhanda, 6139 Grahamstown, South Africa
4 Coastal and Marine Research (CMR), Nelson Mandela University, P.O. Box 77000, 6031 Gqeberha, South Africa
Corresponding author: Matthew S. Bird (mbird@uj.ac.za)

Abstract

Southern Afrotemperate Forest is concentrated in the southern Cape region of South Africa and whilst it is relatively well known botanically, the fauna, specifically the aquatic invertebrate fauna, is poorly documented. The majority of remaining intact forest habitat is contained within the Garden Route National Park (GRNP), which straddles the provincial boundary between the Western and Eastern Cape. This study undertakes a survey of the water beetle fauna inhabiting the GRNP. The aquatic ecosystems within temperate forests of the region are poorly researched from an ecological and biodiversity perspective, despite being known to harbour endemic invertebrate elements. We collected water beetles and in situ physico-chemical data from a total of 31 waterbodies across the park over two seasons (summer and late winter) in 2017. The waterbodies sampled were mostly small freshwater perennial streams and isolated forest ponds. A total of 61 beetle taxa was recorded (29 Adephaga, 32 Polyphaga) from these waterbodies. The water beetle fauna of these forests appears to be diverse and contains many species endemic to the fynbos-dominated Cape Floristic Region, but very few of the species appear to be forest specialists. This is in contrast to the fynbos heathland habitat of the region, which harbours a high number of water beetle species endemic to this habitat, often with Gondwanan affinity. Our study is the first to document the water beetles of Afrotemperate Forests in the southern Cape region and provides an important baseline for future work on such habitats in the region and in other parts of southern Africa.

Key words: aquatic Coleoptera, aquatic invertebrates, biodiversity census, forest conservation, freshwater biodiversity, southern Cape, temperate forests

Academic editor: Christopher Majka
Received: 1 March 2023
Accepted: 16 May 2023
Published: 19 October 2023

ZooBank: https://zoobank.org/38368875-C0E0-4924-A44B-9CD2781B46EC

Citation: Bird MS, Bilton DT, Mlambo MC, Perissinotto R (2023) Water beetles (Coleoptera) associated with Afrotemperate Forest patches in the Garden Route National Park, South Africa. ZooKeys 1182: 237–258. https://doi.org/10.3897/zookeys.1182.102866

Introduction

Closed-canopy evergreen indigenous forest is a relatively scarce biome in southern Africa, most of this vegetation type in South Africa being located in the east and north of the country (Mucina and Geldenhuys 2006). Remaining forests in southern Africa are highly fragmented, existing as a series of ecological islands within a mosaic of other biomes, including savannah, grassland, fynbos, alien vegetation and agriculturally transformed lands. Additionally, the majority of remaining forests are small (< 100 ha), the distribution of patches showing what often appears to be a relictual pattern, for example, as fire refugia within other biomes, suggesting that forest fragmentation has been driven substantially by non-anthropogenic factors, particularly the development of fire prone ecosystems since the Miocene-Pliocene (e.g., Eeley et al. 1999). The largest single forest in South Africa is in the vicinity of Knysna in the southern Cape (25,706 ha), itself sitting within a much larger complex of forest patches totalling over 60,000 ha (Mucina and Geldenhuys 2006). The forests in the southern and western Cape regions have floristic affinities with Afromontane Forest in the Drakensberg and on mountains further north into tropical Africa, the southerly latitude allowing these forests to occur at relatively low altitude (Meadows and Linder 1989). These Cape forests are compositionally distinct from those further east and north, however, and usually considered to comprise a separate vegetation unit, Southern Afrotemperate Forest (Mucina and Geldenhuys 2006). Whilst some patches of this habitat occur in fire refugia, such as ravines and mountainsides across the Western Cape Province (and indeed into the Northern Cape), the majority is found in the coastal hills and low mountains that straddle the borders of the Western and Eastern Cape provinces. Whilst most of the historical extent of this forest has been lost to human activities (Geldenhuys 1991), more than 50% of what remains is protected within the Garden Route National Park (Mucina and Geldenhuys 2006).

Our understanding of the biodiversity of Afrotemperate Forests in southern Africa remains limited and patchy, both taxonomically and geographically. Floristic composition and endemism are relatively well understood for most groups; Southern Afrotemperate forests being dominated by palaeoendemic trees such as the podocarps (*Afrocarpus* and *Podocarpus*) and *Cunonia*, *Ocotea*, and *Olea*, but with relatively few strictly endemic plant taxa (Mucina and Geldenhuys 2006). A number of forest birds, including the Knysna Turaco (also known locally as the Knysna Lourie) *Tauraco corythaix* (Wagler, 1827) are near-endemic to the region, and amongst other vertebrates these forests support the near-endemic shrew *Myosorex longicaudatus* Meester & Dippenaar, 1978 (Hilton-Taylor 2000), some near-endemic amphibians (Passmore and Carruthers 1995) and the strictly endemic Knysna Dwarf Chamaleon *Bradypodion damarnum* (Boulenger, 1887) (Tolley et al. 2004; Stuart-Fox and Moussalli 2007). The invertebrate fauna of the southern Cape forests is much more poorly documented, but is known to include a number of apparent endemics (for a review of the soil fauna of South African forests, see Janion-Scheepers et al. 2016), in groups as diverse as land snails (e.g., Moussalli et al. 2009; Perera et al. 2021), millipedes (Hamer 1998), terrestrial isopods (Ferrara and Taiti 1979) and terrestrial beetles (e.g., Solidovnikov and Newton 2004; Janák and Makranczy 2016).

Very little work has been conducted on the freshwaters of Southern Afrotemperate Forests to date. Midgley and Schafer (1992) examined correlates of water colour in southern Cape streams, establishing that black water streams could occur in both fynbos and forested catchments. De Moor and Bellingham (2019) document and discuss the Trichoptera of streams in the region, including forested sites, and highlight the presence of a number of range-restricted Cape Floristic Region (CFR) endemic species. Otherwise, knowledge of the insect fauna of these habitats is largely limited to descriptions in the taxonomic literature (e.g., Solidovnikov and Newton 2004; Perkins 2009; Janák and Makranczy 2016). In South Africa, comparatively less is known about aquatic beetles (but see Perissinotto et al. 2016; Bird et al. 2017) unlike their counterparts in groups such as dung beetles (Davis et al. 2020), canopy beetles (Swart et al. 2021) and fruit chafers (Beinhundner 2017). Beetles have colonised water many times from separate terrestrial ancestors, forming an ecological grouping rather than a clade (Bilton et al. 2019). As a consequence, aquatic beetles are ecologically and functionally diverse and occupy the entire spectrum of freshwater habitats, where they often make up a significant proportion of freshwater macroinvertebrate biodiversity (Jäch and Balke 2008), making them an excellent group for ecological assessment (e.g., Bilton et al. 2006; Sánchez-Fernández et al. 2006; Picazo et al. 2011). The present study aimed to document the water beetle fauna of forested regions of the Garden Route National Park, through targeted surveys. Here we document all water beetle species recorded, together with multivariate analyses of water beetle assemblage composition. Given the general lack of such data from southern Africa (Bird et al. 2019), and Cape forests in particular (de Moor and Day 2013), our study provides a valuable baseline for the study of this key group of freshwater macroinvertebrates in Afrotemperate Forest habitats in southern Africa.

Materials and methods

Study area

Samples were collected from a total of 31 waterbodies spanning the length of the Garden Route National Park (GRNP) along the southern Cape coast of South Africa between the towns of Storms River in the east and George in the west (Fig. 1a, b). This region constitutes the core area of remaining Southern Afrotemperate Forest habitat (sensu Mucina and Geldenhuys 2006), with only small, scattered fragments of this habitat occurring outside of the study area (Fig. 1b). The study area spans the border of the Western Cape and Eastern Cape provinces (Fig. 1a, b) and is part of a relatively moist coastal plain (the Mean Annual Precipitation, MAP, for Southern Afrotemperate Forest is 862 mm; Mucina and Geldenhuys 2006), which gives way to the semi-desert Karoo inland, as apparent in the satellite imagery of Fig. 1a. Despite covering a relatively small area, Southern Afrotemperate Forest habitat is considered 'Least Threatened' (Mucina and Geldenhuys 2006) thanks largely to the statutory protection it receives, with more than half of the extent of these forests falling within the boundaries of the GRNP (Fig. 1b).

Sample collection was performed across two seasons, with 20 sites being sampled in early February 2017 (mid-summer, hereafter 'summer') and 14 sites sampled in mid-September 2017 (late winter, hereafter 'winter'). Three of the sites sampled in summer were sampled again in winter. In terms of waterbody types sampled in this study, 15 of the sites sampled in summer were small perennial streams, whilst four such sites were sampled in winter. Five sites sampled in summer were ponds, whilst nine ponds were sampled in winter. One of the sites sampled in winter was a seepage wetland. The waterbodies were low lying, all occurring at less than 400 m altitude. Several clusters of sites were sampled, with 13 sites occurring in the vicinity of Storms River, 12 sites at Nature's Valley, three at Harkerville, two at Diepwalle and one site was sampled at Wilderness. All sampled sites occurred within patches of Southern

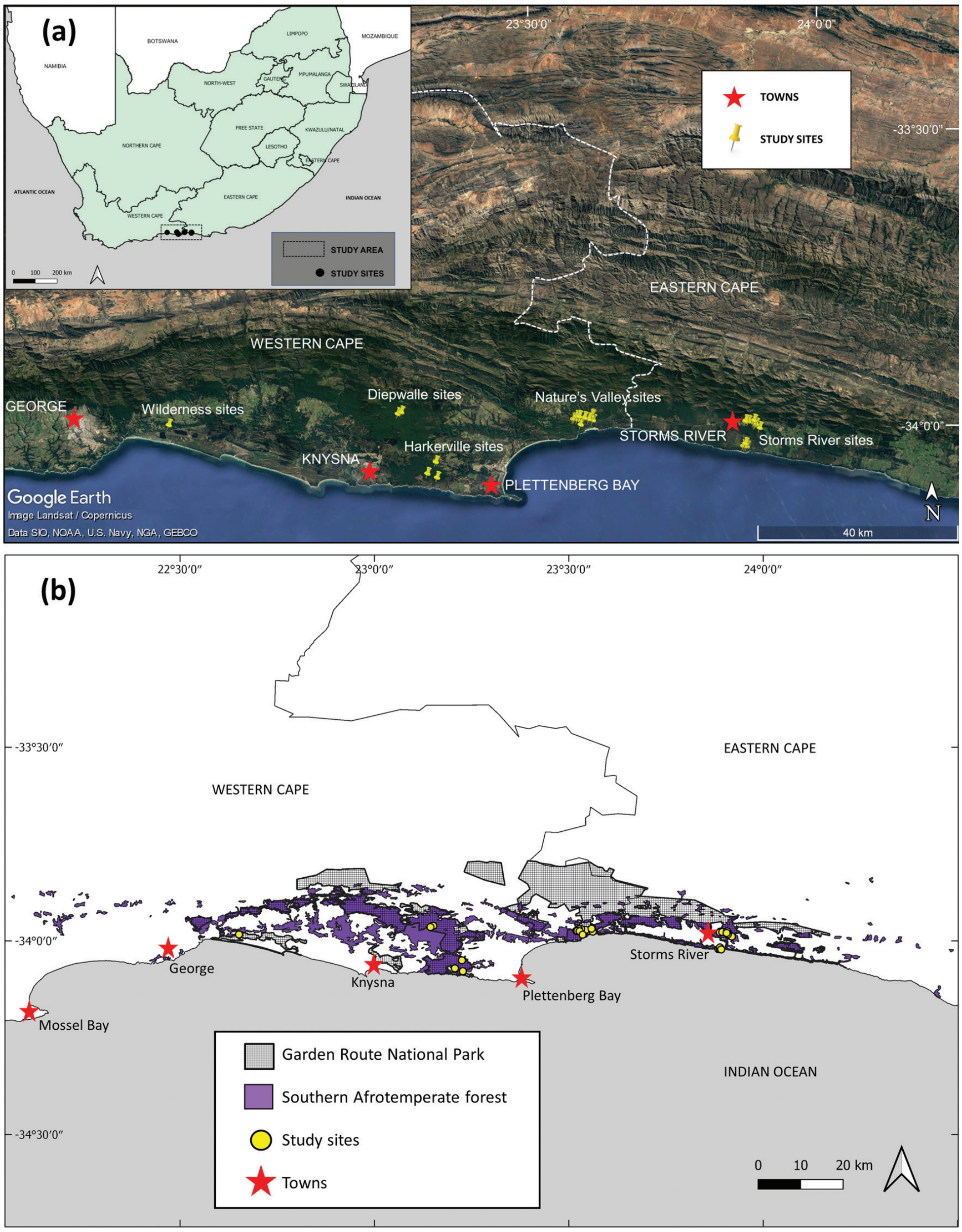

Figure 1. Location of the study sites along the southern Cape coastline of South Africa. Sites were grouped according to five main areas that represent different forest fragments within the Garden Route National Park (GRNP): Storms River; Nature's Valley; Harkerville; Diepwalle and Wilderness (**a**). The position of the study sites in relation to the remaining core Afrotemperate Forest habitat in the region is depicted, as well the boundaries of the GRNP (**b**).

Afrotemperate Forest and were in a relatively pristine condition, being located inside the GRNP. The site locality information for all sampled waterbodies is provided in Table 1 and photographs of typical habitats are provided in Fig. 2.

Field sampling protocol and beetle identification

Water beetles were collected during both seasons using sweep netting. A long-handled square-framed pond net with a 30-cm mouth and 1-mm mesh was used for this purpose. With each sweep the net would be swept from the water surface to the bottom substrate and back to the surface again, in similar

Table 1. Site locality information for waterbodies sampled during this study. Two collection trips were undertaken, the first being during February 2017 (mid-summer) and the second during September 2017 (late winter). SR: Storms River; NV: Nature's Valley; HV: Harkerville; DW: Diepwalle; WN: Wilderness.

Site	Date sampled (dd/mm/yyyy)	GPS (DD)	Altitude (m)	Region	Waterbody type	February (summer)	September (winter)
1	07/02/2017	-34.02138, 23.88472	41	SR	Stream	X	
2	07/02/2017; 14/09/2017	-33.97711, 23.89476	237	SR	Stream	X	X
3	07/02/2017; 14/09/2017	-33.97541, 23.90689	239	SR	Pond	X	X
4	07/02/2017	-33.98300, 23.90829	195	SR	Stream	X	
5	07/02/2017	-33.98180, 23.91132	233	SR	Stream	X	
6	07/02/2017	-33.98871, 23.91929	78	SR	Stream	X	
7	08/02/2017	-33.97638, 23.88886	228	SR	Stream	X	
8	08/02/2017	-33.97800, 23.88846	224	SR	Stream	X	
9	09/02/2017	-33.97403, 23.55288	64	NV	Stream	X	
10	09/02/2017	-33.97158, 23.54332	137	NV	Stream	X	
11	09/02/2017	-33.96859, 23.55978	3	NV	Stream	X	
12	09/02/2017; 15/09/2017	-33.96860, 23.55861	9	NV	Pond	X	X
13	09/02/2017	-33.97605, 23.56169	2	NV	Pond	X	
14	10/02/2017	-33.97428, 23.51926	39	NV	Stream	X	
15	11/02/2017	-34.05024, 23.22491	240	HV	Pond	X	
16	11/02/2017	-34.07092, 23.20679	189	HV	Stream	X	
17	11/02/2017	-34.07839, 23.22742	177	HV	Stream	X	
18	11/02/2017	-33.96131, 23.15123	392	DW	Stream	X	
19	11/02/2017	-33.96436, 23.14399	381	DW	Pond	X	
20	12/02/2017	-33.98355, 22.65148	5	WN	Stream	X	
21	14/09/2017	-34.02140, 23.8886	25	SR	Stream		X
22	15/09/2017	-34.01701, 23.88892	101	SR	Stream		X
23	15/09/2017	-34.02209, 23.89196	68	SR	Pond		X
24	15/09/2017	-33.98311, 23.90889	195	SR	Seep		X
25	15/09/2017	-33.97967, 23.90582	217	SR	Stream		X
26	15/09/2017	-33.96713, 23.56006	3	NV	Pond		X
27	16/09/2017	-33.96937, 23.53168	218	NV	Pond		X
28	16/09/2017	-33.96966, 23.52587	223	NV	Pond		X
29	16/09/2017	-33.97414, 23.52207	36	NV	Pond		X
30	16/09/2017	-33.97509, 23.52778	87	NV	Pond		X
31	16/09/2017	-33.98408, 23.53546	4	NV	Pond		X

fashion to the protocols of Perissinotto et al. (2016) and Bird et al. (2017). Submerged fringing vegetation and the shore margins were targeted, given the authors' previous experience of finding most water beetles in these habitats. Visual searching of the margins of each waterbody for shore beetles and semi-aquatic taxa was conducted in addition to sweep netting. Sampling was

Figure 2. Examples of the waterbodies and habitat types sampled in the Garden Route National Park (pictures taken during the summer survey in mid-February 2017). **a** Stream in the Plaatbos forest, Storms River (site 4) **b** main channel of the Storms River where the bridge crosses near the public picnic site (site 6) **c** the main channel of the Groot River at Nature's Valley (site 13) **d** marshy pond at Plaatbos, Storms River (site 3) **e** stream crossing a hiking trail in the Plaatbos forest, Storms River (site 2) **f** small stream on the Kalanderkloof hiking trail, Nature's Valley (site 9) **g** DTB examining water beetles at a pond in the Harkerville forest (site 15) **h** pond in the Diepwalle forest (site 19) **i** the authors hard at work sampling a pond at Nature's Valley (site 12) adjacent to the Groot River **j** typical Southern Afrotemperate Forest habitat at Harkerville.

continued until no additional new taxa were found, each location typically being worked by the team for ca. 1 h. All beetle specimens were killed using ethyl acetate vapour and preserved in absolute ethanol.

To provide baseline information on the freshwater habitats of GRNP, and an environmental context for the water beetle assemblages, basic in situ physico-chemical parameters were measured at each site. Temperature, conductivity, pH, turbidity, and dissolved oxygen were recorded using a YSI 6600-V2 multi-system probe. Physico-chemical measurements could not be taken from two of the sites during the summer survey due to logistical constraints.

All identifications were conducted by DTB, using a wide range of literature and, in some cases, comparison with reference/voucher material. All identifications were based, at least in part, on the study of male genitalia, unless otherwise stated.

Data analysis

Spatio-temporal patterns in the physico-chemistry of the waterbodies were assessed to determine whether the beetle assemblages mirrored physico-chemical patterns. Differences in physico-chemistry amongst sampled waterbodies were depicted using Principal Components Analysis (PCA), after first normalising the variables in the matrix. The variables constituting each matrix were temperature, conductivity, dissolved oxygen, pH, depth, and turbidity. Physico-chemical differences were compared across three factors of interest, which were overlaid on the PCA plots: season (summer, winter); region (Storms River, Nature's Valley, Harkerville, Diepwalle, Wilderness); and waterbody type (streams, ponds, seeps). Permutational MANOVA (PERMANOVA, Anderson 2001) was used to test for differences in waterbody physico-chemistry across each of the three factors above (i.e., between seasons, regions, and waterbody types). For the regional comparison, 'Wilderness' was excluded as a factor as no physico-chemical data were collected at the Wilderness site. For comparison of waterbody types, 'seeps' was excluded as a factor because only one seep was sampled on one occasion (i.e., streams were compared with ponds).

Spatio-temporal patterns in beetle assemblage composition were depicted using non-metric multidimensional scaling (MDS). The MDS plots were overlaid by the same factors as per the physico-chemical data (seasons, regions, and waterbody types). Beetle presence-absence data were converted to a Bray-Curtis dissimilarity matrix in order to construct the MDS plots. PERMANOVA was used to test for differences in beetle assemblage composition (represented by a Bray-Curtis dissimilarity matrix) between the two seasons sampled (February 2017 – mid-summer vs. September 2017 – late winter) and amongst the different regions (i.e., separate forest patches) sampled along the Tsitsikamma coast (Storms River, Nature's Valley, Harkerville, Diepwalle), as well as between waterbody types (streams vs. ponds). For regional comparisons using PERMANOVA, Wilderness was not included in the test due to only one site being sampled in that region, and similarly seeps were excluded from the comparisons of waterbody types due to only one seep being sampled. Species richness (number of species recorded per waterbody) was similarly compared amongst seasons, regions, and waterbody types. Richness patterns were visually assessed using boxplots and comparisons between seasons, regions and waterbody types were performed using t-tests (two-group comparisons) or one-way ANOVA (three-group comparisons), given that the richness data followed a Gaussian distribution and significant heteroscedasticity was not evident for any of the comparisons (Quinn and Keough 2002). Lastly, beetle assemblage composition was regressed against the various environmental variables recorded in this study to determine what variables best account for the assemblage distribution patterns in the GRNP. The predictor variables here were the spatio-temporal variables (latitude, longitude, altitude, season), regional variables (Storms River, Nature's Valley, Harkerville, Diepwalle), waterbody type (stream, pond, seep) and physico-chemistry (temperature, conductivity, dissolved oxygen, pH, depth, turbidity). Once again, Wilderness was not included as a regional factor (no physico-chemical data for this site). Multivariate regressions were performed using distance-based Redundancy Analysis (dbRDA, Legendre and Anderson 1999; McArdle and Anderson 2001). Separate marginal tests were first run between each environmental variable and beetle assemblage composition, followed by a step-wise selection of the environmental variables using the adjusted Akaike Information Criterion (AICc), which is recommended for small sample sizes (Burnham and Anderson 2002). A 'best' (most parsimonious) overall model was also calculated by considering all variable subsets, with parsimony scored according to the AICc criterion.

All tests were performed using an a priori significance level of $\alpha = 0.05$. P values for PERMANOVA models were tested using 999 unrestricted permutations of the raw data. The PCA, MDS, PERMANOVA and DISTLM procedures were implemented with PRIMER v. 7.0.21 software (Clarke and Gorley 2015) with the PERMANOVA+ add-on (Anderson et al. 2008). Boxplots and univariate tests were performed using GraphPad Prism v. 9.1.0 for Windows (GraphPad Software, San Diego, California USA).

Results

Physico-chemical characteristics of the waterbodies

The waterbodies encountered in the forests of the GRNP were predominantly small perennial rocky streams, although a small proportion of these streams (e.g., sites 9 and 10) are expected to dry up intermittently. There are several larger running waters in the park, such as the Groot, Storms, and Salt rivers, which were also sampled in this study. The second-most abundant waterbody type encountered was ponds (or depression wetlands according to the South African wetland classification system; Ollis et al. 2013), which were all small and shallow and likely dry up on occasion.

Table 2 presents a summary of the physico-chemical variables recorded during each of the two surveys. Surface water temperatures appeared to be somewhat moderated by the shady forest and relatively mild coastal climate in this region, and water temperatures never exceeded 21.5 °C during the mid-summer survey, nor were the minimum winter temperatures extreme, never dropping below 12 °C. Differences in water temperature between summer and winter were not particularly pronounced, with the difference in median temperature of the waterbodies between the two seasons being approximately 5 °C. All the sites sampled were fresh (median summer and winter conductivity was 0.281 $mS.cm^{-1}$ and 0.412 $mS.cm^{-1}$ respectively), with only site 26 being slightly brackish (conductivity of 4.605 $mS.cm^{-1}$). Median pH was circum-neutral in summer (6.76) and no sites were notably alkaline, however five of the sites were genuinely acidic ($pH < 6$). In winter, the sites visited were neutral-to-alkaline, with seven genuinely alkaline sites ($pH > 8$) and median pH was alkaline (8.06). Interestingly, sites 2 and 3, which were revisited in the winter survey, showed a substantial shift in their pH from acidic to alkaline conditions from summer to winter (Table 2).

Sites were generally shallow, being < 1 m in depth (the deepest recording was 0.60 m for sites 16 and 22). However, this does not reflect the true depth of some of the larger rivers such as the Groot River, where water beetles were

Table 2. Physico-chemical variables recorded at each waterbody during the February and September 2017 surveys. Median, minimum, and maximum values are reported for each survey. Readings were not recorded at sites 13 and 20.

Survey date	Site	Temperature (°C)	Conductivity (mS.cm^{-1})	pH	Dissolved O_2 (mg.L^{-1})	Turbidity (NTU)	Depth (m)
February 2017	1	20.41	0.980	7.80	8.45	1.6	0.10
	2	18.54	0.166	4.64	8.19	0.5	0.16
	3	20.41	0.221	6.41	2.53	8.0	0.17
	4	18.71	0.175	5.65	7.63	0.0	0.17
	5	18.64	0.163	5.31	2.35	1.4	0.21
	6	20.61	0.100	4.49	8.76	1.8	0.17
	7	19.95	1.138	6.74	7.53	1.8	0.10
	8	18.51	0.350	7.07	3.48	0.7	0.09
	9	17.51	0.811	6.91	6.22	0.2	0.16
	10	20.38	0.425	7.01	5.68	9.6	0.12
	11	21.44	0.178	6.89	3.83	13.2	0.11
	12	19.57	0.757	7.02	5.90	52.5	0.23
	14	20.93	0.250	5.51	9.09	210.0	0.07
	15	18.90	0.240	6.70	0.56	12.0	0.22
	16	18.50	0.373	6.87	8.82	0.0	0.60
	17	18.71	0.415	6.78	7.56	0.8	0.18
	18	17.52	0.193	6.35	3.31	11.6	0.30
	19	19.38	0.311	6.81	0.72	86.5	0.45
	Median	**19.14**	**0.281**	**6.76**	**6.06**	**1.8**	**0.17**
	Minimum	**17.51**	**0.100**	**4.49**	**0.56**	**0.0**	**0.07**
	Maximum	**21.44**	**1.138**	**7.80**	**9.09**	**210.0**	**0.60**
September 2017	2	13.48	0.955	8.16	9.10	2.1	0.30
	3	12.08	0.140	8.53	1.82	7.1	0.07
	12	14.93	0.802	7.32	1.53	12.9	0.05
	21	13.92	0.761	9.70	9.75	2.2	0.45
	22	13.74	1.724	8.18	2.46	28.6	0.60
	23	14.52	2.245	7.70	0.83	431.0	0.50
	24	12.72	0.454	8.15	3.41	12.5	0.05
	25	14.24	0.138	7.15	7.83	5.1	0.05
	26	14.54	4.605	7.78	5.93	26.2	0.05
	27	14.20	0.159	7.64	7.71	20.1	0.15
	28	15.28	0.334	6.70	6.51	5.2	0.07
	29	15.00	0.359	9.65	3.17	28.4	0.15
	30	17.54	0.279	8.77	6.88	31.5	0.08
	31	15.63	0.370	7.98	4.88	107.0	0.07
	Median	**14.37**	**0.412**	**8.06**	**5.41**	**16.5**	**0.08**
	Minimum	**12.08**	**0.138**	**6.70**	**0.83**	**2.1**	**0.05**
	Maximum	**17.54**	**4.605**	**9.70**	**9.75**	**431.0**	**0.60**

Table 3. Non-parametric permutational MANOVA (PERMANOVA) results for models comparing the physico-chemistry of the waterbodies between (a) seasons, (b) regions and (c) waterbody types. The multivariate models tested for differences between group centroids in multivariate space, represented by Euclidean distance. An asterisk indicates significant P values at α = 0.05.

(a)	df	SS	MS	F	P
Season	1	45.64	45.64	9.75	0.001*
Residual	30	140.35	4.67	–	–
Total	31	186	–	–	–
(b)	**df**	**SS**	**MS**	**F**	**P**
Region	3	12.85	4.28	0.69	0.762
Residual	28	173.15	6.18	–	–
Total	31	186		–	–
(c)	**df**	**SS**	**MS**	**F**	**P**
Waterbody type	1	18.344	18.34	3.26	0.005*
Residual	29	163.04	5.62	–	–
Total	30	181.39	–	–	–

targeted in the shallow marginal vegetation at the edges (e.g., site 13) rather than the deeper middle section of the channel. Although some of the waterbodies were well oxygenated (dissolved oxygen concentrations > 7 mg.L^{-1}), a large proportion of the sites had low dissolved oxygen concentrations, with some of the streams and ponds recording remarkably low values (< 2 mg.L^{-1}, see Table 2). Median dissolved oxygen concentrations were low in both seasons (6.06 and 5.41 mg.L^{-1} for summer and winter respectively). Waterbodies were generally clear, as reflected by the relatively low median turbidity values (< 20 NTU in both seasons), although there were a few high turbidity exceptions (e.g., sites 14, 19, 23 and 31, see Table 2).

According to the PCA plot in Fig. 3, waterbodies varied substantially in their overall physico-chemistry, but consistent gradients for each of the measured variables among the sites were not clear and the overlaid vectors were not well correlated with the sites on the plot. The only possible exceptions are for pH and temperature, with the winter sites towards the bottom right of the plot being associated with higher pH and lower water temperatures, the latter not being surprising. There was a clear distinction between the overall physico-chemical composition of waterbodies sampled in summer vs. winter, as evidenced by their separation on the plot (green vs. blue triangles). This separation was confirmed by the significant PERMANOVA test result for the factor ‘season’ (Table 3 (a)). No significant distinction in physico-chemistry was found among the waterbodies from the different regions of the park (Table 3 (b)), however physico-chemistry did differ between streams and ponds (Table 3 (c)).

Water beetles

The list of water beetles recorded in this study is reported in Table 4. In all 61 taxa were collected from the GRNP over the two surveys of this study, with 47 taxa recorded from the summer survey and 35 from the winter trip. Fifty-three taxa were identified to species level, whilst eight taxa were identified to genus

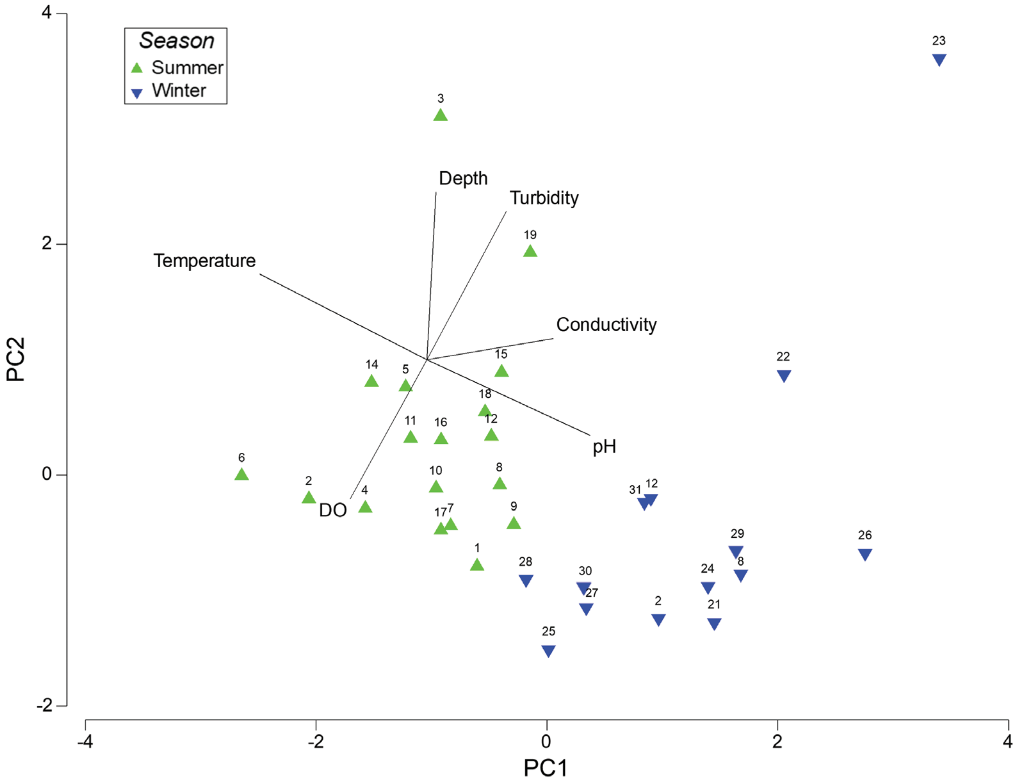

Figure 3. Principal components analysis depicting multivariate differences in the physico-chemistry of the various waterbodies sampled in this study. The site numbers are indicated above the symbol for each site and symbols have been differentiated according to season (summer vs. winter trips). The physico-chemical variables measured at each site have been overlaid as vectors on the plot.

(due to lack of modern revisions) and one to family (Ptilodactylidae larvae). Twenty-nine of the recorded taxa belong to the suborder Adephaga (predaceous water beetles) and 32 belong to the suborder Polyphaga. The richest family collected in this study was the Dytiscidae (Adephaga), with 22 species, followed by the Hydrophilidae (Polyphaga) with 14 taxa, and the Hydraenidae (Polyphaga) with nine species. Similarly, dytiscids were the most widespread family, occurring at 34 sites in the park, followed by the hydrophilids at 23 sites, and hydraenids at 14 sites. *Hydaticus galla* Guérin-Méneville, 1849 (Dytiscidae) was the most widespread species in the GRNP, recorded from 23 waterbodies across the park, followed by *Copelatus caffer* Balfour-Browne, 1939 (Dytiscidae) from 20 of the waterbodies, and *Copelatus capensis* Sharp, 1882 (Dytiscidae) recorded from 17 sites. In contrast, 26 of the taxa were only recorded at a single waterbody. Thus, almost half of the taxa had a very localised distribution in this study.

Mean taxon richness across all sites and sampling trips was 7.1±3.7 (±SD) taxa per site. The most taxa recorded at a single site was 14, recorded at sites 3 and 13, which were both ponds. This was followed by sites 6 (stream) and 27 (pond), where 13 taxa were collected at each of these sites. Therefore, three out of the four richest sites were ponds. The boxplots in Fig. 4 indicate that the median taxon richness of water beetles was higher in summer than winter, but that there was no overall significant difference between the seasons ($t_{32} = 1.604$, $p = 0.119$). In terms of regions, Nature's Valley sites had a higher median richness than for Storms River, but no overall significant difference in richness was reported across the regions

Table 4. Water beetles collected from the Garden Route National Park during the course of this study. The sites are listed from which each taxon was collected on each of the two sampling trips (February and September 2017). Site numbers 1 – 31 correspond to those listed in Table 1. The regions where each taxon occurred are also indicated: SR – Storms River; NR – Nature's Valley; HV – Harkerville; DW – Diepwalle; WN – Wilderness. + Taxa endemic to South Africa.

Taxa	Sampling date		Region				
	February	September	SR	NV	HV	DW	WN
Gyrinidae:							
Dineutus grossus (Modeer, 1776)	1, 6, 8, 14	23	X	X			
+*Aulonogyrus formosus knysnanus* Brinck, 1955	13, 14, 16, 17			X	X		
Aulonogyrus varians Brinck, 1955	6	25	X				
+*Orectogyrus capicola* Brinck, 1955	14			X			
Haliplidae:							
+*Haliplus exsecratus* Guignot, 1936	11, 20			X			X
Noteridae:							
Synchortus simplex Sharp, 1882	3		X				
Dytiscidae:							
+*Agabus austellus* Englund, Bilton & Bergsten, 2020	15				X		
+*Copelatus caffer* Balfour-Browne, 1939	1, 2, 3, 4, 10, 11, 12, 13, 15, 18, 19	2, 3, 12, 21, 23, 24, 25, 26, 30	X	X	X	X	
+*Copelatus capensis* Sharp, 1882	1, 3, 9, 10, 11, 12, 13, 15, 18	3, 12, 21, 23, 24, 26, 28, 30	X	X	X	X	
Copelatus erichsoni Guérin-Méneville, 1849	10, 11, 12	3, 12, 23, 24, 30	X	X			
+*Copelatus notius* Omer-Cooper, 1965		11		X			
Aethionectes apicalis (Boheman, 1848)	12	12		X			
Hydaticus capicola Aubé, 1838	10, 11, 13, 14, 15, 17, 18, 20	12, 23, 27	X	X	X	X	X
Hydaticus dregei Aubé, 1838	8		X				
Hydaticus galla Guérin-Méneville, 1849	1, 3, 4, 5, 7, 8, 10, 11, 12, 13, 14, 15, 16, 18, 19	3, 12, 21, 22, 23, 24, 27, 30	X	X	X	X	
+*Bidessus mundulus* Omer-Cooper, 1965		28		X			
Clypeodytes meridionalis Régimbart, 1895	1, 3, 6, 8, 13,	25	X	X			
Hydroglyphus lineolatus (Boheman, 1848)		27		X			
Uvarus opacus (Gschwendtner, 1935)	3		X				
Yola frontalis Régimbart, 1906	4, 6, 8, 11, 4		X	X			
+*Canthyporus fluviatilis* Omer-Cooper, 1956	3, 15		X		X		
+*Canthyporus hottentottus* (Gemminger & Harold, 1868)	3, 8	26, 27	X	X			
+*Hydrovatus amplicornis* Régimbart, 1895	3	28	X	X			
+*Darwinhydrus solidus* Sharp, 1882	15	27, 28, 29, 31		X	X		
+*Hydropeplus trimaculatus* (Laporte, 1835)		27		X			
+*Hyphydrus soni* Biström, 1982	1, 3, 6, 7, 10, 11, 12, 13, 15, 16, 20	12, 22, 25, 26, 27	X	X	X		X
+*Africophilus jansei* Omer-Cooper & Omer-Cooper, 1957	14			X			
Laccophilus lineatus Aubé, 1838	3, 6, 7, 11, 12, 13, 14, 20	22, 25	X	X			X

Taxa	Sampling date		Region				
	February	**September**	**SR**	**NV**	**HV**	**DW**	**WN**
Hydrochidae							
Hydrochus sp.		27, 28, 29		X			
Spercheidae							
Spercheus cerisyi Guérin-Méneville, 1842		27, 28		X			
Hydrophilidae							
Amphiops globus Erichson, 1843	1, 11, 12, 14, 19	12, 22	X	X		X	
Amphiops senegalensis (Laporte, 1840)	13			X			
+*Anacaena capensis* Hebauer, 1999		25	X				
+*Anacaena glabriventris* Komarek, 2004	10, 14	27		X			
Agraphydrus albescens (Régimbart, 1903)	6, 13		X	X			
+*Enochrus hartmanni* Hebauer, 1998	27, 28, 29			X			
Enochrus (*Methydrus*) sp.	1, 3, 4, 8, 9, 10, 12, 13, 15, 17, 19	23, 24, 30	X	X	X	X	
Helochares longipalpis (Murray, 1859)	3		X				
Helochares sp.	6		X				
+*Limnoxenus sjoestedti* Knisch, 1924		27		X			
Hydrochara elliptica (Fabricius, 1801)		27		X			
Sternolophus mundus (Boheman, 1851)	1, 11, 12, 13	12	X	X			
Laccobius praecipuus Kuwert, 1890	14			X			
Coelostoma sp.	14			X			
Hydraenidae							
Hydraena cooperi Balfour-Browne, 1954	3, 13		X	X			
+*Mesoceration apicalum* Perkins & Balfour-Browne, 1994	2, 4, 16, 17		X		X		
+*Mesoceration barriotum* Perkins, 2008	17				X		
+*Mesoceration dissonum* Perkins & Balfour-Browne, 1994	2, 4, 5		X				
+*Mesoceration distinctum* Perkins & Balfour-Browne, 1994	6		X				
+*Mesoceration integrum* Perkins, 2008	17				X		
+*Nucleotops interceps* Perkins, 2004		29		X			
+*Parhydraena asperita* Perkins, 2009	1, 2, 4, 15, 17	31	X	X	X		
+*Parhydraena seriata* Balfour-Browne, 1954		22, 26, 29	X	X			
Dryopidae							
+*Strina* sp.	6, 17	25	X		X		
Elmidae							
Stenelmis sp.	2		X				
+*Elpidelmis capensis* (Grouvelle, 1890)	2, 4, 6, 17	25	X		X		
+*Elpidelmis fossicollis* Delève, 1966		25	X				
+*Peloriolus* sp. 1	6		X				
+*Peloriolus* sp. 2	2, 5, 6, 17	25	X		X		
Ptilodactylidae							
Ptilodactylidae (larvae)	13			X			

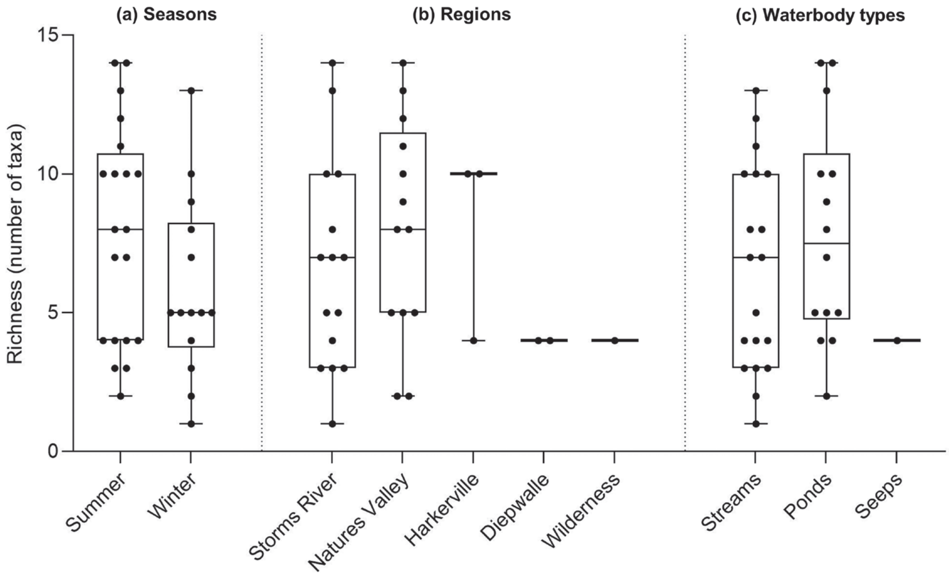

Figure 4. Boxplots comparing the median and spread of water beetle taxon richness (number of taxa per site) between **a** seasons **b** regions and **c** waterbody types at GRNP. The middle line represents the median, whilst the boxes demarcate the interquartile range and the 'whiskers' extend to the maximum and minimum values. The black circles on the graphs represent individual data points (number of taxa) for each site sampled. Unpaired t-tests reported no significant difference in richness between the two seasons (t_{32} = 1.604, p = 0.119) and between the waterbody types (streams vs. ponds, t_{31} = 0.959, p = 0.345). One-way ANOVA reported no significant difference in richness between the regions ($F_{3,29}$ = 0.809, p = 0.499). 'Seeps' was excluded as a factor from the waterbody comparisons due to only one sample being taken from this habitat and 'Wilderness' was similarly excluded from the regional comparison due to only one sample being collected in this region.

($F_{3,29}$ = 0.809, p = 0.499). Ponds had slightly higher median richness than streams, but once again the difference was not significant (t_{31} = 0.959, p = 0.345).

Water beetle assemblage composition differed between seasons, regions, and waterbody types at GRNP, as depicted visually in the MDS plots in Fig. 5. These differences were significant according to the PERMANOVA test results (Table 5). The summer and winter sites do show some overlap in Fig. 5a towards the middle of the plot, but the group centroids are significantly different. In terms of regions, the Nature's Valley sites form a fairly distinct cluster towards the right of the plot (Fig. 5b), with Storms River, Harkerville, and Diepwalle sites mostly overlapping in their beetle assemblage composition (towards the left of the plot). As observed for seasons, the stream and pond waterbody types showed some overlap in their beetle faunas (towards the middle of the plot in Fig. 5c), but overall their group centroids were distinct.

The measured environmental variables in this study were together able to explain approximately 78.5% of the variation in beetle assemblage composition among the waterbodies sampled in the GRNP (Table 6 (a)). Although five of the variables were significantly associated with assemblage composition when considered independently (Table 6 (a)), only pH was selected in the step-wise (Table 6 (b)) and best overall (Table 6 (c)) AICc models when environmental variables were considered non-independently (i.e., accounting for the effects of other variables in the model). The most parsimonious model overall, considering all variable subsets, was that which included only pH. Despite being the most parsimonious, this model only accounts for ~8% of the variation in beetle assemblage composition and thus has very low explanatory power. Taken together, the results in Table 6 (a–c) indicate that, with the possible exception

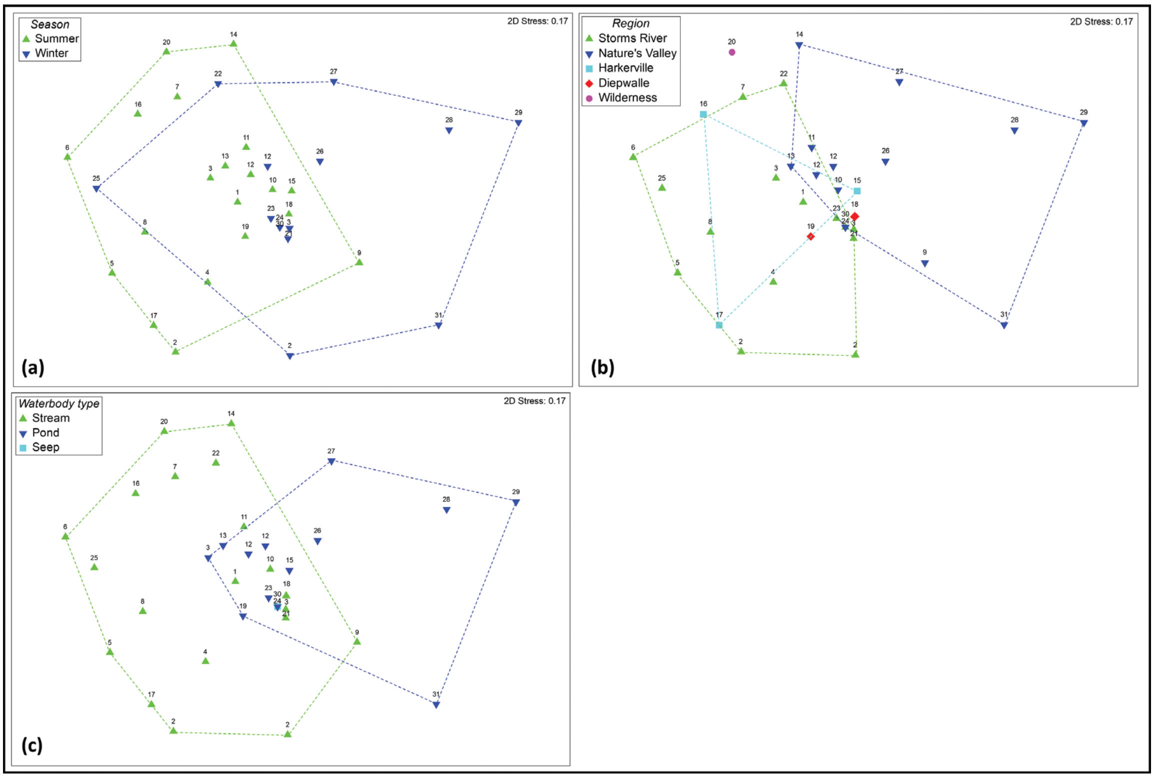

Figure 5. Multidimensional scaling (MDS) plots depicting the similarity of sites sampled at GRNP in terms of their water beetle assemblages. Symbols on the plot have been coded in terms of **a** season **b** region and **c** waterbody type. Convex hulls (dashed lines) have been overlaid on each plot to clarify groupings according to season, region, or waterbody type.

Table 5. Non-parametric permutational MANOVA (PERMANOVA) results for models comparing beetle assemblage composition across (a) seasons, (b) regions and (c) waterbody types. The multivariate models tested for differences between group centroids in Bray-Curtis dissimilarity space. SR: Storms River; NV: Nature's Valley; HV: Harkerville; DW: Diepwalle. For the regional comparison, Wilderness was not included due to only one site being sampled there on one occasion and for the comparison of waterbody types, 'seeps' was excluded as a factor because only one seep was sampled on one occasion (i.e., streams were compared with ponds). An asterisk indicates significant P values at α = 0.05.

(a)	df	SS	MS	F	P			
Season	1	6241.6	6241.6	2.20	0.018*			
Residual	32	90669	2833.4	–	–			
Total	33	96910	–	–	–			
(b)	**df**	**SS**	**MS**	**F**	**P**	***Post hoc pairwise comparisons***		
						Groups	**t**	**P**
Region	3	12497	4165.6	1.51	0.048*	SR, NV	1.477	0.021*
Residual	29	80134	2763.2	–	–	SR, HV	1.238	0.140
Total	32	92630	–	–	–	SR, DW	0.840	0.661
						NV, HV	1.265	0.103
						NV, DW	0.979	0.329
						HV, DW	1.282	0.155
(c)	**df**	**SS**	**MS**	**F**	**P**			
Waterbody type	1	6152.4	6152.4	2.136	0.033*			
Residual	31	89270	2879.7	–	–			
Total	32	95422	–	–	–			

Table 6. Results of the dbRDA multivariate regression tests of environmental variables against beetle assemblage composition. Independent marginal tests are first presented (a), followed by variables selected by the step-wise procedure using the AICc selection criterion (b) and the 'best' (most parsimonious, considering all combinations of variables) overall model according to the AICc criterion (c). '% Var': the percentage of variation in each Bray-Curtis similarity matrix that is explained by the respective predictor variable in each test; 'Cum. % var': the cumulative percentage variation across all tests; 'Res. df': residual degrees of freedom associated with each test. An asterisk indicates significant variables at α = 0.05.

(a) Marginal tests:

Variable	F	P	% Var
Latitude	1.24	0.240	3.99
Longitude	1.20	0.294	3.86
Season	2.01	0.036*	6.31
Altitude	1.05	0.405	3.40
Region: 'Storms River'	1.83	0.065	5.77
Region: 'Nature's Valley'	2.31	0.019*	7.16
Region: 'Harkerville'	1.48	0.136	4.72
Region: 'Diepwalle'	0.70	0.691	2.29
Waterbody type: 'Stream'	2.21	0.021*	6.89
Waterbody type: 'Pond'	2.01	0.042*	6.29
Waterbody type: 'Seep'	0.45	0.842	1.49
Temperature	1.85	0.053	5.84
Conductivity	1.17	0.33	3.78
DO	1.34	0.198	4.29
pH	2.64	0.006*	8.11
Depth	0.68	0.717	2.24
Turbidity	0.66	0.702	2.18
		Total:	78.59

(b) Sequential tests:

Variable	AICc	F	P	% Var.	Res. df
pH	256.1	2.64	0.01*	8.11	30

(c) Best solution:

Variable	AICc	F	P	% Var.	Res. df
pH	256.1	2.64	0.01*	8.11	30

of pH, none of the individual environmental variables had a particularly strong influence on beetle assemblages, but cumulatively they were able to explain most (~ 78.5%) of the variation in assemblage composition between sites. This cumulative amount of explained variation is relatively high, considering that this study did not involve exhaustive sampling of all potential explanatory environmental variables.

Discussion

Our work demonstrates that the waterbodies of forests of the Garden Route National Park support a diverse water beetle fauna, including a number of South African endemics. The total of 61 taxa recorded from the region is, however, considerably lower than the 116 reported from similar surveys by the same team in the subtropical iSimangaliso Wetland Park, further north on the KwaZulu-Natal coast (Perissinotto et al. 2016; Bird et al. 2017). It is also lower than the typical diversity reported from tropical forest systems in Africa and elsewhere. For example, Bilardo and Rocchi (2011) recorded 51 species of aquatic Adephaga (vs. 29 in GRNP) in the Monts de Cristal National Park, Gabon. Apenborn (2013) reported the collection of 122 species of aquatic beetles, representing ten different families, in the Peruvian Amazon near the Panguana Biological Field Station (Hendrich et al. 2015). In northern temperate forests, water beetle biodiversity can also often be higher than we observed in the southern Cape. In Knyszyn Primeval Forest in north-east Poland, for example, Greń et al. (2022) reported 128 species of aquatic Coleoptera from this approximately 1,000 km^2 site.

Of the species recorded here, 32 are endemic to South Africa. The vast majority of these are Cape endemics, more widespread in the fynbos biome to the west, and not tied to forest waterbodies. Such species include the dytiscids *Darwinhydrus solidus* Sharp, 1884 and *Hydropeplus trimaculatus* (Laporte, 1835), both of which are widespread and often abundant in lentic waters in fynbos in the far southwestern Cape, a number of the stream-dwelling *Mesoceration* (Hydraenidae) found in GRNP and the two lotic *Elpidelmis* species (Elmidae). Very few water beetle species found in these forests are either local endemics or forest specialists, the suite of taxa recorded during our surveys being dominated by species typical of fynbos waterbodies of the southern Cape (DTB, pers. obs.). Taxa which appear to be genuinely restricted to this region are *Aulonogyrus formosus knysnanus* Brinck, 1955 (Gyrinidae) and *Parhydraena asperita* Perkins, 2009 (Hydraenidae). Of these two, only the latter appears to be predominantly a forest species, which is particularly abundant in the margins of small standing waters filled with decaying leaf litter, although it has also been reported from stream margins in the nearby Little Karoo (Perkins 2009). Otherwise, the only forest specialist discovered during our surveys is *Aethionectes apicalis* (Boheman, 1848), a relatively widespread, large Afrotropical diving beetle (Omer-Cooper 1966), typically breeding in fish-free temporary waters with dead leaves. Interestingly, this targeted survey did not reveal any species new to science, and forested waterbodies in the region appear to be genuinely almost devoid of narrow-range endemics. This finding is in stark contrast to the situation in fynbos-dominated catchments, particularly further west in the Cape, where recent work has revealed a large number of apparently locally endemic species, particularly in the Hydraenidae (e.g., Bilton 2013a, b, 2014a, b, 2015a, b, c; Bilton and Mlambo 2019). Recent sampling in other remnant patches of Southern Afrotemperate Forest in the Cape (e.g., Grootevanderbosch in the Langberg) have also failed to find any locally endemic water beetles and Southern Afrotemperate Forest streams in general appear to support fewer species and individuals of most water beetle groups than similarly sized systems in fynbos (DTB, pers. obs.). Possible reasons behind this pattern remain unclear, but may relate to palaeogeographic changes (e.g., Lewis 2008; Quick et al. 2016) and levels of autochthonous productivity, particularly biofilm composition and availability, which may be lower in small, heavily shaded catchments. In the case of vertebrates, Lawes et al. (2007) suggested that the relative paucity of local endemics in Southern Afrotemperate Forests has resulted through a combination of climatic extinction filtering during the Pleistocene and the infiltration of assemblages by generalist species from surrounding matrix habitats. The lack of forest-specialist water beetles in GRNP suggests that similar processes may apply to the aquatic insect faunas here.

Our study demonstrates that there are clear, measurable, differences between the aquatic beetle assemblages in different forested sections of the Garden Route National Park, as revealed by nMDS and PERMANOVA analyses, but no significant differences in species richness. Clearly, despite these forested catchments being close geographically, there is significant spatial variation in aquatic habitats, reflected in the different beetle faunas. Interestingly, the relatively few environmental parameters recorded during our study are able to explain almost 79% of the variation in beetle assemblage composition across sites, suggesting that these measures capture the main environmental drivers of species composition in the region. In most studies, even with many more environmental parameters, the proportion of explained variation is typically much lower (e.g., Rundle et al. 2002).

In summary, our study documents the aquatic beetle faunas of southern Cape Afrotemperate Forests for the first time, providing an important baseline for future work in the area and similar habitats in other parts of southern Africa. We show that these systems support a wide range of water beetle species, including a number of South African endemics, but do not, apparently, harbour any truly local endemics, even in running waters. This observation is in marked contrast to streams draining fynbos catchments, particularly further west in the Cape, where high concentrations of locally endemic water beetles are known, many with Gondwanan affinities. Whilst de Moor and Bellingham (2019) note that the Trichoptera of the region includes a number of Cape endemics, the degree to which these are locally endemic to the Garden Route remains unclear.

Acknowledgements

Sampling in the Garden Route National Park was authorised by a research collection permit from South African National Parks (permit number: PERRI-R/2016-023). We are very grateful to Nerina Kruger (Science Liaison & GIS at South African National Parks Scientific Services, Sedgefield) and the managers of the various sections of the GRNP for providing general assistance with the project and logistic support during the two expeditions of this study. We would like to thank Lynette Clennell for assisting with field collections. Albrecht Komarek (Vienna) kindly examined the *Agraphydrus* species. This work is based on the research supported by the South African Research Chairs Initiative of the Department of Science and Technology (DST) and National Research Foundation (NRF) of South Africa. Any opinion, finding and conclusion or recommendation expressed in this material is that of the author(s) and the NRF does not accept any liability in this regard.

Additional information

Conflict of interest

No conflict of interest was declared.

Ethical statement

No ethical statement was reported.

Funding

National Research Foundation (NRF); Department of Science and Technology (DST).

Author contributions

Conceptualization: DTTB, MCM, MSB, RP. Data curation: MCM, DTTB. Formal analysis: MSB, MCM. Funding acquisition: RP. Investigation: DTTB, MCM, MSB, RP. Methodology: DTTB, MCM, RP, MSB. Project administration: RP. Resources: DTTB, RP. Software: MSB. Validation: MCM, DTTB. Visualization: MSB. Writing – original draft: MCM, MSB, RP, DTTB. Writing – review and editing: RP, DTTB, MSB, MCM.

Author ORCIDs

Matthew S. Bird https://orcid.org/0000-0001-9163-1008
David T. Bilton https://orcid.org/0000-0003-1136-0848
Musa C. Mlambo https://orcid.org/0000-0001-7624-5686
Renzo Perissinotto https://orcid.org/0000-0002-9224-3573

Data availability

All of the data that support the findings of this study are available in the main text or Supplementary Information.

References

Anderson MJ (2001) A new method for non-parametric multivariate analysis of variance. Austral Ecology 26: 32–46. https://doi.org/10.1111/j.1442-9993.2001.01070.pp.x

Anderson MJ, Gorley RN, Clarke KR (2008) PERMANOVA+ for PRIMER: Guide to software and statistical methods. PRIMER-E, Plymouth, UK.

Apenborn R (2013) Die Wasserkäferfauna von Panguana – Artenspektrum u Habitatansprüche. Unpublished thesis, Hochschule Zittau/Görlitz, 80 pp.

Beinhundner G (2017) The Cetoniinae of Africa. Gerhard Beinhundner, Euerbach, 1199 pp.

Bilardo A, Rocchi S (2011) Noteridae, Dytiscidae (Coleoptera) du Gabon (8ème partie). Monts de Cristal. Natural History Sciences : Atti della Societa Italiana di Scienze Naturali e del Museo Civico di Storia Naturale in Milano 152(2): 177–231. https://doi.org/10.4081/nhs.2011.177

Bilton DT (2013a) Description of the male of *Sebasthetops omaliniformis* Jäch, 1998 – a phylogenetically isolated water beetle from South Africa, with notes on its ecology (Coleoptera: Hydraenidae). Zootaxa 3635(1): 94–100. https://doi.org/10.11646/zootaxa.3635.1.10

Bilton DT (2013b) *Prosthetops wolfbergensis* sp. nov. – a giant amongst the 'minute moss beetles', with new data on other members of the genus (Coleoptera, Hydraenidae). Zootaxa 3666(3): 345–357. https://doi.org/10.11646/zootaxa.3666.3.5

Bilton DT (2014a) New species and new records of *Pterosthetops*: Eumadicolous water beetles of the South African Cape (Coleoptera, Hydraenidae). Zootaxa 3811(4): 438–462. https://doi.org/10.11646/zootaxa.3811.4.2

Bilton DT (2014b) Two new water beetles from the Hantamsberg, an inselberg in the Northern Cape of South Africa (Coleoptera, Hydraenidae). Zootaxa 3877(4): 471–480. https://doi.org/10.11646/zootaxa.3887.4.5

Bilton DT (2015a) New species and new records of *Mesoceration* from South Africa (Coleoptera: Hydraenidae). Zootaxa 3972: 495–520. https://doi.org/10.11646/zootaxa.3972.4.3

Bilton DT (2015b) Two new species of madicolous water beetle from South Africa (Coleoptera: Hydraenidae). African Invertebrates 56(1): 181–190. https://doi.org/10.5733/afin.056.0114

Bilton DT (2015c) A second *Sebasthetops* from South Africa (Coleoptera, Hydraenidae). Koleopterologische Rundschau 85: 73–80.

Bilton DT, Mlambo MC (2019) Two new *Mesoceration* Janssens, 967 from the Piketberg, South Africa (Coleoptera, Hydraenidae). Zootaxa 4555(2): 268–274. https://doi.org/10.11646/zootaxa.4555.2.7

Bilton DT, McAbendroth L, Bedford A, Ramsay PM (2006) How wide to cast the net? Cross-taxon congruence of species richness, community similarity and indicator taxa in ponds. Freshwater Biology 51(3): 578–590. https://doi.org/10.1111/j.1365-2427.2006.01505.x

Bilton DT, Ribera I, Short AEZ (2019) Water beetles as models in ecology and evolution. Annual Review of Entomology 64(1): 359–377. https://doi.org/10.1146/annurev-ento-011118-111829

Bird MS, Bilton DT, Perissinotto R (2017) Diversity and distribution of polyphagan water beetles (Coleoptera) in the Lake St Lucia system, South Africa. ZooKeys 656: 51–84. https://doi.org/10.3897/zookeys.656.11622

Bird MS, Mlambo MC, Wasserman RJ, Dalu T, Holland AJ, Day JA, Villet MH, Bilton DT, Barber-James HM, Brendonck L (2019) Deeper knowledge of shallow waters: Reviewing the invertebrate fauna of southern African temporary wetlands. Hydrobiologia 827(1): 89–121. https://doi.org/10.1007/s10750-018-3772-z

Burnham KP, Anderson DR (2002) Model selection and multimodel inference: a practical information-theoretic approach, 2nd edn. Springer-Verlag, New York, USA, 488 pp.

Clarke KR, Gorley RN (2015) PRIMER v7: User Manual/Tutorial. PRIMER-E: Plymouth.

Davis AL, Deschodt CM, Scholtz CH (2020) Conservation assessment of Scarabaeine dung beetles in South Africa, Botswana and Namibia: IUCN Red List categories, atlas and ecological notes. Suricata 6. South African National Biodiversity Institute, 799 pp.

de Moor FC, Bellingham TA (2019) Evaluation of the conservation requirements of Trichoptera from the Tsitsikamma mountain streams in South Africa. Zoosymposia 14(1): 151–164. https://doi.org/10.11646/zoosymposia.14.1.17

de Moor F, Day J (2013) Aquatic biodiversity in the mediterranean region of South Africa. Hydrobiologia 719: 237–268. https://doi.org/10.1007/s10750-013-1488-7

Eeley HAC, Lawes MJ, Piper SE (1999) The influence of climate change on the distribution of indigenous forest in KwaZulu-Natal, South Africa. Journal of Biogeography 26(3): 595–617. https://doi.org/10.1046/j.1365-2699.1999.00307.x

Ferrara F, Taiti S (1979) A check-list of terrestrial isopods from Africa (south of the Sahara). Monitore Zoologico Italiano 10(1): 89–215. https://doi.org/10.1080/03749444.1979.10736595

Geldenhuys CJ (1991) Distribution, size and ownership of forests in the southern Cape. Southern African Forestry Journal 158(1): 51–66. https://doi.org/10.1080/00382167.1991.9630375

Greń C, Lubecki K, Sućko K (2022) Chrząszcze wodne (Coleoptera: Hydradephaga, Hydrophiloidea, Hydraenidae, Dryopoidea) Puszczy Knyszyńkiej. Rocznik Muzeum Górnośląskiego Bytomiu Przyroda 28: 1–35.

Hamer ML (1998) A checklist of Southern African millipedes. Annals of the Natal Museum 39: 11–82.

Hendrich L, Apenborn R, Burmeister E-G, Balke M (2015) A new species of *Agaporomorphus* Zimmermann, 1921 from Peru (Coleoptera, Dytiscidae, Copelatinae). ZooKeys 512: 63–76. https://doi.org/10.3897/zookeys.512.9505

Hilton-Taylor C (2000) 2000 IUCN Red List of Threatened Species. IUCN, Gland and Cambridge.

Jäch MA, Balke M (2008) Global diversity of water beetles (Coleoptera) in freshwater. Hydrobiologia 595(1): 419–442. https://doi.org/10.1007/s10750-007-9117-y

Janák J, Makranczy G (2016) Description of a blind and flightless species of *Thinobius* from South Africa (Coleoptera: Staphylinidae: Oxytelinae). Acta Entomologica Musei Nationalis Pragae 56: 203–210.

Janion-Scheepers C, Measey J, Braschler B, Chown SL, Coetzee L, Colville JF, Dames J, Davies AB, Davies SJ, Davis AL, Dippenaar-Schoeman AS, Duffy GA, Fourie D, Griffiths C, Haddad CR, Hamer M, Herbert DG, Hugo-Coetzee EA, Jacobs A, Jacobs K, Rensburg CJ, Lamani S, Lotz LN, Louw SM, Lyle R, Malan AP, Marais M, Neethling J-A, Nxele TC, Plisko DJ, Prendini L, Rink AN, Swart A, Theron P, Truter M, Ueckermann E, Uys VM, Villet MH, Willows-Munro S, Wilson JRU (2016) Soil biota in a megadiverse country: Current knowledge and future research directions in South Africa. Pedobiologia 59(3): 129–174. https://doi.org/10.1016/j.pedobi.2016.03.004

Lawes MJ, Eeley HAC, Findlay NJ, Forbes D (2007) Resilient forest faunal communities in South Africa: A legacy of palaeoclimatic change and extinction filtering? Journal of Biogeography 34(7): 1246–1264. https://doi.org/10.1111/j.1365-2699.2007.01696.x

Legendre P, Anderson MJ (1999) Distance-based redundancy analysis: Testing multi-species responses in multi-factorial ecological experiments. Ecological Monographs 69(1): 1–24. https://doi.org/10.1890/0012-9615(1999)069[0001:DBRATM]2.0.CO;2

Lewis CA (2008) Late Quaternary climatic changes, and associated human responses, during the last ~45 000 yr in the Eastern and adjoining Western Cape, South Africa. Earth-Science Reviews 88(3–4): 167–187. https://doi.org/10.1016/j.earscirev.2008.01.006

McArdle BH, Anderson MJ (2001) Fitting multivariate models to community data: A comment on distance-based redundancy analysis. Ecology 82(1): 290–297. https://doi.org/10.1890/0012-9658(2001)082[0290:FMMTCD]2.0.CO;2

Meadows ME, Linder HP (1989) A reassessment of the biogeography and vegetation history of the southern Afromontane region. In: Geldenhuys CJ (Ed.) Biogeography of the mixed evergreen forests of southern Africa, 15–29. [FRD, Pretoria]

Midgley J, Schafer G (1992) Correlates of water colour in streams rising in Southern Cape catchments vegetated by fynbos and/or forest. Water S.A. 18: 93–100.

Moussalli A, Herbert DG, Stuart-Fox D (2009) A phylogeny of the cannibal snails of southern Africa, genus *Natalina* sensu lato (Pulmonata: Rhytididae): Assessing concordance between morphology and molecular data. Molecular Phylogenetics and Evolution 52(1): 167–182. https://doi.org/10.1016/j.ympev.2009.02.018

Mucina L, Geldenhuys CJ (2006) Afrotemperate, subtropical and azonal forests. In: Mucina L, Rutherford MC (Eds) The vegetation of South Africa, Lesotho and Swaziland. Strelitzia, 584–614.

Ollis D, Snaddon C, Job N, Mbona N (2013) Classification System for Wetlands and other Aquatic Ecosystems in South Africa. User Manual: Inland Systems. SANBI Biodiversity Series 22. South African National Biodiversity Institute, Pretoria, 110 pp.

Omer-Cooper J (1966) Coleoptera: Dytiscidae. Chapter 2. In: Hanström B, Brinck P, Rudebeck G (Eds) South African Animal Life 6: 59–214.

Passmore NI, Carruthers VC (1995) South African frogs. Southern Book Publishers and Witwatersrand University Press, Johannesburg.

Perera SJ, Herbert DG, Procheş Ş, Ramdhani S (2021) Land snail biogeography and endemism in south-eastern Africa: Implications for the Maputaland-Pondoland-Albany biodiversity hotspot. PLoS ONE 16(3): e0248040. https://doi.org/10.1371/journal.pone.0248040

Perissinotto R, Bird MS, Bilton DT (2016) Predaceous water beetles (Coleoptera, Hydradephaga) of the Lake St Lucia system, South Africa: Biodiversity, community ecology and conservation implications. ZooKeys 595: 85–135. https://doi.org/10.3897/zookeys.595.8614

Perkins PD (2009) Revisions of the genera *Parhydraena* Orchymont, *Protozantaena* Perkins, *Decarthrocerus* Orchymont, and *Parhydraenopsis* nomen novum, aquatic and humicolous beetles from Africa and Madagascar, and comparative morphology of the tribe Parhydraenini (Coleoptera: Hydraenidae). Zootaxa 2038(1): 1–119. https://doi.org/10.11646/zootaxa.2038.1.1

Picazo F, Bilton DT, Moreno JL, Sánchez-Fernández D, Millán A (2011) Water beetle biodiversity in Mediterranean standing waters: Assemblage composition, environmental drivers and nestedness patterns. Insect Diversity and Conservation 5(2): 146–158. https://doi.org/10.1111/j.1752-4598.2011.00144.x

Quick LJ, Meadows ME, Bateman MD, Kirsten KL, Mausbcher R, Haberzettl T, Chase BM (2016) Vegetation and climate dynamics during the last glacial period in the fynbos-afrotemperate forest ecotone, southern Cape, South Africa. Quaternary International 404: 136–149. https://doi.org/10.1016/j.quaint.2015.08.027

Quinn GP, Keough MJ (2002) Experimental design and data analysis for biologists. Cambridge University Press, Cambridge, United Kingdom, 537 pp. https://doi.org/10.1017/CBO9780511806384

Rundle SD, Foggo A, Choisel V, Bilton DT (2002) Are distribution patterns linked to dispersal mechanism? An investigation using pond invertebrate assemblages. Freshwater Biology 4(9): 1571–1581. https://doi.org/10.1046/j.1365-2427.2002.00886.x

Sánchez-Fernández D, Abellán P, Mellado A, Velasco J, Millán A (2006) Are water beetles good indicators of biodiversity in Mediterranean aquatic ecosystems? The case of the Segura River basin (SE Spain). Biodiversity and Conservation 15(14): 4507–4520. https://doi.org/10.1007/s10531-005-5101-x

Solidovnikov AYU, Newton AF (2004) Phylogenetic placement of Arrowinini trib.n. within the subfamily Staphylininae (Coleoptera: Staphylinidae), with revision of the relict South African genus *Arrowinus* and description of its larva. Systematic Entomology 30(3): 398–441. https://doi.org/10.1111/j.1365-3113.2004.00283.x

Stuart-Fox D, Moussalli A (2007) Sex-specific ecomorphological variation and the evolution of sexual dimorphism in dwarf chameleons (*Bradypodion* spp.). Journal of Evolutionary Biology 20(3): 1073–1081. https://doi.org/10.1111/j.1420-9101.2007.01295.x

Swart RC, Samways MJ, Roets F (2021) Latitude, paleo-history and forest size matter for Afromontane canopy beetle diversity in a world context. Biodiversity and Conservation 30(3): 659–672. https://doi.org/10.1007/s10531-020-02108-0

Tolley KA, Tilbury CR, Branch WR, Matthee CA (2004) Evolutionary history and phylogenetics of the southern African dwarf chameleons, *Bradypodion*. Molecular Phylogenetics and Evolution 30: 354–365. https://doi.org/10.1016/S1055-7903(03)00211-2

ZooKeys 1182: 259–287 (2023)
DOI: 10.3897/zookeys.1182.105030

Research Article

Phylogeography and genetic diversity of the Japanese mud shrimp *Upogebia major* (Crustacea, Decapoda, Upogebiidae): Natural or anthropogenic dispersal?

Kyosuke Kitabatake[1], Kentaro Izumi[2], Natsuko I. Kondo[3], Kenji Okoshi[1]

1 *Graduate School of Science, Toho University, 2-2-1 Miyama, Funabashi, Chiba 274-8510, Japan*
2 *Faculty and Graduate School of Education, Chiba University, 1-33 Yayoi-cho, Inage-ku, Chiba-shi, Chiba 263-8522, Japan*
3 *Biodiversity Division, National Institute for Environmental Studies, 16-2 Onogawa, Tsukuba, Ibaraki 305-8506, Japan*
Corresponding author: Kyosuke Kitabatake (kyosuke.kitabatake@gmail.com)

Abstract

Upogebia major (De Haan, 1841) is known for forming huge burrows in sandy, intertidal areas that can extend to depths of over 2 m. Despite its widespread distribution in East Asia and Russia, the genetic relatedness of its regional populations remains uncertain, likely owing to difficulties in specimen collection. Therefore, to appraise the phylogeographic patterns, genetic diversity, and morphological variety of *U. major*, the mitochondrial DNA of specimens collected from Japan, Korea and China were subjected to molecular phylogenetic analyses of COI genes, alongside morphological assessment. As a result, we discovered four principal groups; of these, Group 1 consisted predominantly of Japanese specimens, while Groups 3 and 4 were interpreted as having originated from the continent. Group 2 exhibited genetic segregation from both continental and Japanese descent. Group 1 mostly comprising Japanese specimens implies that the planktonic larvae of *U. major* were disseminated north and south by ocean currents encompassing the Japanese archipelago. In contrast, individuals probably originating from the continent were discovered in Lake Notoro, Hokkaido and Matsukawa-ura, Fukushima in northeastern Japan, indicating possible introduction from the continent through ocean currents or unintentional introduction with other organisms imported. Additionally, one of the specimens collected from Matsukawa-ura exhibited significant genetic and morphological differences from other specimens, suggesting the possibility of being a subspecies. The outcomes of this study not only offer valuable insights into the origins of distribution of *U. major* but also introduce a novel challenge of assessing the coexistence of two routes: natural and anthropogenic dispersion.

Key words: Artificial introduction, Geographical distribution, Molecular phylogenetics, Morphological analysis, Ocean current, Topographic change, *Upogebia major*

Academic editor: Célio Magalhães
Received: 19 April 2023
Accepted: 8 August 2023
Published: 19 October 2023

ZooBank: https://zoobank.org/840985BB-25CF-4BEE-830D-172D996A9F26

Citation: Kitabatake K, Izumi K, Kondo NI, Okoshi K (2023) Phylogeography and genetic diversity of the Japanese mud shrimp *Upogebia major* (Crustacea, Decapoda, Upogebiidae): natural or anthropogenic dispersal? ZooKeys 1182: 259–287. https://doi.org/10.3897/zookeys.1182.105030

Introduction

The *Upogebia* genus constitutes a cluster of crustaceans, commonly referred to as mud shrimp, which inhabit all corners of the world and encompass approximately 280 species. Amongst these, the Japanese archipelago harbours 13 species (Komai 2020). Several of these species are characterised by their capacity to construct extensive burrows exceeding depths of 1 m. In particular, *Upogebia major* (De Haan 1841), is renowned for its ability to create large Y-shaped burrow, some exceeding depths of 2 m, in substrates such as slightly silty sand within the shallow waters of the coastal regions of the Japanese archipelago, Korean Peninsula, Shandong Peninsula, and the Russian coast facing the Sea of Japan (Kinoshita 2002; Itani 2004; Sakai 2006; Selin 2017; Kinoshita 2022). Collecting this species poses a considerable challenge because of its deep burrow habitat and poorly understood ecological characteristics. However, *U. major* is an active edificator that plays a pivotal role in shaping the qualitative composition and abundance of benthic organisms (Kinoshita et al. 2008; Hong 2013; Kinoshita 2022). The abundance of *U. major* and its bioturbation activities have made it the subject of increasing scientific interest as an essential contributor to the structure of benthic communities. In particular, this species has garnered attention as a host for numerous symbiotic organisms within its burrows and on its body (Kinoshita et al. 2008; Seike and Goto 2020; Shiozaki and Itani 2020). Similar research has been conducted on closely-related species such as *Upogebia yokoyai* (Henmi and Itani 2014, 2021). Larger specimens of *U. major* are commonly harvested and consumed in Western Japan and South Korea (Sato 2000; Ngoc-Ho 2001; Hong 2013; Das et al. 2017), whereas smaller specimens are employed as fishing bait in Japan (Kitabatake, personal observation). Despite extensive research on the ecology, environment, symbiotic relationships and economic implications of *U. major*, phylogenetic and genetic investigations are limited and the origins of local populations remain largely unknown despite their wide distribution in East Asia and Russia. Recently, genetic analyses utilising complete mitochondrial genomes have elucidated the evolutionary history of *U. major* at the familial and generic levels, indicating its close affiliation with members of the Thalassinidae family, with *U. yokoyai* as its closest relative (Sun and He 2021). Nonetheless, intraspecific research on *U. major* remains limited and a comprehensive assessment of its phylogeography and genetic diversity has yet to be accomplished. These data could shed light on the migration and dispersal processes that underlie the geographical distribution of this species.

The study of the phylogeography and genetic diversity of benthic organisms inhabiting coastal marine waters has been extensively researched on a global scale. For instance, *Oratosquilla oratoria* and *Eriocheir japonica*, crustaceans that inhabit the coast of China facing the East China Sea, display marked genetic divergence between the northern and southern regions of China, primarily because of topographic changes associated with the opening of the Sea of Japan (Zhang et al. 2014). The echinoderm *Ophiura sarsii*, which is widely distributed throughout the Arctic and sub-Arctic regions of the Atlantic and Pacific Oceans, exhibits a marked genetic diversity in the Barents Sea. Their population and spatial expansion are hypothesised to have taken place in the Barents Sea during the Bølling–Allerød interglacial epoch of the melting glacial period in the western margin region of the Barents Sea (Genelt-Yanovskiy et al. 2021). Furthermore, the unintentional migration of the Caribbean polychaete *Branchiomma bairdi*, facilitated by commercial shipping, led to its discovery in Tunisia, where the genetic features of native individuals were similar to those of introduced individuals (Khedhri et al. 2017). Several analogous studies have been documented around the Japanese archipelago, albeit their quantity is limited. For example, *Turbo sa-*

zae, a rocky reef inhabitant and *Batillaria cumingii*, a mud flat dweller, exhibit distinct haplotypes on the Sea of Japan and Pacific sides of the Japanese archipelago (Kojima et al. 1997, 2000, 2004; Yanagimoto et al. 2022). This differentiation is attributed to gene flow via separate ocean currents on the Sea of Japan and the Pacific. Additionally, the crustacean *Tachypleus tridentatus*, distributed from south-eastern to western Japan, was found in Mikawa Bay in central Japan with a haplotype of Chinese origin, likely originating from individuals introduced from China for commercial purposes and is now considered an alien species (Nishida et al. 2015). Thus, a multitude of prior investigations regarding phylogeography and genetic diversity have demonstrated that the geographical distribution of marine benthos results from the complex interplay of physical and anthropogenic factors. Conversely, research on epifaunal organisms, which are readily collected, has taken centre stage, whereas enquiries into infaunal species, such as *U. major*, which are deeply embedded in sediments, appear to be scarce.

In this study, molecular phylogenetic analyses were performed on *U. major* specimens collected from Japan, Korea and China. A phylogenetic tree and haplotype network, based on the cytochrome *c* oxidase subunit I (COI) of mitochondrial DNA, were constructed to reveal detailed interspecific relationships. Furthermore, the calculation of pairwise population differentiation (F_{ST}) and analysis of molecular variance (AMOVA) were performed to scrutinise the genetic variation amongst populations. Morphological measurements were conducted to examine the possible correlations between genetic variation and morphological characteristics. Through these examinations, the phylogeography and genetic diversity of *U. major* were evaluated and the physical and anthropogenic factors responsible for the genetic differentiation of the species in the vicinity of the Japanese archipelago were discussed. The findings of this study provide crucial insights into the geographical origins of *U. major*.

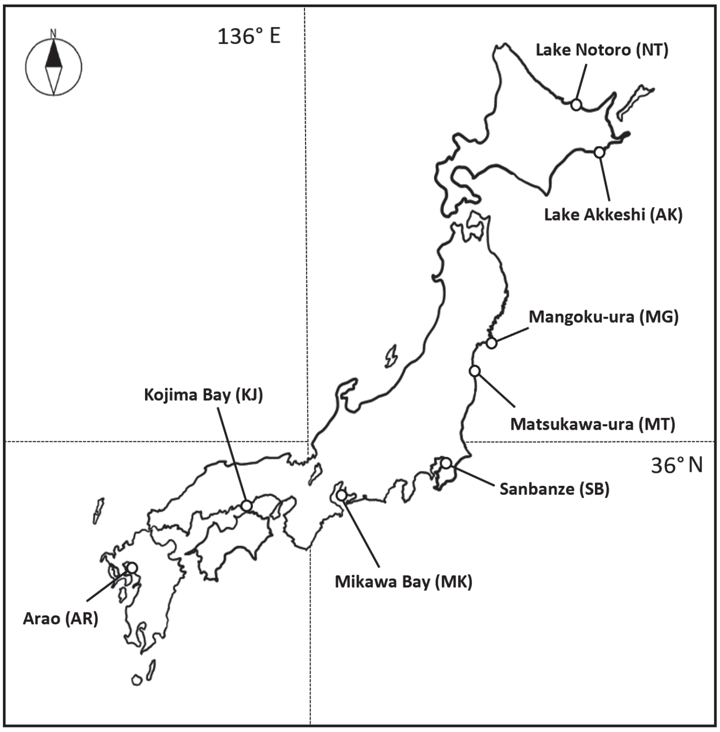

Figure 1. Map of the sampling sites for *Upogebia major* examined in this study.

Materials and methods

Sampling sites

Samples of *U. major* were collected during the period of September 2021 to July 2022 from five sites in east and northern Japan (Fig. 1) by brush and yabbie pump (Poseidon, Aichi, Japan) during low tide. The sampling sites are Lake Notoro (NT) and Lake Akkeshi, Hokkaido (AK), Mangoku-ura, Lagoon (or Inlet), Miyagi (MG), Matsukawa-ura, Lagoon, Fukushima (MT) and Sanbanze, Chiba (SB). *U. major* lived at high densities (at least 20 to over 100 burrows per square metre) at the AK sites. In addition, *U. major* purchased from the following areas at Mikawa Bay, Aichi (MK), Kojima Bay, Okayama (KJ) and Arao, Kumamoto (AR) were stored at -25 °C immediately after collection. A total of 53 samples were analysed: nine from NT, three from AK, seven from MG, seven from MT, five from SB, seven from MK, 11 from KJ and four from AR, respectively (Table 1).

Table 1. (A) Provides a comprehensive representation of *U. major*, a Japanese species, that was obtained for this study. The depiction encompasses a multitude of details, including sample code, collection site, date of collection, isolation source and gene. (B) Depicts nucleotide sequence data obtained from GenBank, including crucial information such as sample code, species, accession number and elaborate information concerning collection location, literature and gene. The collected location of SK-03-05 was procured and has been verified by GBIF (Global Biodiversity Information Facility) (https://www.gbif.org/ja/species/2222995) on the grounds of the voucher number itemised in the registration information of the Accession Number.

A	Sample code	Collected location	Geographical coordinates	Collected date	Isolation source	Gene	Accession No.
	NT-01	Lake Notoro, Hokkaido	44.0425°N, 144.1704°E	29.july.22	Abdomen tissue	COI	LC761102
	NT-02	Lake Notoro, Hokkaido	44.0425°N, 144.1704°E	29.july.22	Abdomen tissue	COI	LC761103
	NT-03	Lake Notoro, Hokkaido	44.0425°N, 144.1704°E	29.july.22	Abdomen tissue	COI	LC761104
	NT-04	Lake Notoro, Hokkaido	44.0425°N, 144.1704°E	29.july.22	Abdomen tissue	COI	LC761105
	NT-05	Lake Notoro, Hokkaido	44.0425°N, 144.1704°E	29.july.22	Abdomen tissue	COI	LC761106
	NT-06	Lake Notoro, Hokkaido	44.0425°N, 144.1704°E	29.july.22	Abdomen tissue	COI	LC761107
	NT-07	Lake Notoro, Hokkaido	44.0425°N, 144.1704°E	29.july.22	Abdomen tissue	COI	LC761108
	NT-08	Lake Notoro, Hokkaido	44.0425°N, 144.1704°E	29.july.22	Abdomen tissue	COI	LC761109
	NT-09	Lake Notoro, Hokkaido	44.0425°N, 144.1704°E	29.july.22	Abdomen tissue	COI	LC761110
	AK-01	Lake Akkeshi, Hokkaido	43.0256°N, 144.8792°E	28.july.22	Abdomen tissue	COI	LC761111
	AK-02	Lake Akkeshi, Hokkaido	43.0256°N, 144.8792°E	28.july.22	Abdomen tissue	COI	LC761112
	AK-03	Lake Akkeshi, Hokkaido	43.0256°N, 144.8792°E	28.july.22	Abdomen tissue	COI	LC761113
	MG-01	Mangoku-ura, Miyagi	38.4185°N, 141.3820°E	22.March.22	Abdomen tissue	COI	LC761114
	MG-02	Mangoku-ura, Miyagi	38.4185°N, 141.3820°E	22.March.22	Abdomen tissue	COI	LC761115
	MG-03	Mangoku-ura, Miyagi	38.4185°N, 141.3820°E	22.March.22	Abdomen tissue	COI	LC761116
	MG-04	Mangoku-ura, Miyagi	38.4185°N, 141.3820°E	22.March.22	Abdomen tissue	COI	LC761117
	MG-05	Mangoku-ura, Miyagi	38.4185°N, 141.3820°E	19.May.22	Abdomen tissue	COI	LC761118
	MG-06	Mangoku-ura, Miyagi	38.4185°N, 141.3820°E	19.May.22	Abdomen tissue	COI	LC761119
	MG-07	Mangoku-ura, Miyagi	38.4185°N, 141.3820°E	19.May.22	Abdomen tissue	COI	LC761120
	MT-01	Matsukaura, Fukushima	37.8128°N, 140.9723°E	21.September.21	Manus tissue	COI	LC761121
	MT-02	Matsukaura, Fukushima	37.8128°N, 140.9723°E	21.September.21	Manus tissue	COI	LC761122
	MT-03	Matsukaura, Fukushima	37.8128°N, 140.9723°E	21.September.21	Manus tissue	COI	LC761123
	MT-04	Matsukaura, Fukushima	37.8128°N, 140.9723°E	20.May.22	Abdomen tissue	COI	LC761124

A	**Sample code**	**Collected location**	**Geographical coordinates**	**Collected date**	**Isolation source**	**Gene**	**Accession No.**
	MT-05	Matsukaura, Fukushima	37.8128°N, 140.9723°E	20.May.22	Abdomen tissue	COI	LC761125
	MT-06	Matsukaura, Fukushima	37.8128°N, 140.9723°E	20.May.22	Abdomen tissue	COI	LC761126
	MT-07	Matsukaura, Fukushima	37.8128°N, 140.9723°E	20.May.22	Abdomen tissue	COI	LC761127
	SB-01	Sanbanze, Chiba	35.6709°N, 139.9689°E	5.October.21	Manus tissue	COI	LC761128
	SB-02	Sanbanze, Chiba	35.6709°N, 139.9689°E	5.October.21	Manus tissue	COI	LC761129
	SB-03	Sanbanze, Chiba	35.6709°N, 139.9689°E	5.October.21	Manus tissue	COI	LC761130
	SB-04	Sanbanze, Chiba	35.6709°N, 139.9689°E	5.October.21	Manus tissue	COI	LC761131
	SB-05	Sanbanze, Chiba	35.6709°N, 139.9689°E	1.july.22	Abdomen tissue	COI	LC761132
	MK-01	Mikawa Bay, Aichi	Unknown	Purchased	Manus tissue	COI	LC761133
	MK-02	Mikawa Bay, Aichi	Unknown	Purchased	Manus tissue	COI	LC761134
	MK-03	Mikawa Bay, Aichi	Unknown	Purchased	Manus tissue	COI	LC761135
	MK-04	Mikawa Bay, Aichi	Unknown	Purchased	Manus tissue	COI	LC761136
	MK-05	Mikawa Bay, Aichi	Unknown	Purchased	Manus tissue	COI	LC761137
	MK-06	Mikawa Bay, Aichi	Unknown	Purchased	Abdomen tissue	COI	LC761138
	MK-07	Mikawa Bay, Aichi	Unknown	Purchased	Abdomen tissue	COI	LC761139
	KJ-01	Kojima Bay, Okayama	Unknown	Purchased	Manus tissue	COI	LC761140
	KJ-02	Kojima Bay, Okayama	Unknown	Purchased	Manus tissue	COI	LC761141
	KJ-03	Kojima Bay, Okayama	Unknown	Purchased	Manus tissue	COI	LC761142
	KJ-04	Kojima Bay, Okayama	Unknown	Purchased	Manus tissue	COI	LC761143
	KJ-05	Kojima Bay, Okayama	Unknown	Purchased	Manus tissue	COI	LC761144
	KJ-06	Kojima Bay, Okayama	Unknown	Purchased	Abdomen tissue	COI	LC761145
	KJ-07	Kojima Bay, Okayama	Unknown	Purchased	Abdomen tissue	COI	LC761146
	KJ-08	Kojima Bay, Okayama	Unknown	Purchased	Abdomen tissue	COI	LC761147
	KJ-09	Kojima Bay, Okayama	Unknown	Purchased	Abdomen tissue	COI	LC761148
	KJ-10	Kojima Bay, Okayama	Unknown	Purchased	Abdomen tissue	COI	LC761149
	KJ-11	Kojima Bay, Okayama	Unknown	Purchased	Abdomen tissue	COI	LC761150
	AR-01	Arao, Kumamoto	Unknown	Purchased	Manus tissue	COI	LC761151
	AR-02	Arao, Kumamoto	Unknown	Purchased	Manus tissue	COI	LC761152
	AR-03	Arao, Kumamoto	Unknown	Purchased	Manus tissue	COI	LC761153
	AR-04	Arao, Kumamoto	Unknown	Purchased	Manus tissue	COI	LC761154
B	**Sample code, Species**	**Collected location**	**Gene**	**Reffrence**	**Accession No.**		
	SK-01	Seosan, South Korea	COI	Kim et al. (2011)	JF793665.1		
	SK-02	South Korea	COI	Kim et al. (Unpublished)	JX502989.1		
	SK-03	South Korea	COI	Kim et al. (Unpublished)	JX502990.1		
	SK-04	Gyeonggi-do, South Korea	COI	Kim, (Unpublished)	OL876961.1		
	SK-05	Gyeonggi-do, South Korea	COI	Kim, (Unpublished)	OL876962.1		
	SK-06	Gyeonggi-do, South Korea	COI	Kim, (Unpublished)	OL876963.1		
	CH-01	Qingdao, China	COI	Liu et al. (2012)	JN897377.1		
	Upogebia yokoyai	Jeju-do, Korea	COI	Yang et al. (2014)	NC_025943.1		
	Wolffogebia heterocheir	India	COI	Rengaiyan et al. (2019)	MN579655.1		

DNA extraction, PCR amplification and Sequencing

Less than 10 mg of abdominal tissue was removed from adult samples for DNA analysis. DNA was extracted using the ISOSPIN Tissue DNA Kit (NIPPON GENE, Tokyo, Japan) and stored at -25 °C until use.

Polymerase chain reaction (PCR) was used to amplify the COI region of the mitochondrial DNA. Up to 658 bp from the COI region was amplified using the universal primers LCO1490: 5'-GGTCAACAAATCATAAAGATATTG-3' and HCO2198: 5'-TAAACTTCAGGGTGACCAAAAAATCA-3' (Folmer et al. 1994). Each 20 μl PCR reaction consisted of 2.0 μl of extracted DNA (undiluted solution), 0.4 μl of KOD FX (1.0 U/μl) (TOYOBO, Osaka, Japan), 4.0 μl of 2.0 mM of each dNTP, 10 μl of 2× PCR buffer for KOD FX, 2.4 μl Nuclease-free water (Thermo Fisher Scientific, Waltham, MA, USA) and 0.6 μl of each primer (10 pmol/μl). Gene Atlas 322 (ASTEC, Fukuoka, Japan) was used as the thermal cycler for PCR. The PCR reactions consisted of an initial denaturation cycle at 94 °C for 2 min, 40 cycles of 98 °C for 10 s, 40 °C for 30 s, 68 °C for 1 min, and a final cycle at 10 °C for 1 min. PCR products were loaded onto an agarose gel with MIDORI Green Advance Agarose Tablets (Nippon Genetics, Tokyo, Japan) and separated by electrophoresis in 1× TAE buffer. Separated DNA fragments were observed under blue/green LED light. All PCR products were purified using Illustra ExoProStar (GE Healthcare, Chicago, USA) and sequenced with a Big Dye Terminator v.3.1 Cycle Sequencing Kit (Thermo Fisher Scientific, Waltham, MA, USA) by contracting to the FASMAC sequencing service (FASMAC, Kanagawa, Japan).

Population and phylogenetic analyses

We conducted sequence analyses on 53 specimens of *U. major* for the COI gene, incorporating data obtained from GenBank for three species: *U. major* from Korea (Accession numbers: JF793665, JX502989, JX502990, OL876961, OL876962, OL876963) and China (JN897377), the closest relative species *U. yokoyai* (NC_025943) and *Wolffogebia heterocheire* (MN579655) as an outgroup, all with COI gene sequences (Table 1). All sequences were aligned using the MEGA X software (Kumar et al. 2018) and adjusted using the BioEdit v.7.0.5.3 software (http://www.mbio.ncsu.edu/BioEdit/bioedit.html). The assembled sequences were manually inspected for quality. Unique haplotypes were identified and used for further analyses. Obtained haplotypes are deposited via DNA Data Bank of Japan (DDBJ) with DDBJ/EMBL/GenBank accession numbers (LC761102–LC761154). Phylogenetic trees were constructed using the maximum-likelihood (ML) method, based on the Tamura 3-parameter model with a discrete gamma distribution (T92 + G) (Suppl. material 1: appendix S1) and the reliability of the trees was tested with 1,000 bootstrap replicates (Felsenstein 1985) using MEGA X software (Kumar et al. 2018). The MEGA X software was utilised to ascertain the differential count of bases between sequences through the application of the “No. for the difference” metric. The “Kimura 2-parameter model” was used to determine the genetic distance between the sequences.

The estimation of haplotypes, haplotype diversity (*h*) and nucleotide diversity (π) was performed through the utilisation of DnaSP v.6.12.03. The F_{ST} values between populations were executed using Arlequin v.3.5.2.2 and the K2P distance metric (Kimura 1980). A haplotype network was constructed to visually depict the genetic distances between haplotypes using Network 10 (Forster et al. 1996). Furthermore, AMOVA was carried out by utilising Arlequin v.3.5.2.2 to identify any disparities in genetic structure amongst the groups. The haplotype data and the preparation of datasets in .hap and .arp format were performed through the use of DnaSP v.6.10.01. The relevant *p*-values were determined through 1023 permutations.

Morphological examination

The parts for morphometric measurements are shown in Fig. 2. An electronic caliper (Shinwa, Niigata, Japan) was employed to ascertain the carapace length and width (CL, CW), as well as the length of the six pleomeres (PL 1 to 6). Additionally, measurements were obtained for the telson length and width (TL, TW). The propodus length (PRL) and the width of the manus (MW) were also determined bilaterally. Furthermore, considering the fact that at least female individuals achieve sexual maturity upon attaining a minimum CL of 25 mm (Kinoshita et al. 2003), we probed the correlation between CL and other morphological

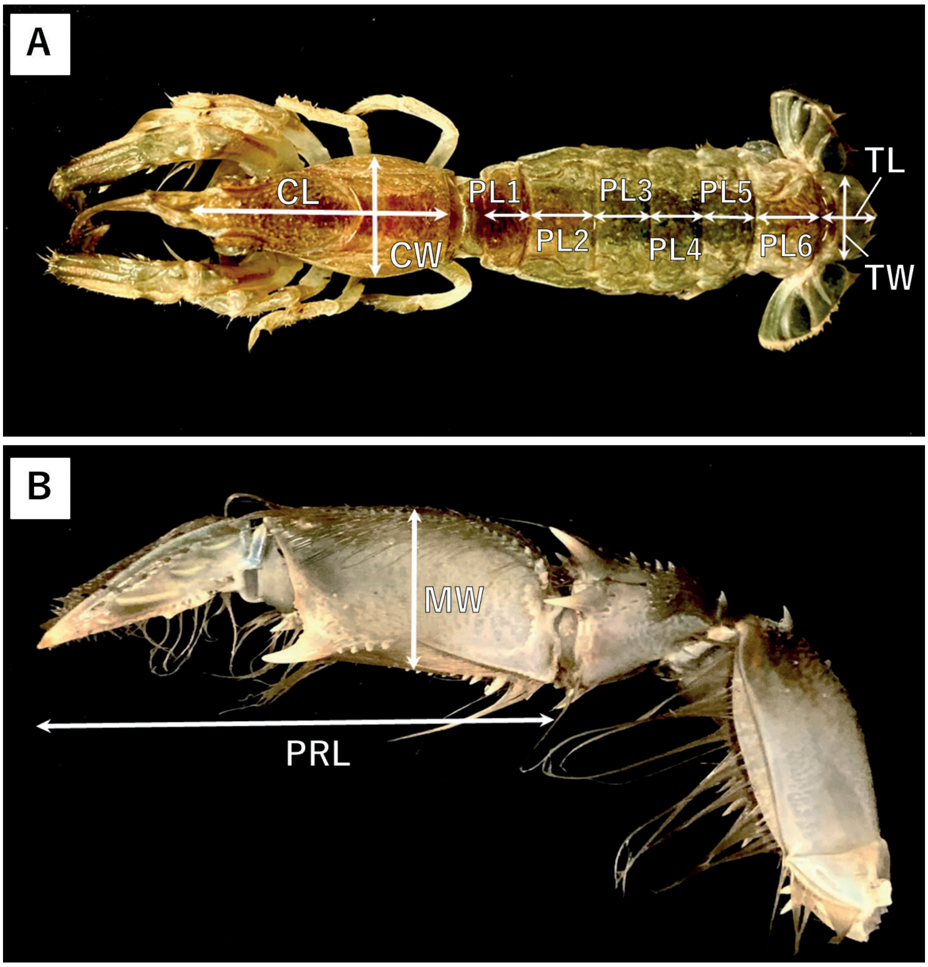

Figure 2. The site at which the morphometric assessments were conducted of *U. major* **A** CL: Carapace Length, CW: Carapace Width, PL 1–6: Pleomeres Length, 1–6, PTL: Pleomeres Total Length, TL: Telson Length, TW: Telson Width **B** MW: Manus Width, PRL: Propodus Length.

parameters in individuals with a CL greater than 25 mm. It is worth noting that the measurement data of adult *U. yokoyai* (n = 8), the closest relative species, were also included in this analysis to examine the inter-species differences in morphology. The specimens of *U. yokoyai* used in this study were collected in Uranouchi Inlet, Kochi, Southwest Japan in October 2021. All measurements were performed to the nearest 0.01 mm. To discriminate variations in morphological characteristics, we performed an extensive observation and analysis of all traits, including the parts where morphometric measurements were taken, by utilising the AndonStar ADSM302 video microscope.

Data resources

The data underpinning the analysis reported in this paper are deposited at GBIF, the Global Biodiversity Information Facility and are available at https://doi.org/10.15468/wmdf6k.

Results

Molecular phylogeny and genetic diversity

The final compilation of data comprised 637 bp of COI sequences from a total of 62 samples of *U. major*, outgroup species *W. heterocheire* and the closely-related outgroup species *U. yokoyai*.

Concatenate sequences are shown in Fig. 3. Based on the ML analyses, *U. major* is distinctly separated from its outgroups and closest species, forming its own clade, in which four groups were recognised. Group 1 constitutes a clade primarily composed of Japanese specimens, with only one individual

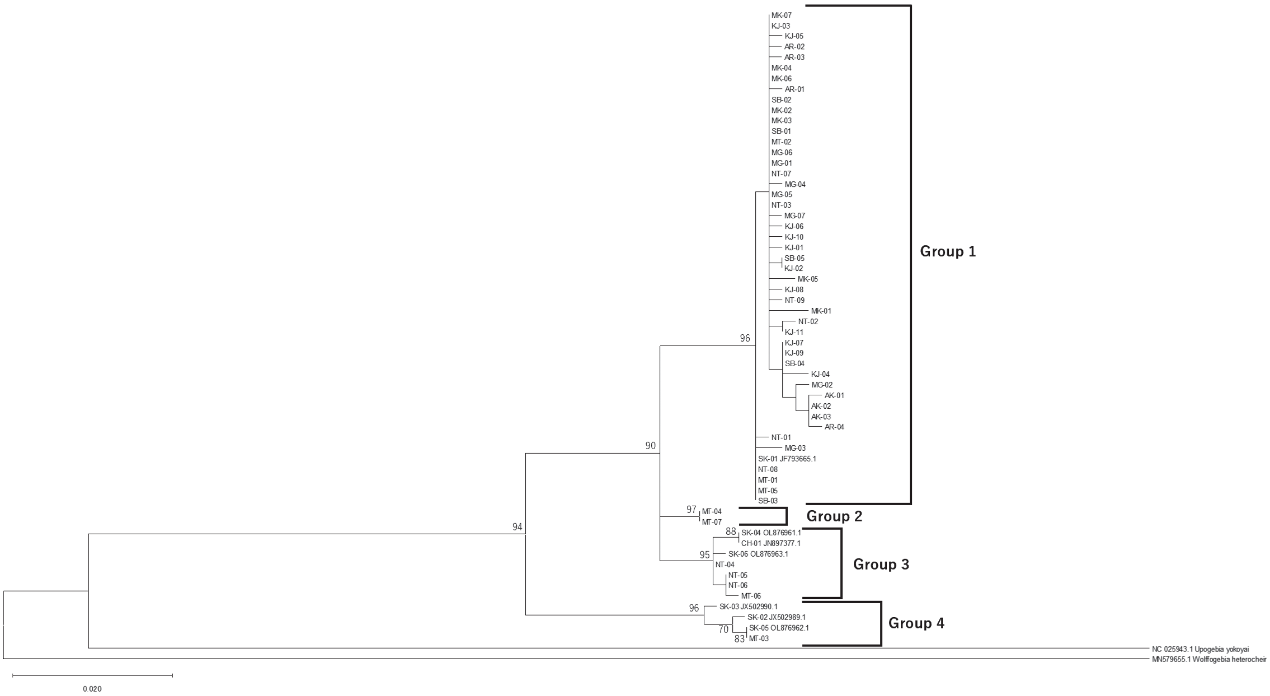

Figure 3. Maximum likelihood tree of concatenated COI sequences. Only bootstrap values exceeding a threshold of 70% were exhibited.

from South Korea (SK-01) included. Conversely, Group 2 forms a clade exclusively comprised of Matsukawa-ura specimens (MT-04, 07). Group 3 encompasses specimens from Lake Notoro, Matsukawa-ura, Korea and China. Group 4, in contrast, constitutes an independent clade comprised of three specimens from Korea and one from Matsukawa-ura (MT-03). Groups 1 and 2 were of Japanese descent, except for one specimen, whereas Groups 3 and 4 consist of both Japanese and continental specimens forming the clade.

The disparity in base number between Group 2 and Group 3 was found to be minimal, ranging from 7 to 9 bp, while Group 1 and Group 4 showed a significant difference of 29 to 34 bp (Table 2A). Additionally, the genetic distance between Group 2 and Group 3 was small, ranging from 0.011 to 0.014, whereas Group 1 and Group 4 displayed a larger difference, ranging from 0.047 to 0.056 (Table 2B). In particular, MT-03, a specimen of Group 4, exhibited a maximum disparity of 34 bp in base counts and a maximum genetic distance of 0.056 from MT-02, the Matsukawa-ura specimen pertaining to Group 1, thereby rendering them genetically remote from each other. These findings imply that Matsukawa-ura harbours *U. major* with highly divergent genetic characteristics within a single location.

Utilisation of the DnaSP software yielded 35 COI haplotypes (Table 3). Lake Notoro and Matsukawa-ura exhibited a predilection for elevated levels of haplotype diversity (h: 0.944, 0.905) and nucleotide diversity (π: 0.0115, 0.0224), respectively, in comparison to the remaining populations. In contrast, Sanbanze and Kojima Bay displayed higher values of haplotype diversity within the range of 0.900, but comparatively lower base diversity. Haplotype network analysis revealed that the haplotypes of *U. major* could be segregated into four principal groups (Fig. 4), which revealed the genetic distances between the four groups shown in the phylogenetic tree. Moreover, it was explicitly demonstrated that Group 4, which encompasses MT-03, is genetically distant from other groups.

Pairwise F_{ST} revealed genetic differentiation in all groups (F_{ST} = 0.7931 to 0.9388, p < 0.05) (Table 4). The F_{ST} values between Groups 1 and 2, primarily comprising Japanese specimens, and Group 3, consisting of continental specimens, were 0.8445 and 0.7931, respectively. Group 2 demonstrated substantial

Table 2. (A) The maximum, minimum, mean and standard deviation of the base number differences between groups. (B) The maximum, minimum, mean and standard deviation of the genetic distance between groups.

		Between Group 1 and Group 2	Between Group 1 and Group 3	Between Group 1 and Group 4	Between Group 2 and Group 3	Between Group 2 and Group 4	Between Group 3 and Group 4
A	Maximum	14	17	34	9	27	29
	Minimum	10	11	29	7	25	25
	Mean	11.5	13.8	31.3	8.3	26.0	26.8
	Standard deviation	0.862	1.114	1.271	0.699	1.000	1.115
B	Maximum	0.022	0.027	0.056	0.014	0.044	0.047
	Minimum	0.016	0.018	0.047	0.011	0.041	0.041
	Mean	0.018	0.022	0.051	0.013	0.042	0.043
	Standard deviation	0.001	0.002	0.002	0.001	0.002	0.002

Table 3. Frequencies of selected haplotypes, haplotype diversity (*h*) and nucleotide diversity (*π*) in local samples from Japan, South Korea and China.

COI haplotype	Local populations									Total
	SK/CH	NT	AK	MG	MT	SB	MK	KJ	AR	
H_1	1	0	0	0	0	0	0	0	0	1
H_2	1	0	0	0	0	0	0	0	0	1
H_3	1	0	0	0	0	0	0	0	0	1
H_4	1	0	0	0	1	0	0	0	0	2
H_5	2	0	0	0	0	0	0	0	0	2
H_6	1	1	0	0	2	1	0	0	0	5
H_7	0	0	1	0	0	0	0	0	0	1
H_8	0	0	2	0	0	0	0	0	0	2
H_9	0	1	0	0	0	0	0	0	0	1
H_10	0	1	0	0	0	0	0	0	0	1
H_11	0	2	0	3	1	2	5	1	0	14
H_12	0	1	0	0	0	0	0	0	0	1
H_13	0	2	0	0	0	0	0	0	0	2
H_14	0	1	0	0	0	0	0	0	0	1
H_15	0	0	0	0	0	0	0	0	1	1
H_16	0	0	0	0	0	0	0	0	1	1
H_17	0	0	0	0	0	0	0	0	1	1
H_18	0	0	0	0	0	0	0	0	1	1
H_19	0	0	0	0	2	0	0	0	0	2
H_20	0	0	0	0	1	0	0	0	0	1
H_21	0	0	0	0	0	0	1	0	0	1
H_22	0	0	0	0	0	0	1	0	0	1
H_23	0	0	0	0	0	0	0	1	0	1
H_24	0	0	0	0	0	1	0	1	0	2
H_25	0	0	0	0	0	0	0	1	0	1
H_26	0	0	0	0	0	0	0	1	0	1
H_27	0	0	0	0	0	0	0	1	0	1
H_28	0	0	0	0	0	1	0	2	0	3
H_29	0	0	0	0	0	0	0	1	0	1
H_30	0	0	0	0	0	0	0	1	0	1
H_31	0	0	0	0	0	0	0	1	0	1
H_32	0	0	0	1	0	0	0	0	0	1
H_33	0	0	0	1	0	0	0	0	0	1
H_34	0	0	0	1	0	0	0	0	0	1
H_35	0	0	0	1	0	0	0	0	0	1
h	0.952	0.944	0.667	0.857	0.905	0.900	0.524	0.982	1.000	60
π	0.02841	0.01151	0.00105	0.00344	0.02235	0.00188	0.00224	0.00320	0.00471	

genetic divergence from both groups, although it was only marginally closely related to Group 3. The most notable genetic difference was observed between the Group 1 and 4 populations, with a recorded F_{ST} value of 0.9388.

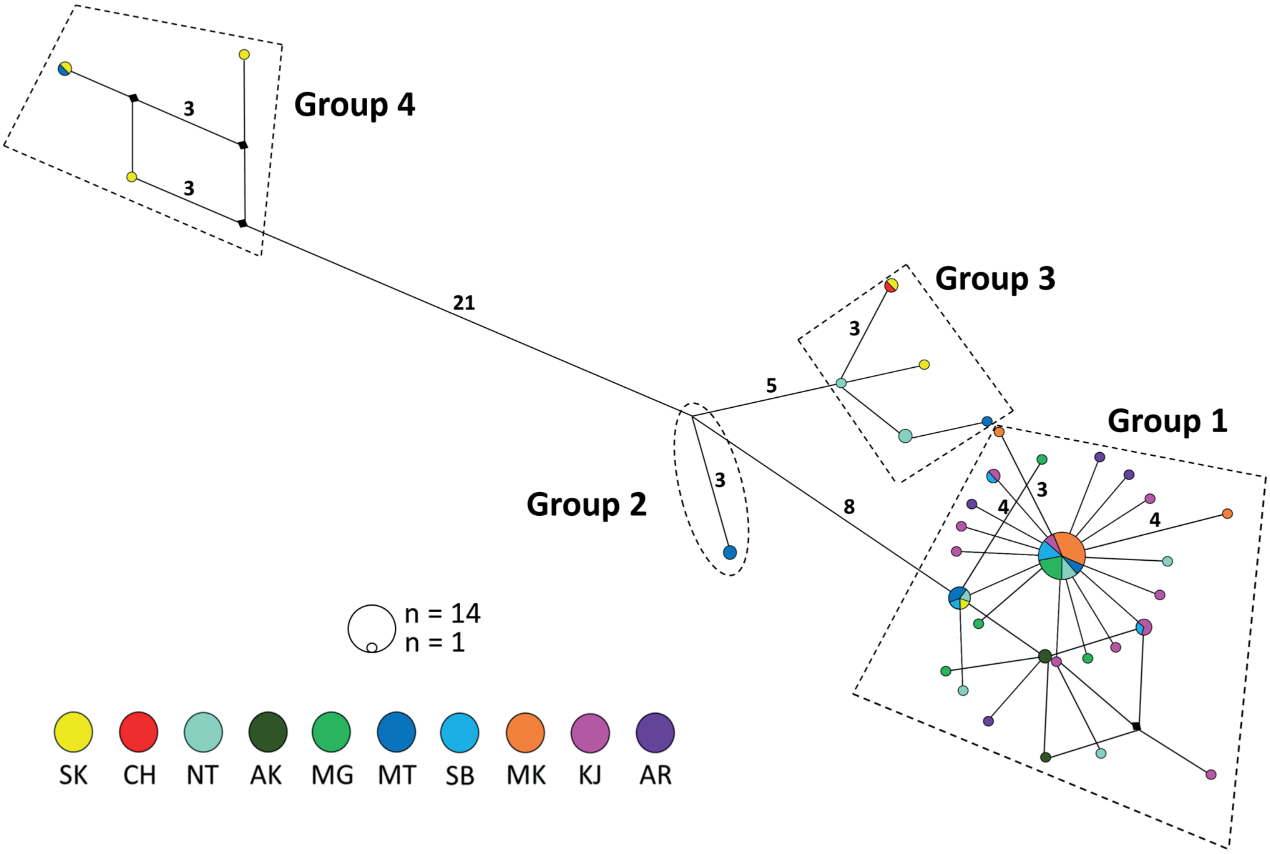

Figure 4. Median-joining haplotype networks, based on COI sequences. The circle size is proportional to the frequency of haplotypes. Black circles represent missing haplotypes. Each line represents a double mutation step, otherwise step numbers are indicated.

Table 4. Pairwise F_{ST} values amongst groups.

	Group 1	Group 2	Group 3	Group 4
Group 1	0.0000			
Group 2	0.8445	0.0000		
Group 3	0.8608	0.7931	0.0000	
Group 4	0.9388	0.9256	0.9177	0.0000

Table 5. AMOVA for COI sequences of *U. major* populations used in this study. *d.f.* indicates degrees of freedom. * indicates $p < 0.01$.

Source of variation	*d.f.*	Sum of squares	% of variation	Fixation index
Among Groups	3	197.197	86.97	F_{ST} = 0.900*
Within Groups	56	54.772	9.20	

A quantitative assessment of the genetic structural disparities between each group was conducted using AMOVA (Table 5). The analysis showed significant differences in the genetic structure between the groups, with most genetic differentiation occurring amongst the groups (86.97%, F_{ST} = 0.900). Conversely, the variation within each group was observed to be quite minimal, measuring at a mere 9.20%.

Morphological characteristics

All measures of morphological traits of Japanese *U. major* are presented in Table 6 (see Suppl. material 1: appendix S4 for data distinguished by sex). The data gathered were evaluated for size disparities amongst groups and genders using the Tukey test. The results showed statistically significant differences only in the MW (right) size between the genders, while no other significant differences were observed (refer to Suppl. material 1: appendix S5). It should be noted that the between-group testing was restricted to Group 1 versus Group 3, considering the limited sample sizes of Groups 2 and 4 (n = 1–2). Furthermore, the relationship between CL and each morphological parameter was analysed to determine variations amongst groups, as shown in Fig. 5 (see also Suppl. ma-

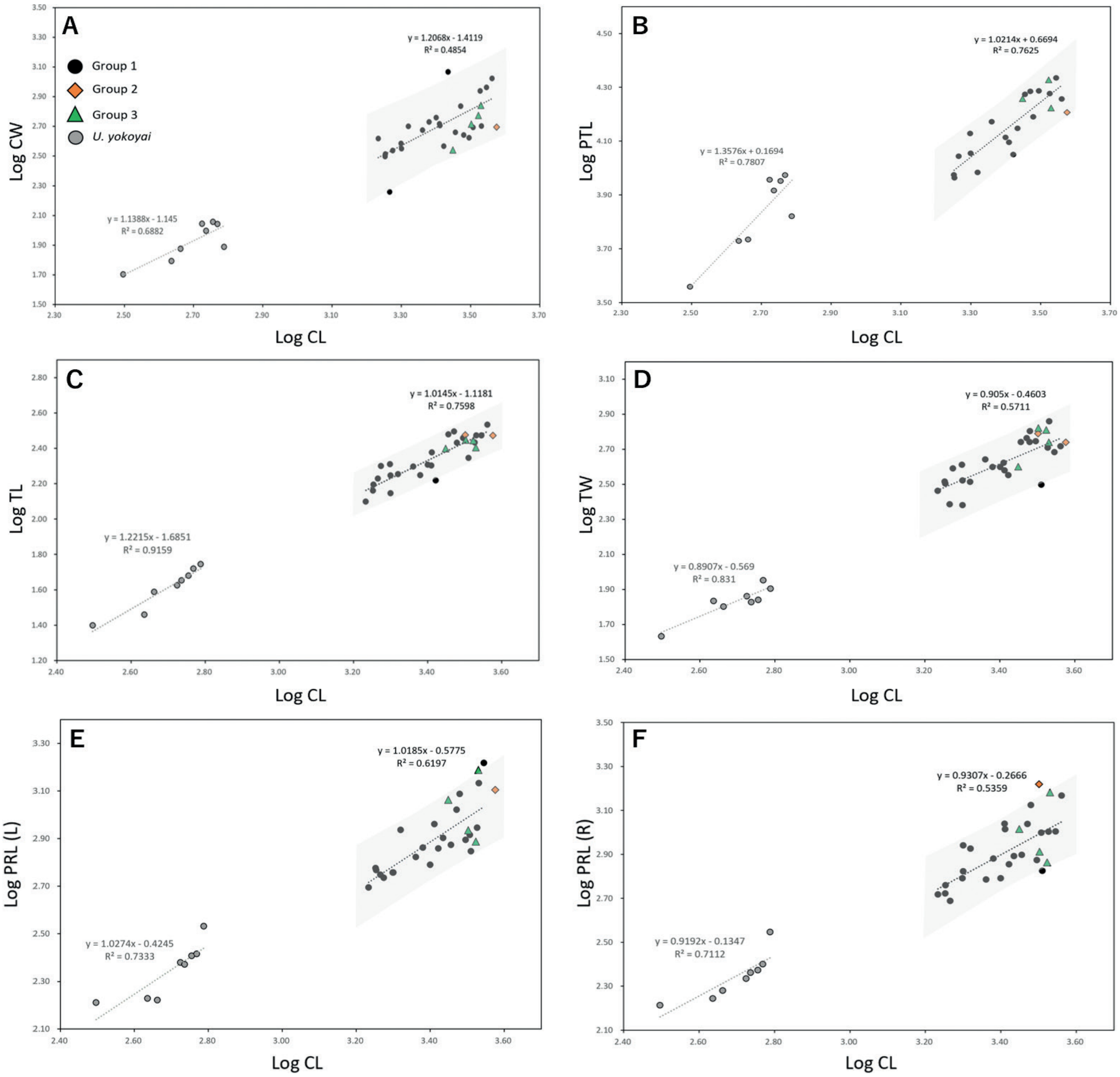

Figure 5. The size of each of the morphological parameters relative to carapace length (CL) **A** Carapace Width (CW) **B** Pleomere Total Length (PTL) **C** Telson Length (TL) **D** Telson Width (TW) **E** Left Propodus Length (PRL (L)), and **F** Right Propodus Length (PRL (R)). Shaded areas show the 95% confidence interval. Note that Group 4 was excluded from the analysis due to the carapace of the MT-03 being damaged, rendering the measurement of CL impossible.

Table 6. The morphometric measurements' outcomes have been tabulated by group. The maximum and minimum values and the corresponding standard deviation, have been presented for each Group, except for group 4 (n = 1). The symbol "-" denotes that the observation was unattainable due to impairment.

Group	Sample Code	Sex	CL	CW	PL1	PL2	PL3	PL4	PL5	PL6	PTL	TL	TW	MW		PRL	
														Left	Right	Left	Right
1	NT-01	Male	32.46	14.06	10.17	-	9.05	8.70	9.58	11.01	-	-	16.51	7.96	7.88	21.92	22.74
	NT-02	Male	34.17	14.92	10.49	14.89	9.93	-	10.25	11.64	-	11.85	17.48	8.26	-	22.93	-
	NT-03	Male	-	-	11.94	8.71	-	-	8.06	11.13	-	10.48	14.13	8.33	8.31	23.40	8.31
	NT-07	Female	31.69	14.31	11.57	11.10	9.28	8.94	10.68	11.23	71.74	11.93	15.53	5.11	4.95	17.70	18.13
	NT-08	Female	32.97	13.79	10.60	12.61	10.13	9.44	9.05	11.39	72.66	11.68	15.60	5.79	5.22	18.07	17.71
	NT-09	Female	33.36	14.79	11.49	11.69	9.95	10.92	10.74	-	-	-	-	5.47	6.33	18.45	20.04
	AK-01	Female	33.46	-	-	-	-	8.63	7.20	10.25	-	10.44	12.17	5.56	5.24	17.23	16.85
	AK-02	Female	-	-	-	-	-	-	-	-	-	-	-	7.87	-	23.67	-
	AK-03	Female	-	-	-	-	-	-	-	-	-	-	-	-	8.24	-	24.48
	MG-01	Female	26.43	12.65	9.38	11.07	-	8.27	9.07	10.68	-	9.97	13.35	5.00	-	15.41	-
	MG-02	Male	31.03	21.49	10.21	11.17	8.19	7.68	8.70	9.61	63.24	-	-	6.06	6.22	18.22	18.03
	MG-03	Female	-	-	11.15	12.58	10.35	9.57	-	12.51	65.73	11.51	14.76	-	-	-	-
	MG-04	Female	19.26	8.57	6.10	-	-	-	5.86	7.49	-	7.02	8.60	3.24	3.12	10.81	10.77
	MG-05	Female	18.81	11.07	6.34	-	5.34	5.17	5.68	7.79	-	6.71	7.76	3.42	3.39	11.04	11.60
	MG-06	Male	21.95	8.73	6.87	8.09	-	-	5.97	7.51	-	6.71	9.83	4.10	3.72	13.23	12.52
	MG-07	Male	30.32	14.99	9.87	-	8.51	7.72	8.60	9.66	-	10.77	13.21	6.62	7.02	19.31	20.38
	MT-01	Female	32.44	-	10.13	12.63	9.13	7.58	7.46	11.49	66.00	11.38	15.51	-	-	-	-
	MT-02	Male	26.20	9.59	8.31	11.23	6.98	6.90	7.56	9.12	57.00	9.29	10.88	4.67	4.54	15.61	14.69
	MT-05	Male	-	-	-	-	-	-	-	-	-	11.49	15.33	-	8.89	-	23.64
	SB-01	Male	27.12	-	8.70	9.87	6.67	6.98	9.18	9.27	57.65	9.45	12.47	-	5.58	-	18.92
	SB-02	Female	27.08	13.28	9.87	11.50	8.76	6.82	8.81	9.47	62.05	10.07	13.64	4.67	4.97	15.75	16.30
	SB-03	Male	25.37	13.72	6.52	8.85	-	6.02	7.53	8.22	-	8.15	11.75	5.24	5.39	14.79	15.14
	SB-04	Female	-	-	9.18	10.43	-	-	-	-	-	-	-	5.14	-	16.09	-
	SB-05	Male	29.38	15.34	-	-	-	-	-	9.45	-	9.46	13.46	5.71	6.34	17.49	17.83
	MK-01	Male	25.89	12.36	8.68	10.14	6.85	5.99	6.40	8.57	52.62	8.98	12.24	5.09	4.81	15.93	15.78
	MK-02	Male	30.27	15.14	9.43	10.72	7.56	7.20	8.34	9.56	60.01	10.00	13.79	-	7.17	-	20.88
	MK-03	Male	30.64	13.03	9.29	10.38	7.60	6.96	7.53	8.66	57.38	9.19	12.85	6.08	6.00	17.44	17.36
	MK-04	Male	27.66	14.91	9.14	9.52	6.50	6.45	6.82	8.81	53.69	9.52	12.37	6.03	6.15	18.84	18.65
	MK-05	Male	23.85	11.81	8.01	8.49	5.82	6.68	7.30	7.40	50.38	8.37	11.08	4.74	4.82	14.47	15.39
	MK-06	Female	28.82	14.53	9.75	11.36	8.19	8.36	9.12	9.64	64.78	9.94	14.05	5.16	5.05	16.81	16.21
	MK-07	Female	29.97	15.79	9.58	10.91	7.30	7.39	8.79	9.78	61.14	10.05	13.46	4.91	5.38	16.28	16.30
	KJ-01	Female	23.99	12.76	8.30	9.51	6.25	6.10	6.43	8.13	50.82	8.52	11.46	5.57	5.66	16.09	17.35
	KJ-02	Female	22.16	10.00	6.93	6.84	5.69	4.72	5.63	7.05	41.58	7.19	9.76	3.98	4.36	12.05	13.10
	KJ-03	Female	23.34	10.59	7.42	8.63	6.18	6.13	6.46	7.77	48.72	7.65	11.01	4.36	4.33	13.25	13.30
	KJ-04	Male	25.86	12.17	8.03	9.56	6.94	6.67	7.31	8.03	53.21	8.68	12.39	5.32	5.03	16.06	15.21
	KJ-05	Male	20.88	11.04	7.08	8.21	5.63	5.38	6.02	7.08	44.78	6.96	9.65	4.62	4.61	13.99	13.53
	KJ-06	Female	19.61	10.56	6.93	8.06	5.07	-	5.82	6.78	-	6.98	9.61	4.13	4.05	12.62	12.66
	KJ-07	Male	27.12	12.82	8.53	10.12	6.65	-	7.13	8.05	-	8.55	10.83	5.28	5.89	15.75	16.82
	KJ-08	Female	22.82	11.21	7.36	8.63	6.04	4.67	7.00	7.57	45.94	7.66	10.99	4.71	4.65	13.98	13.70
	KJ-09	Female	22.42	10.01	7.91	9.01	6.20	6.03	6.50	7.58	49.26	7.92	10.27	4.90	4.78	14.16	14.33

Group	Sample Code	Sex	CL	CW	PL1	PL2	PL3	PL4	PL5	PL6	PTL	TL	TW	MW		PRL	
														Left	Right	Left	Right
1	KJ-10	Male	22.16	10.69	6.74	8.62	5.97	5.88	6.42	7.39	46.90	7.90	10.17	4.81	5.09	14.52	14.33
	KJ-11	Female	23.85	11.17	7.41	9.41	6.15	6.94	7.10	7.37	51.32	7.82	10.18	4.61	4.71	15.31	14.67
	AR-01	Male	35.22	20.57	10.58	11.36	9.24	8.72	10.39	11.53	70.54	12.60	15.14	-	9.95	-	23.75
	AR-02	Female	32.18	17.08	11.50	12.10	10.03	8.84	10.35	10.86	72.52	12.12	15.88	6.73	6.41	20.51	20.85
	AR-03	Female	34.03	18.91	12.42	11.84	9.16	8.62	9.97	11.33	71.96	11.39	15.03	6.22	6.40	19.02	20.14
	AR-04	Female	34.66	19.36	12.19	12.52	9.80	9.83	10.29	11.82	76.28	11.86	14.65	11.48	6.64	24.97	20.17
	Maximum		35.22	21.49	12.42	14.89	10.35	10.92	10.74	12.51	76.28	12.60	17.48	11.48	9.95	24.97	24.48
	Minimum		18.81	8.57	6.10	6.84	5.07	4.67	5.63	6.78	41.58	6.71	7.76	3.24	3.12	10.81	8.31
	Mean		27.5	13.5	9.1	10.3	7.6	7.3	7.9	9.3	58.6	9.5	12.7	5.6	5.7	16.7	16.8
	Standard deviation		4.717	3.093	1.739	1.673	1.608	1.493	1.554	1.620	9.675	1.722	2.316	1.523	1.464	3.362	3.638
2	MT-04	Male	33.17	-	11.89	13.14	8.60	8.15	-	11.24	-	11.89	16.27	-	9.29	-	25.02
	MT-07	Male	35.72	14.80	11.31	11.15	9.14	8.22	8.88	10.21	67.13	11.86	15.49	7.94	-	22.30	-
	Maximum		35.72	14.80	11.89	13.14	9.14	8.22	8.88	11.24	67.13	11.89	16.27	7.94	9.29	22.30	25.02
	Minimum		33.17	14.80	11.31	11.15	8.60	8.15	8.88	10.21	67.13	11.86	15.49	7.94	9.29	22.30	25.02
	Mean		34.4	14.8	11.6	12.1	8.9	8.2	8.9	10.7	67.1	11.9	15.9	7.9	9.3	22.3	25.02
	Standard deviation		1.275	0.000	0.290	0.995	0.270	0.035	0.000	0.515	0.000	0.015	0.390	0.000	0.000	0.000	0.000
3	NT-04	Female	33.89	16.03	11.71	11.12	10.43	9.56	11.70	11.69	75.77	11.53	16.61	5.92	5.58	17.94	17.52
	NT-05	Male	31.46	12.69	11.36	11.03	8.42	9.18	9.76	11.70	70.63	11.01	15.49	7.34	7.14	21.38	20.40
	NT-06	Female	33.20	15.12	-	12.05	9.70	9.66	10.74	12.36	-	11.56	16.80	5.24	5.26	18.83	18.39
	MT-06	Male	34.13	17.16	10.19	12.12	8.82	8.26	9.87	10.70	68.22	11.07	15.49	8.16	7.96	24.26	24.10
	Maximum		34.13	17.16	11.71	12.12	10.43	9.66	11.70	12.36	75.77	11.56	16.80	8.16	7.96	24.26	24.10
	Minimum		31.46	12.69	10.19	11.03	8.42	8.26	9.76	10.70	68.22	11.01	15.49	5.24	5.26	17.94	17.52
	Mean		33.2	15.3	11.1	11.6	9.3	9.2	10.5	11.6	71.5	11.3	16.1	6.7	6.5	20.6	20.1
	Standard deviation		1.045	1.645	0.650	0.507	0.780	0.552	0.781	0.593	3.149	0.254	0.611	1.149	1.110	2.460	2.533
4	MT-03	Male	-	-	-	11.21	9.33	8.26	8.49	11.96	-	11.58	15.63	-	7.39	-	23.68

terial 1: appendix S6). By utilising Group 1 as the benchmark, which possesses the largest sample size in this study, and establishing 95% confidence intervals, the male samples originating from Groups 2 and 3 exhibited marginally higher PRL/CL ratios than those from Group 1 (Fig. 5E, F and Suppl. material 1: appendix S6E (a), see F (a) for more detail). Additionally, the F-test conducted on the slopes of the data for Group 1 and *U. yokoyai* did not reveal any statistically significant differences, except for PTL (Male) (Suppl. material 1: appendix S7). This suggests that the two species share similar growth patterns, but exhibit distinct size variations. However, due to the small sample size, the statistical analysis of the slope was not performed for all groups except Group 1. Therefore, it cannot be ruled out that the other groups may have different slopes for Group 1, indicating that Groups 2 and 3 may display divergent growth patterns from Group 1. To investigate this possibility, it would be necessary to augment the sample size in each group. On the other hand, the analysis of morphological features involved quantification of the number of projections located below the manus (NPLBM) and the number of projections above the propodal finger (NPAPF) and

tabulation of the number of ventral projections of pereopod 2 (NVPP2) (Fig. 6A, B). Note that this analysis specifically focused on specimens possessing a CL of 25 mm or larger. The results demonstrate that NPLBM, NPAPF and NVPP2 had a range of 3 to 7, 2 to 9 and 1 to 3, respectively, in Group 1 of Japanese descent, while NPLBM ranged from 4 to 7, NPAPF from 6 to 9 and NVPP2 from 1 to 2 in the continental Group 3 (Table 7). Moreover, amongst the parameters, NPAPF was the only one that exhibited a significant difference between males and females, with a range of 3 to 9 in males and 2 to 8 in females (see Suppl. material 1: appendix S8). Despite the variability in the number of projections, the Tukey test revealed no statistically significant differences in any of the parameters between groups or genders (Suppl. material 1: appendix S9). By contrast, there were noticeable disparities in the morphology of the telson apices between the sexes (Suppl. material 1: appendix S8). In males, approximately 90% displayed a concave shape in the median, whereas all females demonstrated a linear shape (Fig. 6C). Amongst the specimens, one stands out as particularly distinctive: MT-03, a male individual from Group 4, which exhibits a conspic-

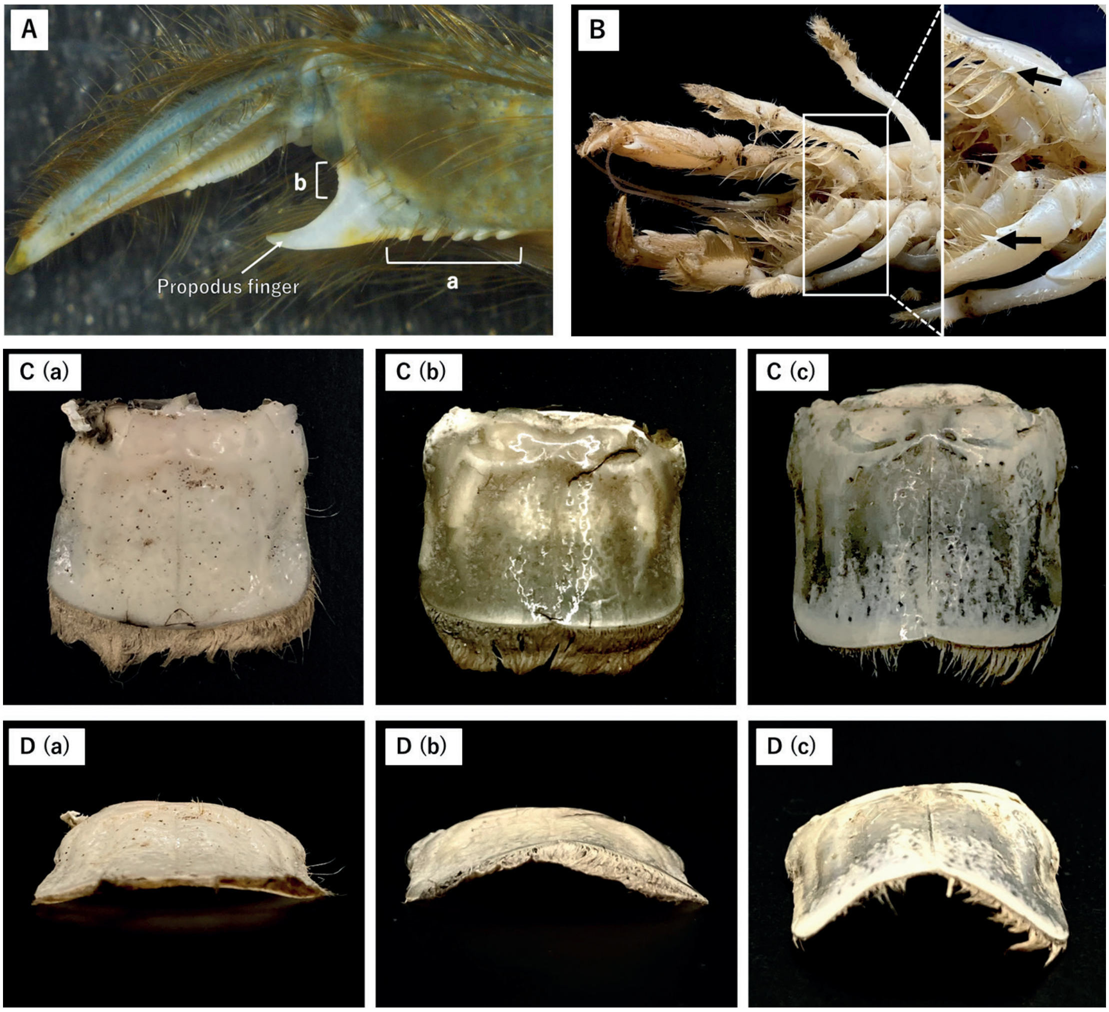

Figure 6. Morphological traits observed in this study **A** projections located beneath the manus (a) and above the propodal finger (b) **B** ventral projections of pereopod 2 (arrow) **C** telson tip. (a) Linear shape, Female, MT-01 (b) Slightly concave shape, Male, MT-02 (c) Concave shape, MT-03 specimen from Matsukawa-ura **D** cross-sectional profile of the telson. (a) Linear shape, Female, MT-01 (b) Slightly arched shape, Male, MT-02 (c) Arched shape, MT-03

Table 7. The results of morphometric observations are summarised by group. NPLBM: Number of projections located beneath the manus, NPAPF: Number of projections above the propodal finger, NVPP2: Number of ventral projections of pereopod 2, MTT: Morphology of the telson tip, CST: Cross-sectional shape of the telson, L: Linear, SC: Slightly concave, C: Concave, SA: Slightly arched, A: Arched. The maximum and minimum values and the corresponding standard deviations are given for each group, except for Group 4, where the sample size is 1. Additionally, the percentage of MTT and CST traits are presented. The symbol "-" indicates an unattainable observation due to impairment.

Group	Sample code	Sex	NPLBM		NPAPF		NVPP2			MTT	CST
			Left	Right	Left	Right	Left	Right			
1	NT-01	Male	5	4	8	8	–	1		SC	L
	NT-02	Male	5	–	6	–	2	1		SC	L
	NT-07	Female	4	5	4	7	2	2		L	L
	NT-08	Female	6	5	7	4	1	1		L	L
	NT-09	Female	5	4	–	2	–	1		L	L
	AK-01	Female	5	6	5	4	1	1		L	L
	MG-01	Female	4	–	–	–	–	2		L	L
	MG-02	Male	3	4	8	9	3	2		SC	L
	MG-07	Male	5	4	5	6	2	2		L	L
	MT-01	Female	–	–	–	–	–	1		L	L
	MT-02	Male	4	5	4	6	2	2		SC	SA
	SB-01	Male	–	5	–	6	2	–		SC	L
	SB-02	Female	–	3	–	8	2	1		L	L
	SB-03	Male	5	6	4	5	2	1		SC	L
	SB-05	Male	6	5	4	6	2	2		SC	L
	MK-01	Male	7	6	4	3	2	2		SC	L
	MK-02	Male	–	4	–	6	2	2		SC	L
	MK-03	Male	6	6	6	5	2	2		SC	L
	MK-04	Male	5	5	7	5	2	2		SC	L
	MK-06	Female	4	4	6	4	2	2		L	L
	MK-07	Female	5	6	4	6	3	2		L	L
	KJ-04	Male	6	5	5	5	–	–		SC	L
	KJ-05	Male	4	4	7	5	2	2		SC	L
	AR-01	Male	–	5	–	6	2	1		SC	L
	AR-02	Female	4	5	5	2	2	2		L	L
	AR-03	Female	4	4	5	4	2	2		L	L
	AR-04	Female	5	4	5	5	2	2		L	L
	Maximum		7	6	8	9	3	2	%	L = 48.1	L = 96.3
	Minimum		3	3	4	2	1	1		SC = 51.9	SA = 3.7
	Mean		4.9	4.8	5.5	5.3	2.0	1.6		C = 0.0	A = 0.0
	Standard deviation		0.919	0.829	1.322	1.695	0.426	0.480			
2	MT-04	Male	–	6	–	8	1	–		SC	L
	MT-07	Male	4	–	8	–	–	2		SC	L
	Maximum		4	6	8	8	1	2	%	L = 100	L = 100
	Minimum		4	6	8	8	1	2		SC = 0.0	SA = 0.0
	Mean		4.0	6.0	8.0	8.0	1.0	2.0		C = 0.0	A = 0.0
	Standard deviation		0.000	0.000	0.000	0.000	0.000	0.000			

Group	Sample code	Sex	NPLBM		NPAPF		NVPP2			MTT	CST
			Left	Right	Left	Right	Left	Right			
3	NT-04	Female	7	6	–	–	1	2		L	L
	NT-05	Male	4	5	8	7	2	1		SC	L
	NT-06	Female	5	4	6	6	2	2		L	L
	MT-06	Male	5	4	8	9	2	1		SC	L
	Maximum		7	6	8	9	2	2	%	L = 50.0	L = 100
	Minimum		4	4	6	6	1	1		SC = 50.0	SA = 0.0
	Mean		5.3	4.8	7.3	7.3	1.8	1.5		C = 0.0	A = 0.0
	Standard deviation		1.090	0.829	0.943	1.247	0.433	0.500			
4	MT-03	Male	–	4	–	9	–	–		C	A

uously concave-shaped tip, a trait that is absent in all other specimens. Additionally, the majority of the talus cross-sectional shapes were linear, exceeding 90% in both groups and genders, with only a minority of specimens displaying a slightly arched talus. In contrast, MT-03 presented a marked arch shape, providing a distinct contrast from the other specimens (Fig. 6D).

Discussion

The COI phylogenetic tree analysis reveals that *U. major* is distinctly separated from its outgroups and closest species, forming its own clade comprising four groups (Fig. 3). Group 1 is predominantly made up of Japanese specimens, while Groups 3 and 4 consist of continental specimens, categorising them broadly as Japanese and continental, respectively. However, Group 2 specimens from Matsukawa-ura exhibit genetic differentiation from both continental and Japanese descent and the presence of Japanese individuals from Matsukawa-ura and Lake Notoro in Groups 3 and 4, along with significantly larger PRL of Group 2 and 3 individuals of males in comparison to Group 1, suggest that genetically and morphologically distinct *U. major* is prevalent in Japan.

Although the precise origin of *U. major* remains unknown, the oldest lineage traced in the inferred phylogenetic tree belongs to Group 4, with the South Korean sample (SK-03) being the first to diverge within this group. Thus, it is plausible that the coastal waters of Korea could serve as the putative origin of *U. major*. This study assumes that the origin of *U. major* is situated around South Korea and conducts an extensive evaluation of the genetic differentiation of this species throughout the entirety of the Japanese archipelago, taking into account various physical and anthropogenic factors.

The dispersion of genes in marine benthos influenced by physical factors

Marine benthos possessing planktonic larval stages have the potential to increase their geographic range owing to their floating period and the hydrodynamic properties of ocean currents. Specifically, around the Japanese archipelago, three prominent oceanic currents exist: the warm Tsushima Current, the Kuroshio Current and the cold Oyashio Current (Fig. 7). According to the Japan Meteorological Agency, the Kuroshio Current, which flows eastwards along the Pacific coast of the Japanese archipelago, usually reaches the Boso Peninsula, where

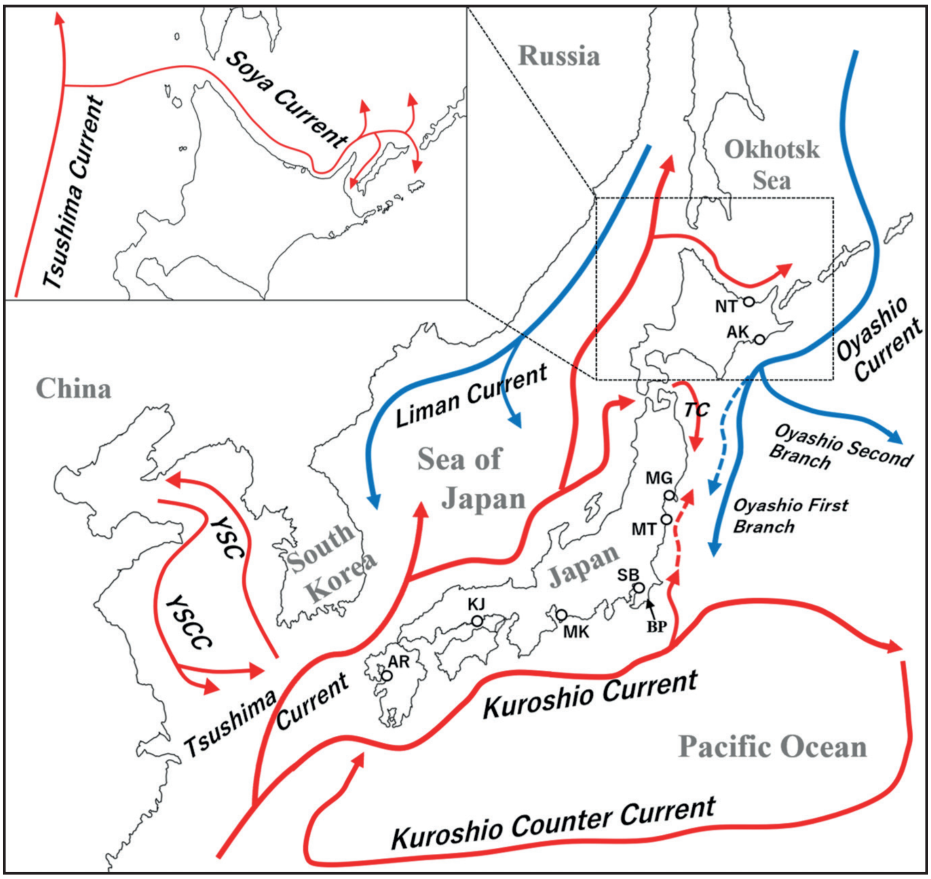

Figure 7. Designations of the oceanic currents and their respective flow patterns in the Japanese archipelago. The Blue dotted arrow denotes the southern extremity of the First branch of the Oyashio current during its attenuation, while the Red dotted arrow demarcates the northern boundary of the Kuroshio Basin at that particular juncture. TC: Tsugaru Current, YSC: Yellow Sea Current, YSCC: Yellow Sea Counter Current, BP: Boso Peninsula.

Sanbanze is located. However, when the first branch of the Oyashio Current, flowing southwards from the north, is weakened, the Kuroshio Current extends northwards off the coast of Miyagi Prefecture, where Mangoku-ura is located. Additionally, the Kuroshio Current which flows offshore of the Boso Peninsula into the Pacific Ocean, voyages towards the south along the southern extent of the Japanese archipelago as the Kuroshio Counter Current, meandering westwards and ultimately reunites with the principal Kuroshio Current. The Tsushima Current, a warm current, flows through the Sea of Japan, and a segment thereof permeates the Pacific Ocean as the Tsugaru Current. The Soya Current is the constituent that transits through the Soya Strait and infiltrates the Sea of Okhotsk.

Thus, ocean currents circulate around the Japanese archipelago. *U. major* has three larval stages and one decapod stage and its planktonic larval period is estimated to be approximately one month or more for individuals inhabiting Tokyo Bay (Kinoshita et al. 2003). The flow velocity of major ocean currents near Japan varies seasonally, but generally, the Kuroshio flows at 2 to 3 knots (3.7 to 5.6 km/h), the Tsushima Current at 1 to 1.5 knots (1.9 to 2.8 km/h) and the Oyashio at approximately 1 knot (Japan Coast Guard 2023). Assuming a planktonic larval period of 31 d for *U. major*, maximum displacement distances of up to 4,166 km in the Kuroshio region, 2,083 km in the Tsushima Current region and 1,414 km in the Oyashio region are possible.

The presence of *U. major* individuals belonging to Groups 3 and 4 in Lake Notoro and Matsukawa-ura, respectively, implies the potential for passive continental invasion of the species into Japan through the agency of oceanic currents. Included in Groups 3 and 4 were specimens from Gyeonggi-do, a coastal region situated in the western part of South Korea, as well as specimens from the Qingdao Peninsula in China and South Korean specimens with unspecified collection locations. To reach Lake Notoro, these individuals must follow the Yellow Sea Coastal Current and subsequently merge with the Tsushima Current before finally riding along the Soya Current (Fig. 8). A similar example of marine organisms expanding their range through such mechanisms is demonstrated by *Nemopilema nomurai*. This species is known to inhabit the Bohai, Yellow and East China Seas before infiltrating the Sea of Japan via the Tsushima Current (Uye 2008; Moon et al. 2010). Therefore, it is possible that planktonic larvae of continental *U. major* might have traversed the Sea of Japan through this route. Nevertheless, the velocity of ocean currents and the duration of *U. major* planktonic larvae render direct transport from the Yellow Sea arduous, which indicates the possibility of an intermediate relay point on the Sea of Japan side of the Japanese archipelago. Additionally, this species has been sighted in several regions of Russia, including Vladivostok, Vostok Bay, Olga Bay and Sakhalin Island, but without any corresponding genetic data (Makarov 1938; Urita 1942; Vinogradov 1950; Selin 2017).

While no prior research has documented the transfer of organisms from the Russian coastline to the Japanese archipelago via the Liman Current merging with the Tsushima Current, it is possible that *U. major* larvae from Russia may have travelled this route and ultimately arrived at Lake Notoro. Moreover, it is worth noting that although a greater distance must be traversed to reach Matsukawa-ura, two potential routes may be posited: one involves planktonic larvae of continental *U. major* inhabiting Lake Notoro riding the Soya Current into the Pacific Ocean and then utilising the Oyashio Current to reach Matsukawa-ura and the other involves reaching Matsukawa-ura via the Tsugaru Current from an intermediate relay point on the Sea of Japan (Fig. 8).

While the sample size is not extensive, the evident genetic and morphological heterogeneity exhibited by the *U. major* population in Matsukawa-ura is noteworthy. This diversity may, to some extent, be influenced by changes in coastal topography. The Tohoku region, where Matsukawa-ura is situated, experiences significant earthquakes once every 500–800 years (Sawai et al. 2012), which can trigger tsunamis leading to alterations in coastal topography. The most recent such occurrence was the Great East Japan Earthquake in March 2011, which resulted in the destruction of the sandbar in Matsukawa-ura and allowed coastal water to inundate the area, significantly modifying the topography (Nishi et al. 2012). However, such disturbances can also increase species diversity. For example, after the Great East Japan Earthquake, the range of *Gasterosteus* genera in the Tohoku region expanded due to changes in topography, resulting in hybridisation and increased genetic and morphological diversity (Hosoki et al. 2019). Additionally, the distribution range of oysters expanded as a result of wide-scale transport of oyster reefs by tsunamis generated during the earthquake (Okoshi 2016). There have been no reports indicating changes in the distribution range of *U. major* after the Great East Japan Earthquake. There have been no reports indicating changes in the distribution range of *U. major*

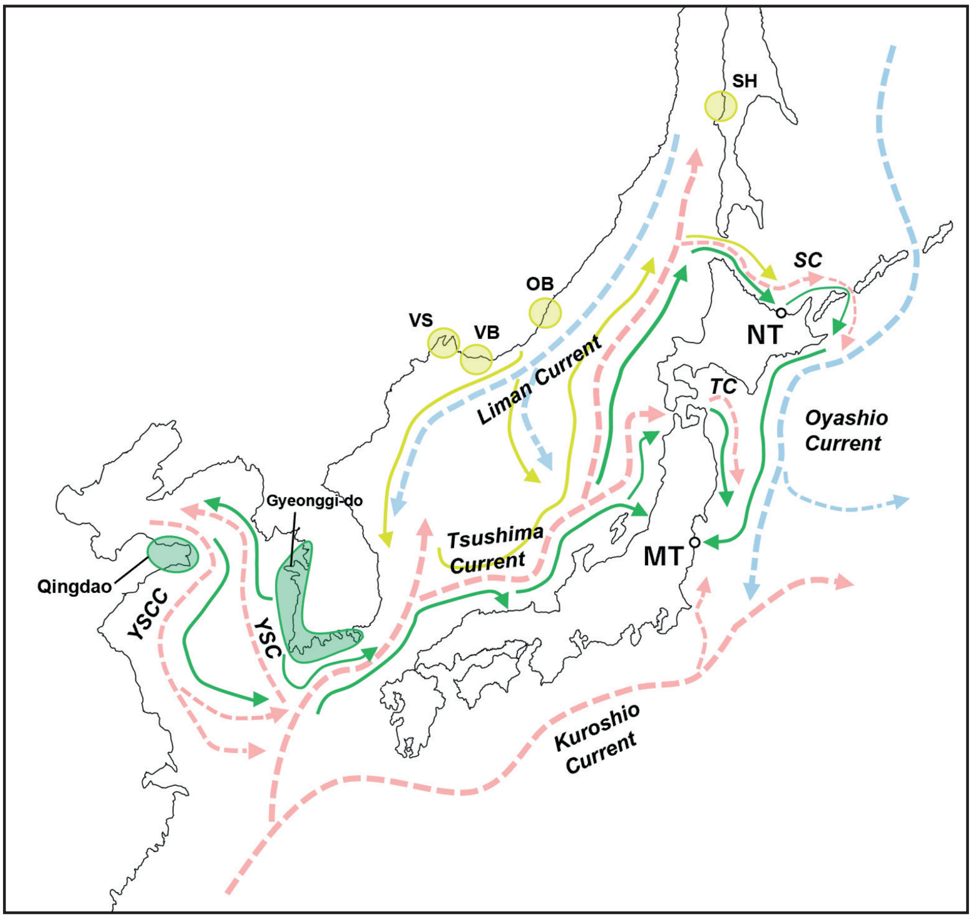

Figure 8. Possible routes for *U. major* larvae from South Korea, China and Russia to Lake Notoro and Matsukawa-ura. The warm currents are denoted by red dotted arrows, while the cold currents are denoted by blue dotted arrows. The collection sites of specimens from Korea and China used in this study are indicated by green circles, while the localities of *U. major* in Russia are denoted by yellow circles (The exact collection site in Sakhalin Island is unknown). Furthermore, potential dispersal routes of *U. major* larvae from South Korean/Chinese specimens and Russian specimens are shown in green and yellow arrows, respectively. SC: Soya Current, TC: Tsugaru Current, YSC: Yellow Sea Current, YSCC: Yellow Sea Counter Current, VS: Vladivostok, VB: Vostok Bay, OB: Olga Bay, SH: Sakhalin Island.

after the Great East Japan Earthquake. However, there is a possibility that the alterations in coastal topography caused by the earthquake and tsunami, along with the influx of coastal water, may have advanced genetic differentiation.

Additionally, an example of the spread of organisms of continental origin across the Japanese archipelago is evident in the "continental relict species". During the Pleistocene glacial period, the southern coast of Korea and the present-day Ariake Sea were united by land, but regression of the Ariake Sea during the postglacial period resulted in their separation (Emery et al. 1971; Wang and Wang 1980). Consequently, the habitats of living beings have also separated and, today, the Ariake Sea is a habitat for many benthic organisms that possess continental genes (Sato 2010). However, the distribution of many continental relict species in the Ariake Sea has not expanded. This could be due to the difficulty of maintaining a shared inner bay environment with continental coasts in Japan, which are isolated from the continent (Sato 2010). Initially, it remains uncertain whether *U. major* was extant during the time in question, given the lack of fossil evidence. Nevertheless, based on current perspectives, it appears somewhat improbable that this species is a relict of a continental nature. Furthermore, all specimens from the Ariake Sea are included in Group 1 and their genetic relationships with continental species cannot be determined. To evaluate this hypothesis, more comprehensive examinations of Ariake Sea specimens are required, followed by an estimation of their divergence ages and other relevant details.

Group 1 individuals shared the haplotype H_11 at six different sites in Japan (Lake Notoro, Mangoku-ura, Matsukawa-ura, Sanbanze, Mikawa Bay and Kojima Bay) and displayed a trend of low genetic diversity, indicating that their planktonic larvae were dispersed over a broad north-south range by ocean currents surrounding the Japanese archipelago. *Panulirus japonicus*, a decapod crustacean resembling *U. major*, is broadly distributed in the Kuroshio region, but there is no identifiable genetic variation within populations. With a planktonic larval duration of about one year, it is speculated that *P. japonicus* with the same haplotype has moved long distances over an extended period through the Kuroshio region (Inoue et al. 2007). *Macrophthalmus japonicus*, extensively distributed across the intertidal zones of Japan, possesses an extended planktonic larval phase exceeding one month, enabling extensive dispersal throughout the region through the influence of the Kuroshio Current. As a consequence, this species demonstrates limited genetic diversity and lacks clear population structuring throughout the Japanese archipelago (Kobayashi et al. 2023). Moreover, marine gastropods of the genus *Monodonta*, also widely distributed in Japan, exhibit a briefer planktonic larval period of approximately 3 to 5 days; however, they reveal genetically distinct populations broadly distributed between the Japan Sea side and the Pacific side, facilitated by dispersal via the Tsushima Current and the Kuroshio Current (Yamazaki et al. 2017). Therefore, it is possible that *U. major* also follows a similar dispersal pattern. The dispersal range of marine benthic larvae is affected by a variety of environmental factors, including water temperature, pH, salinity, dissolved oxygen concentration, ultraviolet radiation and turbidity, as well as biological factors, such as the availability of food and the presence of predators and habitat preferences (Cowen and Sponaugle 2009; Yamazaki et al. 2020; Bashevkin et al. 2020). Thus, it is improbable that the larvae of *U. major* dispersed passively solely through the influence of ocean currents; however, it cannot be excluded that they may have disseminated throughout the entire coastal area of Japan by utilising ocean currents for transportation.

In contrast, two specimens (MT-04 and 07) from Matsukawa-ura, belonging to Group 2, exhibited a slight difference in PRL compared to Group 1 and no discernible morphological distinctions were noted between Group 2 and Group 3. Nevertheless, they exhibited a distinctive haplotype, which may suggest phenotypic plasticity. This occurrence is well established in marine snails, as demonstrated in previous studies (e.g. Hollander et al. (2006); Kurihara et al. (2006)). Furthermore, Matsukawa-ura was found to harbor individuals from all four groups, but it is plausible that the specimens belonging to Group 2 may have migrated from collection sites not surveyed in this study. Alternatively, the individuals in Group 2 may have differentiated within Matsukawa-ura, with the subsequent movement of individuals from Groups 1, 3 and 4 to this location. To determine the exact distribution range of Group 2, a more extensive collection survey is necessary.

The dispersion of species as a consequence of anthropogenic activities

In addition to physical factors, it is possible that species dispersion occurs because of anthropogenic activities. Japan began importing the Manila clam *Ruditapes philippinarum*, from China and North Korea in the 1980s. Jute bags of imported clams contain live organisms other than clams, which are released into domestic clam fisheries or added to aquaculture farms every year (Okoshi 2004; Okoshi and Sato-Okoshi 2011). One species, the moon snail *Laguncula pulchella*, is established throughout Japan and is a significant predator of clams. Additionally, crustacean species, such as *Philyra pisum* and *Pagurus* sp., have also been found inside the bags (Okoshi 2004; Okoshi and Sato-Okoshi 2011). Owing to its soft-bodied morphology, *U. major* may potentially exhibit a diminished likelihood of prosperous establishment when contrasted with organisms possessing rigid exoskeletal structures, such as select crustaceans and molluscs. Nevertheless, the surface of jute bags contains moisture and there are spaces between the shells inside, making it highly plausible that small larvae and juveniles of *U. major* measuring less than 1 cm in total length could survive within the bag. The amounts of organisms introduced into Japan from the coasts of China and the Korean Peninsula, along with imported clams, have already exceeded 10,000 tonnes; however, it is not known whether they have survived or died, except for moon snails, whose presence was manifested by eating clams. In the clam-producing areas, Matsukawa-ura transplanted clams from abroad until 2010, a year before the Great East Japan Earthquake, when they were cultivated, enlarged and shipped. The damage to clams caused by moon snails was also serious and the number of egg masses that the fishery cooperative had to exterminate each year amounted to several hundred kilograms. Considering the prolonged release of foreign clams, it is irrefutable that *U. major* may have been unintentionally introduced into Japan. Additionally, fishing bait can lead to the introduction of non-native species. In Japan, the worm bait *Perinereis aibuhitensis*, which is imported from China and other countries, has successfully established itself in certain areas (Iwasaki 2006). *U. major* is also used as fishing bait in western Japan and some areas import live organisms from China and Korea. An interview was conducted with seven fishing tackle establishments in the vicinity of Matsukawa-ura to enquire whether they had any prior experience in retailing *U. major*. Note that this interview was carried out after detailed information on the morphological characteristics had been communicated. The findings revealed that one establishment had, indeed, vended specimens of indeterminate provenance in the past. If these individuals hailed from the continental origin, there exists a potential for gene dissemination through fishing bait. Upon being released into the marine environment, these entities are commonly presumed to fall prey to a myriad of organisms, such as fish (Kaifu et al. 2013a, b). Nevertheless, there is also the likelihood of certain individuals evading predation. Furthermore, in the event that the bait individuals were bearing eggs, there is a prospect for the hatching of their larvae and subsequent dispersion of continental origin individuals within Matsukawa-ura. It is also possible that Matsukawa-ura receives *U. major* larvae from both the Kuroshio and Oyashio currents, but despite Mangoku-ura being only approximately 100 km away, continental species have not been identified there. Therefore, there is the possibility of anthropogenic introduction to Matsukawa-ura.

Conversely, in Lake Notoro, a specimen of continental origin was also detected, but there was no record of the introduction of *R. philippinarum* from China or Korea and none of the ten surrounding fishing tackle stores handled *U. major* as bait. Based on the current findings, it is highly probable that the introduction to Lake Notoro was natural and occurred via ocean currents.

Possibility of subspecies

In this study, we focused on various morphological traits, including spines and hairs and counted, measured and compared them amongst individuals. We identified several traits that were characteristic of the comparisons amongst individuals. The divergence exhibited by MT-03, which is affiliated with Group 4, is particularly noteworthy regarding the morphology of its telson tip and section. Additionally, genetic analysis revealed a significant genetic distance of up to 0.056 from the other Japanese specimens of Groups 1, 2 and 3, indicating that it might be considered a subspecies. However, there is a lack of available morphological data for SK-02, 03, and 05, which also belong to Group 4. Therefore, further investigation is required to confirm their classification as subspecies through continuous surveys in Matsukawa-ura and Korea.

Group 4 has been proposed as the most primordial lineage that diverged within the species *U. major*, with the potential occurrence of subspecies within this particular group.

Conclusions

We conducted morphological evaluations in conjunction with molecular phylogenetic analyses of COI genes, extracted from specimens collected in Japan, Korea, and China, to ascertain the phylogeographic patterns and genetic as well as morphological, diversity in *Upogebia major*. As a consequence of our analysis, *U. major* was classified into four primary groups: one with predominantly Japanese descent, two other groups inferred to have originated from the continent, and the other group genetically segregated from both Continental and Japanese descent. The group exclusively comprising Japanese specimens suggests that the planktonic larvae of this species are widely dispersed by ocean currents surrounding the Japanese Archipelago. In contrast, several Japanese specimens were included in the continental group, which may be due to the introduction of individuals from the continent via ocean currents, the possibility that this species being a continental relict or the unintentional introduction of biota imported from Korea and China. Matsukawa-ura demonstrated high genetic diversity, with specimens from all groups present. Moreover, one specimen sampled from Matsukawa-ura (MT-03) presented noteworthy genetic and morphological variances compared with the other specimens, indicating the possibility of its being a subspecies. A specimen from Gyeonggi-do, Korea, obtained from GenBank, was classified into the same group as MT-03, although information on its morphology was unavailable because the reference paper remains unpublished. To confirm these findings, further morphological and genetic investigations and analyses encompassing Matsukawa-ura and other sites are necessary.

The genetic dispersal of *U. major* suggests the existence of both natural and anthropogenic dissemination pathways, implying their intricate interplay in the shaping of regional populations. The outcomes of this study underscore the potential for analogous occurrences in all organisms, irrespective of intentional or unintentional introduction and release from neighboring regions, transcending the boundaries of this particular species. These insights not only contribute to a deeper understanding of the origins of distribution of *U. major* but also introduce a novel challenge of assessing the coexistence of these two dispersion routes.

Acknowledgements

We appreciate Mr. Satoru Takeyama, Director of Akkeshi Oyster Seeding Center, the Nishi-Abashiri Fisheries Cooperative Association in Hokkaido, the Ishinomaki Bay Branch of the Miyagi Prefecture Fisheries Cooperative Association and the Matsukawa-ura Branch of the Soma Futaba Fisheries Cooperative Association in Fukushima Prefecture for their understanding of the field survey and cooperation in transporting the samples. We also thank Ms. Rumiko Kaneko and Ms. Makoto Suzuki for their assistance during morphometric measurements. We would like to thank Editage (www.editage.com) for their English language editing. The comments received from Dr. Célio Magalhães, the subject editor, and the two anonymous reviewers have significantly contributed to the substantial improvement of our manuscript.

Additional information

Conflict of interest

The authors have declared that no competing interests exist.

Ethical statement

No ethical statement was reported.

Funding

This study was partly funded by JSPS KAKENHI Grant Number JP23H03519, the Sasakawa Scientific Research Grant from The Japan Science Society and The Research Institute of Marine Invertebrates.

Author contributions

KK conceived and designed the study, conducted the sampling, performed molecular and morphometric analyses and interpreted the data, as well as writing the manuscript. IK participated in the field survey and contributed to manuscript writing. KIN provided assistance with molecular analysis, as well as contributing to manuscript writing. OK oversaw the research, contributed to the sampling and reviewed and revised the manuscript. All authors have thoroughly reviewed and approved the final version of the manuscript.

Author ORCIDs

Kyosuke Kitabatake https://orcid.org/0009-0006-4150-9622
Kentaro Izumi https://orcid.org/0000-0001-9802-071X
Natsuko I. Kondo https://orcid.org/0000-0002-0883-0506
Kenji Okoshi https://orcid.org/0000-0003-0421-2812

Data availability

All of the data that support the findings of this study are available in the main text or Supplementary Information.

References

Bashevkin SM, Dibble CD, Dunn RP, Hollarsmith JA, Ng G, Satterthwaite EV, Morgan SG (2020) Larval dispersal in a changing ocean with an emphasis on upwelling regions. Ecosphere 11(1): e03015. https://doi.org/10.1002/ecs2.3015

Cowen RK, Sponaugle S (2009) Larval dispersal and marine population connectivity. Annual Review of Marine Science 1(1): 443–466. https://doi.org/10.1146/annurev.marine.010908.163757

Das S, Tseng LC, Wang L, Hwang JS (2017) Burrow characteristics of the mud shrimp *Austinogebia edulis*, an ecological engineer causing sediment modification of a tidal flat. PLoS ONE 12(12): e0187647. https://doi.org/10.1371/journal.pone.0187647

Emery KO, Niino H, Sullivan B (1971): Post-Pleistocene levels of the East China Sea. In: Turekian (Ed.) Late Cenozoic Glacial Ages. Yale University Press, New Haven, 381–390.

Felsenstein J (1985) Confidence limits on phylogenies: An approach using the bootstrap. Evolution; International Journal of Organic Evolution 39(4): 783–791. https://doi.org/10.2307/2408678

Folmer O, Black M, Hoeh W, Lutz R, Vrijenhoek R (1994) DNA primers for amplification of mt cytochrome c oxidase subunit I from diverse metazoan invertebrates. Molecular Marine Biology and Biotechnology 3(5): 294–299. https://pubmed.ncbi.nlm.nih.gov/7881515/

Forster P, Harding R, Torroni A, Bandelt HJ (1996) Origin and evolution of Native American mtDNA variation: A reappraisal. American Journal of Human Genetics 59(4): 935–945. https://pubmed.ncbi.nlm.nih.gov/8808611/

Genelt-Yanovskiy E, Li Y, Stratanenko E, Zhuravleva N, Strelkova N, Xu Q, Nazarova S (2021) Phylogeography of the Brittle Star *Ophiura sarsii* Lütken, 1855 (Echinodermata: Ophiuroidea) from the Barents Sea and East Atlantic. Diversity 13(2): 1–40. https://doi.org/10.3390/d13020040

Henmi Y, Itani G (2014) Burrow utilization in the Goby *Eutaeniichthys gilli* associated with the Mud Shrimp *Upogebia yokoyai*. Zoological Science 31(8): 523–528. https://doi.org/10.2108/zs140055

Henmi Y, Itani G (2021) Species-specific patterns of the use of burrows of *Upogebia* Leach, 1814 (Decapoda: Gebiidea: Upogebiidae) by the symbiotic alpheid shrimps *Stenalpheops anacanthus* Miya, 1997 and *Athanas japonicus* Kubo, 1936 (Decapoda: Caridea: Alpheidae) as revealed by laboratory quantification. Journal of Crustacean Biology 41(1): 1–7. https://doi.org/10.1093/jcbiol/ruaa095

Hollander J, Collyer ML, Adams DC, Johannesson K (2006) Phenotypic plasticity in two marine snails: Constraints superseding life history. Evolution; International Journal of Organic Evolution 60(12): 1861–1872. https://doi.org/10.1111/j.0014-3820.2006.tb01884.x

Hong J-S (2013) Biology of the Mud Shrimp *Upogebia major* (de Haan, 1841) with particular reference to pest management for shrimp control in manila clam bed in the West Coast of Korea. Ocean and Polar Research 35(4): 323–349. https://doi.org/10.4217/OPR.2013.35.4.323

Hosoki T, Mori S, Nishida S, Kume M, Sumi T, Kitano J (2019) Diversity of gill raker number and diets among stickleback populations in novel habitats created by the 2011

Tohoku earthquake and tsunami. Evolutionary Ecology Research 20(2): 213–230. http://evolutionary-ecology.com/abstracts/v20/3168.html

Inoue N, Watanabe H, Kojima S, Sekiguchi H (2007) Population structure of Japanese spiny lobster *Panulirus japonicus* inferred by nucleotide sequence analysis of mitochondrial COI gene. Fisheries Science 73(3): 550–556. https://doi.org/10.1111/j.1444-2906.2007.01367.x

Itani G (2004) Distribution of intertidal upogebiid shrimp (Crustacea: Decapoda: Thalassinidea) in Japan. Contributions from the Biological Laboratory. Kyoto University 29: 383–399.

Iwasaki K (2006) Human-mediated introduction of marine organisms in Japan: a review. In: Koike F, Clout MN, Kawamichi M, De Poorter M, Kunio Iwatsuki K (Eds) Assessment and Control of Biological Invasion Risks. IUCN, Shoukadoh Book Sellers, Kyoto and Gland, 104–112. http://vege1.kan.ynu.ac.jp/isp/PDF/Iwasaki.pdf

Japan Coast Guard (2023) Japan Coast Guard. https://www1.kaiho.mlit.go.jp/KANKYO/KAIYO/qboc/

Kaifu K, Miller MJ, Yada T, Aoyama J, Washitani I, Tsukamoto K (2013a) Growth differences of Japanese eels *Anguilla japonica* between fresh and brackish water habitats in relation to annual food consumption in the Kojima Bay-Asahi River system, Japan. Ecology Freshwater Fish 22(1): 127–136. https://doi.org/10.1111/eff.12010

Kaifu K, Miller MJ, Aoyama J, Washitani I, Tsukamoto K (2013b) Evidence of niche segregation between freshwater eels and conger eels in Kojima Bay, Japan. Fisheries Science 79(4): 593–603. https://doi.org/10.1007/s12562-013-0628-3

Khedhri I, Tovar-Hernández M, Bonifácio P, Ahmed A, Aleya L (2017) First report of the invasive species *Branchiomma bairdi* McIntosh, 1885 (Annelida: Sabellidae) along the Tunisian coast (Mediterranean Sea). BioInvasions Records 6(2): 139–145. https://doi.org/10.3391/bir.2017.6.2.09

Kimura M (1980) A simple method for estimating evolutionary rate of base substitutions through comparative studies of nucleotide sequences. Journal of Molecular Evolution 16(2): 111–120. https://doi.org/10.1007/BF01731581

Kinoshita K (2002) Burrow structure of the mud shrimp *Upogebia major* (Decapoda: Thalassinidea: Upogebiidae). Journal of Crustacean Biology 22(2): 474–480. https://doi.org/10.1163/20021975-99990255

Kinoshita K (2022) Life history characteristics and burrow structure of the mud shrimp (Decapoda: Upogebiidae). Plankton & Benthos Research 17(4): 327–337. https://doi.org/10.3800/pbr.17.327

Kinoshita K, Nakayama S, Frota T (2003) Life cycle characteristics of the deep-burrowing mud shrimp *Upogebia major* (Thalassinidea: Upogebiidae) on a tidal flat along the northern coast of Tokyo Bay. Journal of Crustacean Biology 23(2): 318–327. https://doi.org/10.1163/20021975-99990342

Kinoshita K, Wada M, Kogure K, Furota T (2008) Microbial activity and accumulation of organic matter in the burrow of the mud shrimp, *Upogebia major* (Crustacea: Thalassinidea). Marine Biology 153(3): 277–283. https://doi.org/10.1007/s00227-007-0802-1

Kobayashi G, Itoh H, Kanaya G, Abe H, Kojima S (2023) Genetically isolated population of the coastal species with high dispersal potential: the case of the sentinel crab *Macrophthalmus japonicus* (Brachyura: Macrophthalmidae) in Japan. Plankton & Benthos Research 18(1): 13–20. https://doi.org/10.3800/pbr.18.13

Kojima S, Segawa R, Hayashi I (1997) Genetic differentiation among populations of the Japanese turban shell *Turbo* (*Batillus*) *cornutus* corresponding to war m currents. Marine Ecology Progress Series 150: 149–155. https://doi.org/10.3354/meps150149

Kojima S, Segawa R, Hayashi I (2000) Stability of the courses of the warm coastal currents along the Kyushu Island suggested by the population structure of the Japanese turban shell, *Turbo* (*Batillus*) *cornutus*. Journal of Oceanography 56(5): 601–604. https://doi.org/10.1023/A:1011113430343

Kojima S, Hayashi I, Kim D, Iijima A, Furota T (2004) Phylogeography of an intertidal direct-developing gastropod *Batillaria cumingi* around the Japanese Islands. Marine Ecology Progress Series 276(1): 161–172. https://doi.org/10.3354/meps276161

Komai T (2020) Confirmation of the occurrence of a little known upogebiid mudshrimp *Upogebia pugnax* de Man, 1905 (Decapoda: Gebiidea) in Japanese waters. Fauna Ryukyuana 53: 19–29. http://purl.org/coar/access_right/c_abf2

Kumar S, Stecher G, Li M, Knyaz C, Tamura K (2018) MEGA X: Molecular evolutionary genetics analysis across computing platforms. Molecular Biology and Evolution 35(6): 1547–1549. https://doi.org/10.1093/molbev/msy096

Kurihara T, Shikatani M, Nakayama K, Nishida M (2006) Proximate mechanisms causing morphological variation in a turban snail among different shores. Zoological Science 23(11): 999–1008. https://doi.org/10.2108/zsj.23.999

Makarov VV (1938) Anomura, in Fauna SSSR, Rakoobraznye (The Fauna of the USSR: Crustaceans). Akad. Nauk SSSR 10(3): 1–324.

Moon JH, Pang IC, Yang JY, Yoon WD (2010) Behavior of the giant jellyfish *Nemopilema nomurai* in the East China Sea and East/Japan Sea during summer 2005: A numerical model approach using a particle-tracking experiment. Journal of Marine Systems 80(1): 101–114. https://doi.org/10.1016/j.jmarsys.2009.10.015

Ngoc-Ho N (2001) *Austinogebia*, a new genus in the Upogebiidae and rediagnosis of its close relative, *Gebiacantha* Ngoc-Ho, 1989 (Crustacea: Decapoda: Thalassinidea). Hydrobiologia 449(1/3): 47–58. https://doi.org/10.1023/A:1017516331683

Nishi R, Manu J, Jansen T, Hayashi K (2012): Scarp generation behind a dune and shore protection structure by Tsunami on March 11, 2011. Journal of Japan Society of Civil Engineers Series B3 (Ocean Engineering) 68: 198–203. [In Japanese] https://doi.org/10.2208/jscejoe.68.I_198

Nishida S, Kuroyanagi K, Koike H (2015) Genetic features of *Tachypleus tridentatus* in Japan and an alien (non-native) population founded at Ise-Mikawa Bay, Chubu region, central Japan. In: Carmichael RH, Botton ML, Shin PKS, CheungSG (Eds) Changing Global Perspectives on Horseshoe Crab Biology, Conservation and Management. Springer, 129–146. https://doi.org/10.1007/978-3-319-19542-1_6

Okoshi K (2004) Alien species introduced with imported clams: the clam-eating moon snail *Euspira fortunei* and other unintentionally introduced species. Japanese Journal of Benthology 59: 74–82. [In Japanese with English abstract] https://doi.org/10.5179/benthos.59.74

Okoshi K (2016) The Effects of Liquefaction, Tsunami, and Land Subsidence on Intertidal Mollusks Following the Great East Japan Earthquake. Ecological Impacts of Tsunamis on Coastal Ecosystems. Springer, 165–178. https://doi.org/10.1007/978-4-431-56448-5_12

Okoshi K, Sato-Okoshi W (2011) *Euspira fortunei*: Biology and Fisheries Science of Invasive Species. Kouseisyakouseikaku, Tokyo, 225 pp. [In Japanese] http://www.kouseisha.com/book/b212112.html

Sakai K (2006) Upogebiidae of the world (Decapoda, Thalassinidea). Crustaceana Monographs 6: 1–185. https://doi.org/10.1163/9789047418580

Sato M (2000) Life in Ariake Sea: Biodiversity in Tidal Flats and Estuaries. Kaiyusha, Tokyo, 396 pp. [In Japanese]

Sato M (2010) Anthropogenic decline of the peculiar fauna of estuarine mudflats in Japan. Plankton & Benthos Research 5(Supplement): 202–213. https://doi.org/10.3800/pbr.5.202

Sawai Y, Namegaya Y, Okamura Y, Satake K, Shishikura M (2012) Challenges of anticipating the 2011 Tohoku earthquake and tsunami using coastal geology. Geophysical Research Letters 39: L21309. https://doi.org/10.1029/2012GL053692

Seike K, Goto R (2020) Trophic segregation in a burrow: The stable carbon and nitrogen isotope ratios of the burrowing shrimp *Upogebia major* and its commensal bivalve *Cryptomya busoensis*. Plankton & Benthos Research 15(3): 220–227. https://doi.org/10.3800/pbr.15.220

Selin NI (2017) The population dynamics and growth of the mud shrimp *Upogebia major* (De Haan, 1841) (Crustacea: Decapoda) from Peter the Great Bay,Sea of Japan. Russian Journal of Marine Biology 43(4): 270–275. https://doi.org/10.1134/S1063074017040101

Shiozaki Y, Itani G (2020) Behavioural strategy of the ectosymbiotic crab (*Sestrostoma* sp.) during ecdysis of the crab and its upogebiid shrimp host. Journal of the Marine Biological Association of the United Kingdom 100(5): 753–758. https://doi.org/10.1017/S0025315420000594

Sun X, He J (2021) The complete mitochondrial genome and phylogenetic analysis of *Upogebia major* (De Haan, 1841). Mitochondrial DNA, Part B, Resources 6(3): 970–971. https://doi.org/10.1080/23802359.2020.1870898

Urita T (1942) Decapod crustaceans from Saghalien, Japan. Nihon Seibutsu Chiri Gakkai Kaiho 12(1): 1–78.

Uye SI (2008) Blooms of the giant jellyfish *Nemopilema nomurai*: A threat to the fisheries sustainability of the East Asian marginal seas. Plankton & Benthos Research 3(Suppl.): 125–131. https://doi.org/10.3800/pbr.3.125

Vinogradov LG (1950) Keys for the identification of shrimps, prawns and crabs of the Far East, Izv. Tikhookean. Nauchno-Issled. Inst. Rybn. Khoz. Okeanogr 33: 179–358.

Wang JT, Wang PX (1980) Relationship between sea-level changes and climatic fluctuations in East China since late Pleistocene. Acta Genetica Sinica 35: 299–312. [In Chinese with English abstract] https://doi.org/10.11821/xb198004003

Yamazaki D, Miura O, Ikeda M, Kijima A, Van TD, Sasaki T, Chiba S (2017) Genetic diversification of intertidal gastropoda in an archipelago: The effects of islands, oceanic currents, and ecology. Marine Biology 164(9): e184. https://doi.org/10.1007/s00227-017-3207-9

Yamazaki D, Aota T, Chiba S (2020) The genetic structure of the marine flatworm *Stylochoplana pusilla* (Rhabditophora: Polycladida) and its use of intertidal snails. Journal of the Marine Biological Association of the United Kingdom 100(5): 1–5. https://doi.org/10.1017/S0025315420000570

Yanagimoto T, Chow S, Sakai T, Sawayama S, Hayashi Y, Saito K, Wakabayas T, Yamamoto J (2022) Genetic and morphological differentiation among local populations of Japanese top shell *Turbo sazae*. Nippon Suisan Gakkaishi 88(5): 396–406. https://doi.org/10.2331/suisan.22-00005

Zhang D, Ding G, Ge B, Zhang H, Tang B, Yang G (2014) Comparative phylogeography of two marine species of crustacean: Recent divergence and expansion due to environmental changes. Gene 550(1): 141–147. https://doi.org/10.1016/j.gene.2014.08.006

Supplementary material 1

Molecular and morphometric analyses of *Upogebia major*

Authors: Kyosuke Kitabatake, Kentaro Izumi, Natsuko I. Kondo, Kenji Okoshi

Data type: xlsx

Explanation note: The appendix contains certain outcomes of molecular analyses, such as variations in nucleotide numbers and genetic disparities, as well as the results and tests of morphometric analyses stratified by gender.

Link: https://doi.org/10.3897/zookeys.1182.105030.suppl1

ZooKeys 1182: 289–306 (2023)
DOI: 10.3897/zookeys.1182.105449

Research Article

New species and newly recorded species of *Anisandrus* Ferrari, 1867 ambrosia beetles from Thailand (Coleoptera, Curculionidae, Scolytinae, Xyleborini)

Wisut Sittichaya[1], Sarah M. Smith[2], Roger A. Beaver[3]

1 *Agricultural Innovation and Management Division, Faculty of Natural Resources, Prince of Songkla University, Songkhla, 90110, Thailand*
2 *Department of Entomology, Michigan State University, 288 Farm Lane, 243 Natural Science Bldg, East Lansing, MI 48824, USA*
3 *161/2 Mu 5, Soi Wat Pranon, T. Donkaew, A. Maerim, Chiangmai 50180, Thailand*
Corresponding author: Wisut Sittichaya (wanakorn62@hotmail.com)

Abstract

Five new species, *Anisandrus montanus* **sp. nov.**, *A. phithakpa* **sp. nov.**, *A. tanaosi* **sp. nov.**, *A. triton* **sp. nov.**, and *A. uniseriatus* **sp. nov.** are described from Thailand. *Anisandrus carinensis* (Eggers, 1923) is reported from Thailand for the first time and *A. apicalis* is removed from the Thai fauna. With the inclusion of the species described and recorded here, the diversity of *Anisandrus* is increased to 40 species, of which 11 occur in Thailand. A synoptic list and a key to the *Anisandrus* of Thailand are presented.

Key words: Key, new records, Oriental region, Thai fauna

Academic editor: M. Alonso-Zarazaga
Received: 25 April 2023
Accepted: 30 September 2023
Published: 20 October 2023

ZooBank: https://zoobank.org/2C0E1229-A614-47E1-BDE8-E88F1674DE35

Citation: Sittichaya W, Smith SM, Beaver RA (2023) New species and newly recorded species of *Anisandrus* Ferrari, 1867 ambrosia beetles from Thailand (Coleoptera, Curculionidae, Scolytinae, Xyleborini). ZooKeys 1182: 289–306. https://doi.org/10.3897/zookeys.1182.105449

Introduction

The ambrosia beetle genus *Anisandrus* Ferrari, 1867, was erected for *Xyleborus dispar* (Fabricius, 1792) because of its antennal club and mouth parts which differ from other *Xyleborus* Eichhoff, 1864 species (Ferrari 1867). *Anisandrus* currently contains 35 species distributed through the Palearctic region, from Europe to Japan, and through the Oriental region to New Guinea and the Solomon Islands. A single species occurs in Madagascar, but the genus is not known from the African continent. Two species, *A. obesus* (LeConte, 1868) and *A. sayi* Hopkins, 1915, are indigenous to the Nearctic region, and two Palearctic species, *A. dispar* (Fabricius, 1792), and *A. maiche* (Kurentsov, 1941) have been introduced to and established in the USA (Wood 1977; Rabaglia et al. 2009; Gomez et al. 2018). *Anisandrus maiche* is also established in Italy and Ukraine (Nikulina et al. 2015; Colombari et al. 2022). In Thailand, six *Anisandrus* species were previously recorded (Hutacharern and Tubtim 1995; Beaver and Liu 2010; Beaver et al. 2014; Smith et al. 2020), but one species, *A. apicalis* (Blandford, 1894) must be removed from the fauna following the recognition of closely similar species with which it was previously confused (see below). In the present study, we describe five new species and report one new species from Thailand, increasing the diversity of the Thai fauna to 11 *Anisandrus* species and that of the genus to 40. We also provide a key and synoptic list of the *Anisandrus* of Thailand.

Materials and methods

Specimens were collected at 27 study sites in 24 conservation areas across all regions of Thailand as detailed and illustrated by Sittichaya and Smith (2022), with the addition of 10 study sites in the Tanaosi (Tenasserim) mountain range in western Thailand between September and December 2022 using the same collecting methods. Photographs were taken with a Canon 5D digital camera with a Canon MP-E 65 mm macro lens (Canon, Tokyo, Japan) and StackShot-Macrorail (Cognisys, Traverse City, Michigan, USA). The photos were then combined with Helicon Focus v. 6.8.0. (Helicon Soft, Kharkiv, Ukraine) and all photos were improved with Adobe Photoshop CS6 (Adobe Systems, San Jose, California, USA). The antennal and pronotum types and characters follow those proposed by Hulcr et al. (2007) and subsequently elaborated by Smith et al. (2020). Length was measured from pronotal apex to the apex of the declivity, and width was measured at the widest part of the specimen. Pronotal length included the anterior serrations and elytral length was measured from the anterior margin to the apex along the elytral medial suture. Pedicel is excluded from the number of funicle segments.

Abbreviations used for entomological collections:

MSUC	Albert J. Cook Arthropod Research Collection, Michigan State University, East Lansing, USA
NHMW	Naturhistorisches Museum Wien, Austria
QSBG	Queen Sirikit Botanical Garden, Chiang Mai, Thailand
RABC	Roger A. Beaver collection, Chiang Mai, Thailand
THNHM	Natural History Museum of the National Science Museum, Thailand
WSTC	Private collection of Wisut Sittichaya, Songkhla, Thailand

Taxonomic treatment

Xyleborini LeConte, 1876

Anisandrus Ferrari, 1867

Anisandrus Ferrari, 1867: 24.

Type species. *Apate dispar* Fabricius, 1792, by monotypy.

Differential diagnosis. Antennal club obliquely truncate, type 1 (except *A. achaete* Smith, Beaver & Cognato, 2020, which is type 2) (Hulcr et al 2007; Smith et al. 2020), club taller than wide (except *A. achaete* wider than tall); procoxae contiguous or narrowly separated; protibiae slender, obliquely or distinctly triangular, outer margin with 5–8 large socketed denticles on distal half, posterior face flat, unarmed, or with a few small granules; mesonotal mycangial tufts present (except *A. achaete*, *A. carinensis* (Eggers, 1923), *A. paragogus* Smith, Beaver & Cognato, 2020, and *A. uniseriatus* sp. nov.) along the pronotal base either as a small tuft the length of the scutellum and directly opposite it or extending laterally from the scutellum to striae 3 and with elytral base broadly, shallowly emarginated from the scutellum to striae 3; pronotum anterior margin with a row of serrations, pronotum lateral margins obliquely costate (Smith et al. 2020).

Some *Anisandrus* species have a median pair of pronotal serrations larger than the remaining serrations and superficially resemble *Cnestus* Sampson species. The genera are easily separated by the lateral margin of the pronotum which is costate in *Anisandrus* and carinate in *Cnestus*.

New species

Anisandrus montanus **Sittichaya, Smith & Beaver, sp. nov.**

https://zoobank.org/A68B1284-FBA2-4172-AE79-02DBACC5BDD9
Fig. 1

Type materials. ***Holotype*****:** female, THAILAND, Chiangmai Province, Chom Thong District, Doi Inthanon National Park, 18°32'03.1"N, 98°29'55.2"E, 1680m, high montane forest, ethanol-baited traps, 01.vi.[20]20, W. Sittichaya (MSUC). ***Paratypes*****:** same as holotype except: 18°35'10.5"N, 98°29'13.1"E, 2,550 m, 01.iv.[20]19, W. Sittichaya (2, WSTC; 1, THNHM); Chiang Mai, Doi Inthanon NP, Kaew Maepan Trail, 18°33.162'N, 98°28.810'E, 2250 m, Malaise trap, 10–17.xi.2006, Y. Areeluck (1, RABC); as previous except: 18°35.361'N, 98°29.157'E, summit forest, 2500 m, 9–16.viii.2006 (1, RABC); as previous except: 6–13.ix.2006 (1, QSBG).

Similar species. *A. eggersi* (Beeson, 1930), *A. improbus* (Sampson, 1913).

Differential diagnosis. 2.80–2.92 mm long (mean 2.86, *n* = 4); 2.33–2.43× as long as wide. This species is similar to *A. eggersi*, but the body is smaller and more elongate, the declivity is less laterally broadened, and the posterolateral margin is not feebly costate. It is also similar to *A. improbus* but is distinguished by the following characteristics (*A. improbus* given first): sparse pubescence vs moderate pubescence, body 3.3–3.4 mm long vs 2.80–2.92 mm long, and body form more elongate, 2.43–2.54× as long as wide, vs stouter, 2.33–2.43× as long as wide.

Description. Female. 2.80–2.92 mm long (mean 2.86, *n* = 4); 2.33–2.43× as long as wide. Body shiny and black, except appendages yellowish brown; body moderately densely covered with long, yellowish-brown, hair-like setae. ***Head***: epistoma entire, transverse, with a row of hair-like setae; setae moderately long, sparse. Frons feebly convex to upper level of eyes, smooth, moderately shining, rather sparsely punctured, except close to epistoma; punctures bearing long, fine, hair-like setae. Frons with a weakly elevated, glabrous median ridge from epistoma to mid-point; above the eyes slightly domed, less shiny, coriaceous. Eyes shallowly emarginate just above antennal insertion, upper part smaller than lower part. Submentum triangular, large, slightly impressed. Antennal scape regularly thick, slightly longer than club (1.1:1). Pedicel as wide as scape, half as long as funicle. Funicle 4-segmented, segment 1 shorter than pedicel. Club longer than wide, obliquely truncate, type 1; segment 1 corneous, encircling anterior face, with sharp marginal carina; segment 2 narrow, concave, corneous on anterior face; sutures absent on posterior face. ***Pronotum***: 0.90× as long as wide, in dorsal view rounded, type 1, sides convex, rounded anteriorly; anterior margin with a row of six small serrations; serrations not larger than asperities behind. In lateral view short and tall, type 3, disc as long as anterior slope, summit at midpoint; summit from lateral view weakly raised, disc flat. Anterior slope with moderately spaced, medium-sized, coarse asperities, becoming lower and more strongly transverse towards summit. Disc alutaceous, subshining,

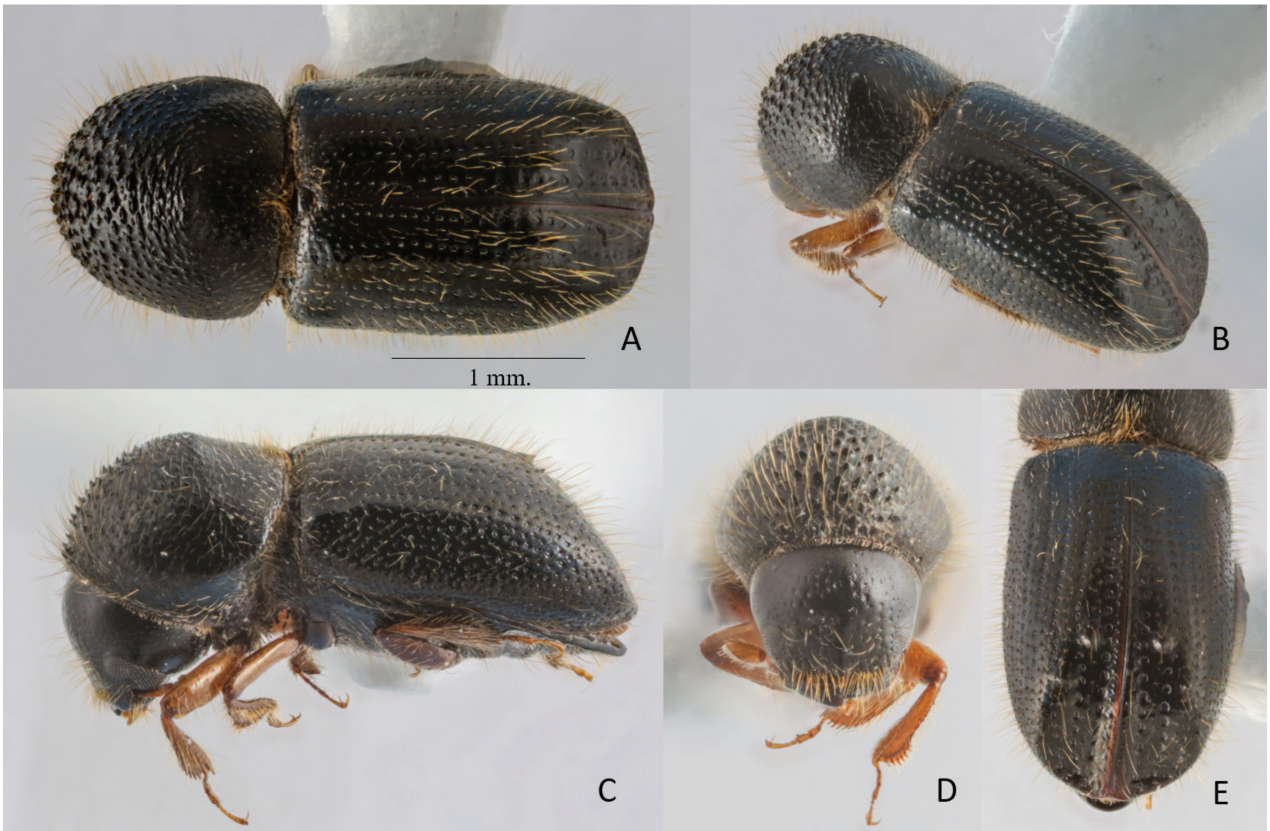

Figure 1. *Anisandrus montanus* sp. nov. holotype female **A** dorsal view **B** postero-lateral view **C** lateral view **D** frons **E** declivital face.

sparsely granulate-punctate, with a semi-recumbent, moderately long, fine, forwardly directed, hair-like seta arising from just anterior to each granule. Lateral margins obliquely costate; costa long, slightly elevated. Base slightly, broadly concave; posterior angles angulate. Mycangial tuft present along basal margin; tuft moderately setose, approximately equal to width of scutellum. ***Elytra***: 1.44× as long as wide, 1.63× as long as pronotum. Scutellum moderate in size, flat. Base transverse, edge oblique, humeral angles rounded, parallel-sided in basal 5/8, then broadly rounded to apex; surface shiny. Disc shiny, moderately convex, without transverse saddle-like depression; striae with broad, shallow punctures separated by 1/2 diameter of a puncture, setose, setae slightly longer than two diameters of a puncture, semi-recumbent, hair-like; interstriae flat, 2–3× as wide as striae, punctate; punctures uniseriate, minute, setose; setae long, erect, hair-like, becoming longer posteriorly; interstriae 2 weakly raised near declivital summit, so that first striae and interstriae appear shallowly sulcate. Declivity occupying approximately 1/3 of elytra, evenly rounded, declivital face narrow, opalescent, weakly bisulcate, moderately impressed between interstriae 1 and 3 in upper part, interstriae 3 weakly inflated near summit, flat below. Declivital striae weakly impressed, strial punctures moderately larger and deeper than those of disc, with setae as described for disc; interstriae impunctate, sparsely minutely granulate; setae 2–3× width of interstriae 2, erect, hair-like; interstriae 2 either as wide as or narrower than interstriae 3 at midpoint of declivity. Declivital summit armed with a small, sharp, backwardly pointed spine on interstriae 2 and 3; spine on interstriae 2 stronger. Posterolateral margin costate to interstriae 5. ***Legs***: procoxae contiguous. Protibiae obliquely triangular, broadest at apical 1/3; posterior face of protibiae punctate, with some punctures near base and inner margin with small, sparse granules; apical ½ of outer margin with six large, socketed denticles, their length longer than basal width. Meso- and metatibiae flattened; outer margins evenly rounded with nine and 10 large socketed denticles, respectively.

Male. Unknown.

Etymology. Latin adjective *montanus*, found on mountains. The species is known only from Doi Inthanon, the highest mountain in Thailand, at 1680–2550 m.

Distribution. Thailand (Chiangmai Province).

Biology. This species prefers montane forest.

Remarks. Three of the paratypes listed above were previously reported as *A. apicalis* by Beaver et al. (2014).

Anisandrus phithakpa **Sittichaya, Smith & Beaver, sp. nov.**

https://zoobank.org/80EC9C36-187D-40F2-A37C-A62B879D2C47
Fig. 2

Type materials. *Holotype*: female, THAILAND, Phetchaburi Province, Kaeng Krachan District, Kaeng Krachan National Park, 12°49'43.6"N, 99°21'45.2"E, 900 m, low montane forest, ex *Lithocarpus* sp., 04.x.22, W. Sittichaya (MSUC). ***Paratypes*:** Kanchanaburi Province, Thong Pha Phum District, Thong Pha Phum National Park, 14°41'40.6"N, 98°23'51.9"E, 940 m, low montane forest, ethanol-baited trap, 11.xii.22, W. Sittichaya (1, WSTC; 1, THNHM; 1, RABC).

Similar species. *A. apicalis*, *A. congruens* Smith, Beaver & Cognato, 2020, *A. cristatus* (Hagedorn, 1908).

Differential diagnosis. 2.88–3.02 mm long (mean 2.96 mm, *n* = 4); 2.06–2.17× as long as wide. Stout species; elytral disc saddle-like, bearing a pair of small spines on interstriae 2. Declivity broad; declivital face with striae 1 and 2 weakly impressed; interstriae 1 and 3 slightly elevated; posterolateral margin rounded, costate only near apex. The species is similar to *A. apicalis*, *A. congruens*, and *A. cristatus*. *Anisandrus congruens* and *A. cristatus* are distinguished by the presence on declivital interstriae 3 of a row of 5–7 regularly spaced, backwardly directed, sharply pointed spines; in *A. phithakpa* and *A. apicalis* these are reduced to small granules. *Anisandrus phithakpa* is distinguished from *A. apicalis* by the following characters (*A. phithakpa* given first): declivital interstriae with a pair of minute, pointed granules on interstriae 1, and an equally sized pair on interstriae 2 and 3 vs no granules on interstriae 1, and interstriae 2 with a pair of small, backwardly directed, sharply pointed teeth which are considerably larger than the pointed granules on interstriae 3.

Description. Female. 2.88–3.02 mm long (mean 2.96 mm; *n* = 4); 2.06–2.17× as long as wide (mean 2.12× as long as wide; *n* = 4). ***Body colors***: dark brown to black, appendages paler brown. ***Head***: epistoma entire, transverse, with a row of hair-like, moderately long, sparse setae. Frons weakly convex to upper level of eyes, reticulate, subshining, with sparse widely separated, small, shallow, setose punctures each with a long, erect hair-like seta. Medial area inconspicuous, feebly convex (flat in one paratype), glabrous. Eyes shallowly emarginate just above antennal insertion, upper part smaller than lower part. Submentum mod-

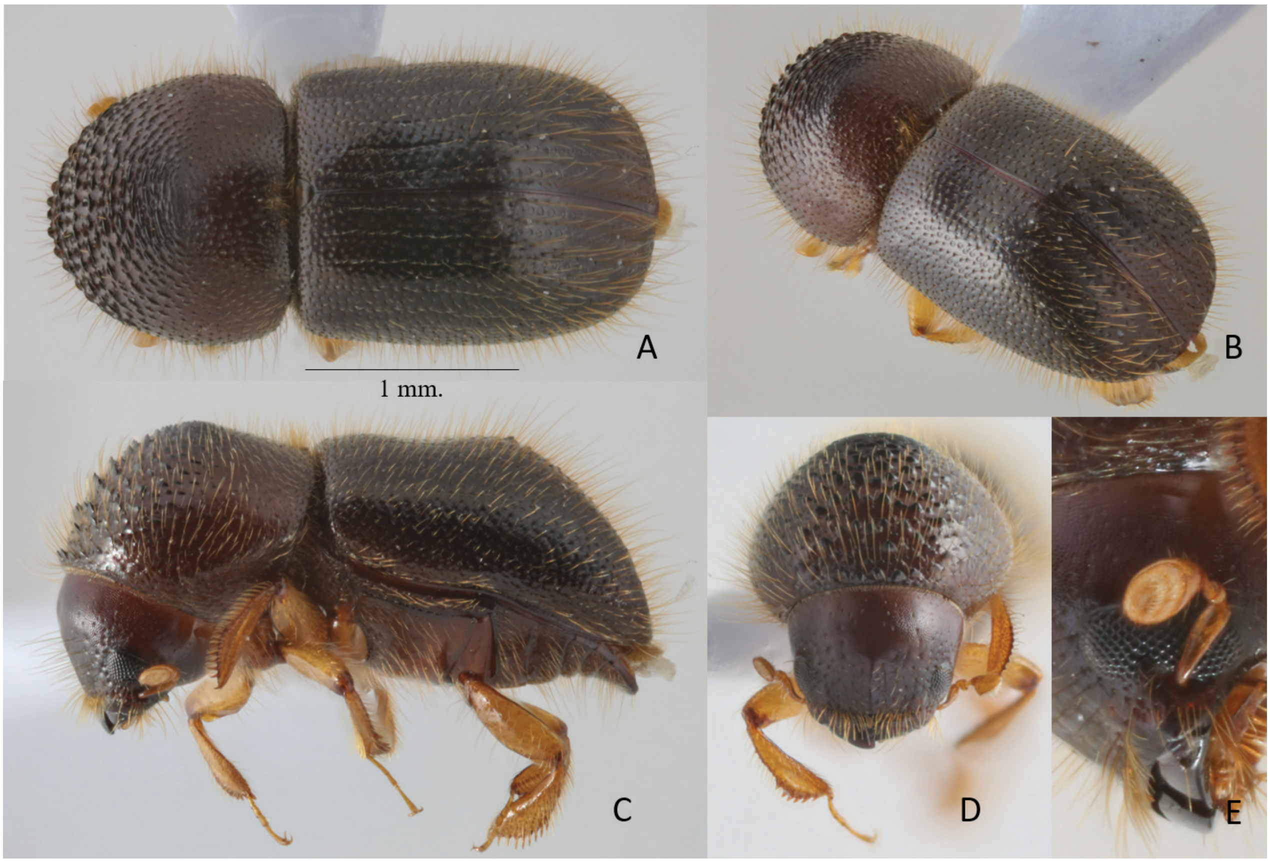

Figure 2. *Anisandrus phithakpa* sp. nov. holotype female **A** dorsal view **B** postero-lateral view **C** lateral view **D** frons **E** antenna.

erate, distinctly triangular, slightly impressed. Antennal scape regularly thick, 1.2× as long as club. Pedicel as wide as scape, shorter than funicle. Funicle 4-segmented; segment 1 shorter than pedicel. Club longer than wide, obliquely truncate, type 1; segment 1 corneous, encircling anterior face; segment 2 narrow, concave, corneous; sutures absent on posterior face. ***Pronotum***: 0.98× as long as wide, in dorsal view rounded, type 1; sides convex, rounded anteriorly; anterior margin with a row of eight small serrations of same size as asperities above; in lateral view, short and tall, type 3; disc as long as anterior slope, summit at midpoint. Anterior slope with densely spaced, very large, coarse asperities, becoming lower and more strongly transverse towards summit. Disc alutaceous, subshiny with moderately dense, large, shallow punctures; punctures with moderate, semi-recumbent, hair-like setae; some longer hair-like setae at margins. Lateral margins obliquely costate. Base transverse with posterior angles rounded. Mycangial tuft present along basal margin; tuft moderately setose, approximately the width of scutellum. ***Elytra***: 1.5× as long as wide, 1.5× as long as pronotum. Scutellum broad, large, linguiform, flush with elytra, flat, shiny. Elytral base transverse; edge oblique; humeral angles rounded; elytra parallel-sided in basal ½, then broadly rounded to apex; surface shiny. Disc shiny, with a distinct medial, transverse, saddle-like depression; depressed areas opalescent; striae not impressed; with broad shallow punctures separated by areas less than a diameter of a puncture, setose; setae 2–3× as long as a puncture, recumbent, hair-like; interstriae flat, punctate, with 2 or 3 confused lines of minute punctures, setose; setae long, 1–1.5× width of interstriae 2, erect, hair-like, unarmed by granules. Declivity occupying approximately 1/3 elytra; apex evenly rounded; declivital summit with a pair of minute, pointed granules on interstriae 1, and a slightly larger pair on both interstriae 2 and 3 placed progressively further towards apex; declivital face feebly bisulcate; striae 1 and 2 impressed; interstriae 3 inflated and armed, with 2 or 3 minute granules; strial punctures of similar size and depth to those of disc, bearing setae as described for disc; interstriae impunctate, sparsely, minutely granulate; setae 2× width of interstriae 2, erect, hair-like; interstriae 2 as wide as or narrower than interstriae 3 at midpoint of declivity. Posterolateral margin costate to interstriae 5. ***Legs***: procoxae contiguous; prosternal coxal piece short, inconspicuous. Protibiae obliquely triangular, broadest at apical 1/3; posterior face inflated, punctate, punctures minute; apical 1/2 of outer margin with six socketed denticles, their length 2× their basal as basal width. Meso- and metatibiae flattened; outer margins evenly rounded with seven and eight long slender socketed denticles, respectively.

Male. Unknown.

Etymology. Thai (พิทักษ์ป่า) “Phithakpa”, forest rangers. The species name indicates our deep appreciation for Thai forest rangers for their hard and selfless work to protect conservation areas in Thailand. Noun in apposition.

Distribution. Thailand (Kanchanaburi and Phetchaburi provinces).

Biology. Recorded from *Lithocarpus* sp. (Fagaceae).

Remarks. The paler body colors (brown) of the holotype and some paratypes suggest that they are teneral. One paratype has a consistently dark-brown body with pale appendages.

Anisandrus tanaosi Sittichaya, Smith & Beaver, sp. nov.

https://zoobank.org/4B554589-BDE9-460C-AEAA-6D7208213A80

Fig. 3

Type materials. ***Holotype*:** female, Thailand, Phetchaburi Province, Kaeng Krachan District, Kaeng Krachan National Park, 12°49'43.6"N, 99°21'45.2"E, 900 m, low montane forest, ex. *Lithocarpus* sp., 04.x.22, W. Sittichaya (MSUC). ***Paratype*:** Kanchanaburi Province, Thong Pha Phum District, Thong Pha Phum National Park, 14°41'40.6"N, 98°23'51.9"E, 940 m, low montane forest, ethanol-baited trap, 11.xii.22, W. Sittichaya (1 WSTC).

Similar species. *A. auco* Smith, Beaver & Cognato, 2020, *A. cryphaloides* Smith, Beaver & Cognato, 2020, *A. triton* sp. nov.

Differential diagnosis. 2.31–2.70 mm long (mean 2.5; $n = 2$); 2.20–2.25× as long as wide (mean = 2.23; $n = 2$). Small and stout species. Pronotal anterior margin slightly angularly projecting; elytral disc convex, without a saddle-like impression, declivital summit armed with a pair of minute, spinulose granules on interstriae 2, declivital face feebly convex, unarmed. Posterolateral margin rounded, costate only near apex. The species is similar to *A. auco* and *A. cryphaloides*. It can be distinguished from *A. auco* by the following characters (*A. tanaosi* given first): smaller size (2.3–2.7 mm long vs 2.9–3.0 mm); anterior margin of pronotum with seven moderately sized asperities vs four large coarse asperities; more steeply sloping elytral declivity occupying 3/8 of elytral length vs more gently sloping occupying 3/5 of length; dark-brown to black body vs light brown to reddish brown. It can be distinguished from *A. cryphaloides* by the

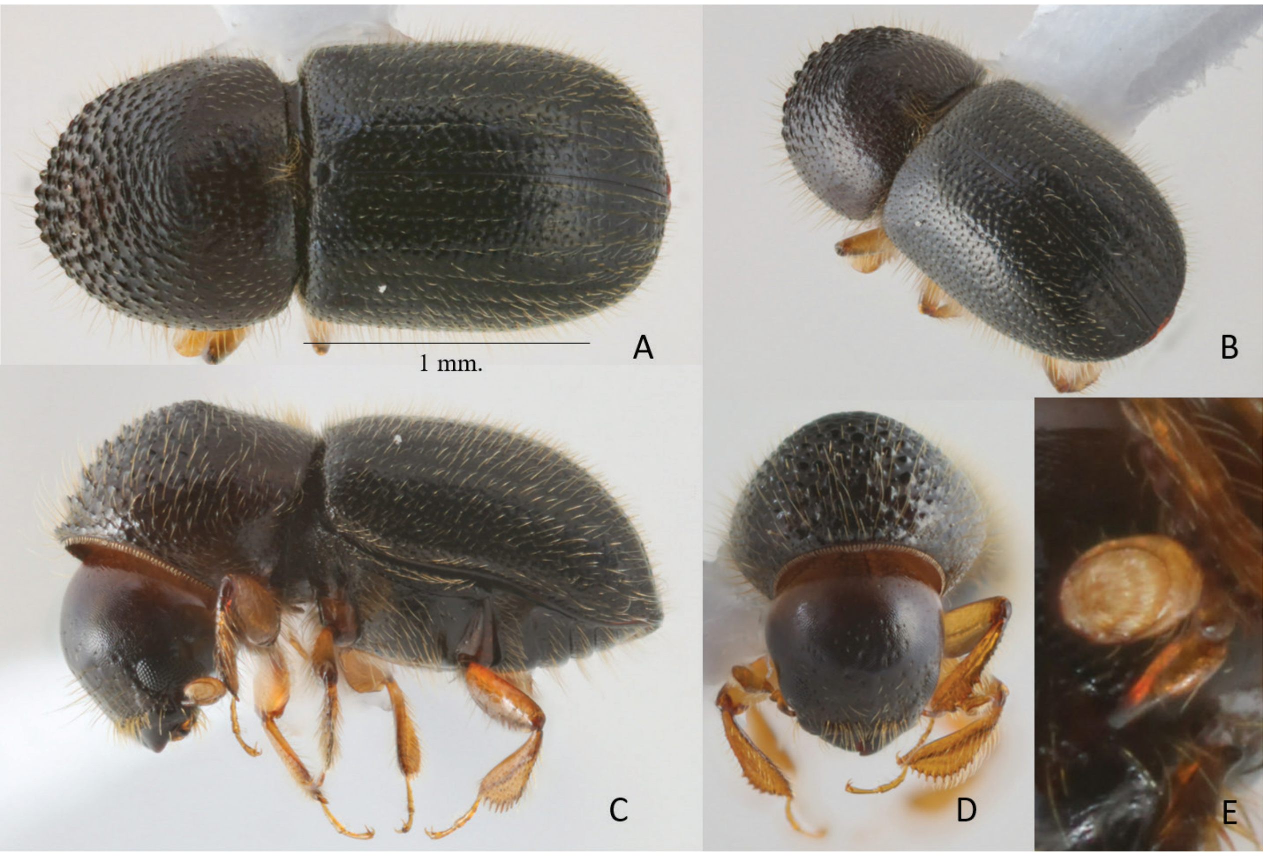

Figure 3. *Anisandrus tanaosi* sp. nov. holotype female **A** dorsal view **B** postero-lateral view **C** lateral view **D** frons **E** antenna.

following characters (*A. tanaosi* given first): pronotum in dorsal view type 0, anterior margin only slightly projecting, with asperities of equal size vs pronotum more strongly conical, type 6, median pair of asperities larger than lateral pairs.

Description. Female. 2.31–2.70 mm long (mean 2.5; *n* = 2); 2.20–2.25× as long as wide (mean 2.23; *n* = 2). Body dark brown to black, head and prothorax dark brown, elytra and venter black, appendages yellowish brown. Antennae and legs light brown. Body densely covered with greyish-brown setae. ***Head***: epistoma entire, transverse, with a row of short hair-like setae, setae sparse. Frons feebly convex to upper level of eyes, weakly reticulate, rugulose-punctate, some rugulosities forming longitudinal lines; each puncture with a moderately long, fine, hair-like setae; a weak, impunctate median ridge extends to upper level of eyes. Eyes feebly emarginate just above antennal insertion, upper part slightly smaller than lower part. Submentum triangular, small, slightly impressed. Antennal scape regularly thick, short, as long as club. Pedicel as wide as scape, shorter than funicle. Funicle 4-segmented, segment 1 as long as pedicel. Club longer than wide, obliquely truncate, type 1; segment 1 corneous, encircling anterior face; segment 2 concave, soft and narrow; sutures absent on posterior face. ***Pronotum*:** 0.90× as long as wide. In dorsal view, type 0, feebly conical anteriorly, sides convex; anterior margin with a row of seven small, slightly protruding serrations, equal in size to those on anterior slope. In lateral view type 3, short and tall; disc as long as anterior slope, summit at midpoint. Anterior slope with moderately densely spaced, large coarse asperities, becoming lower and more strongly transverse towards summit. Disc alutaceous, subshining with moderately dense, minute granulate punctures, each bearing a short, semi-recumbent, hair-like seta, some longer hair-like setae at margins. Lateral margins obliquely costate. Base transverse, posterior angles angularly rounded. Mycangial tuft present along basal margin, tuft moderately setose, approximately the width of scutellum. ***Elytra***: 1.22× as long as wide, 1.42× as long as pronotum. Scutellum broad, large, linguiform, flush with elytra, flat, shiny. Elytral base transverse, edge oblique, humeral angles rounded, parallel-sided in basal 2/3, then broadly rounded to apex. Disc subshiny, broadly convex; striae not impressed, with small, shallow, setose punctures separated by 1.5–2× diameters of a puncture, setae 3× as long as diameter of punctures, recumbent, hair-like; interstriae flat; punctures strongly confused, without granules, setose; setae short, as long as strial setae, erect hair-like. Declivity occupying approximately 3/8 elytra; summit with a pair of spinulose granules on interstriae 2; declivital face feebly convex above, flattened below from interstriae 1–3; striae weakly impressed; strial punctures somewhat larger and deeper than those of disc; interstriae sparsely uniseriate punctate, setae 2× width of an interstria, erect, hair-like. Posterolateral margin rounded, unarmed by granules, costate only close to apex. ***Legs***: procoxae contiguous; prosternal coxal piece short, inconspicuous. Protibiae obliquely triangular, broadest at apical 1/3; posterior face minutely granulate; apical 1/3 of outer margin with six small, socketed denticles, their length as long as basal width. Meso- and metatibiae flattened; outer margins evenly rounded with eight large, socketed denticles.

Male. Unknown.

Etymology. Tanaosi (ตะนาวศรี), Thai name of the Tenasserim mountain range, in reference to the collection locality of the holotype. Noun in apposition.

Distribution. Thailand (Kanchanaburi and Phetchaburi provinces).

Biology. Unknown.

Anisandrus triton **Sittichaya, Smith & Beaver, sp. nov.**

https://zoobank.org/411AD77C-E814-4329-9ACC-145754A53EDB
Fig. 4

Type material. ***Holotype*:** female, THAILAND, Kanchanaburi Province, Thong Pha Phum District, Thong Pha Phum National Park, 14°41'40.6"N, 98°23'51.9"E, 940m, low montane forest, ethanol-baited trap, 11.xii.22, W. Sittichaya (MSUC).

Similar species. *Anisandrus auco*, *A. cryphaloides*.

Differential diagnosis. 4.22 mm long; 1.94× as long as wide. Large, broad, stout species. Elytral disc with a saddle-like, weak impression on middle of disc; declivity longer than disc; interstriae 2 armed with two pairs of spines, backwardly incurved on declivital summit and one additional smaller sized spine on upper portion of declivital face; interstriae 3 armed with a row of 3–5 unequally sized spines and granules; declivital face feebly convex, apex broadly rounded; posterolateral margin rounded, with a short costa near apex. The species is similar to *Anisandrus auco*, *A. cryphaloides*, and *A. tanaosi*. It can be distinguished from them by the following characters (*A. triton* given first): greater size (4.2 mm long vs 2.1–3.0 mm) and stouter body (1.94× longer than wide vs 2.2–2.4×; elytral disc with a weak, saddle-like depression vs elytral disc flat; upper margin of the elytral declivity with a pair of backwardly directed, sharply pointed spines vs a pair of minute, pointed granules.

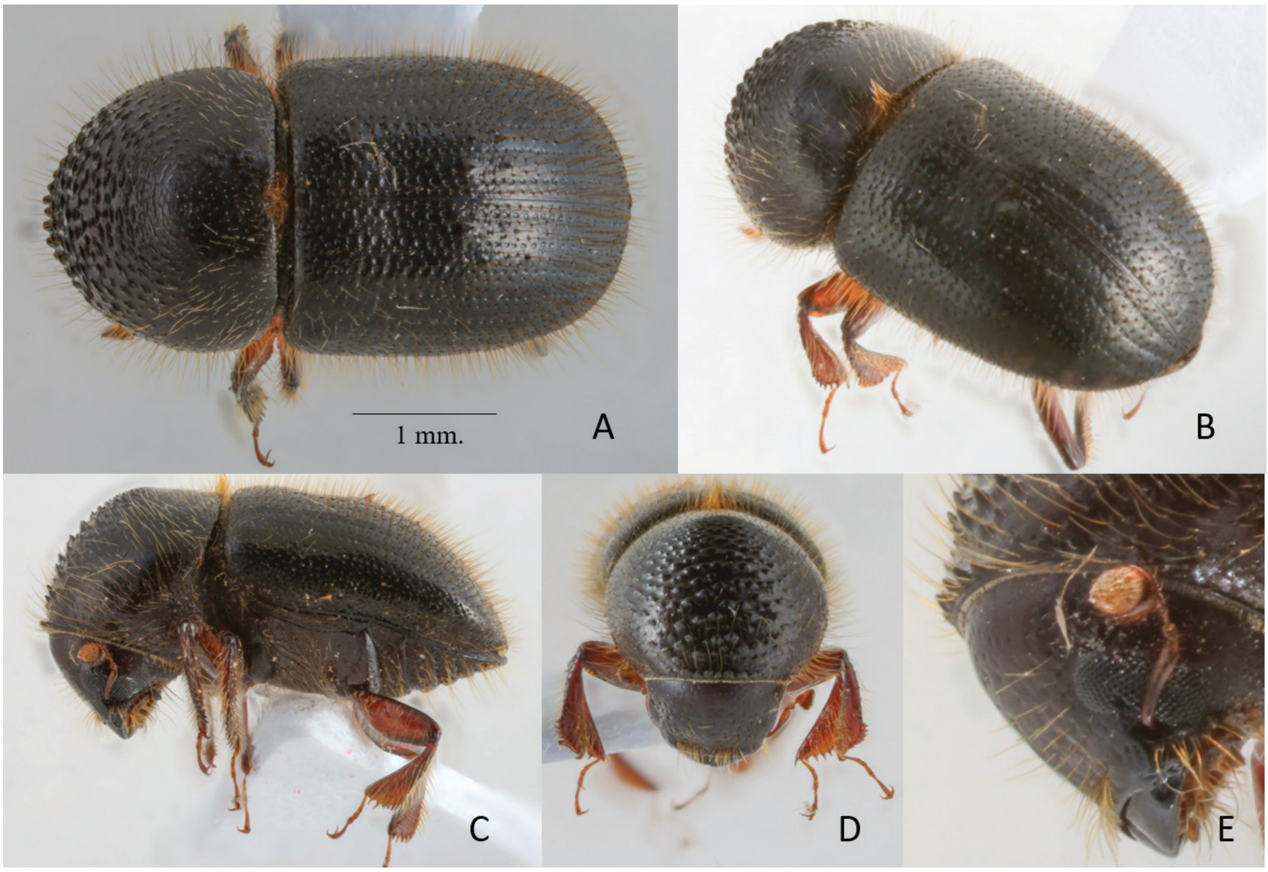

Figure 4. *Anisandrus triton* sp. nov. holotype female **A** dorsal view **B** postero-lateral view **C** lateral view **D** frons **E** antenna.

Description. Female. 4.22 mm long (*n* = 1); 1.94× as long as wide. Body black except appendages brown; body densely covered with long, erect, yellowish-brown, hair-like setae. ***Head***: epistoma entire, transverse, with a row of short and sparse, hair-like setae, sparser in the middle and on lateral margins below eyes. Frons with a weak median ridge extending to upper margin of eyes, weakly impressed on each side near epistoma, becoming flattened and weakly convex above, reticulate, subshining, with sparse, large, shallow, punctures, each puncture bearing a shorter, finer, erect hair-like seta than those on epistoma; punctures becoming smaller and shallower towards vertex. Eyes large, feebly emarginate just above antennal insertion; upper part of eyes much smaller than lower part. Submentum transversely long, narrowly triangular, slightly impressed. Antennal scape slender, 1.4× as long as club. Pedicel as wide as scape, shorter than funicle. Funicle 4-segmented, segment 1 as long as pedicel. Club longer than wide, obliquely truncate, type 1; segment 1 corneous, encircling anterior face; segment 2 narrow, corneous on anterior face only; sutures absent on posterior face. ***Pronotum*****:** 0.83× as long as wide. In dorsal view, between type 0 and type 6, sides convex, strongly narrowed anteriorly; anterior margin with a row of seven medium-sized serrations. In lateral view, short and tall, type 3; disc slightly shorter than anterior slope. Anterior slope with moderately dense, large, coarse asperities, becoming lower and more strongly transverse towards summit. Disc convex, moderately shiny with moderately dense, minute, punctures bearing two types of setae: moderately long, erect, hair-like setae and short, semi-recumbent, hair-like setae; some longer, hair-like setae at margins. Base transverse; posterior angles broadly rounded. Mycangial tuft present along basal margin; tuft dense, long, setose, approximately 2× width of scutellum. ***Elytra***: 1.18× as long as wide, 1.63× as long as pronotum. Scutellum small, broad, linguiform, shiny, slightly convex, flush with elytra. Elytral base transverse, edge oblique, humeral angles rounded, parallel-sided in basal ½, then broadly rounded to apex; surface shining. Disc shallowly, transversely impressed; striae not impressed, with medium-sized, shallow punctures separated by the diameter of a puncture; strial setae 1.5× as long as punctures, semi-recumbent, hair-like; discal interstriae 1 and 3 flat, interstriae 4 and 5 weakly convex; near upper margin of declivity, interstriae 1–5 weakly convex; interstriae biseriate punctate, punctures minute, shallow, each bearing an erect hair-like seta; setae on disc as long as interstrial width, some longer setae present on lateral and apical margins of elytra; punctures on lateral margins and near declivital summit replaced by small granules. Declivity occupying approximately 1/2 elytra, evenly rounded, declivital face convex; striae feebly impressed, strial punctures the same size and depth as those of disc; interstriae feebly convex, 1–3 of equal width, biseriate granulate; setae 2× width of an interstria, erect, hair-like; declivital interstria 2 armed with two pairs of spines; the larger on declivital summit backwardly hooked, the smaller on upper portion of declivital face pointed; interstria 3 armed by a row of 5 spinulose granules, the upper two pairs slightly backwardly hooked. Posterolateral margin of declivity rounded, with a short costa near apex, unarmed by granules. ***Legs***: procoxae slightly separated; prosternal coxal piece short, inconspicuous. Protibiae obliquely triangular, broadest at apical 1/3; posterior face inflated, unarmed; apical 1/2 of outer margin with six moderately sized socketed denticles, length approximately equal to basal width. Meso- and metatibiae flattened; outer margins evenly rounded each with eight moderately sized socketed denticles.

Male. Unknown.

Etymology. Ancient Greek, *triton* is a fish-tailed sea-god, named after a veteran vehicle used in beetle surveys by the senior author.

Distribution. Thailand (Kanchanaburi Province).

Biology. Unknown.

Anisandrus uniseriatus Sittichaya, Smith & Beaver, sp. nov.

https://zoobank.org/A00B2A08-2C6F-4922-8620-4EBDF881F1A4

Fig. 5

Type material. ***Holotype***, female, Thailand, Nan Province, Pua District, Doi Phu Kha National Park, 19°10'27.4"N, 101°06'19.7"E, 1660 m, montane forest, ethanol-baited traps, 01.viii.19 W. Sittichaya (MSUC). ***Paratypes*:** same as holotype except: 30.vi.19 (2) (1, NHMW; 1, RABC); same as holotype except: 10.x.19 (2) (1, THNHM; 1, WSTC).

Similar species. *Anisandrus carinensis*.

Differential diagnosis. 4.0–4.32 mm long (mean 4.20 mm; *n* = 5); 2.32–2.60× as long as wide (mean 2.44 mm; *n* = 5). Species large, robust; body yellowish brown, covered with long erect hair-like setae; pronotal anterior margin broadly rounded and armed with a row of serrations; mesonotal mycangial tuft absent; antennal club type 1 with segment 1 encircling anterior face; elytral disc with a

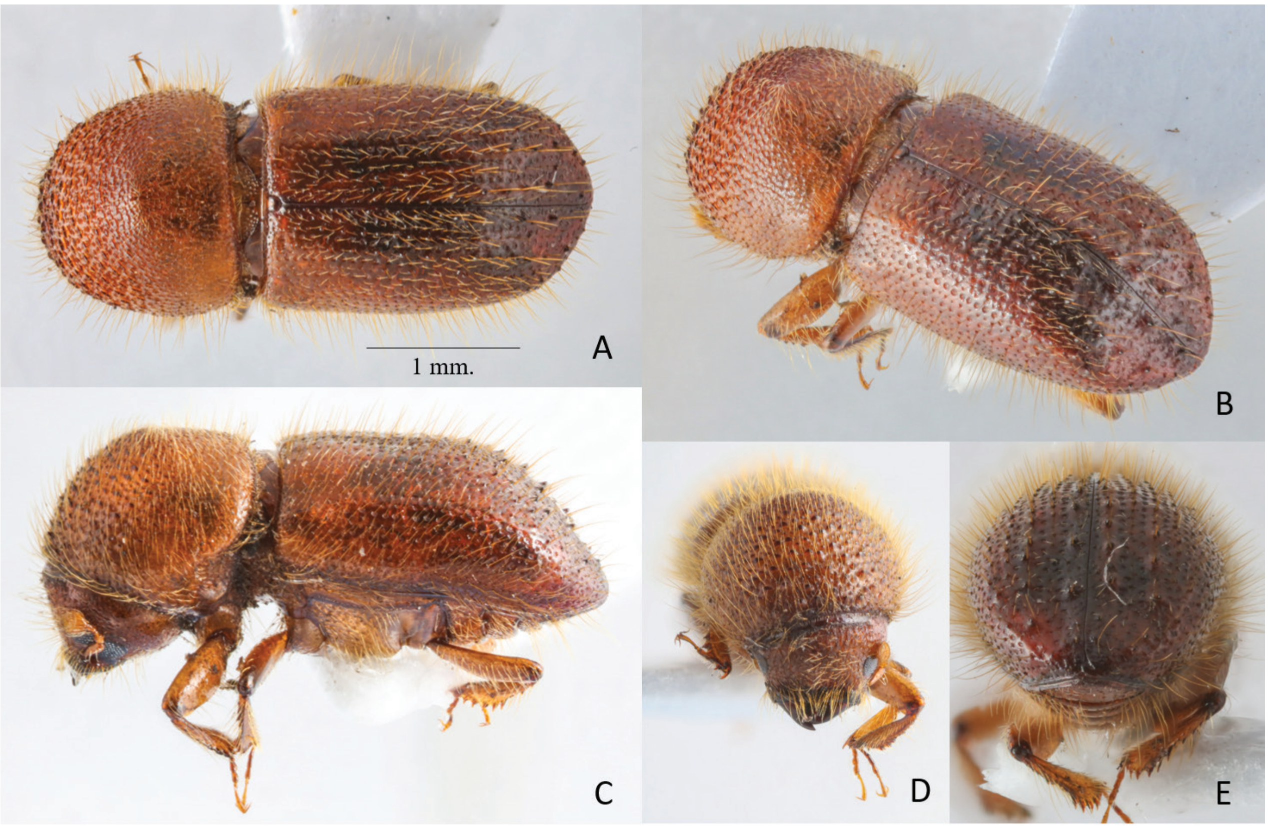

Figure 5. *Anisandrus uniseriatus* **sp. nov.** holotype female **A** dorsal view **B** lateral view **C** postero-lateral view **D** frons **E** venter and antennae **F** declivital face.

weak transverse saddle-like depression; interstriae uniseriate granulate; declivital interstriae 1 and 3 armed by four or five unequally sized tubercles; elytral apex angularly rounded.

This species is closely related to *A. carinensis* but is distinguished by the following characteristics (*A. uniseriatus* given first): discal interstria uniseriate granulate-punctate vs biseriate granulate-punctate; angularly rounded apex vs broadly rounded elytral apex.

Description. Female. 4.0–4.32 mm long (mean 4.20 mm; *n* = 5); 2.32–2.60× as long as wide (mean 2.44 mm; *n* = 5). Body yellowish brown to reddish brown, declivity darker. Head, legs, and antennae light brown. ***Head*:** epistoma entire, transverse, with a row of golden, long and thick hair-like setae. Frons flat to upper level of eyes, shining, with sparse small granules, each with a fine, long, erect hair-like seta; median line narrowly elevated to upper margin of eyes, glabrous strongly shining. Vertex convex, reticulate, with longitudinal shallow rugae and punctures. Eyes shallowly emarginate just above antennal insertion, upper part smaller than lower part. Submentum large, distinctly triangular, slightly impressed. Antennal scape regularly thick, as long as club. Pedicel as wide as scape, shorter than funicle. Funicle 4-segmented, segment 1 shorter than pedicel. Club wider than long, obliquely truncate, type 1; segment 1 corneous, transverse, occupying basal 2/5, encircling anterior face; segment 2 narrow, concave, corneous; sutures absent on posterior face. ***Pronotum*:** 0.89× as long as wide. In dorsal view basic, type 2, sides parallel in basal 1/2, rounded anteriorly; anterior margin without distinct serrations. In lateral view basic, type 0, disc as long as anterior slope, summit at apical 2/5. Anterior slope with densely placed asperities of very variable size, becoming lower and more strongly transverse towards summit. Disc shining, with densely placed, minute asperities and granules, arranged approximately concentrically behind summit; vestiture of long, erect hair-like setae interspersed with shorter, more abundant, semi-recumbent setae directed antero-medially; some longer hair-like setae on convex lateral margins. Base transverse, posterior angles rounded. Mycangial tuft absent. ***Elytra*:** 1.55× as long as wide, 1.75× as long as pronotum. Scutellum narrow, moderately sized, linguiform, flush with elytra, flat, shiny. Elytral bases transverse, edge oblique, humeral angles rounded; elytra parallel-sided in basal 2/3, then broadly rounded to apex; surface shiny. Disc with a very slight, transverse, saddle-like depression in middle; only striae 1 impressed, its punctures coarse, shallow, regularly placed, separated by about the diameter of a puncture, and bearing fine, moderately long, hair-like setae; interstriae finely punctate, with some punctures (approximately every second puncture) granulate; interstria 1 uniseriately punctured, but with 2–3 rows of punctures where widened posteriorly close to declivity; interstria 2 uniseriately punctate along its length; interstriae 3–5 biseriately punctate close to base, uniseriate posteriorly; granulate punctures on interstriae bearing long, fine, erect hairlike setae, non-granulate punctures with shorter, semi-recumbent setae. Declivity occupying approximately 1/3 of elytra, steeply sloping; declivital face weakly bisulcate between raised interstriae 1 and 3; strial punctures larger and deeper than those of disc; interstriae uniseriate with some punctures replaced by granules or tubercles; interstriae 1 widest at mid-declivity, with 4–6 larger pointed tubercles, and some smaller granules; interstriae 2 with a few small granules at top of declivity only, narrowed towards apex; interstriae 3 with 5–7 pointed tubercles, a little smaller than those on interstriae 1; interstrial tubercles and granules bearing long, erect setae 1.5× width of interstriae 2; interstrial punctures with finer, shorter setae. Posterolateral margin of elytra rounded, costate only near apex, unarmed by granules. ***Legs*:** procoxae contiguous, prosternal coxal piece tall and pointed. Protibiae distinctly triangular, broadest at apical 4/5, posterior face smooth; apical 1/2 of outer margin with five moderately sized socketed denticles, their length slightly longer than basal width. Meso- and metatibiae flattened, obliquely triangular, their apical 1/2 with 5- or 6-socketed denticles on outer margin.

Male. Unknown.

Etymology. Latin *uniseriatus*: uni- meaning one; series meaning row, in reference to a single row of interstrial setae.

Distribution. Thailand (Nan Province).

Biology. Unknown.

New country record

Anisandrus carinensis (Eggers, 1923)

Fig. 6

Differential diagnosis. 3.70–4.26 mm long (mean 4.08; $n = 7$); 2.27–2.35× as long as wide (mean 2.31×; $n = 7$). Moderate to large in size, robust form; body yellowish brown, covered with long erect hair-like setae; pronotal anterior margin broadly rounded and armed with a row of serrations on anterior margin of

Figure 6. *Anisandrus carinensis* female. **A** dorsal view **B** lateral view.

pronotum; mesonotal mycangial tuft absent; antennal club type 1 with segment 1 encircling anterior face; elytral disc with a weak transverse saddle-like depression; interstriae biseriate granulate; declivital interstriae 1 and 3 armed by four or five unequally sized tubercles; elytral apex broadly rounded.

Thai distribution. S: Ranong Province, Suk Samran District, Klong Naka Wildlife Sanctuary, 9°27'42.8"N, 98°32'23.3"E, 320 m, tropical lowland forest, ethanol-baited traps, 01.iv.14 (4); Suratthani Province, Ban Ta Khun District, Khao Sok National Park, 8°55'25.6"N, 98°31'19.2"E, 380 m, tropical rain forest, ethanol-baited trap, 01.v.14 (10). W: Kanchanaburi Province, Thong Pha Phum District, Thong Pha Phum National Park, 14°41'40.6"N, 98°23'51.9"E, 940 m, montane forest, ethanol baited trap, 10.ix.22 (3); all W. Sittichaya.

Other distribution. Myanmar (Smith et al. 2020).

Correction to faunal list for Thailand

Anisandrus apicalis (Blandford, 1894)

Notes. Seven specimens were recorded from Chiang Mai province under this name by Beaver et al. (2014). Three of these specimens are now included in the closely similar species, *A. montanus* sp. nov. (see above). The other four specimens belong to *A. cristatus*, which was considered a synonym of *A. apicalis* at the time of Beaver et al.'s publication. It was reinstated as a distinct species by Smith et al. (2020). We know of no specimens of *A. apicalis* from Thailand, and the species must be removed from the faunal list.

Discussion

Anisandrus has recently been the focus of intense study, with 18 species described since 2020, including those described here (Smith et al. 2020, 2022).

Table 1. Synoptic list and habitat types of the *Anisandrus* fauna of Thailand. References are to records of the species in Thailand. Thai distribution follows that of Sittichaya and Smith (2022) which lists the following abbreviations: C = Central; N = North; NE = Northeast; S = South.

Species	Thai distribution	Habitat types	References
Anisandrus carinensis (Eggers, 1923)	W: Kanchanaburi; S: Ranong, Suratthani	Tropical rain forest, low montane forest	This publication
Anisandrus congruens Smith, Beaver & Cognato, 2020	N: Chiang Mai, Nan	Montane forest	Smith et al. 2020; W. Sittichaya (unpublished)
Anisandrus cristatus (Hagedorn, 1908)	N: Chiang Mai, Nan	Montane forest	Smith et al. 2020; W. Sittichaya (unpublished)
Anisandrus eggersi (Beeson, 1930)	N: Chiang Mai, Nan; NE: Loei	Montane forest	Smith et al. 2020; W. Sittichaya (unpublished)
Anisandrus hirtus (Hagedorn, 1904)	N: Chiang Mai, Nan; NE: Loei; S: Nakhon Sri Thammarat, Narathiwat, Phang Nga, Ranong, Songkhla, Suratthani, Trang	Dry dipterocarp forest, Montane forest, Tropical rain forest	Beaver and Liu 2010; Beaver et al. 2014
Anisandrus montanus sp. nov.	N: Chiang Mai	Montane forest	This publication
Anisandrus phithakpa sp. nov.	C: Phetchaburi; W: Kanchanaburi	Low montane forest	This publication
Anisandrus tanaosi sp. nov.	C: Phetchaburi; W: Kanchanaburi	Low montane forest	This publication
Anisandrus triton sp. nov.	W: Kanchanaburi	Low montane forest	This publication
Anisandrus uniseriatus sp. nov.	N: Nan	Montane forest	This publication
Anisandrus ursulus (Eggers, 1923)	C: Chanthaburi, Nakhon Nayok, Phetchaburi; N: Chiang Mai, Tak; NE: Loei, Nakhon Ratchasima; S: Nakhon Sri Thammarat, Surat Thani	Dry dipterocarp forest, Dry evergreen forest, Montane forest, Tropical rain forest	Hutacharern and Tubtim 1995; Beaver et al. 2014

The genus is diverse in montane forest habitats in Southeast Asia, and Thailand in particular (Table 1). There is no doubt that additional species await discovery in unsampled mountain ranges throughout Southeast Asia.

Key to *Anisandrus* species present in Thailand (females only)

1 Mycangial tuft present, just anterior and roughly equal in width to scutellum, lightly to moderately setose **2**

– Mycangial tuft absent **10**

2 Interstriae 2 without spines or granules on upper margin of elytral declivity. Large. densely hairy species, 3.4–4.9 mm long. Median pair of asperities on anterior margin of pronotum distinctly larger than outer pair........ **3**

– Interstriae 2 with spines, spinulose granules or blunt tubercles on upper margin of elytral declivity. Usually smaller, less densely hairy species. Median pair of asperities on anterior margin of pronotum not distinctly larger than outer pair(s)............ **4**

3 Larger, stouter species, 4.3–4.9 mm long, 1.9–2.0× longer than wide. Declivital striae not impressed............ ***A. ursulus* (Eggers)**

– Smaller, more elongate species, 3.4–4.5 mm long, 2.1–2.5× longer than wide. Declivital striae impressed............ ***A. hirtus* (Hagedorn)**

4 Interstriae 2 with a sharp, hooked spine on summit of elytral declivity........ **5**

– Interstriae 2 with rounded or spinulose granules, never with a sharp, hooked spine on summit of elytral declivity **8**

5 Large, stout species, 4.2 mm long, 1.95× as long as wide; elytral declivity weakly convex .... ***A. triton* sp. nov.**

– Smaller, more elongate species, 2.6–3.7 mm long, 2.2–2.5× as long as wide; elytral declivity impressed, often bisulcate.......................................**6**

6 Interstriae 3 on elytral declivity armed with a row of 4 or 5 backwardly pointed spines, its upper portion elevated to middle of declivity..............**7**

– Interstriae 3 on elytral declivity armed only with 1 or 2 backwardly pointed spines; upper portion of declivital interstriae flat, not elevated ....***A. montanus* sp. nov.**

7 Smaller species, 2.6–2.8 mm long. Spines on declivital interstriae 3 sharply pointed but not backwardly hooked .... ***A. congruens* Smith, Beaver & Cognato**

– Larger species, 3.3–3.7 mm long. Spines on declivital interstriae 3 sharply pointed and backwardly hooked .... ***A. cristatus* (Hagedorn)**

8 Declivital interstriae impunctate, punctures replaced by minute granules, especially on interstriae 1–3; declivital summit armed with two pairs of distinct spinulose granules on interstriae 2 and 3; posterolateral margin of elytra strongly or weakly costate to interstriae 5 ....**9**

– Declivital striae punctate; declivital summit armed only by a pair of minute, spinulose granules on interstriae 2; posterolateral margin of elytra costate only close to apex..***A. tanaosi* sp. nov.**

9 Elytral disc with a weak, transverse, saddle-like depression; posterolateral margin of elytra weakly costate ....***A. phithakpa* sp. nov.**

– Elytral disc without a weak, transverse, saddle-like depression; posterolateral margin of elytra strongly costate .... ***A. eggersi* (Beeson)**

10 Interstriae on elytral declivity irregularly biseriate granulate-punctate, elytral apex broadly rounded ....***A. carinensis* (Eggers)**

– Interstriae on elytral declivity uniseriate granulate-punctate, elytral apex angulately rounded..***A. uniseriatus* sp. nov.**

Acknowledgements

We are most grateful to Harald Schillhammer (NHMW) for access to specimens. Special thanks also go to members of the National Parks staff for facilitating collecting.

Additional information

Conflict of interest

The authors have declared that no competing interests exist.

Ethical statement

No ethical statement was reported.

Funding

This research was supported by Prince of Songkla University (Grant No. NAT6502010S), an NSF-PEET grant (DEB-0328920 awarded to Anthony Cognato, Michigan State University) and a Cooperative Agreement (IP00533923 to Anthony Cognato) from the United

States Department of Agriculture's Animal and Plant Health Inspection Service (APHIS). It may not necessarily express APHIS' views.

Author contributions

Data curation: WS. Resources: WS. Writing – original draft: WS. Writing – review and editing: RAB, SMS.

Author ORCIDs

Wisut Sittichaya https://orcid.org/0000-0001-6200-1285
Sarah M. Smith https://orcid.org/0000-0002-5173-3736
Roger A. Beaver https://orcid.org/0000-0003-1932-3208

Data availability

All of the data that support the findings of this study are available in the main text.

References

Beaver RA, Liu L-Y (2010) An annotated synopsis of Taiwanese bark and ambrosia beetles, with new synonymy, new combinations and new records (Coleoptera: Curculionidae: Scolytinae). Zootaxa 2602(1): 1–47. https://doi.org/10.11646/zootaxa.2602.1.1

Beaver RA, Sittichaya W, Liu L-Y (2014) A synopsis of the scolytine ambrosia beetles of Thailand (Coleoptera: Curculionidae: Scolytinae). Zootaxa 3875(1): 1–82. https://doi.org/10.11646/zootaxa.3875.1.1

Colombari F, Martinez-Sañudo I, Battisti A (2022) First report of the alien ambrosia beetle *Cnestus mutilatus* and further finding of *Anisandrus maiche* in the European part of the EPPO region (Coleoptera: Curculionidae: Scolytinae: Xyleborini). Bulletin OEPP. EPPO Bulletin. European and Mediterranean Plant Protection Organisation 52(2): 446–450. https://doi.org/10.1111/epp.12840

Ferrari JA (1867) Die Forst- und Baumzuchtschädlichen Borkenkäfer (Tomicides Lac.) aus der Familie der Holzverderber (Scolytides Lac.), mit Besonderer Berücksichtigung Vorzüglich der Europäischen Formen, und der Sammlung des k. k. Zoologischen Kabinets in Wien. Carl Gerold's Sohn, Wien, 96 pp.

Gomez DF, Rabaglia RJ, Fairbanks KEO, Hulcr J (2018) North American Xyleborini north of Mexico: A review and key to genera and species (Coleoptera, Curculionidae, Scolytinae). ZooKeys 768: 19–68. https://doi.org/10.3897/zookeys.768.24697

Hulcr J, Dole SA, Beaver RA, Cognato AI (2007) Cladistic review of generic taxonomic characters in Xyleborina (Coleoptera: Curculionidae: Scolytinae). Systematic Entomology 32(3): 568–584. https://doi.org/10.1111/j.1365-3113.2007.00386.x

Hutacharern C, Tubtim N (1995) Checklist of Forest Insects of Thailand. Office of Environmental Policy and Planning, Bangkok, 392 pp.

Nikulina T, Mandelshtam M, Petrov A, Nazarenko V, Yunakov N (2015) A survey of the weevils of Ukraine. Bark and ambrosia beetles (Coleoptera: Curculionidae: Platypodinae and Scolytinae). Zootaxa 3912: 1–61. https://doi.org/10.11646/zootaxa.3912.1.1

Rabaglia RJ, Vandenburg N, Acciavatti RE (2009) First records of *Anisandrus maiche* Stark (Coleoptera: Curculionidae: Scolytinae) from North America. Zootaxa 2137(1): 23–28. https://doi.org/10.11646/zootaxa.2137.1.2

Sittichaya W, Smith SM (2022) New species and new records of *Amasa* Lea, 1894 ambrosia beetles from Thailand (Coleoptera: Curculionidae: Scolytinae: Xyleborini). Zootaxa 5196(2): 197–210. https://doi.org/10.11646/zootaxa.5196.2.2

Smith SM, Beaver RA, Cognato AI (2020) A monograph of the Xyleborini (Coleoptera, Curculionidae, Scolytinae) of the Indochinese Peninsula (except Malaysia) and China. ZooKeys 983: 1–442. https://doi.org/10.3897/zookeys.983.52630

Smith SM, Beaver RA, Pham HT, Cognato AI (2022) New species and new records of Xyleborini from the Oriental region, Japan and Papua New Guinea (Coleoptera: Curculionidae: Scolytinae). Zootaxa 5209(1): 1–33. https://doi.org/10.11646/zootaxa.5209.1.1

Wood SL (1977) Introduced and exported American Scolytidae (Coleoptera). The Great Basin Naturalist 37: 67–74.

ZooKeys 1182: 307–329 (2023)
DOI: 10.3897/zookeys.1182.106828

Research Article

A new species of *Xenophrys* (Amphibia, Anura, Megophryidae) from southern Tibet, China

Guocheng Shu[1,2], Ke Li[1], Yayong Wu[1], Qin Liu[1], Zhongping He[1], Ling Li[1,3], He Zhang[1,3], Peng Guo[1]

1 *Faculty of Agriculture, Forest and Food Engineering, Yibin University, Yibin 644007, China*
2 *Key Lab of Aromatic Plant Resources Exploitation and Utilization in Sichuan Higher Education, Yibin 644007, China*
3 *College of Life Sciences, Shenyang Normal University, Shenyang 110034, China*
Corresponding author: Peng Guo (ybguop@163.com)

Abstract

A new species of *Xenophrys* is described from Yadong County, Tibet Autonomous Region, China based on morphological and molecular evidence. Phylogenetic analyses based on the mitochondrial genes 16S rRNA and COI indicated that this new species represents an independent lineage and the minimum *p*-distance based on 16S rRNA between this species and its congeners is 4.4%. Additionally, the new species is distinguished from its congeners by a combination of the following morphological characters: (1) small body size, SVL 17.9–22.2 mm in adult males and SVL 23.4 mm in the single adult female; (2) tympanum indistinct, supratympanic fold distinct; (3) canthus rostralis well-developed, snout tip far beyond the margin of the lower lip; (5) pupil vertical; (6) vomerine teeth present, maxillary teeth present; (7) tongue notched posteriorly; (8) supernumerary tubercles absent, subarticular, metacarpal and metatarsal tubercles indistinct; (9) relative finger lengths I < II < IV < III, finger tips rounded, slightly expanded relative to digit widths; (10) toes with narrow lateral fringes and tarsal folds; (11) a dark triangular marking with light edge between eyes, a dark ")("-shaped marking, with light edge, present on center of dorsum, pectoral glands on sides of the breast.

Key words: Morphology, phylogenetic analyses, taxonomy, *Xenophrys pangdaensis* sp. nov., Yadong County

Academic editor: Annemarie Ohler
Received: 23 May 2023
Accepted: 13 September 2023
Published: 20 October 2023

ZooBank: https://zoobank.org/64598C08-BB92-49D8-B852-E4CE7B01FD6F

Citation: Shu G, Li K, Wu Y, Liu Q, He Z, Li L, Zhang H, Guo P (2023) A new species of *Xenophrys* (Amphibia, Anura, Megophryidae) from southern Tibet, China. ZooKeys 1182: 307–329. https://doi.org/10.3897/zookeys.1182.106828

Introduction

The Asian horned toad Megophryinae are widely distributed from northern India (west of Nepal) to eastern China and south to the Sundas and the Philippines (Frost 2023). Currently, 132 species have been described until July 2023, more than half of which have been named since the turn of the century (Frost 2023). There has been controversy about the generic classification of this group for a long time (e.g., Huang and Fei 1981; Tian and Hu 1983; Dubois 1987; Lathrop 1997; Rao and Yang 1997; Jiang et al. 2003; Delorme et al. 2006; Fei et al. 2009; Fei and Ye 2016; Chen et al. 2017; Mahony et al. 2017; Liu et al. 2018; Dubois et al. 2021; Lyu et al. 2021, 2023; Frost 2023). So far, the Megophryinae were defined as comprising ten clades by recent multilocus phylogenetic studies, including *Atympanophrys*, *Brachytarsophrys*, *Megophrys*, *Ophryophryne*, *Boulenophrys*, *Pelobatrachus*, *Grillitschia*, *Jingophrys*, *Sarawakiphrys*, and *Xenophrys* (Lyu et al. 2023). Previously, most authors regarded these clades as five or seven genera (Chen et al. 2017; Liu et al. 2018), while few researchers held a conservative attitude and regarded them as seven subgenera (Mahony et al. 2017; Shi et al. 2020). The genus *Panophrys* was established by Rao and Yang (1997); however, Dubois et al. (2021) noted that the generic name was preoccupied by *Panophrys* Dujardin, 1840 (Protozoa), so they chose *Boulenophrys* to replace it under the Principle of Homonymy.

In this study, we followed the classification system in Dubois et al. (2021) and Lyu et al. (2023) that Megophryidae contains ten genera (*Atympanophrys*, *Brachytarsophrys*, *Megophrys*, *Ophryophryne*, *Boulenophrys*, *Pelobatrachus*, *Grillitschia*, *Jingophrys*, *Sarawakiphrys*, and *Xenophrys*). Currently, the genus *Xenophrys* contains 28 recognized species in the world, which are distributed in Nepal, Bhutan, Bangladesh, India, Myanmar, Thailand, Cambodia, Vietnam, Cambodia, China, and Malaysia, of which ten are recorded in China (Frost 2023). In fact, nearly one third of the species in the genus were described in the last five years (Mahony et al. 2018, 2020; Shi et al. 2020; Luong et al. 2022), so the species diversity of the genus may have been underestimated. The eastern Himalaya is one of the 36 global biodiversity hotspots (Basnet et al. 2019), many new species have been discovered and named in this region in recent years (e.g., Jiang et al. 2016a, b, c; Shi et al. 2020). Over the past two years, several field surveys were conducted in this area and specimens of the family Megophryidae were collected. Also, a new bush frog, *Raorchestes yadongensis* Zhang, Shu, Liu, Dong, & Guo, 2022, was recently found and described (Zhang et al. 2022). Based on morphological comparison and molecular phylogenetic analyses, some specimens were identified a new member of *Xenophrys*.

Materials and methods

Sampling

Field surveys were conducted in August 2020 and July 2021. In total, seven adult specimens of *Xenophrys* were collected from two sites in Yadong County, Tibet Autonomous Region, China (Fig. 1). Thirteen tadpoles of the new taxon were also collected in a puddle where the new taxon was found. In the field, after taking photographs, the toads were euthanized using isoflurane, and then specimens were fixed in 75% ethanol. Tissue samples were taken and preserved separately in 95% ethanol prior to fixation. Specimens collected in this work were deposited in Yibin University. The Animal Care and Use Committee of Yibin University provided full approval for this research (No. 202003).

Molecular phylogenetic analysis

Total genomic DNA was extracted using TIANamp Genomic DNA Purification Kit (TIANGEN Bio-tech Co., Ltd., Beijing, China), following manufacturer instructions. Two fragments of mitochondrial genes, 16S ribosomal RNA gene (16S) and the cytochrome C oxidase 1 gene (COI), were amplified and sequenced. Primer sequences were retrieved from the literature for 16S (Simon et al. 1994) and COI (Che et al. 2011), respectively. PCR amplifications were performed in a 25 μl vol-

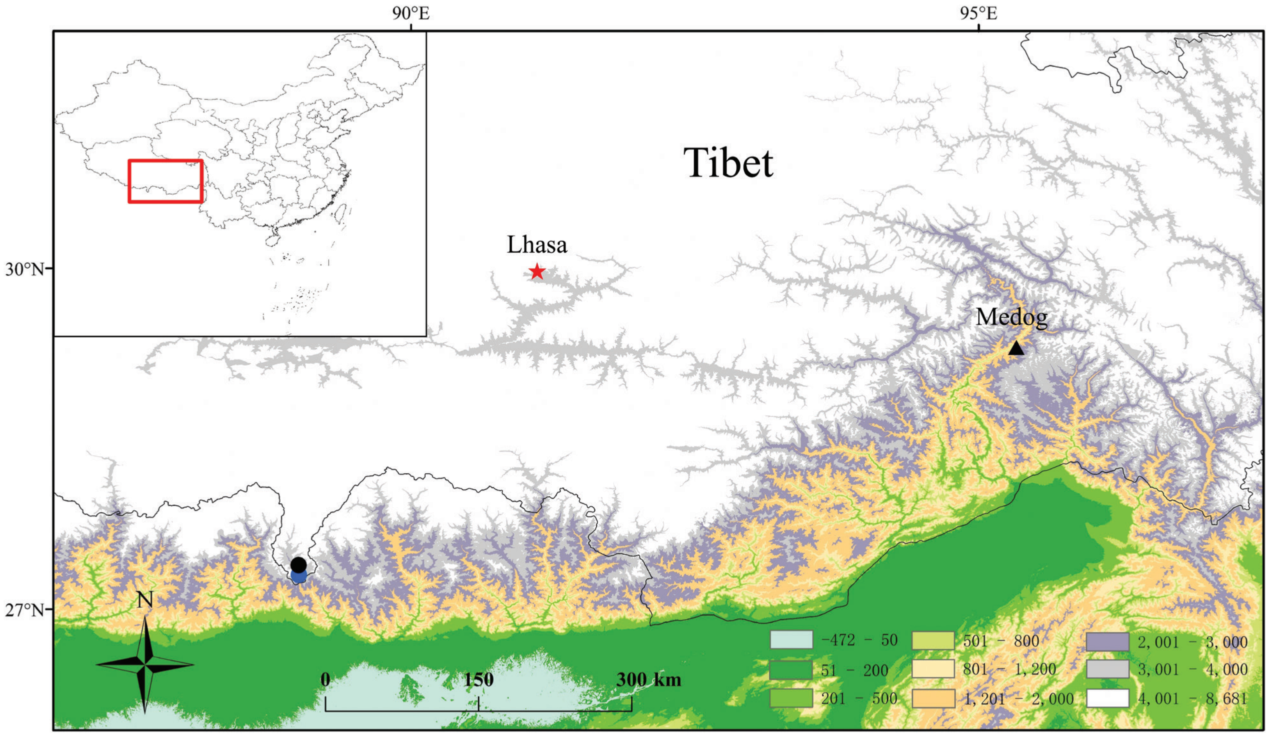

Figure 1. Type locality of the new species *Xenophrys* in Yadong County, Tibet Autonomous Region, China. The red star indicates the provincial capital, the black triangle indicates Medog County, the blue and black spots indicate the type locality and collection site of some tadpoles, respectively.

ume reaction with the following conditions: an initial denaturing step at 95 °C for 4 min; 36 cycles of denaturing at 95 °C for 40 s, annealing at 55 °C (for 16S)/52 °C (for COI) for 40 s and extending at 72 °C for 70 s, and a final extending step of 72 °C for 10 min. PCR products were sequenced with both forward and reverse primers same as used in PCR. Sequencing was conducted using an ABI3730 automated DNA sequencer in Sangon Biotechnologies Co., Ltd. (Shanghai, China). New sequences were uploaded to GenBank (for accession numbers see Table 1).

For molecular analyses, the available sequences of *Xenophrys* species were downloaded from GenBank, especially for their holotypes and/or topotypes for which comparable sequences were available (Table 1). Representative species sequences for all recognized megophryid genera were also downloaded for phylogenetic analysis (also including two controversial species *X. katabhako* comb. nov. and *X. sanu* comb. nov.). Sequences were assembled and aligned using the Clustalw module in BioEdit 7.0.9.0 (Hall 1999) with default settings. Alignments were checked by eye and revised manually if necessary. PartitionFinder v. 2.1.1 (Lanfear et al. 2017) was used to select the corresponding best-fit nucleotide substitution models for 16S gene/each codon position of COI gene under the Akaike Information Criteria (AIC). Phylogenetic analyses of the concatenated-sequence matrix were conducted in MrBayes v. 3.2.4 (Ronquist et al. 2012). Two independent runs were conducted in the BI analysis, and each run consisted of 5×10^7 generations, sampled every 1000 generations. Runs were considered to have converged when the average standard deviation of split frequencies (ASDSF) was less than 0.01. The first 25% of generations were removed as the "burn-in" stage followed by calculation of Bayesian posterior probabilities (BPP) and the 50% majority-rule consensus of the post burn-in

Table 1. Information of samples used in the molecular analyses.

Species	Voucher ID	16S	COI	References
A. gigantica	SYS a003934	MH406766	MH406225	Liu et al. 2018
A. shapingensis	SYS a005310; KIZ YPX37515	MH406890	MH406352	Liu et al. 2018
A. wawuensis	SYS a005311	MH406891	MH406353	Liu et al. 2018
Bo. binglingensis	SYS a005313; KIZ 025807; FMNH 232874	MH406892	MH406354	Liu et al. 2018; Chen et al. 2017; Mahony et al. 2017
Bo. boettgeri	SYS a004149; KIZ YPXJK033	MF667878	MH406247	Liu et al. 2018; Chen et al. 2017
Bo. brachykolos	SYS a002258; ROM 16634	KJ560403	MH406120	Liu et al. 2018; Chen et al. 2017
Bo. cheni	SYS a004050	MF667873	MH406241	Liu et al. 2018
Bo. chishuiensis	SYS a005307; KIZ 025788	MH406888	MH406350	Liu et al. 2018; Chen et al. 2017
Bo. daoji	SYS a004089	MH406783	MH406243	Liu et al. 2018
Bo. fansipanensis	VNMN 2018.01	MH514886	MW086544	Tapley et al. 2021
Bo. frigida	AMS R186131	MT364279	MW086550	Tapley et al. 2021
Bo. huangshanensis	SYS a002702; KIZ 022004	MF667882	MH406160	Liu et al. 2018; Chen et al. 2017
Bo. kuatunensis	SYS a003449	MF667881	MH406206	Liu et al. 2018
Bo. minor	SYS a003212; KIZ YPX37545	MF667865	MH406197	Liu et al. 2018; Chen et al. 2017
Bo. nanlingensis	SYS a001962	MH406645	MH406081	Liu et al. 2018
Bo. sangzhiensis	SYS a004313; KIZ YPX11006	MH406802	MH406264	Liu et al. 2018; Chen et al. 2017
Bo. spinata	SYS a002226; KIZ 016100	MH406675	MH406115	Liu et al. 2018; Chen et al. 2017
Bo. wushanensis	SYS a003009; KIZ 045469	MH406733	MH406185	Liu et al. 2018; Chen et al. 2017
Br. chuannanensis	SYS a004927	MH406902	MH406365	Liu et al. 2018
Br. feae	SYS a003913; KIZ 046706	MH406900	MH406363	Liu et al. 2018; Chen et al. 2017
Br. orientalis	SYS a004225	OQ180989	MT162625	Li et al. 2020; Lyu et al.2023
Br. platyparietus	SYS a005919	OQ180990	MT162633	Li et al. 2020; Lyu et al. 2023
Br. popei	SYS a001864	KM504256	MH406361	Liu et al. 2018
G. aceras	LSUHC 7038	GQ995534	N	Chen et al. 2017
G. longipes	IABHU 21101	AB530656	N	Hasan et al. 2014
J. cf. *pachyproctus*	CIB022017061805	MN963228	MN964303	Shi et al. 2020
J. vegrandis	Z11605 HT	KY022305	MH647530	Mahony et al. 2020
J. yeae	CIB201706MT02	MN963216	MN964313	Shi et al.2020
J. zhoui	CIBMT171053	MN963207	MN964322	Shi et al.2020
J. feii	SYS a003876	OQ181007	OQ180893	Lyu et al. 2023
Lep. alpina	SYS a003927	MH406905	MH406368	Liu et al. 2018
Lep. laui	SYS a003471	MH406903	MH406366	Liu et al. 2018
M. acehensis	MZB Amph 26098	MT710708	N	Munir et al. 2021
M. lancip	ENS 7577	KX773567	N	Mahony et al. 2017
M. montana	LSUMZ 81916; UTA A-53736, ENS 7381	KX811927	KX812163	Chen et al. 2017; Mahony et al. 2017
M. parallela	RMAS 022	KY679898	N	Munir et al. 2018
M. selatanensis	MZB Amph 22411	MT710704	N	Munir et al. 2021
O. hansi	AMNH 169285	KY022204	KX812155	Mahony et al. 2017; Chen et al. 2017
O. microstoma	AMNH 168682	KY022199	N	Mahony et al. 2017
O. poilani	AMNH 169287	KY022202	N	Mahony et al. 2017
P. baluensis	IRSNB 15926	DQ642121	N	Mahony et al. 2017
P. edwardinae	FMNH 273694	KX811918	KX812050	Chen et al. 2017
P. kalimantanensis	KUHE 53577	AB719248	N	Hamidy et al. 2012
P. kobayashii	UNIMAS 8148	KJ831313	N	Oberhummer et al. 2014
P. ligayae	KUKUH309095; ZMMUNAP-05015	KY022192	KX812051	Mahony et al. 2017; Chen et al. 2017
P. stejnegeri	FMNH 250842; KU 314303	KY022190	KX812052	Mahony et al. 2017; Chen et al. 2017
S. dringi	UNIMAS 8948	KJ831316	N	Oberhummer et al. 2014
X. ancrae	Z11606 [S2011.307] HT	MN734391	N	Mahony et al. 2020

Species	Voucher ID	16S	COI	References
X. auralensis	NCSM 79599	KX811807	N	Mahony et al. 2018
X. awuh	BN6069 PT	KY022319	N	Mahony et al. 2020
X. dzukou	BN6072 HT	KY022324	N	Mahony et al. 2020
X. flavipunctata	SDBDU 2009.297 TT	KY022307	MH647536	Mahony et al. 2018
X. glandulosa	SYSa003795	MH406760	MH406219	Shi et al.2021
X. himalayana	BNHS 6050	MH647526	N	Mahony et al. 2018
X. lekaguli	FMNH 265955 PT	KY022214	N	Mahony et al. 2017
X. major	SDBDU 2007.229	MH647514	N	Mahony et al. 2018
X. mangshanensis	KIZ021786	KX811790	KX812079	Shi et al.2020
X. maosonensis	ROM 16679	KX811784	KX812081	Shi et al.2020
X. medogensis	CIB022017062002	MN963219	MN964310	Shi et al.2020
X. megacephala	ZSIC A 11213 HT	KY022315	MH647533	Mahony et al. 2018
X. monticola	SDBDU 2011.1047	KY022312	N	Mahony et al. 2017
X. numhbumaeng	BN6076 PT	MN734393	N	Mahony et al. 2020
X. oreocrypta	BN6046 PT	KY022306	N	Mahony et al. 2020
X. oropedion	SDBDU 2009.299	KY022317	MH647534	Mahony et al. 2018
X. pangdaensis sp. nov.	YBU21248 HT	OR026569	OR026034	This study
X. pangdaensis sp. nov.	YBU21259 PT	OR026570	OR026035	This study
X. pangdaensis sp. nov.	YBU21260 PT	OR026571	OR026036	This study
X. pangdaensis sp. nov.	YBU21261 PT	OR026572	OR026037	This study
X. pangdaensis sp. nov.	YBU21262 PT	OR026573	OR026038	This study
X. pangdaensis sp. nov.	YBU21269 PT	OR026574	OR026039	This study
X. periosa	BNHS 6061 PT	KY022309	MH647528	Mahony et al. 2018
X. robusta	SDBDU 2011.1057 TT	KY022314	MH647535	Mahony et al. 2018
X. serchhipii	SDBDU 2009.612	KY022323	MH647532	Mahony et al. 2018
X. takensis	FMNH 261711	KY022215	N	Mahony et al. 2017
X. truongsonensis	IEBR A.4952	ON146202	N	Luong et al. 2022
X. zhangi	KIZ014278	KX811765	KX812084	Mahony et al. 2018
X. zunhebotoensis	RGK 0041 TT	KY022322	N	Mahony et al. 2018,
X. dehongensis	SYS a003443; KIZ 048507	MH406746	MH406204	Liu et al. 2018; Chen et al. 2017
X. katabhako	K5204/ZSI 11401 HT	KX894667	N	Deuti et al. 2017
X. lancangica	SYS a002961; KIZ01464; AMNH168679	MH406728	MH406180	Liu et al. 2018; Chen et al. 2017; Mahony et al. 2017
X. parva	SYS a003042; KIZ YPX27643	MH406737	MH406189	Liu et al. 2018; Chen et al. 2017
X. sanu	K5197/ZSI 11392 HT	KX894678	N	Deuti et al. 2017

Specimen status: HT, holotype; PT, paratype; TT, topotype.

trees sampled at stationarity. The phylogenetic trees were visualized using FigTree 1.4.3 (Rambaut 2016). Mean genetic distances between *Xenophrys* species were calculated in MEGA 7 (Kumar et al. 2016) using the uncorrected p-distance model based on 16S gene (some species lack of COI gene).

Morphological analysis

A total of seven adult specimens were measured. The terminology and methods followed Mahony (2011). Measurements were taken with a dial caliper to the nearest 0.1 mm. Thirty characters of adult specimens were measured:

EL eye length (horizontal distance between the anterior and posterior borders of orbit);

EN	eye-nostril length (distance from front of eye to the center of nostril);
FAL	forearm length (distance from elbow to wrist);
FIL	first finger length (distance from the tip of the first digit to its base where it joins the second digit);
FIIL	second finger length (distance from the tip of the second digit to its base where it joins the first digit);
FIIIL	third finger length (distance from the tip of the third digit to its base where it joins the second digit);
FIVL	fourth finger length (measured from the tip of the fourth digit to its base where it joins the third digit);
FIIIW	minimum third finger width (taken at the base of the terminal portion of the digit, which is expanded on some species);
FIIIDW	maximum width of the third fingertip;
FOL	foot length (distance from the proximal end of the inner metatarsal tubercle to the tip of the fourth digit);
HAL	hand length (distance from wrist to tip of third digit);
HL	head length (distance from the rear of the mandible to the tip of the snout);
HLL	hindlimb length;
HW	head width (distance between the posterior angles of jaw);
IBE	internal back of eyes (the shortest distance between the posterior borders of the orbits);
IFE	internal front of eyes (shortest distance between the anterior borders of orbits);
IMT	length of the inner metatarsal tubercle;
IN	internarial distance (shortest distance between two nostrils);
IUE	inter upper eyelid width (shortest distance between upper eyelids);
SHL	shank length (distance from knee to ankle);
SL	snout length (distance from tip of snout to anterior border of the orbit);
SN	nostril-snout length (distance from center of the nostril to tip of the snout);
SVL	snout-vent length (distance from the tip of the snout to the posterior edge of the vent);
TFOL	tarsal-foot length (distance from heel to the tip of the fourth digit);
TIVW	minimum fourth toe width (taken at the base of the terminal portion of the digit, which is expanded on some species);
TIVDW	maximum width of the fourth toe tip;
TL	thigh length (distance from cloaca to knee);
TYD	largest tympanum diameter;
TYE	tympanum-eye distance (distance from the anterior border of the tympanum to the posterior orbital border);
UEW	maximum upper eyelid width.

Thirteen tadpoles of the new taxon were measured. The stages of tadpoles were identified following Gosner (1960). Seventeen morphometric characters of tadpoles were measured:

BH	maximum body height;
BL	body length (distance from tip of snout to trunk-tail junction);
BW	maximum body width;
ED	maximum eye diameter;

IND	internasal distance (distance between center of two naris);
LF	maximum height of lower tail fin;
NE	naris-eye distance (distance from center of naris to anterior corner of eye);
ODW	oral disc width (largest width of oral disc);
PP	interpupilar distance;
RN	rostro-narial distance (distance from tip of snout to center of naris);
SS	snout-spiracle distance (distance from tip of snout to opening of spiracle);
SU	snout-upper fin distance (distance from snout to beginning of upper tail fin);
TAL	tail length (distance between posterior side of opening of cloaca to tip of tail);
TMH	maximum tail muscle height;
TMW	maximum tail muscle width;
TOL	total length;
UF	maximum height of upper tail fin.

Sex and maturity of the specimens were confirmed by direct examination of secondary sexual characters, including vocal sacs, nuptial pads, and the gonadal inspection (Fei and Ye 2016; Mahony et al. 2020). For webbing description, we followed Glaw and Vences (2007). We compared the morphological characters of the new species with literature data for 28 other species of *Xenophrys*.

Results

Phylogenetic analyses

The aligned sequence matrix of 16S and COI genes contained 574 bps and 663 bps, respectively. Except *X. damrei*, all other species of *Xenophrys* were included in the phylogenetic analysis. The model selection suggested that GTR+I+G as the best model for 16S rRNA fragment, and GTR+I+G, GTR+I+G, and HKY+I as the best model for the first, second and third codon position of COI gene, respectively. The BI phylogenetic tree is shown in Fig. 2 with Bayesian posterior probabilities (BPP) for major nodes. The phylogenetic tree showed that all *Xenophrys* species formed a monophyletic lineage containing 11 independent clades, though some relationships were not resolved in the tree. Those clades correspond exactly to the ten genera previously recognized, including *Pelobatrachus* (clade A), *Sarawakiphrys* (clade B), *Megophrys* (clade C), *Brachytarsophrys* (clade D), *Atympanophrys* (clade E), *Grillitschia* (clade F), *Ophryophryne* (clade G), *Boulenophrys* (clade H). *Jingophrys* (clade I), *Xenophrys* (clade J), and clade K. Significantly, *J.* cf. *pachyproctus* alone formed a clade. All samples from Yadong were strongly supported to be a monophyletic group and formed sister relationships with *X. flavipunctata*, *X. glandulosa*, *X. himalayana*, *X. periosa*, *X. robusta*, *X. mangshanensis*, *X. maosonensis*, *X. truongsonensis*, *X. medogensis*, *X. megdogensis*, *X. monticola*, and *X. zhangi*. *X. katabhako* comb. nov. and *X. monticola* formed a clade. *X. sanu* comb. nov. and *X. zhangi* clustered into another clade.

Interspecific uncorrected *p*-distance of the *Xenophrys* species ranged from 0.0 (*X. zhangi* and *X. sanu* comb. nov.) to 18.7% (*X. awuh* and *X. dzukou*) (Table 2). The minimum *p*-distance between the unidentified specimens and any other species of *Xenophrys* was 4.4% (with *X. glandulosa*) (Table 2).

Table 2. Uncorrected pairwise sequence divergences (*p*-distance, in %) based on 16S ribosomal RNA sequences.

No.	Species	1	2	3	4	5	6	7	8	9	10	11	12	13	14	15	16	17	18	19	20	21	22	23	24	25	26	27	28	29	30
1	*X. ancrae*																														
2	*X. auralensis*	9.4																													
3	*X. awuh*	9.9	14.7																												
4	*X. dzukou*	6.9	9	18.7																											
5	*X. flavipunctata*	8.5	9.4	13.6	10.2																										
6	*X. glandulosa*	7.7	7.1	12.1	7.5	4.6																									
7	*X. himalayana*	7.9	6.7	10.5	8.6	5.2	3.3																								
8	*X. legkaguli*	8.4	4	14.8	8.9	9.6	7.8	7.6																							
9	*X. major*	7.9	7.7	11.4	8.9	6.6	5.5	4.7	8.8																						
10	*X. mangshanensis*	8.2	8	11.5	9.7	5.7	5.6	5.7	9.3	6.9																					
11	*X. maosonensis*	7.9	8.4	12.4	9.7	6.1	5.6	5.2	9	6.5	1.9																				
12	*X. medogensis*	7	7.4	11.7	8.2	5	3.8	3.3	7.8	5.2	5.4	5																			
13	*X. monticola*	9.7	7.5	13.3	10.2	7	5.2	5.6	9	7.4	6.3	6.9	6.7																		
14	*X. megacephala*	7.1	9.5	12.1	8.2	9.8	9.1	8.6	8.6	8.4	8.7	8.9	9	10.2																	
15	*X. numhbumaeng*	8.2	10.2	10.7	12.2	10	9.8	10	11.5	9.8	10.7	10.9	9.5	11	7.8																
16	*X. oreocrypta*	9.1	8.6	14.5	10.2	7.4	6.9	6.6	8.4	7	8.4	7.8	7.5	8.5	9.4	10.5															
17	*X. oropedion*	8.5	11.1	13.4	11.8	11.3	10.7	10.5	11.2	10.5	10.1	10.7	10.5	11.3	7.8	5.1	11.1														
18	*X. periosa*	8.7	7.3	12.2	8.9	5.6	3.1	2.5	7.8	6	6.1	5.9	3.3	6.2	8.6	10.2	7.2	10.7													
19	*X. robusta*	9.9	8.8	13.3	11.5	6.2	4.4	4.6	9.2	6.8	6.9	6.9	4.8	6.2	10.4	10.6	7.8	11.9	4.1												
20	*X. serchhipii*	8.3	11.4	8.7	11.5	10.2	10.6	10	10.9	10	9.4	10.2	10.4	12.4	8.5	9.2	11.6	10.3	10.4	11.6											
21	*X. takensis*	9.5	4	14.2	9.9	9.4	7.2	6.8	4.7	8.4	8.2	8.4	6.7	8.6	8.8	10.9	9	11.4	7.4	8.6	10.8										
22	*X. truongsonensis*	8	7.7	12.4	10.6	7.2	6.3	6.5	7.9	6.5	3.6	3.3	5.2	7.8	9.1	10.7	7.7	10.4	7.2	7.2	9.9	9									
23	*X. zhangi*	7	6.5	11.4	9	5.6	3.8	4	7.4	4.8	5.2	5	3.6	4.4	9.3	8.9	7.3	10.5	4.4	4.8	10.6	6.7	5								
24	*X. zunhebotoensis*	7.2	12.2	8.1	10.2	10.7	9.9	10.4	12.2	10.6	10.8	11	9.7	11.7	9.2	8.3	11.6	10	10.9	11.9	8.3	11.4	10.9	10.3							
25	*X. katabhako*	8.4	9.5	12.9	9.6	7.3	4.9	5.9	9.3	7.1	5.7	6.3	5.9	2.7	10.1	11.9	8.9	12.5	6.8	6.2	12.2	8.7	7.4	4.3	11						
26	*X. lancangica*	7	7.8	13.6	8.2	7.7	5.9	6.7	7.6	6.9	8.1	7.7	6.7	9.2	8.8	10	7.7	11.3	7.7	7.5	10.8	8.2	7.5	7.1	10.5	8.1					
27	*X. sanu*	8.1	8.6	13.3	9.6	6.8	4.9	4.6	8.7	5.7	6.8	6.5	4.3	5.1	10.5	10.8	8.7	12.8	5.4	5.7	12.2	8.2	6.3	0	11.5	4.3	8.9				
28	*X. dehongensis*	9.9	6.4	16.3	10.1	9.7	7.1	8.2	7.4	9.1	9.3	9.9	8.3	9.7	10.2	11.6	8.5	12.7	8.4	8.4	13.5	7.2	9.5	7.3	13.2	10.4	7.9	9.3			
29	*X. parva*	10.5	6.7	15.9	10.8	10.1	7.5	7.8	7.4	8	8.9	9.1	7.7	9.2	10.2	12	8.6	12.3	8	8.2	12.2	7.4	8.4	7.5	12.7	9.9	7.5	9	6.8		
30	*X. pangdaensis* sp.nov.	7.3	6.5	12.5	9.5	6	4.4	5.6	7.4	6.2	6.1	5.7	4.6	6.2	9.8	10	7.4	11.3	5	5.2	11	7.6	6.1	4.6	10	6.5	5.9	6.3	8.3	7.7	

Morphological analysis

All samples from Yadong shared many morphological characters with *Xenophrys* species, including dorsal skin texture basically smooth, vomerine teeth present, ventral colorations, lateral fringes and webbings on toes, tongues notched posteriorly, maxillary teeth present, and tympanum indistinct. However, they can be distinguished from all recognized congeners by a combination of distinctive morphological characters (see taxonomic accounts below) and these specimens are therefore described as a new species based on the phylogenetic analyses and morphological comparisons.

Taxonomic accounts

Xenophrys pangdaensis **sp. nov.**

https://zoobank.org/262319B9-D690-4FDB-9A44-621FD390956E
Fig. 3

Type material. *Holotype*. YBU21248, adult male, collected by Ke Li and He Zhang on 28 August 2021 from Pangda Village (27°17.25'N, 89°0.42'E; ca. 2000 m a.s.l.), Yadong Town, Yadong County, Tibet Autonomous Region, China.

***Paratypes*.** Six adult specimens (males: YBU21258, YBU21259, YBU21260, YBU21261, YBU21269; female: YBU21262) were collected from two very close sites in Yadong Town by Ke Li and He Zhang on 28 August 2021.

Other specimens examined. Thirteen tadpoles were collected by Ke Li and He Zhang on 4 September 2021. Five tadpoles were collected from Pangda Village (17 km, 27°18.18'N, 89°0.34'E), Yadong Town. The other tadpoles were collected from Pangda Village (27°17.25'N, 89°0.42'E) together with the holotype.

Etymology. The species name *pangdaensis* indicates the type locality of Pangda Village, Yadong County, Tibet Autonomous Region, China.

Suggested name. Pangda Horned Toad (English), and Pang Da Jiao Chan (庞达角蟾, Chinese).

Diagnoses. (1) Small body size, SVL 17.9–22.2 mm (20.5±1.8, *n* = 6) in adult males and SVL 23.4 mm (*n* = 1) in the adult female (Table 3); (2) tympanum indistinct, supratympanic fold distinct; (3) canthus rostralis well-developed, snout tip far beyond the margin of the lower lip; (5) pupil vertical; (6) vomerine teeth present, maxillary teeth present; (7) tongue notched terminally; (8) supernumerary tubercles absent, subarticular, metacarpal and metatarsal tubercles indistinct; (9) relative finger lengths I < II < IV < III, finger tips rounded, slightly expanded relative to digit widths; (10) toes with narrow lateral fringes and tarsal folds; (11) a dark triangular marking with light edge between eyes, a dark)(-shaped marking, with light edge, present on center of dorsum, pectoral glands on sides of the breast.

Holotype description. Measurements in mm. Mature male, body slender, extremely small (SVL 21.5) (Fig. 3); small protuberance beyond cloaca from dorsal view, not visible from ventral view, not swollen; head moderate, longer than wide (HW 7.0, HL 7.6, IFE 2.8, IBE 3.7); snout nearly rounded in dorsal view, slightly protruding beyond lower jaw, angular in anterior and lateral view; loreal region acute, concave; canthus rostralis angular; dorsal surface of snout slightly concave; nostril oval, closer to eye than tip of snout (SN 1.5, EN 1.6); internarial distance greater than eyelid width, and shorter than narrowest point between upper eye-

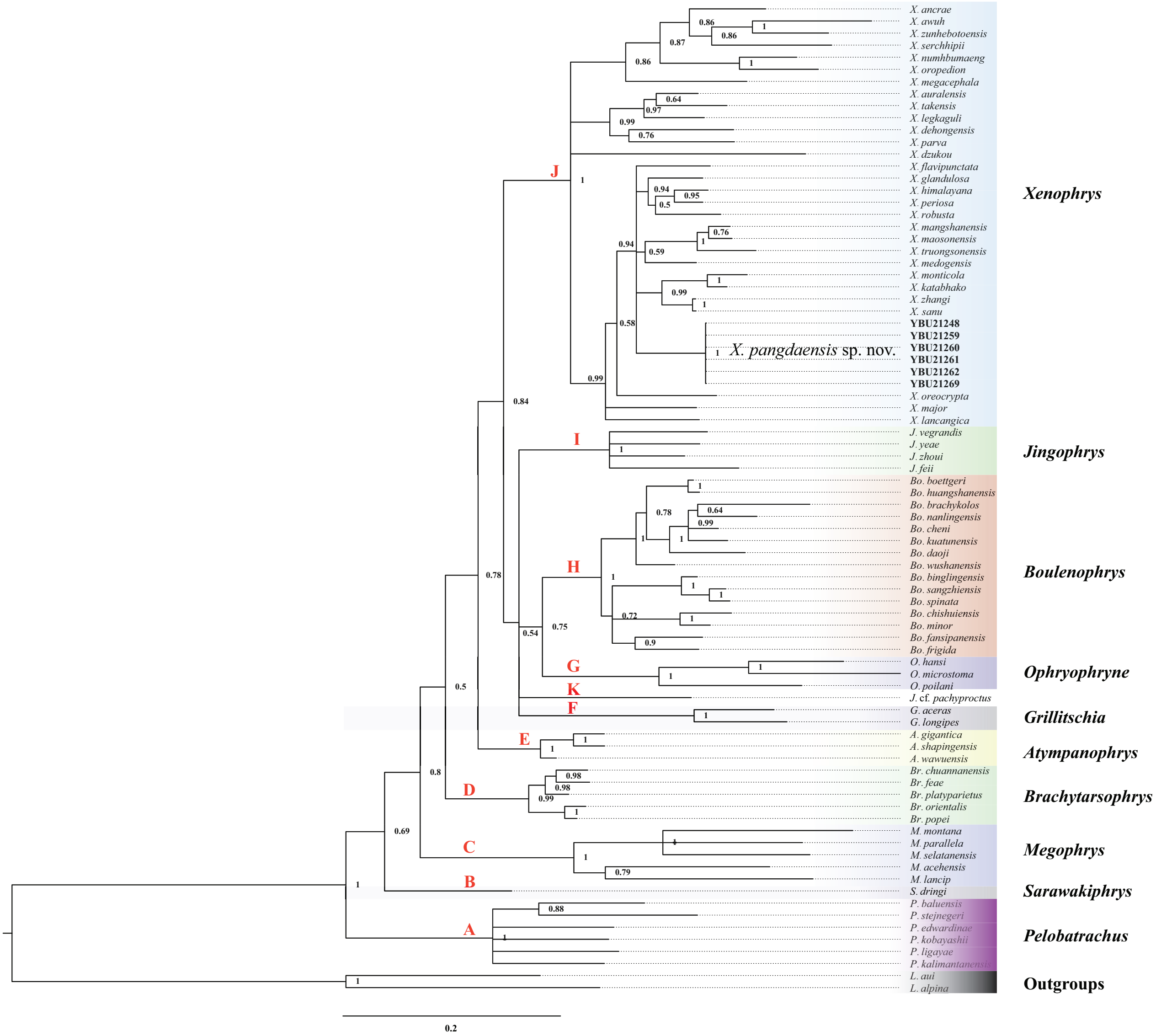

Figure 2. Phylogenetic tree of the genus *Xenophrys* inferred from two mitochondrial gene fragments by Bayesian inference.

lids (IN 2.5, UEW 1.9, IUE 2.9); eye diameter 1.5 × maximum diameter of visible portion of tympanum, and shorter than snout (EL 2.7, TYD 1.8, SL 3.3); eye-tympanum distance (TYE 1.7) shorter than diameter of visible portion of tympanum; tympanum oval-shaped, slightly oblique, upper border concealed by supratympanic ridge; pupil in life vertically elliptical; pineal ocellus not visible externally; vomerine ridges medium sized, orientated acutely, positioned between to slightly posterior to choanae, vomerine teeth small; maxillary teeth present; tongue moderately large, feebly notched posteriorly, medial lingual process absent.

Forelimbs moderately long and thin; forearm slender, shorter than hand (FAL 3.4, HAL 6.5); fingers moderately long, with narrow lateral fringes and rudimentary webbing (Fig. 2); finger length formula I < II < IV < III (FIL 2.6, FIIL 3.6, FIIIL 6.0, FIVL 4.4); supernumerary, thenar and metacarpal tubercles absent, with slightly visible subarticular tubercles; finger tips rounded, with subcircular pads, without terminal grooves, slightly expanded relative to digit widths (FIIIW 0.2, FIIIDW 0.3).

Hindlimbs long and thin, heels overlapping when hindlimbs held at right angles to body; thighs slightly shorter than shanks and feet (TL 9.1, SHL 10.9,

Table 3. Measurements (in mm) of the type series of *Xenophrys pangdaensis* sp. nov.

	YBU21248 (holotype)	YBU21262 (paratype)	YBU21261 (paratype)	YBU21259 (paratype)	YBU21260 (paratype)	YBU21269 (paratype)	YBU21258 (paratype)
Sex	male	female	male	male	male	male	male
SVL	21.5	23.4	21.7	20.9	18.6	17.9	22.2
FAL	3.4	5.9	7.5	5.5	4.3	3.6	4.6
HAL	6.5	6.3	7.2	5.2	5.1	5.8	8.0
HLL	30.4	33.5	30.5	34.9	30.4	26.6	35.4
SHL	10.9	11.4	11.3	9.8	9.1	9.2	11.6
SL	3.3	3.0	3.1	2.6	2.7	1.8	3.0
FOL	10.8	10.1	11.2	9.7	6.5	8.9	10.9
IN	2.5	2.9	2.1	2.4	2.9	3.1	2.7
IUE	2.9	2.3	2.4	2.1	3.3	2.5	3.4
UEW	1.9	2.0	1.6	1.3	2.11	2.5	1.9
TYD	1.8	1.1	1.7	1.7	1.8	1.6	1.5
HL	7.6	6.7	7.6	6.3	5.4	6.2	7.4
HW	6.9	7.1	7.0	6.2	6.2	6.5	8.5
FIL	2.6	2.6	3.3	2.3	2.2	2.5	3.2
FIIL	3.6	3.9	3.9	3.4	2.6	2.8	3.3
FIIIL	6.0	5.9	5.4	4.8	4.8	5.1	4.9
FIVL	4.4	3.9	4.6	3.7	3.1	3.8	3.3
SN	1.5	1.3	1.8	1.4	1.3	1.4	1.8
EN	1.6	1.4	2.4	1.5	1.5	1.8	1.9
EL	2.7	2.5	2.9	2.6	2.7	2.2	3.1
IFE	2.8	2.9	3.0	3.1	2.9	2.9	3.4
IBE	3.7	3.4	3.3	3.4	3.1	3.1	4.1
TYE	1.7	1.9	1.7	1.4	1.2	1.2	1.9
FIIIW	0.2	0.2	0.9	0.2	0.3	0.2	0.4
FIIIDW	0.3	0.3	0.3	0.3	0.3	0.3	0.4
TIVW	0.4	0.4	0.5	0.4	0.4	0.4	0.5
TIVDW	0.3	0.4	0.4	0.3	0.3	0.3	0.4
TL	9.1	8.9	8.6	9.1	8.9	9.2	10.1
TFOL	14.2	14.4	15.0	13.6	11.9	12.2	16.3
IMT	1.0	0.8	1.1	0.7	0.6	0.7	1.1

FOL 10.8); toes with narrow lateral fringes, rudimentary webbing; relative toe lengths I < II < V < III < IV; toe tips rounded, with subcircular pads, terminal grooves absent; supernumerary, subarticular and outer metatarsal tubercles absent; inner metatarsal tubercles indistinct.

Skin of dorsal and ventral surfaces of head, body and limbs basically smooth; dorsal skin with very small densely-distributed granules; tympanum smooth with borders slightly raised; supratympanic ridges thin before and above departure with tympanum and gradually expanding beyond posterior edge of tympanum; skin ridges formed by small disconnected tubercles;)(-shaped skin ridge on center of dorsum, its anterior ends extending posteriorly from above tympanum; flanks with two slender skin ridges, started at the shoulder and ended on both sides of the back of the cloaca; two small pectoral glands positioned on level with axilla; femoral glands moderate, positioned posterior surface of thigh, sub-equally distant from knee and cloaca.

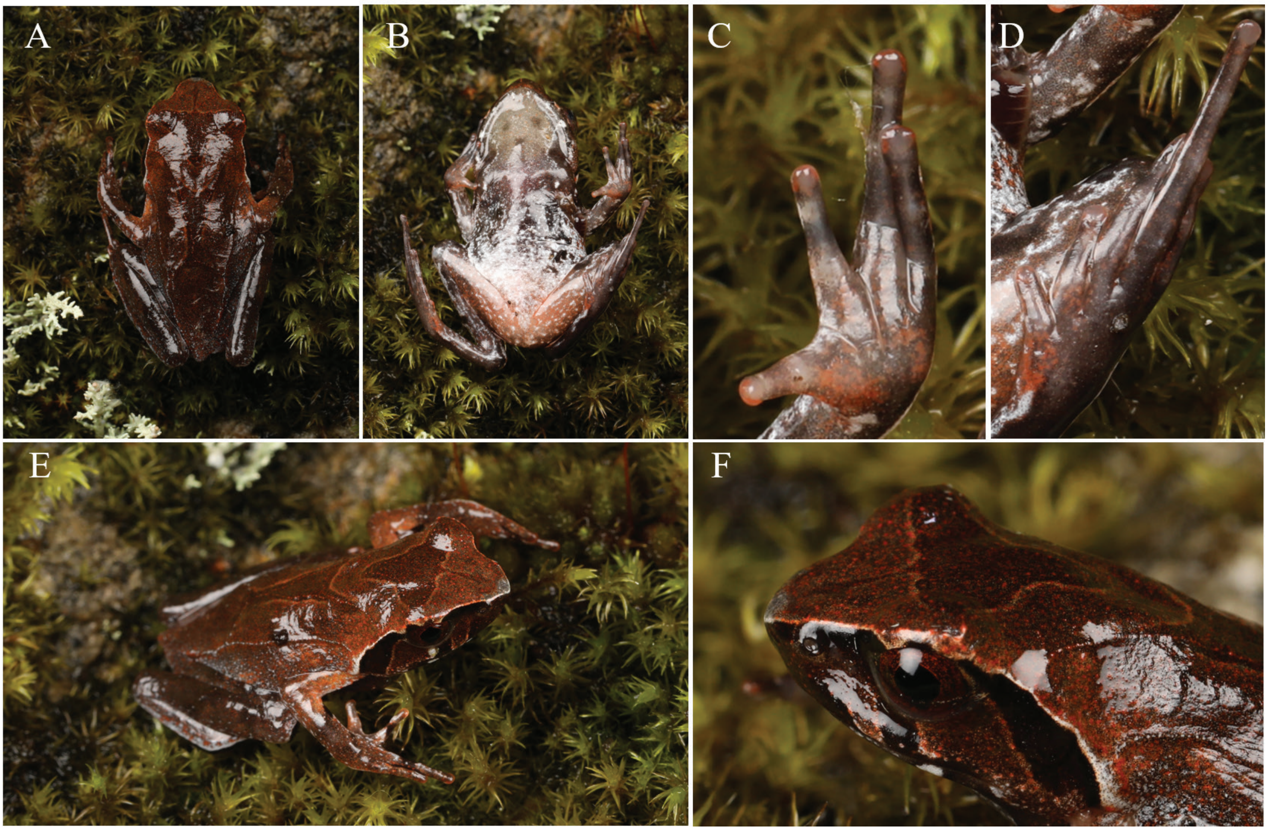

Figure 3. *Xenophrys pangdaensis* sp. nov. in life. **A** dorsal view of body **B** ventral view of body **C** ventral view of hand **D** ventral view of foot **E** lateral view of body **F** lateral view of head.

Coloration in life. Dorsal surface basically saddle brown, darker on anterior and hindlimbs than on posterior; orange-red granules scattered on surface; dark brown)(-shaped marking with orange edge on central dorsum; ventrolateral trunk with white spots and orange dots; dark brown triangular pattern with orange edges presents between eyes, and dark brown rod-like pattern positioned in front of triangular pattern; supratympanic fold white mingled with orange flecks; temporal region under supratympanic ridge black; two dark brown patches present on upper lips under eye and nostril on side of head; eight relatively large white patches present on lower lip, symmetrically distributed; two white symmetrically curved lines on both sides of throat; many orange-red dots scattered on surface of throat; iris orange-red; two dark transverse bands on each forearm; finger tips orange-red; large white blotches on belly and ventral surfaces of hindlimbs; three dark transverse bands on anterior surface of thigh and shank; femoral glands white on thigh.

Coloration in preservative. After preservation in ethanol, dorsal surface primarily brown; dark brown triangular pattern with white edges presents between eyes; brown)(-shaped marking with white edge on central dorsum; two white slender skin ridges in flanks; two dark transverse bands on each forearm; dark brown band with white dots in middle of thigh and shank; throat pale brownish grey, two white symmetrically curved lines distinct; eight distinct white patches on lower lip; chest brown with two white pectoral glands; belly pale gray-white with large black-brown blotches on sides; posterior ventral body surface, thigh, and upper part of tibia pale brown with scattered white spots; ventral surfaces of fingers and toes dark brown with white blotches.

Variations. Paratypes generally resemble the holotype but with some differences. For example, a few specimens (YBU21258, YBU21262 and YBU21269) have the head width greater than the head length; YBU21258 had more and larger maxillary teeth, the tongue thinner; rod-like patterns on the top of head different between specimens. Coloration varied on ventral body, with some specimens being darker. The tips of the fingers in some specimens were not orange-red.

Sexual dimorphism. Males: external vocal sac indistinct; internal vocal slit present on floor of mouth near rear of mandible, one on each side; vocal sac, vocal slits, and enlarged forearms all absent in female.

Tadpole. Gosner stages 25–36. Body length range from 6.3–13.8 mm (Table 4); oral disk funnel like, positioned anterior-dorsal, large, width average 1.5× (1.1–1.7, *n* = 13) maximum body width, rice-like submarginal papillae scattered on lower and upper lips and pointed towards oral cavity; nares oval and closer to eye than to snout (RN 1.0, NE 0.4); internarial distance nearly equal to interorbital distance (IND 2.8, PP 2.7); eyes dorsolateral, pupils rounded; spiracle opens left of body in dorsal view, spiracular tube positioned equidistant between tip of the snout and trunk-tail junction; the tail accounts for 0.7 of the total length (TOL 37.0, TAL 26.6); dorsal fin arise near middle of tail, upper tail fin higher than lower tail, and approximately half of tail muscle height (UF 1.5, LF 1.1, TMW 2.8)(Fig. 4).

Coloration in preservative. Dorsal and lateral parts of body greyish white, mixed with brown patches; lateral tail semi-transparent brown, muscle scattered with many distinct brown patches; no pigment on upper and lower fins; ventral body semi-transparent white, with tiny gray pigment scattered on it, the viscera can almost be seen; lips semi-transparent white, papillae brown. Coloration in life were not noted.

Table 4. Measurements (in mm) of the tadpoles of *Xenophrys pangdaensis* sp. nov. N indicates missing data. Character abbreviations are provided in the text.

Characters	1	2	3	4	5	6	7	8	9	10	11	12	13
Stage	36	31	31	31	33	31	35	32	31	27	25	29	36
BH	4.8	4.7	4.5	4.0	4.4	4.3	4.7	6.6	6.1	4.6	2.6	6.2	4.8
BL	11.4	10.3	10.8	10.4	11.0	11.5	10.9	13.8	11.8	10.4	6.3	11.9	10.6
BW	5.5	4.8	4.7	4.3	4.8	4.8	4.9	7.6	6.5	4.8	2.9	7.1	4.5
ED	0.9	1.1	1.0	1.0	1.0	1.0	1.0	1.2	1.0	0.9	0.8	1.0	1.3
IND	2.6	2.7	2.5	2.7	2.8	2.8	2.8	3.5	3.2	2.5	2.0	3.3	N
LF	1.0	1.2	1.1	1.2	1.2	1.0	1.2	1.2	1.2	1.1	0.7	1.2	1.1
NE	0.5	0.4	0.3	0.4	0.6	0.5	0.4	0.5	0.7	0.3	0.3	0.6	0.3
ODW	7.9	7.4	8.1	7.1	7.9	7.2	7.7	8.7	8.3	7.9	4.8	10.1	5.6
PP	3.1	2.7	2.5	2.8	2.8	2.5	2.9	3.3	2.9	2.6	1.6	3.3	N
RN	1.1	0.8	0.9	0.5	0.9	1.0	0.9	1.8	1.2	1.0	0.8	1.4	0.9
SS	5.8	5.8	5.6	5.7	5.7	5.4	5.7	7.4	6.8	5.4	3.7	6.4	5.3
SU	9.0	8.7	9.9	9.0	10.2	9.8	9.8	11.2	10.9	11.1	5.7	12.2	10.3
TAL	30.4	30.6	27.2	27.2	27.1	23.5	28.1	N	31.6	23.4	15.6	30.5	23.7
TMH	1.1	1.3	1.1	1.5	1.5	1.5	1.7	2.7	2.1	1.3	1.1	2.2	2.2
TMW	3.2	2.1	2.1	1.9	2.4	2.9	2.7	4.8	3.5	2.4	1.5	4.6	2.7
TOL	41.4	39.2	37.7	37.7	37.5	34.4	38.6	N	43.0	34.1	22.6	41.7	36.4
UF	1.9	1.4	1.6	1.3	1.4	1.4	1.3	2.1	1.8	1.3	0.9	1.5	1.3
TH	5.5	5.0	5.1	4.4	4.8	5.4	5.2	7.8	5.8	5.0	3.1	7.1	5.1

Figure 4. Tadpole of *Xenophrys pangdaensis* sp. nov. (Gonser stage 29) from Yadong County, Tibet Autonomous Region, China. **A** dorsal view of the tadpole **B** ventral view of the tadpole **C** lateral view of the tadpole. All photographs of just-preserved specimens.

Distribution and ecology. *Xenophrys pangdaensis* sp. nov. is only known from the type locality, Yadong Town, Yadong County, Tibet Autonomous Region, China at elevations of 2003–2972 m. All calling males were recorded in August and September on ferns near or on a small stream in the tropical forest (Fig. 5). The tadpoles collected from near the type locality were from Gosner stages 25–36. The habitat is located in the small gully, both sides covered with ferns and other vegetation. None of the adults or tadpoles were found in July, and all specimens were found in late August and early September, implying that the breeding season included August and September. The sympatric species, *Raorchestes yadongensis* Zhang, Shu, Liu, Dong & Guo, 2022, *Nanorana blanfordii* (Boulenger, 1882), *Duttaphrynus himalayanus* (Günther, 1864), and *Nanorana liebigii* (Günther, 1860) were also recorded.

Comparisons. *Xenophrys pangdaensis* sp. nov. is here compared with all 28 recognized species of the *Xenophrys* (Table 5). The smallest recognized species of *Xenophrys* is *X. zunhebotoensis* (male 28.4–33.9, females 37–39.5). So, by having small body size (males 18.0–22.2 mm, *n* = 6; female 23.4 mm, *n* = 1), *Xenophrys pangdaensis* sp. nov. differs from all congeners from *Xenophrys*.

Xenophrys pangdaensis sp. nov. differs from *X. awuh*, *X. damrei, X. dzukou*, *X. flavipunctata*, *X. glandulosa*, *X. megacephala*, *X. numhbumaeng*, *X. oropedion*, *X. serchhipii*, *X. takensis*, *X. truongsonensis*, *X. zhangi*, *X. zunhebotoensis*, *X. pava*, *X. dehongensis*, *and X. lancangica* by the presence of a horn-like tubercle laterally on the upper eyelid (vs absence of horn-like tubercle at edge of upper eyelid).

Figure 5. Habitat of *Xenophrys pangdaensis* sp. nov. in the type locality, Pangda Village, Yadong County, Tibet Autonomous Region, China.

Xenophrys pangdaensis sp. nov. differs from *X. awuh*, *X. monticola*, *X. robusta*, and *X. zunhebotoensis* by presence of vomerine teeth (vs absence of vomerine teeth).

Xenophrys pangdaensis sp. nov. differs from *X. lekaguli*, *X. truongsonensis* by presence of vocal sac (vs absence of vocal sac).

Xenophrys pangdaensis sp. nov. differs from *X. ancrae*, *X. awuh*, *X. dzukou*, *X. flavipunctata*, *X. himalayana*, *X. major*, *X. megacephala*, *X. monticola*, *X. numhbumaeng*, *X. oropedion*, *X. periosa*, *X. robusta*, *X. serchhipii*, *X. takensis*, *X. zhangi*, *X. zunhebotoensis*, *X. pava*, *X. dehongensis* and *X. lancangica* by absence of nuptial pads on fingers (vs presence of nuptial pads on fingers).

Xenophrys pangdaensis sp. nov. differs from *X. ancrae*, *X. awuh*, *X. dzukou*, *X. glandulosa*, *X. major*, *X. mangshanensis*, *X. maosonensis*, *X. medogensis*, *X. monticola*, *X. numhbumaeng*, *X. oropedion*, *X. truongsonensis*, *X. zhangi*, *X. zunhebotoensis*, *X. pava*, *X. lancangica* (vs tongue feebly notched), *X. auralensis*, *X. lekaguli*, *X. megacephala*, *X. robusta*, *X. takensis*, *X. dehongensis* by tongue distinctly notched (vs tongue not notched).

Xenophrys pangdaensis sp. nov. differs from *X. ancrae*, *X. awuh*, *X. auralensis*, *X. damrei*, *X. lekaguli*, *X. mangshanensis*, *X. maosonensis*, *X. medogensis*, *X. megacephala*, *X. numhbumaeng*, *X. oreocrypta*, *X. oropedion*, *X. periosa*, *X. robusta*, *X. serchhipii*, *X. takensis*, *X. zunhebotoensis*, *X. pava*, and *X. dehongensis* by having narrow lateral fringes on toes (vs lateral fringes on toes absent), and *X. glandulosa* (vs lateral fringes on toes wide).

Xenophrys pangdaensis sp. nov. differs from *X. dzukou*, *X. mangshanensis*, *X. oropedion*, *X. zhangi*, *X. pava*, and *X. zunhebotoensis* by toes with rudiment of webbing (vs toes without webbing), *X. flavipunctata*, and *X. maosonensis* (vs at most one-fourth webbed).

Table 5. Morphological comparison between *Xenophrys pangdaensis* sp. nov. and 28 recognized species: 1. SVL in males (mm); 2. SVL in females (mm); 3. ratio TYD/EL in males; 4. ratio TYD/EL in females; 5. ratio SHL/SVL in males; 6. ratio SHL/SVL in females; 7. Horn-like tubercle at edge of upper eyelid absent (0), small (1), slightly larger (2), long point (3); 8. Vomerine teeth absent (0), present (1); 9. Vocal sac absent (0), present (1); 10. Tongue not notched (0), feebly notched(1), notched (2); 11. Lateral fringes on toes absent (0), narrow (1), wide (2); 12. Toes without webbing (0), with rudiment of webbing (1), at most one-fourth webbed (2), at least one-fourth webbed (3); 13. Subarticular tubercles on toes absent (0), indistinct (1), distinct (2); 14. Relative finger lengths; 15. Nuptial pads on finger absent (0), present (1). 16. Dorsal skin texture: smooth (0), smooth with small tubercles (1), rough (2). ? = data not available. ts= this study. Data sources: (a) Boulenger (1908), (b) Bourret (1937), (c) Bourret (1942), (d)Fei at al. (1983), (e) Ye and Fei (1992),(f) Fei et al. (1992), ((g) Huang et al. (1998), (h) Ohler et al. (2002), (i) Stuart et al. (2006), (j)Mathew and Sen (2007), (k) Fei et al. (2009), (l) Fei et al. (2012), (m) Mahony (2011), (n) Mahony et al. (2011), (o) Mahony et al. (2013), (p) Neang et al. (2013), (q)Fei and Ye (2016), (r) Deuti et al.(2017), (s) Mahony et al. (2018), (t) Shi et al. (2020), (u) Mahony et al. (2020), (v) Luong et al. (2022), (w) Lyu et al. (2023).

Species	1	2	3	4	5	6	7	8	9	10	11	12	13	14	15	16	References
X. pangdaensis sp. nov.	18.0–22.2	21.7–23.4	0.50–0.69	0.48–0.58	0.47–0.52	0.49–0.52	1	1	1	2	1	1	1	I<II<IV<III	0	1	t, s
X. ancrae	39.1–45.0	48.9	0.5–0.63	0.5–0.63	0.46–0.53	0.49	1	1	?	1	0	1	0	I<II<IV<III	1	1	o
X. awuh	35.7–41.1	43.7–48	0.56–0.64	0.61–0.63	0.49–0.55	0.50–0.53	0	0	1	1	0	1	0	I=II<IV<III	1	0	u
X. auralensis	60.1–76.7	?	0.6	?	0.51	?	1	0/1	1	0	0	1	1	II<I<IV<III	0	1	h, p
X. damrei	47.7–57.1	69.1	0.58	0.58	0.51	0.50	0	1	1	2	0	1	0	IV<I<II<III	0	0	n, p
X. dzukou	34.2–35.3	?	0.45–0.59	?	0.47–0.53	?	0	1	1	1	1	0	0	I=II<IV<III	1	0	u
X. flavipunctata	56.9–68.4	68–74.6	0.41–0.51	0.46–0.51	0.54–0.61	0.54–0.58	0	1	1	2	1	2	0	IV<I=II<III	1	1	s
X. glandulosa	76.3–81	76.5–99.5	0.51–0.65	?77	0.58–0.60	0.5–0.55	0	1	1	1	2	1	0	II=I<IV<III/ IV<II<I<III	0	0	f, g, k, l, q, s
X. himalayana	68–73.5	83.9	0.54	0.48	0.50–0.54	0.54	1	1	1	2	1	1	0	I<II<V<III<IV	1	1	s
X. lekaguli	40.1–66.6	58.6–94	0.59–0.74	0.58–0.64	0.47–0.52	0.44–0.52	1	1	0	0	0	1	0	IV<II<I<III	0	0	i, p
X. major	71.6–87.5	85.6–98.2	0.33–0.48	0.40–0.41	0.50–0.58	0.50–0.57	1	1	1	1	1	1	0	IV<II=I<III	1	1	q, u
X. mangshanensis	62.5	73	?	?	0.52	0.54	1	1	1	1	0	0	0	II<I<IV<III	0	0	f, g, k, l, q
X. maosonensis	58–76	68–93.5	0.5	?	0.5–0.6	?	1	1	?	1	0	2	0	?	?	0	b, c
X. medogensis	57.2–68	75.7–85.5	?	?	0.56	?	1	1	1	1	0	1/0	0	I<II<IV<III	0	1	d, k, l, q, t
X. megacephala	48.4–53.4	49.3–64.4	0.54–0.71	0.56–0.82	0.41–0.49	0.41–0.47	0	1	1	0	0	1	0	IV<II<I<III	1	1	m, u
X. monticola	37.8–49.1	40.5–51.1	0.38–0.59	0.44–0.71	0.45–0.51	0.46–0.51	1	0	1	1	1	1	0	I<II<IV<III	1	1	r, s
X. numhbumaeng	33.8–34.6	?	0.45–0.46	?	0.52–0.58	?	0	1	1	1	0	1	0	I=II<IV<III	1	0	u
X. oreocrypta	?	94.9	?	0.52	?	0.51	1	1	?	?	0	1	0	IV<II<I<III	?	1	s
X. oropedion	32.8–39.2	44.1–48.7	0.54–0.65	0.62–0.69	0.43–0.48	0.42–0.43	0	1	1	1	0	0	0	I=II=IV<III	1	1	o
X. periosa	71.3–93.8	112	0.44–0.58	0.45	0.51–0.58	0.51	1	1	1	?	0	1	0	IV<II<I<III	1	0	s
X. robusta	73.5–83.1	81.3–114	0.38–0.52	0.40–0.74	0.51–0.57	0.46–0.54	1	0	1	0	0	1	0	IV<I=II<III	1	1	a, s
X. serchhipii	36.1–46.7	46.1–53	0.47–0.66	0.50–0.55	0.46–0.53	0.47–0.51	0	1	1	?	0	1	0	IV<I=II<III	1	1	j, u
X. takensis	47.3–53	72.9	0.42–0.48	0.53	0.41–0.49	0.45	0	1	1	0	0	1	0	IV≤II<I<III/ IV=I<II<III	1	1	s, u

Species	1	2	3	4	5	6	7	8	9	10	11	12	13	14	15	16	References
X. truongsonensis	58.8–71.4	65.6–87.3	0.51–0.67	0.53–0.59	0.55–0.64	0.54–0.58	0	1	0	1	1	1	0	I<II<IV<III	0	0	v
X. zhangi	32.5–37.2	?	0.5	?	0.49	?	0	1	1	1	1	0	0	II=I <IV<III	1	1	e, k, l, q
X. zunhebotoensis	28.4–33.9	37–39.5	0.43–0.58	0.48–0.59	0.45–0.54	0.47–0.50	0	0	1	1	0	0	0	IV<I<II≤III I≤II<IV<III	1	1	j, u
X. pava	36.6–42.9	41.4–52.1	0.40–0.49	0.44–0.55	0.46–0.48	0.43–0.44	0	1	1	0/1	0	0	0	II<IV<I<III	1	1	u, w
X. dehongensis	34.8–36.7	45.7–46.8	0.34–0.45	0.43–0.44	0.43–0.50	0.46–0.50	0	1	1	0	0	1	0	II<I<IV<III	1	2	w
X. lancangica	64.0–65.4	75.0–88.6	0.63–0.74	0.59–0.77	0.54–0.57	0.56–0.58	0	1	1	1	1	1	0	II<IV<I<III	1	1	w

Xenophrys pangdaensis sp. nov. differs from *X. ancrae*, *X. awuh*, *X. damrei*, *X. dzukou*, *X. flavipunctata*, *X. glandulosa*, *X. himalayana*, *X. lekaguli*, *X. major*, *X. mangshanensis*, *X. maosonensis*, *X. medogensis*, *X. megacephala*, *X. monticola*, *X. numhbumaeng*, *X. oreocrypta*, *X. oropedion*, *X. periosa*, *X. robusta*, *X. serchhipii*, *X. takensis*, *X. truongsonensis*, *X. zhangi*, *X. zunhebotoensis*, *X. pava*, *X. lancangica* and *X. dehongensis* by presence of indistinct subarticular tubercles on toes (vs absence of subarticular tubercles on toes).

Xenophrys pangdaensis sp. nov. differs from *X. awuh*, *X. damrei*, *X. dzukou*, *X. glandulosa*, *X. lekaguli*, *X. mangshanensis*, *X. maosonensis*, *X. numhbumaeng*, *X. periosa*, and *X. truongsonensis* by dorsal skin texture smooth with small tubercles (vs dorsal skin texture smooth), *X. dehongensis* (vs dorsal skin rough).

Discussion

The genus *Megophrys* sensu lato is a large group with extremely high species diversity. With the description of this new species, the members of the group will be 133. *Xenophrys pangdaensis* sp. nov. represents the 29th known species of *Xenophrys* in China and the ninth known species of the Asian horned toads from Tibet, China (Shi et al. 2020; Frost 2023). In fact, there are still some pending species whose taxonomic status needs further confirmation between Northeast India and adjacent China. Deuti et al. (2017) who described two small sized new species, *X. katabhako* and *X. sanu*, based on morphological and molecular sampling. However, Mahony et al. (2018) found that *X. katabhako* and *X. sanu* are nested within the concept of *X. monticola*. Also, similar results were obtained in this study. *X. katabhako* and *X. monticola* formed a clade. *X. sanu* and *X. zhangi* clustered into another clade. Finally, they all formed monophyletic group, but the two clades diverged considerably. For the moment, it is necessary to further investigate the taxonomic affinities of these populations by integrating more evidence. Thus, there may be some cryptic species in this group and it should be continuously paid more attentions on the species diversity of the *Megophrys sensu lato*. Southern Tibet is located in the eastern of Himalayas, which is one of 36 biodiversity hotspots in the world (Basnet et al. 2019). This region is extremely unique and deserves our continued attention. In recent years, many new species have been gradually discovered in this area (Jiang et al. 2012, 2016a, 2016b, 2016c; Shi et al. 2020; Che et al. 2020; Zhang et al. 2022). There is also high species diversity in the middle and lower reaches of the Yarlung Zangbo Grand Canyon, for example, Mahony et al. (2018) revealed cryptic diversity within the *Megophrys major* species group, which suggests that the species diversity in this area may have been previously underestimated and therefore needs to be further investigated.

The body length (SVL) of the new species ranges from 18.0 to 22.4 mm in males and from 23.4 mm in female, however, the minimum SVL of the other recognized congeners is 28.4–33.9 mm (*X. zunhebotoensis*) in males and 37–39.5 mm (*X. zunhebotoensis*) in females. Thus, *X. pangdaensis* sp. nov. is likely to be the smallest member of all recognized species in *Xenophrys*. In addition, the members of the *Xenophrys* are very variable in body length; for example, *X. glandulosa* reaches approximately 80 mm in males and 76.5–99.5 mm in females, and the body length of *X. robusta* are even more than 100 mm in females (81.3–114.0 mm). So, it indicates that species of the same genus have a large span in body length. This also reflects the strong morphological plasticity of the Asian horned toads.

It has always been difficult to identify horned toads, especially the species with similar body length. Liu et al. (2018) recognized one sample SYSa002934 from Medog County as *X.* cf. *pachyproctus*; however, this sample clustered in a clade with *X. medogensis* in the results of Shi et al. (2020). Additionally, the evolutionary branch length in the phylogenetic tree between the two species was much shorter than between any other species, and further analysis showed that the genetic divergence between them is only 0.57% based on 16S gene. It is probable that this specimen may be misidentified previously and should be reexamined (Shi et al. 2020; this study). Furthermore, another specimen (CIB022017061805) from Bari, Medog, Tibet, China formed an independent clade in our analysis. Shi et al. (2020) treated it as *M.* cf. *pachyproctus*. So far, there is only a morphological description and no available molecular evidence from samples of the type locality (Gelin) for *J. pachyproctus*. Thus, we suggest that further sampling at Gelin would help to resolve the taxonomic problem of *J. pachyproctus* in the future.

Acknowledgements

We thank Forest Department of Yadong County for permission for field work and specimen collection. We are grateful to Dr. J. Che (Kunming Institute of Zoology, Chinese Academy of Sciences) and Dr. W. Y. Duan (Kunming Institute of Botany, Chinese Academy of Sciences) for their assistance.

Additional information

Conflict of interest

The authors have declared that no competing interests exist.

Ethical statement

No ethical statement was reported.

Funding

This research is supported by the Second Tibetan Plateau Scientific Expedition and Research Program (STEP) (No. 2019QZKK0501), Strategic Priority Research Program of the Chinese Academy of Sciences (No. XDA 20050201), National Natural Science Foundation of Sichuan (No. 2023NSFSC1157), Sailing Project of Yibin University (No. 2020QH07), and Key Lab of Aromatic Plant Resources Exploitation and Utilization in Sichuan Higher Education (No.21XLY03).

Author contributions

Guocheng Shu, Conceptualization- Equal, Data curation-Lead, Formal analysis-Lead, Methodology-Lead, Resources-Equal, Software-Equal, Validation- Lead, Visualization-Lead, Writing-original draft-Lead, Writing-review and editing-Lead; Ke Li, Data curation-Supporting, Formal analysis-Equal, Investigation-Lead; Yayong Wu, Writing-review & editing-Equal, Formal analysis-Equal, Methodology-Equal; Qin Liu, Data curation-Supporting, Formal analysis-Supporting, Writing-review & editing-Equal; Zhongping He, Data curation-Supporting, Formal analysis-Supporting, Writing-review and editing-Equal; Ling Li, Formal analysis-Supporting, Visualization-Equal; He Zhang, Data curation-Supporting, Investigation-Equal; Peng Guo, Conceptualization-Equal, Data curation-Equal, Funding acquisition-Lead, Investigation-Equal, Project administration-Lead, Resources-Equal, Supervision-Lead, Validation-Equal, Writing-review and editing-Lead.

Author ORCIDs

Guocheng Shu https://orcid.org/0000-0003-1590-6510
Ke Li https://orcid.org/0000-0001-9695-4236
Yayong Wu https://orcid.org/0000-0003-2752-4085
Qin Liu https://orcid.org/0000-0001-8402-6491
Zhongping He https://orcid.org/0009-0005-7077-8074
Ling Li https://orcid.org/0000-0002-7650-2280
He Zhang https://orcid.org/0000-0002-9511-2552
Peng Guo https://orcid.org/0000-0001-5585-292X

Data availability

All of the data that support the findings of this study are available in the main text or Supplementary Information.

References

Basnet D, Kandel P, Chettri N, Yang Y, Lodhi MS, Htun NZ, Uddin K, Sharma E (2019) Biodiversity research trends and gaps from the confluence of three global biodiversity hotspots in the far-eastern Himalaya. International Journal of Ecology 2019: 1–14. https://doi.org/10.1155/2019/1323419

Boulenger GA (1908) A revision of the Oriental pelobatid batrachians (genus *Megalophrys*). Proceedings of the Zoological Society of London 78(2): 407–430. https://doi.org/10.1111/j.1096-3642.1908.tb01852.x

Bourret R (1937) Notes herpétologiques sur l'Indochine française. XIV. Les Batraciens de la collection du Laboratoire des Sciences Naturelles de l'Université. Descriptions de quinze espèces ou variétés nouvelles. Annexe au Bulletin Général de l'Instruction Publique 4: 5–56. [In French]

Bourret R (1942) Les batrachians de l'Indochine. Institut Océanographique de l'Indochine, Hanoi, 547 + X pp. [pls 1–4] [In French]

Che J, Chen H, Yang J, Jin J, Jiang K, Yuan ZY, Murphy RW, Zhang Y-P (2011) Universal COI primers for DNA barcoding amphibians. Molecular Ecology Resources 12(2): 247–258. https://doi.org/10.1111/j.1755-0998.2011.03090.x

Che J, Jiang K, Yan F, Zhang YP (2020) Amphibians and Reptiles in Tibet – Diversity and Evolution. Science Press, Beijing, 836 pp. [In Chinese]

Chen JM, Zhou WW, Poyarkov Jr NA, Stuart BL, Brown RM, Lathrop A, Wang YY, Yuan ZY, Jiang K, Hou M, Chen HM, Suwannapoom C, Nguyen SN, Duong TV, Papenfuss

TJ, Murphy RW, Zhang YP, Che J (2017) A novel multilocus phylogenetic estimation reveals unrecognized diversity in Asian horned toads, genus *Megophrys sensu lato* (Anura: Megophryidae). Molecular Phylogenetics and Evolution 106: 28–43. https://doi.org/10.1016/j.ympev.2016.09.004

Delorme M, Dubois A, Grosjean S, Ohler A (2006) Une nouvelle ergotaxinomie des Megophryidae (Amphibia, Anura). Alytes 24: 6–21.

Deuti K, Grosjean S, Nicolas V, Vasudevan K, Ohler A (2017) Nomenclatural puzzle in early *Xenophrys nomina* (Anura, Megophryidae) solved with description of two new species from India (Darjeeling hills and Sikkim). Alytes 34: 20–48.

Dubois A (1987) ("1986") Miscellanea taxinomica batrachologica (I). Alytes 5: 7–95.

Dubois A, Ohler A, Pyron RA (2021) New concepts and methods for phylogenetic taxonomy and nomenclature in zoology, exemplified by a new ranked cladonomy of recent amphibians (Lissamphibia). Megataxa 5(1): 1–738. https://doi.org/10.11646/megataxa.5.1.1

Fei L, Ye CY (2016) Amphibians of China, Volume 1. Science Press, Beijing, 611–735.

Fei L, Ye CY, Huang YZ (1983) Two new subspecies of *Megophrys omeimontis* Liu from China (Amphibia, Pelobatidae). Acta Herpetologica Sinica/ Liangqi baxing dongwu yanjiu. New Series. Chengdu 2(2): 49–52. [In Chinese with English abstract]

Fei L, Ye CY, Huang Y (1992) Description of two new species of the genus *Megophrys*, Pelobatidae (Amphibia: Anura) from China. Zoological Research 13: 5–12. [In Chinese] https://doi.org/10.5479/si.23317515.118.12

Fei L, Hu SQ, Ye CY, Huang YZ (2009) Fauna Sinica. Amphibia. Volume 2. Anura. Science Press, Beijing, 328–481. [In Chinese]

Fei L, Ye CY, Jiang JP (2012) Coloured Atlas of Chinese Amphibians and their Distributions. Sichuan Publishing House of Science & Technology, Sichuan, 209–246. [In Chinese]

Frost DR (2023) Amphibian Species of the World: an Online Reference. Version 6.1 (January 10, 2023). American Museum of Natural History, New York, USA. https://amphibiansoftheworld.amnh.org/index.php

Glaw F, Vences M (2007) A field guide to the amphibians and reptiles of Madagascar. 3rd edn. Frosch Verlag, Cologne, 496 pp.

Gosner KL (1960) A simplified table for staging anuran embryos and larvae with notes on identification. Herpetologica 16(3): 183–190.

Hall TA (1999) BIOEDIT: A user-friendly biological sequence alignment editor and analysis program for Windows 95/98/NT. Nucleic Acids Symposium Series 41(41): 95–98.

Hasan M, Islam M, Khan M, Igawa T, Alam MS, Djong HT, Kurniawan N, Joshy H, Sen YH, Bflabut DM, Kurabayashi A, Kuramoto M, Sumida M (2014) Genetic divergences of South and Southeast Asian frogs: A case study of several taxa based on 16S ribosomal RNA gene data with notes on the generic name *Fejervarya*. Turkish Journal of Zoology 38(4): 389–411. https://doi.org/10.3906/zoo-1308-36

Huang YZ, Fei L (1981) Two new species of amphibians from Xizang. Acta Zootaxonomica Sinica/ Dong wu fen lei xue bao. Beijing 6: 211–215.

Huang CM, Lathrop A, Murphy RW (1998) Translations of "Two new species of amphibian in Tibet" Huang & Fei 1981 and "Description of two new species of the genus *Megophrys*" Fei, Ye, & Huang 1995. Smithsonian Herpetological Information Service 118: 1–20. https://doi.org/10.5479/si.23317515.118.3

Jiang JP, Yuan FR, Xie F, Zheng ZH (2003) Phylogenetic relationships of some species and genera in megophryids inferred from partial sequences of mitochondrial 12S and 16S rRNA genes. Zoological Research 24: 241–248.

Jiang K, Rao DQ, Yuan SQ, Wang JS, Li PP, Hou M, Che M, Che J (2012) A new species of the genus *Scutiger* (Anura: Megophryidae) from southeastern Tibet, China. Zootaxa 3388(1): 29–40. https://doi.org/10.11646/zootaxa.3388.1.3

Jiang K, Wang K, Xie J, Zou DH, Liu WL, Jiang JP, Li C, Che J (2016a) A new species of the genus *Amolops* (Amphibia: Ranidae) from southeastern Tibet, China. Zoological Research 37: 31–40. https://doi.org/10.13918/j.issn.2095-8137.2016.1.31

Jiang K, Wang K, Zou DH, Yan F, Li PP, Che J (2016b) A new species of the genus *Scutiger* (Anura: Megophryidae) from Medog of southeastern Tibet, China. Zoological Research 37: 21–30. https://doi.org/10.13918/j.issn.2095-8137.2016.1.21

Jiang K, Yan F, Wang K, Zou DH, Li C, Che J (2016c) A new genus and species of treefrog from Medog, southeastern Tibet, China (Anura, Rhacophoridae). Zoological Research 37: 15–20. https://doi.org/10.13918/j.issn.2095-8137.2016.1.15

Kumar S, Stecher G, Tamura K (2016) MEGA7: Molecular Evolutionary Genetics Analysis Version 7.0 for Bigger Datasets. Molecular Biology and Evolution 33(7): 1870–1874. https://doi.org/10.1093/molbev/msw054

Lanfear R, Frandsen PB, Wright AM, Senfeld T, Calcott B (2017) Partitionfinder 2: New methods for selecting partitioned models of evolution for molecular and morphological phylogenetic analyses. Molecular Biology and Evolution 34(3): 772–773. https://doi.org/10.1093/molbev/msw260

Lathrop A (1997) Taxonomic review of the megophryid frogs (Anura: Pelobatoidea). Asiatic Herpetological Research 7: 68–79. https://doi.org/10.5962/bhl.part.18857

Liu Z, Chen G, Zhu T, Zeng Z, Lyu Z, Wang J, Messenger K, Greenberg AJ, Guo ZX, Yang ZH, Shi SH, Wang YY (2018) Prevalence of cryptic species in morphologically uniform taxa-fast speciation and evolutionary radiation in Asian frogs. Molecular Phylogenetics and Evolution 127: 723–731. https://doi.org/10.1016/j.ympev.2018.06.020

Luong AM, Hoang CV, Pham CT, Nguyen TT, Orlov N, Ziegler T, Nguyen TQ (2022) A new species of *Xenophrys* (Amphibia: Anura: Megophryidae) from Truong Son Range, Vietnam. Zootaxa 5150(3): 333–356. https://doi.org/10.11646/zootaxa.5150.3.2

Lyu ZT, Zeng Z, Wang J, Liu ZY, Huang YQ, Li WZ, Wang YY (2021) Four new species of *Panophrys* (Anura, Megophryidae) from eastern China, with discussion on the recognition of *Panophrys* as a distinct genus. Zootaxa 4927(1): 9–40. https://doi.org/10.11646/zootaxa.4927.1.2

Lyu ZT, Qi S, Wang J, Zhang SY, Zhao J, Zeng ZC, Wang H, Yang JH, Mo YM, Wang YY (2023) Generic classification of Asian horned toads (Anura: Megophryidae: Megophryinae) and monograph of Chinese species. Zoological Research 44(2): 380–450. https://doi.org/10.24272/j.issn.2095-8137.2022.372

Mahony S (2011) Two new species of *Megophrys* Kuhl and van Hasselt (Amphibia: Megophryidae), from western Thailand and southern Cambodia. Zootaxa 2734(1): 23–39. https://doi.org/10.11646/zootaxa.2734.1.2

Mahony S, Sengupta S, Kamei RG, Biju SD (2011) A new low altitude species of *Megophrys* Kuhl & van Hasselt (Amphibia: Megophryidae), from Assam, Northeast India. Zootaxa 3059 (1): 36–46. https://doi.org/10.11646/zootaxa.3059.1.2

Mahony S, Teeling EC, Biju SD (2013) Three new species of horned frogs, *Megophrys* (Amphibia: Megophryidae), from northeast India, with a resolution to the identity of *Megophrys boettgeri* populations reported from the region. Zootaxa 3722 (2): 143–169. https://doi.org/10.11646/zootaxa.3931.2.3

Mahony S, Foley NM, Biju SD, Teeling EC (2017) Evolutionary history of the Asian Horned Frogs (Megophryinae): integrative approaches to timetree dating in the absence of a fossil record. Molecular biology and evolution 34(3): 744–771. https://doi.org/10.1093/molbev/msw267

Mahony S, Kamei RG, Teeling EC, Biju SD (2018) Cryptic diversity within the *Megophrys major* species group (Amphibia: Megophryidae) of the Asian Horned Frogs: Phylogenetic perspectives and a taxonomic revision of South Asian taxa, with descriptions of four new species. Zootaxa 4523(1): 1–96. https://doi.org/10.11646/zootaxa.4523.1.1

Mahony S, Kamei RG, Teeling EC, Biju SD (2020) Taxonomic review of the Asian Horned Frogs (Amphibia: *Megophrys* Kuhl & Van Hasselt) of Northeast India and Bangladesh previously misidentified as M. parva (Boulenger), with descriptions of three new species. Journal of Natural History 54(1–4): 119–194. https://doi.org/10.1080/00222933.2020.1736679

Mathew R, Sen N (2007) Description of two new species of *Xenophrys* (Amphibia: Anura: Megophryidae) from north-east India. Cobra 1(2): 18–28.

Munir M, Hamidy A, Farajallah A, Smith EN (2018) A new *Megophrys* Kuhl and Van Hasselt (Amphibia: Megophryidae) from southwestern Sumatra, Indonesia. Zootaxa 4442(3): 389–412. https://doi.org/10.11646/zootaxa.4442.3.3

Munir M, Nishikawa K, Hamidy A, Smith EN (2021) Two new species of *Megophrys* Kuhl and Van Hasselt (Amphibia: Megophryidae) from Sumatra, Indonesia. Zootaxa 5057(4): 503–529. https://doi.org/10.11646/zootaxa.5057.4.3

Neang T, Chin S, Meang M, Hun S (2013) Confirmation of three species of megophryid frogs (Amphibia: Megophryidae) from the Cardamom Mountains of Southwest Cambodia, with the rediscovery of a long lost species. Cambodian Journal of Natural History 2013(2): 66–72.

Oberhummer E, Barten C, Schweizer M, Das I, Haas A, Hertwig ST (2014) Description of the tadpoles of three rare species of megophryid frogs (Amphibia: Anura: Megophryidae) from Gunung Mulu, Sarawak, Malaysia. Zootaxa 3835(1): 59–79. https://doi.org/10.11646/zootaxa.3835.1.3

Ohler A, Swan SR, Daltry JC (2002) A recent survey of the amphibian fauna of the Cardomom Mountains, Southwest Cambodia with descriptions of three new species. Raffles Bulletin of Zoology 50 (2): 465–481.

Rambaut A (2016) FigTree v1.4.3. Molecular Evolution, Phylogenetics and Epidemiology. http://tree.bio.ed.ac.uk/software/figtree/

Rao DQ, Yang DT (1997) The karyotypes of Megophryinae (Pelobatidae) with a discussion on their classification and phylogenetic relationships. Asian Herpetological Research 7: 93–102. https://doi.org/10.5962/bhl.part.18858

Ronquist F, Teslenko M, Paul VDM, Ayres DL, Darling A, Höhna S, Larget B, Liu L, Suchard MA, Huelsenbeck JP (2012) MrBayes 3.2: Efficient Bayesian phylogenetic inference and model choice across a large model space. Systematic Biology 61(3): 539–542. https://doi.org/10.1093/sysbio/sys029

Shi S, Zhang M, Xie F, Jiang J, Liu W, Ding L, Luan L, Wang B (2020) Multiple data revealed two new species of the Asian horned toad *Megophrys* Kuhl & Van Hasselt, 1822 (Anura, Megophryidae) from the eastern corner of the Himalayas. ZooKeys 977: 101–161. https://doi.org/10.3897/zookeys.977.55693

Simon C, Frati F, Beckenbach A, Crespi B, Liu H, Flook P (1994) Evolution, weighting and phylogenetic utility of mitochondrial gene sequences and a compilation of conserved polymerase chain reaction primers. Annals of the Entomological Society of America 87(6): 651–701. https://doi.org/10.1093/aesa/87.6.651

Stuart BL, Chuaynkern Y, Chan-ard T, Inger RF (2006) Three new species of frogs and a new tadpole from eastern Thailand. Fieldiana 111: 1–19. https://doi.org/10.3158/0015-0754(2006)187[1:TNSOFA]2.0.CO;2

Tian WS, Hu QX (1983) Taxonomic study on genus *Megophrys*, with descriptions of two new genera. Acta Herpetologica Sinica New Series 2: 41–48.

Ye CY, Fei L (1992) A new pelobatid toad of the genus *Megophrys* from Xizang, China. Acta Herpetologica Sinica/Liangqi baxing dongwu yanjiu 1(2): 50–52.

Zhang H, Shu GC, Shu F, Li K, Liu Q, Wu YY, Dong BJ, Guo P (2022) A new species of bush frog (Anura, Rhacophoridae, *Raorchestes*) from southern Xizang, China. Zootaxa 5195(2): 125–142. https://doi.org/10.11646/zootaxa.5195.2.2

Supplementary material 1

References utilized for morphological characters of congeners of the genus *Xenophrys*

Authors: Guocheng Shu, Ke Li, Yayong Wu, Qin Liu, Zhongping He, Ling Li, He Zhang, Peng Guo

Data type: xlsx

Link: https://doi.org/10.3897/zookeys.1182.106828.suppl1

ZooKeys 1182: 331–338 (2023)
DOI: 10.3897/zookeys.1182.108219

Research Article

Renicoris robustus, a new genus and species of the subfamily Harpactorinae (Hemiptera, Reduviidae) from China

Jianyun Wang[1], Zhuo Chen[2], Ping Zhao[3], Wanzhi Cai[2]

1 *Environment and Plant Protection Institute, Chinese Academy of Tropical Agricultural Sciences, Haikou, Hainan, 571101, China*
2 *Department of Entomology and MOA Key Lab of Pest Monitoring and Green Management, College of Plant Protection, China Agricultural University, Yuanmingyuan West Road, Beijing 100193, China*
3 *Key Laboratory of Environment Change and Resources Use in Beibu Gulf (Ministry of Education) and Guangxi Key Laboratory of Earth Surface Processes and Intelligent Simulation, Nanning Normal University, Nanning 530001, China*
Corresponding authors: Ping Zhao (zpyayjl@126.com); Wanzhi Cai (caiwz@cau.edu.cn)

Abstract

Renicoris **gen. nov.** and its type species *Renicoris robustus* **sp. nov.** (Hemiptera: Heteroptera: Reduviidae: Harpactorinae) from Yunnan, China, are described and illustrated. A key to separate the new genus and its closely related genera is provided.

Key words: Assassin bug, Euagorasini, key, morphology, new species, taxonomy

Academic editor: Jader Oliveira
Received: 22 July 2023
Accepted: 6 September 2023
Published: 20 October 2023

ZooBank: https://zoobank.org/D94364C3-71CE-4628-AC95-9A865C16531E

Citation: Wang J, Chen Z, Zhao P, Cai W (2023) *Renicoris robustus*, a new genus and species of the subfamily Harpactorinae (Hemiptera, Reduviidae) from China. ZooKeys 1182: 331–338. https://doi.org/10.3897/zookeys.1182.108219

Introduction

Harpactorinae is the largest subfamily of Reduviidae, including more than 2000 species and 300 genera worldwide, and 191 spe`cies and 55 genera in China (Maldonado-Capriles 1990; Zhao et al. 2009, 2014a, b, 2015a, b, 2021; Chen et al. 2020, 2022). However, the tribe-level systematic relationship in Harpactorinae is in debate due to the complex morphological variation and the high biodiversity within the subfamily. The taxonomic status of several harpactorine tribes, Euagorasini Distant, 1904, Rhaphidosomoni Jeannal, 1919, Rhynocorini Villiers, 1982 and Sycanini Dohrn, 1859 are not recognized by all taxonomists (Distant 1904; Hsiao and Ren 1981; Forero 2011). It is worthwhile to study whether some generic groups should be promoted to tribal level.

During fieldwork to Yunnan Province in southwestern China, we discovered an undescribed, rare, and unique species belonging to the tribe Euagorasini. Euagorasini was established by Distant (1904) based on the following characters: body slender; head with a pair of spines or tubercules at the base of the antennae; lateral pronotal angles generally produced into spines. The tribe consists of 29 genera and 76 species in China (Hsiao and Ren 1981; Cai and Tomokuni 2003; Chen et al. 2005; Truong et al. 2005; Zhao et al. 2006a, b, 2014a, 2021; Huang et al. 2007; Chen et al. 2020). The head of the undescribed species has a small round tubercle behind the base of the antennal tubercle, which is an important common character for all genera of Euagorasini (Distant 1904; Hsiao and Ren 1981). We could not assign it to any known genus and have therefore erected a new monotypic genus to accommodate it. A key to the new genus and related genera is provided.

Material and method

This study is based on material deposited in the Entomological Museum of China Agricultural University (CAU), Beijing, China. External structures were examined using a binocular dissecting microscope. Male genitalia were soaked in hot 90% lactic acid for ~10 min to remove soft tissue, then rinsed in hot distilled water and dissected under a microscope. Dissected parts of the genitalic structures were placed in a plastic microvial with lactic acid under the corresponding specimen. All habitus photographs were taken using Canon D60 SLR camera (Canon Inc., Tokyo, Japan). All photographs of the male genitalia were taken with the aid of the Research Stereo Microscope SMZ25 (Nikon Corporation, Tokyo, Japan). Measurements were obtained using a calibrated micrometer; body length was measured from the apex of the head to the tip of the fore wings in a resting position; maximum width of the pronotum was measured across humeral angles. All measurements are given in millimeters. Morphological terminology and the classification system mainly followed those of Cai and Tomokuni (2003), Davis (1966) and Hsiao and Ren (1981).

Taxonomy

Subfamily Harpactorinae Amyot & Servile, 1843
Tribe Euagorasini Distant, 1904

Renicoris gen. nov.

https://zoobank.org/96E69160-7238-483C-8CD0-22F155C20036
Figs 1–3

Type species. *Renicoris robustus* sp. nov.

Type locality. China, Yunnan, Lvchun, Huanglian Mountain.

Diagnosis. *Renicoris* gen. nov. resembles *Chenicoris* Chen & Cai, 2020 in the structure of the head and the male genitalia (Figs 1–3). However, in the new genus, the pronotum is trapezoidal and its median transversal constriction is indistinct (Figs 1, 2); the posterior pronotal lobe is not enlarged, the lateral pronotal angle is spine-shaped; the lateral margin of pronotum is straight (Figs 1, 2); the abdomen is rhomboid, and the fourth to sixth connexival segments of the abdomen are produced laterally (Fig. 1); the median pygophore process is bifid with acute angles (Fig. 3a, b) (vs. in *Chenicoris*, the pronotum is not trapezoidal due to its median transversal strong constriction; the posterior pronotal lobe is much enlarged and the lateral pronotal angle is rounded; the lateral margin of pronotum is distinctly constricted in the middle; the abdomen is not rhomboid, the fourth to sixth connexival segments of the abdomen are produced laterally, especially the lateral angle of the fifth segment which is dilated and round; the median pygophore process is absent). The genera morphologically related to the new genus can be separated using the following key.

Generic character. Body somewhat robust (Figs 1, 2). Head shorter than pronotum, with a small round tubercle behind base of each antennal tubercle (Figs 1a, 2a); eyes large and protruded laterally (Figs 1, 2a–c); ocelli elevated; anteocular part slightly longer than postocular part, transversely constricted between eyes; postocular part posteriorly narrower (Figs 1, 2a–c); first

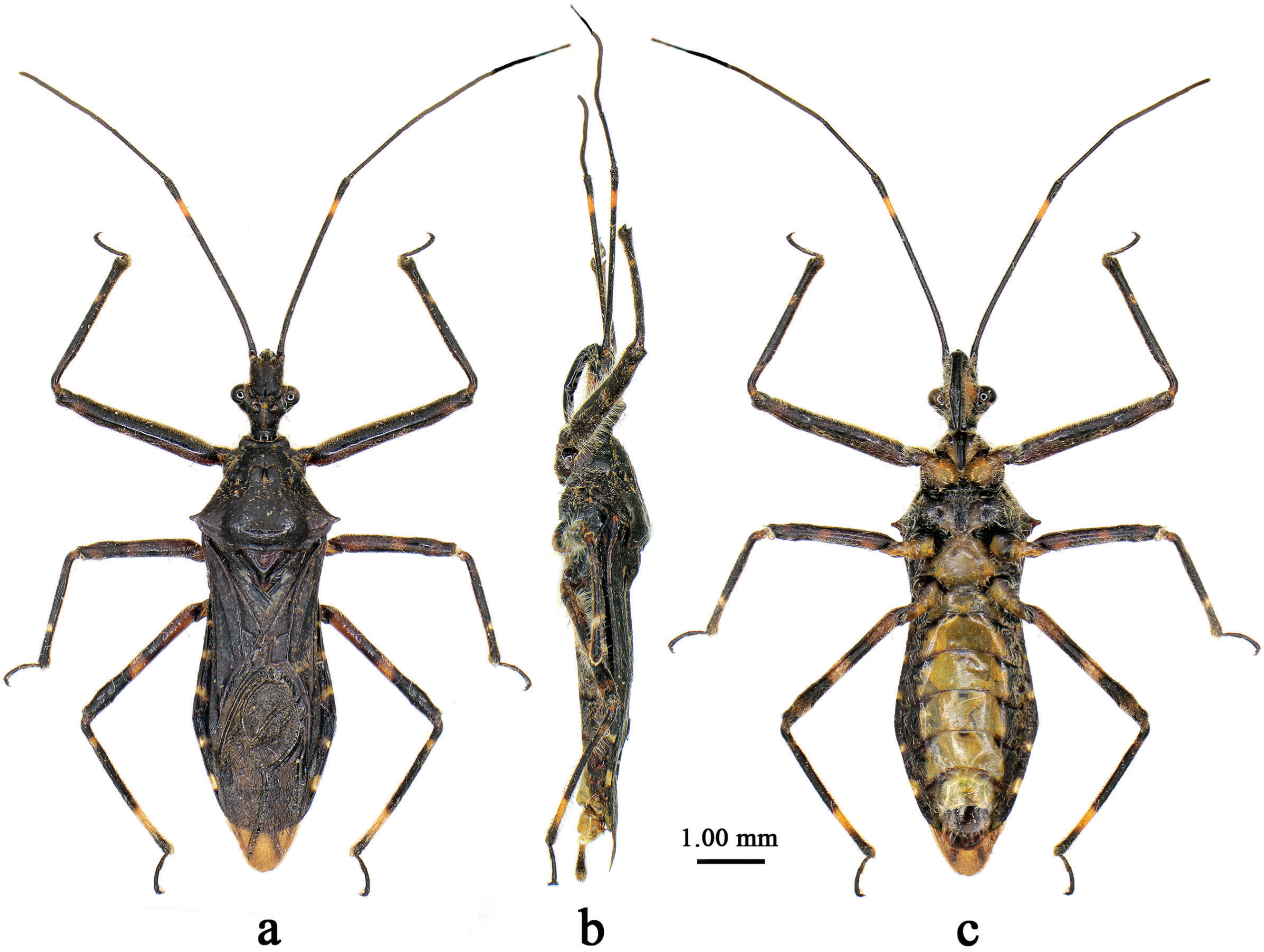

Figure 1. *Renicoris robustus* sp. nov., male, holotype, habitus **a** dorsal view **b** lateral view **c** ventral view.

antennal segment nearly as long as head and pronotum together in length; first rostral segment longest and extending to middle of eyes (Fig. 2b). Pronotum dorsally slightly flat, somewhat anteriorly declining, medially with indistinct transversal constriction; lateral margin nearly straight; anterior angle round; anterior pronotal lobe 1/2 as long as posterior lobe; middle part of posterior lobe faintly bulgy, two sides with lateral sulci; lateral pronotal angles produced laterally, short spine-shaped, with round protuberance behind it; posterior and posterolateral margins nearly straight; posterior angle round; scutellum subtriangular with Y-shaped ridge (Figs 1, 2a–c). Legs thick and robust, fore legs somewhat thickened (Figs 1, 2). Fore wing with inner cell wider than outer cell at base. Fourth to sixth connexival segments of abdomen laterally slightly rhombus-shaped dilated.

Distribution. China (Yunnan).

Etymology. The genus is named after the Chinese entomologist Shu-Zhi Ren (Nankai University, Tianjin, China), for her great contribution to the taxonomy of Chinese Heteroptera. The Greek noun *coris* means "bug". Gender masculine.

A key to *Renicoris* gen. nov. and its morphologically similar genera

1 Apical part of fore tibia distinctly bent..**2**
– Apical part of fore tibia straight..**5**

2 Fore femur prominently thickened and robust .... ***Agyrius* Stål, 1863**

– Fore femur somewhat thickened **3**

3 Inner side of subapical part of fore tibia armed with a long spur .... ***Rihirbus* Stål, 1861**

– Fore tibia unarmed **4**

4 Pronotum conspicuously anteriorly declining; posterior pronotal lobe anteriorly faintly elevated, and two sides without lateral sulci .... ***Flexitibia* Zhao & Cai, 2014**

– Pronotum not declining; posterior pronotal lobe not elevated, middle part feebly concave and two sides with lateral sulci .... ***Camptibia* Cai & Tomokuni, 2003**

5 Posterior part of lateral margin of anterior pronotal lobe with a distinct protuberance.. ***Isyndus* Stål 1858**

– Lateral margin of pronotum without protuberance **6**

6 Fourth to sixth connexival segments of abdomen laterally dilated, fifth connexival segment prominently roundly-produced laterally .... ***Chenicoris* Chen & Cai, 2020**

– Fourth to sixth connexival segments of abdomen laterally slightly rhombus-shaped, dilated .... ***Renicoris* gen. nov.**

***Renicoris robustus* sp. nov.**

https://zoobank.org/C1D2BEB1-1835-4FA8-82BE-EEE732D93AB9
Figs 1–3

Type material. ***Holotype*** (♂): CHINA, Yunnan, Lvchun, Huanglian Mountain, Yakou, Yijiao Center, 22°53'48.9"N, 102°18'23.4"E, 1938 m, 2015-VI-8, Jianyun Wang leg. (CAU).

Diagnosis. As for the genus by monotypy.

Description. Macropterous male. ***Coloration*.** Body dorsally bluish-black to black with milky white to yellowish markings, ventrally paler (Fig. 1a–c). Ventral surface of head (Figs 1c, 2c), one small round spot of vertex, ocellus (Figs 1a, 2a), one distinct annular marking of subapical part of first antennal segment (Fig. 1a–c), coxae, trochanters (Figs 1c, 2c), three faint annular markings of basal, median and apical parts of fore and mid femora (Figs 1, 2d, e), one distinct annular marking of median part and two faint markings of basal and apical parts of hind femera (Figs 1, 2f), one faint marking of basal part and one distinct marking of subapical part of fore and mid tibiae (Figs 1, 2d, e), one distinct annular marking of subapical part and one small marking of subbasal part of hind tibiae (Fig. 2f), sterna of pro- and metathoraxes (Figs 1c, 2c), sterna of abdomen (except connexivum and lateral margins) (Fig. 1c), and markings of posterior margins of connexival segments, milky white to yellowish (Fig. 1).

***Structure*.** Body of medium size, somewhat flattened dorsoventrally (Fig. 1). Head, thorax, abdomen, and legs covered with white short bent procumbent pubescence and sub-erect setae; first antennal segment sparsely clothed with erect setae, second to fourth segments densely clothed with procumbent pubescence; fore femur and tibia ventrally clothed with dense short setae (Figs 1, 2). Head width subequal to or slightly shorter than length; interocular

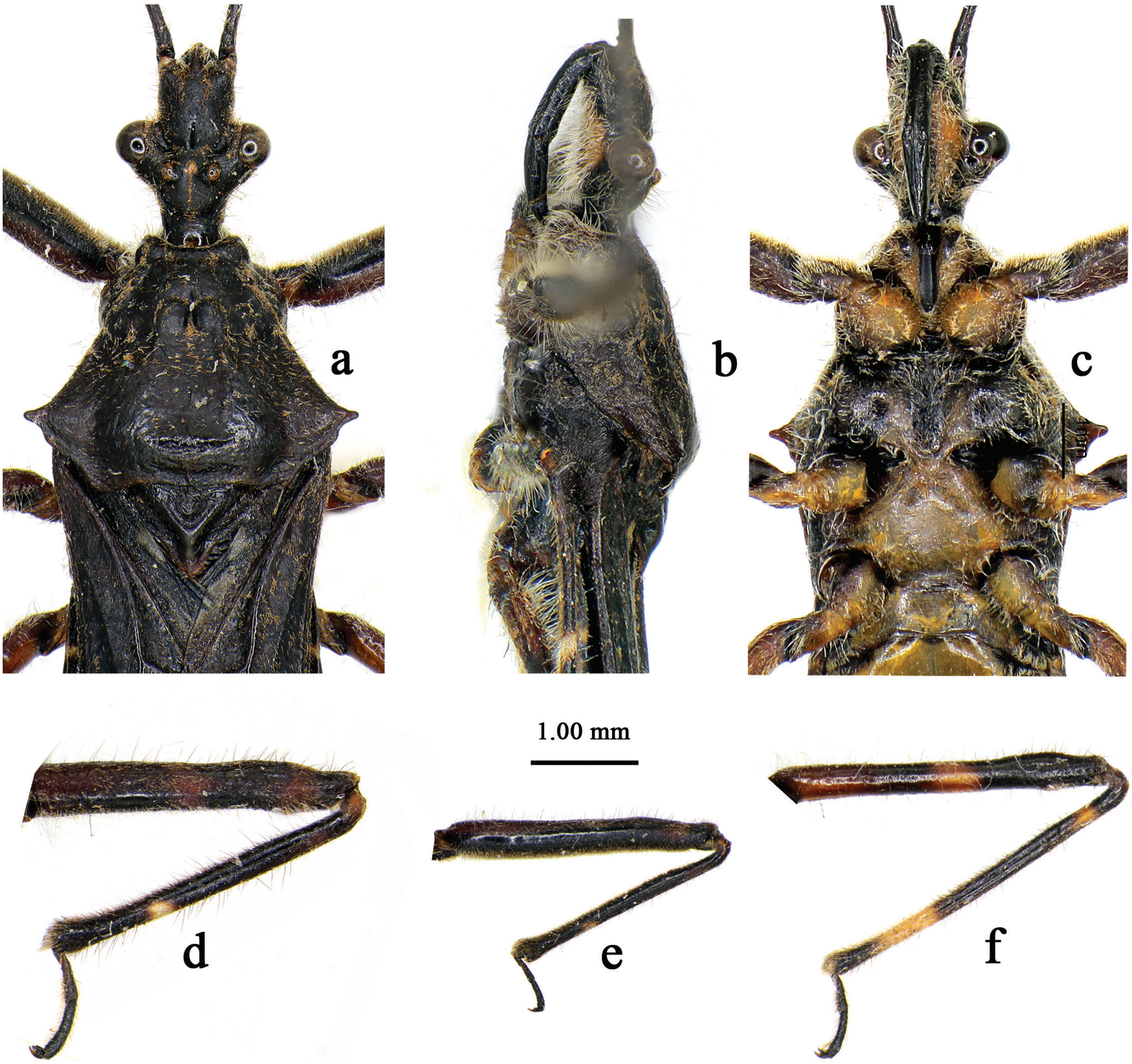

Figure 2. *Renicoris robustus* sp. nov., male, holotype **a–c** head and pronotum, with antennae and legs not shown **d** fore leg **e** mid leg **f** hind leg. **a** dorsal view **b, d–f** lateral view **c** ventral view.

space more than 2× interocellar space; rostrum robust, first segment subequal to second and third segments together in length (Fig. 2b, c). Anterior pronotal lobe basally centrally sulcate and laterally with shallow arc-shaped glabrous area; middle part of posterior pronotal lobe somewhat concaved; lateral pronotal angles acutely produced, short (Figs 1a, 2a). Fore wing surpassing abdominal tip by 0.7 mm (Fig. 1).

***Male genitalia*.** Pygophore oblong, median pygophore process bifid with acute angles (Fig. 3a, b); paramere clavate, slightly curved, middle part twisted (Fig. 3a–c); basal plate of phallobase longer and thicker than basal plate bridge, pedicel short (Fig. 3d, e). Phallosome elliptical (Fig. 3e–g); dorsal phallothecal sclerite well sclerotized, apical part concave, lateral arm subequal to strut in length (Fig. 3e); apical part of endosome armed with a pair of leaflike sclerites (Fig. 3e, f).

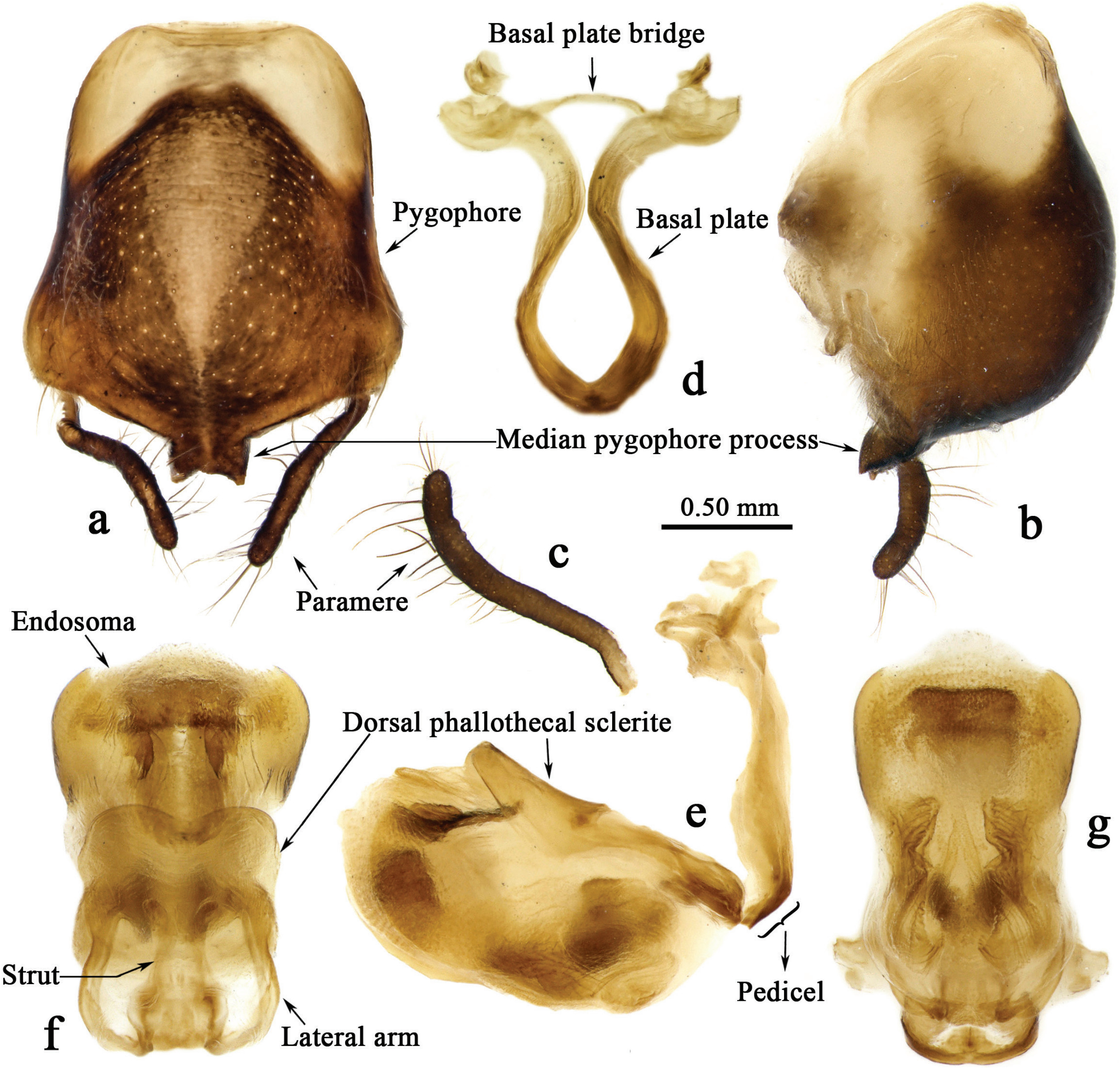

Figure 3. *Renicoris robustus* sp. nov., male, holotype, genitalia **a** pygophore with two parameres **b** pygophore with a paramere previously extracted **c** paramere **d** phallobase **e** phallus **f, g** phallosoma **a, g** ventral view **e, b** lateral view **f** dorsal view.

Measurements [male (*N* = 1), in mm]. Body length 14.4 (to tip of abdomen) / 15.1 (to tips of fore wings). Length of head 2.6 (with neck) / 2.4 (without neck); length of anteocular part 1.0; length of postocular part 0.75; width across eyes 2.1; interocular space 1.2; interocellar space 0.45; length of antennal segments I–IV 5.5, 2.0, 3.2, 1.8; length of rostral segments I–III 1.4, 0.9, 0.5. Length of anterior pronotal lobe 1.2; length of posterior pronotal lobe 2.0; length of pronotum 3.2; width of anterior pronotal lobe 2.2; width of posterior pronotal lobe 4.3; basal width of scutellum 1.6; median length of scutellum 1.1; length of fore wing 9.9; length of fore femur / tibia / tarsus 4.9 / 4.5 / 1.1; length of mid femur / tibia / tarsus 3.5 / 3.2 / 1.1; length of hind femur / tibia / tarsus 4.7 / 4.7 / 1.1. Length of abdomen 7.2; maximum width of abdomen 4.2.

Distribution. China (Yunnan).

Etymology. The specific name alludes to the robust body shape of the new species. The Latin noun *robustus* means “sturdy, strong”.

Biology. Unknown.

Additional information

Conflict of interest

The authors have declared that no competing interests exist.

Ethical statement

No ethical statement was reported.

Funding

This research is supported by grants from the National Natural Science Foundation of China (No. 32270474); the Natural Science Foundation of Hainan Province of China (No. 322QN361); the Guangxi Natural Science Foundation of China (No. 2021GXNSFAA220106).

Author contributions

Conceptualization: WC. Funding acquisition: PZ. Investigation: JW. Supervision: WC. Visualization: JW. Writing - original draft: PZ. Writing - review and editing: WC, ZC.

Author ORCIDs

Jianyun Wang https://orcid.org/0000-0002-8466-3252
Zhuo Chen https://orcid.org/0000-0003-3393-0338
Ping Zhao https://orcid.org/0000-0001-9315-2756

Data availability

All of the data that support the findings of this study are available in the main text.

References

Cai WZ, Tomokuni M (2003) *Camptibia obscura* gen. et sp. nov. (Heteroptera: Reduviidae: Harpactorinae) from China. European Journal of Entomology 100(1): 181–185. https://doi.org/10.14411/eje.2003.028

Chen W, Zhao P, Cai WZ (2005) The discovery of the genus *Irantha* Stål, 1861 (Heteroptera: Reduviidae: Harpactorinae) from China, with the description of a new species. Annales Zoologici 55(1): 107–109. https://doi.org/10.3161/0003454053642130

Chen Z, Wang JY, Li H, Cai WZ (2020) *Chenicoris dilatatus*, a remarkable new genus and new species of assassin bug (Hemiptera: Heteroptera: Reduviidae: Harpactorinae) from southern China. European Journal of Entomology 117(1): 252–259. https://doi.org/10.14411/eje.2020.027

Chen Z, Liu YQ, Wu YF, Lee M, Li H, Cai WZ (2022) A survey of the tribe Ectinoderini (Hemiptera: Reduviidae: Harpactorinae) of China, with the description of a new *Ectinoderus* species. Journal of Asia-Pacific Entomology 25(4): 101974. https://doi.org/10.1016/j.aspen.2022.101974

Davis NT (1966) Contribution to the morphology and phylogeny of the Reduvioidea (Hemiptera: Heteroptera). Part III. The male and female genitalia. Annals of the Entomological Society of America 59(5): 911–924. https://doi.org/10.1093/aesa/59.5.911

Distant WL (1904) The Fauna of British India, Including Ceylon and Burma. Rhynchota 2 (Heteroptera). Taylor and Francis, London, 503 pp. [pp 1–242, 1903; pp i–xvii, 243–503, 1904] https://doi.org/10.1080/00222930408562466

Forero D (2011) Classification of Harpactorinae assassin bugs (Hemiptera: Heteroptera: Reduviidae). Boletin del Museo Entomológico Francisco Luís Gallego 3(1): 9–24.

Hsiao TY, Ren SZ (1981) Reduviidae. In: Hsiao TY, Ren SZ, Zheng LY, Jing XL, Zou HG, Liu SL (Eds) A Handbook for the Determination of the Chinese Hemiptera-Heteroptera. Vol. II. Science Press, Beijing, 390–538. [In Chinese with English summary]

Huang X, Zhao P, Zhao SY, Cai WZ (2007) A taxonomic review of genus *Scipinia* Stål (Hemiptera: Reduviidae: Harpactorinae) from China. Zootaxa 1507(1): 57–67. https://doi.org/10.11646/zootaxa.1507.1.2

Maldonado-Capriles J (1990) Systematic Catalogue of the Reduviidae of the World (Insecta: Heteroptera). A special edition of Caribbean Journal of Science, Puerto Rico, 694 pp.

Truong XL, Cai WZ, Wang YZ (2005) *Agyrius watanabeorum* Ishikawa, a new record genus and species from China and Vietnam (Heteroptera: Reduviidae). Entomotaxonomia 27: 23–26. http://en.cnki.com.cn/Article_en/CJFDTotal-KCFL200501005.htm

Zhao P, Cai WZ, Ren D (2006a) The reduviid genus *Nagustoides* Miller (Heteroptera: Reduviidae: Harpactorinae) found in China, with description of a new species. Zootaxa 1176(1): 17–25. https://doi.org/10.11646/zootaxa.1176.1.2

Zhao P, Yang CW, Cai WZ (2006b) First record of the genus *Platerus* Distant (Heteroptera: Reduviidae: Harpactorinae) from China, with the description of a third species of the genus. Zootaxa 1286: 23–31. https://doi.org/10.11646/zootaxa.1286.1.3

Zhao P, Luo ZH, Cai WZ (2009) *Iocoris nodulifemoralis*, a new genus and new species of Harpactorinae (Hemiptera: Heteroptera: Reduviidae) from China. Zootaxa 2129(1): 63–68. https://doi.org/10.11646/zootaxa.2129.1.4

Zhao P, Pham M, Truong XL, Cai WZ (2014a) *Flexitibia*, a new genus of Harpactorinae (Hemiptera: Heteroptera: Reduviidae), with a discussion on the functional morphology of forelegs of the related genera. Zootaxa 3795(5): 564–570. https://doi.org/10.11646/zootaxa.3795.5.5

Zhao P, Wang JY, Cai WZ (2014b) Description of a new species of the genus *Henricohahnia* Breddin (Hemiptera: Heteroptera: Reduviidae: Harpactorinae) from China, with a key to Chinese species. Zootaxa 3811(3811): 367–373. https://doi.org/10.11646/zootaxa.3811.3.7

Zhao P, Ren SZ, Wang BH, Cai WZ (2015a) A new species of the genus *Sphedanolestes* Stål 1866 (Hemiptera: Reduviidae: Harpactorinae) from China, with a key to Chinese species. Zootaxa 3985(4): 591–599. https://doi.org/10.11646/zootaxa.3985.4.8

Zhao P, Ren SZ, Wang BH, Cai WZ (2015b) *Cosmosycanus perelegans* (Hemiptera: Reduviidae: Harpactorinae), a new record from China, with report of its female genitalia. Zootaxa 3936(4): 567–574. https://doi.org/10.11646/zootaxa.3936.4.6

Zhao P, Du ZY, Zhao Q, Li DH, Shao XL, Li H, Cai WZ (2021) Integrative taxonomy of the spinous assassin bug genus *Sclomina* (Heteroptera: Reduviidae: Harpactorinae) reveals three cryptic species based on DNA barcoding and morphological evidence. Insects 12(3): 251. https://doi.org/10.3390/insects12030251

ZooKeys 1182: 339–359 (2023)
DOI: 10.3897/zookeys.1182.111297

Research Article

Morphological and ultrastructural studies of the internal reproductive systems of two deltocephaline leafhoppers, *Nephotettix cincticeps* and *Deltocephalus vulgaris* (Hemiptera, Cicadellidae, Deltocephalinae)

Jiarui Chen[1]*, Jing Zhang[1]*, Wei Liu[1,2]*, Bismillah Shah[1,3], Christopher H. Dietrich[4], Yani Duan[1]

1 *Anhui Province Key Laboratory of Integrated Pest Management on Crops, Key Laboratory of Biology and Sustainable Management of Plant Diseases and Pests of Anhui Higher Education Institutes, School of Plant Protection, Anhui Agricultural University, Hefei, Anhui 230036, China*
2 *Jingxian Agricultural and Rural Bureau, Xuancheng, Anhui 242500, China*
3 *Department of Forestry Protection, School of Forestry and Biotechnology, Zhejiang A&F University, 666 Wusu Street, Linan, Hangzhou, Zhejiang 311300, China*
4 *Illinois Natural History Survey, Prairie Research Institute, University of Illinois, Champaign, IL 61820, USA*
Corresponding author: Yani Duan (duanyani@hotmail.com)

Academic editor: J. A.Pinedo-Escatel
Received: 17 August 2023
Accepted: 2 October 2023
Published: 20 October 2023

ZooBank: https://zoobank.org/117A3B21-A629-4295-ADD8-5E7B77972A6B

Citation: Chen J, Zhang J, Liu W, Shah B, Dietrich CH, Duan Y (2023) Morphological and ultrastructural studies of the internal reproductive systems of two deltocephaline leafhoppers, *Nephotettix cincticeps* and *Deltocephalus vulgaris* (Hemiptera, Cicadellidae, Deltocephalinae). ZooKeys 1182: 339–359. https://doi.org/10.3897/zookeys.1182.111297

Abstract

Insects have highly variable reproductive systems, reflecting a diversity of reproductive strategies and adaptations. Such variation has been widely used to classify and estimate phylogenetic relationships. Here, the morphology and ultrastructure of the internal reproductive systems of two leafhopper species are described and illustrated, using both light and transmission electron microscopy, and representing two tribes of Deltocephalinae: in Chiasmini, *Nephotettix cincticeps* (Uhler, 1896), and in Deltocephalini, *Deltocephalus vulgaris* (Dash & Viraktamath, 1998). Tables comparing the morphology of male and female internal reproductive structures of these studied species are provided and indicate that the main differences are in the relative shapes, sizes, and colors of these structures. The overall structure and organization, including details of the ultrastructure, of these two leafhopper species' male and female internal reproductive systems are very similar to those of previously studied leafhoppers. The main differences observed among species include the number of testicular follicles, the relative position of seminal vesicles and the degree of development of the accessory glands in the male, the number of ovaries, and the shape and color of the vagina and spermatheca in the female.

Key words: Auchenorrhyncha, comparative study, Memberacoidea, transmission electron microscope

Introduction

Insects are the dominant component of terrestrial biodiversity. Their ability to survive across complex and varied natural environments is closely related to their strong reproductive capacity. The structures of the insect reproductive system are complex and varied, reflecting different reproductive strategies (Song 2011). The reproductive system of insects consists of multiple organs in the abdominal cavity that work together to produce sperm or ova and facilitate

---

* These authors contributed equally to this work.

copulation. A study of the insect reproductive system is needed to improve the understanding of insect reproductive potential and oviposition mode, which may ultimately facilitate pest management (Lei and Rong 2003). Comparative study of the reproductive structures of different insects also increases our understanding of the evolution and phylogeny of insects.

Despite leafhoppers' high diversity and economic importance and the widespread use of the external sclerotized structures of their genitalia for taxonomy and phylogenetics, their internal reproductive organs remain little studied. Helms (1968) described in detail the morphology of the leafhopper *Empoasca fabae* (Harris, 1841) male reproductive system. The adult male consists of two testes (each composed of four follicles), vasa deferentia with seminal vesicles, paired accessory glands, paired ejaculatory ducts, and a median ejaculatory bulb. Moreover, Mishra (1979) concluded in the comparison of male leafhoppers *Cofana spectra* (Distant, 1908), *C. unimaculata* (Signoret, 1854), and *Amritodus atkinsoni* (Lethierry, 1889) that the number of testicular follicles is different, and the corresponding accessory glands also differ in shape. Similarly, Tsai and Perrier (1996) studied the morphology of male reproductive systems of the two deltocephaline leafhoppers representing different tribes, *Dalbulus maidis* (DeLong, 1923) and *Graminella nigrifrons* (Forbes, 1885). They found that the males of these species have two lateral testes (each with six follicles). A pair of accessory glands arise at the posterior of each seminal vesicle and open into a lateral ejaculatory duct. Hayashi and Kamimura (2002) conducted a specific study on the leafhopper *Bothrogonia ferruginea* Fabricius, 1787 and found that during the process from production to entry into the female body, male sperm first transported to the female's bursa copulatrix through a spermatophore. After successful mating, the sperm enters the spermatheca for fertilization. At this stage, the sperm-binding material (trypsin degradable proteins) and the spermatophore disappear in the bursa and an enlarged portion of the genital duct. They suggested that females could incorporate proteinaceous material derived from male spermatophores and/or sperm-binding material into their oocytes. Tian et al. (2006) compared the male reproductive systems of 39 species of Cicadellidae and focused on spermatogenesis, classifying the testes into two types according to the presence or absence of the sheath. Their results revealed that the testicular follicles of Cicadellidae are spherical, while testicular follicles in Heteroptera are lamellar and sheathed. Su et al. (2014) compared the ultrastructure of the male reproductive systems of *Psammotettix striatus* (Linnaeus, 1758) and *Exitianus indicus* (Distant, 1908) (Deltocephalinae) and described the morphology and ultrastructure of the sperm of these two species. The sperm of both species have a 9+9+2 axonemal pattern, as in other Auchenorrhyncha, and provide a reference for the comparative study and phylogeny of other groups. Vitale et al. (2015) analyzed the morphology of the male reproductive system of *Balclutha brevis* (Lindberg, 1954). Their results showed that secretory activity occurring mainly in the lateral ejaculatory ducts and the accessory glands. The ultrastructural features of the seminal vesicle differed from those of the lateral ejaculatory duct, suggesting that these structures play distinct roles in the organization of the sperm bundles. Recently, Zhang et al. (2016) found differences in the organizational structure of the male reproductive systems of the closely related cicadelline leafhoppers *Cicadella viridis* (Linnaeus, 1758) and *Kolla paulula* (Walker, 1858).

Similarly, Helms (1968) found that the female reproductive system of *E. fabae* (Harris, 1841) consists of two ovaries (each composed of four telotrophic ovarioles), lateral oviducts, a median oviduct, a spermatheca, a genital chamber with a pair of spermatozoal pouches, and a median accessory gland. Additionally, Cheung (1994, 1995) studied the female reproductive system of *Euscelidium variegatus* Kirschbaum, 1858; it was clear that the ovary is endotrophic, and the main source of nutrition for growth and development is also completed by trophoblasts. Studies on the ultrastructure of the cicada reproductive system have found ovarian sheaths and tracheae on the periphery of the ovarian tubes, which are called perimetrium. Similarly, Tsai and Perrier (1996) also compared the morphology of the female reproductive systems of *D. maidis* (DeLong, 1923) and *G. nigrifrons* (Forbes, 1885) and found that ovaries of these species contain six ovarioles, each with six follicles. In *G. nigrifrons* each ovariole usually contains only one egg within the last follicle, whereas the ovarioles of *D. maidis* usually contain two eggs. The ovarioles open into the lateral oviduct, common oviduct, and the vagina. Besides, Hummel et al. (2006) studied the development of the ovaries in *Homalodisca vitripennis* (Germar, 1821) and found that a single ovary is composed of 10 ovarioles, and the development of an ovary occurred in seven stages. Recently, Pappalardo et al. (2016) studied the ultrastructure of the female reproductive system of *Balclutha brevis* (Lindberg, 1954). Their results showed that the female reproductive system has a morphological configuration comparable to most species of Auchenorrhyncha.

These previous studies indicate that characteristics of the reproductive system may provide a basis for phylogenetic analysis and classification. However, the available data are scattered, and studies have focused on different reproductive characteristics. Thus, additional comparative analyses are needed.

Materials and methods

Source of specimens

Specimens of deltocephaline leafhopper *Nephotettix cincticeps* were collected in mid-June 2020 and *Deltocephalus vulgaris* in early September 2020 using light-trap and net-sweeping techniques. The collection sites were concentrated in the urban area of Hefei in Anhui Province. Individual adult leafhoppers were collected into tubes, classified, identified, and placed into insect cages to reside and feed on relevant hosts for 3–5 days before being processed for anatomical study. The samples *N. cincticeps* contained five males and two females, while *D. vulgaris* contained five males and nine females. We used specimens without well-developed eggs in ovarioles for drawings and descriptions of females.

Light microscopy

Fresh adult leafhoppers were placed in a −36 °C freezer for 5–10 min. The leafhopper's abdomen was then immediately dissected under a light microscope (Motic, K-700HS). The abdominal epidermis was carefully removed with a dissecting needle to reveal the complete internal reproductive system of the leafhopper and transferred into a new concave slide with glycerin. It was then observed and photographed under a stereoscope (Nikon, SMZ1500). Photographs were edited using Adobe Photoshop CS6.

Transmission electron microscope

Fresh adult samples were dried for 15 min before the dissection of the internal reproductive system. Samples were fixed in 2.5% glutaraldehyde in a 0.1 M phosphate-buffered saline (PBS) (pH 7.2) and washed several times in the same phosphate-buffered saline. The samples were then fixed with 1% osmium tetroxide for 1–2 h. Later, the samples were serially dehydrated with 30%, 50%, 70%, 80%, 90% and 95% ethanol solutions for 15 min each, then treated with 100% ethanol for 20 min. After dehydration, all samples were treated with pure acetone for 20 min and then with a pure embedding agent for 24 h. Infiltrated samples were embedded by heating them at 70 °C for 24 h to obtain an embedded sample block. The embedded block was then sectioned in an ultra-microtome to obtain sections of 100 nm which could be observed under a transmission electron microscope (Hitachi, HT-7700). Micrographs of each species were obtained from a single male and a single female.

Morphological terminology

The morphological terminology used here mainly follows Tsai and Perrier (1996).

Results

Morphological observation of the internal reproductive systems

Nephotettix cincticeps

The male internal reproductive system of *N. cincticeps* consists of a pair of testes, a pair of vasa deferentia, a pair of seminal vesicles, a pair of accessory glands, a pair of lateral ejaculatory ducts, and a single common ejaculatory duct. The testes consist of six testicular follicles of similar size and shape, which are droplet-shaped and pale blue, and their distal ends are connected to the slender vasa deferentia. The seminal vesicle is oval, outward spreading, and pale blue (same as the testicular follicles). The accessory glands are well developed, with a long, tubular structure and bilateral symmetry. The distal end of the seminal vesicle is contracted and joined to the lateral ejaculatory duct, a slender, tubular structure. The distal ends converge and expand into the common ejaculatory duct, which is straight and connected with the external genitalia (Fig. 1).

The female internal reproductive system comprises a pair of ovaries, two lateral oviducts, a common oviduct, a colleterial gland, a vagina, and a spermatheca. A pair of accessory glands may also be present, but their degree of development varies according to the age and physiological state of the individual female (Hummel et al. 2006). The ovary is composed of six ovarioles of similar shape and size. The individual ovarioles are milky white, tubular, rounded at the top, and confluent at the distal ends to meet the lateral oviduct. The lateral

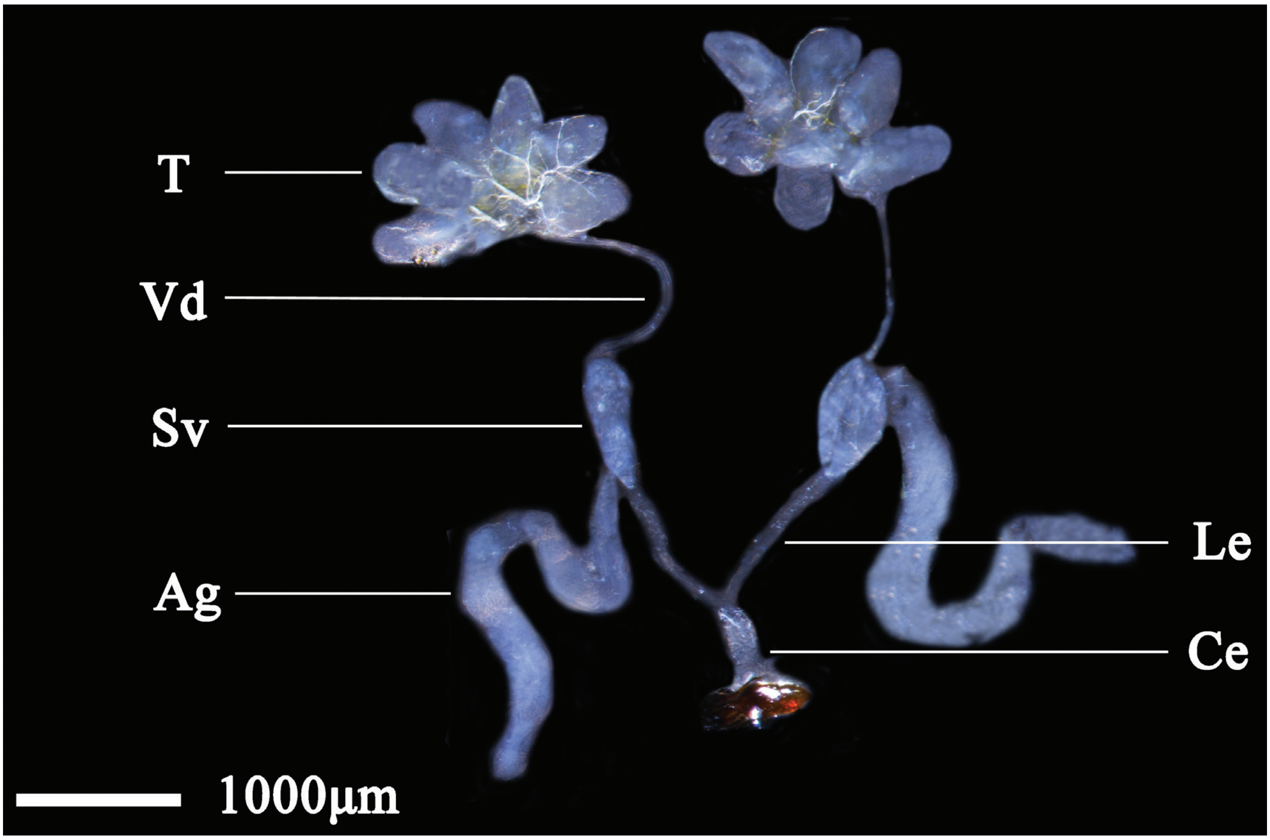

Figure 1. Male internal reproductive system of *N. cincticeps* (Uhler, 1896). Abbreviations: T – testis, Vd – vas deferens, Sv – seminal vesicle, Le – lateral ejaculatory duct, Ag – accessory gland, Ce – common ejaculatory duct.

oviducts are slender, tubular structures whose two distal ends fuse to converge with the common oviduct. The anterior part of the spermatheca is a slender, tubular structure. The termination of the common oviducts adheres to the vagina. The colleterial gland has a developed, tubular structure. The spermatheca is yellowish white and digitate in appearance (Fig. 2).

Deltocephalus vulgaris

The male internal reproductive system of *D. vulgaris* consists of a pair of testes, a pair of vasa deferentia, a pair of seminal vesicles, a pair of accessory glands, a pair of lateral ejaculatory ducts, and a single common ejaculatory duct. The testes are composed of five independent testicular follicles, which are pale blue with obvious bright spots, resemble a series of water droplets, and are connected to the vasa deferentia. The vasa deferentia are linear, slender, and connected to the seminal vesicle. The whole seminal vesicle is pale blue, translucent, and ovoid. The accessory glands are developed, the anterior segment is protuberant, the middle segment is contracted, the distal end is rod-like, the whole is milky white, and both sides are symmetrical. The lateral ejaculatory sac joins the common ejaculatory duct, which connects with the external genitalia (Fig. 3).

The female internal reproductive system consists of a pair of ovaries, lateral oviducts, a common oviduct, a colleterial gland, a vagina, and a spermatheca. The ovaries on both sides are symmetrically unfolded in a “Y” shape. Each

Figure 2. Female internal reproductive system of *N. cincticeps* (Uhler, 1896). Abbreviations: O – ovary, Lo – lateral oviduct, S – spermatheca, V – vagina, Cg – colleterial gland, Co – common oviduct.

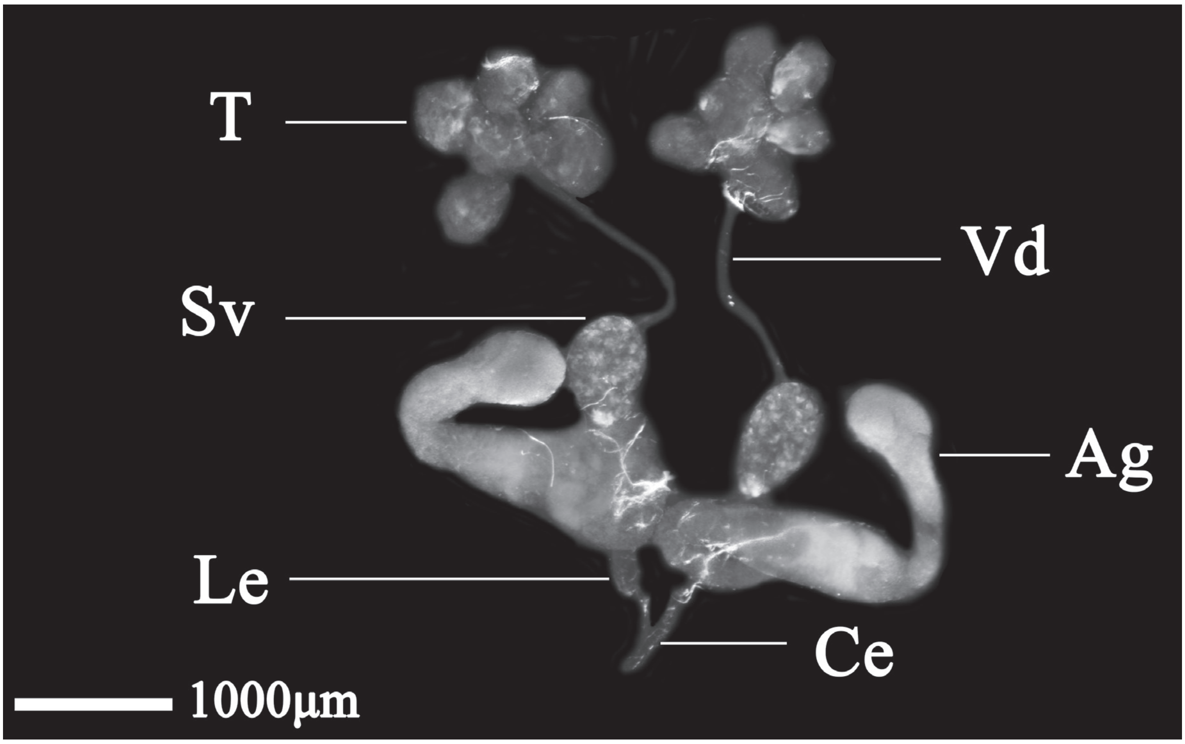

Figure 3. Male internal reproductive system of *D. vulgaris* (Dash & Viraktamath, 1998). Abbreviations: T – testis, Vd – vas deferens, Sv – seminal vesicle, Ag – accessory gland, Le – lateral ejaculatory duct, Ce – common ejaculatory duct.

ovary is made up of six ovarioles of similar shape and size. Individual ovarioles are milky white tubules, rounded at the top, and confluent at the distal ends to meet the lateral oviduct. The lateral oviduct is slender, thin, closed at both distal ends, and converges with the common oviduct. The distal end of the common oviduct adheres to the vagina. The spermatheca is light yellow and shaped like an irregular cone (Fig. 4).

Ultrastructure of the internal reproductive systems

Ultrastructure of the male internal reproductive system of *N. cincticeps*

Testis

The testis comprises six droplet-shaped testicular follicles of similar size and shape. The testis is symmetrical, without a sheath, and the surface is pale blue. The testicular follicles comprise a follicle membrane, muscular sheath, epithelium, and lumen with sperm at different developmental stages. There are tracheoles between the testicular follicle membrane and the muscle sheath and vesicles in the epithelium. Many endoplasmic reticula surround epithelial cell nucleus. Many sperm gather in the testicular follicles, and a

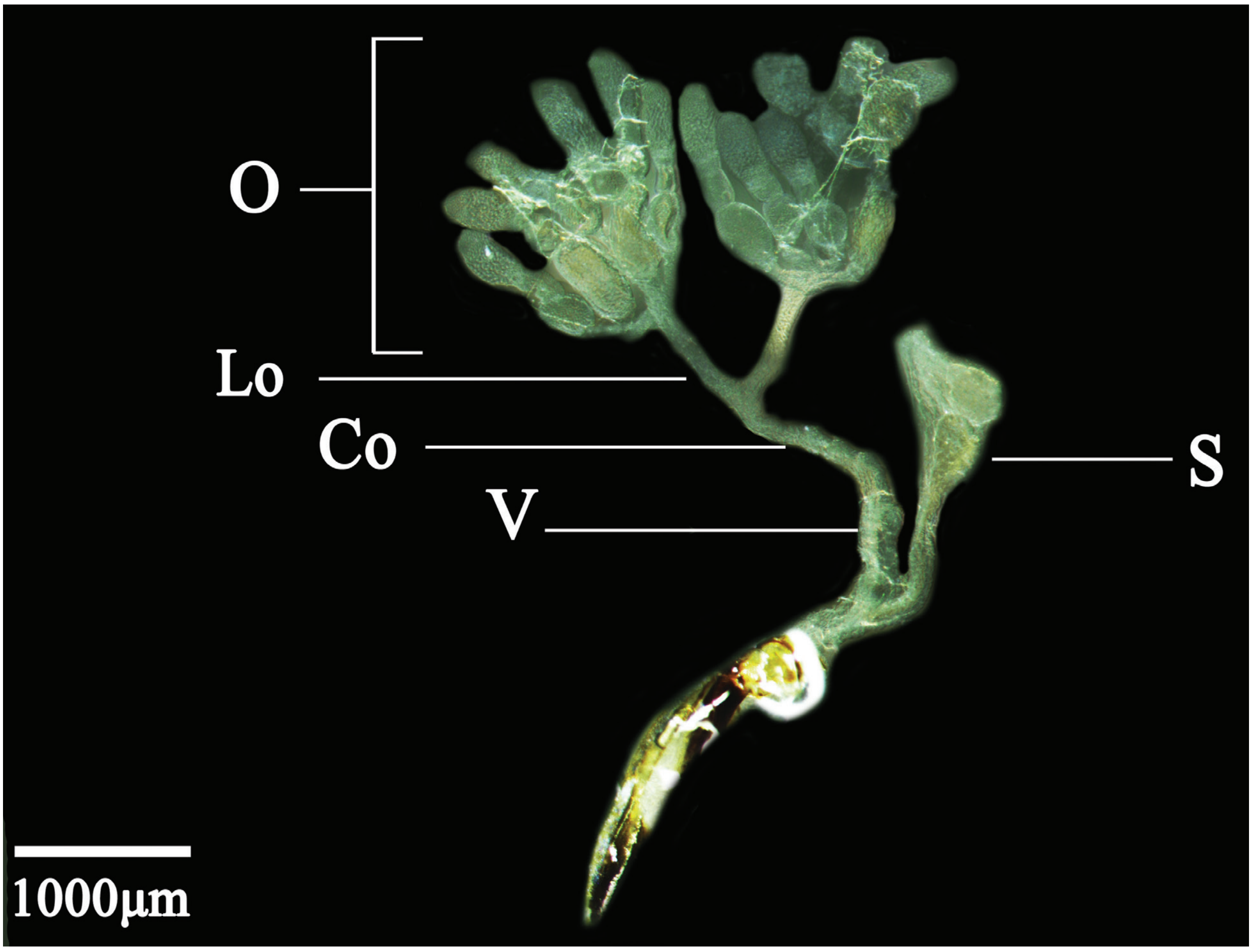

Figure 4. Female internal reproductive system of *D. vulgaris* (Dash & Viraktamath, 1998). Abbreviations: O – ovary, Lo – lateral oviduct, Co – common oviduct, S – spermatheca, V – vagina.

thick basal membrane is present (Fig. 5A, B). During the growth and development of the sperm, the sperm bundle is formed and is free to the edge of the basal membrane, at the same time, the phenomenon of partition appears (Fig. 5C, D).

Seminal vesicle

The edge of the seminal vesicle is clear, with starlike spots, almost oval, and pale blue. The tunica external tightly wraps the seminal vesicle, and the overall structure comprises four parts: tunica external, muscular sheath, epithelium, and lumen. There are some differences in sperm at different developmental stages (Fig. 6A, B). A long, narrow intercellular space exists between the

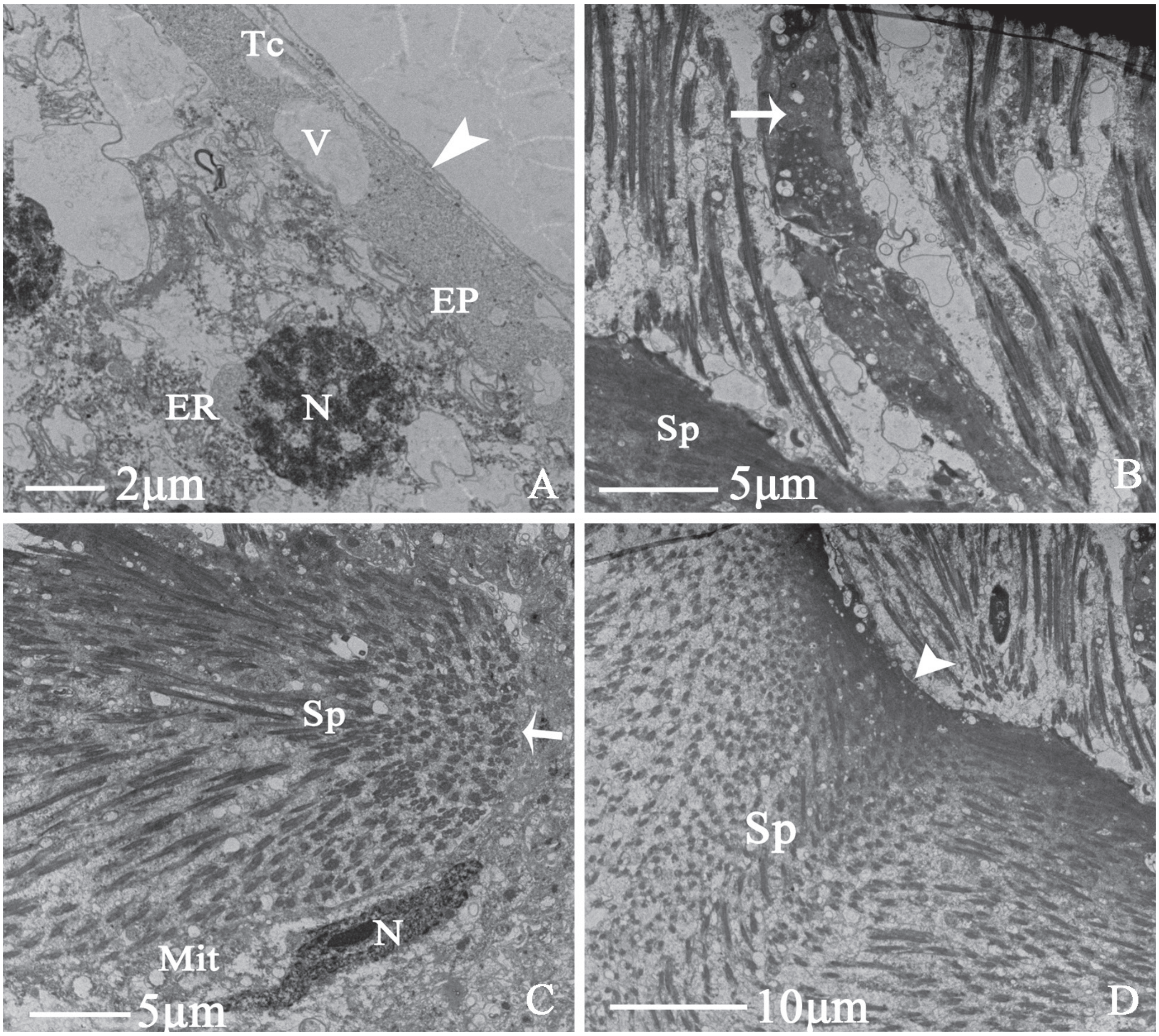

Figure 5. Ultrastructure of testicular follicle of *N. cincticeps* (Uhler, 1896) **A, B** cross-section of testicular follicle, showing (Tc) tracheole, (V) vesicle, (ER) endoplasmic reticulum, (EP) epithelium, (N) epithelial cell nucleus, (Sp) spermatid, (TM) the triangular arrowhead indicates testicular follicle membrane, (BM) the long arrow indicates thick basal membrane **C, D** showing (Sp) spermatid, (Mit) numerous mitochondria, (N) epithelial cell nucleus, (BL) the long arrow indicates basal lamina, (BM) the triangular arrowhead indicates thick basal membrane.

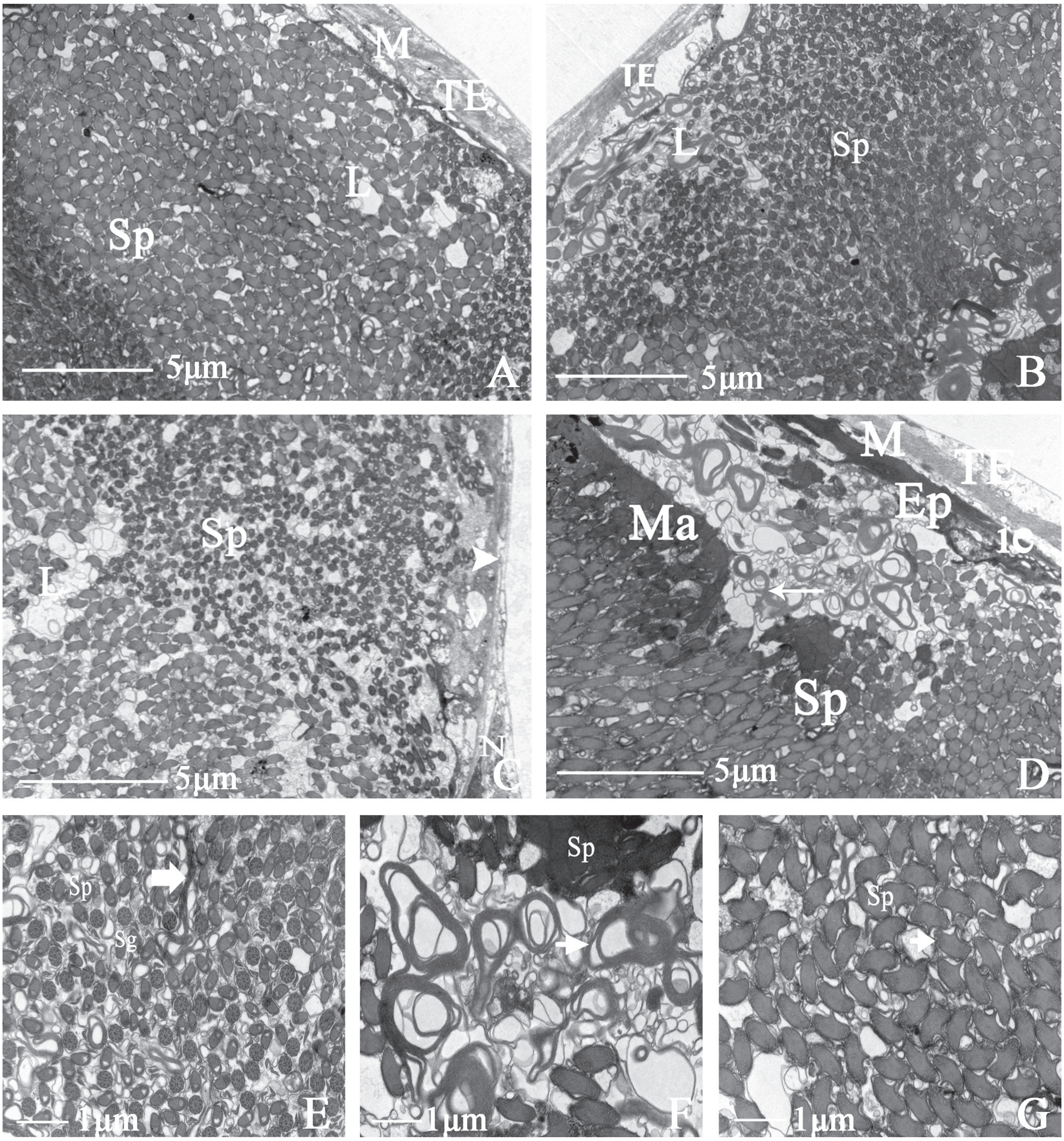

Figure 6. Ultrastructure of seminal vesicle of *N. cincticeps* (Uhler, 1896) **A, B** cross-section of seminal vesicle, showing (TE) tunica external, (M) muscle sheath, (Sp) sperm, (L) lumen **C** showing (L) lumen, (Sp) sperm **D** showing (TE) tunica external, (M) muscle sheath, (EP) epithelium, (ie) intercellular spaces, (Sp) sperm, (Ma) head of sperm embedded in the homogenous matrix in lumen **E** showing (Sp) sperm and (Sg) secretory granules in lumen, accompanied by plasma membrane to gap (arrow) **F** the arrow indicates lamellar bodies **G** cross-section of thumbtack nuclei of sperm.

epithelium and the muscular sheath. The lumen contains much sperm, and their heads are inserted into the matrix to form sperm bundles (Fig. 6C, D). Sperm and secretory cells appear simultaneously, with distinct plasma membrane spacing and lamellar bodies appearing in clumps in the lumen. In the cross-section of the seminal vesicle, the thumbtack-shaped nuclei and surrounding microtubules are visible (Fig. 6E–G).

Accessory glands

The accessory glands of *N. cincticeps* are long, tubular structures with bilateral symmetry. Their structure is relatively simple, consisting of a muscular sheath, epithelium, and basal lamina from the outside to the inside (Fig. 7A). The central part of the tube has a large amount of secretory material. Secretory granules with variable margins and vesicles surround epithelial nuclei. Multiple secretory granules gather to form a secretory center surrounded by mitochondria (Fig. 7B–D).

Ultrastructure of the female internal reproductive system of *N. cincticeps*

Vagina

The vagina of *N. cincticeps* is a simple, short, thick tubular structure. Transmission electron microscopy shows that it is composed of a muscular sheath, epithelium, and lumen. There are abundant mitochondria at the junction between

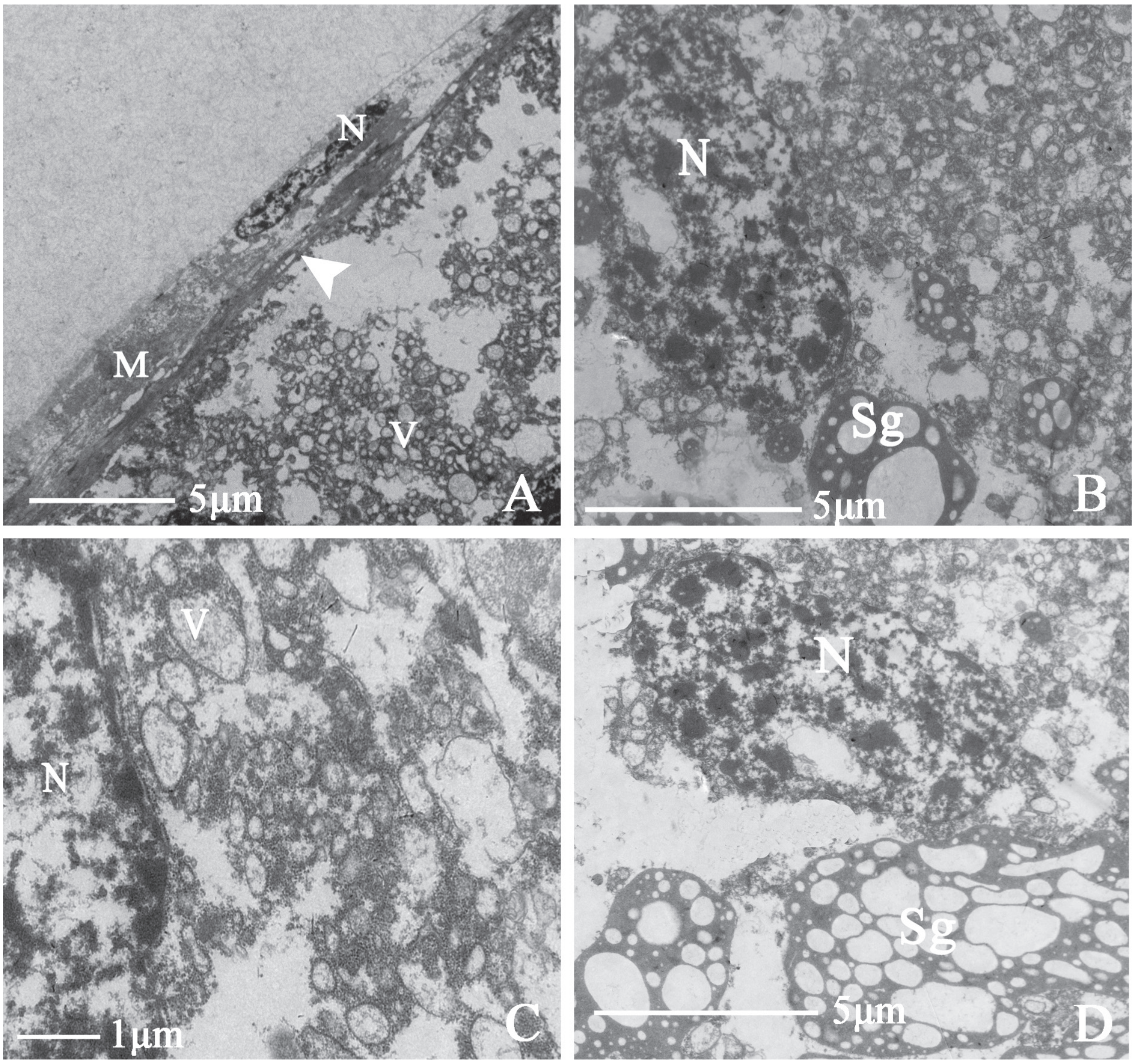

Figure 7. Ultrastructure of male accessory gland of *N. cincticeps* (Uhler, 1896) **A** cross-section of accessory gland, showing (M) muscle sheath, (N) epithelial cell nucleus, (BL) the white-arrowhead indicates basal lamina **B–D** showing (N) epithelial cell nucleus, (V) vesicle, (Sg) secretory granules.

the muscular sheath and lumen. The endoplasmic reticulum surrounds the epithelial cell nucleus. The core of the illustrated specimen is occupied by much sperm (Fig. 8A, B). Sperm swim in the lumen in the direction of the matrix (Fig. 8C, D).

Spermatheca

The spermatheca base is slender and tubular, the distal end is enlarged to about 90° and bent outward, and the whole structure is pale yellow. Under transmission electron microscopy, the spermatheca is shown to be composed of a muscular sheath, epithelium, and lumen. The spermatheca has a hollow lumen filled with

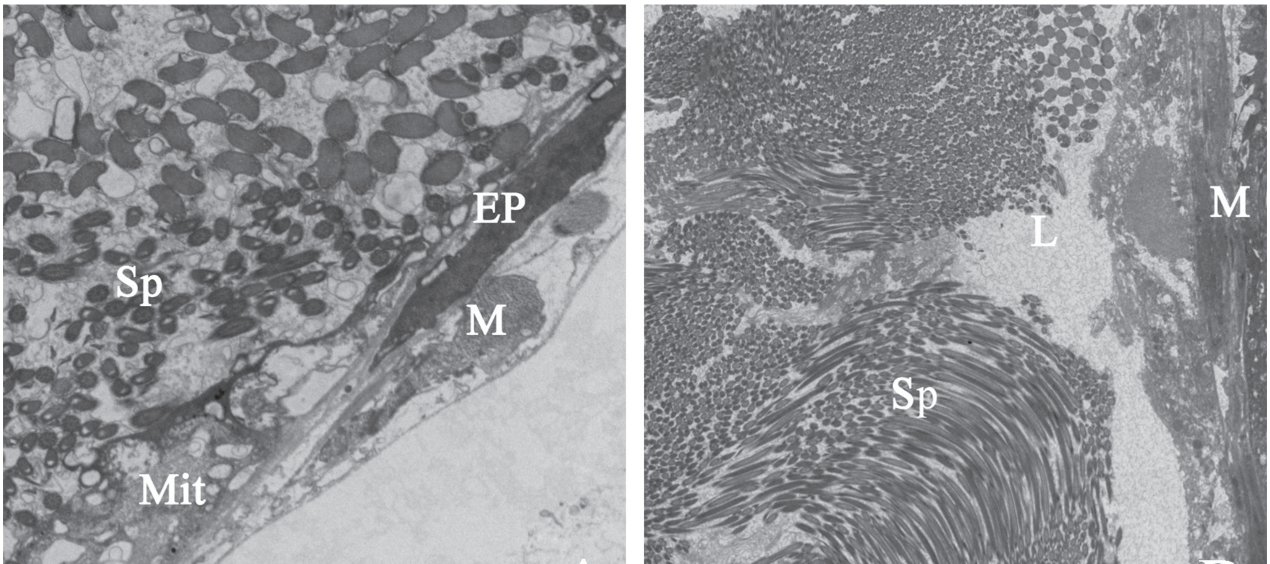

Figure 8. Ultrastructure of vagina of *N. cincticeps* (Uhler, 1896) **A, B** cross-section of vagina, showing (M) muscle sheath, (EP) epithelium, (Mit) mitochondria, (Sp) sperm, (L) lumen **C, D** showing (N) epithelial cell nucleus, (ER) endoplasmic reticulum, (L) lumen, (Sp) sperm, (Mit) mitochondria.

many sperm. Muscle texture is clearly visible in the muscular sheath, and a few tracheoles are observed at the junction with the epithelium (Fig. 9A). Infolding is present at the interval between the epithelium and the basal lamina. Numerous mitochondria and vesicles surround epithelial cell nucleus (Fig. 9B, C). Sperm swim in the matrix, which is covered by abundant lamellar bodies (Fig. 9D).

Ultrastructure of the male internal reproductive system of *D. vulgaris*

Testis

The testis has a clear margin and comprises six droplet-shaped testicular follicles of similar size and shape. The testis is symmetrical, without a sheath,

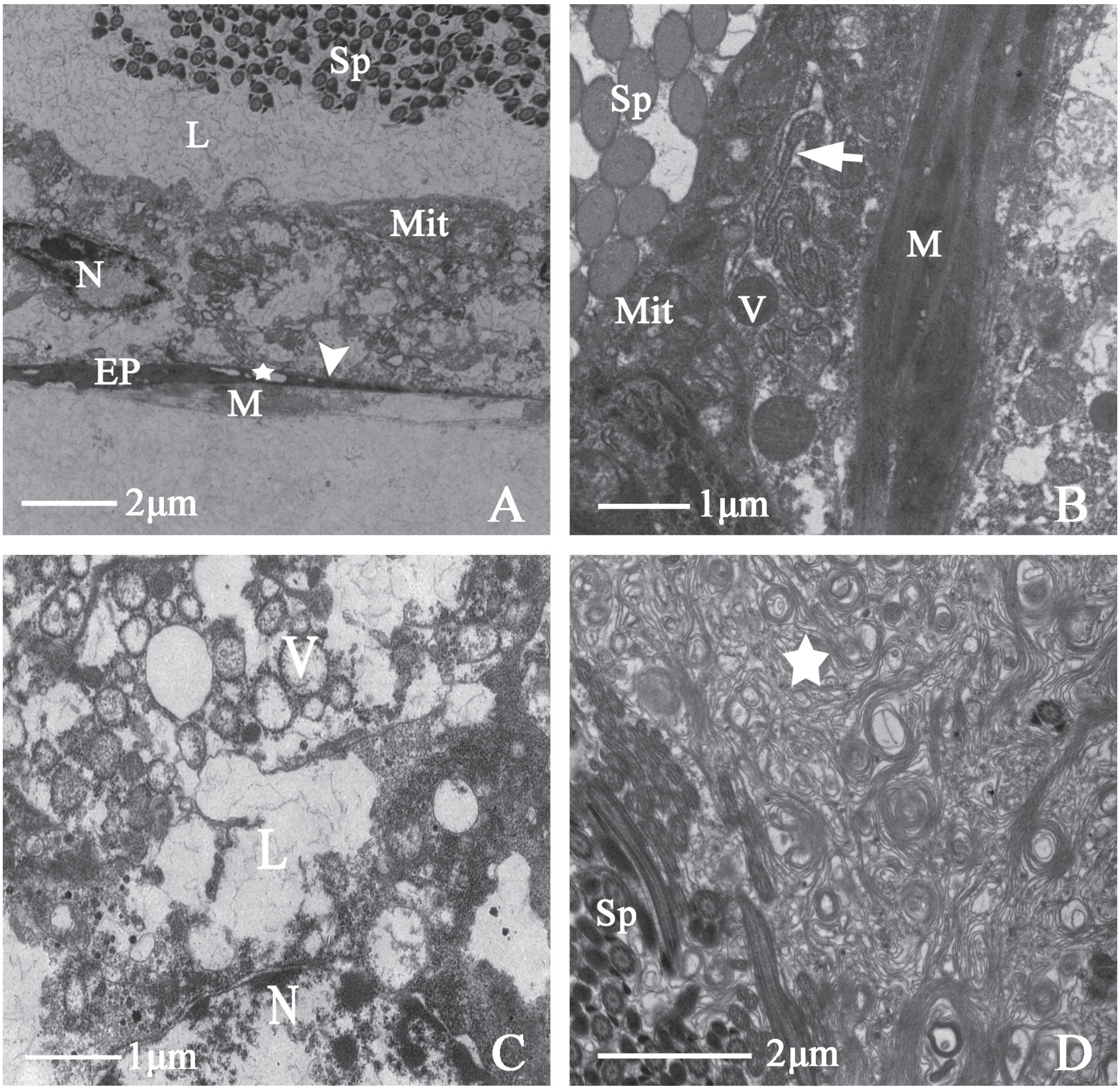

Figure 9. Ultrastructure of spermatheca of *N. cincticeps* (Uhler, 1896) **A** cross-section of spermatheca, showing (M) muscle sheath, (EP) epithelium, (L) lumen, (N) epithelial cell nucleus, (Sp) sperm, (BL) black triangular arrowhead indicates basal lamina **B, C** showing (M) muscle sheath, (V) vesicles, (Mit) mitochondria, (Sp) sperm, (L) lumen, (if) black arrowhead indicates infolding **D** showing (Sp) sperm.

and the surface is pale blue. The testicular follicles comprise a testicular follicle membrane, muscular sheath, epithelium, and lumen with sperm at different developmental stages. Mitochondria surround epithelial cell nucleus. Microtubule material besides the epithelial cell nucleus converges at both distal ends (Fig. 10A). There is a clear dividing line between the sperm and epithelium. Spermatogenesis and development occur in the lumen (Fig. 10B). A single sperm has a cell boundary and a thick basal lamina. There are a few vesicles between spermatozoa (Fig. 10C). Secretory cells are close to sperm cells. Sperm have a typical 9+9+2 axonemal pattern (Fig. 10D).

Seminal vesicle

The edge of the seminal vesicle is clear, and the seminal vesicle has star-like spots, is almost oval, and pale blue. The structure of the seminal vesicle

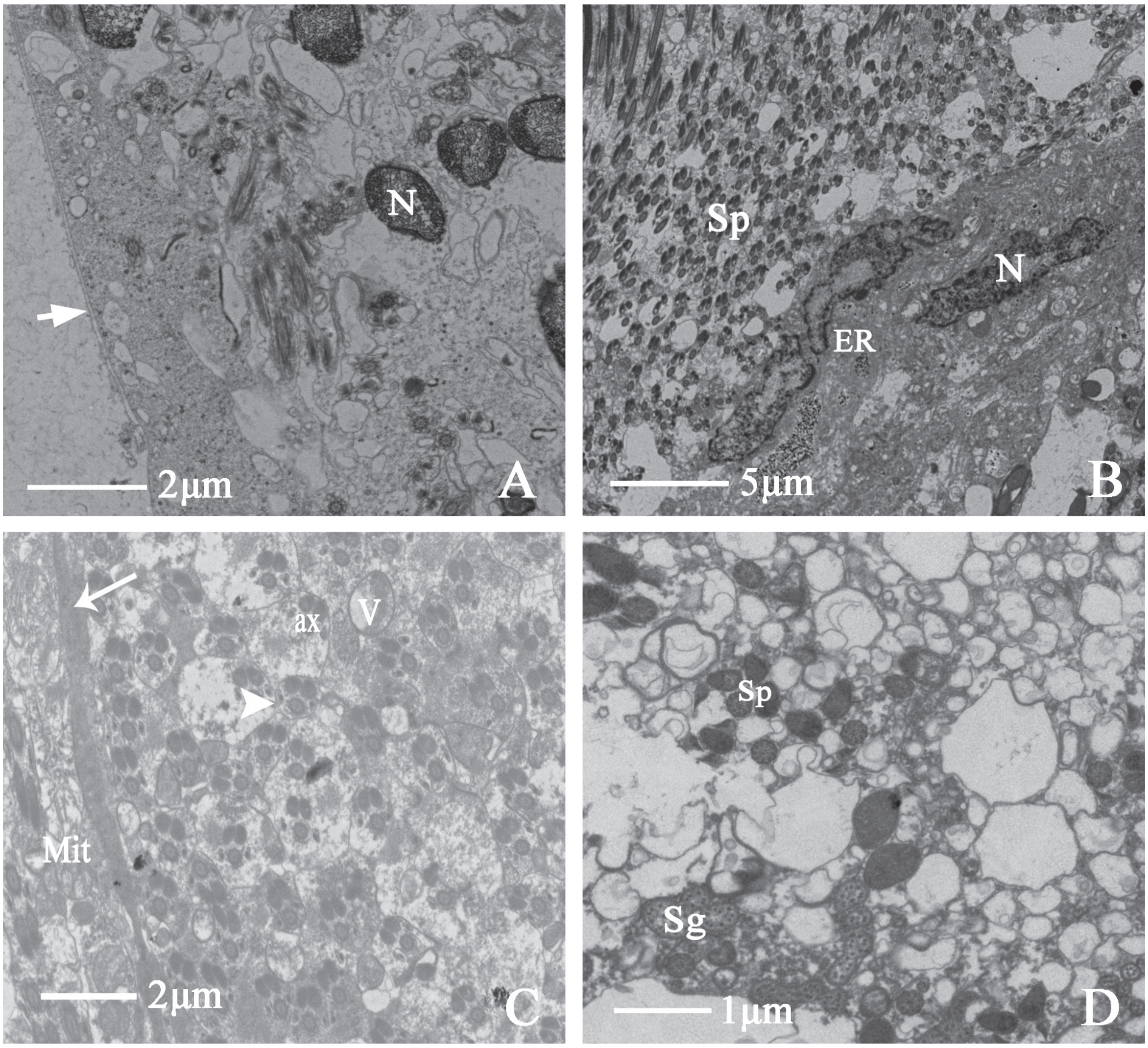

Figure 10. Ultrastructure of testicular follicle of *D. vulgaris* (Dash & Viraktamath, 1998) **A** cross-section of testicular follicle, showing (TM) testicular follicle membrane, (N) epithelial cell nucleus, (TM) the arrow indicates testicular follicle membrane **B** showing (Sp) spermatid, (ER) endoplasmic reticulum, (N) epithelial cell nucleus **C** showing (ax) axoneme, (V) vesicle, (Mit) mitochondria, (BM) the long arrow indicates thick basal membrane, (Sj) the triangular arrowhead indicates septate junction **D** showing (Sp) spermatid, (Sg) secretory granules.

consists of four parts: the tunica external, muscular sheath, epithelium, and lumen. The lumen contains many sperm at different stages of development, the sperm heads are inserted into the homogenous matrix, and there is an intercellular septum between sperm. There is an intercellular space between the tunica external and the muscular sheath. The muscles of the muscular sheath are clearly textured and striated. The basal lamina at the edge of the epithelium folds inward (Fig. 11A, B). Microvilli in the epithelium increase the area of the secretory surfaces (Fig. 11C–E).

Accessory gland

The accessory gland of *D. vulgaris* is relatively large and with bilateral symmetry. The front segment of the accessory gland protrudes, while the middle segment is contracted; the distal end is rod-like, and the whole is milky white. Its structure comprises a muscular sheath, epithelium, basal lamina, and numerous secretory granules. A dark basal lamina is formed at the edge of the epithelium, accompanied by basal lamina folding (Fig. 12A, B). Around the secretory granules, many weakly electron-dense vesicles congregate in the secretory cell

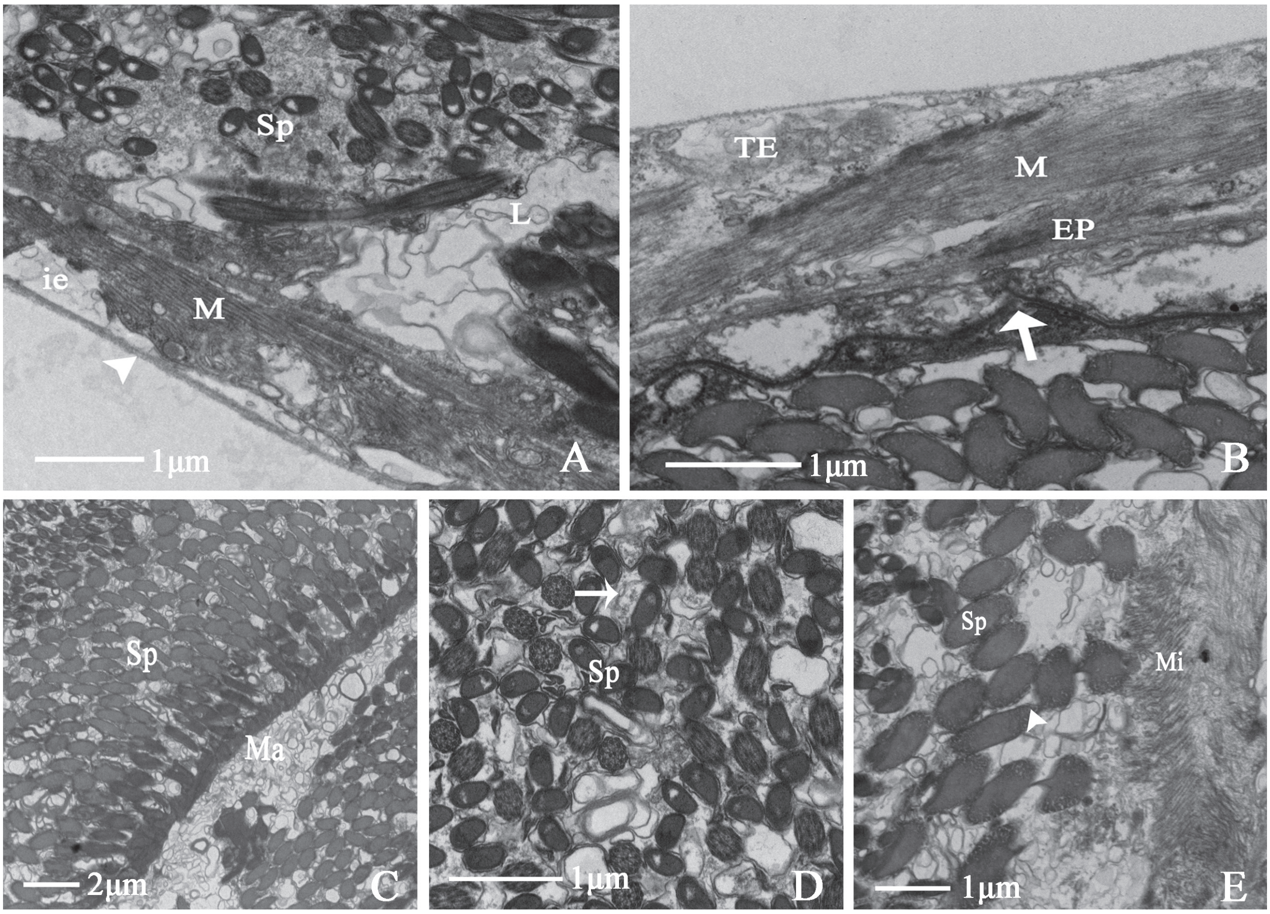

Figure 11. Ultrastructure of seminal vesicle of *D. vulgaris* (Dash & Viraktamath, 1998) **A, B** cross-section of seminal vesicle, showing (TE) tunica external, (M) muscle sheath, (EP) epithelium, (N) epithelial cell nucleus, (Sp) sperm, (L) lumen, (ie) intercellular spaces, (TE) the triangular arrowhead indicates tunica external, (BL) the long arrow indicates basal lamina **C–E** showing (Ma) head of sperm embedded in the homogenous matrix in lumen, (Sp) spermatid, (Sj) the arrow indicates a septate junction, (Mi) microvillus.

center, the margin is oval and surrounded by endoplasmic reticulum (Fig. 12C). Based on their morphology and composition, secretory granules can be divided into Sg1 and Sg2 (Fig. 12D).

Ultrastructure of the female internal reproductive system of *D. vulgaris*

Ovary

The ovaries of *D. vulgaris* are symmetrically expanded. A single ovariole is a milky-white tubular structure, rounded at the apex, with its distal end joining the lateral oviduct. At low magnification under transmission electron microscopy, the ovaries are oval and contain oocytes, fat droplets, and yolk granules. The margin of the basal lamina is clear, and the intercellular space is visible

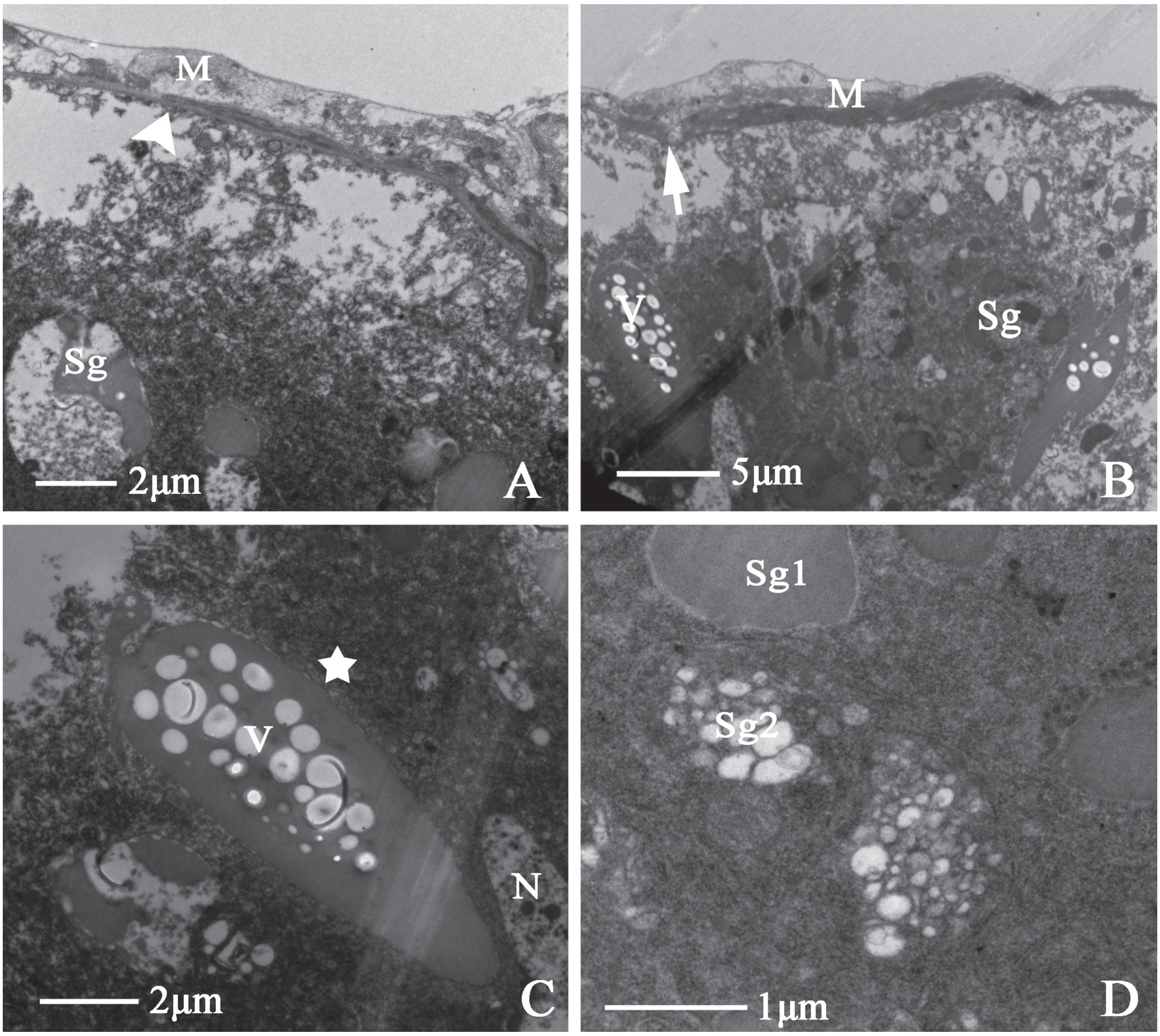

Figure 12. Ultrastructure of male accessory gland of *D. vulgaris* (Dash & Viraktamath, 1998) **A, B** cross-section of accessory gland showing (M) muscle sheath, (BL) triangular arrowhead indicates basal lamina, (if) the arrowhead indicates infolding, (Sg) secretory granules **C, D** showing (V) vesicle collection, (ER) the asterisk indicates endoplasmic reticulum, (N) epithelial cell nucleus, (Sg1) secretory granules 1, (Sg2) secretory granules 2.

(Fig. 13A, B). Many yolk granules, fat droplets, and lipid granules surround the oocyte. Trophocytes vary in morphology (Fig. 13C). Yolk granules and fat droplets embed into each other, enlarging as the ovariole develops. There are multiple vesicles (Fig. 13D).

Vagina

The vagina of *D. vulgaris* is a tubular structure and connects with the distal end of the common oviduct. Transmission electron microscopy shows that it is composed of a muscular sheath, epithelium, and lumen. The epithelium is

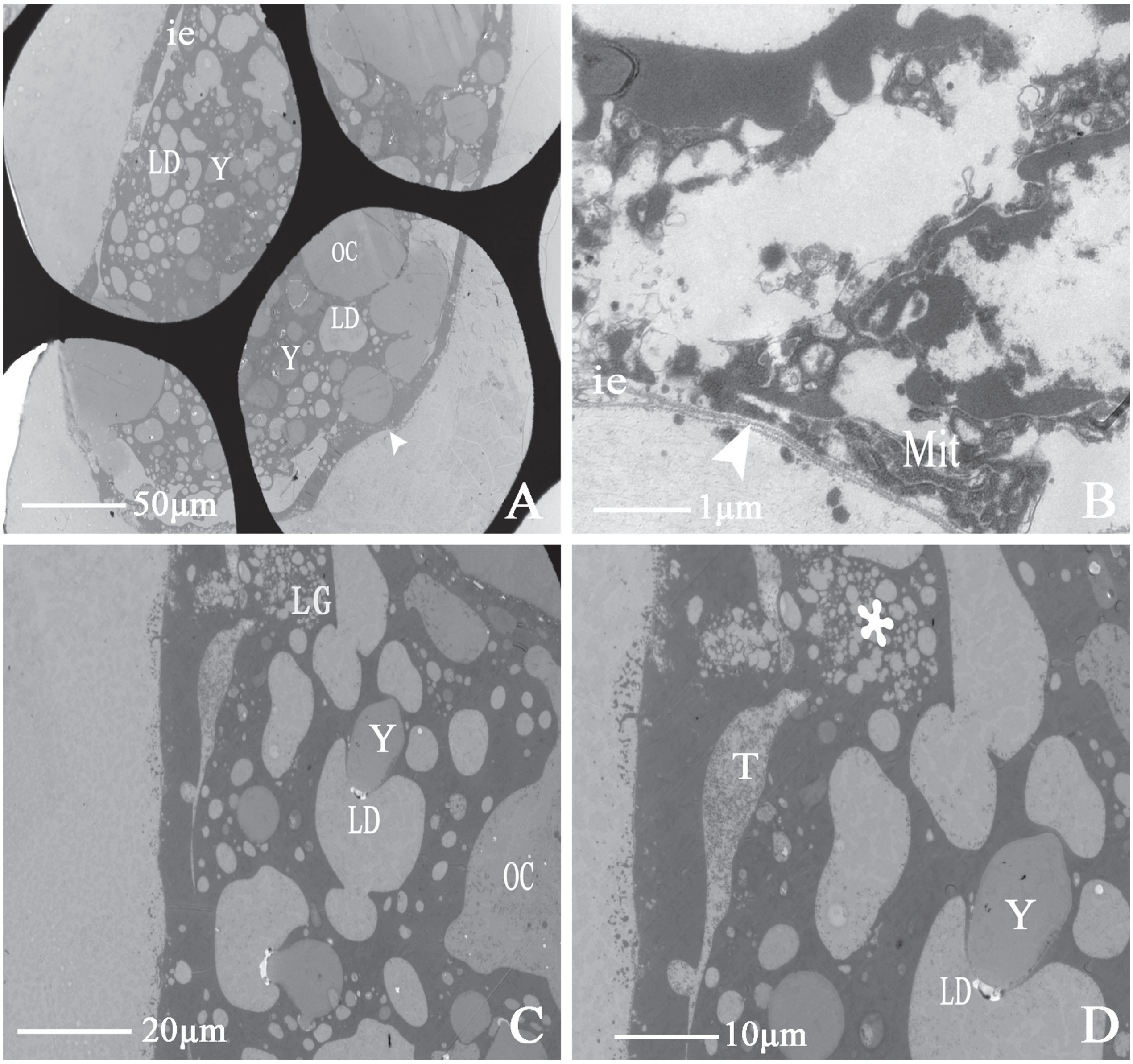

Figure 13. Ultrastructure of ovariole of *D. vulgaris* (Dash & Viraktamath, 1998) **A, B** cross-section of ovarioles, showing (OC) oocytes, (LD) lipid drop, (Y) yolk granule, (ie) intercellular spaces, (Mit) mitochondria, (BL) the arrow indicates basal lamina **C** showing (OC) oocytes, (LD) lipid drop, (Y) yolk granule, (LG) lipid granules **D** showing (T) trophocytes, (LD) lipid drop, (Y) yolk granule, (MB) the asterisk indicates a multivesicular body.

thicker, mottled, and stretched into strips (Fig. 14A). Tracheoles are present at the junction of the muscular sheath (Fig. 14B). Epithelial nuclei are surrounded by abundant mitochondria and an endoplasmic reticulum. No sperm was observed in the vagina of the specimen illustrated here. Cells are separated by a curved intercellular septum (Fig. 14C). Microvilli are observed in the epithelium (Fig. 14D). There are scattered unidentified, black, granular materials in the epithelium, accompanied by lamellar bodies (Fig. 14E).

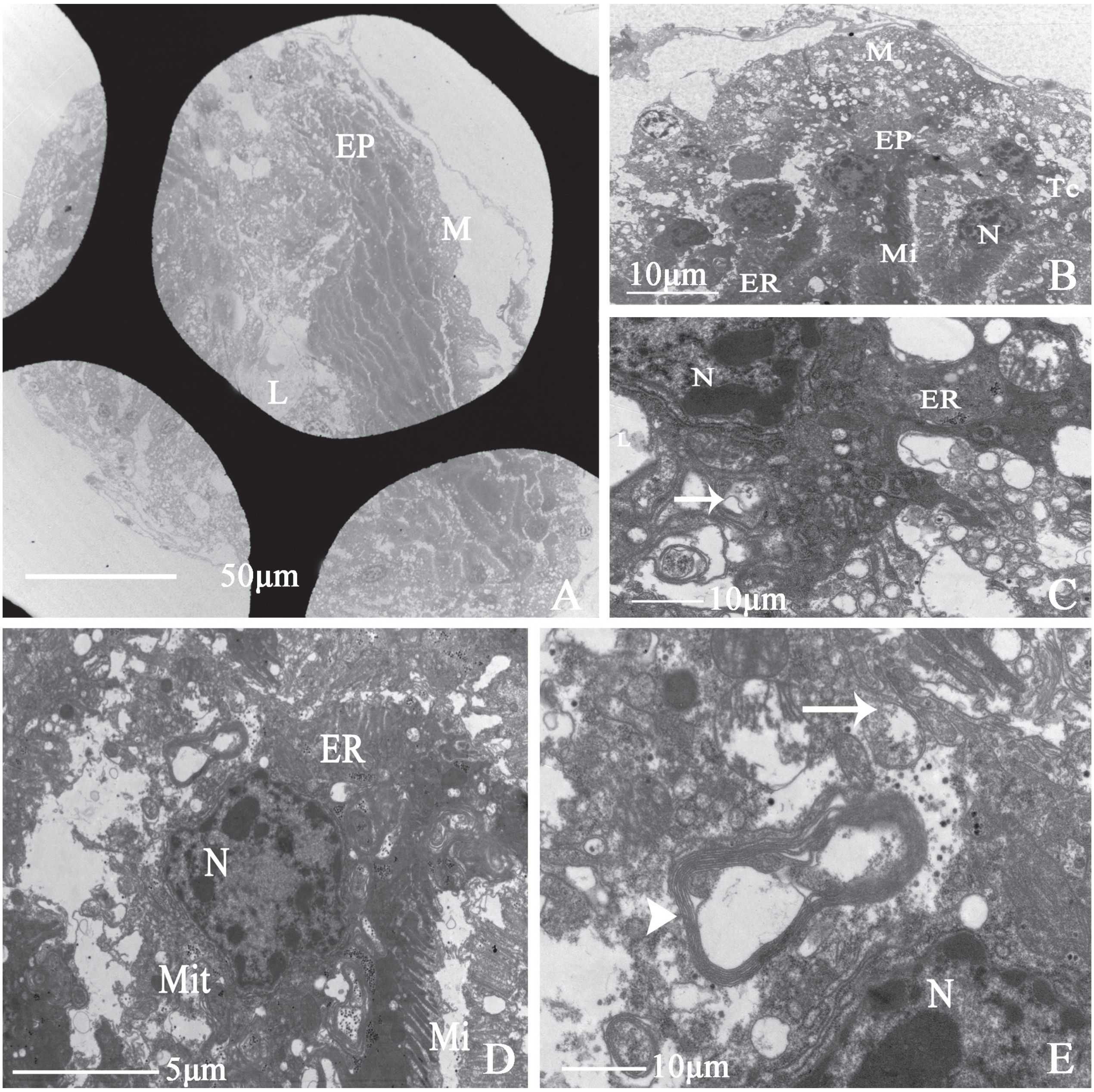

Figure 14. Ultrastructure of vagina of *D. vulgaris* (Dash & Viraktamath, 1998) **A** cross-section of vagina, showing (M) muscle sheath, (EP) epithelium, (L) lumen **B, C** showing (M) muscle sheath, (EP) epithelium, (ER) endoplasmic reticulum, (Mit) mitochondria, (Tc) tracheole, (Sj) the arrow indicates septate junction **D** showing (N) epithelial cell nucleus, (ER) endoplasmic reticulum, (Mit) mitochondria, (Mi) microvillus; (E) showing (N) epithelial cell nucleus, (Sj) the long arrow indicates the septate junction.

Discussion

In this study, the overall morphology and ultrastructure of the male and female internal reproductive systems of two species of Deltocephalinae are described and illustrated for the first time. The overall composition and structure of the internal genitalia of these species are similar to those of other studied leafhoppers. Although we observed some differences between *N. cincticeps* and *D. vulgaris*, further study will be needed to determine whether such differences, e.g., in the color of the seminal vesicles of the males and degree of development of the spermatheca and accessory glands of the females, are consistent or whether they may reflect different ages or physiological stages of the studied individuals.

Comparing our observations to the few published observations of the male internal reproductive organs of other leafhopper species (Table 1), we note that, in contrast to the two species of Deltocephalinae studied here, in which males have the seminal vesicles well separated from each other, as in the megophthalmine leafhopper *Agallia constricta* (Gil-Fernandez & Black, 1965), another deltocephaline species, *B. brevis* (tribe Macrostelini) has the seminal vesicles joined to each other medially (Vitale et al. 2015). Two previously studied species of sharpshooters (subfamily Cicadellinae) also have paired seminal vesicles joined

Table 1. Main features of male internal reproductive systems of Cicadellidae.

Subfamily	Tribe	Species	Testicular follicles	Seminal vesicle	Accessory gland	Lateral ejaculatory sac	Common ejaculatory duct	Reference
Cicadellinae	Cicadellini	*Bothrogonia ferruginea*	11–13, globular	2, oval, close integration	2, tubular, developed	Long, slender, tubular	Globular	Hayashi and Kamimura 2002
		Cicadella viridis	6, globular	2, columnar, close integration	2, tubular, short, white	Long, slender, tubular	Globular	Zhang et al. 2016
		Cofana spectra	3, oval	2, close integration	2, wide tubes	Long, straight	Expanded	Mishra 1979
		Cofana unimaculata	5	2, close integration	2, wide tubes	Long, convoluted	Expanded	Mishra 1979
		Kolla paulula	5, globular	2, teardrop, close integration	2, tubular, long, peachblow	Long, slender, tubular	Globular	Zhang et al. 2016
Deltocephalinae	Chiasmini	*Exitianus indicus*	6, dacryoid, yellow	2, immediate, columnar, forsythia	2, tubular, short, white	Short, thick, straight	Sausage, white	Su et al. 2014
		Nephotettix cincticeps	6, teardrop, baby blue	2, expanded, oval, baby blue	2, tubular, developed, white, transparent	Long, slender, tubular	Tubular, white	Here examined
	Deltocephalini	*Deltocephalus vulgaris*	6, teardrop, baby blue	2, expanded, oval, baby blue	2, tubular, milky white	Short, slender, tubular	Tubular, white	Here examined
		Graminella nigrifrons	6, oval	2, elliptical, immediate	2, tubular, long, thick	Long, thin, straight	Elliptical, white	Tsai and Perrier 1996
	Macrostelini	*Balclutha brevis*	6, oval	2, immediate, yellow	2, tubular, distal 2/3 yellow/brown, proximal 1/3 white/ opalescent	Long, thin, straight	Elliptical, white	Vitale et al. 2015
		Dalbulus maidis	6, oval	2, elliptical, immediate	2, tubular, long, thick	Long, thin, straight	Elliptical, white	Tsai and Perrier 1996
	Paralimnini	*Psammotettix striatus*	6, dacryoid, yellow	2, immediate, splayed, yellow	2, tubular, short, thick, white	Heliciform	Globular, white	Su et al. 2014
Eurymelinae	Idiocerini	*Amritodus atkinsoni*	6	2, separate	2, long, narrow, coiled	Short, straight	Expanded	Mishra 1979
Typhlocybinae	Empoascini	*Empoasca fabae*	4	2, oval	2, tubular	Short, tubular	Globular	Helms 1968

Table 2. Main features of female internal reproductive systems of Cicadellidae.

Subfamily	Tribe	Species	Ovariole	Common oviduct	Colleterial gland	Vagina	Spermatheca	Reference
Cicadellidae	Cicadellini	*Bothrogonia ferruginea*	—	Short, tubular	—	Globular	Expand	Hayashi and Kamimura 2002
	Proconiini	*Homalodisca vitripennis*	10, perlitic, milky white	—	1, tubular	Globular	Bursiform, 4 compartments	Hummel et al. 2006
Deltocephalinae	Athysanini	*Euscelidius variegatus*	7	Tubular	1, tubular	Globular	—	Cheung 1994, 1995
	Chiasmini	*Nephotettix cincticeps*	6, tubular, milk white	Short, tubular	1, tubular, developed	Tubular, milk white	Crooked, tubular, faintly yellow	Here examined
	Deltocephalini	*Deltocephalus vulgaris*	6, tubular, milk white	Short, tubular	1, tubular, underdeveloped	Tubular, faint yellow	Triangular, faintly yellow	Here examined
		Graminella nigrifrons	6	—	1, tubular, underdeveloped	Globular, white	Globular, small	Tsai and Perrier 1996
	Macrostelini	*Balclutha brevis*	6	Tubular, convoluted	—	Sac-shaped	Globular, small, brown	Pappalardo et al. 2016
		Dalbulus maidis	6	—	1, tubular, underdeveloped	Globular, small	Globular, small	Tsai and Perrier 1996
Typhlocybinae	Empoascini	*Empoasca fabae*	4	Tubular, convoluted	1, tubular	Club-shaped	Kidney-shaped	Helms 1968

Note: "—" information not reported.

medially (Tian et al. 2006; Zhang et al. 2016). Vitale et al. (2015) also noted that the male accessory glands of *B. brevis* are divided into distinct proximal and distal sections distinguishable by color. Such sections are evident in the accessory glands of *K. paulula* but not in *C. viridis*, based on illustrations by Zhang et al. (2016), and we also did not observe distinct regions in the two species examined here. However, the distal section of the accessory gland of *D. vulgaris* is somewhat paler than the darker proximal section. In other respects, leafhoppers' male internal reproductive structures appear to be highly conservative, although differences among species in the number of testicular follicles have been reported (Vitale et al. 2015), as observed among the two species studied here.

Comparing our observations to the few published observations of the female internal reproductive organs of other leafhopper species (Table 2), we note that, among female leafhoppers, the most obvious differences among species in the internal reproductive structures seem to be the number of ovarioles. The two studied species each had six ovarioles per ovary, as in most previously studied leafhopper species. However, the number of ovarioles may be much larger and vary within a species, e.g., 8–10 in *H. vitripennis* (Hummel et al. 2006). The structure of individual ovarioles may also vary among species, which may reflect differences in fecundity (Tsai and Perrier 1996), although such variation also occurs within individuals at different stages of development and vitellogenesis (Hummel et al. 2006). Much more comparative study, including the variation among individuals of the same species at different stages of development, is needed to elucidate further the morphological variability of leafhoppers' male and female internal reproductive structures.

Conclusion

The overall structure and organization, including details of the ultrastructure, of the male and female reproductive systems of *Nephotettix cincticeps* (Uhler,

1896) and *Deltocephalus vulgaris* (Dash & Viraktamath, 1998) are very similar to those of previously studied leafhoppers. The main differences observed among species include the number of testicular follicles, the relative position of seminal vesicles, the degree of development of the accessory glands in the male, the number of ovarioles, and the shape and color of the vagina and spermatheca in the female. This suggests that, compared to the external genitalia, which highly varies among species and is often used in taxonomy, the internal reproductive structures of leafhoppers offer relatively few characters useful for classification and phylogenetics. Nevertheless, relatively few species have so far been studied in detail. Future work should focus on representatives of the many additional leafhopper subfamilies that have not yet been studied in detail.

Acknowledgments

We sincerely thank J.R. Schrock, Emporia State University, USA, for commenting on an earlier draft of this paper and anonymous referees and the subject editor for constructive criticism.

Additional information

Conflict of interest

The authors have declared that no competing interests exist.

Ethical statement

No ethical statement was reported.

Funding

This research was funded by the Anhui Provincial Colleges and Universities Natural Science Foundation (2022AH050868), the National Natural Science Foundation of China (31000968) and the Innovation and Entrepreneurship Training Program for College Students (X202210364112).

Author contributions

Conceptualization: YD; Methodology: WL; Investigation: JC, WL; Data Acquisition: WL; Data Analysis: YD; Writing-Original Draft Preparation: JC, JZ, BS; Writing-Review & Editing: all authors; Supervision: CHD; Funding Acquisition: YD.

Author ORCIDs

Jiarui Chen https://orcid.org/0009-0002-7919-1972
Jing Zhang https://orcid.org/0000-0002-9354-786X
Wei Liu https://orcid.org/0009-0001-1727-0280
Bismillah Shah https://orcid.org/0000-0002-8407-8627
Christopher H. Dietrich https://orcid.org/0000-0003-4005-4305
Yani Duan https://orcid.org/0000-0002-5952-0778

Data availability

All of the data that support the findings of this study are available in the main text.

References

Cheung WWK (1994) Ultrastructural studies on the female reproductive system of the leafhopper *Euscelidium variegatus* Kirshbaum (Homoptera, Cicadellidae) I. The germarium. Cytologia 59(1): 93–101. https://doi.org/10.1508/cytologia.59.93

Cheung WWK (1995) Ultrastructural studies on the female reproductive system of the leafhopper *Euscelidium variegatus* Kirshbaum (Homoptera, Cicadellidae) II. The vitellarium oocytes and follicular epithelium. Cytologia 60(4): 395–405. https://doi.org/10.1508/cytologia.60.395

Hayashi F, Kamimura Y (2002) The potential for incorporation of male derived proteins into developing eggs in the leafhopper *Bothrogonia ferruginea*. Journal of Insect Physiology 48(2): 153–159. https://doi.org/10.1016/S0022-1910(01)00159-7

Helms TJ (1968) Postembryonic reproductive systems development in *Empoasca fabae*. Annals of the Entomological Society of America 61(2): 316–332. https://doi.org/10.1093/aesa/61.2.316

Hummel NA, Zalom FG, Peng CYS (2006) Anatomy and histology of reproductive organs of female *Homalodisca coagulata* (Hemiptera, Cicadellidae, Proconiini), with special emphasis on categorization of vitellogenic oocytes. Annals of the Entomological Society of America 99(5): 920–932. https://doi.org/10.1603/0013-8746(2006)99[920:AAHORO]2.0.CO;2

Lei CL, Rong XL (2003) Reproductive system and physiology of insects. In: Lei CL, Rong XL (Eds) General Entomology (2nd edn.). China Agriculture Press, Beijing, 300–316.

Mishra RK (1979) Male reproductive organs of five species of Auchenorrhyncha (Homoptera). Acta Entomologica Bohemoslovaca 76: 162–168.

Pappalardo AM, D'Urso V, Viscuso R, Ferrito V, Giunta MC, Cupani S, Vitale DGM (2016) Morphostructural investigation of the female reproductive system and molecular evidence for *Wolbachia* in *Balclutha brevis* Lindberg, 1954 (Hemiptera, Cicadellidae). Micron 81: 23–33. https://doi.org/10.1016/j.micron.2015.12.003

Song DL (2011) The reproductive system of the insects. In: Cai WZ, Pang XF, Hua BZ, Liang GW, Song DL (Eds) General Entomology, Second Edition. China Agricultural University Press, Beijing, 178–184.

Su M, Dietrich CH, Zhang YL, Dai W (2014) Ultrastructure of the spermatozoa of *Psammotettix striatus* (Linnaeus) and *Exitianus nanus* (Distant) (Hemiptera, Auchenorrhyncha, Cicadellidae, Deltocephalinae). Arthropod Structure & Development 43(6): 559–570. https://doi.org/10.1016/j.asd.2014.06.003

Tian RG, Yuan F, Zhang YL (2006) Male reproductive system and spermatogenesis in Homoptera (Insecta, Hemiptera). Entomotaxonomia 28(4): 241–253.

Tsai JH, Perrier JL (1996) Morphology of the digestive and reproductive system of *Dalbulus maidis* and *Graminella nigrifrons* (Homoptera, Cicadellidae). The Florida Entomologist 79(4): 563–578. https://doi.org/10.2307/3496069

Vitale DGM, Viscuso R, D'Urso V, Gibilras S, Sardella A, Marletta A, Pappalardo AM (2015) Morphostructural analysis of the male reproductive system and DNA barcoding in *Balclutha brevis* Lindberg 1954 (Homoptera, Cicadellidae). Micron 79: 36–45. https://doi.org/10.1016/j.micron.2015.08.002

Zhang BB, Zhang CN, Dietrich C, Dai W (2016) Anatomy and ultrastructure of male reproductive system in two leafhoppers *Cicadella viridis* and *Kolla paulula* (Hemiptera, Auchenorrhyncha, Cicadellidae). Annals of the Entomological Society of America 109(3): 447–462. https://doi.org/10.1093/aesa/saw016